Appendix II-F2

Avian Appendix

May 2024

Appendix II-F2

Supporting Material for Avian Assessment:

Data Sources, Methods, and Results

December 17, 2021
Updated August 23, 2022

Prepared by:

Biodiversity Research Institute

276 Canco Road

Portland, ME 04103

Table of Contents

List of Figures

List of Tables

List of Acronyms and Abbreviations

BOEM	Bureau of Ocean Energy Management
COP	Construction and Operations Plan
dBBMM	dynamic Brownian-bridge movement model
ECC	Export cable corridor
EIS	Environmental Impact Statement
ESA	Endangered Species Act
ft	feet
GPS	Global Positioning System
GSD	ground sampling distance
INLA	Integrated nested Laplace approximation
IPaC	Information for Planning and Consultation
km	kilometer
m	meter
MDAT	Marine-life Data and Analysis Team
mi	mile
MLLW	Mean Lower Low Water
MW	megawatt
NCCOS	National Center for Coastal Ocean Science
nm	nautical mile
NJDEP	New Jersey Department of Environmental Protection
NOAA	National Oceanic and Atmospheric Administration
OCS	Outer Continental Shelf
OSS	offshore substation
PiF	Partners in Flight
POI	Point of Interconnection
PTT	Argos platform terminal transmitter
RSZ	rotor swept zone
SDJV	Sea Duck Joint Venture
UD	Utilization distribution
UK	United Kingdom of Great Britain and Northern Ireland
US	United States
USFWS	United States Fish and Wildlife Service
WEA	Wind Energy Area
WTA	Wind Turbine Area
WTG	Wind Turbine Generator

1 Summary

Atlantic Shores Offshore Wind, LLC ("Atlantic Shores") proposes to construct, operate, and decommission two offshore renewable wind energy projects in the southern portion of Bureau of Ocean Energy Management (BOEM) Lease Area OCS-A 0499 (Lease Area), within the New Jersey Wind Energy Area (NJWEA), along with associated offshore and onshore cabling, onshore substations and/or converter stations, landfall sites, and an onshore Operations and Maintenance (O&M) Facility and associated parking structure. Section 4.3 of Atlantic Shores' Construction and Operation Plan (COP) describes the presence of birds and suitable bird habitat in the Offshore Project Area (including the Wind Turbine Area [WTA], composed of Project 1, Project 2, and an Overlap Area), and the Onshore Project Area. Potential project-related impacts to birds and suitable bird habitat are also discussed. This Appendix to the COP provides detailed supporting information for both the offshore and onshore components of the Projects.

Offshore, there are taxonomic sections on avian exposure (likelihood of occurrence) and vulnerability. Exposure to the WTA is assessed using project specific digital aerial surveys, New Jersey boat-based surveys, regional models, and tracking data.

<u>Aerial surveys</u>: A series of eight digital aerial surveys were flown across the Lease Area, from October 2020 to May 2021. Spatially-explicit models were fit to the year-round and seasonal survey data, by species and taxa group using integrated nested Laplace approximation (INLA), to model the observation density and account for the spatial dependence among observations. The surveys provide density estimates for three seasons to support understanding individual level exposure and the spatial models provide information on how birds are distributed across the Lease Area.

<u>Boat-based surveys</u>: The New Jersey Department of Environmental Protection (NJDEP) Ocean/Wind Power Ecological Baseline Studies (NJDEP Baseline Studies) included monthly boat-based avian surveys conducted coastally and further offshore of New Jersey between January 2008 and December 2009. An effort was made to distance correct the data using community distance models and standard distance correction methods, but the models had a poor fit and correction was not applied. The naïve density estimates were used in the exposure assessment to determine how the density of birds in the WTA compare surveys in other areas during the NJDEP Baseline Studies.

<u>MDAT models</u>: Seasonal predictions of bird density were developed by National Oceanic and Atmospheric Administration (NOAA) to support Atlantic marine renewable energy planning, which describe regional-scale patterns of abundance. The models were used in the exposure assessment to determine how the density of birds in the WTA compare to other areas along the Atlantic OCS. These models, along with the boat-based surveys, and modeled digital surveys are presented for each species and season at the end of the Appendix.

<u>Tracking data</u>: Numerous tracking studies are available along the Atlantic Outer Continental Shelf (OCS) to improve the understanding of bird exposure to the WTA. Atlantic Shores conducted a GPS tracking study of Red Knots (*Calidris canutus rufa*) in coastal New Jersey; U.S.

Fish and Wildlife (USFWS) tracked shorebirds (Red Knot, Piping Plover [*Charadrius melodus*], Roseate Tern [*Sterna dougallii*]) with nanotags; BOEM supported satellite tracking of diving birds (Red-throated Loon [*Gavia stellate*], Northern Gannet [*Morus bassanus*], and Surf Scoter [*Melanitta perspicillata*]); and other researchers have tracked sea ducks, herons, falcons, and Osprey (*Pandion haliaetus*). Collectively, these data provide information on the potential exposure of these species to the WTA.

Vulnerability: For the birds exposed to the WTA, vulnerability to collision and displacement was then assessed for marine birds using a scoring process and the literature for nonmarine birds. This assessment of vulnerability focused on documented avoidance behaviors, estimated flight heights, and other factors. Flight heights used in the assessment were gathered from the datasets in the Northwest Atlantic Seabird Catalog.

The onshore section includes maps of the cable landfall areas, interconnection cable routes, substation and/or converter station locations, and points of interconnection (POIs). Tables detail the habitat types associated with the each of the onshore Project components and the degree that they are co-located with existing development. A list of birds that may occur is presented based on eBird records within 9.3 mi (15 km) of onshore components as well as monthly eBird records of Red Knot and Piping Plover detections. Maps and tables provide estimates on the distance of know Piping Plover nesting locations in relation to cable landfall sits as well as areas being considered for Red Knot critical habitat. Overall, these robust datasets provide support for the offshore and onshore risk assessment detailed in the COP.

2 Introduction

This Appendix provides support for the detailed avian assessment provided in Section 4.3 of COP Volume II. Section 3 of this Appendix focuses on the birds in the onshore environment; Section 4 provides specific details on the methods used for the offshore assessment; Section 5 focuses on birds in the offshore environment and includes details on seasonal densities of birds exposed to the southern portion of Lease Area OCS-A 0499 (Lease Area); Section 6 lists the literature cited, Section 7 describes the methods for applying a community distance model to correct density estimates of seabirds in New Jersey waters; Section 8 provides an analysis of NJDEP baseline density estimates relative to a 15-mile offshore boundary section; and Section 9 provides seasonal exposure maps for marine birds.

2.1 Project Description

Atlantic Shores Offshore Wind, LLC ("Atlantic Shores") proposes to construct, operate, and eventually decommission two offshore renewable wind energy facilities in the southern portion of Bureau of Ocean Energy Management (BOEM) the Lease Area, within the New Jersey Wind Energy Area (NJWEA), along with associated offshore and onshore cables, onshore substations and/or converter stations, POIs and an onshore O&M Facility with an associated parking structure. The southern portion of the Lease Area (referred to herein as the Wind Turbine Area, or WTA, contains Project 1, Project 2, and the Overlap Area, which include an array of up to 200 wind turbine generators (WTGs)[1] and multiple offshore substations (OSSs). Meteorological (met) towers and/or meteorological and oceanographic (metocean) buoys may also be installed in the WTA. Offshore export cables will transmit electricity from the WTA to onshore transmission systems via landfalls in Atlantic City and Monmouth, New Jersey (Figure 2-1).

The WTA is approximately 102,055 acres (413 km^2), and approximately 8.7 miles (mi) (14 kilometers [km]) from the New Jersey shoreline, at its closest point. The structures (WTGs and OSSs) will be aligned in a uniform east-northeast/west-southwest grid pattern, designed to maximize offshore renewable wind energy production while minimizing effects on existing marine uses in the Atlantic Shores Offshore Project Area. The Projects are in an area of shelf water (62 to 121 ft [19 to 37 m]) that is generally devoid of significant underwater features, such as shoals, that would provide regionally important foraging areas (Figure 2-2), although there is a diverse group of birds that have the potential to use the WTA (Table 2-1).

[1] Project 1 will have a minimum of 105, up to a maximum of 136 WTGs. Project 2 will have a minimum of 64, up to a maximum of 95 WTGs. The Overlap Area includes 31 turbine locations that could be used by Project 1 or Project 2.

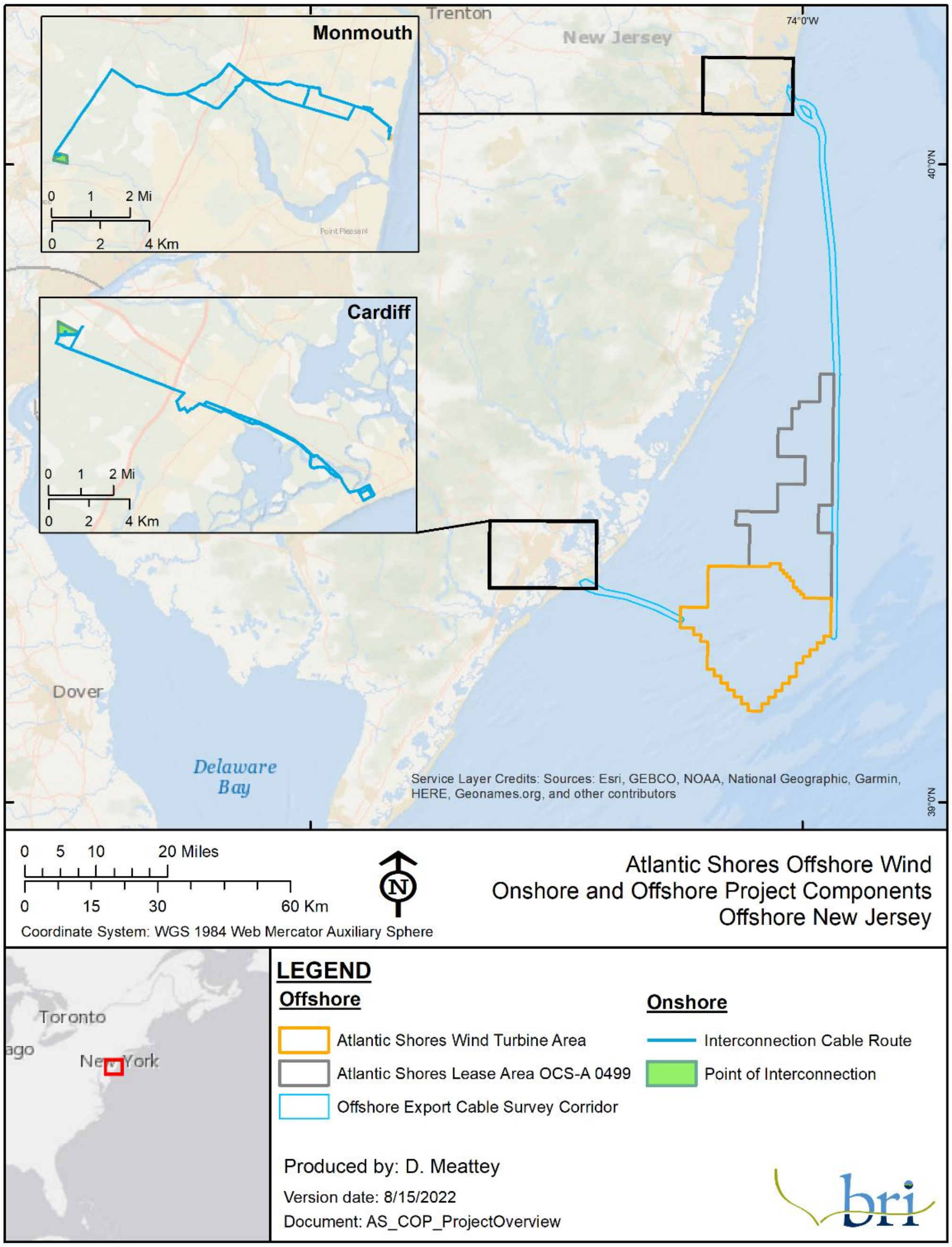

Figure 2-1: Overview of Onshore and Offshore Project Components.

2.2 Methods Overview

Offshore

For each subject group addressed under this assessment, species occurrence and area use were identified and evaluated using multiple data sources, including but not limited to: Lease Area specific digital aerial surveys (APEM), NJDEP Baseline Studies boat-based surveys, National Oceanic and Atmospheric Administration (NOAA) Marine-Life Data and Analysis Team (MDAT) bird distribution models, Northwest Atlantic Seabird Catalog, eBird and other occurrence and phenology data, individual tracking studies, relevant current literature, and species accounts.

Most species were assessed within general taxonomic groups (e.g., wading birds), however, species with federal listing status, or candidate species, were individually assessed, namely the Piping Plover (*Charadrius melodus*), Red Knot (*Calidris canutus rufa*), Roseate Tern (*Sterna dougallii*), and Black-capped Petrel (*Pterodroma hasitata*).

The results section of this Appendix addresses exposure and vulnerability of coastal birds and marine birds separately and includes maps, tables, and figures for each major taxonomic group. Exposure assessment maps, tables, and figures are presented for both coastal and marine birds based on the aforementioned data sources.

For the offshore assessment, a semi-quantitative approach was taken that first describes the species that would potentially be exposed to the WTA, and the vulnerability of the species exposed. The assessment process was as follows:

- *Exposure* – The first step in the process was to assess exposure for each species and each taxonomic group, where 'exposure' is defined as the extent of overlap between a species' seasonal or annual distribution and the WTA. For species where site-specific data was available, a semi-quantitative exposure assessment was conducted. This exposure assessment was focused exclusively on the horizontal, or two-dimensional, likelihood that a bird would use the WTA.

- *Relative Vulnerability* – Potential vulnerability was then assessed for marine birds using a scoring process. For the purposes of this analysis, 'behavioral vulnerability' is defined as the degree to which a species is expected to be affected by WTGs in the WTA based on known responses to similar offshore developments. This assessment of behavioral vulnerability focused on documented avoidance behaviors, estimated flight heights, and other factors. Flight heights used in the assessment were gathered from the NJDEP Baseline Studies (local) and non-digital aerial survey datasets in the Northwest Atlantic Seabird Catalog (regional).

Onshore

The onshore section includes maps of the landfall sites, interconnection cable routes, substation and/or converter station locations, and POIs. Tables detail the habitat types associated with the each of the onshore project components and the degree that they are co-located with existing development. A list of birds that may occur is presented based on eBird records within 9.3 mi (15 km) of onshore components as well as monthly eBird records of Red Knot and Piping Plover detections. Since eBird effort is inconsistent, the 9.3 mi buffer was used to include more sites where birds were observed to ensure most species using the general area were recorded. Maps and tables provide estimates on the distance of known Piping Plover nesting locations in relation to cable landfall sits as well as areas being considered for Red Knot critical habitat.

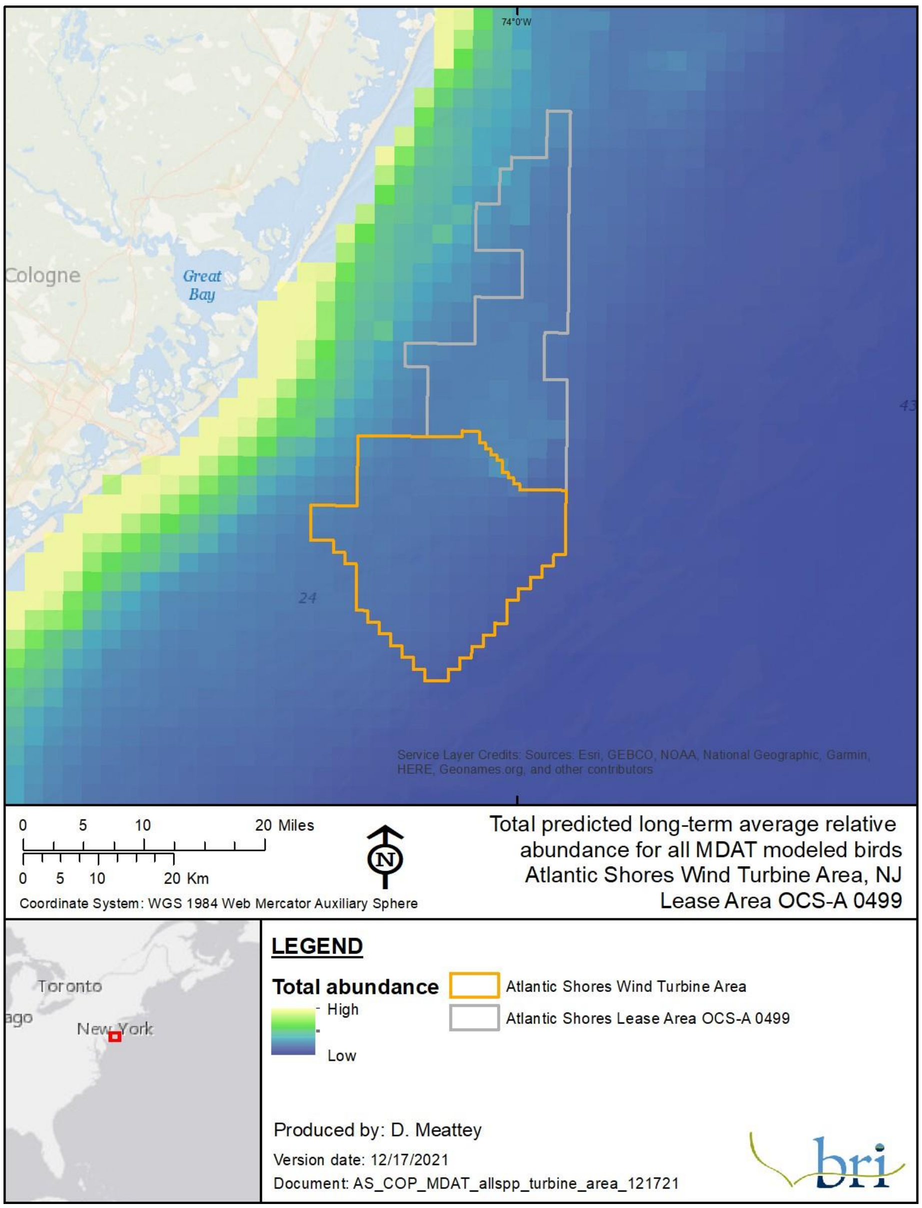

Figure 2-2: Estimated total bird abundance from the MDAT models. The models highlight that overall abundance is lower in the WTA than adjacent nearshore waters.

Table 2-1: List of species detected within the WTA in various data sources (NJDEP, MDAT, APEM, IPaC), plus federally-listed species that may occur in the area, and their conservation status.

Common Name	Latin Name	Source				Conservation Status[1]	
		NJDEP	MDAT	APEM	IPaC	Federal	State
Ducks, geese, and swans							
Snow Goose	*Anser caerulescens*	•					
American Black Duck	*Anas rubripes*	•					
Sea ducks							
Surf Scoter	*Melanitta perspicillata*	•	•		•		
White-winged Scoter	*Melanitta fusca*	•	•	•	•		
Black Scoter	*Melanitta americana*	•	•		•		
Red-breasted Merganser	*Mergus serrator*	•	•		•		
Loons							
Red-throated Loon	*Gavia stellata*	•	•	•	•		
Common Loon	*Gavia immer*	•	•	•	•		
Herons and egrets							
Great Blue Heron	*Ardea herodias*	•					SC
Black-crowned Night-Heron	*Nycticorax nycticorax*	•					T
Shearwaters and petrels							
Black-capped Petrel	*Pterodroma hasitata*					Cand.	
Cory's Shearwater	*Calonectris diomedea*	•	•			BCC	
Sooty Shearwater	*Ardenna grisea*	•	•				
Great Shearwater	*Ardenna gravis*	•	•		•		
Audubon's Shearwater	*Puffinus lherminieri*	•	•			BCC	
Wilson's Storm-Petrel	*Oceanites oceanicus*	•	•		•		
Gannets							
Northern Gannet	*Morus bassanus*	•	•	•			
Cormorants and pelicans							
Double-crested Cormorant	*Phalacrocorax auritus*	•	•		•		
Brown Pelican	*Pelecanus occidentalis*	•	•		•		
Jaegers and gulls							
Parasitic Jaeger	*Stercorarius parasiticus*	•	•				
Black-legged Kittiwake	*Rissa tridactyla*	•	•	•			
Bonaparte's Gull	*Chroicocephalus philadelphia*	•	•	•			
Laughing Gull	*Leucophaeus atricilla*	•	•	•			
Ring-billed Gull	*Larus delawarensis*	•	•		•		
Herring Gull	*Larus argentatus*	•	•	•			
Great Black-backed Gull	*Larus marinus*	•	•	•			
Terns							
Black Tern	*Chlidonias niger*	•					
Common Tern	*Sterna hirundo*	•	•				SC
Forster's Tern	*Sterna forsteri*	•					
Roseate Tern	*Sterna dougallii*	•			•	E	E

Common Name	Latin Name	Source				Conservation Status[1]	
		NJDEP	MDAT	APEM	IPaC	Federal	State
Royal Tern	*Thalasseus maximus*	•	•		•		
Auks							
Dovekie	*Alle alle*	•	•		•		
Common Murre	*Uria aalge*	•	•		•		
Razorbill	*Alca torda*	•	•		•		
Atlantic Puffin	*Fratercula arctica*	•	•		•		
Shorebirds							
Black-bellied Plover	*Pluvialis squatarola*	•					
Piping Plover	*Charadrius melodus*					T	E
Red Knot	*Calidris canutus rufa*					T	E
Sanderling	*Calidris alba*	•					SC
Least Sandpiper	*Calidris minutilla*	•					
Red-necked Phalarope	*Phalaropus lobatus*	•	•				
Red Phalarope	*Phalaropus fulicarius*	•	•				
Passerines							
Purple Martin	*Progne subis*	•					
Tree Swallow	*Tachycineta bicolor*	•					
Barn Swallow	*Hirundo rustica*	•					
House Finch	*Haemorhous mexicanus*	•					
Pine Siskin	*Spinus pinus*	•					
American Goldfinch	*Spinus tristis*	•					
Song Sparrow	*Melospiza melodia*	•					
Red-winged Blackbird	*Agelaius phoeniceus*	•					
Brown-headed Cowbird	*Molothrus ater*	•					
Northern Waterthrush	*Parkesia noveboracensis*	•					
Northern Parula	*Setophaga americana*	•					SC
Yellow-rumped Warbler	*Setophaga coronata*	•					
Black-throated Green Warbler	*Setophaga virens*	•					

[1] E=Endangered, T=Threatened, SC=Special Concern, Cand.=Candidate for listing under ESA, BCC=Birds of Conservation Concern

3 Birds – Onshore Methods and Results

This section provides tables, maps, and figures to support the discussion in Section 4.3 of the COP Volume II about the birds that may be impacted by construction and operation of the onshore project components, including landfall sites, onshore interconnection cables, onshore substations and/or converter stations, POIs, and the O&M Facility. The habitat that would be modified by onshore project components is described and the birds likely to occur in the habitat are provided. Additional information is provided on federally-listed species.

3.1 Assessment Methods and Data Sources

3.1.1 Onshore Interconnection Cable Route Habitat Assessment

The habitat potentially to be disturbed by the onshore project components was assessed by calculating the overlap of the interconnection cable routes with local habitat types; and then by calculating the percentage each route was co-located with existing development. The habitat types were determined for each cable route using the Land Use/Land Cover of New Jersey 2015 data set available from the NJDEP Bureau of GIS[2]. The classification system used was a modified Anderson (1976) classification system. A 100 ft (30 m) buffer was applied to either side of each proposed cable route. This buffer width was expected to account for potential disturbance across the construction ROW. The area of each landscape type within each buffered cable route was calculated using the Intersect tool in ArcGIS (ESRI v10.8.1).

Co-occurrence of the interconnection cable route options with existing linear infrastructure was also assessed in ArcGIS (ESRI v10.8.1). Road centerlines for the state of New Jersey were downloaded from the New Jersey Geographic Information Network (NJGIN) and clipped to the buffered cable route layers. All road features that ran parallel to the cable route were manually selected and summed for total road length and percentage of total route length. These same methods were used to assess total, and percentage co-occurrence with existing transmission line corridors using an Electrical Power Transmission Lines layer developed for the Homeland Infrastructure Foundation-Level Data (HIFLD[3]).

3.1.2 Avian Data Sources and Methods

Data on possible bird species present, including Red Knot and Piping Plover, were primarily compiled from eBird citizen science data (Sullivan et al. 2009) from within a 9.3 mi (15 km) buffer of the center of the onshore sites and was temporally constrained to the prior 10 years of data (2011-2021). In addition, the USFWS IPaC database (USFWS 2020) was queried using a polygon encompassing the entire Onshore Project Area. Piping Plover nesting sites in coastal New Jersey were mapped based on sites identified in Heiser and Davis (2020).

---

[2] https://gisdata-njdep.opendata.arcgis.com/

[3] https://gii.dhs.gov/HIFLD

3.2 Affected Habitat

The Projects include landfall sites and associated onshore interconnection cable routes and substations and/or converter stations.

3.2.1 Landfall Areas

The Monmouth Landfall Site is located within the Borough of Sea Girt in Monmouth County, New Jersey, at the Army National Guard Training Center (NGTC) (Figure 3-1). The proposed Larrabeeonshore interconnection cable route passes through Sea Girt Borough, Manasquan Borough, Wall Township, and Howell Township.

The Atlantic Landfall Site will be located in an area generally situated between Albany Avenue and California Avenue within high-density urban development within Atlantic City, New Jersey (Figure 3-2). The proposed Cardiff onshore interconnection cable route runs from the Atlantic Landfall Site in Atlantic City northwest through Pleasantville Township andinto Egg Harbor Township.

Figure 3-1. Approximate Monmouth Landfall Area and Larrabee Onshore Interconnection Cable Route.

Figure 3-2. Atlantic Landfall Site and Cardiff Onshore Interconnection Cable Route.

3.2.2 Onshore Interconnection Cable Routes

Onshore interconnection cables will travel underground primarily along existing roadways, utility rights-of-way (ROWs), and/or along bike paths (Figure 3-3, Figure 3-4, Table 3-1, Table 3-2).

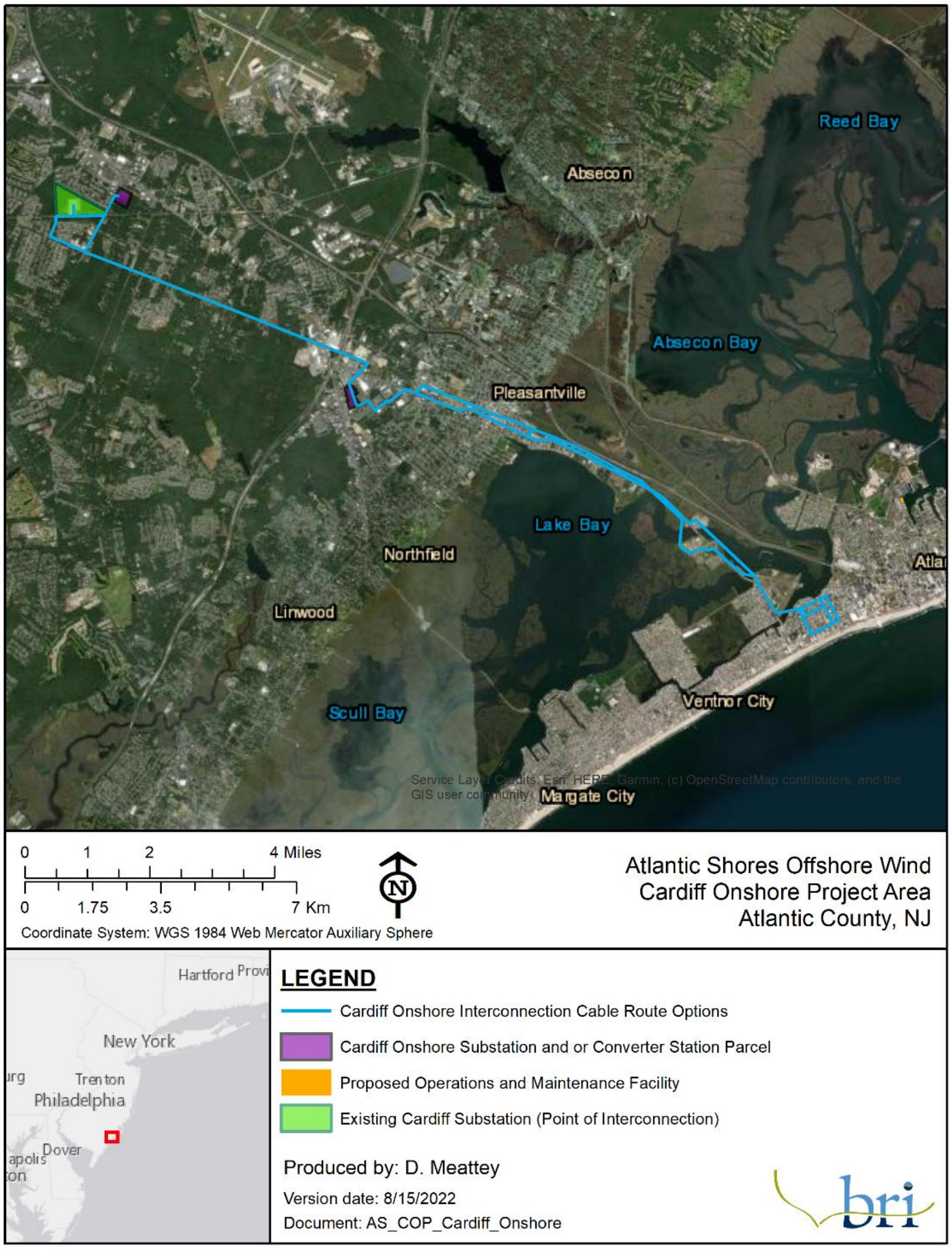

Figure 3-3. Cardiff Onshore Project Area.

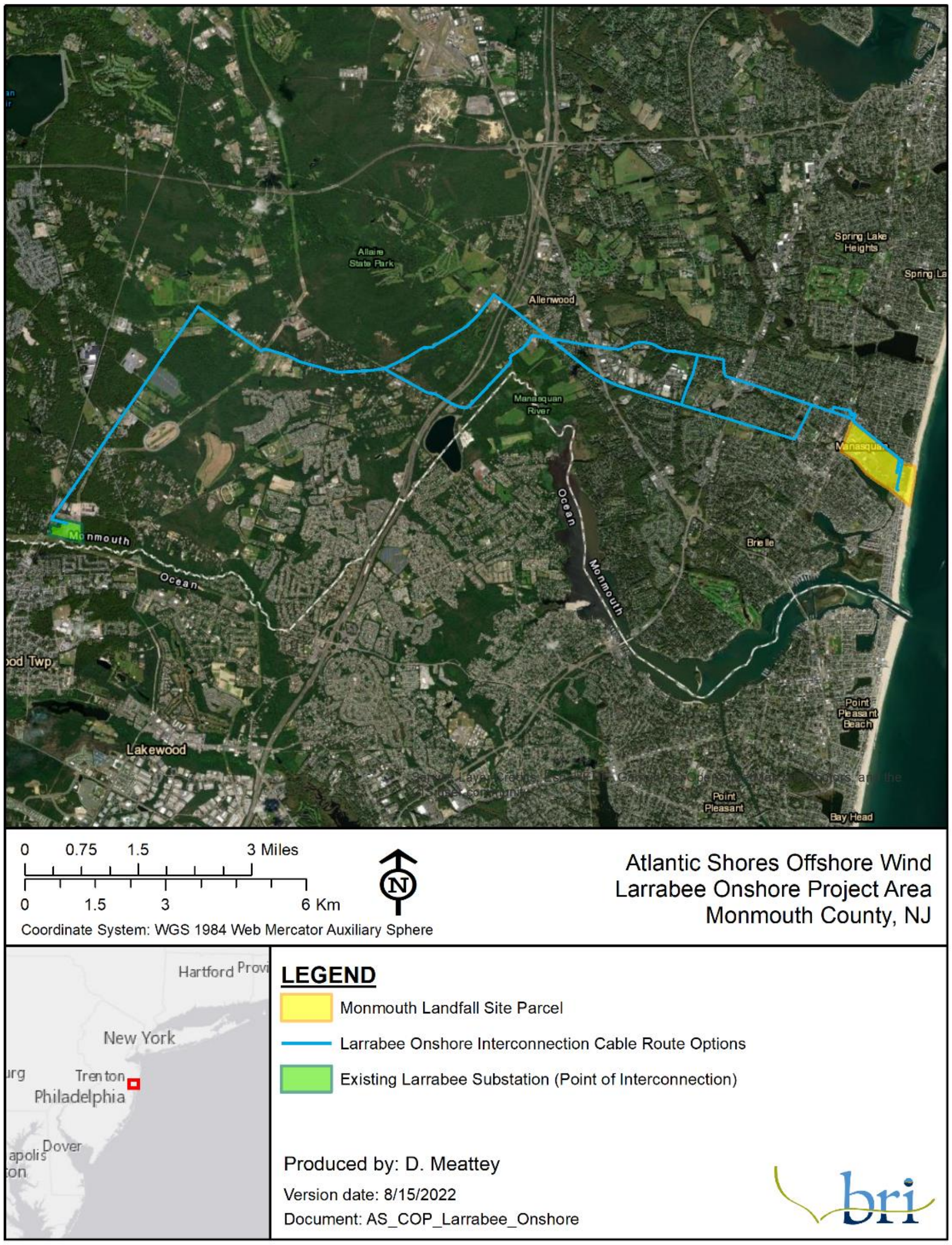

Figure 3-4. Larrabee Onshore Project Area.

Table 3-1. Road and transmission line co-occurrence of Onshore Interconnection Cable Route Options.

Onshore Area	Route Name	Co-occurrence with Existing Roads and Transmission Lines		
		Total Length (ft)	Co-located (ft)	% of Total Length
Larrabee	Onshore Interconnection Cable Route	93,563.9	58,147.7	62.1
Cardiff	Onshore Interconnection Cable Route	111,484.2	79,188.8	71.0

Table 3-2. Habitat associations of Onshore Interconnection Cable Options.

Onshore Area	Route Name	Total Area (sq. km)	Habitat Type (% of Total Area)					
			Open Water	Developed	Barren Land[1]	Forested	Field/ Agriculture	Wetland
Larrabee	Onshore Interconnection Cable Route	1.7	0.0	50.5	1.7	22.9	4.7	7.1
Cardiff	Onshore Interconnection Cable Route	2.0	7.0	71.0	0.0	2.5	0.5	4.5

[1] Barren Land includes classifications of Dry Salt Flats, Beaches, Sandy Areas other than Beaches, Bare Exposed Rock, Strip Mines, Quarries, Gravel Pits, Transitional Areas, and Mixed Barren Land.

3.2.3 Onshore Points of Interconnections

The onshore POIs associated with the Projects are existing substations that are primarily located in areasof existing development with fragmented habitat (Figure 3-5, Figure 3-6).

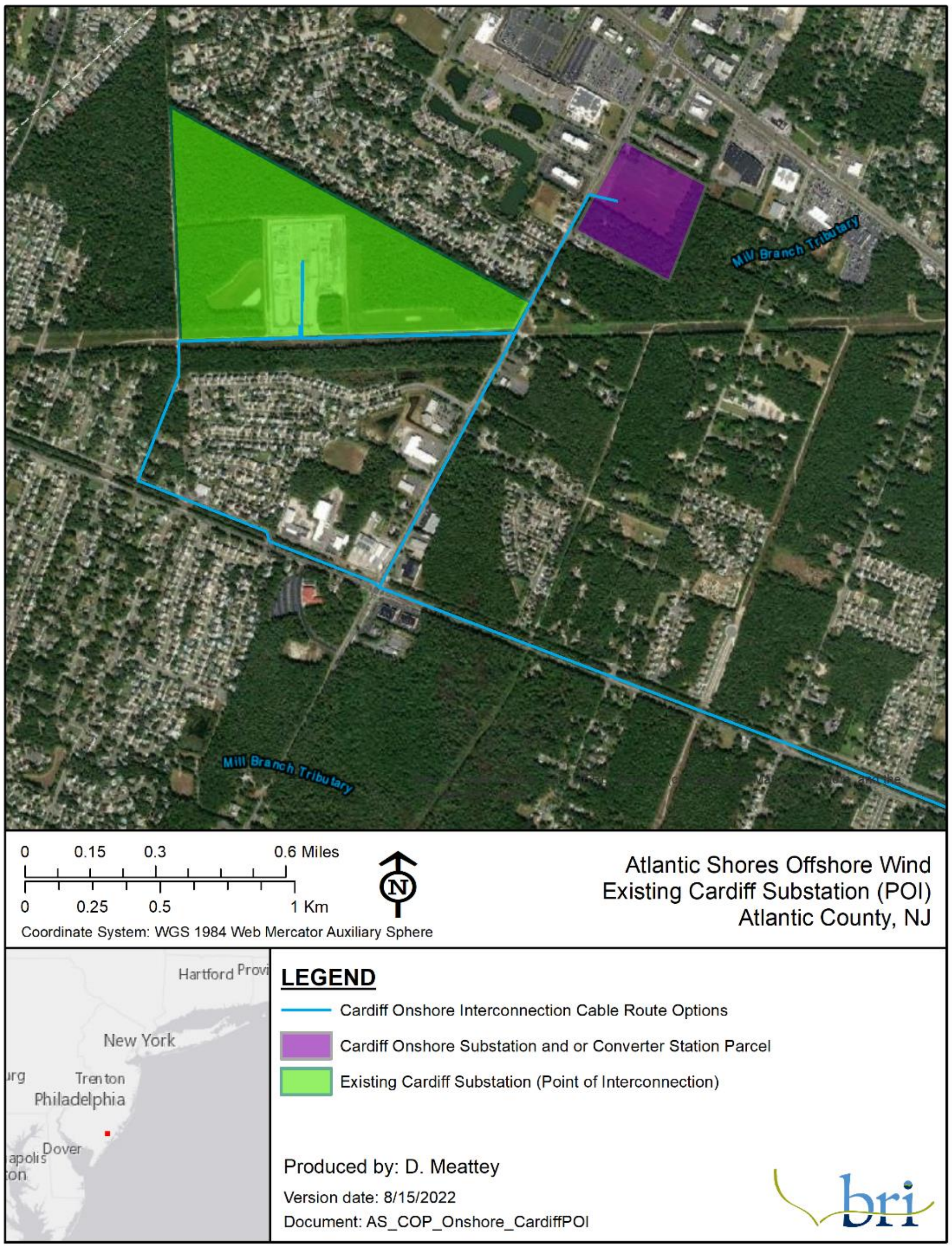

Figure 3-5. Existing Cardiff Substation (Point of Interconnection) and Cardiff Onshore Interconnection Cable Route Options.

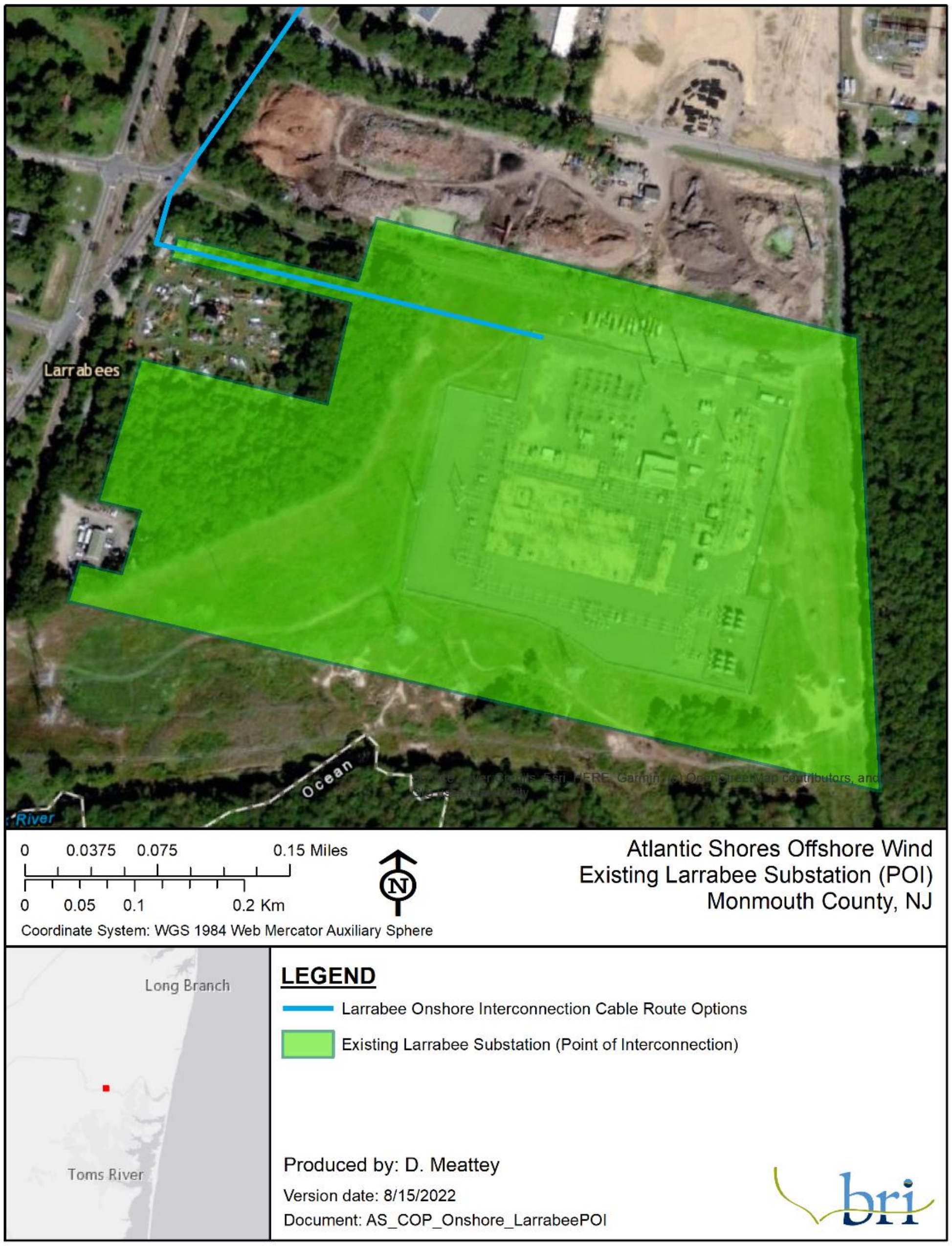

Figure 3-6. Existing Larrabee Substation (Point of Interconnection).

3.3 Birds likely to occupy existing habitat

Due to the mobility of birds, a variety of species have the potential to pass through the habitats within or adjacent to the Onshore Project Area. Below, Table 3-4 lists species of conservation concern identified in the eBird database within 9.3 mi (15 km) of the Onshore Project Area and habitat associations; and Table 3-4 lists all species identified in the eBird database within 9.3 (15 km) of the Onshore Project Area.

3.4 Endangered and Threatened Species

3.4.1 Red Knot

In 2014, the U.S. Fish and Wildlife Service (USFWS) listed the North Atlantic subspecies of Red Knot (*Calidris canutus rufa*) as Threatened under the Endangered Species Act of 1973 (USFWS 2015). The *rufa* subspecies breeds in the Arctic and winters at sites as far south as Tierra del Fuego, Argentina. During both migrations, Red Knots use key staging and stopover areas to rest and feed where they utilize habitats including sandy coastal beaches, at or near tidal inlets, or the mouths of bays and estuaries, salt marshes, tidal mudflats, and sandy/gravel beaches where they feed on clams, crustaceans, and invertebrates. The highest numbers of Red Knots are detected during spring and fall migration (Figure 3-7) and the cable landfall sites do not overlap with proposed Red Knot Critical Habitat (Figure 3-8)

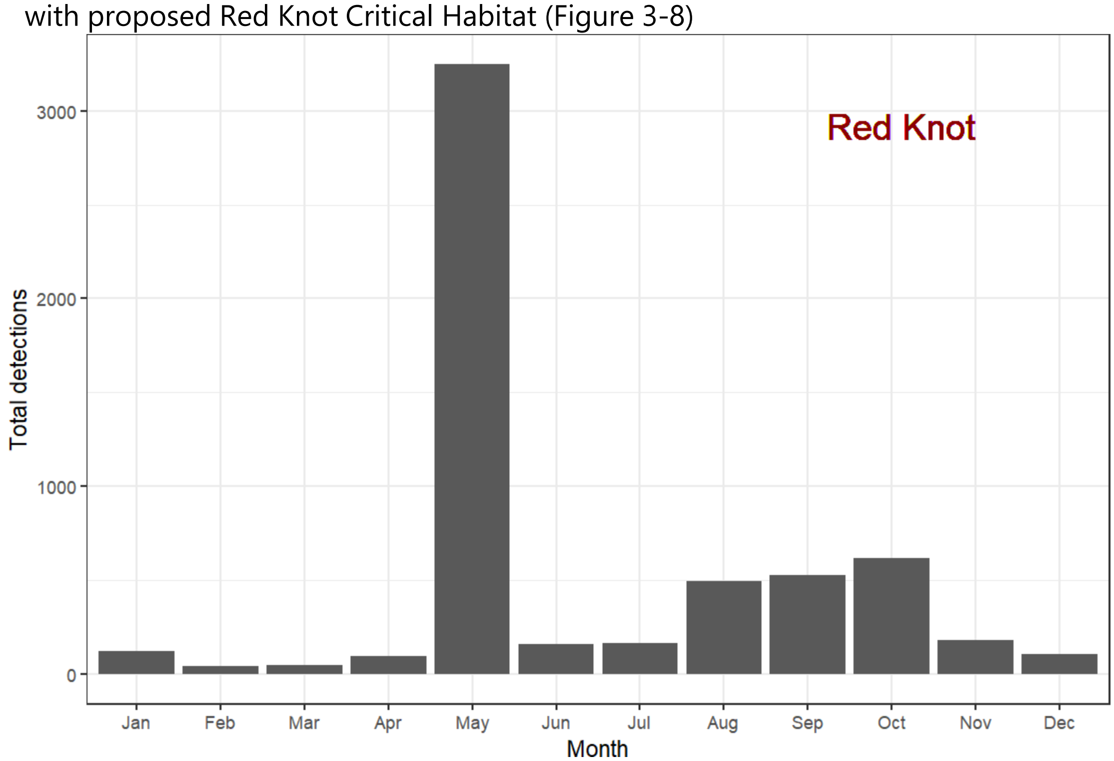

Figure 3-7: 10-year monthly averages of Red Knot detections in coastal New Jersey, derived from the eBird database.

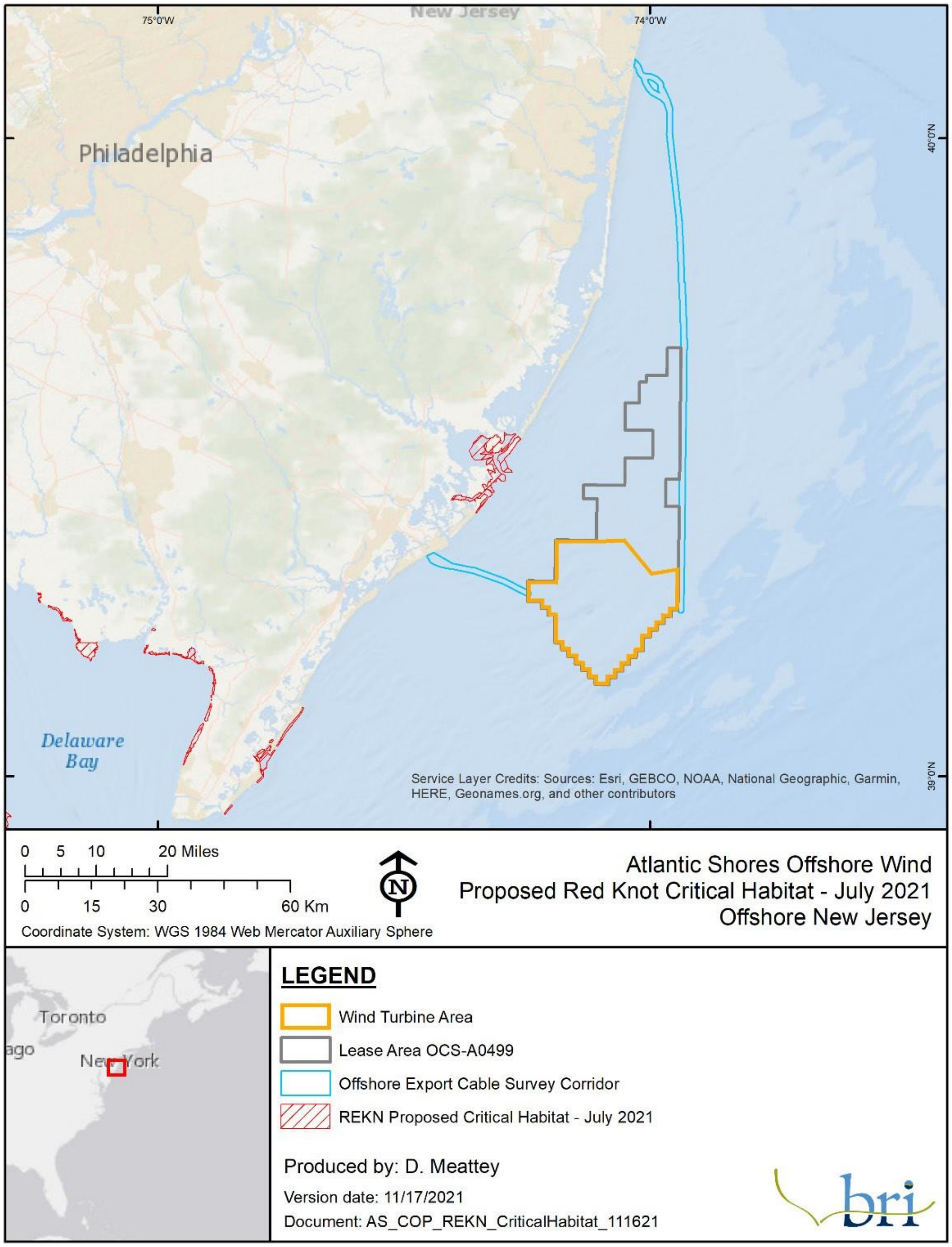

Figure 3-8: USFWS Proposed Red Knot Critical Habitat (as of July 2021) in relation to Onshore and Offshore Project Areas

3.4.2 Piping Plover

The Atlantic Coast population of the Piping Plover was federally-listed as Threatened in 1986, and is also listed by the State of New Jersey. Piping Plovers nest on coastal beaches, sandflats at the ends of sand spits and barrier islands, gently sloped foredunes, sparsely vegetated dunes, and washover areas cut into or between dunes. Breeding plovers feed on exposed wet sand in wash zones; intertidal ocean beach; wrack lines; washover passes; mud, sand, and algal flats; and shorelines of streams, ephemeral ponds, lagoons, and salt marshes by probing for invertebrates at or just below the surface. They use beaches adjacent to foraging areas for roosting and preening. Small sand dunes, debris, and sparse vegetation within adjacent beaches provides shelter from wind and extreme temperatures. Plovers arrive in New Jersey in March and leave by October (Figure 3-9). Plovers nest along the New Jersey coast (Figure 3-10), and the closest nesting site in 2020 (Heiser and Davis 2020) was 0.75 mi from the Monmouth Landfall Area (Table 3-3).

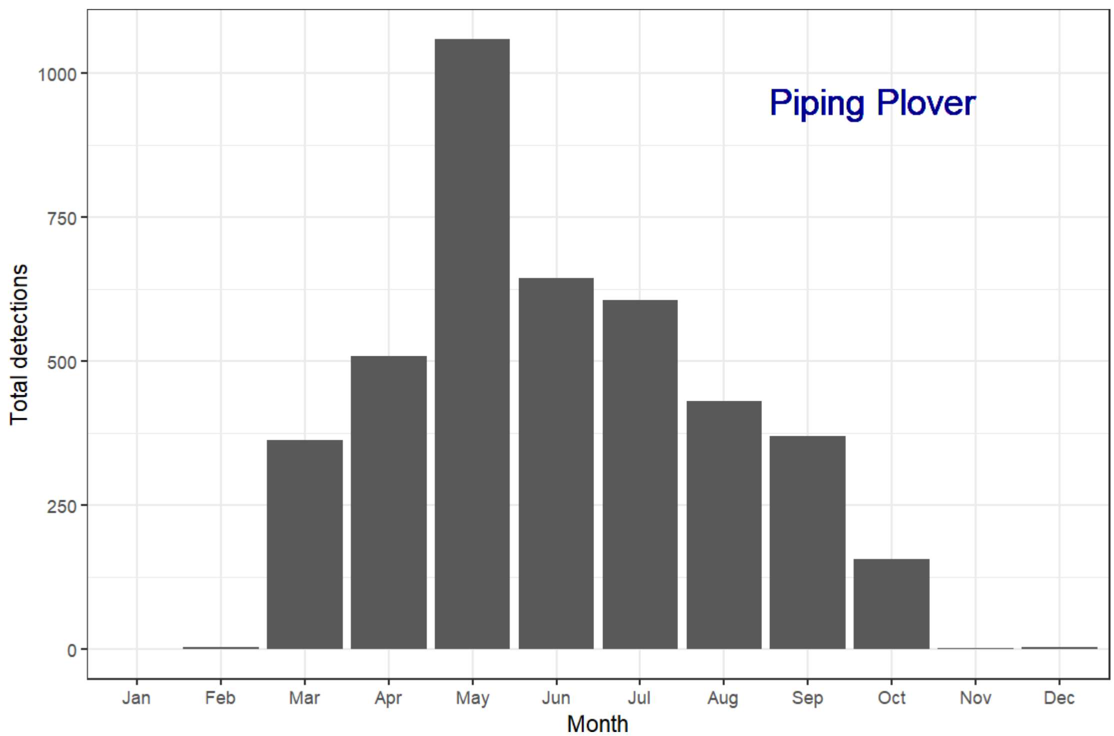

Figure 3-9: 10-year monthly averages of Piping Plover detections in coastal New Jersey, derived from the eBird database.

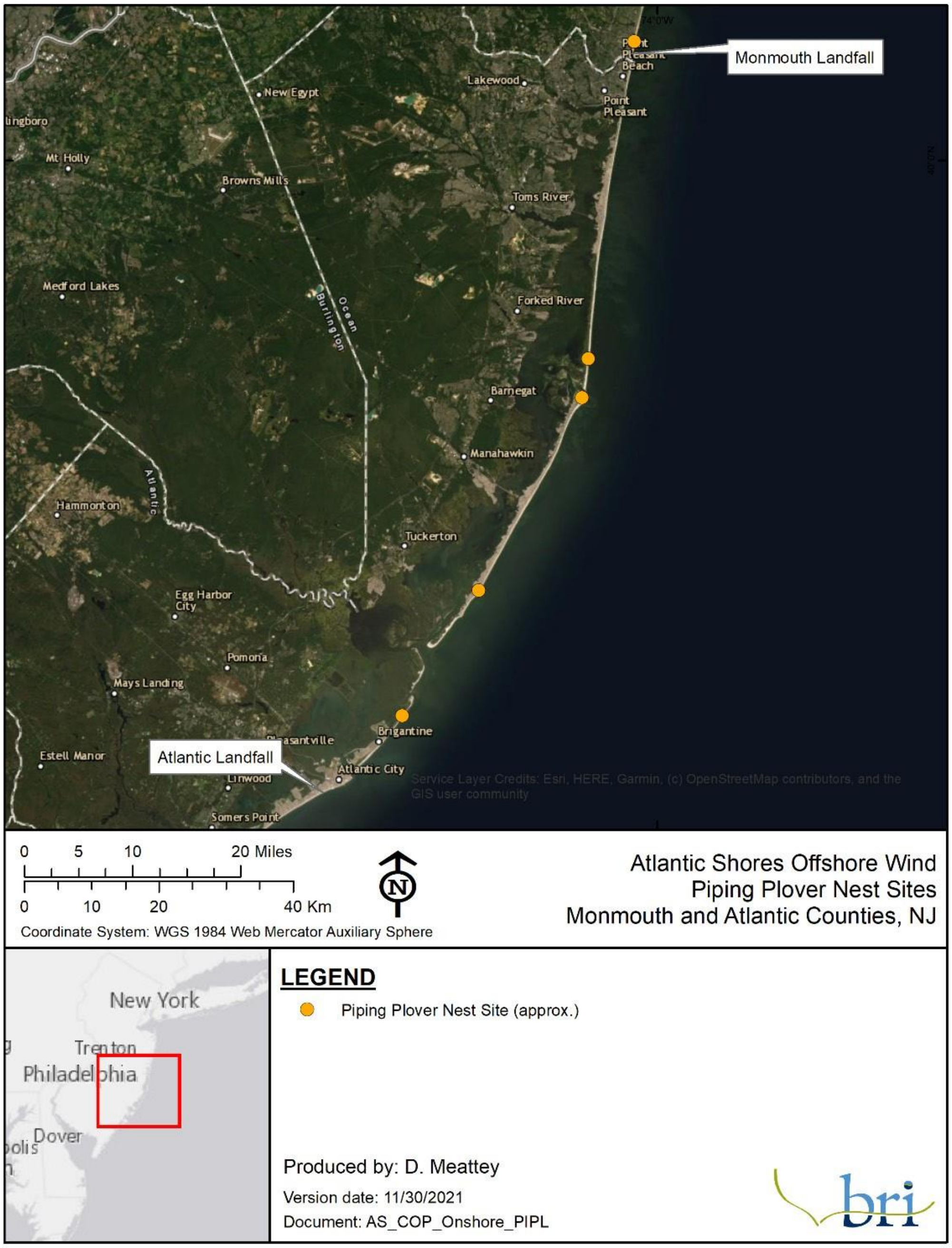

Figure 3-10: Approximate Piping Plover nest sites (2020) in relation to the Project Landfall Areas.

Table 3-3: Nesting sites of Piping Plovers in 2020, and distance (mi) to Landfall Areas.

Nesting Site	Distance to Potential Atlantic Landfall Parcels (mi)	Distance to Monmouth Landfall Area (mi)
Sandy Hook NRA		
Coast Guard	80	25
North Beach	80	25
North Beach Recreational	80	25
North Gunnison	80	20
South Gunnison	80	20
Critical Zone	unknown	unknown
Fee Beach	unknown	unknown
South Fee Beach	unknown	unknown
Sea Bright - North	75	20
Monmouth Beach - North	70	15
Sea Girt - NGCT	60	0.75
Island Beach SP NNA	35	20
Barnegat Light	33	25
EB Forsythe NWR		
Holgate	25	40
Little Beach	10	45
North Brigantine	8	50
Ocean City North	10	65
Corson's Inlet SP	15	70
Stone Harbor Point	25	80
Coast Guard - TRACEN	35	90

Table 3-4: List of species observed by eBird users in the general Onshore Project Area, and their primary and general breeding habitats. Site: C = Cardiff, L = Larrabee.

Common Name	Scientific Name	Primary Habitat	General Breeding Habitat	Conservation Status	Site
American Black Duck	*Anas rubripes*	Freshwater	Wetland	SGCN	C, L
Northern Pintail	*Anas acuta*	Freshwater, Coastal	Wetland	SGCN	C, L
Common Eider	*Somateria mollissima*	Marine	Intertidal, Wetland	SGCN	C, L
Hooded Merganser	*Lophodytes cucullatus*	Freshwater	Forest, Wetland	STE	C, L
Pied-billed Grebe	*Podilymbus podiceps*	Freshwater, Marine	Wetland	STE, F-SGCN	C, L
Black-billed Cuckoo	*Coccyzus erythropthalmus*	Terrestrial	Forest, Shrubland	STE, SGCN	C, L
Common Nighthawk	*Chordeiles minor*	Terrestrial	Grassland, Forest, Wetland	STE, SGCN	C, L
Chuck-will's-widow	*Antrostomus carolinensis*	Terrestrial	Forest, Grassland, Shrubland	SGCN	C
Chimney Swift	*Chaetura pelagica*	Terrestrial	Forest	SGCN	C, L
King Rail	*Rallus elegans*	Freshwater	Wetland	STE, SGCN	C
Clapper Rail	*Rallus crepitans*	Freshwater	Wetland, Forest	SGCN	C, L
Virginia Rail	*Rallus limicola*	Freshwater	Wetland	STE	C
Sora	*Porzana carolina*	Freshwater	Wetland	STE, SGCN	C
Common Gallinule	*Gallinula galeata*	Freshwater	Wetland	STE	C
American Oystercatcher	*Haematopus palliatus*	Marine	Intertidal, Beach	STE, F-SGCN	C, L
Piping Plover	*Charadrius melodus*	Marine	Intertidal, Beach	FTE, STE, F-SGCN	C, L
Whimbrel	*Numenius phaeopus*	Terrestrial, Coastal	Forest, Grassland, Shrubland	STE, SGCN	C
Marbled Godwit	*Limosa fedoa*	Terrestrial, Coastal	Grassland, Wetland	SGCN	C
Ruddy Turnstone	*Arenaria interpres*	Terrestrial, Coastal	Grassland, Wetland	F-SGCN	C, L
Red Knot	*Calidris canutus*	Terrestrial, Coastal	Grassland, Wetland	FTE, STE, F-SGCN	C
Sanderling	*Calidris alba*	Terrestrial, Coastal	Grassland, Wetland	STE, SGCN	C, L
Purple Sandpiper	*Calidris maritima*	Terrestrial, Coastal	Grassland, Wetland	SGCN	C, L
Semipalmated Sandpiper	*Calidris pusilla*	Terrestrial, Coastal	Grassland, Wetland	STE, SGCN	C, L
American Woodcock	*Scolopax minor*	Terrestrial	Forest	F-SGCN	C, L

Common Name	Scientific Name	Primary Habitat	General Breeding Habitat	Conservation Status	Site
Wilson's Phalarope	*Phalaropus tricolor*	Freshwater, Marine	Wetland, Grassland, Forest	SGCN	C
Spotted Sandpiper	*Actitis macularius*	Freshwater, Coastal	Wetland	STE	C, L
Willet	*Tringa semipalmata*	Terrestrial, Coastal	Intertidal, Wetland	SGCN	C, L
Least Tern	*Sternula antillarum*	Marine, Coastal	Intertidal	STE, F-SGCN	C, L
Gull-billed Tern	*Gelochelidon nilotica*	Marine, Coastal	Intertidal, Wetland	STE, SGCN	C
Caspian Tern	*Hydroprogne caspia*	Marine, Coastal	Wetland, Intertidal	STE	C, L
Black Tern	*Chlidonias niger*	Marine, Coastal	Wetland	SGCN	C
Common Tern	*Sterna hirundo*	Marine, Coastal	Intertidal, Wetland	STE, F-SGCN	C, L
Forster's Tern	*Sterna forsteri*	Marine, Coastal	Wetland	F-SGCN	C, L
Black Skimmer	*Rynchops niger*	Marine, Coastal	Intertidal, Wetland	STE, F-SGCN	C, L
Common Loon	*Gavia immer*	Freshwater, Marine	Wetland	SGCN	C, L
American Bittern	*Botaurus lentiginosus*	Freshwater	Wetland	STE, SGCN	C
Least Bittern	*Ixobrychus exilis*	Freshwater	Wetland, Forest	STE, SGCN	C
Great Blue Heron	*Ardea herodias*	Freshwater, Marine	Wetland, Intertidal, Forest	STE	C, L
Snowy Egret	*Egretta thula*	Freshwater, Marine	Wetland, Intertidal	STE, F-SGCN	C, L
Little Blue Heron	*Egretta caerulea*	Freshwater, Marine	Wetland, Intertidal, Forest	STE, F-SGCN	C, L
Tricolored Heron	*Egretta tricolor*	Freshwater, Marine	Wetland, Intertidal, Forest	STE, F-SGCN	C
Cattle Egret	*Bubulcus ibis*	Freshwater	Grassland, Wetland	STE, SGCN	C
Black-crowned Night-Heron	*Nycticorax nycticorax*	Freshwater, Marine	Forest, Intertidal, Wetland	STE, SGCN	C, L
Yellow-crowned Night-Heron	*Nyctanassa violacea*	Freshwater, Marine	Forest, Intertidal, Wetland	STE, SGCN	C, L
Glossy Ibis	*Plegadis falcinellus*	Freshwater, Coastal	Wetland	STE	C, L
Osprey	*Pandion haliaetus*	Freshwater, Coastal	Forest, Wetland, Intertidal	STE, SGCN	C, L
Golden Eagle	*Aquila chrysaetos*	Terrestrial	Grassland, Forest, Shrubland	SGCN	C
Northern Harrier	*Circus hudsonius*	Terrestrial, Freshwater	Forest, Grassland, Shrubland, Wetland	STE, F-SGCN	C, L
Sharp-shinned Hawk	*Accipiter striatus*	Terrestrial	Forest, Shrubland	STE	C, L
Cooper's Hawk	*Accipiter cooperii*	Terrestrial	Forest	STE	C, L
Bald Eagle	*Haliaeetus leucocephalus*	Freshwater, Coastal	Wetland Forest, Intertidal	STE, SGCN	C, L

Common Name	Scientific Name	Primary Habitat	General Breeding Habitat	Conservation Status	Site
Red-shouldered Hawk	*Buteo lineatus*	Terrestrial	Forest	STE, SGCN	C, L
Broad-winged Hawk	*Buteo platypterus*	Terrestrial	Forest	STE, SGCN	C, L
Barred Owl	*Strix varia*	Terrestrial	Forest, Wetland	STE, SGCN	C, L
Short-eared Owl	*Asio flammeus*	Terrestrial	Grassland	STE, SGCN	C
Red-headed Woodpecker	*Melanerpes erythrocephalus*	Terrestrial	Forest, Grassland	STE, F-SGCN	C
American Kestrel	*Falco sparverius*	Terrestrial	Forest, Grassland, Shrubland	STE, SGCN	C, L
Peregrine Falcon	*Falco peregrinus*	Terrestrial, Coastal	Forest, Grassland, Intertidal, Shrubland	STE, F-SGCN	C, L
Acadian Flycatcher	*Empidonax virescens*	Terrestrial	Forest, Wetland	SGCN	C, L
Willow Flycatcher	*Empidonax traillii*	Terrestrial	Shrubland, Wetland	SGCN	C, L
Least Flycatcher	*Empidonax minimus*	Terrestrial	Forest, Shrubland	STE	C, L
Yellow-throated Vireo	*Vireo flavifrons*	Terrestrial	Forest	SGCN	C, L
Blue-headed Vireo	*Vireo solitarius*	Terrestrial	Forest	STE	C, L
Horned Lark	*Eremophila alpestris*	Terrestrial	Grassland, Shrubland	STE, SGCN	C, L
Bank Swallow	*Riparia riparia*	Terrestrial, Freshwater	Grassland, Wetland	SGCN	C, L
Cliff Swallow	*Petrochelidon pyrrhonota*	Terrestrial, Freshwater	Forest, Grassland, Wetland	STE	C, L
Winter Wren	*Troglodytes hiemalis*	Terrestrial	Forest, Shrubland	STE	C, L
Marsh Wren	*Cistothorus palustris*	Terrestrial, Freshwater	Wetlands, Intertidal	SGCN	C, L
Brown Thrasher	*Toxostoma rufum*	Terrestrial	Shrubland, Forest	STE, SGCN	C, L
Veery	*Catharus fuscescens*	Terrestrial	Forest	STE, SGCN	C, L
Wood Thrush	*Hylocichla mustelina*	Terrestrial	Forest	STE, F-SGCN	C, L
Grasshopper Sparrow	*Ammodramus savannarum*	Terrestrial	Grassland, Shrubland	STE, F-SGCN	C, L
Field Sparrow	*Spizella pusilla*	Terrestrial	Forest, Grassland, Shrubland	SGCN	C, L
Vesper Sparrow	*Pooecetes gramineus*	Terrestrial	Grassland, Shrubland	STE, F-SGCN	C
Seaside Sparrow	*Ammospiza maritima*	Terrestrial	Intertidal	SGCN	C
Saltmarsh Sparrow	*Ammospiza caudacuta*	Terrestrial, Coastal	Intertidal	STE, SGCN	C
Savannah Sparrow	*Passerculus sandwichensis*	Terrestrial, Freshwater, Coastal	Grassland, Shrubland, Wetland	STE, SGCN	C, L

Common Name	Scientific Name	Primary Habitat	General Breeding Habitat	Conservation Status	Site
Eastern Towhee	*Pipilo erythrophthalmus*	Terrestrial	Forest, Shrubland	SGCN	C, L
Yellow-breasted Chat	*Icteria virens*	Terrestrial	Forest, Shrubland	STE, SGCN	C
Bobolink	*Dolichonyx oryzivorus*	Terrestrial	Grassland	STE, F-SGCN	C
Eastern Meadowlark	*Sturnella magna*	Terrestrial	Grassland, Shrubland	STE, F-SGCN	C, L
Rusty Blackbird	*Euphagus carolinus*	Terrestrial, Freshwater	Wetland	SGCN	C
Worm-eating Warbler	*Helmitheros vermivorum*	Terrestrial	Forest	STE, SGCN	C, L
Blue-winged Warbler	*Vermivora cyanoptera*	Terrestrial	Grassland, Shrubland	F-SGCN	C, L
Black-and-white Warbler	*Mniotilta varia*	Terrestrial	Forest	SGCN	C, L
Prothonotary Warbler	*Protonotaria citrea*	Terrestrial	Forest	F-SGCN	L
Nashville Warbler	*Leiothlypis ruficapilla*	Terrestrial	Forest	STE	C, L
Hooded Warbler	*Setophaga citrina*	Terrestrial	Forest	STE, SGCN	C, L
Cape May Warbler	*Setophaga tigrina*	Terrestrial	Forest	SGCN	C, L
Northern Parula	*Setophaga americana*	Terrestrial	Forest	STE, SGCN	C, L
Bay-breasted Warbler	*Setophaga castanea*	Terrestrial	Forest	SGCN	C, L
Blackburnian Warbler	*Setophaga fusca*	Terrestrial	Forest	STE, SGCN	C, L
Black-throated Blue Warbler	*Setophaga caerulescens*	Terrestrial	Forest	STE, SGCN	C, L
Prairie Warbler	*Setophaga discolor*	Terrestrial	Shrubland, Forest	SGCN	C, L
Black-throated Green Warbler	*Setophaga virens*	Terrestrial	Forest, Wetland	STE, SGCN	C, L
Canada Warbler	*Cardellina canadensis*	Terrestrial	Forest	STE, SGCN	C, L
Scarlet Tanager	*Piranga olivacea*	Terrestrial	Forest	F-SGCN	C, L
Dickcissel	*Spiza americana*	Terrestrial	Grassland	SGCN	C

Note: Species reported on at least 30 separate days over the last 10 years and designated as one or more of the following: SGCN = Species of Greatest Conservation Need for NJ, F-SGCN = focal Species of Greatest Conservation Need for NJ, STE = state-listed species, and FTE = federally-listed species (bolded).

Table 3-5: Complete list of species observed by eBird users in the general Onshore Project Area, and their conversation status.

Species	Scientific Name	Cardiff	Larra-bee	Federal Status	State Status	Priority SGCN	Focal SGCN	IPaC
Black-bellied Whistling-Duck	*Dendrocygna autumnalis*	•						
Snow Goose	*Anser caerulescens*	•	•					
Ross's Goose	*Anser rossii*	•						
Pink-footed Goose	*Anser brachyrhynchus*		•					
Brant	*Branta bernicla*	•	•			•		
Canada Goose	*Branta canadensis*	•	•					
Mute Swan	*Cygnus olor*	•	•					
Tundra Swan	*Cygnus columbianus*	•						
Wood Duck	*Aix sponsa*	•	•					
Blue-winged Teal	*Spatula discors*	•	•					
Northern Shoveler	*Spatula clypeata*	•	•					
Gadwall	*Mareca strepera*	•	•					
Eurasian Wigeon	*Mareca penelope*	•	•					
American Wigeon	*Mareca americana*	•	•					
Mallard	*Anas platyrhynchos*	•	•					
American Black Duck	*Anas rubripes*	•	•			•		
Northern Pintail	*Anas acuta*	•	•			•		
Green-winged Teal	*Anas crecca*	•	•					
Canvasback	*Aythya valisineria*	•	•					
Redhead	*Aythya americana*	•	•					
Ring-necked Duck	*Aythya collaris*	•	•					
Greater Scaup	*Aythya marila*	•	•					
Lesser Scaup	*Aythya affinis*	•	•					
King Eider	*Somateria spectabilis*		•					
Common Eider	*Somateria mollissima*	•	•			•		•
Harlequin Duck	*Histrionicus histrionicus*		•					
Surf Scoter	*Melanitta perspicillata*	•	•					•
White-winged Scoter	*Melanitta deglandi*		•					•
Black Scoter	*Melanitta americana*	•	•					•
Long-tailed Duck	*Clangula hyemalis*	•	•					•
Bufflehead	*Bucephala albeola*	•	•					
Common Goldeneye	*Bucephala clangula*	•	•					
Hooded Merganser	*Lophodytes cucullatus*	•	•		•			
Common Merganser	*Mergus merganser*	•	•					
Red-breasted Merganser	*Mergus serrator*	•	•					•
Ruddy Duck	*Oxyura jamaicensis*	•	•					
Northern Bobwhite	*Colinus virginianus*					•	•	
Ruffed Grouse	*Bonasa umbellus*					•		
Wild Turkey	*Meleagris gallopavo*	•	•					
Pied-billed Grebe	*Podilymbus podiceps*	•	•		•	•	•	
Horned Grebe	*Podiceps auritus*	•	•					
Red-necked Grebe	*Podiceps grisegena*	•	•					
Rock Pigeon	*Columba livia*	•	•					
Mourning Dove	*Zenaida macroura*	•	•					
Yellow-billed Cuckoo	*Coccyzus americanus*	•	•					
Black-billed Cuckoo	*Coccyzus erythropthalmus*	•	•		•	•		•
Common Nighthawk	*Chordeiles minor*	•	•		•	•		
Chuck-will's-widow	*Antrostomus carolinensis*	•				•		
Eastern Whip-poor-will	*Antrostomus vociferus*	•			•			•
Chimney Swift	*Chaetura pelagica*	•	•			•		
Ruby-throated Hummingbird	*Archilochus colubris*	•	•					

Species	Scientific Name	Cardiff	Larra-bee	Federal Status	State Status	Priority SGCN	Focal SGCN	IPaC
King Rail	*Rallus elegans*	•			•	•		•
Clapper Rail	*Rallus crepitans*	•	•			•		
Virginia Rail	*Rallus limicola*	•			•			
Sora	*Porzana carolina*	•			•	•		
Common Gallinule	*Gallinula galeata*	•			•			
American Coot	*Fulica americana*	•	•					
Black Rail	*Laterallus jamaicensis*				•	•	•	
Black-necked Stilt	*Himantopus mexicanus*	•						
American Avocet	*Recurvirostra americana*	•						
American Oystercatcher	*Haematopus palliatus*	•	•		•	•	•	•
Black-bellied Plover	*Pluvialis squatarola*	•	•					
American Golden-Plover	*Pluvialis dominica*	•						
Semipalmated Plover	*Charadrius semipalmatus*	•	•					
Piping Plover	*Charadrius melodus*	•	•	•	•	•	•	
Killdeer	*Charadrius vociferus*	•	•					
Whimbrel	*Numenius phaeopus*	•			•	•		
Hudsonian Godwit	*Limosa haemastica*	•						•
Marbled Godwit	*Limosa fedoa*	•				•		
Ruddy Turnstone	*Arenaria interpres*	•	•			•	•	•
Red Knot	*Calidris canutus*	•		•	•	•	•	
Upland Sandpiper	*Bartramia longicauda*				•	•		
Stilt Sandpiper	*Calidris himantopus*	•						
Sanderling	*Calidris alba*	•	•		•	•		
Dunlin	*Calidris alpina*	•	•					
Purple Sandpiper	*Calidris maritima*	•	•			•		•
Baird's Sandpiper	*Calidris bairdii*	•						
Least Sandpiper	*Calidris minutilla*	•	•					
White-rumped Sandpiper	*Calidris fuscicollis*	•						
Buff-breasted Sandpiper	*Calidris subruficollis*	•						
Pectoral Sandpiper	*Calidris melanotos*	•						
Semipalmated Sandpiper	*Calidris pusilla*	•	•		•	•		
Western Sandpiper	*Calidris mauri*	•						
Short-billed Dowitcher	*Limnodromus griseus*	•	•					•
Long-billed Dowitcher	*Limnodromus scolopaceus*	•						
American Woodcock	*Scolopax minor*	•	•			•	•	
Wilson's Snipe	*Gallinago delicata*	•	•					
Wilson's Phalarope	*Phalaropus tricolor*	•				•		
Red-necked Phalarope	*Phalaropus lobatus*	•						•
Spotted Sandpiper	*Actitis macularius*	•	•		•			
Solitary Sandpiper	*Tringa solitaria*	•	•					
Greater Yellowlegs	*Tringa melanoleuca*	•	•					
Willet	*Tringa semipalmata*	•	•			•		•
Lesser Yellowlegs	*Tringa flavipes*	•	•					•
Razorbill	*Alca torda*		•					•
Bonaparte's Gull	*Chroicocephalus philadelphia*	•	•					
Black-headed Gull	*Chroicocephalus ridibundus*	•	•					
Laughing Gull	*Leucophaeus atricilla*	•	•					
Ring-billed Gull	*Larus delawarensis*	•	•					•
Herring Gull	*Larus argentatus*	•	•					
Iceland Gull	*Larus glaucoides*		•					
Lesser Black-backed Gull	*Larus fuscus*	•	•					
Glaucous Gull	*Larus hyperboreus*		•					
Great Black-backed Gull	*Larus marinus*	•	•					
Least Tern	*Sternula antillarum*	•	•		•	•	•	

Species	Scientific Name	Cardiff	Larra-bee	Federal Status	State Status	Priority SGCN	Focal SGCN	IPaC
Gull-billed Tern	*Gelochelidon nilotica*	•			•	•		•
Caspian Tern	*Hydroprogne caspia*	•	•		•			
Black Tern	*Chlidonias niger*	•				•		
Common Tern	*Sterna hirundo*	•	•		•	•	•	
Forster's Tern	*Sterna forsteri*	•	•			•	•	
Royal Tern	*Thalasseus maximus*	•	•					•
Black Skimmer	*Rynchops niger*	•	•		•	•	•	•
Roseate Tern	*Sterna dougallii*			•	•	•		•
Red-throated Loon	*Gavia stellata*	•	•					•
Common Loon	*Gavia immer*	•	•			•		•
Wilson's Storm-Petrel	*Oceanites oceanicus*		•					•
Northern Gannet	*Morus bassanus*	•	•					
Great Cormorant	*Phalacrocorax carbo*		•					
Double-crested Cormorant	*Phalacrocorax auritus*	•	•					•
American White Pelican	*Pelecanus erythrorhynchos*	•						
Brown Pelican	*Pelecanus occidentalis*	•	•					•
American Bittern	*Botaurus lentiginosus*	•			•	•		
Least Bittern	*Ixobrychus exilis*	•			•	•		
Great Blue Heron	*Ardea herodias*	•	•		•			
Great Egret	*Ardea alba*	•	•					
Snowy Egret	*Egretta thula*	•	•		•	•	•	
Little Blue Heron	*Egretta caerulea*	•	•		•	•	•	
Tricolored Heron	*Egretta tricolor*	•			•	•	•	
Cattle Egret	*Bubulcus ibis*	•			•	•		
Green Heron	*Butorides virescens*	•	•					
Black-crowned Night-Heron	*Nycticorax nycticorax*	•	•		•	•		
Yellow-crowned Night-Heron	*Nyctanassa violacea*	•	•		•	•		
White Ibis	*Eudocimus albus*	•						
Glossy Ibis	*Plegadis falcinellus*	•	•		•			
White-faced Ibis	*Plegadis chihi*	•						
Black Vulture	*Coragyps atratus*	•	•					
Turkey Vulture	*Cathartes aura*	•	•					
Osprey	*Pandion haliaetus*	•	•		•	•		
Golden Eagle	*Aquila chrysaetos*	•				•		•
Northern Harrier	*Circus hudsonius*	•	•		•	•	•	
Sharp-shinned Hawk	*Accipiter striatus*	•	•		•			
Cooper's Hawk	*Accipiter cooperii*	•	•		•			
Bald Eagle	*Haliaeetus leucocephalus*	•	•		•	•		•
Northern Goshawk	*Accipiter gentilis*				•	•		
Red-shouldered Hawk	*Buteo lineatus*	•	•		•	•		
Broad-winged Hawk	*Buteo platypterus*	•	•		•	•		
Red-tailed Hawk	*Buteo jamaicensis*	•	•					
Rough-legged Hawk	*Buteo lagopus*	•						
Barn Owl	*Tyto alba*				•	•		
Eastern Screech-Owl	*Megascops asio*	•	•					
Great Horned Owl	*Bubo virginianus*	•	•					
Snowy Owl	*Bubo scandiacus*	•						
Barred Owl	*Strix varia*	•	•		•	•		
Short-eared Owl	*Asio flammeus*	•			•	•		
Long-eared Owl	*Asio otus*				•	•		•
Belted Kingfisher	*Megaceryle alcyon*	•	•					
Yellow-bellied Sapsucker	*Sphyrapicus varius*	•	•					
Red-headed Woodpecker	*Melanerpes erythrocephalus*	•			•	•	•	•
Red-bellied Woodpecker	*Melanerpes carolinus*	•	•					

Species	Scientific Name	Cardiff	Larra-bee	Federal Status	State Status	Priority SGCN	Focal SGCN	IPaC
Downy Woodpecker	*Dryobates pubescens*	•	•					
Hairy Woodpecker	*Dryobates villosus*	•	•					
Pileated Woodpecker	*Dryocopus pileatus*		•					
Northern Flicker	*Colaptes auratus*	•	•					
American Kestrel	*Falco sparverius*	•	•		•	•		
Merlin	*Falco columbarius*	•	•					
Peregrine Falcon	*Falco peregrinus*	•	•		•	•	•	
Eastern Wood-Pewee	*Contopus virens*	•	•					
Acadian Flycatcher	*Empidonax virescens*	•	•			•		
Willow Flycatcher	*Empidonax traillii*	•	•			•		
Least Flycatcher	*Empidonax minimus*	•	•		•			
Olive-sided Flycatcher	*Contopus cooperi*					•		
Eastern Phoebe	*Sayornis phoebe*	•	•					
Great Crested Flycatcher	*Myiarchus crinitus*	•	•					
Eastern Kingbird	*Tyrannus tyrannus*	•	•					
White-eyed Vireo	*Vireo griseus*	•	•					
Yellow-throated Vireo	*Vireo flavifrons*	•	•			•		
Blue-headed Vireo	*Vireo solitarius*	•	•		•			
Philadelphia Vireo	*Vireo philadelphicus*	•						
Warbling Vireo	*Vireo gilvus*	•	•					
Red-eyed Vireo	*Vireo olivaceus*	•	•					
Loggerhead Shrike	*Lanius ludovicianus*				•	•		
Blue Jay	*Cyanocitta cristata*	•	•					
American Crow	*Corvus brachyrhynchos*	•	•					
Fish Crow	*Corvus ossifragus*	•	•					
Common Raven	*Corvus corax*	•	•					
Carolina Chickadee	*Poecile carolinensis*	•	•					
Tufted Titmouse	*Baeolophus bicolor*	•	•					
Horned Lark	*Eremophila alpestris*	•	•		•	•		
Northern Rough-winged Swallow	*Stelgidopteryx serripennis*	•	•					
Purple Martin	*Progne subis*	•	•					
Tree Swallow	*Tachycineta bicolor*	•	•					
Bank Swallow	*Riparia riparia*	•	•			•		
Barn Swallow	*Hirundo rustica*	•	•					
Cliff Swallow	*Petrochelidon pyrrhonota*	•	•		•			
Golden-crowned Kinglet	*Regulus satrapa*	•	•					
Ruby-crowned Kinglet	*Regulus calendula*	•	•					
Red-breasted Nuthatch	*Sitta canadensis*	•	•					
White-breasted Nuthatch	*Sitta carolinensis*	•	•					
Brown Creeper	*Certhia americana*	•	•					
Blue-gray Gnatcatcher	*Polioptila caerulea*	•	•					
House Wren	*Troglodytes aedon*	•	•					
Winter Wren	*Troglodytes hiemalis*	•	•		•			
Marsh Wren	*Cistothorus palustris*	•	•			•		
Carolina Wren	*Thryothorus ludovicianus*	•	•					
Sedge Wren	*Cistothorus stellaris*				•	•		
European Starling	*Sturnus vulgaris*	•	•					
Gray Catbird	*Dumetella carolinensis*	•	•					
Brown Thrasher	*Toxostoma rufum*	•	•		•	•		
Northern Mockingbird	*Mimus polyglottos*	•	•					
Eastern Bluebird	*Sialia sialis*	•	•					
Veery	*Catharus fuscescens*	•	•		•	•		
Swainson's Thrush	*Catharus ustulatus*	•	•					

Species	Scientific Name	Cardiff	Larra-bee	Federal Status	State Status	Priority SGCN	Focal SGCN	IPaC
Hermit Thrush	*Catharus guttatus*	•	•					
Wood Thrush	*Hylocichla mustelina*	•	•		•	•	•	•
Gray-cheeked Thrush	*Catharus minimus*				•			
Bicknell's Thrush	*Catharus bicknelli*					•		
American Robin	*Turdus migratorius*	•	•					
Cedar Waxwing	*Bombycilla cedrorum*	•	•					
House Sparrow	*Passer domesticus*	•	•					
American Pipit	*Anthus rubescens*	•						
House Finch	*Haemorhous mexicanus*	•	•					
Purple Finch	*Haemorhous purpureus*	•	•					
Pine Siskin	*Spinus pinus*	•	•					
American Goldfinch	*Spinus tristis*	•	•					
Lapland Longspur	*Calcarius lapponicus*	•						
Snow Bunting	*Plectrophenax nivalis*	•						
Grasshopper Sparrow	*Ammodramus savannarum*	•	•		•	•	•	
Chipping Sparrow	*Spizella passerina*	•	•					
Field Sparrow	*Spizella pusilla*	•	•			•		
American Tree Sparrow	*Spizelloides arborea*	•	•					
Fox Sparrow	*Passerella iliaca*	•	•					
Dark-eyed Junco	*Junco hyemalis*	•	•					
White-crowned Sparrow	*Zonotrichia leucophrys*	•	•					
White-throated Sparrow	*Zonotrichia albicollis*	•	•					
Vesper Sparrow	*Pooecetes gramineus*	•			•	•	•	
Seaside Sparrow	*Ammospiza maritima*	•				•		
Nelson's Sparrow	*Ammospiza nelsoni*	•						
Saltmarsh Sparrow	*Ammospiza caudacuta*	•			•	•		
Savannah Sparrow	*Passerculus sandwichensis*	•	•		•	•		
Song Sparrow	*Melospiza melodia*	•	•					
Lincoln's Sparrow	*Melospiza lincolnii*		•					
Swamp Sparrow	*Melospiza georgiana*	•	•					
Eastern Towhee	*Pipilo erythrophthalmus*	•	•			•		
Henslow's Sparrow	*Centronyx henslowii*				•	•		
Yellow-breasted Chat	*Icteria virens*	•			•	•		
Yellow-headed Blackbird	*Xanthocephalus xanthocephalus*	•						
Bobolink	*Dolichonyx oryzivorus*	•			•	•	•	•
Eastern Meadowlark	*Sturnella magna*	•	•		•	•	•	
Orchard Oriole	*Icterus spurius*	•	•					
Baltimore Oriole	*Icterus galbula*	•	•					
Red-winged Blackbird	*Agelaius phoeniceus*	•	•					
Brown-headed Cowbird	*Molothrus ater*	•	•					
Rusty Blackbird	*Euphagus carolinus*	•				•		•
Common Grackle	*Quiscalus quiscula*	•	•					
Boat-tailed Grackle	*Quiscalus major*	•	•					
Ovenbird	*Seiurus aurocapilla*	•	•					
Worm-eating Warbler	*Helmitheros vermivorum*	•	•		•	•		
Northern Waterthrush	*Parkesia noveboracensis*	•	•					
Blue-winged Warbler	*Vermivora cyanoptera*	•	•			•	•	•
Black-and-white Warbler	*Mniotilta varia*	•	•			•		
Prothonotary Warbler	*Protonotaria citrea*		•			•	•	•
Tennessee Warbler	*Leiothlypis peregrina*	•						
Orange-crowned Warbler	*Leiothlypis celata*	•	•					
Nashville Warbler	*Leiothlypis ruficapilla*	•	•		•			
Common Yellowthroat	*Geothlypis trichas*	•	•					

Species	Scientific Name	Cardiff	Larra-bee	Federal Status	State Status	Priority SGCN	Focal SGCN	IPaC
Hooded Warbler	*Setophaga citrina*	•	•		•	•		
American Redstart	*Setophaga ruticilla*	•	•					
Cape May Warbler	*Setophaga tigrina*	•	•			•		
Northern Parula	*Setophaga americana*	•	•		•	•		
Magnolia Warbler	*Setophaga magnolia*	•	•					
Bay-breasted Warbler	*Setophaga castanea*	•	•			•		
Blackburnian Warbler	*Setophaga fusca*	•	•		•	•		
Yellow Warbler	*Setophaga petechia*	•	•					
Chestnut-sided Warbler	*Setophaga pensylvanica*	•	•					
Blackpoll Warbler	*Setophaga striata*	•	•					
Black-throated Blue Warbler	*Setophaga caerulescens*	•	•		•	•		
Palm Warbler	*Setophaga palmarum*	•	•					
Louisiana Waterthrush	*Parkesia motacilla*					•		
Pine Warbler	*Setophaga pinus*	•	•					
Golden-winged Warbler	*Vermivora chrysoptera*				•	•	•	
Yellow-rumped Warbler	*Setophaga coronata*	•	•					
Swainson's Warbler	*Limnothlypis swainsonii*					•		
Yellow-throated Warbler	*Setophaga dominica*	•						
Prairie Warbler	*Setophaga discolor*	•	•			•		•
Black-throated Green Warbler	*Setophaga virens*	•	•		•	•		
Kentucky Warbler	*Geothlypis formosa*				•	•	•	•
Cerulean Warbler	*Setophaga cerulea*				•	•	•	
Canada Warbler	*Cardellina canadensis*	•	•		•	•		•
Wilson's Warbler	*Cardellina pusilla*	•	•					
Scarlet Tanager	*Piranga olivacea*	•	•			•	•	
Northern Cardinal	*Cardinalis cardinalis*	•	•					
Rose-breasted Grosbeak	*Pheucticus ludovicianus*	•	•					
Blue Grosbeak	*Passerina caerulea*	•	•					
Indigo Bunting	*Passerina cyanea*	•	•					
Summer Tanager	*Piranga rubra*					•		
Dickcissel	*Spiza americana*	•				•		

4 Birds – Offshore: Methods

This section provides a detailed overview of the data sources and methods used in the exposure and vulnerability assessments. Exposure was assessed for each species and taxonomic group, where 'exposure' is defined as the extent of overlap between a species' seasonal or annual distribution and the WTA. Potential vulnerability was then assessed for marine birds using a scoring process focused on documented avoidance behaviors, estimated flight heights, and other factors.

4.1.1 Exposure Framework

Exposure has both a horizontal and vertical component. The exposure assessment focused exclusively on the horizontal exposure of birds. Vertical exposure (i.e., flight height) was considered within the assessment of vulnerability. The exposure assessment was quantitative where site-specific survey data was available. For birds with no available site-specific data, species accounts and the literature were used to conduct a qualitative assessment. For all marine birds, exposure was considered both in the context of the proportion of the population predicted to be exposed to the WTA as well as absolute numbers of individuals. The following sections introduce the data sources used in the analysis, the methods used to map species exposure, methods used to assign an exposure metric, methods to aggregate scores to year and taxonomic group, and interpretation of exposure scores.

4.1.1.1 Exposure Assessment Data Sources and Coverage

To assess the proportion of marine bird populations exposed to the WTA, three primary data sources were used to evaluate local and regional marine bird use: (1) digital aerial surveys, conducted by APEM, (2) the NJDEP Baseline Studies conducted by Geo-Marine, Inc. (2010), and (3) version 2 of the MDAT marine bird relative density and distribution models (Curtice et al. 2019). The APEM surveys provide the most current local coverage across the WTA plus buffer and the NJDEP Baseline Studies provide an important local context. The MDAT models are modeled abundance data providing a large regional context for the WTA but are built from offshore survey data collected from 1978–2016. Each of these primary sources is described in more detail below, along with additional data sources that inform the avian impact assessment. Data collected during these surveys are in general agreement with BOEM guidelines and the goals detailed above and described below.

4.1.1.1.1 APEM Digital Aerial Surveys

A series of 8 digital aerial surveys were flown across the Lease Area, from October 2020 to May 2021 (Figure 4-1). Note: no surveys were flown in summer months (see Figure 4-2 for seasonal effort). Approximately 40% of the Lease Area plus a 2.5 nm (4 km) buffer was surveyed; but only a quarter of the resulting images (representing ~10% of the Lease Area [including the WTA]) were analyzed. These surveys were flown at an altitude of 1,360 ft (415 m) and collected photographic imagery at a resolution of 0.6 in (1.5 cm) ground sampling distance (GSD). Using APEM's Shearwater III camera system, each image footprint was approximately 0.027 mi^2 (0.043 km^2).

Surveys were conducted in weather conditions that did not limit the ability to identify marine fauna at or near the water surface – cloud base >1,400 ft (427 m), visibility >3 mi (5 km), wind speed <30 knots (35 mph), and a Beaufort Scale sea state of 3 (small waves with few whitecaps) or less, ideally 2 (small waves with no whitecaps) or less to maximize accuracy of identifications. On days with little cloud cover, surveys avoided the middle of the day to minimize glint (strong reflected light off the sea) that makes finding and subsequently identifying the marine fauna recorded in the images more difficult. The onboard camera technician continuously monitored the images collected and, if they ceased to be of sufficient quality, surveys were ceased until suitable conditions returned.

On completion of each survey flight, all images were saved and backed up locally. Management of the data was overseen in the US with a secondary data manager in the United Kingdom. Once the images had been processed and screened for potential targets, data was examined by taxonomic experts for completion of species identifications and associated QA/QC.

Table 4-1: Digital aerial survey dates

Survey	Year	Date	Season
1	2020	15 October	fall
2		07 November	
3		03 December	winter
4	2021	06 January	
5		06 March	spring
6		20 March	
7		20 April	
8		07 May	

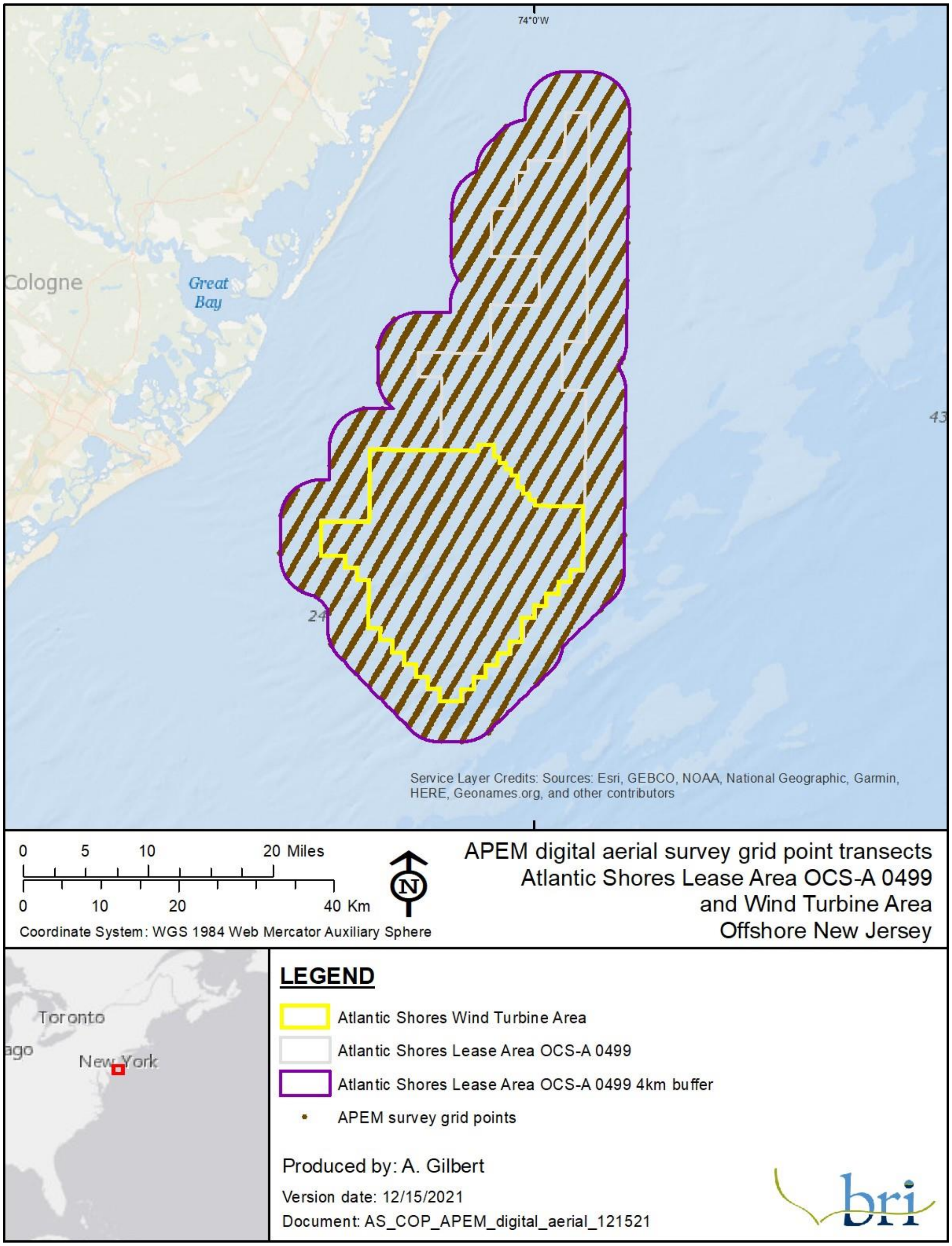

Figure 4-1: Map of digital aerial survey transects across the Lease Area.

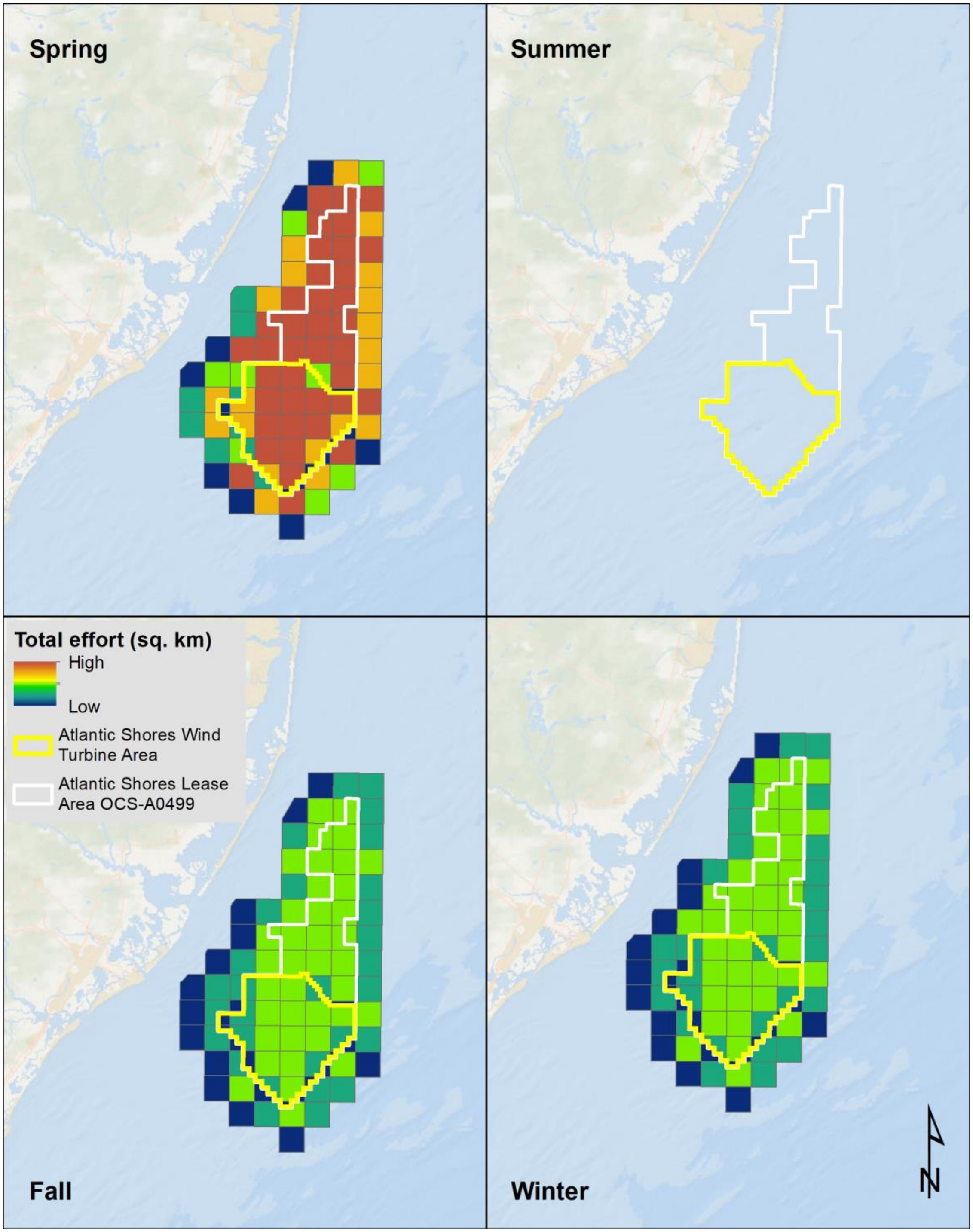

NOTE: The seasonal effort is the total number of square km of effort flown in each lease block in each season. Since there was unbalanced effort seasonally, there is greater effort in spring and none in summer. The season definitions and effort are detailed in Table 4-1.

Figure 4-2: Seasonal survey effort of Atlantic Shores APEM digital aerial surveys. Survey effort totaled within each full or partial lease block.

4.1.1.1.2 NJDEP Baseline Studies

The NJDEP Baseline Studies included monthly boat-based avian surveys conducted coastally and further offshore of New Jersey (Geo-Marine 2010). The offshore study area covered from approximately the 32 ft (10 m) isobath to an outer boundary at 20 nm (~37 km) from shore, and extended from Hereford Inlet, just north of Cape May, north to the Route 37 bridge at Seaside Heights (Figure 4-3). Shipboard surveys were conducted between January of 2008 and December of 2009. Due to weather, February 2008 and December 2009 survey effort was less than typical, but all other surveys were conducted in a double saw-tooth design covering the entire NJDEP Baseline Studies study area. In addition, supplemental offshore saw-tooth surveys were conducted between August and December 2009, and 6 days of offshore surveys were conducted in concert with sea watches (land-based seaward counts) at Barnegat Light and north end of Avalon. The supplemental surveys were meant to determine if increased survey effort had an effect on abundance estimates.

Offshore and coastal surveys were conducted using a hybrid distance sampling/strip transect method, while the boat was traveling at 10 knots during daylight hours, and visibility was at least 4.3 mi (7 km). Observers recorded distance and angle to all animals, focusing effort within 984 ft (300 m) ahead and to the side of the survey vessel. Observers viewed within a 90-degree bow-to-beam arc off either side of the vessel. During offshore saw-tooth surveys, a closing method for marine mammals was used where, when marine mammals were sighted, the vessel went off transect to identify the species present and estimate the group size (if more than one was present). During these off-transect periods, observations were designated as "off" until they returned to the original transect line, when they were designated as "on". This approach increases the chances of double-counting but should improve estimates of marine mammal group size and identification rates. Estimated flight heights were recorded during surveys (as 1 ft [0.3 m], 25 ft [7.6 m], 50 ft [15.2 m], 100 ft [30.5 m], 200 ft [70 m], 300 ft [91 m], 500 ft [152 m], and 1,000+ ft [305 m] above sea-level) and basic behavioral states were noted.

During both coastal and boat-based surveys, a total of 176,217 birds was recorded, consisting of 153 species, including many migrant land birds. The addition of non-target taxa (e.g., bats, butterflies, marine mammals) resulted in a total of 201 identification codes, some of which are not identified to species (e.g., unknown small tern). The overall patterns indicate higher species densities closer to shore, although spring and summer appear to show higher relative densities offshore. No federally-listed bird species were detected during these surveys. As discussed below, the NJDEP Baseline Studies boat-based survey data are displayed as proportions of total effort-corrected counts and displayed as quantiles.

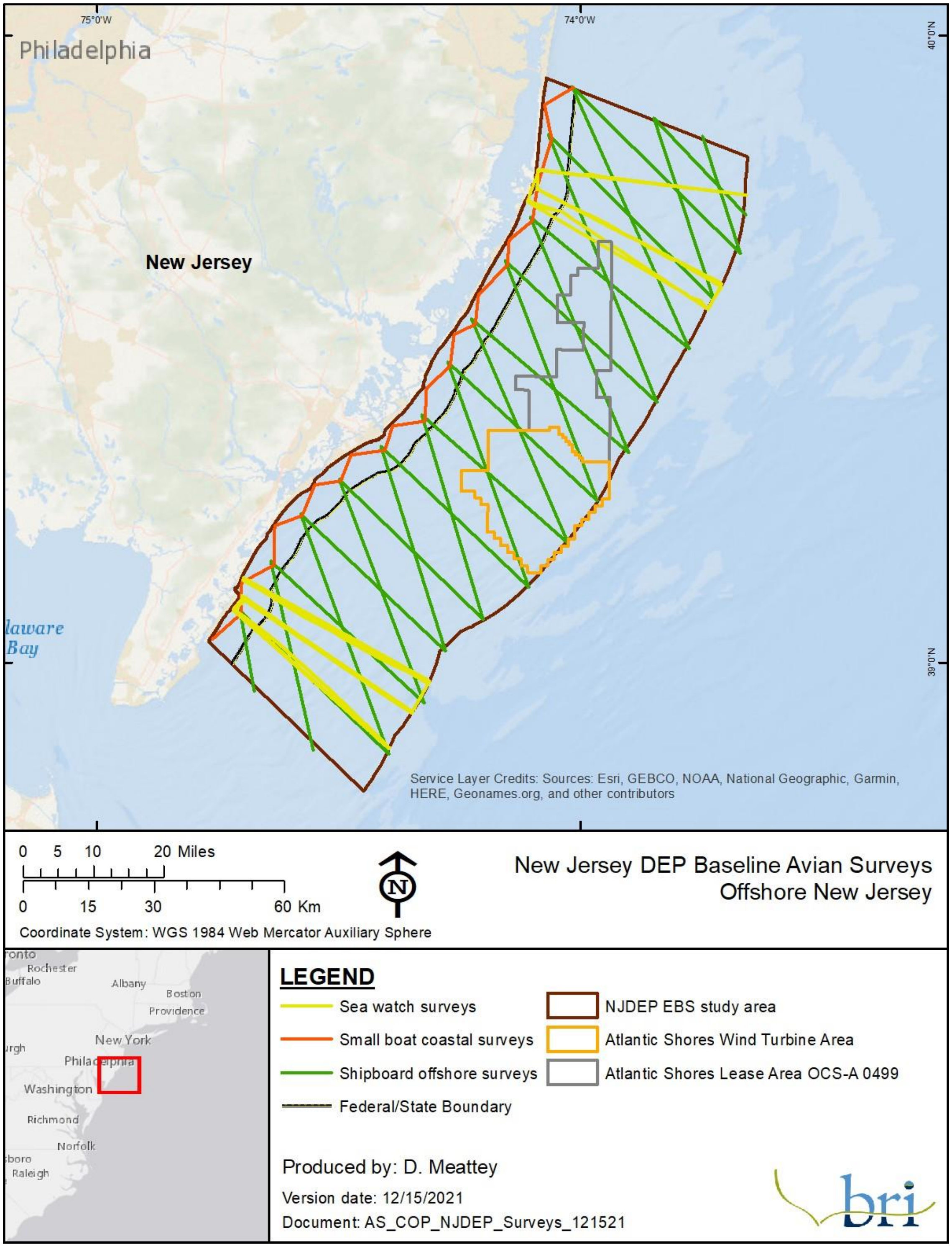

Figure 4-3: Map of NJDEP Baseline Studies survey transects and the Atlantic Shores WTA.

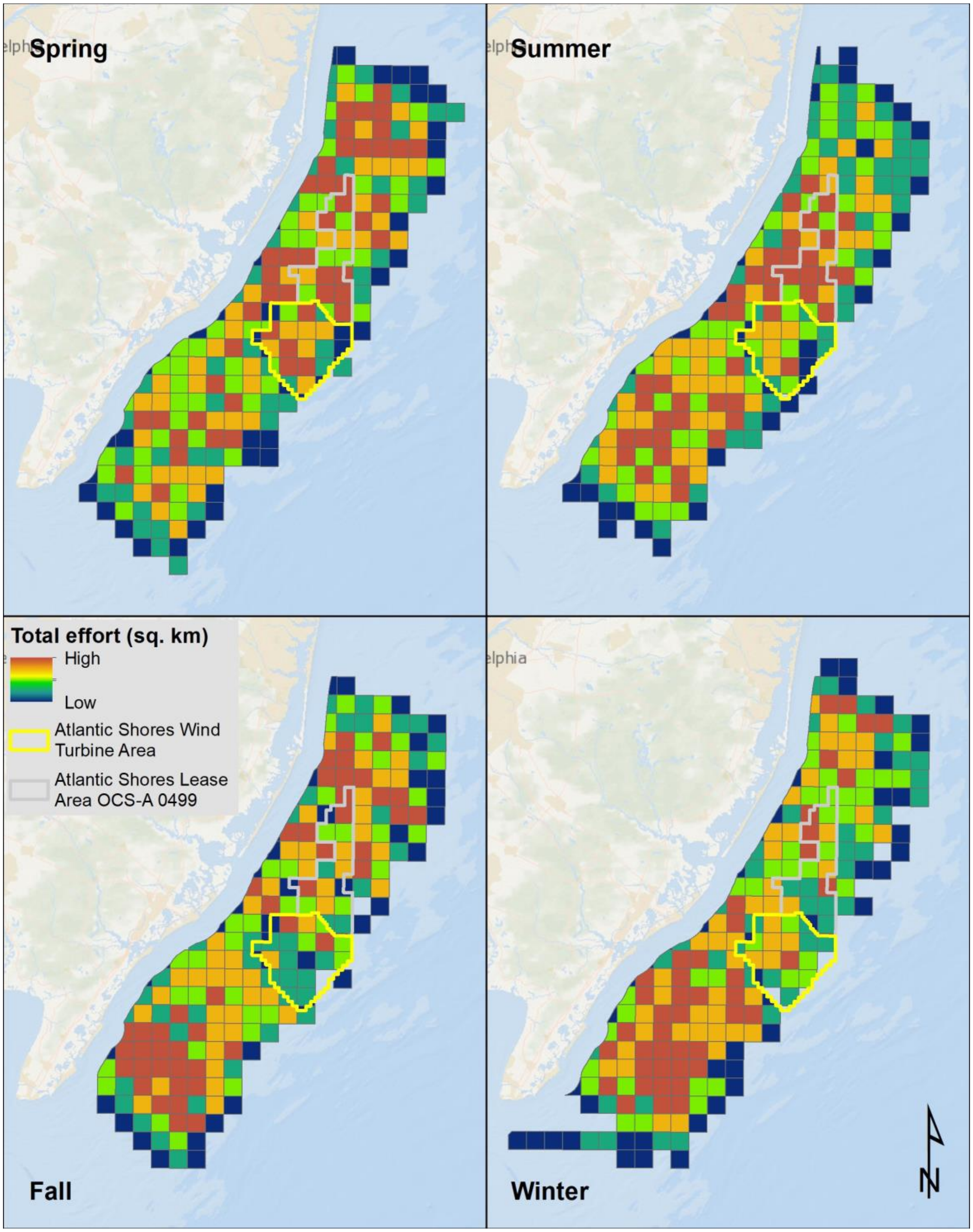

NOTE: Relative effort (in sq. km) is shown across the study area by season. Red=higher effort (more sq. km covered) blue is lowest effort.

Figure 4-4: NJDEP Baseline Studies survey effort by season. While effort varied by OCS lease block and season, the entire study area, including the WTA, was thoroughly surveyed each season.

4.1.1.1.3 The MDAT Marine Bird Abundance and Occurrence Models (Version 2)

Seasonal predictions of density were developed to support Atlantic marine renewable energy planning. Distributed as MDAT bird models (Winship et al. 2018; Curtice et al. 2019), they describe regional-scale patterns of abundance. Updates to these models (Version 2) are available directly from Duke University's Marine Geospatial Ecology Lab MDAT model web page[4]. The MDAT analysis integrated survey data (1978–2016) from the Atlantic Offshore Seabird Dataset Catalog[5] with a range of environmental predictor variables to produce long-term average annual and seasonal models (Figure 4-5). These models were developed to support marine spatial planning in the Atlantic. In Version 2, relative abundance and distribution models were produced for 47 avian species using Atlantic waters in the United States (US) from Florida to Maine; this resource provides an excellent regional context to local relative densities estimated from boat-based surveys.

The digital aerial surveys, NJDEP Baseline Studies, and MDAT models each have strengths and weaknesses. The data from the digital aerial surveys and NJDEP Baseline Studies were collected in a standardized, comprehensive way, and are relatively recent, so they describe recent distribution patterns in the WTA and surrounding areas. However, these surveys covered a fairly small area relative to the Northwest Atlantic distribution of most marine bird species, and the limited number of surveys conducted in each season means that individual observations (or lack of observations, for rare species) may in some cases carry substantial weight in determining seasonal exposure.

The MDAT models, in contrast to the baseline surveys, include data collected at much larger geographic and temporal scales, and use a range of survey methods. The larger geographic scale is helpful for determining the importance of the WTA to marine birds, relative to other available locations in the Northwest Atlantic, and is thus essential for determining overall exposure. However, these models are based on data from decades of surveys and long-term climatological averages of dynamic covariates; given changing climate conditions, these models may no longer accurately reflect current distribution patterns. Model outputs that incorporate environmental covariates to predict distributions across a broad spatial scale may also vary in the accuracy of those predictions at a local scale.

---

[4] http://seamap.env.duke.edu/models/mdat/

[5] https://coast.noaa.gov/digitalcoast/data/atloffshoreseabird.html

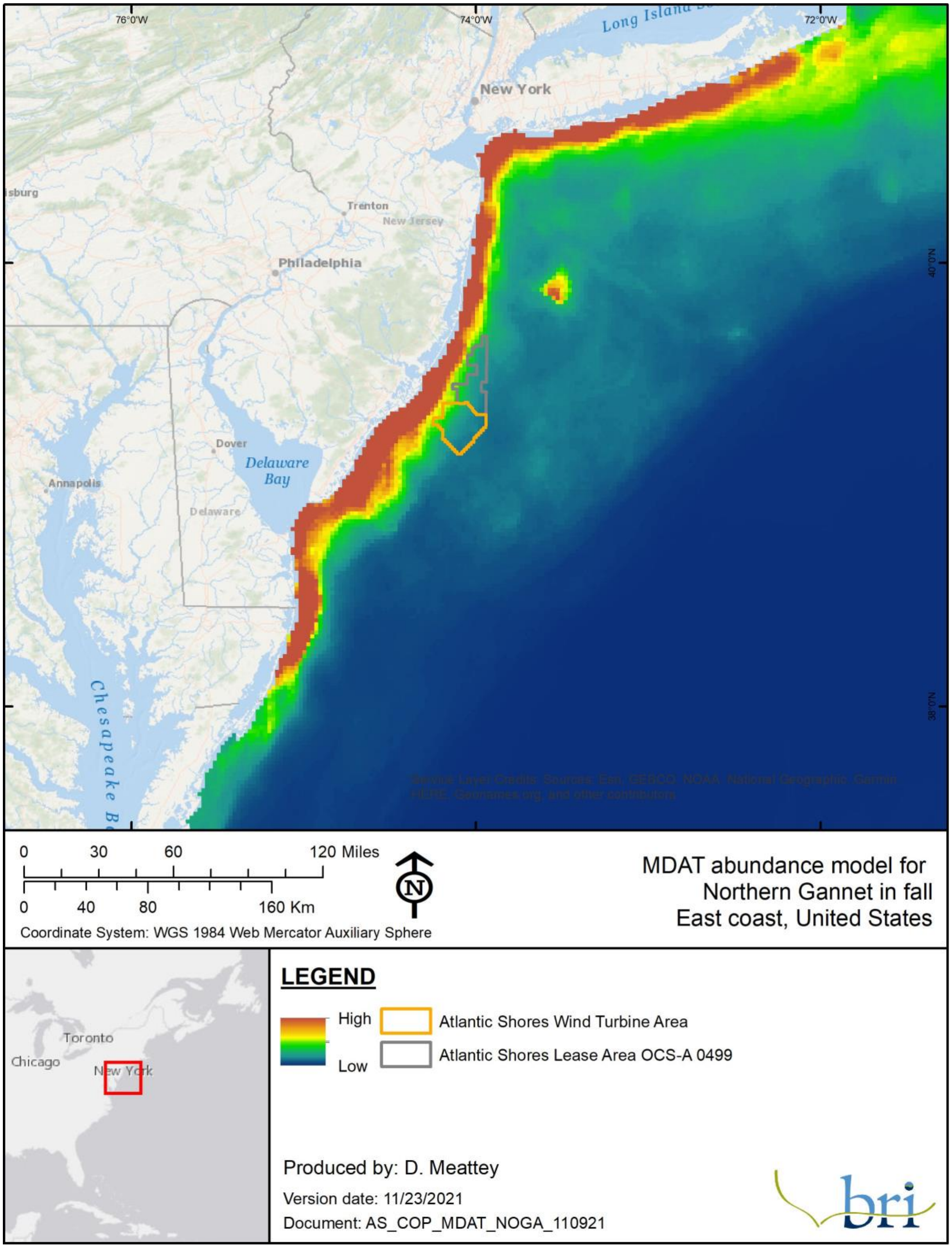

Figure 4-5: Example MDAT abundance model for the Northern Gannet (*Morus bassanus*) in fall.

4.1.1.1.4 Secondary Sources

4.1.1.1.4.1 Northwest Atlantic Seabird Catalog

The Northwest Atlantic Seabird Catalog is the comprehensive database for offshore and coastal seabird surveys conducted in US Atlantic waters from Maine to Florida. The database contains records from 1938–2019, having more than 200 datasets and approximately 750,000 observation records along with associated effort information (Arliss Winship, pers. comm., 17 Nov 2021). The database is currently being managed by NOAAs National Center for Coastal Ocean Science (NCCOS). With BOEM's approval, NOAA provided the Catalog database to BRI to make queries for this assessment. All relevant data from the Catalog were mapped to determine the occurrence of rare species within the WTA.

4.1.1.1.4.2 Mid-Atlantic Diving Bird Tracking Study

A satellite telemetry tracking study in the mid-Atlantic was developed and supported by BOEM and the USFWS with objectives aimed at determining fine scale use and movement patterns of three species of marine diving birds during migration and winter (Spiegel et al. 2017; Stenhouse et al. 2020). These species – the Red-throated Loon, Surf Scoter, and Northern Gannet– are all considered species of conservation concern and exhibit various traits that make them vulnerable to offshore wind development. Nearly 400 individuals were tracked using satellite transmitters, Argos platform terminal transmitters (PTT), over the course of five years (2012–2016), including some Surf Scoters tagged as part of the Atlantic and Great Lakes Sea Duck Migration Study by the Sea Duck Joint Venture (SDJV)[6]. Results provide a better understanding of how these diving birds use offshore areas of the mid-Atlantic Outer Continental Shelf (OCS) and beyond.

Utilization distributions (UDs) were determined for each species by calculating individual level dynamic Brownian-bridge movement model (dBBMM) surfaces (Kranstauber et al. 2012) using package Move for R (Kranstauber and Smolla 2016). Separate dBBMM surfaces were calculated for each of two winters with at least five days of data and combined into a weighted mean surface for each animal (as a percentage of the total number of days represented in the surface) with a minimum 30 total combined days of data. This method of combining multiple seasons was used for the migration periods as well, but with relaxed requirements for days of data, requiring only five days per year and seven total days per period since migration duration often occurred over a much shorter time period. Utilization contour levels of 50%, 75%, and 95% were calculated for the mean UD surface. The final UD was cropped to the 95% contour for mapping and further analyses (Spiegel et al. 2017).

4.1.1.1.4.3 Migrant Raptor Studies

Falcons

To facilitate research efforts on migrant raptors [i.e., migration routes, stopover sites, space use relative to Atlantic OCS wintering/summer range, origins, contaminant exposure], BRI has deployed satellite transmitters on fall migrating raptors at three different raptor migration

[6] https://seaduckjv.org/science-resources/atlantic-and-great-lakes-sea-duck-migration-study/

research stations along the north Atlantic coast (DeSorbo et al. 2012; DeSorbo, Gilpatrick, et al. 2018; DeSorbo, Persico, et al. 2018). Research stations include Block Island in Rhode Island, Monhegan Island in Maine, and Cutler in Maine.

Data from satellite-tagged Peregrine Falcons (*Falco prergrinus*) and Merlins (*F. columbarius*) identifies fall migration routes along the Atlantic Flyway. Positional data was filtered to remove poor quality locations using the Douglas Argos Filtering tool (Douglas et al. 2012), available online on the Movebank data repository[7], where these data are stored and processed. A request for data use was made to Chris DeSorbo, Raptor Program Director at BRI, who provided permission to utilize the results of the migrant raptor studies.

Osprey

Between 2000 and 2019, 106 tracking devices were fitted to Ospreys (*Pandion haliaetus*) predominantly at Chesapeake Bay and in northern New Hampshire (www.ospreytrax.com). This data set includes both adults and juvenile Ospreys but represents the first dedicated study of dispersal and migration in juveniles. Satellite transmitters were used in early years, but beginning in 2012, higher resolution cellular GPS transmitters were deployed on adult males to better document their migration (Horton et al. 2014).

Separately, Argos satellite transmitters were deployed on Ospreys in the US and Canada between 1995 and 2001 (Martell et al. 2001; Martell and Douglas 2019). Tagging locations included areas in Oregon, Washington, Minnesota, New York, and New Jersey. Birds tagged in eastern states generally migrated along the Atlantic coast.

To characterize potential utilization of the offshore environment by Ospreys, UDs were generated for individual animals using a dBBMM (Kranstauber et al. 2012). Both Argos satellite data and GPS-derived positional data were used from the two different telemetry datasets from Movebank. Both datasets were compiled and a max speed filter by animal was applied, which excluded locations with instantaneous speeds greater than 62 mph (100 kmph) and also filtered points outside of an extent including the eastern US and Atlantic Canada (including all offshore points for this region). Individual dBBMMs were generated for the last 365 consecutive days of available data per tag (or less if the tags provide less than 365 consecutive days), thus representing an annual cycle within the US. Models were composited into a weighted UD for the sampled population, weighting each animal's UD by the number of days data were available of the total number of days of all animals providing models.

4.1.1.1.4.4 Tracking movements of vulnerable terns and shorebirds in the Northwest Atlantic using nanotags

Since 2013, BOEM and the USFWS have supported a study using nanotags (coded VHF tags) and an array of automated very high frequency (VHF) radio telemetry stations to track the movements of vulnerable terns and shorebirds. The study was designed to assess the degree to which these species use offshore federal waters during breeding, pre-migratory staging periods,

[7] https://www.movebank.org/

and on their migrations. In a pilot study in 2013, researchers attached nanotags to Common Terns (*Sterna hirundo*) and American Oystercatchers (*Haematopus palliatus*) and set up eight automated sentry stations (Loring et al. 2017). Having proved the methods successful, the study was expanded to 16 automated stations in 2014, and from 2015–2017, tagging efforts included ESA-listed species, Piping Plovers and Roseate Terns. This study provided new information on the offshore movements and flight altitudes for these species gathered from a total of 33 automated telemetry stations deployed across Atlantic coastal states, including areas of Massachusetts, New York, New Jersey, Delaware, and Virginia (Loring et al. 2019).

4.1.1.1.4.5 Tracking movements of Red Knots in US Atlantic Outer Continental Shelf Waters

Building from a previous tracking study, Red Knots of the *rufa* subspecies were fitted with digital VHF transmitters during their 2016 southbound migration at stopover locations and along the Atlantic coast in both Canada and the US. Individuals were tracked using radio telemetry stations within the study area that extended from Cape Cod, Massachusetts to Back Bay, Virginia. Modeling techniques were developed to describe the frequency and offshore movements over Federal waters and specific WEAs within the study area. The primary study objectives were to: develop models related to offshore movements for Red Knots; assess the exposure to each WEA during southbound migration; and examine WEA exposure and migratory departure movements in relation to meteorological conditions (Loring et al. 2018).

4.1.1.1.4.6 Sea Duck Tracking Studies

The Atlantic and Great Lakes Sea Duck Migration Study, a multi-partner collaboration, was initiated by the SDJV in 2009 with the goals of: (1) fully describing full annual cycle migration patterns for four species of sea ducks (Surf Scoter, Black Scoter [*Melanitta americana*], White-winged Scoter [*Melanitta deglandi*], and Long-tailed Duck [*Clangula hyemalis*]), (2) mapping local movements and estimating length-of-stay during winter for individual radio-marked ducks in areas proposed for placement of WTGs, (3) identifying nearshore and offshore habitats of high significance to sea ducks to help inform habitat conservation efforts, and (4) estimating rates of annual site fidelity to wintering areas, breeding areas, and molting areas for all four focal species in the Atlantic flyway. To date, over 500 transmitters have been deployed in the US and Canada by a broad range of project partners. These collective studies have led to increased understanding of annual cycle dynamics of sea ducks, as well as potential interactions with and impacts from offshore wind energy development (Loring et al. 2014; SDJV 2015; Meattey et al. 2018; Meattey et al. 2019).

As part of a satellite telemetry tracking study in the mid-Atlantic, BOEM and the USFWS also partnered with the SDJV during 2012–2016 to deploy transmitters in Surf Scoters, with the aim of determining fine scale use and movement patterns of three species of marine diving birds during migration and winter (Spiegel et al. 2017).

UDs were determined for each species by calculating individual level dBBMM surfaces (Kranstauber et al. 2012) using package Move for R (Kranstauber and Smolla 2016). Separate dBBMM surfaces were calculate for each of two winters with at least five days of data and combined into a weighted mean surface for each animal (as a percentage of the total number of days represented in the surface) with a minimum 30 total combined days of data. This method of combining multiple seasons was used for the migration periods as well, but with relaxed requirements for days of data, requiring only five days per year and seven total days per period since migration duration often occurred over a much shorter time period. Utilization contour levels of 50%, 75%, and 95% were calculated for the mean UD surface. The final UD was cropped to the 95% contour for mapping and further analyses (Spiegel et al. 2017).

4.1.1.2 Spatial Density Modeling Using Digital Aerial Survey Data

Data Compilation

Bird observations were collected from eight digital aerial surveys conducted approximately monthly from October 2020 to May 2021, covering fall, winter, and spring seasons. These aerial surveys were conducted using the standard APEM protocol (see Section 4.1.1.1.1). Bird observations were identified from digital images using a combination of automated (AI) and manual (seabird experts) methods. Birds were identified to species level when possible and were otherwise assigned to the lowest possible taxonomic group (i.e., Auk-species unknown or Murre-species unknown). Taxa groups were created to include species-unknown observations with taxonomically similar species (i.e., all identified Scoter species plus unknown scoter category). In sum, the observation data included 17 species (Table 4-2) and nine taxonomic groups (Table 4-3). Along with the full year-round data set, each species/group was subset into three seasonal data sets for density modeling. Only species/groups with greater than 10 observations in the given season were used to build spatial models.

Data Analysis

To model the observation density and account for the spatial dependence among observations, we fit spatially-explicit log Gaussian Cox Poisson (LGCP) process models to the year-round and seasonal survey data by species and taxa group using INLA, integrated nested Laplace approximation (Rue et al. 2009) for approximate Bayesian inference. The spatial dependence in the data is accounted for by incorporating a Gaussian Markov Random Field (GMRF) into the models. Briefly, LGCP models estimate the point density using a log link function such that the log of the spatial inhomogeneous intensity function (λ) at any point is assumed to be normally distributed (GMRF; Møller & Waagepetersen 2007). We implemented the stochastic partial differential equations (SPDE) approach (Lindgren et al. 2011) to incorporate the spatial random effect as a latent Gaussian Field (GF) with a Matérn covariance structure to account for the spatial dependence in the data. Put another way, densities are more likely to be similar in adjacent spatial units than remote units, and these models estimate these spatial correlations to estimate changes in density over space.

To approximate the continuous space of the data, we constructed a constrained refined Delaunay triangulation spatial mesh covering the entire Atlantic Shores survey area (Figure 4-6). An area of coarser density mesh (10% of the survey area diameter) was added beyond that to remove boundary effects that cause increased variance at the borders (Lindgren et al. 2011). We built the mesh using all bird observations points as the initial triangulation nodes, with a maximum triangle edge of 700 m for the inner mesh (i.e., survey area) and 7,000 m for the outer mesh. To avoid very small triangles, we also set a cutoff of 1000 m, such that points at a closer distance than this are replaced by a single vertex prior to mesh creation. We estimated smooth density surfaces by modeling the intensity (λ) at each spatial location (s) as a function of the spatial random effect (*u*).

$$\lambda(s) = \exp(\beta_0 + AA(s))$$

where β_0 is an intercept term that we set to zero and **u** is the GF representing the spatial random effect. The spatial effect **u** can be approximated at any point within the triangulated domain, using the projector matrix **A** to link the spatial GF (defined by the mesh vertices or nodes) to the locations of the observed data, s (Krainski et al. 2018). The Matérn covariance matrix for the spatial effect was parameterized using penalized complexity (PC) priors (Fuglstad et al. 2018), where the hyperparameters of range (*r*) and the marginalized standard deviation of the field (σ) define the spatial random effect so that $P(r > r_0) = p$ and $P(\sigma > \sigma_0) = p$. For these models, we used uninformed priors, so the prior probability of the spatial range being less than 9000 was 0.001 and the probability of spatial variance being less than 900 was 0.001.

Species/group density predictions were made to the BOEM ~1,200 m resolution aliquot grid encompassing the Atlantic Shores lease block area with a 4 km buffer. Density predictions of all species/groups were converted into density proportions by dividing the expected density at each prediction point by the sum of that group's expected density across the prediction grid. All models were fit in R version 4.0.2, (R Core Team 2020), using the R-INLA (version 21.02.23, https://www.r-inla.org, Lindgren & Rue 2015) and inlabru (version 2.3.1, Bachl et al. 2019) packages.

Table 4-2: Avian species identified in the digital aerial survey imagery.

Common Name	Scientific Name	Total Observations
Atlantic Puffin	*Fratercula arctica*	2
Black-legged Kittiwake	*Rissa tridactyla*	24
Black Scoter	*Melanitta americana*	44
Bonaparte's Gull	*Chroicocephalus philadelphia*	1218
Common Loon	*Gavia immer*	1241
Gadwall	*Mareca strepera*	1
Great Black-backed Gull	*Larus marinus*	181
Herring Gull	*Larus argentatus*	138
Laughing Gull	*Leucophaeus atricilla*	452
Manx Shearwater	*Puffinus puffinus*	1
Northern Gannet	*Morus bassanus*	934
Razorbill	*Alca torda*	9
Red-throated Loon	*Gavia stellata*	129
Red Phalarope	*Phalaropus fulicarius*	41
Ring-billed Gull	*Larus delawarensis*	2

Common Name	Scientific Name	Total Observations
Surf Scoter	*Melanitta perspicillata*	1
White-winged Scoter	*Melanitta deglandi*	505

Table 4-3: Species and categories included in each taxonomic group.

Group	Categories in Group	Total Observations
Terns	Common Tern, Forster's Tern	5
Murres	Common Murre, Thick-billed Murre	26
Auks	Atlantic Puffin, Auk-species unknown, Common Murre, Thick-billed Murre, Murre/Razorbill, Razorbill	116
Gulls, small	Bonaparte's Gull, Gull-species unknown–Small	1537
Gulls, medium	Black-legged Kittiwake, Laughing Gull, Ring-billed Gull	478
Gulls, large	Great Black-backed Gull, Herring Gull, Gull-species unknown–Large	340
Loons	Common Loon, Loon-species unknown, Red-throated Loon	1418
Scoters	Black Scoter, Scoter unid., Surf Scoter, White-winged Scoter	1912

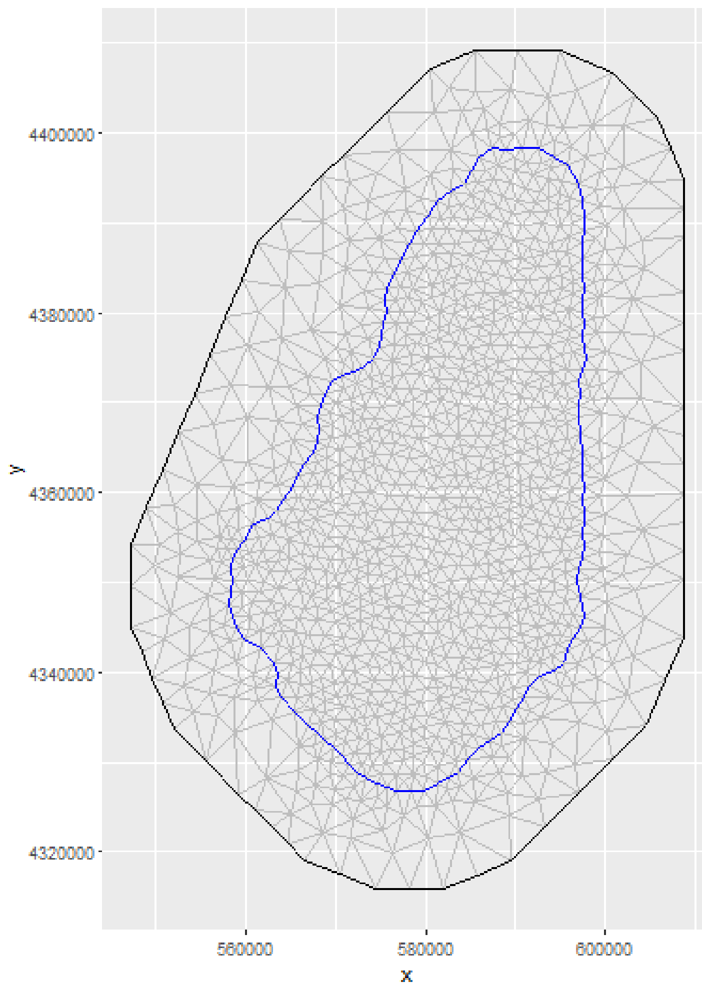

Figure 4-6: Constrained refined Delaunay triangulation spatial mesh.

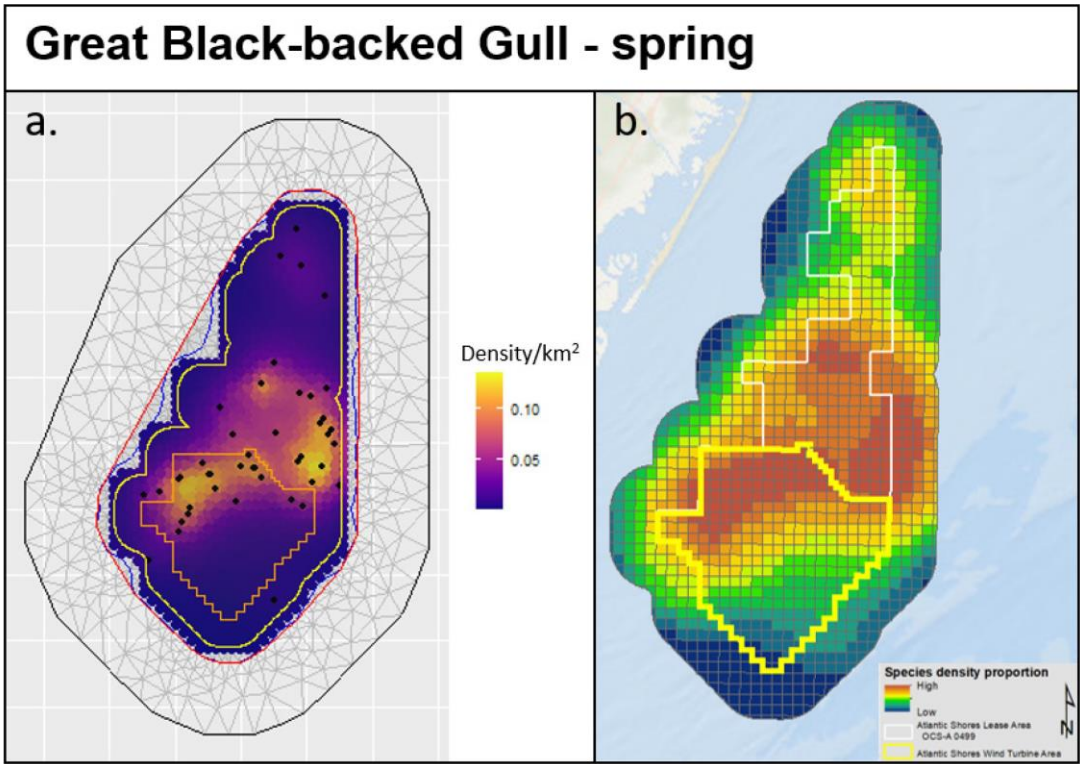

NOTE: The density estimates from the models were converted to density quantiles by dividing the density at each prediction point by the sum of that species/group's density across the prediction grid. These standardized density quantiles were then categorized into 10 percentile groups for visualization purposes, ranging from low to high standardized density proportion. The raw model output (**a.**) shows the triangulation mesh used for the INLA model estimation, the inner mesh boundary (blue outline), the inner mesh prediction area (red outline), the Atlantic Shores Lease Area prediction grid (yellow outline), and the Atlantic Shores WTA (orange outline). Prediction points in **a.** are sized to present a continuous density surface.

Figure 4-7: Example of the **a.** non-standardized mean density/km^2 estimates from the INLA models with the raw observations (black points) overlaid and the **b.** standardized density proportions (of total density) visualized as percentiles.

4.1.1.3 Community Distance Modeling Using NJDEP Baseline Studies Boat Survey Data

Boat-based surveys are a standardized methodology to describe patterns of distribution and abundance in the marine environment. A known bias in this method is that individuals farther from the transect line are more difficult to detect than those closer to the center (Buckland et al. 2001). This bias causes surveyors to underestimate the total number of animals in the survey area (Camphuysen et al. 2004). Estimating detection probability for rare species can also be difficult due to a lack of observations, so researchers have developed new methods for estimating detection probabilities of communities to address this issue (Sollmann et al. 2016). These community-based methods can be beneficial for surveys of wind energy projects as they can help account for problems relating to surveys of relatively small areas or including data from rare species.

We attempted to distance correct the NJDEP boat-based survey data using community distance models. However, while model convergence was adequate, and this modeling approach often fitted reasonable detection curves for some species groups, there were several indications that the models did not reliably correct density estimates across all species groups. Thus, we chose not to use the modeled values and instead relied on naïve density estimates in the exposure assessment (see Section 6 for further details).

Given that the exposure assessment examines the relative differences in densities across the survey area on a species/season basis across the survey area, we expect the detection bias inherent in the boat-based data should have no effect on the exposure results because of any correction for differences in detectability would scale all density results equally for any season/species combination. However, because the detection probability of the APEM digital aerial surveys is expected to be near 100%, we recommend that the digital aerial surveys be considered to have the most current and accurate density estimates for the WTA for those species in which data are available.

4.1.1.4 Exposure Mapping

Maps were developed to display local and regional context for exposure assessments. A three-panel map was created for each species-season (winter: December–February; spring: March–May; summer: June–August; and fall: September–November) combination that includes MDAT models, regional NJDEP baselines survey data, and spatial models of local APEM digital aerial data. Any species-season combination which did not at least have modeled APEM digital aerial data, MDAT model, or NJDEP survey data (i.e., blank maps) were left out of the final map set. An example map for Northern Gannet in fall is provided below (Figure 4-8), while the complete set of species-season maps can be found in Section 7.

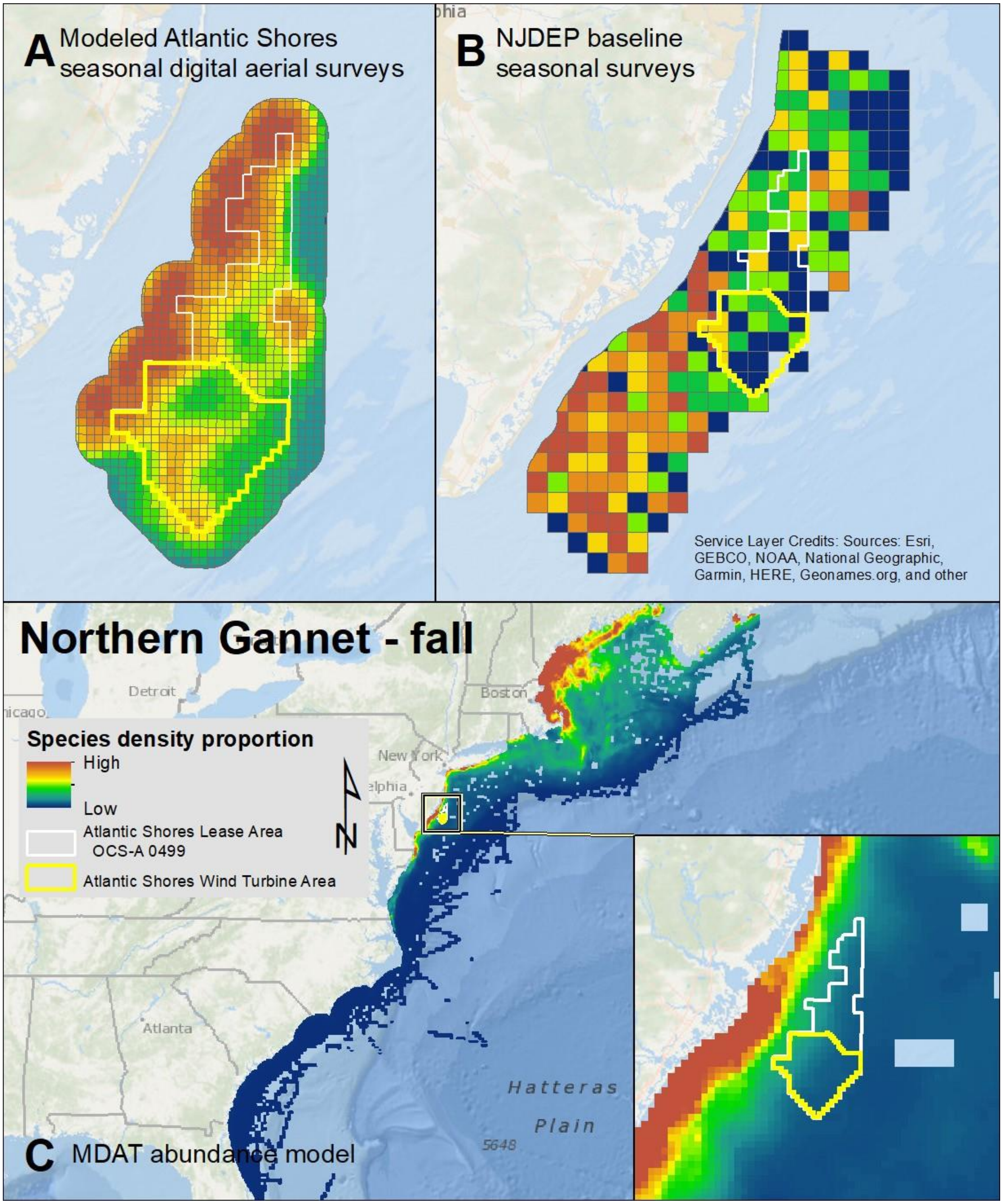

Figure 4-8: Example map of relative density proportions locally and regionally for the Northern Gannet in fall.

Panel A presents the standardized digital aerial survey data visualized as percentiles derived standardized density proportions (of total density). Standardized density proportions were calculated from modeled mean density/km^2 estimates from the INLA models as described above in 4.1.1.2. The density estimates from the models were converted to density quantiles by dividing the density at each prediction point by the sum of that species/group's density across the prediction grid. These standardized density quantiles were then categorized into 10 percentile groups for visualization purposes, ranging from low to high standardized density proportion.

Panel B presents the NJDEP Baseline Studies boat-based survey data as proportions of total effort-corrected counts and displayed as quantiles. The proportion of the total effort-corrected counts (total counts per square kilometer of survey area) was calculated for each BOEM designated OCS[8] Lease Block[9], across all surveys in each season. This method was useful as it scaled all effort-corrected count data from 0–1 to standardize data visualizations among species. Standardized effort-corrected count data were categorized into 6 quantiles for all non-zero data plus a zero category since data were often highly skewed towards 0.

Panel C includes data from MDAT models presented at two different scales – the density models over the US Atlantic coast, and, in an inset map, a zoom in on the modeled densities similar to the map display in panel B. Density data are scaled in a similar way to the baseline survey data, so that the low–high designation for density is similar across species and datasets. However, there are no true zeroes in the MDAT model outputs, and thus no special category for them in the MDAT maps. All MDAT models were masked to remove areas of zero effort within a season. These zero-effort areas do have density estimates, but generally are of low confidence, so they were excluded from mapping and analysis to reduce anomalies in predicted species densities and to strengthen the analysis. While the color scale for the MDAT data is approximately matched to that used for the baseline survey data, the values that underlie them are different (the MDAT data are symbolized using an ArcMap default color scale, which uses standard deviations from the mean to determine the color scale rather than quantiles).

Overall, these maps should be viewed in a broadly relative way between local, regional, and coast-wide assessments, and even across species.

---

[8] The OCS is defined by the US Department of the Interior (https://www.bsee.gov/newsroom/library/glossary) as "All submerged lands seaward and outside the area of lands beneath navigable waters. Lands beneath navigable waters are interpreted as extending from the coastline 3 nautical miles into the Atlantic Ocean, the Pacific Ocean, the Arctic Ocean, and the Gulf of Mexico excluding the coastal waters off Texas and western Florida. Lands beneath navigable waters are interpreted as extending from the coastline 3 marine leagues into the Gulf of Mexico off Texas and western Florida."

[9] OCS Lease Blocks are defined (https://catalog.data.gov/dataset/outer-continental-shelf-lease-blocks-atlantic-region-nad83) as "small geographic areas within an Official Protraction Diagram (OPD) for leasing and administrative purposes. These blocks have been clipped along the Submerged Lands Act (SLA) boundary and along the Continental Shelf Boundaries. Additional details are available from: https://www.boem.gov/BOEM-Newsroom/Library/Publications/1999/99-0006-pdf.aspx"

4.1.1.5 Exposure Assessment Metrics

Avian exposure to the WTA was assessed for each species by calculating effort-corrected counts for the NJDEP boat-based surveys on a local level and using the MDAT models on a regional level. The exposure scores were developed from the NJDEP boat-based surveys and MDAT models by comparing bird densities in the WTA with all other possible WTA-sized areas within the survey area for each dataset. For each species the mean densities were compiled for each WTA-sized area, quantiles calculated for the set of all WTA-sized areas, and a categorical score was assigned to each quantile. If the WTA was in the top quartile, a bird would get a high exposure score; if it was in the bottom, a minimal score. The analysis was done in the following two steps:

Step 1, assess regional exposure using MDAT models: Using the MDAT data, masked to remove zero-effort predicted cells, the predicted seasonal density surface for a given species was aggregated into a series of rectangles that were approximately the same size as the WTA, and the mean density estimate of each rectangle was calculated. This process compiled a dataset of density estimates for all species surveyed, for areas the same size as the WTA. The 25^{th}, 50^{th}, and 75^{th} weighted quantiles of this dataset were calculated, and the quantile into which the density estimate for the WTA fell for a given species and season combination was identified. Quantiles were weighted by using the proportion of the total density across the entire modeled area that each sample represented. Thus, quantile breaks represent proportions of the total seabird density rather than proportions of the raw data. A categorical score was assigned to the WTA for each season-species: 0 (Minimal) was assigned when the density estimate for the WTA was in the bottom 25%; 1 (Low) when it was between 25% and 50%; 2 (Medium) when it was between 50% and 75%; and 3 (High) when it was in the top quartile (greater than 75%). While a "high" score does suggest importance within a regional scale, these scores need to be considered in context of scores at each spatial scale when assessing overall importance to the species in a season.

Step 2, assess local exposure using the NJDEP boat-based survey: A similar process was used to categorize each species-season combination using the baseline survey data. To compare the WTA to other locations within the survey region, the nearest 26 OCS full or partial Lease Blocks to each OCS Lease Block surveyed in the NJDEP boat-based survey area in each season (winter, n = 228; spring, n = 241; summer, n = 225; and fall, n = 225) were identified and the relative density of each OCS Lease Block group was calculated. Thus, a dataset of relative densities for all possible WTA-sized OCS Lease Block groups was generated within the survey region using the baseline survey data. This data set was used to assign scores to all species-season combinations, based on the same quartile categories described for the MDAT models above. If a score for a species-season combination was not available using the baseline survey data (local assessment), and because the avian surveys made every effort to survey all species, then the local assessment score was assigned a zero because no animals were sighted for that species-season combination.

4.1.1.6 Species Exposure Scoring

To determine the relative exposure for a given species and season in the WTA compared to all other areas, the MDAT quartile score and baseline survey data quartile score were added together to create a final exposure metric that ranged from 0 to 6. The density information at both spatial scales were equally weighted, and thus represent both the local and regional importance of the WTA to a given species during a given season. However, if a species-season combination was not available for the MDAT regional assessment, then the score from the local assessment (baseline survey data) was accepted as the best available information for that species-season, and it was scaled to range from 0 to 6 (e.g., essentially doubled to match the final combined score).

The exposure score was categorized as Minimum (a combined score of 0), Low (combined score of 1–2), Medium (combined score of 3–4), or High (combined score of 5–6; Table 4-4). In general terms, species-season combinations labeled as 'Minimum' had low densities at both the local and regional spatial scales. 'Low' exposure was assessed for species with below-average densities at both spatial scales, or above-average density at one of the two spatial scales and low density at the other scale. 'Medium' exposure describes several different combinations of densities; one or both spatial scales must be at least above-average density, but this category can also include species-season combinations where density was high for one spatial scale and low for another. 'High' exposure is when density is high at both spatial scales, or one is high and the other is above average. Both local and regional exposure scores were viewed as equal in importance in the assessment of exposure. All exposure determinations are highlighted in bold throughout the text.

Table 4-4: Definitions of exposure levels developed for the avian assessment for each species and season.

NOTE: The listed scores represent the exposure scores from the local NJDEP boat-based survey data and the regional MDAT on the left and right, respectively.

Exposure Level	Definition	Scores
Minimal	Densities at both local and regional scales are below the 25th percentile.	0, 0
Low	Local and/or regional density is between the 25th and 50th percentiles. **OR** Local density is between the 50th and 75th percentiles and regional density is below the 25th percentile, or vice versa.	1, 1 2, 0
Medium	Local or regional density is between the 50th and 75th percentiles. **OR** Local density is between the 50th and 75th percentiles and regional density between the 25th and 50th percentiles, or vice versa. **OR** Local density is greater than the 75th percentile and regional density is below the 25th percentile, or vice versa. **OR**	2, 2 2, 1 3, 0

Exposure Level	Definition	Scores
	Local density is greater than the 75th percentile of all densities and regional density is between the 25th and 50th percentiles of all densities (or vice versa).	3, 1
High	Densities at both local and regional scales are above the 75th percentile. **OR** Local densities are greater than the 75th percentile and regional densities are between the 50th and 75th percentiles, or vice versa.	3, 3 3, 2

4.1.1.7 Aggregated Annual Exposure Scores

To understand the total exposure across the annual cycle for each species, seasonal scores were summed to obtain an annual score that ranged from 0–12. These annual scores were then mapped to exposure categories of Minimal (0–2), Low (3–5), Medium (6–8), and High (9–12). The annual exposure category for a species represents the seasonally integrated risk across the annual cycle.

Finally, because these scores are relative to seasonal distribution, estimates of count density were provided within the WTA and over the entire survey area for each species from the baseline survey data. Uncommon species with few detections in the WTA may be somewhat over-rated for exposure using this method, while common species with relatively few detections in the WTA may be effectively under-rated in terms of total exposure to the WTA. Density estimates (count per sq. km) are presented to provide context for the exposure scores.

4.1.1.8 Interpreting Exposure Scores

The final exposure scores for each species and season, as well as the aggregated annual scores, should be interpreted as a measure of the relative importance of the WTA for a species, as compared to other surveyed areas in the region and in the Northwest Atlantic. It does not indicate the absolute number of individuals likely to be exposed. Rather, the exposure score attempts to provide regional and population-level context for each species.

A High exposure score indicates that the observed and predicted densities of the species in the WTA were high relative to densities of that species in other surveyed areas. Conversely, a Low or Minimal exposure score means that the species was predicted to occur at lower densities in the WTA than in other locations. A Minimal exposure score should not be interpreted to mean there are no individuals of that species in the WTA. In fact, common species may receive a Minimal exposure score even if there are substantial numbers of individuals in the WTA, so long as their predicted densities *outside* the WTA are comparatively higher. The quantitative annual exposure score was then considered with additional species-specific information, along with expert opinion, to place each species within a final exposure category (described below in section 4.1.1.9).

4.1.1.9 *Exposure Categories*

The quantitative assessment of exposure (described above), other locally available data, existing literature, and species accounts were utilized to develop a final qualitative exposure determination. Final exposure level categories used in this assessment are described in Table 4-5 below.

Table 4-5: Assessment criteria used for assigning species to final exposure levels.

Final Exposure Level	Definition
Minimal	Minimal seasonal exposure scores in all seasons or Minimal score in all but one season. **OR** Based on the literature—and, if available, other locally available tracking or survey data—little to no evidence of use of the WTA or offshore environment for breeding, wintering, or staging, and low predicted use during migration.
Low	Low exposure scores in two or more seasons, or Medium exposure score in one season. **OR** Based on the literature—and, if available, other locally available tracking or survey data—low evidence of use of the WTA or offshore environment during any season.
Medium	Medium exposure scores in two or more seasons, or High exposure score in one season. **OR** Based on the literature—and, if available, other locally available tracking or survey data—moderate evidence of the WTA or use of the offshore environment during any season.
High	High exposure scores in two or more seasons. **OR** Based on the literature—and, if available, other locally available tracking or survey data—high evidence of use of the WTA or offshore environment, and the offshore environment is primary habitat during any season.

4.1.2 Vulnerability Framework

Researchers in Europe and the US have assessed the vulnerability of birds to offshore wind farms and general disturbance by combining ordinal scores across a range of key variables (Furness et al. 2013; Willmott et al. 2013; Wade et al. 2016; Kelsey et al. 2018; Fliessbach et al. 2019). The purpose of these indices was to prioritize species in environmental assessments (Desholm 2009), and provide a relative rank of vulnerability (Willmott et al. 2013). Importantly, past assessments and the one conducted here are intended to support decision-making by ranking the relative likelihood that a species will be sensitive to offshore wind farms but should not be interpreted as an absolute determination that there will or will not be collision mortality or habitat loss. Therefore, the results should be interpreted as a guide to species that have a higher likelihood of vulnerability.

The existing vulnerability methods assess individual-level vulnerability to collision and displacement independently and then incorporate population-level vulnerability to develop a final *species-specific* vulnerability score. These past efforts provide useful rankings across a region but are not designed to assess the vulnerability of birds to a particular wind farm or certain WTG designs. Collision risk models (e.g., Band 2012) do estimate site-specific mortality, but are substantially influenced by assumptions about avoidance rates (Chamberlain et al. 2006). Furthermore, collision risk models do not explicitly assess vulnerability to displacement (i.e., macro avoidance behaviors, leading to temporarily or permanently displacement from a wind farm area, which can cause effective habitat loss). Thus, there is a need to develop a *project-specific* vulnerability score for each species that is inclusive of both collision and displacement and has fewer assumptions.

The scoring process in this assessment builds from the existing methods, incorporates the specifications of the WTGs being considered by Atlantic Shores, utilizes local bird conservation status, and limits the vulnerability score to the species observed in the local surveys. The results from this scoring method may differ for some species from the qualitative determinations made in other Construction and Operations Plan (COP) assessments because the input parameters use specific categorical definitions that in some cases are conservative (e.g., > 40% macro-avoidance receives the highest score; see below and

Table 4-7). The literature is also used to interpret scoring results, and, if empirical studies indicate a lower or higher vulnerability, a range is added to the final score (see uncertainty discussion below). For species or species groups for which inputs are lacking, the literature is used to qualitatively determine a vulnerability ranking using the criteria in Table 4-6. Below is a description of the scoring approach.

Table 4-6: Assessment criteria used for assigning species to each behavioral vulnerability level.

Behavioral Vulnerability Level	Definition
Minimal	0–0.25 ranking for collision or displacement risk in vulnerability scoring. **OR** No evidence of collisions or displacement in the literature. Unlikely to fly within the rotor-swept zone (RSZ).
Low	0.26–0.5 ranking for collision or displacement risk in vulnerability scoring. **OR** Little evidence of collisions or displacement in the literature. Rarely flies within the RSZ.
Medium	0.51–0.75 ranking for collision or displacement risk in vulnerability scoring. **OR**

Behavioral Vulnerability Level	Definition
	Evidence of collisions or displacement in the literature. Occasionally flies within the RSZ.
High	0.76–1.0 ranking for collision or displacement risk in vulnerability scoring. **OR** Significant evidence of collisions or displacement in the literature. Regularly flies within the RSZ.

4.1.2.1 Population Vulnerability

Many factors contribute to how sensitive a population is to mortality or habitat loss related to the presence of a wind farm, including vital rates, existing population trends, and relative abundance of birds (Goodale and Stenhouse 2016). In this avian risk assessment, the relative abundance of birds is accounted for by the exposure analysis described above. The vulnerability assessment creates a population vulnerability (PV) score by using Partners in Flight (PiF) "continental combined score" (CCSmax), a local "state status" (SSmax), and adult survival score (AS; (Equation 1 below). Survival is included as an independent variable that is not accounted for in the CCSmax. This approach is based upon methods used by Kelsey et al. (2018) and Fliessbach et al. (2019).

Each factor included in this assessment (CCSmax, SSmax, and AS) is weighted equally and receives a categorical score of 1–5 (Table 4-7). The final population level vulnerability scores are rescaled to a 0–1 scale, divided into quartiles, and are then translated into four final vulnerability categories (Table 4-6). As using quartiles creates hard cut-off points and there is uncertainty present in all inputs (see discussion on uncertainty below), using scores alone can potentially misrepresent vulnerability (e.g., a 0.545 PV score leading to a ***minimal*** category). To account for this, the scores are considered along with information in existing literature. If there is evidence in the literature that conflicts with the vulnerability score, then the score will be appropriately adjusted (up or down) according to documented empirical evidence. For example, if a PV score was assessed as ***low***, but a paper indicated an increasing population, the score would be adjusted up to include a range of ***minimal–low***.

$$PV = CCSmax + SSmax + AS \qquad \textit{Equation 1}$$

Specifics for each factor in PV are as follows:

- *CCSmax* is included in scoring because it integrates various factors PiF used to indicate global population health. It represents the maximum value for breeding and non-breeding birds developed by PiF, and combines the scores for population size, distribution, global threat status, and population trend (Panjabi et al. 2019). The CCSmax score from PiF was rescaled to a 1–5 scale to achieve consistent scoring among factors.

- *SSmax* is included in scoring to account for local conservation status, which is not included in the CCSmax. Local conservation status is generally determined independently by states and accounts for the local population size, population trends, and stressors on a species within a particular state. It was developed following methods by (Adams et al. 2016) in which the state conservation status for the relevant adjacent states is placed within five categories (1 = no ranking to 5 = endangered), and then, for each species, the maximum state ranking is selected.

- *AS* is included in the scoring because species with higher adult survival rates are more sensitive to increases in adult mortality because they tend to be species that are also long-lived and have low annual reproductive success (e.g., K strategists) (Desholm 2009; Adams et al. 2016). The five categories are based upon those used in several vulnerability assessments (Willmott et al. 2013; Kelsey et al. 2018; Fliessbach et al. 2019), and the species-specific values were used from (Willmott et al. 2013).

Table 4-7: Data sources and scoring of factors used in the vulnerability assessment.

Vulnerability Component	Factor	Definition and Source	Scoring
Population Vulnerability (PV)	continental combined score *(CCSmax)*	CCSmax is Partners in Flight continental combined score: pif.birdconservancy.org/ACAD/Database.aspx.	1 = Minor population sensitivity 2 = Low population sensitivity 3 = Medium population sensitivity 4 = High population sensitivity 5 = Very-High population sensitivity
	state status *(SSmax)*	SSmax from New Jersey from Adams et al. (2016).	1 = No Ranking[1] 2 = State/Federal Special Concern 3 = State/Federal Threatened 4 = State/Federal Endangered 5 = State & Federal End and/or Thr

Vulnerability Component	Factor	Definition and Source	Scoring
	adult survival (AS)	AS score: scores and categories taken from Willmott et al. (2013).	1 = <0.75 2 = 0.75 to 0.80 3 = >0.80 to 0.85 4 = >0.85 to 0.90 5 = >0.90
Collision Vulnerability (CV)	*rotor swept zone (RSZt)*	WTG specific percentage of flight heights in RSZ. Flight heights modeled from Northwest Atlantic Seabird Catalog. Categories from Kelsey et al. (2018).	1 = < 5% in RSZ 3 = 5–20% in RSZ 5 = > 20% in RSZ
	macro-avoidance (MAc)	Avoidance rates and scoring categories from Willmott et al. (2013) and Kelsey et al. (2018).	1 = >40% avoidance 2 = 30 to 40% avoidance 3 = 18 to 29% avoidance 4 = 6 to 17% avoidance 5 = 0 to 5% avoidance
	Nocturnal Flight Activity (NFA); Diurnal Flight Activity (DFA).	NFA scores were taken from Willmot et al. (2013); DFA was calculated using NJDEP boat-based survey data that records behavior including if birds are sitting or flying.	1 = 0–20% 2 = 21–40% 3 = 41–60% 4 = 61–80% 5 = 81–100%
Displacement Vulnerability (DV)	*MAd*	Macro-avoidance rates (MAd) that would decrease collision risk from Willmott et al. (2013) and Kelsey et al. (2018).	1 = 0–5% avoidance 2 = 6–17% avoidance 3 = 18–29% avoidance 4 = 30–40% avoidance 5 = > 40% avoidance
	Habitat flexibility (HF)	The degree to which a species is considered a habitat generalist (i.e., can forage in a variety of habitats) or a specialist (i.e., requires specific habitat and prey type). HF score and categories taken from Willmott et al. (2013).	0 = species does not forage in the Atlantic Outer Continental Shelf 1 = species uses a wide range of habitats over a large area and usually has a wide range of prey available to them 2 to 4 = grades of behavior between scores 1 and 5 5 = species with habitat- and prey-specific requirements that do not have much flexibility in diving-depth or choice of prey species

[1] Note actual definitions for state conservation ranking may be adjusted to follow individual state language.

4.1.2.2 Collision Vulnerability

Collision vulnerability (CV) assessments can include a variety of factors including nocturnal flight activity, diurnal flight activity, avoidance, proportion of time within the RSZ, maneuverability in flight, and percentage of time flying (Furness et al. 2013; Willmott et al. 2013; Kelsey et al. 2018). The assessment process conducted here follows Kelsey et al. (2018) and includes proportion of time within the RSZ (RSZt), a measure of avoidance (MAc), and flight activity (NFA and DFA; Equation 2 below). Each factor was weighted equally and given a categorical score of 1–5 (Table 4-7). The final collision vulnerability scores were rescaled to a 0–1 scale, divided into quartiles, and then translated into four final vulnerability categories (Table 4-6). As described in the PV section, the score is then considered along with information available in existing literature; if there is sufficient evidence to deviate from the quantitative score, a CV categorical range is assigned for each species.

$$CV = RSZt + MAc + (NFA + DFA)/2 \qquad \text{Equation 2}$$

Specifics for each factor in CV are as follows:

- RSZt is included in the score to account for the probability that a bird may fly through the RSZ. Flight height data was selected from the Northwest Atlantic Seabird Catalog and included NJDEP boat-based surveys. Flight heights calculated from digital aerial survey methods were excluded because the methods have not been validated (Thaxter et al. 2015) and the standard flight height data used in European collision assessments (Masden 2019) is modeled primarily from boat-based survey (Johnston et al. 2014). Three additional boat-based datasets were excluded because there was low confidence in the data (collected by citizen science efforts, less standardized, and of lower quality) or estimated flight heights only included part of the air space below 300 m (984 ft).

Many of the boat-based datasets provided flight heights as categorical ranges for which the mid-value of the range in meters were determined, as well as the lower and upper bounds of the category. Upper bounds that were given as greater than X m (or ft) were capped at 300 m (984 ft) to estimate upper bounds. A few datasets provided exact flight height estimates which resulted in upper and lower ranges being the same as the mid-value. A total of 100 randomized datasets were generated per species using the uniform distribution to select possible flight height values between lower and upper flight height bounds. Similar to methods from Johnston et al. (2014), flight heights were modeled using a smooth spline of the square root of the binned counts in 10-m (32-ft) bins. The integration of the smooth spline model count within each 1 m (3 ft) increment was calculated and the mean and standard deviation of all 100 models were calculated across all 1 m (3 ft) increments. The proportion of animals within each RSZ was estimated by summing the 1 m (3 ft) count integrations and dividing by the total estimate count of animals across all RSZ zones, then values were converted to a 1–5 scale based upon the categories used by Kelsey et al. (2018; see Table 4-7). The RSZ was defined by minimum and maximum WTG options being considered for WTA (two different power unit ranges at two different tower heights; Table 4-8). The analysis was conducted in R Version 3.5.3.[10] Of note, there are several important uncertainties in flight height estimates: flight heights from boats can be skewed low; flight heights are generally recorded during daylight and in fair weather; and flight heights may change when WTGs are present.

Table 4-8: WTG specifications used in the vulnerability analysis; mean Lower Low Water (MLLW) is the average height of the lowest tide recorded at a tide station each day during the recording period.

WTG Parameter	Project Design Options	
	Minimum	Maximum
Maximum tip height (MLLW)	891.3 ft (271.68 m)	1,048.8 ft (319.68 m)
Maximum hub height (MLLW)	497.6 ft (151.68 m)	576.4 ft (175.68 m)
Maximum rotor diameter	787.4 ft (240 m)	918.6 ft (280 m)
Minimum tip clearance/air gap (MLLW)	78.0 ft (23.78 m)	78.0 ft (23.78 m)
Maximum blade chord	19.7 ft (6 m)	32.8 ft (10 m)
Maximum tower diameter	26.2 ft (8 m)	32.8 ft (10 m)

- MAc is included in the score to account for macro-avoidance rates that would decrease collision risk. Macro-avoidance is defined as a bird's ability to change course to avoid the entire wind farm area (Kelsey et al. 2018), versus meso-avoidance (avoiding individual WTGs), and micro-avoidance (avoiding WTG blades; Skov et al. 2018). The scores used in the assessment were based on Willmott et al. (2013), who conducted a literature review to determine known macro-avoidance rates and then converted them to a 1–5 score based upon the categories in Table 4-7. The MAc indicates that this factor is used in the CV versus the MAd, which was used in the displacement vulnerability (DV) score (described below). For the assessment conducted here, Willmott et al. (2013) avoidance rates were updated to reflect the most recent empirical studies (Krijgsveld et al. 2011; Cook et al. 2012; Vanermen et al. 2015; Cook et al. 2018), and indexes (Garthe and Hüppop 2004; Furness et al. 2013; Bradbury et al. 2014; Adams et al. 2016; Wade et al. 2016; Kelsey et al. 2018). For the empirical studies, the average avoidance was used when a range was provided in a paper. For the indices, the scores were converted to a continuous value using the median of a scores range; only one value was entered for related indices (e.g., Adams et al. 2016 and Kelsey et al. 2018). When multiple values were available for a species, the mean value was calculated. For some species, averaging

[10] R Core Team (2019). R: A language and environment for statistical computing. R Foundation for Statistical Computing, Vienna, Austria. URL https://www.R-project.org/

the avoidance rates across both the empirical studies and indices led to some studies being counted multiple times. Indices were included to capture how the authors interpreted the avoidance studies and determined avoidance rates for species where data was not available. There are several important uncertainties in determining avoidances rates: the studies were all conducted in Europe; the studies were conducted at wind farms with WTGs smaller than are proposed for the WTA; the methods used to record avoidance rates varied and included surveys, radar, and observers; the analytical methods used to estimate avoidance rates also varied significantly between studies; and the avoidance rate for species where empirical data is not available were assumed to be similar to closely-related species.

- NFA and DFA include scores of estimate percentage of time spent flying at night and during the day based upon the assumption that more time spent flying would increase collision risk. The NFA scores were taken directly from the scores, based upon literature review, from Willmott et al. (2013). The DFA score were calculated from the baseline survey data that categorized if a bird was sitting or flying for each bird observation. Per Kelsey et al. (2018), the NFA and DFA scores were equally weighted and averaged.

4.1.2.3 Displacement Vulnerability

Rankings of DV account for two factors: (1) disturbance from ship/helicopter traffic and the wind farm structures (MAd), and (2) habitat flexibility (HF; Furness et al. 2013; Kelsey et al. 2018). This assessment combines these two factors, weights them equally, and categorizes them from 1–5 (Equation 3 below; Table 4-6). It is worth noting that while Furness et al. (2013) down-weighted the DV score by dividing by 10 (they assumed displacement would have lower impacts on the population), the assessment conducted here maintains the two scores on the same scale. Empirical studies indicate that for some species, particularly sea ducks, avoidance behavior may change through time and that several years after projects have been built some individuals may forage within the wind farm. The taxonomic specific text indicates whether there is evidence that displacement may be partially temporary. The final displacement vulnerability scores are rescaled to a 0–1 scale, divided into quartiles, and translated into four final vulnerability categories (Table 4-7). As described in the PV section, the score is then considered along with the literature; if there is sufficient evidence to deviate from the quantitative score, a DV categorical range is assigned for each species.

$$DV = MAd + HF \qquad \textit{Equation 3}$$

Specifics for each factor in DV are as follows:

- *MAd* is included to account for behavioral responses from birds that lead to macro-avoidance of wind farms, and that have the potential to cause effective habitat loss if the birds are permanently displaced (Fox et al. 2006). The MAd scores used in the assessment were based on Willmott et al. (2013), but updated to reflect the most recent empirical studies (Krijgsveld et al. 2011; Cook et al. 2012; Vanermen et al. 2015; Cook et al. 2018; Skov et al. 2018), and indexes (Garthe and Hüppop 2004; Furness et al. 2013; Bradbury et al. 2014; Adams et al. 2016; Wade et al. 2016; Kelsey et al. 2018). See MAc above for further details. The scores are the same as the MAc scores described above, but, following methods from Kelsey et al. (2018), are inverted so that a high avoidance rate (greater than 40%) is scored as a 5. Since the greater than 40% cutoff is a low threshold, many species can receive a high 5 score; there is a large range within this high category that includes species documented to have moderate avoidance rates (e.g., terns) and species with near complete avoidance (e.g., loons).

- *HF* accounts for the degree to which a species is considered a habitat generalist (i.e., can forage in a variety of habitats) or a specialist (i.e., requires specific habitat and prey type). The assumption is that generalists are less likely to be affected by displacement, whereas specialists are more likely to be affected (Kelsey et al. 2018). The values for HF used in this assessment were taken from Willmott et al. (2013). Note that Willmott et al. (2013) used a 1–5 scale plus a "0" to indicate that a species does not forage in the OCS.

4.1.3 Uncertainty

Uncertainty is recognized in this assessment for both exposure and vulnerability. Given the natural variability of ecosystems and recognized knowledge gaps, assessing how anthropogenic actions will affect the environment inherently involves a degree of uncertainty (Walker et al. 2003). Broadly defined, uncertainty is incomplete information about a subject (Masden et al. 2015) or a deviation from absolute determinism (Walker et al. 2003). In the risk assessment conducted here, uncertainty is broadly recognized as a factor in the process, and is accounted for by including, based upon the best available data, a range for the exposure, vulnerability, and population scores when appropriate.

For offshore wind avian assessments, uncertainty primarily arises from two sources: predictions of bird use of a project area and region (i.e., exposure); and our understanding of how birds interact with WTGs (i.e., vulnerability). While uncertainty will always be present in any assessment of offshore wind and acquiring data on bird movements during hours of darkness and in poor weather is difficult, overall knowledge on bird use of the marine environment has improved substantially in recent years through local survey efforts, revised regional modeling efforts, and individual tracking studies. For many species, multiple data sources may be available to make an exposure assessment, such as survey and individual tracking data. If the data sources show differing patterns in use of the wind farm area, then a range of exposure is provided (e.g., minimal–low) to account for all available data and to capture knowledge gaps and general uncertainty about bird movements.

Similarly, knowledge has been increasing on the vulnerability of birds to offshore wind facilities in Europe (e.g., Skov et al. 2018). Vulnerability assessments have either incorporated uncertainty into the scoring process to calculate a range of ranks (Willmott et al. 2013; Kelsey et al. 2018), or have developed separate standalone tables (Wade et al. 2016). In order to keep the scoring process as simple as possible, this assessment does not directly include uncertainty in the scoring, rather it uses the uncertainty assessment conducted by Wade et al. (2016) as a reference (Table **4-9**) and references all available literature. Like exposure, if there is evidence in the literature, or from other data sources, that conflicts with the vulnerability score, the score will be adjusted up or down, as appropriate, to include a range that extends into the next category. This approach accounts for knowledge gaps and general uncertainty about vulnerability.

Table 4-9: Vulnerability uncertainty from Wade et al. (2016).

[illegible]	Uncertainty Level: % of time at altitudes overlapping with turbine blades	[illegible]	Uncertainty Level: Displacement caused by structures	[illegible]	Uncertainty Level: Displacement caused by vessels and/or helicopters	[illegible]	Uncertainty Level Use of tidal races	[illegible]	[illegible]
European storm-petrel	Very high	1	Very high	1	High	2	Very high	1	5
Leach's storm-petrel	Very high	1	Very high	1	High	2	Very high	1	5
Sooty shearwater	Very high	1	Very high	1	High	2	Very high	1	S
Arctic skua	Moderate	3	Very high	1	Very high	1	Very high	1	6
Common goldeneye	Very high	1	Very high	1	High	2	High	2	6
Greater scaup	Very high	1	Very high	1	High	2	High	2	6
Manx shearwater	High	2	Very high	1	High	2	Very high	1	6
Slavonian grebe	Very high	1	High	2	High	2	Very high	1	6
White-tailed eagle	Very high	1	High	2	High	2	Very high	1	6
Great-crested grebe	High	2	High	2	High	2	Very high	1	7
Long-tailed duck	Very high	1	High	2	High	2	High	2	7
Roseate tern	Very high	1	High	2	High	2	High	2	7
Great skua	Moderate	3	High	2	High	2	Very high	1	8
Little tern	Very high	1	Moderate	3	Very high	1	Moderate	3	8
Velvet seater	High	2	Very high	1	Moderate	3	High	2	8
Black-headed gull	Moderate	3	Moderate	3	High	2	Very high	1	9
Northern fulmar	Low	4	High	2	High	2	Very high	1	9
Arctic tern	Moderate	3	Moderate	3	High	2	High	2	10
Great northern diver	High	2	High	2	Very high	1	Very low	5	10
Little auk	Very high	1	Low	4	Low	4	Very high	1	10
Black-throated diver	High	2	Moderate	3	High	2	Low	4	11
Common gull	Low	4	Low	4	High	2	Very high	1	11
Common eider	Moderate	3	Moderate	3	Moderate	3	Moderate	3	12
Sandwich tern	Low	4	Low	4	High	2	High	2	12
Black guillemot	Very high	1	High	2	Very low	5	Very low	5	13
European shag	High	2	Low	4	High	2	Very low	5	13
Great black-backed gull	Low	4	Very low	S	Moderate	3	Very high	1	13
Great cormorant	Moderate	3	Very low	S	High	2	Moderate	3	13
Black-legged kittiwake	Very low	5	Very low	5	High	2	High	2	14
Common tern	Very low	5	Low	4	High	2	Moderate	3	14
Herring gull	Very low	5	Very low	5	Moderate	3	Very high	1	14
Lesser black-backed gull	Very low	5	Very low	5	Moderate	3	Very high	1	14
Northern gannet	Very low	5	Very low	5	High	2	High	2	14
Red-throated diver	Low	4	Low	4	High	2	Low	4	14
Common seater	Low	4	Very low	5	Low	4	High	2	15
Atlantic puffin	Moderate	3	Moderate	3	Very low	5	Very low	5	16
Razorbill	Low	4	Very low	5	Very low	5	Low	4	18
Common guillemot	Low	4	Very low	5	Very low	5	Very low	5	19

5 Birds – Offshore: Results

Interpretation of the results are presented in the body of the COP (Volume II, Section 4.3). The results provided below are organized by sections addressing exposure and vulnerability of coastal birds and marine birds separately and include maps, tables, and figures for each species or species group. ESA-listed and candidate species are assessed individually.

5.1 Coastal birds

The following section presents results of the coastal bird exposure assessment. Exposure assessment maps, tables, and figures are presented based on numerous references and data sets, including, but not limited to, the APEM digital aerial surveys, NJDEP boat-based surveys, Northwest Atlantic Seabird Catalog data, occurrence data, individual tracking data, relevant literature, and species accounts. Since there is a diversity of data sources, a variety of data analysis methods are used that all support exposure and vulnerability assessments. For coastal birds, the relative behavioral vulnerability assessment is discussed in the body of the COP (Volume II, Section 4.3) and is primarily based upon the literature and expert opinion.

5.1.1 Shorebirds

5.1.1.1 Maps

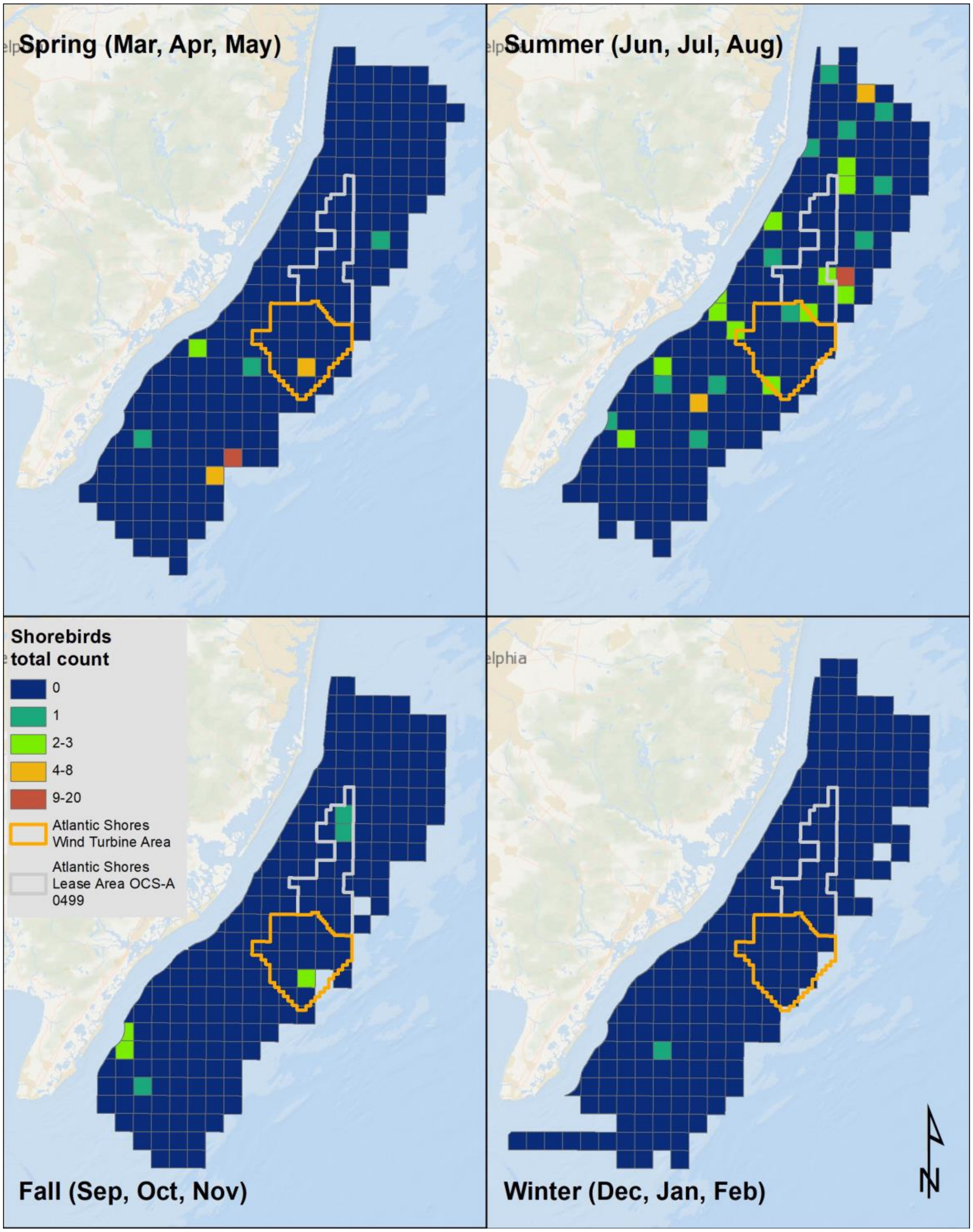

Figure 5-1: Shorebirds observed in the NJDEP boat-based surveys, by season.

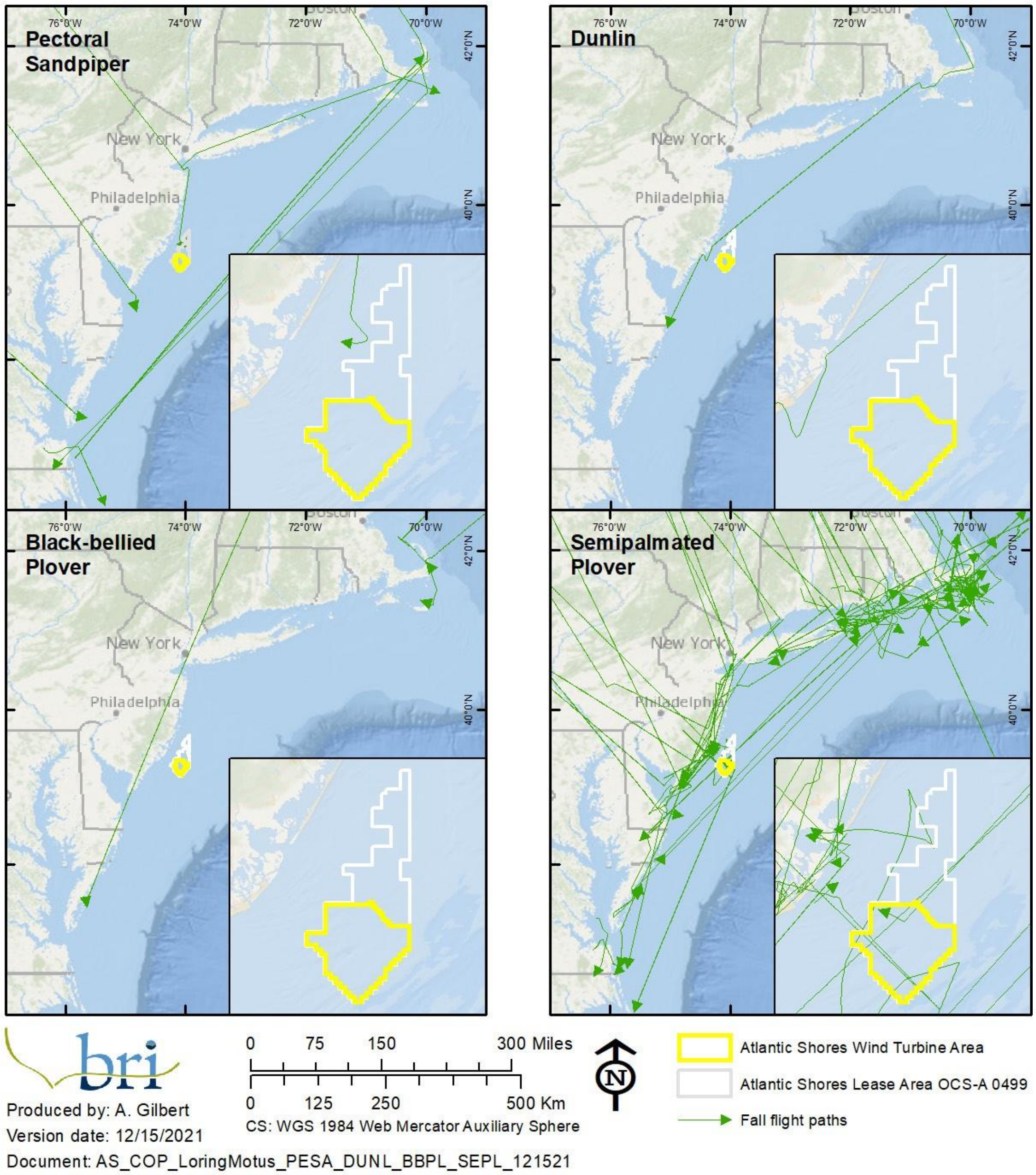

Pectoral Sandpiper
Dunlin
Black-bellied Plover
Semipalmated Plover
New York
Philadelphia
76°0'W
74°0'W
72°0'W
70°0'W
42°0'N
40°0'N
0 75 150 300 Miles
0 125 250 500 Km
CS: WGS 1984 Web Mercator Auxiliary Sphere
N
Atlantic Shores Wind Turbine Area
Atlantic Shores Lease Area OCS-A 0499
Fall flight paths
Produced by: A. Gilbert
Version date: 12/15/2021
Document: AS_COP_LoringMotus_PESA_DUNL_BBPL_SEPL_121521

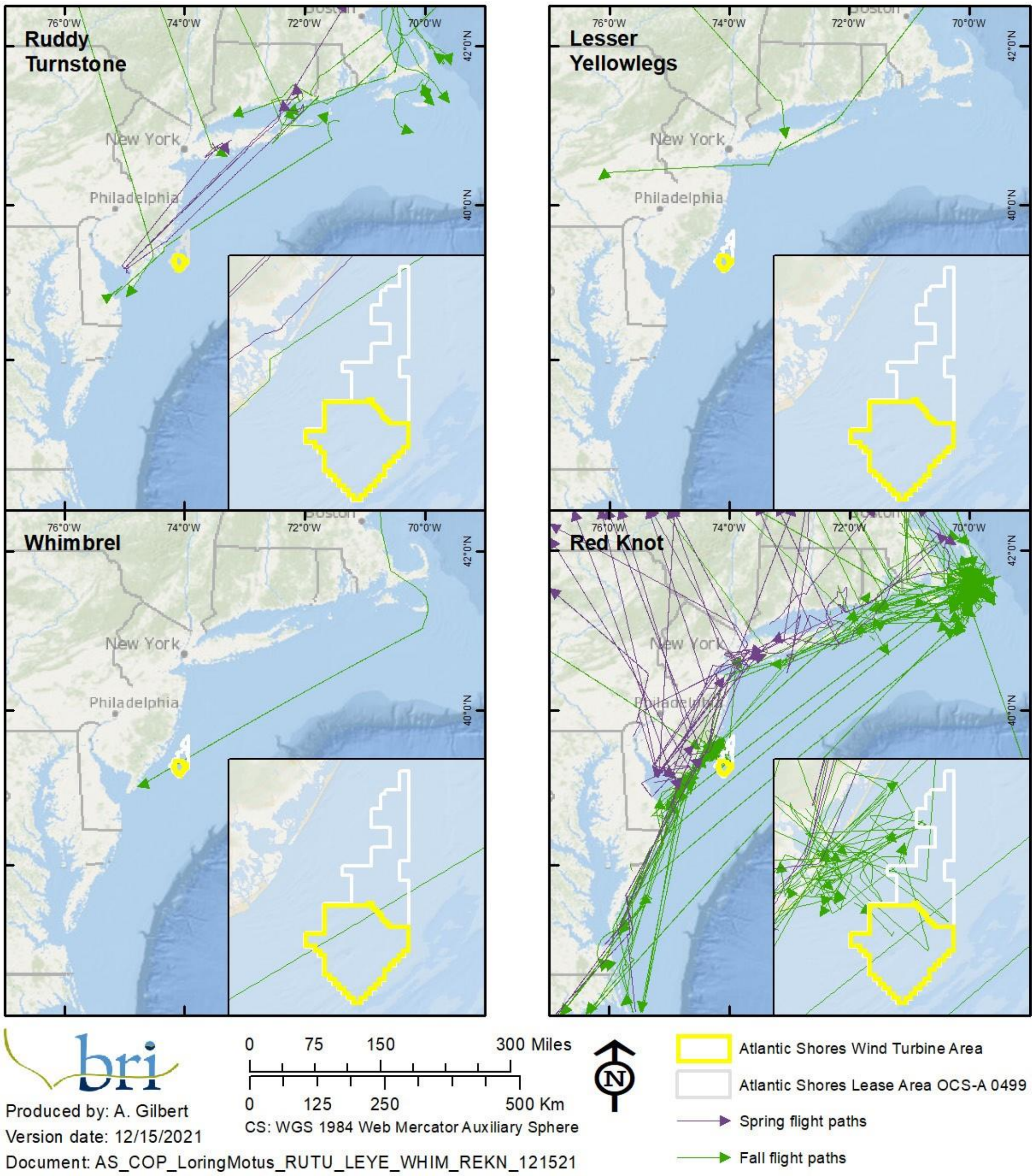
Ruddy Turnstone
Lesser Yellowlegs
Whimbrel
Red Knot
New York
Philadelphia
76°0'W
74°0'W
72°0'W
70°0'W
42°0'N
40°0'N
Produced by: A. Gilbert
Version date: 12/15/2021
Document: AS_COP_LoringMotus_RUTU_LEYE_WHIM_REKN_121521
0 75 150 300 Miles
0 125 250 500 Km
CS: WGS 1984 Web Mercator Auxiliary Sphere
N
Atlantic Shores Wind Turbine Area
Atlantic Shores Lease Area OCS-A 0499
Spring flight paths
Fall flight paths

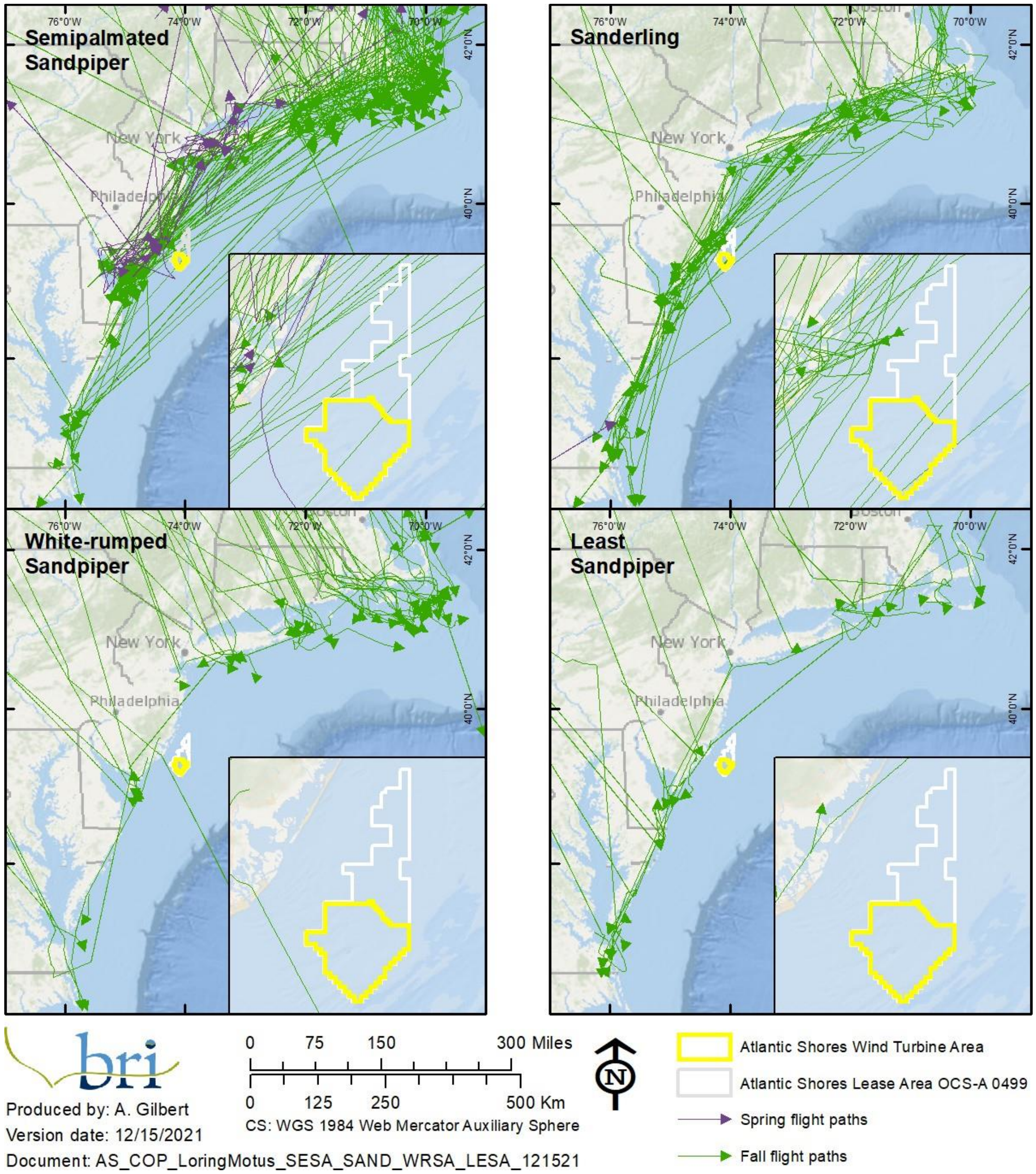

NOTE: All data are not actual flight paths but interpolated (model generated) flight paths. Flight paths were modeled by detections of movements between land-based towers. Towers had a typical detection range <15 km, so birds were only detected when flying within approximately 15 km of one of the towers. (See Fig. 5 (tower locations) in Loring et al. [2019] and Appendix K (detection probability) for details. Appendices are found at: https://espis.boem.gov/final%20reports/BOEM_2019-018a.pdf. Data provided by USFWS and used with permission.

Figure 5-2: Modeled flight paths of migratory shorebirds equipped with nanotags (Loring et al. 2020).

5.1.2 Endangered Shorebird Species

5.1.2.1 Piping Plover

5.1.2.1.1 Maps

Page left intentionally blank

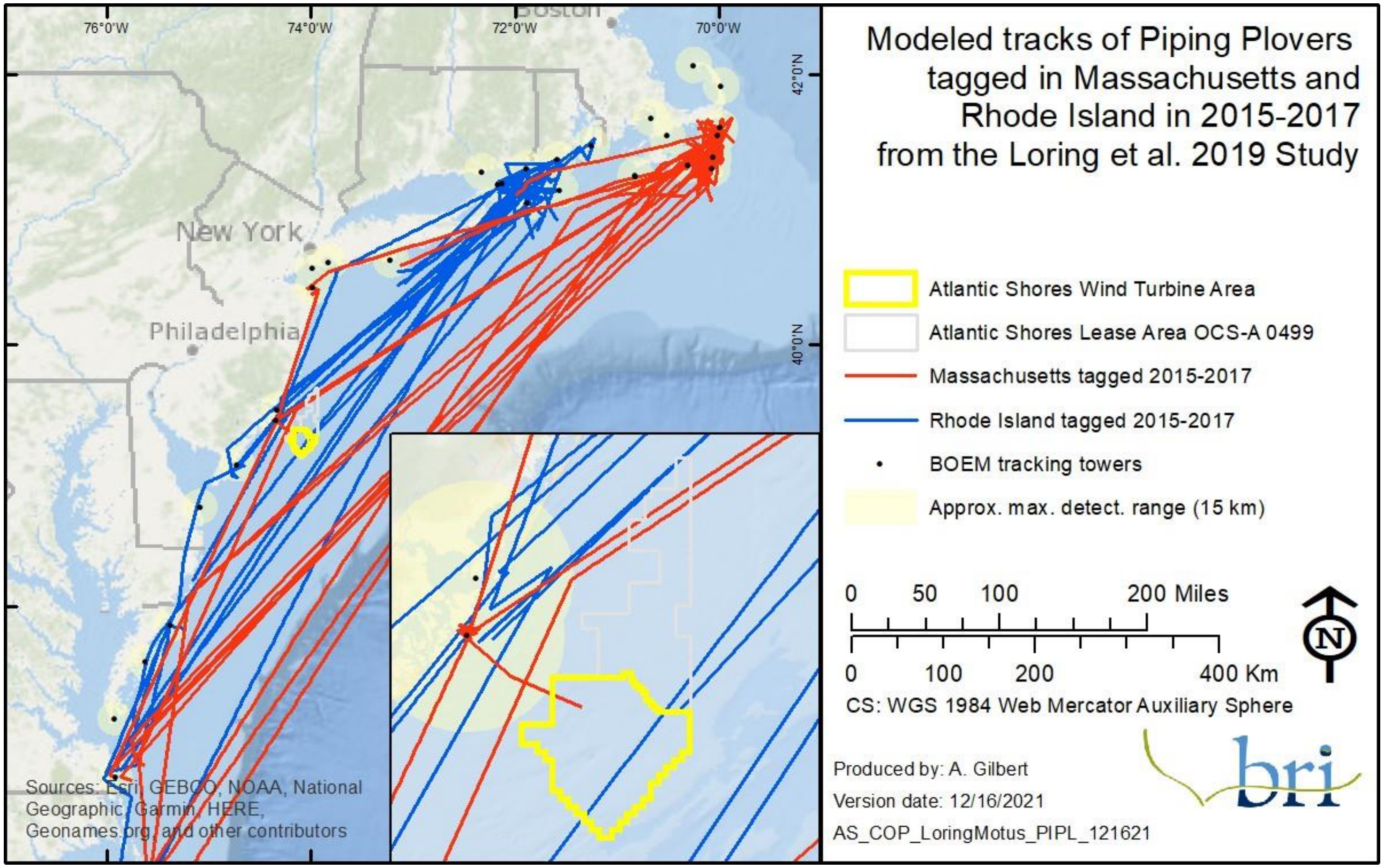

NOTE: All data are not actual flight paths but interpolated (model generated) flight paths. Flight paths were modeled by detections of movements between land-based towers. Towers had a typical detection range < 15 km, so birds were only detected when flying within approximately 15 km of one of the towers. (See Fig 5 [tower locations] in Loring et al. [2019] and Appendix K [detection probability] for details). Appendices are found at: https://espis.boem.gov/final%20reports/BOEM_2019-017a.pdf. Data provided by USFWS and used with permission.

Figure 5-3: Modeled flight paths of migratory Piping Plovers equipped with nanotags (Loring et al. 2019).

Red Knot

5.1.2.1.2 Maps

Page left intentionally blank

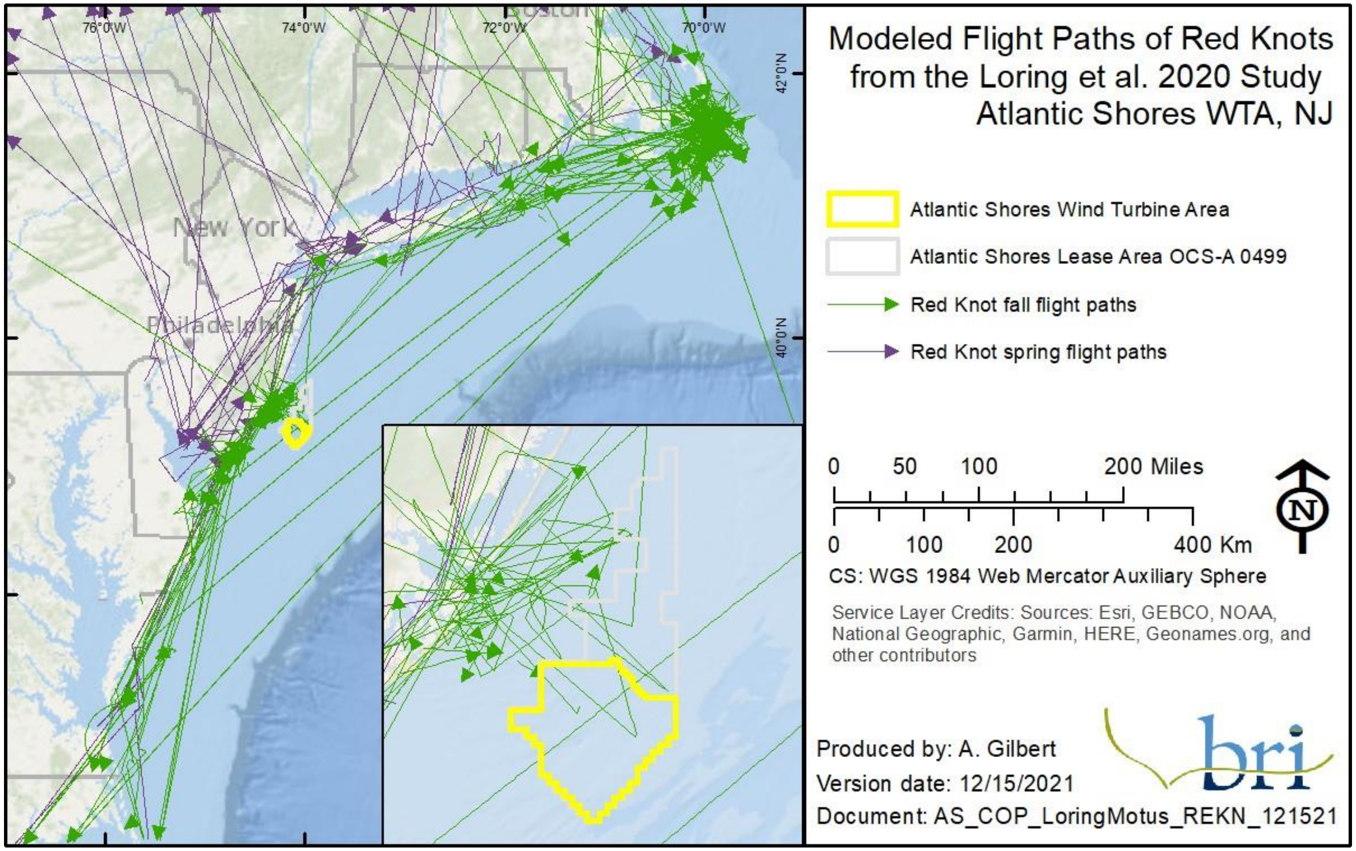

NOTE: All data are not actual flight paths but interpolated (model generated) flight paths. Flight paths were modeled by detections of movements between land-based towers. Towers had a typical detection range < 15 km, so birds were only detected when flying within approximately 15 km of one of the towers. (See Fig 5 [tower locations] in Loring et al. [2019] and Appendix K [detection probability] for details). Appendices are found at: https://espis.boem.gov/final%20reports/BOEM_2019-017a.pdf. Data provided by USFWS and used with permission.

Figure 5-4: Modeled flight paths of migratory Red Knots equipped with nanotags (Loring et al. 2020).

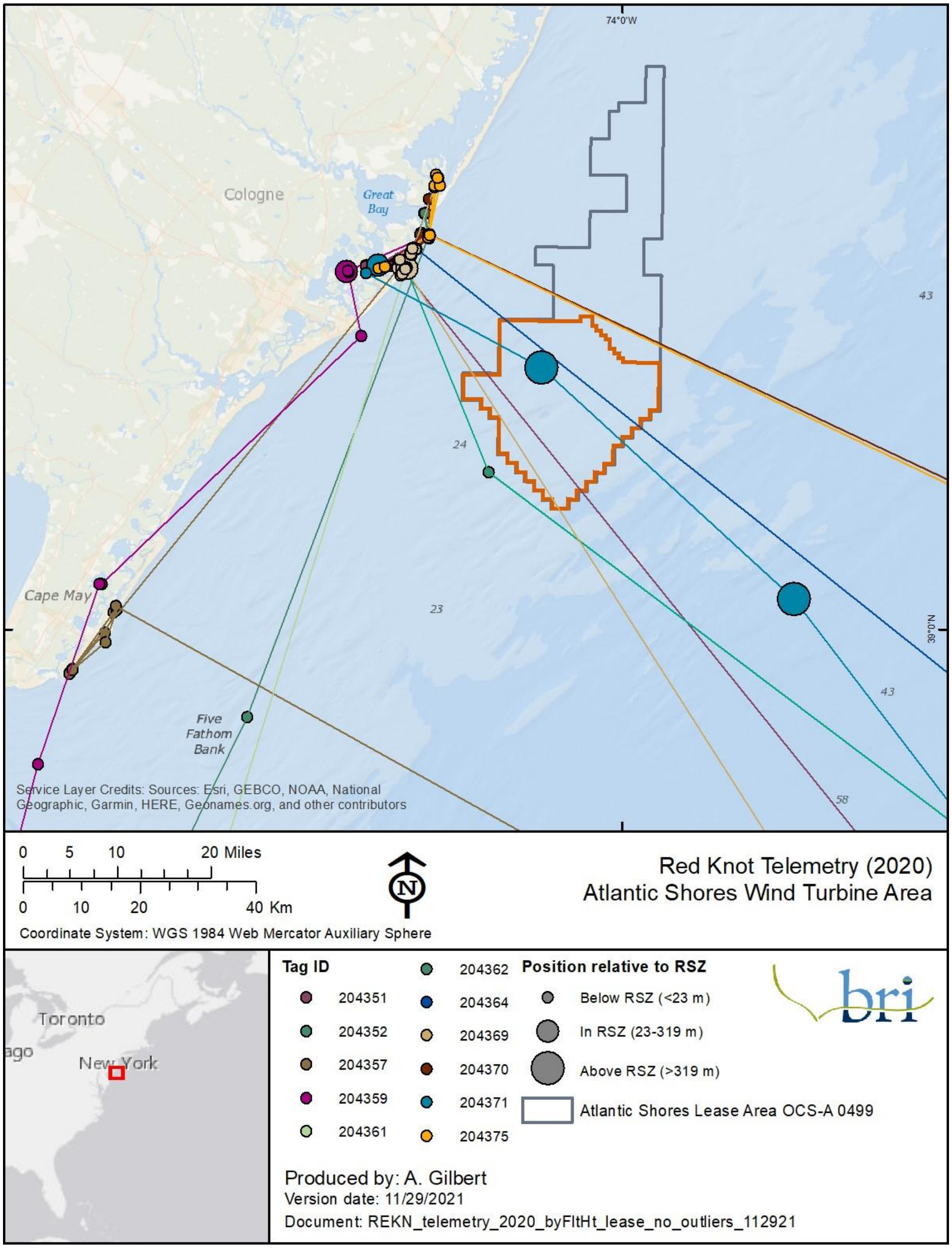

NOTE: All data points are connected by straight lines, and each point for which there is altitudinal data is assigned to a flight height category (below, within, or above the anticipated RSZ) indicated by point size. Further details provided in Appendix II_F3.

Figure 5-5: Movements of 11 Red Knots tagged at Brigantine, NJ, in 2020, as they depart on migration.

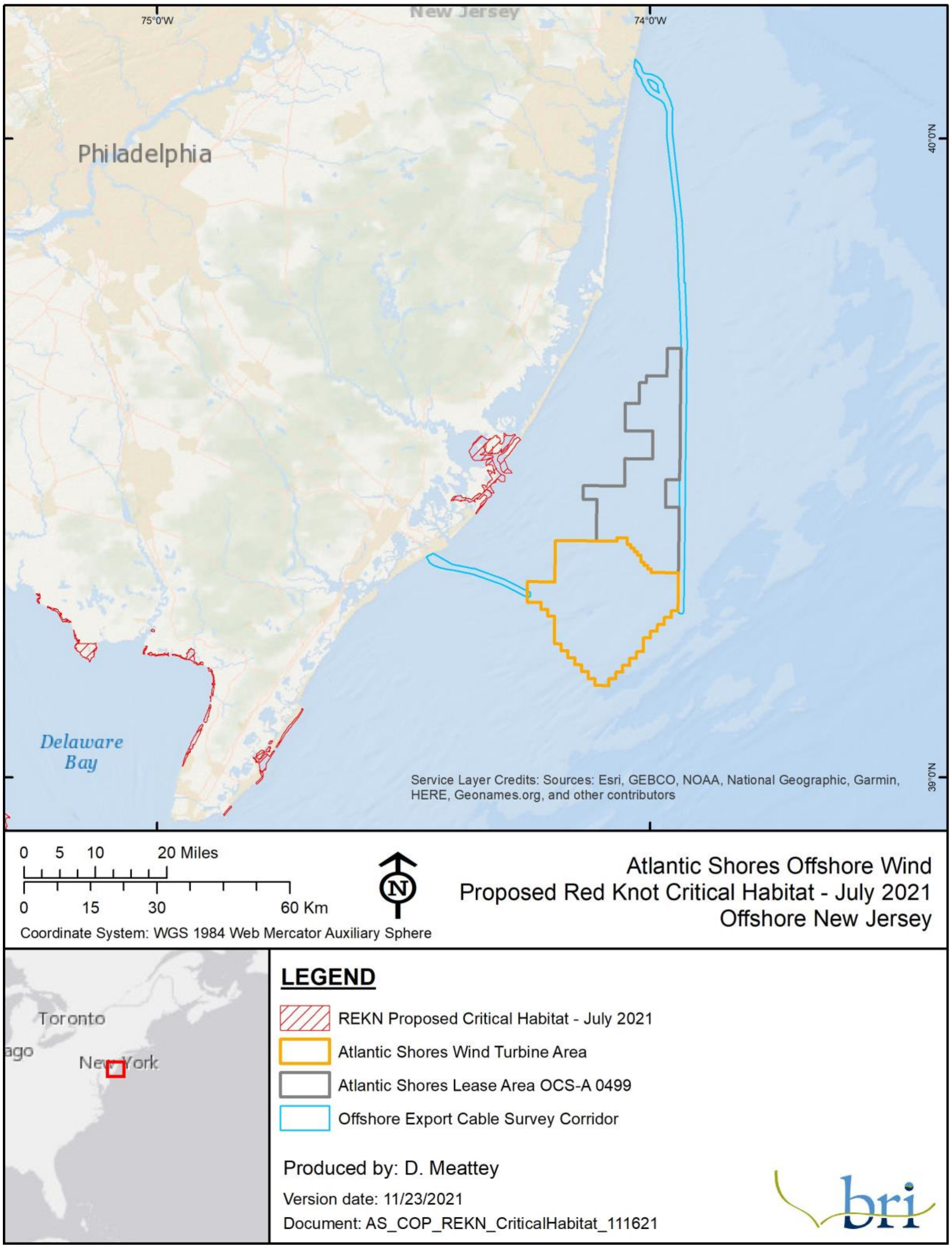

Figure 5-6: Proposed Critical Habitat for Red Knots in New Jersey. Data provided by USFWS, and used with permission.

5.1.3 Coastal Waterbirds (waterfowl)

5.1.3.1 Maps

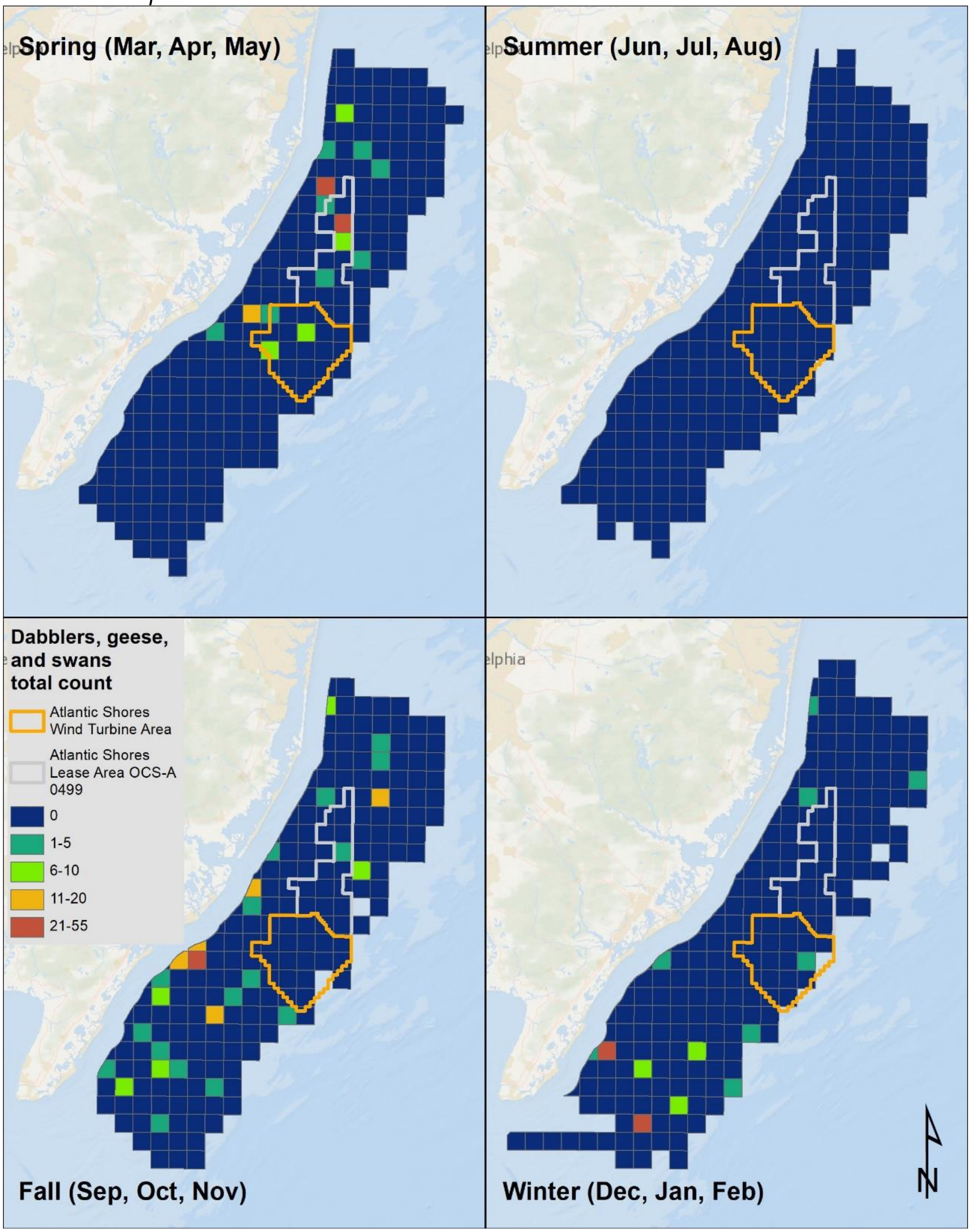

Figure 5-7: Coastal dabbling ducks, geese, and swans observed in the NJDEP boat-based surveys, by season.

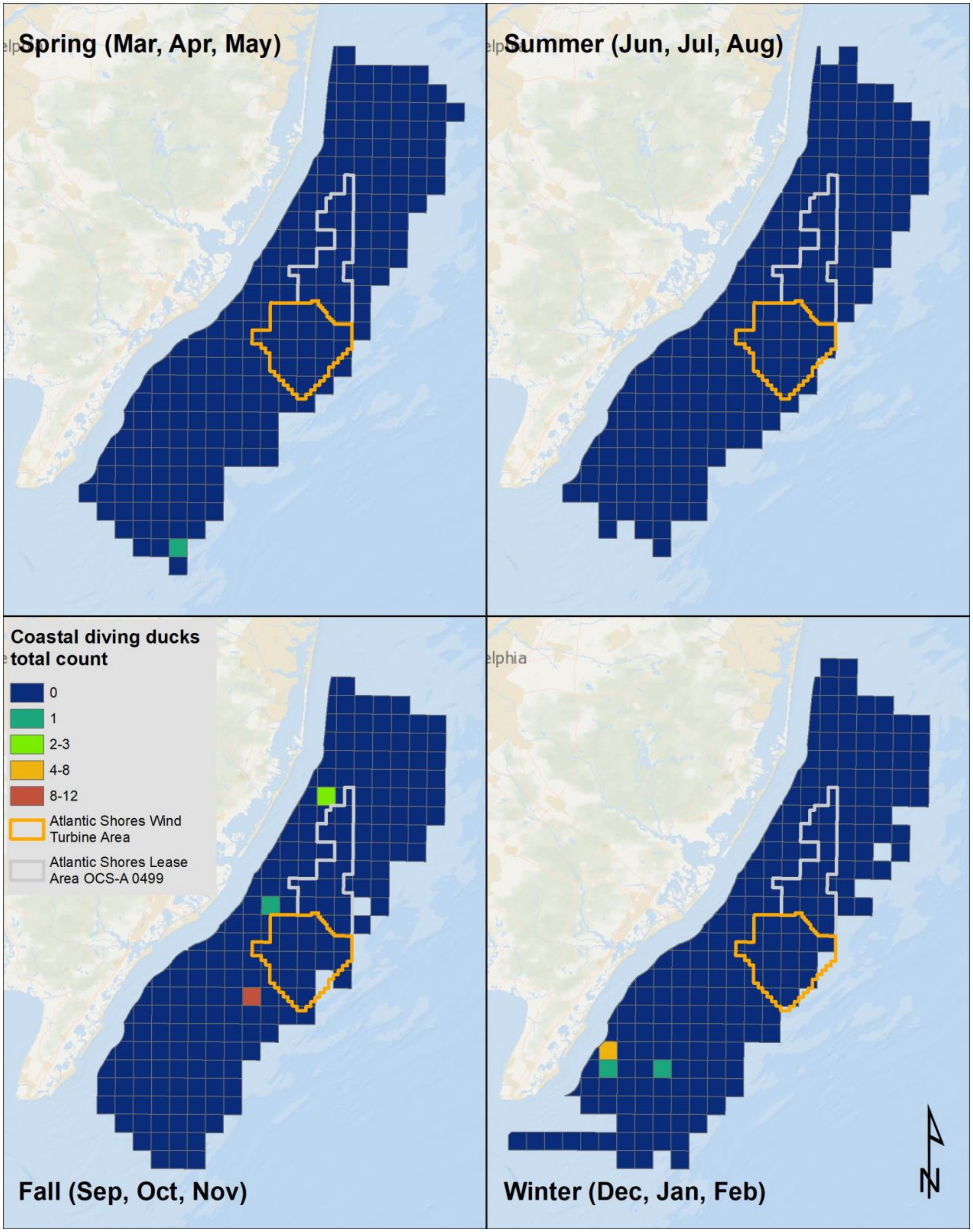

Figure 5-8: Coastal diving ducks observed in the NJDEP boat-based surveys, by season.

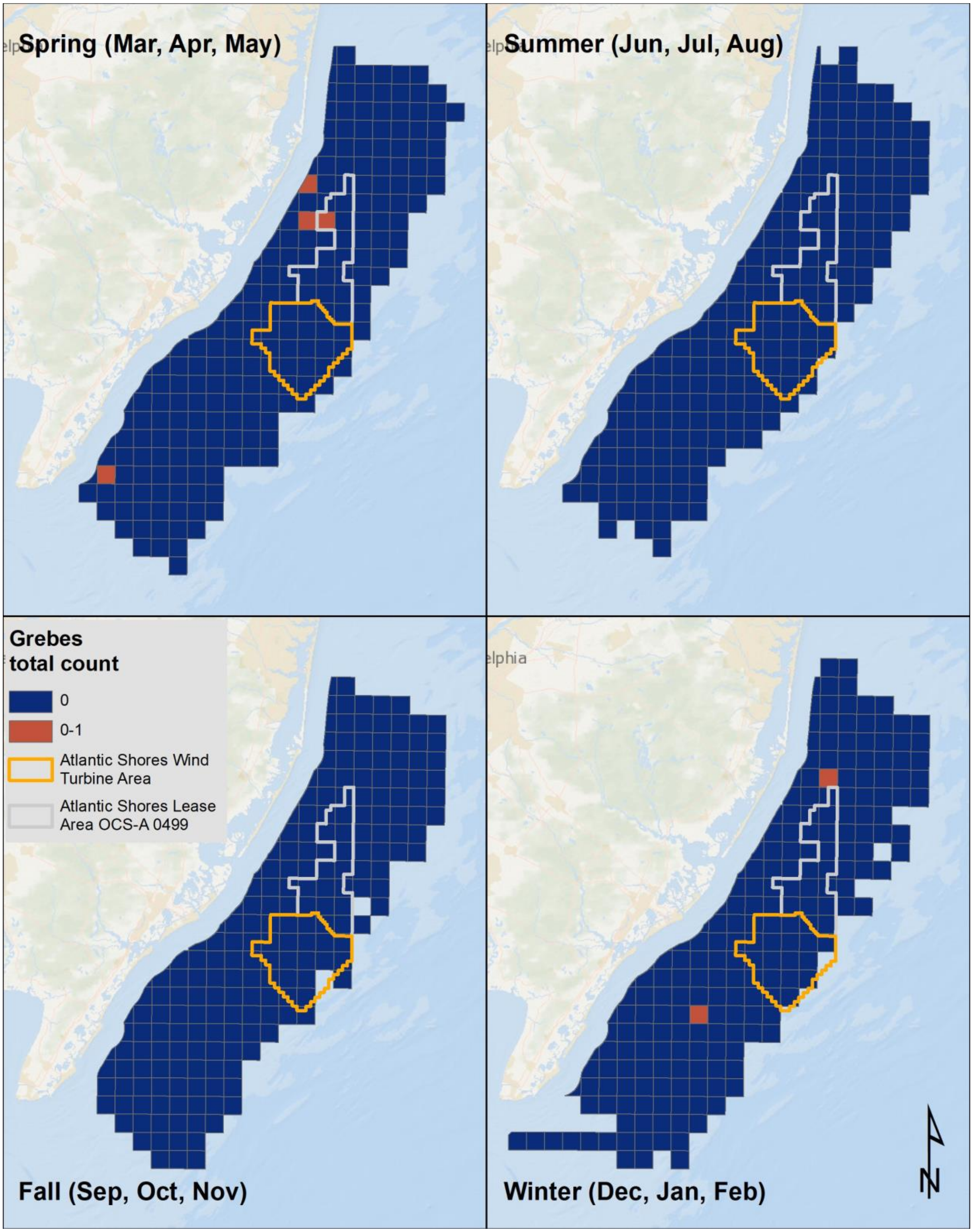

Figure 5-9: Grebes observed in the NJDEP boat-based surveys, by season.

5.1.4 Wading Birds

5.1.4.1 Maps and Figures

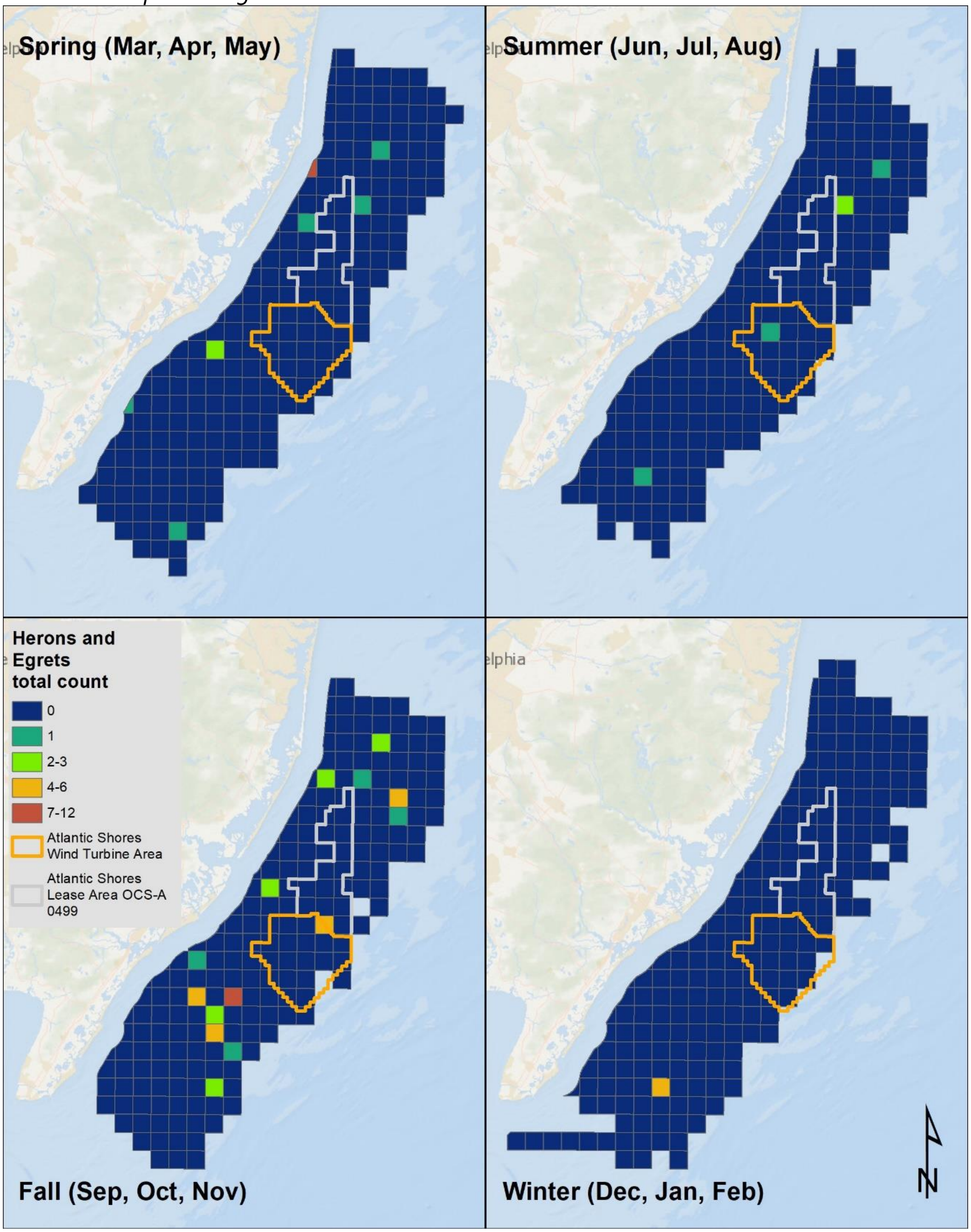

Figure 5-10: Herons and egrets observed in the NJDEP boat-based surveys, by season.

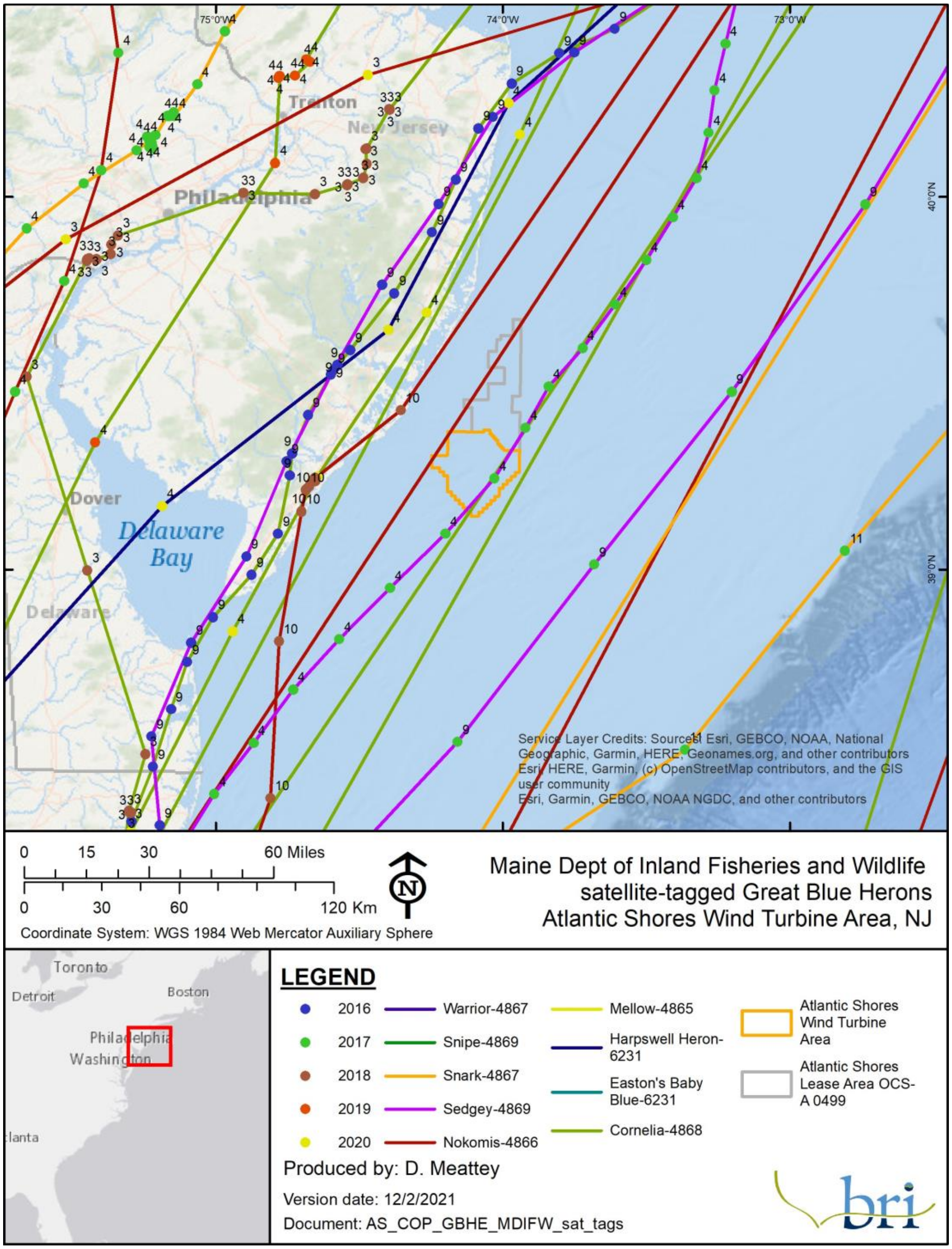

Figure 5-11: Track lines of Great Blue Herons captured in Maine and equipped with satellite transmitters provided by Maine Department of Inland Fisheries and Wildlife.

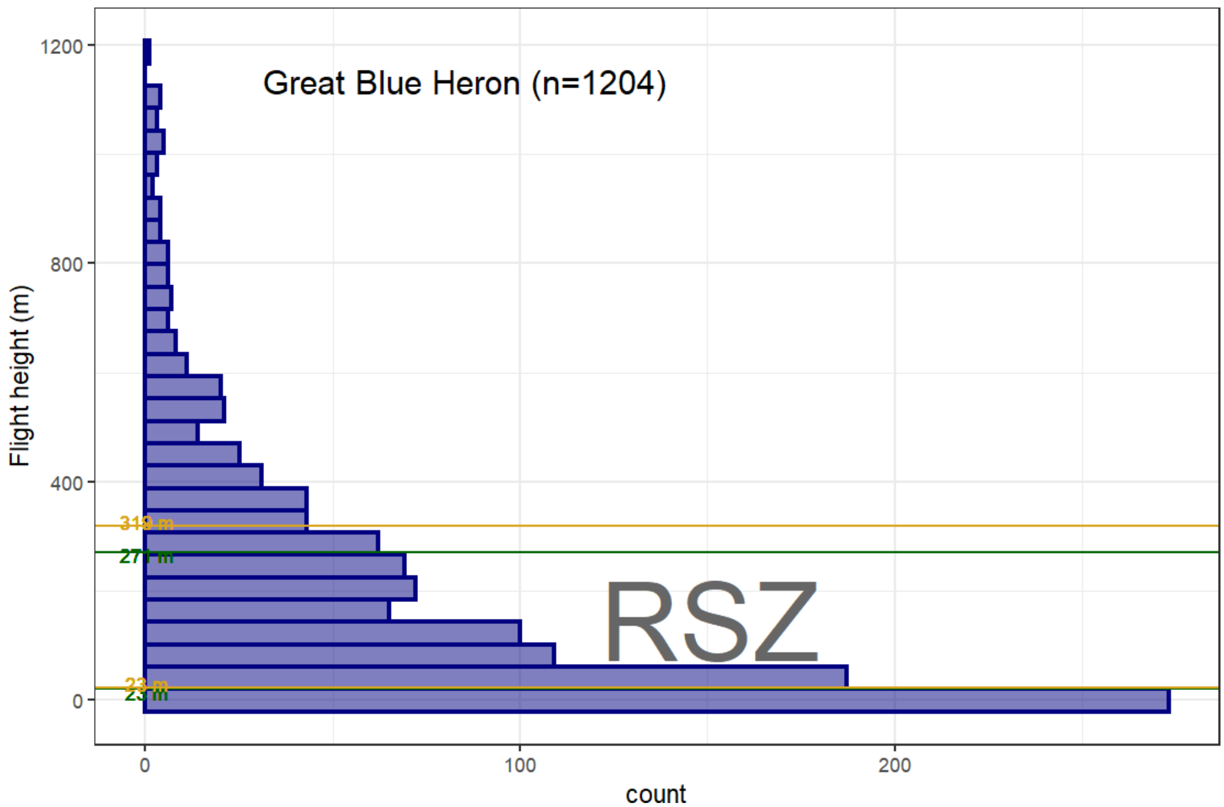

Figure 5-12: Flight heights (m) of Great Blue Herons satellite-tagged in Maine, flying over the Atlantic OCS, in relation to the upper and lower limits of the RSZ for a minimum (green: 23-271 m [75-889 ft]) and maximum WTG (gold: 23-319 m [75-1,046 ft]).

5.1.5 Raptors

5.1.5.1 Maps

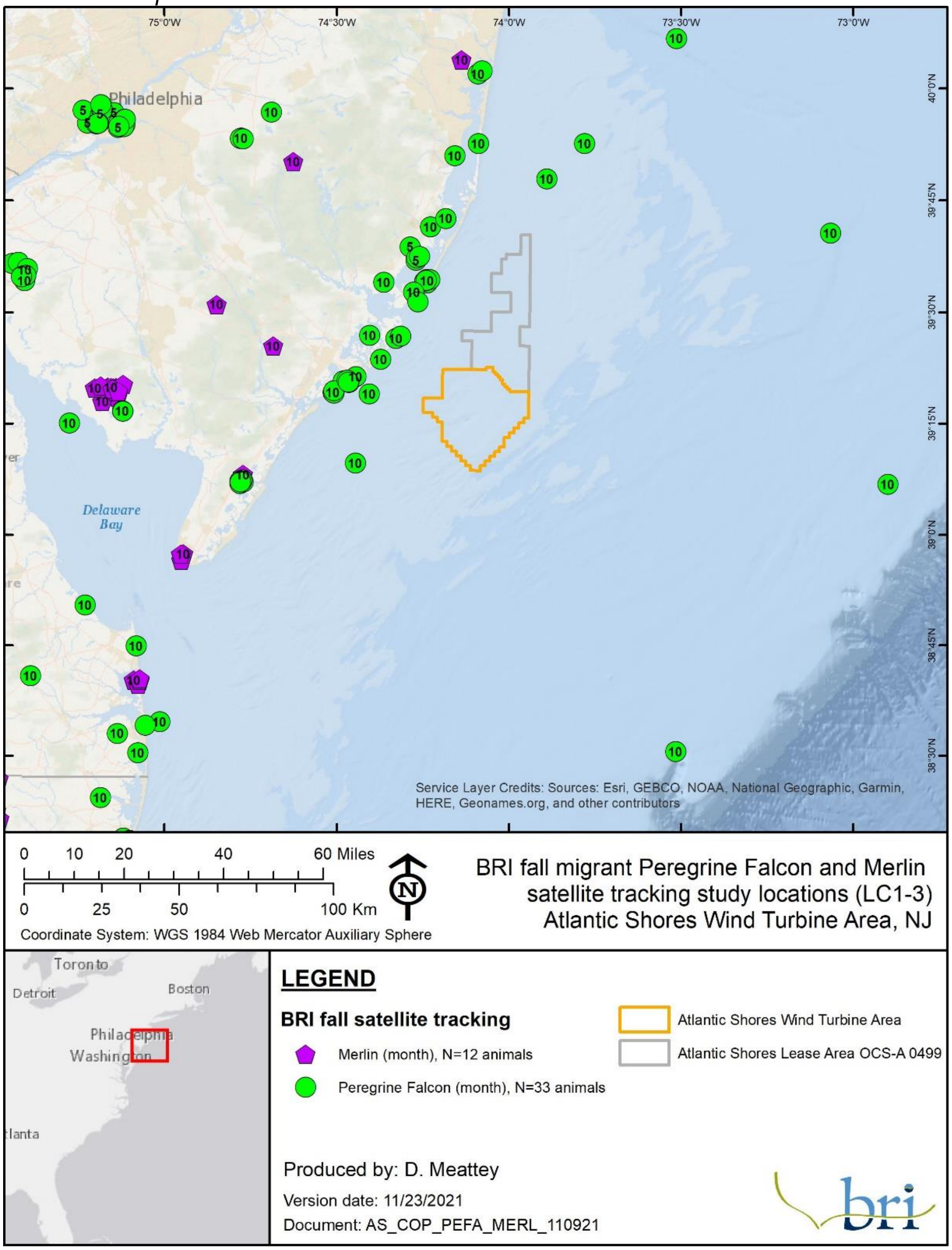

Figure 5-13: Location estimates from satellite transmitters on Peregrine Falcons and Merlins tracked from three raptor research stations along the Atlantic coast, 2010–2018 (DeSorbo, Persico, et al. 2018).

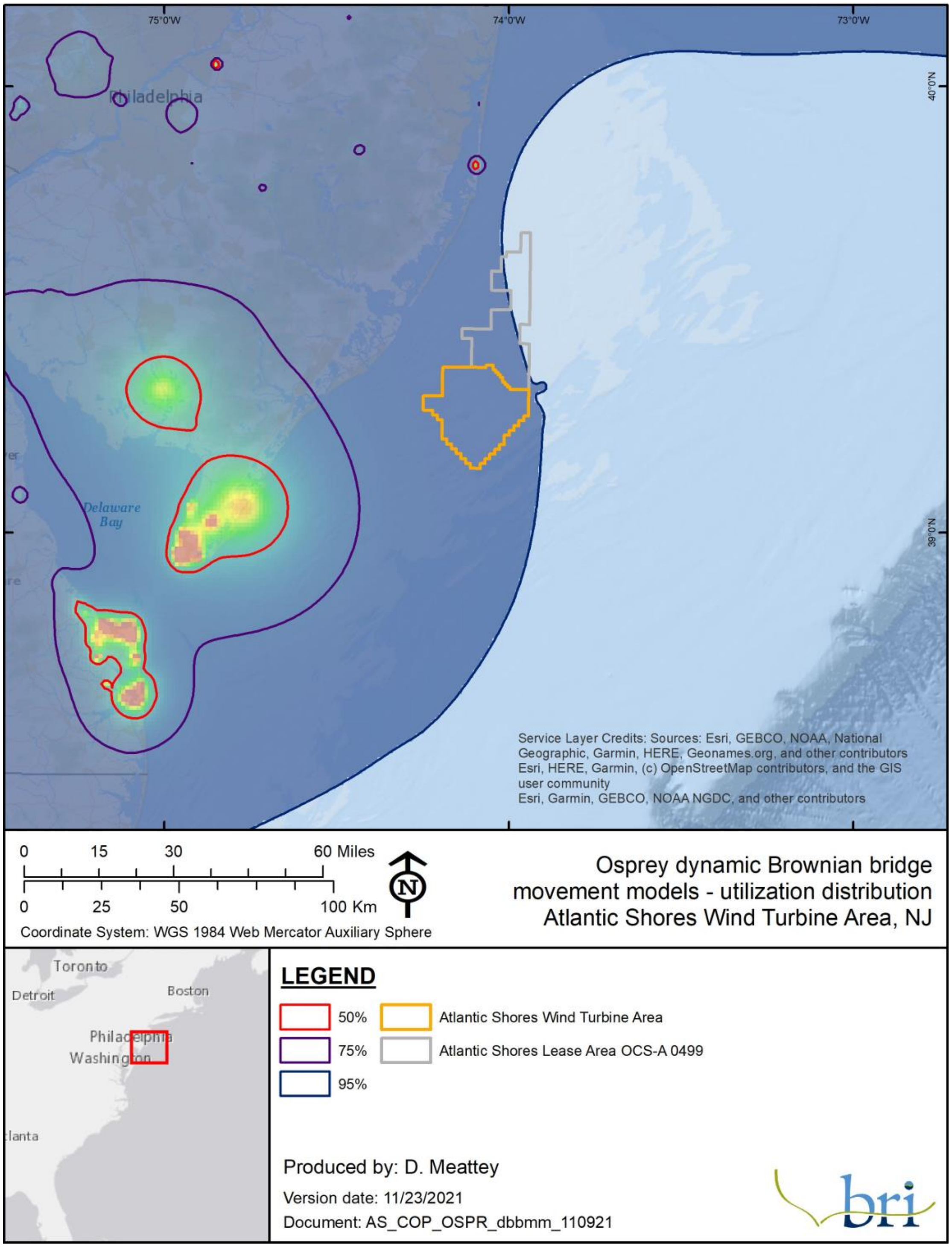

NOTE: The contours represent the percentage of the use area across the UD surface and represent various levels of use from 50% (core use) to 95% (home range).

Figure 5-14: Dynamic Brownian bridge movement models for Osprey (n=127) that were tracked with satellite transmitters.

5.1.6 Songbirds

Maps

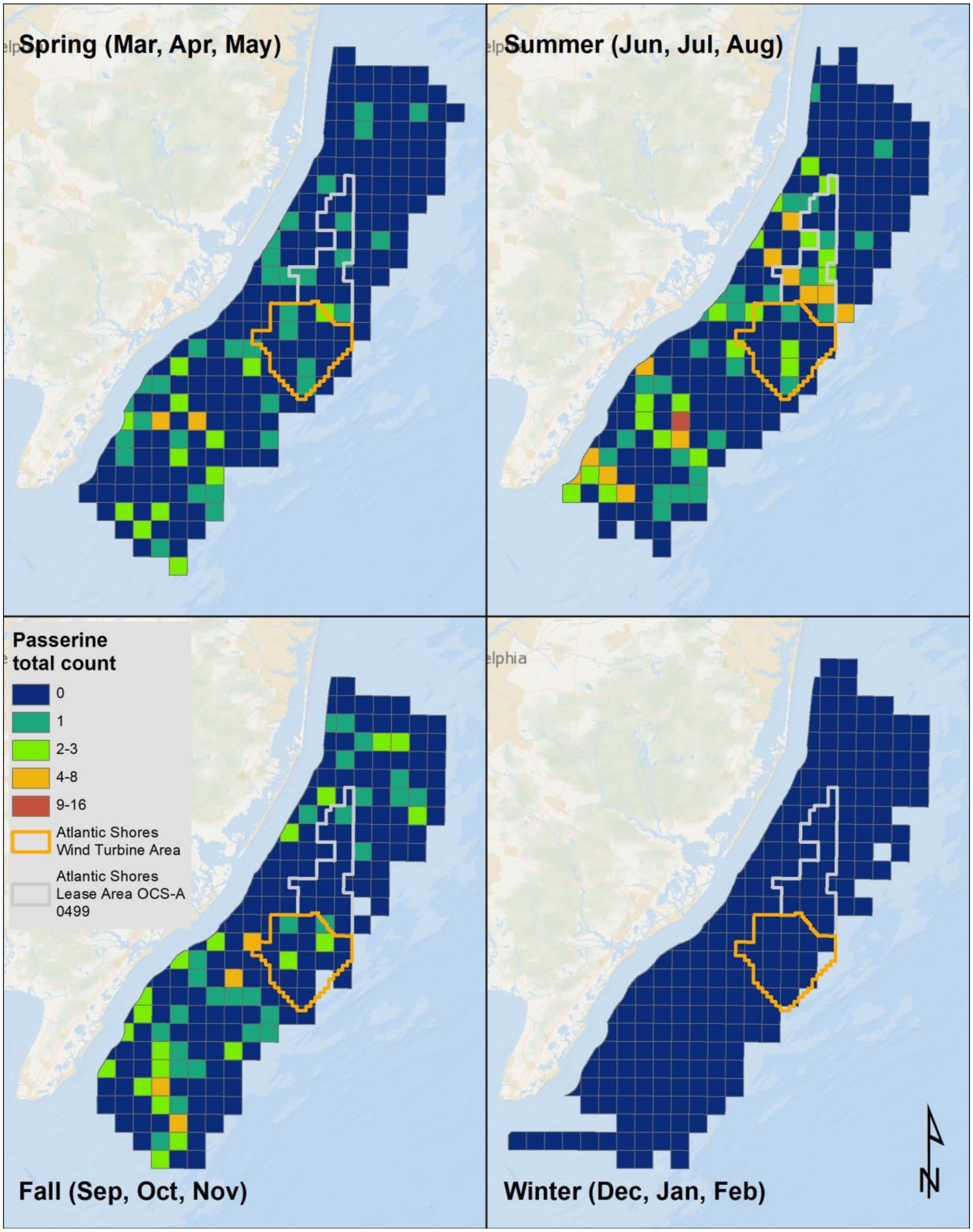

Figure 5-15: Songbirds (Passerines) observed in the NJDEP boat-based surveys, by season.

5.2 Marine birds

The following section presents results of marine bird exposure and vulnerability assessments. Marine birds were assessed by species within each major taxonomic group (Table 5-1), which included loons, sea ducks, petrels and allies, gannets and allies, gulls and allies, terns, and auks. Exposure assessment maps, tables, and figures are presented based on numerous references and data sets including, but not limited to, the APEM digital aerial surveys (Figure 4-1), NJDEP boat-based surveys (Figure 4-3), NOAA MDAT models (Figure 2-2), occurrence data, individual tracking data, relevant literature, and species accounts.

There are noticeable differences in the mean densities of animals detected within the WTA when comparing values from NJDEP boat-based surveys to the modeled APEM digital aerial surveys. A number of factors come into play that each contribute to these observed differences: temporal variation, platform (boat vs. aerial), and analysis. Species-specific density estimates are affected differently by each of these factors.

Temporal variability (seasonal and annual differences) in species density are prevalent, which is why surveys are ideally conducted for multiple seasons and over several years (Camphuysen et al. 2004). The NJDEP boat-based surveys were conducted in 2008–2009 (2+ years), while digital aerial surveys were conducted in 2020–2021 (1 year). Temporal differences can be explained by variation in tides, weather patterns, prey distribution, population differences, timing of survey (i.e., when during the day or even month), and other factors (Camphuysen et al. 2004; Bolduc and Fifield 2017). These factors do not affect species the same, thus, temporal differences may be important (to a greater or lesser degree) in explaining differences between the two surveys, depending on the species.

In the sections below, a relative behavioral vulnerability assessment, including flight height data relative to proposed WTG parameters, is presented for each species. Flight heights are presented at the taxonomic level for brevity, though species-specific flight heights are accounted for in each vulnerability assessment. Flight heights used in the assessment were gathered from datasets in the Northwest Atlantic Seabird Catalog including the NJDEP boat-based surveys.

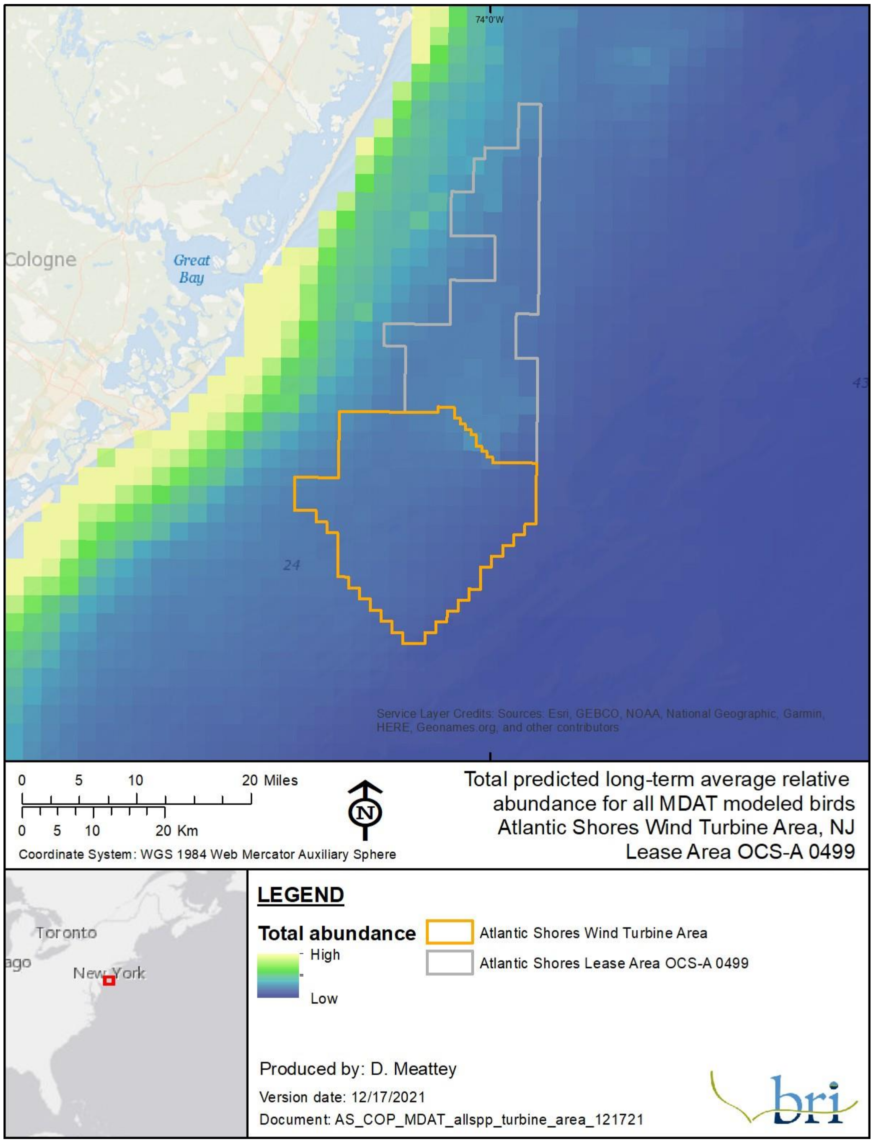

NOTE: For all avian species together, the total relative abundance maps are calculated by stacking each individual species' predicted annual long-term average relative density layers and summing the values of the cells. The result is the total predicted long-term average relative abundance of all individuals (of the included species in the group) in that cell. It is important to note these products represent and reflect relative abundance, not predicted absolute abundance. This caveat is based on the properties of the base layer products being aggregated – the base layer avian products do not predict absolute abundance. In addition, individual species base layers were normalized to their mean prior to summation. This type of group product informs where areas of higher abundances of groups of species may be found relative to other areas (paraphrased from Curtice *et al.* 2019).

Figure 5-16: Bird abundance estimates (all species) from the MDAT avian models. Data provided by NOAA and used with permission.

Table 5-1: Mean annual naive densities (uncorrected count/km^2 of survey transect) within the Atlantic Shores WTA and the NJDEP boat-based survey area on the Atlantic OCS.

Species	Mean relative density (total count/sq. km) in Atlantic Shores WTA	Mean relative density (total count/sq. km) in NJDEP OCS survey area
Sea ducks		
Common Eider	0	0.001
Surf Scoter	0.165	0.461
White-winged Scoter	0	0.038
Black Scoter	0.006	0.274
Long-tailed Duck	0	0.083
Red-breasted Merganser	0.006	0.004
Unidentified scoter	0.148	0.086
Unidentified diving/sea duck	0	0
Loons		
Red-throated Loon	0.129	0.228
Common Loon	0.536	0.485
Unidentified loon	0.01	0.002
Shearwaters and Petrels		
Wilson's Storm-Petrel	0.155	0.496
Leach's Storm-Petrel	0	0
Northern Fulmar	0	0.001
Cory's Shearwater	0.05	0.043
Sooty Shearwater	0.006	0.002
Great Shearwater	0.001	0.005
Manx Shearwater	0	0.001
Audubon's Shearwater	0.001	0
Unidentified shearwater	0.001	0
Unidentified storm-petrel	0	0.001
Gannet		
Northern Gannet	0.454	1.597
Cormorants and Pelicans		
Double-crested Cormorant	0.003	0.19
Great Cormorant	0	0.001
Brown Pelican	0.001	0.001
Unidentified cormorant	0	0
Gulls and Jaegers		
Pomarine Jaeger	0	0
Parasitic Jaeger	0.003	0.004
Black-legged Kittiwake	0.035	0.027
Sabine's Gull	0	0.001
Bonaparte's Gull	0.12	0.125
Little Gull	0	0
Laughing Gull	0.272	0.572
Ring-billed Gull	0.008	0.015
Herring Gull	0.308	0.554
Iceland Gull	0	0
Lesser Black-backed Gull	0	0.001
Great Black-backed Gull	0.144	0.288

Species	Mean relative density (total count/sq. km) in Atlantic Shores WTA	Mean relative density (total count/sq. km) in NJDEP OCS survey area
Unidentified small gull	0.016	0.002
Unidentified jaeger	0	0
Unidentified large gull	0.004	0.021
Terns		
Least Tern	0	0.002
Caspian Tern	0	0
Black Tern	0.001	0.001
Common Tern	0.149	0.272
Forster's Tern	0.01	0.073
Royal Tern	0.004	0.02
Unidentified small gull/tern	0	0
Unidentified small tern	0.024	0.023
Unidentified large tern	0	0
Auks		
Dovekie	0.011	0.019
Common Murre	0.008	0.006
Thick-billed Murre	0	0.002
Razorbill	0.15	0.109
Black Guillemot	0	0
Atlantic Puffin	0.001	0
Unidentified auk	0.001	0.011

Table 5-2: Seasonal species naive densities (uncorrected count/km^2 of survey transect).

NOTE: Table displays densities within the Atlantic Shores WTA and the NJDEP boat-based survey area on the Atlantic OCS and modeled densities (animals/km2) from the APEM digital aerial surveys within the Atlantic Shores WTA and the APEM digital aerial survey area.

	Mean naive density (uncorrected count/sq. km)											Modeled density (animals/sq. km)					
	Atlantic Shores WTA					NJDEP OCS survey area						WTA			APEM survey area		
Species	annual	winter	spring	summ.	fall	annual	winter	spring	summ.	fall	Total count	winter	spring	fall	winter	spring	fall
Sea ducks																	
Common Eider	0	0	0	0	0	<0.001	0	0	0	0.004	6	·	·	·	·	·	·
Surf Scoter	0.165	0	0.717	0	0.021	0.461	0.102	0.585	0	1.009	2574	·	·	·	·	·	·
White-winged Scoter	0	0	0	0	0	0.038	0.119	0.053	0	0.005	238	0.003	0.023	·	0.098	0.122	·
Black Scoter	0.006	0	0.025	0	0	0.274	0.220	0.433	0	0.470	1530	·	·	0	·	·	0.002
Long-tailed Duck	0	0	0	0	0	0.083	0.274	0.159	0	0	393	·	·	·	·	·	·
Red-breasted Merganser	0.005	0	0.024	0	0	0.004	0.009	0.004	0	0.003	18	·	·	·	·	·	·
Unidentified Scoter	0.148	0	0.606	0	0	0.086	0.044	0.219	0	0.179	532	·	·	·	·	·	·
Loons																	
Red-throated Loon	0.129	0.047	0.393	0	0.038	0.228	0.367	0.477	0	0.070	929	0.015	0.065	·	0.016	0.050	·
Common Loon	0.536	0.398	1.109	0.005	1.162	0.484	0.614	0.867	0.042	0.405	2221	0.453	0.320	0.146	0.339	0.236	0.130
Unidentified Loon	0.010	0.026	0	0	0	0.002	0.005	0.002	0	<0.001	9	·	·	·	·	·	·
Shearwaters and Petrels																	
Wilson's Storm-Petrel	0.155	0	0	0.654	0.031	0.496	0	0	2.499	0.146	2566	·	·	·	·	·	·
Leach's Storm-Petrel	0	0	0	0	0	<0.001	0	0	0.001	0	2	·	·	·	·	·	·
Northern Fulmar	0	0	0	0	0	<0.001	0.001	0	0	<0.001	3	·	·	·	·	·	·
Cory's Shearwater	0.050	0	0	0.194	0.027	0.043	0	0	0.144	0.034	220	·	·	·	·	·	·
Sooty Shearwater	0.006	0	0	0.028	0	0.002	0	0	0.007	0	8	·	·	·	·	·	·
Great Shearwater	0.002	0	0	0.005	0	0.005	0	0	0.006	0.016	33	·	·	·	·	·	·
Manx Shearwater	0	0	0	0	0	<0.001	<0.001	0.004	<0.001	0	6	·	·	·	·	·	·
Audubon's Shearwater	0.001	0	0	0	0.011	<0.001	0	0	0	0.001	1	·	·	·	·	·	·
Unidentified Shearwater	0.001	0	0	0	0.011	<0.001	0	0	0	0.001	1	·	·	·	·	·	·
Unidentified Storm-petrel	0	0	0	0	0	<0.001	0	0	0.001	0.001	4	·	·	·	·	·	·
Gannet																	

	Mean naive density (uncorrected count/sq. km)											Modeled density (animals/sq. km)					
	Atlantic Shores WTA					NJDEP OCS survey area						WTA			APEM survey area		
Species	annual	winter	spring	summ.	fall	annual	winter	spring	summ.	fall	Total count	winter	spring	fall	winter	spring	fall
Northern Gannet	0.454	0.443	0.996	0.146	0.230	1.597	1.748	1.979	0.276	1.818	7478	0.183	0.501	0.050	0.173	0.264	0.089
Cormorants and Pelicans																	
Double-crested Cormorant	0.003	0	0	0.011	0	0.190	0.017	0.040	0.010	0.793	1348	·	·	·	·	·	·
Great Cormorant	0	0	0	0	0	<0.001	0	0	0	0.002	3	·	·	·	·	·	·
Brown Pelican	0.001	0	0	0.003	0	0.001	0	0	0.004	<0.001	8	·	·	·	·	·	·
Gulls and Jaegers																	
Pomarine Jaeger	0	0	0	0	0	<0.001	0	0	0	0.001	2	·	·	·	·	·	·
Parasitic Jaeger	0.003	0	0.006	0	0.010	0.004	0	<0.001	0.002	0.013	24	·	·	·	·	·	·
Black-legged Kittiwake	0.035	0.127	0	0	0	0.028	0.038	0	0	0.157	146	0.014	·	·	0.012	·	·
Sabine's Gull	0	0	0	0	0	0.001	0	0	0.008	<0.001	2	·	·	·	·	·	·
Bonaparte's Gull	0.120	0.209	0.521	0	0	0.125	0.198	0.175	0	0.131	554	0.517	·	0.108	0.307	·	0.104
Little Gull	0	0	0	0	0	<0.001	0	<0.001	0	<0.001	2	·	·	·	·	·	·
Laughing Gull	0.272	0	0.184	0.788	0.245	0.572	0.007	0.180	0.918	1.248	3279	0.126	·	·	0.194	·	·
Ring-billed Gull	0.008	0	0.016	0	0.012	0.015	0.017	0.002	0	0.065	59	·	·	·	·	·	·
Herring Gull	0.308	0.498	0.646	0.014	0.200	0.554	0.553	1.024	0.087	0.478	2605	0.021	0.046	0.003	0.033	0.032	0.004
Iceland Gull	0	0	0	0	0	<0.001	0.001	0	0	0	1	·	·	·	·	·	·
Lesser Black-backed Gull	0	0	0	0	0	0.001	0	0.002	<0.001	0.002	8	·	·	·	·	·	·
Great Black-backed Gull	0.144	0.108	0.190	0.109	0.228	0.288	0.212	0.300	0.147	0.438	1259	0.080	0.037	0.008	0.061	0.028	0.010
Unidentified small gull	0.016	0.039	0	0	0	0.002	0.004	0	0	0	3	·	·	·	·	·	·
Unidentified Jaeger	0	0	0	0	0	<0.001	0	0	<0.001	0	1	·	·	·	·	·	·
Unidentified Large Gull	0.004	0	0.006	0	0.021	0.021	0.040	0.018	0.001	0.017	105	·	·	·	·	·	·
Terns																	
Least Tern	0	0	0	0	0	0.002	0	0.001	0.004	0	2	·	·	·	·	·	·
Caspian Tern	0	0	0	0	0	<0.001	0	<0.001	0	<0.001	2	·	·	·	·	·	·
Black Tern	0.001	0	0	0.004	0	0.001	0	0	0.004	<0.001	9	·	·	·	·	·	·
Common Tern	0.149	0	0.153	0.446	0	0.272	0	0.166	0.781	0.104	1484	·	·	·	·	·	·
Forster's Tern	0.010	0	0.039	0	0	0.073	0	0.046	0.018	0.335	431	·	·	·	·	·	·
Royal Tern	0.004	0	0	0	0.026	0.020	0	<0.001	0.052	0.032	79	·	·	·	·	·	·
Unidentified small Tern	0.024	0	0.084	0.017	0	0.023	0	0.050	0.031	0.031	136	·	·	·	·	·	·

Species	Mean naive density (uncorrected count/sq. km)											Modeled density (animals/sq. km)					
	Atlantic Shores WTA					NJDEP OCS survey area						WTA			APEM survey area		
	annual	winter	spring	summ.	fall	annual	winter	spring	summ.	fall	Total count	winter	spring	fall	winter	spring	fall
Auks																	
Dovekie	0.012	0.058	0.011	0	0	0.018	0.068	0.008	0	0	95	·	·	·	·	·	·
Common Murre	0.008	0.013	0.012	0	0	0.005	0.018	0.009	0	0	22	·	·	·	·	·	·
Thick-billed Murre	0	0	0	0	0	0.002	0.005	0.005	0	0	8	·	·	·	·	·	·
Razorbill	0.150	0.177	0.433	0	0	0.109	0.150	0.358	0	0	677	·	·	·	·	·	·
Black Guillemot	0	0	0	0	0	<0.001	0	<0.001	0	0	1	·	·	·	·	·	·
Atlantic Puffin	0.001	0.013	0	0	0	<0.001	0.001	0	0	0	1	·	·	·	·	·	·
Unidentified Alcid	0.001	0	0.006	0	0	0.011	0.016	0.016	0	0	36	·	·	·	·	·	·

Table 5-3: Vulnerability assessment rankings by species within each broad taxonomic grouping.

Species	Collision Vulnerability		DV	PV
	Turbine Opt. 1	Turbine Opt. 2		
Sea ducks				
Black Scoter	low (0.37)	low (0.37)	high (0.9)	low (0.4)
Common Eider	low (0.3)	low (0.3)	high (0.9)	low (0.47)
Long-tailed Duck	low (0.33)	low (0.33)	high (0.9)	low (0.27)
Red-breasted Merganser	low (0.4)	low (0.4)	medium (0.5)	low (0.27)
Surf Scoter	low (0.33)	low (0.33)	high (0.9)	medium (0.53)
White-winged Scoter	low (0.37)	low (0.37)	high (0.8)	medium (0.53)
Auks				
Atlantic Puffin	minimal (0.2)	minimal (0.2)	high (0.8)	medium (0.53)
Black Guillemot	low (0.33)	low (0.33)	high (0.9)	low (0.4)
Common Murre	low (0.27)	low (0.27)	high (0.8)	low (0.4)
Dovekie	low (0.27)	low (0.27)	medium (0.7)	low (0.4)
Razorbill	minimal (0.23)	minimal (0.23)	high (0.8)	medium (0.6)
Gulls				
Black-legged Kittiwake	low (0.43)	low (0.43)	medium (0.6)	low (0.33)
Bonaparte's Gull	low (0.43)	low (0.43)	medium (0.5)	low (0.33)
Great Black-backed Gull	medium (0.6)	medium (0.6)	medium (0.7)	minimal (0.2)
Herring Gull	medium (0.67)	medium (0.67)	medium (0.5)	medium (0.53)
Laughing Gull	medium (0.53)	medium (0.53)	medium (0.5)	low (0.4)
Parasitic Jaeger	medium (0.57)	medium (0.57)	low (0.3)	low (0.4)
Pomarine Jaeger	medium (0.67)	medium (0.67)	low (0.3)	low (0.4)
Ring-billed Gull	medium (0.6)	medium (0.6)	low (0.4)	low (0.33)
Terns				
Common Tern	low (0.33)	low (0.33)	high (0.8)	medium (0.6)
Forster's Tern	low (0.47)	low (0.47)	medium (0.5)	low (0.4)
Roseate Tern	low (0.3)	low (0.3)	high (0.8)	high (0.87)
Royal Tern	low (0.43)	low (0.43)	medium (0.5)	medium (0.53)
Loons				
Common Loon	low (0.33)	low (0.33)	high (0.8)	medium (0.53)
Red-throated Loon	low (0.43)	low (0.43)	high (0.9)	low (0.47)
Shearwaters and Petrels				
Audubon's Shearwater	low (0.4)	low (0.4)	medium (0.6)	medium (0.73)
Cory's Shearwater	low (0.4)	low (0.4)	medium (0.6)	medium (0.6)
Great Shearwater	low (0.37)	low (0.37)	medium (0.6)	medium (0.67)
Leach's Storm-Petrel	low (0.43)	low (0.43)	medium (0.6)	low (0.47)
Manx Shearwater	low (0.4)	low (0.4)	medium (0.6)	medium (0.53)
Northern Fulmar	low (0.4)	low (0.4)	medium (0.6)	low (0.47)
Sooty Shearwater	low (0.37)	low (0.37)	medium (0.6)	medium (0.53)
Wilson's Storm-Petrel	low (0.43)	low (0.43)	medium (0.6)	low (0.4)
Gannet				
Northern Gannet	low (0.47)	low (0.47)	medium (0.6)	low (0.47)
Cormorants and Pelicans				
Brown Pelican	low (0.37)	low (0.37)	medium (0.5)	low (0.4)
Double-crested Cormorant	medium (0.73)	medium (0.73)	low (0.4)	minimal (0.13)

5.2.1 Loons

5.2.1.1 Exposure Tables, Maps, and Figures

Table 5-4: Seasonal exposure rankings for the loon group.

Species	Season	Local Rank	Regional Rank	Total Rank	Exposure Score
Red-throated Loon	Winter	0	1	1	low
	Spring	1	1	2	low
	Summer	0	·	0	minimal
	Fall	0	1	1	low
Common Loon	Winter	0	2	2	low
	Spring	3	3	6	high
	Summer	0	1	1	low
	Fall	2	1	3	medium

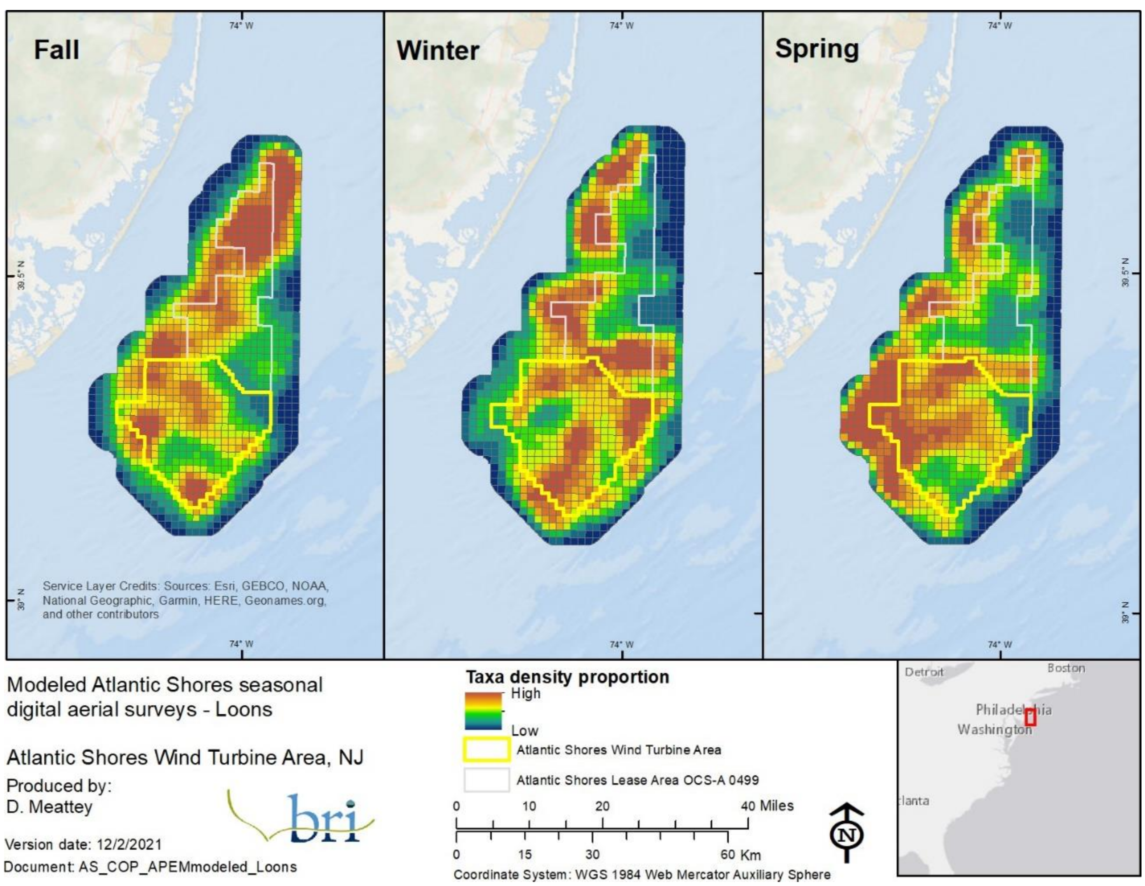

Figure 5-17: Seasonal distributions of loons across the WTA and broader Lease Area, modeled from monthly digital aerial surveys carried out in the area from October 2020–May 2021.

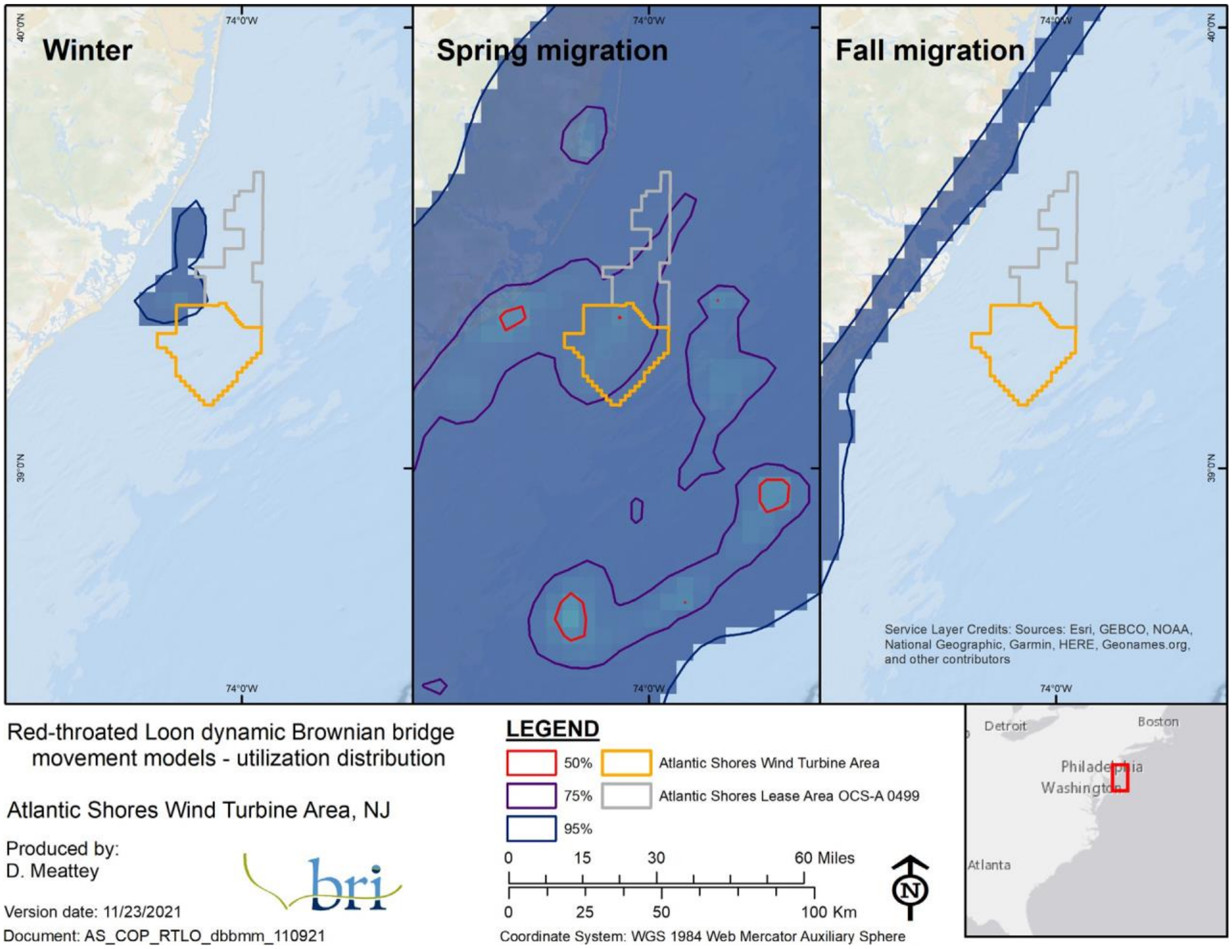

NOTE: (n=46, 46, 31 [winter, spring, fall]) that were tracked with satellite transmitters; the contours represent the percentage of the use area across the UD surface and represent various levels of use from 50% (core use) to 95% (home range). Data provided by BOEM and used with permission.

Figure 5-18: Dynamic Brownian bridge movement models for Red-throated Loons.

5.2.1.2 Relative Behavioral Vulnerability Figures and Tables

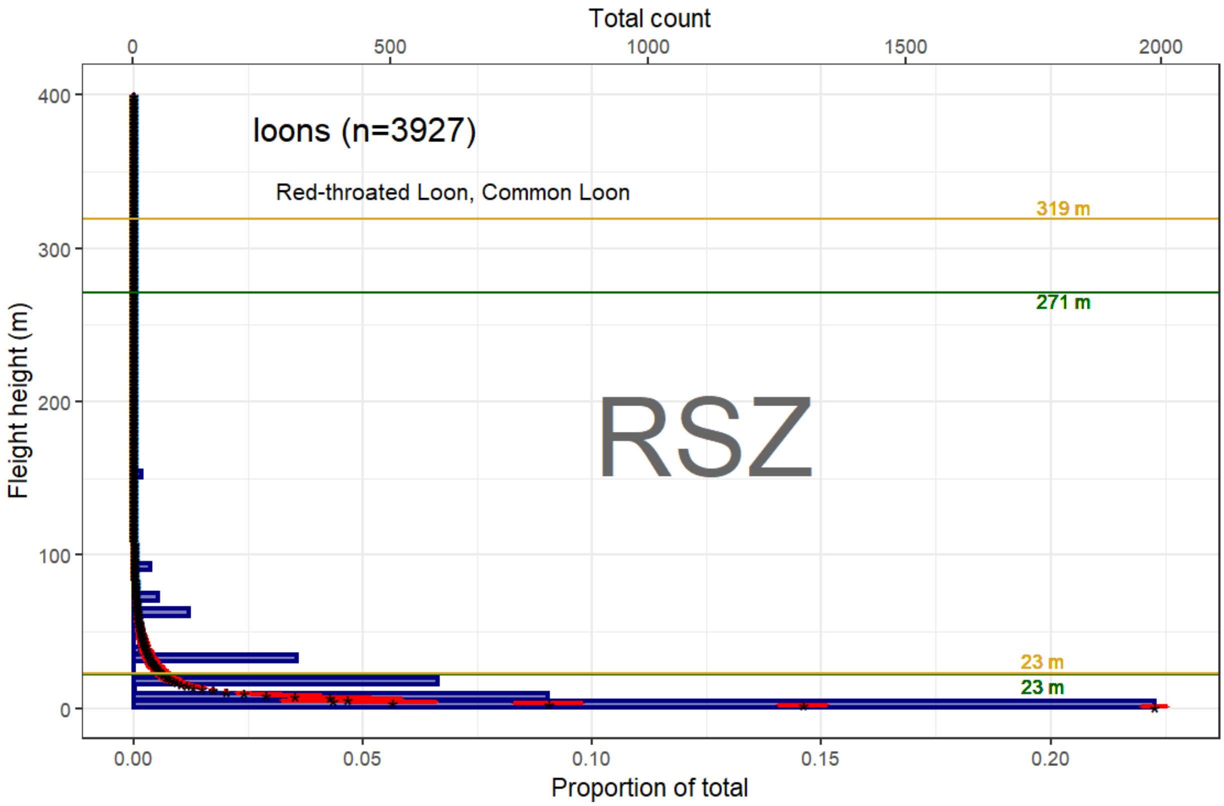

NOTE: Figure shows the actual number of birds in 5 m intervals (blue bars), and the modeled average flight height in 1 m intervals (asterisk) and the standard deviation (red lines), in relation to the upper and lower limits of the RSZ for a minimum (green: 23-271 m [75-889 ft]) and maximum WTG (gold: 23-319 m [75-1,046 ft]).

Figure 5-19: Flight heights of loons (m) derived from the Northwest Atlantic Seabird Catalog.

Table 5-5: Vulnerability assessment rankings by species for the loon group.

Species	Collision Vulnerability		DV	PV
	Turbine Opt. 1	Turbine Opt. 2		
Common Loon	low (0.33)	low (0.33)	high (0.8)	medium (0.53)
Red-throated Loon	low (0.43)	low (0.43)	high (0.9)	low (0.47)

5.2.2 Sea Ducks

5.2.2.1 Exposure Tables, Maps, and Figures

Table 5-6: Seasonal exposure rankings for the sea duck group.

Species	Season	Local Rank	Regional Rank	Total Rank	Exposure Score
Common Eider	Winter	0	0	0	minimal
	Spring	0	0	0	minimal
	Summer	0	0	0	minimal
	Fall	0	1	1	low
Surf Scoter	Winter	0	1	1	low
	Spring	1	0	1	low
	Summer	0	·	0	minimal
	Fall	0	1	1	low
White-winged Scoter	Winter	0	1	1	low
	Spring	0	2	2	low
	Summer	0	·	0	minimal
	Fall	0	0	0	minimal
Black Scoter	Winter	0	0	0	minimal
	Spring	0	0	0	minimal
	Summer	0	·	0	minimal
	Fall	0	1	1	low
Long-tailed Duck	Winter	0	0	0	minimal
	Spring	0	0	0	minimal
	Summer	0	·	0	minimal
	Fall	0	1	1	low
Red-breasted Merganser	Winter	0	1	1	low
	Spring	3	0	3	medium
	Summer	0	·	0	minimal
	Fall	0	·	0	minimal

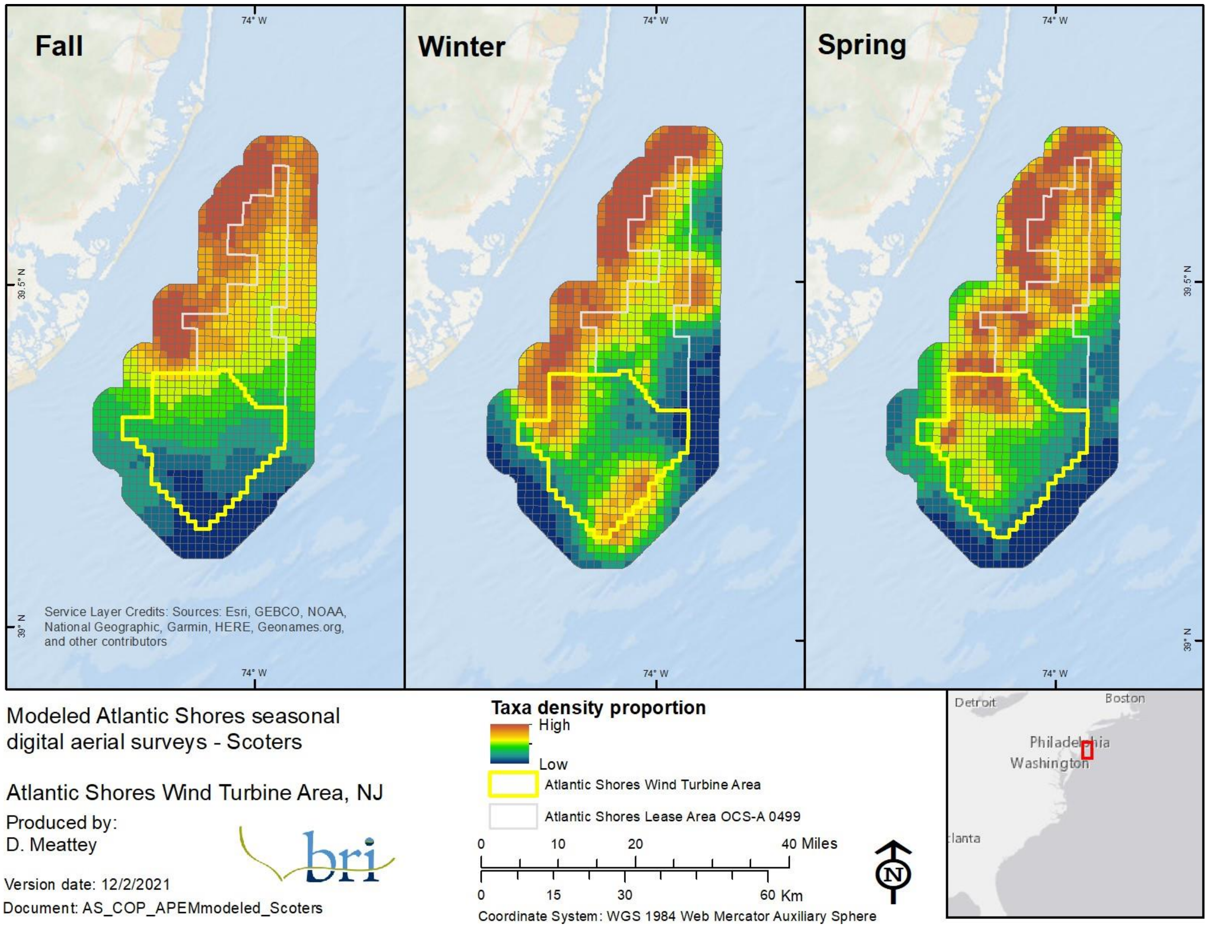

Figure 5-20: Seasonal distributions of scoters across the WTA and broader Lease Area, modeled from monthly digital aerial surveys carried out in the area from October 2020–May 2021.

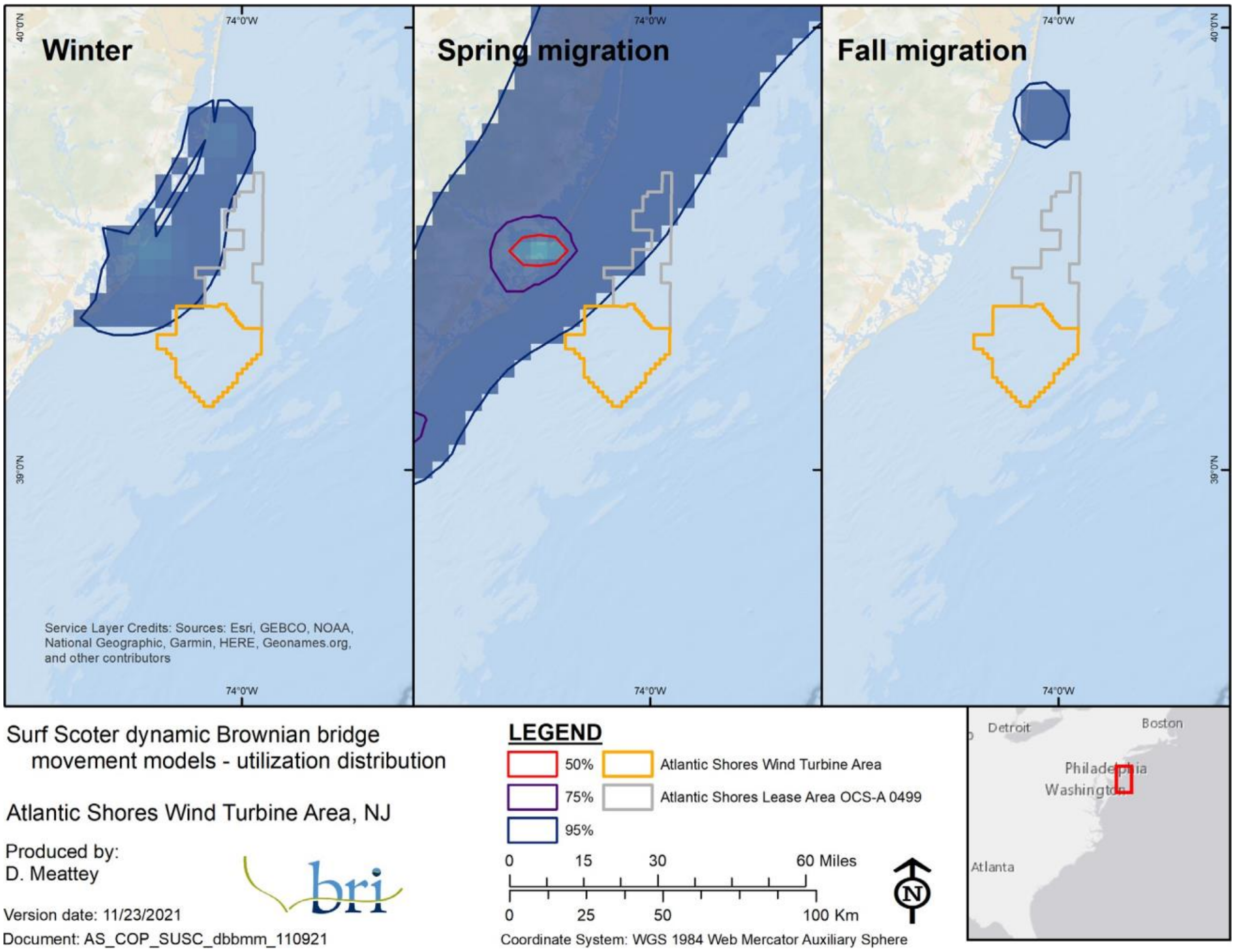

NOTE: (n=78, 87, 83 [winter, spring, fall]) that were tracked with satellite transmitters; the contours represent the percentage of the use area across the UD surface and represent various levels of use from 50% (core use) to 95% (home range). Data provided by multiple sea duck researchers and used with permission.

Figure 5-21: Dynamic Brownian bridge movement models for Surf Scoter.

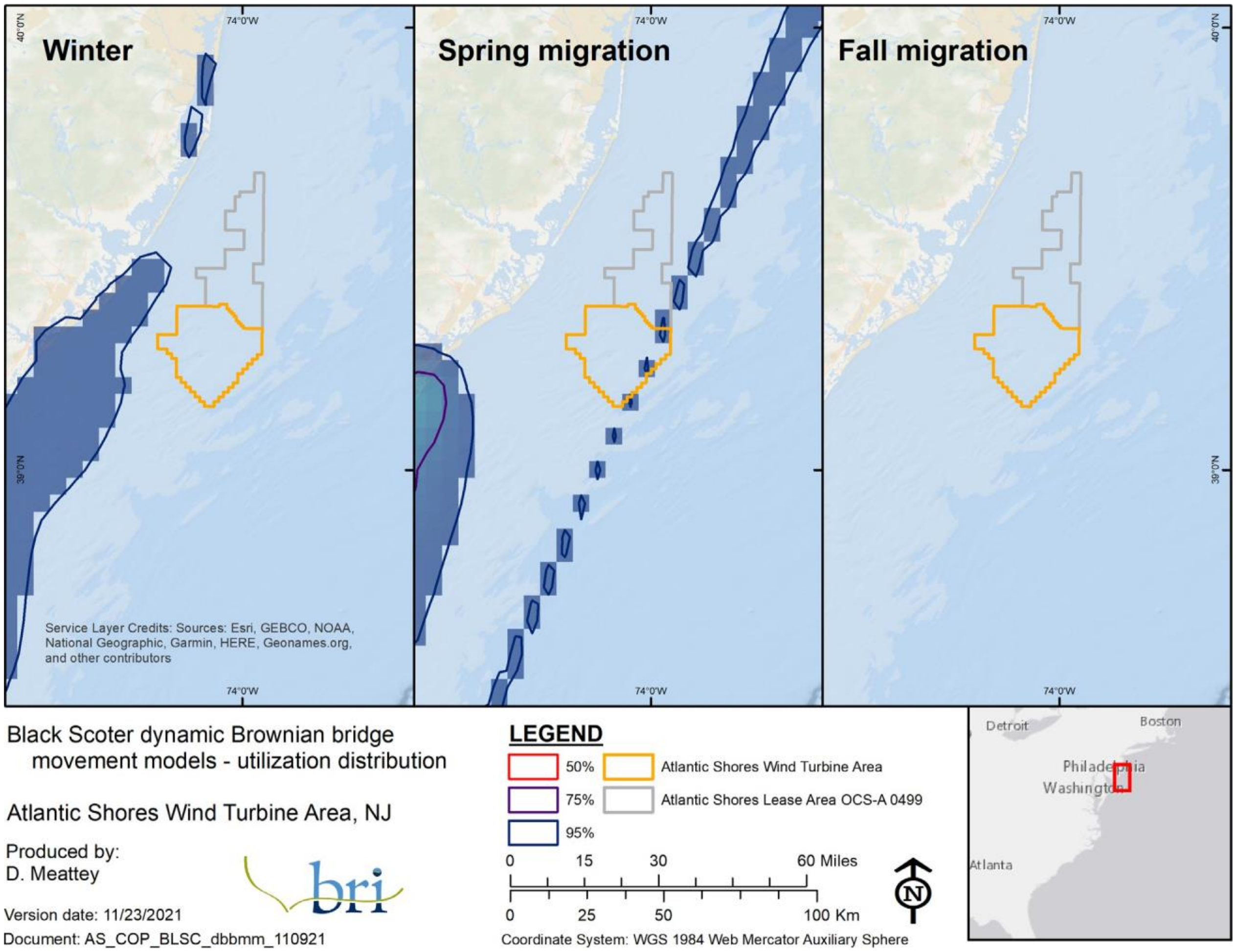

NOTE: (n=61, 76, 80 [winter, spring, fall]) that were tracked with satellite transmitters; the contours represent the percentage of the use area across the UD surface and represent various levels of use from 50% (core use) to 95% (home range). Data provided by multiple sea duck researchers and used with permission.

Figure 5-22: Dynamic Brownian bridge movement models for Black Scoter.

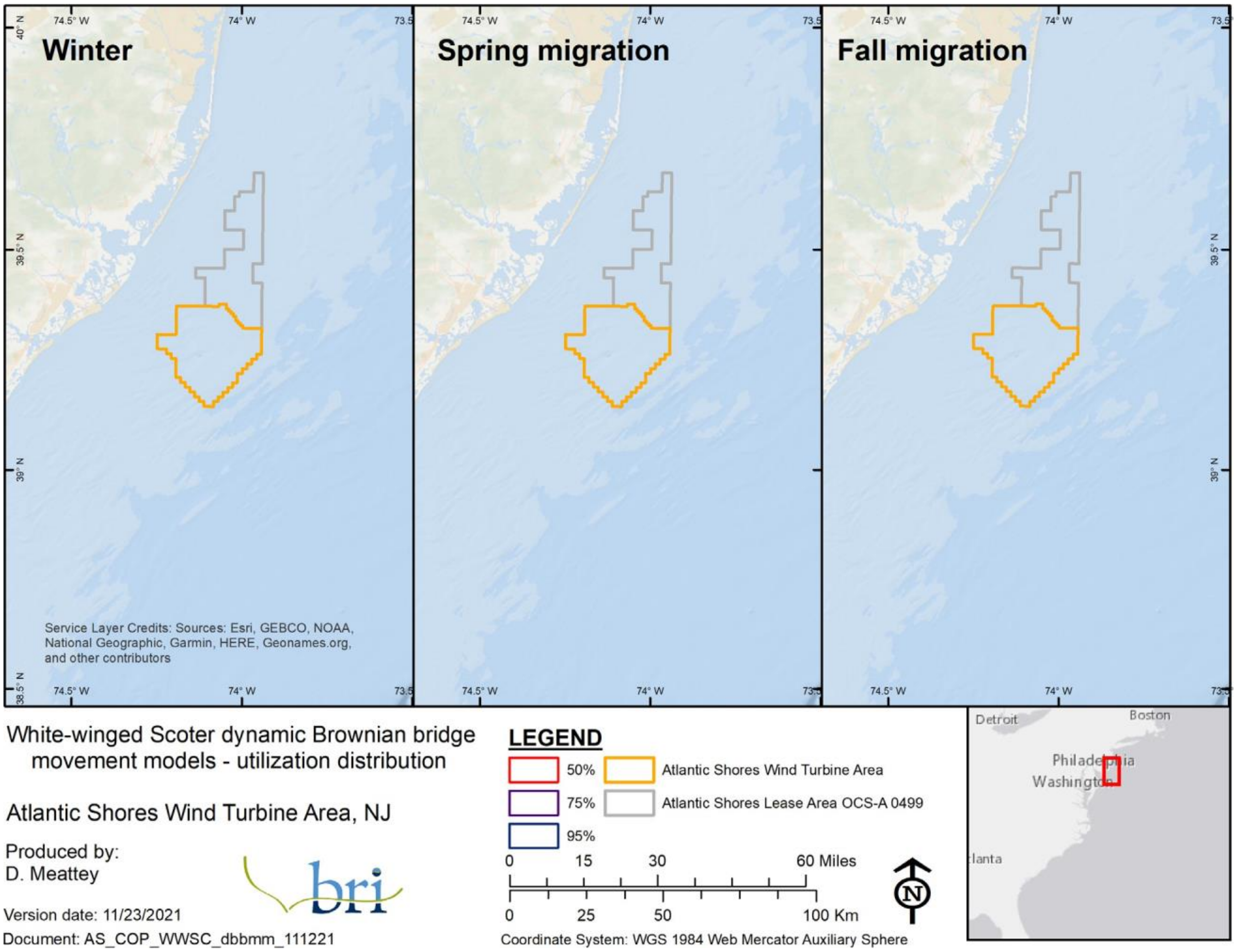

NOTE: (n=66, 45, 62 [winter, spring, fall]) that were tracked with satellite transmitters: the contours represent the percentage of the use area across the UD surface and represent various levels of use from 50% (core use) to 95% (home range). Data provided by multiple sea duck researchers and used with permission.

Figure 5-23: Dynamic Brownian bridge movement models for White-winged Scoter.

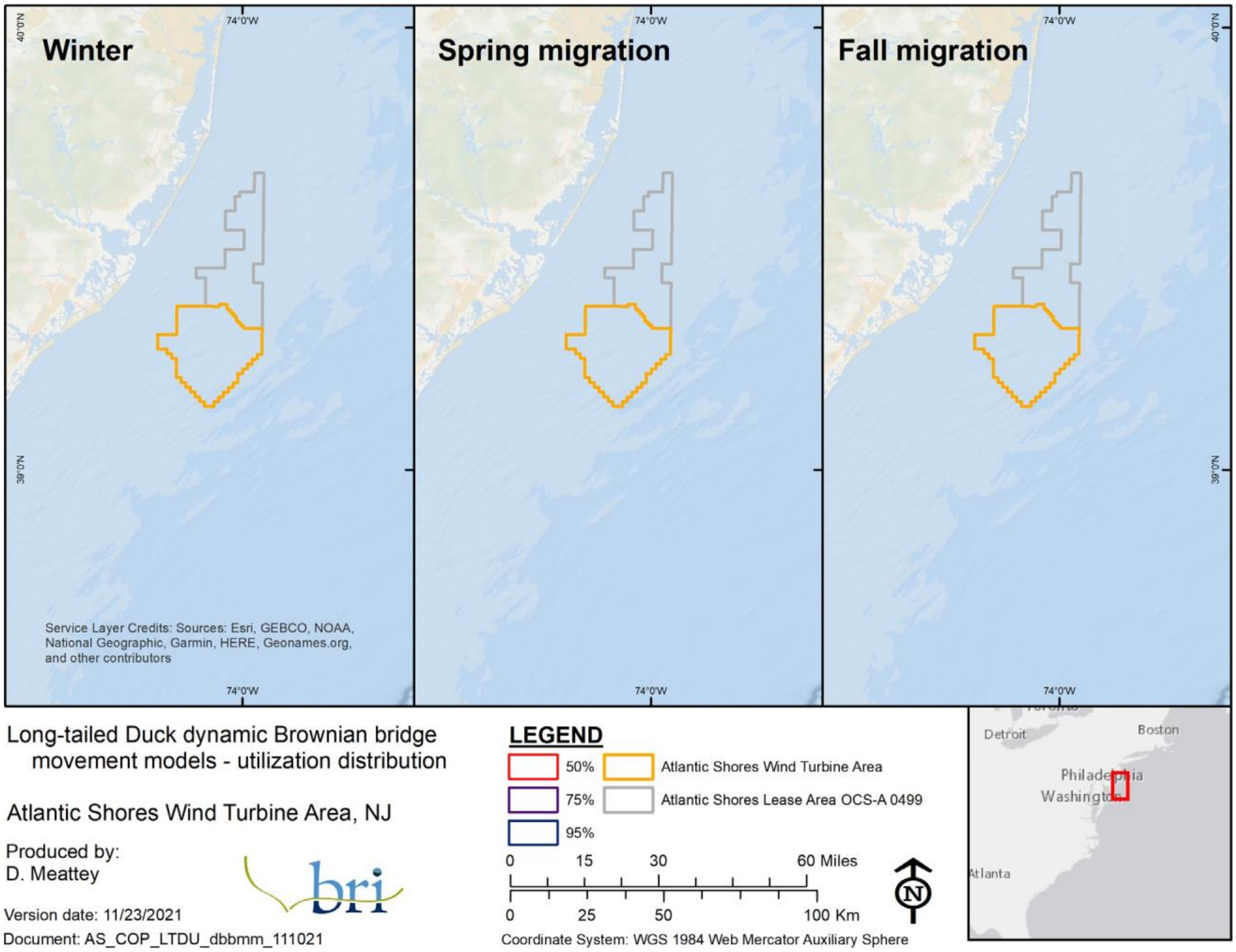

NOTE: (n=49, 60, 37 [winter, spring, fall]) that were tracked with satellite transmitters; the contours represent the percentage of the use area across the UD surface and represent various levels of use from 50% (core use) to 95% (home range). Data provided by multiple sea duck researchers and used with permission.

Figure 5-24: Dynamic Brownian bridge movement models for Long-tailed Duck.

5.2.2.2 Relative Behavioral Vulnerability Figures and Tables

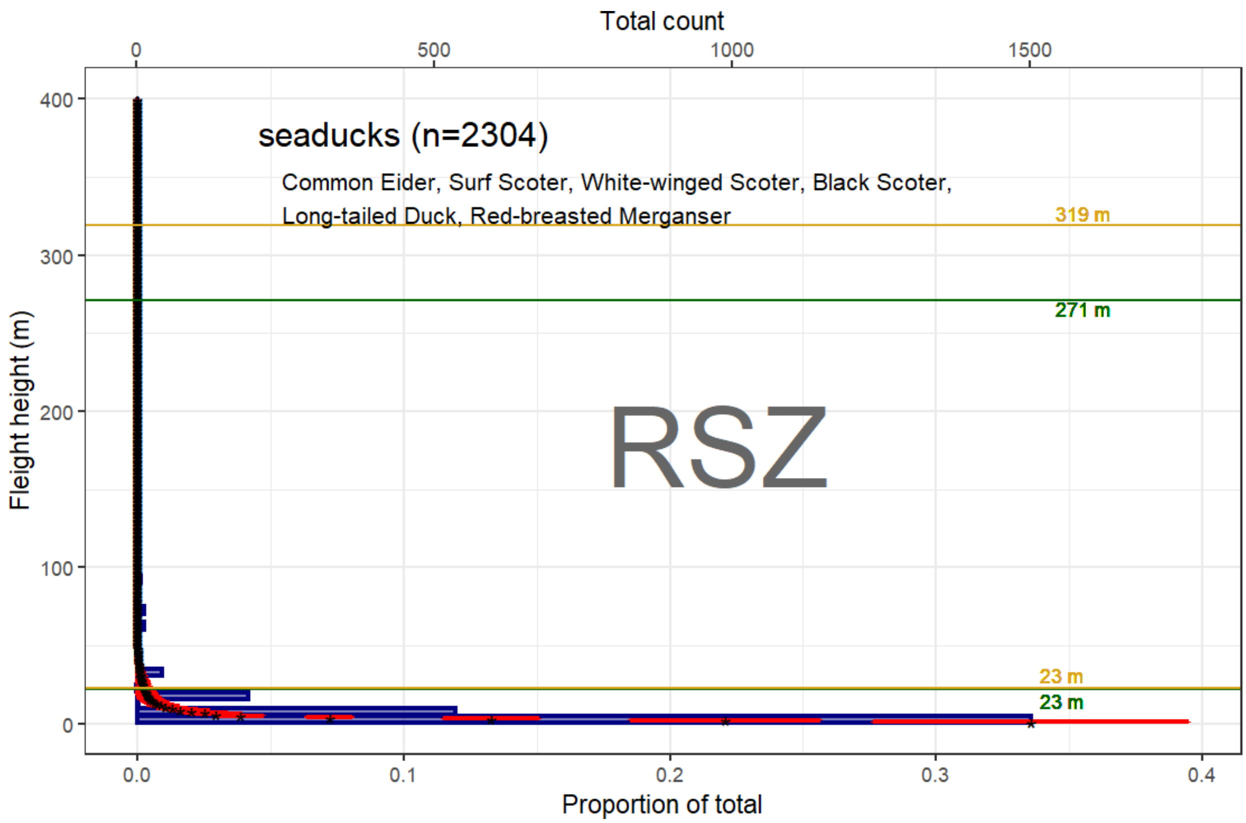

NOTE: Figure shows the actual number of birds in 5 m intervals (blue bars), and the modeled average flight height in 1 m intervals (asterisk) and the standard deviation (red lines), in relation to the upper and lower limits of the RSZ for a minimum (green: 23-271 m [75-889 ft]) and maximum WTG (gold: 23-319 m [75-1,046 ft]).

Figure 5-25: Flight heights of sea ducks (m) derived from the Northwest Atlantic Seabird Catalog.

Table 5-7: Vulnerability assessment rankings by species for the sea duck group.

Species	Collision Vulnerability		DV	PV
	Turbine Opt. 1	Turbine Opt. 2		
Black Scoter	low (0.37)	low (0.37)	high (0.9)	low (0.4)
Common Eider	low (0.3)	low (0.3)	high (0.9)	low (0.47)
Long-tailed Duck	low (0.33)	low (0.33)	high (0.9)	low (0.27)
Red-breasted Merganser	low (0.4)	low (0.4)	medium (0.5)	low (0.27)
Surf Scoter	low (0.33)	low (0.33)	high (0.9)	medium (0.53)
White-winged Scoter	low (0.37)	low (0.37)	high (0.8)	medium (0.53)

* Note: in the COP, "medium" is added to the DV score because there is evidence in the literature that some sea ducks will return to offshore wind farms several years after operation.

Shearwaters and Petrels

5.2.2.3 *Exposure Tables, Maps, and Figures*

Table 5-8: Seasonal exposure rankings for the shearwater and petrel group.

Species	Season	Local Rank	Regional Rank	Total Rank	Exposure Score
Northern Fulmar	Winter	0	0	0	minimal
	Spring	0	0	0	minimal
	Summer	0	0	0	minimal
	Fall	0	0	0	minimal
Cory's Shearwater	Winter	0	·	0	minimal
	Spring	0	0	0	minimal
	Summer	2	0	2	low
	Fall	1	0	1	low
Sooty Shearwater	Winter	0	·	0	minimal
	Spring	0	0	0	minimal
	Summer	3	0	3	medium
	Fall	0	0	0	minimal
Great Shearwater	Winter	0	0	0	minimal
	Spring	0	0	0	minimal
	Summer	0	0	0	minimal
	Fall	0	0	0	minimal
Manx Shearwater	Winter	0	·	0	minimal
	Spring	0	0	0	minimal
	Summer	0	0	0	minimal
	Fall	0	0	0	minimal
Audubon's Shearwater	Winter	0	0	0	minimal
	Spring	0	0	0	minimal
	Summer	0	0	0	minimal
	Fall	3	0	3	medium
Wilson's Storm-Petrel	Winter	0	·	0	minimal
	Spring	0	0	0	minimal
	Summer	0	0	0	minimal
	Fall	0	0	0	minimal
Leach's Storm-Petrel	Winter	0	·	0	minimal
	Spring	0	0	0	minimal
	Summer	0	0	0	minimal
	Fall	0	0	0	minimal

5.2.2.4 Relative Behavioral Vulnerability Figures and Tables

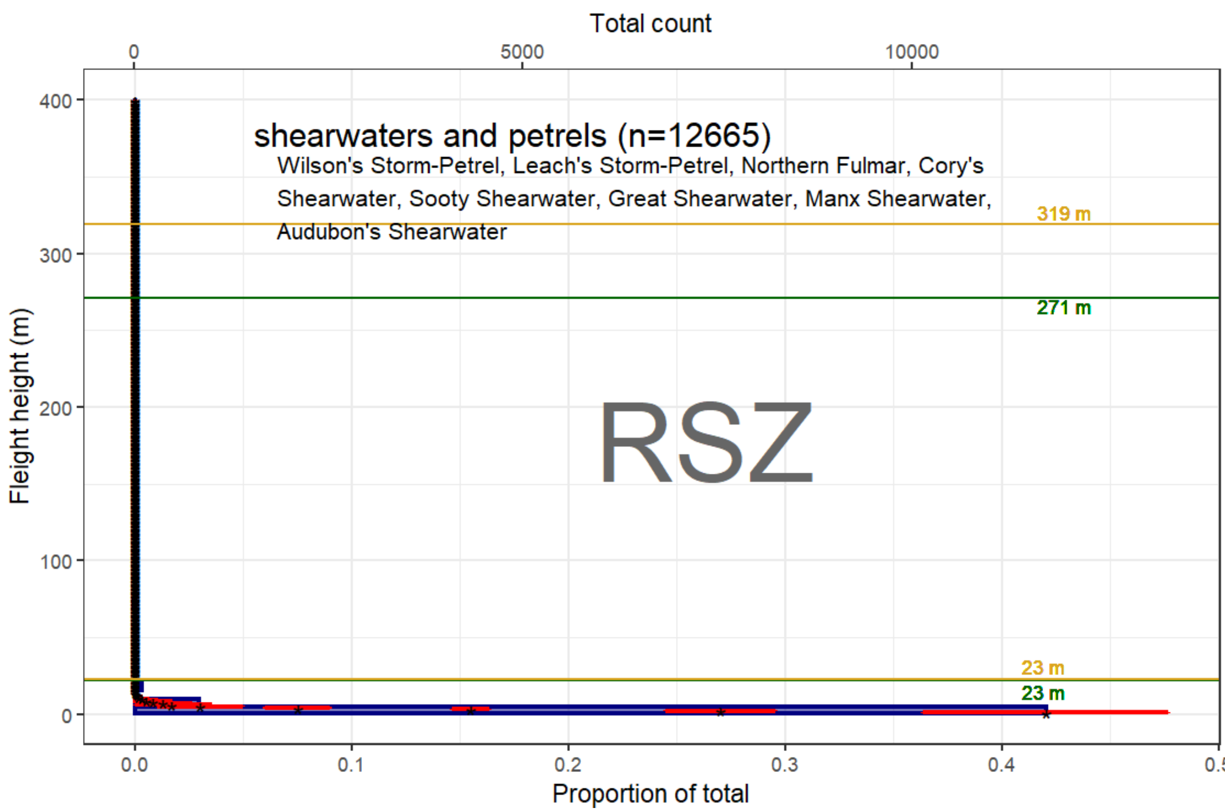

NOTE: Figures shows the actual number of birds in 5 m intervals (blue bars), and the modeled average flight height in 1 m intervals (asterisk) and the standard deviation (red lines), in relation to the upper and lower limits of the RSZ for a minimum (green: 23-271 m [75-889 ft]) and maximum WTG (gold: 23-319 m [75-1,046 ft]).

Figure 5-26: Flight heights of shearwaters, petrels, and storm-petrels (m) derived from the Northwest Atlantic Seabird Catalog.

Table 5-9: Vulnerability assessment rankings by species for the shearwater and petrel group.

Species	Collision Vulnerability		DV	PV
	Turbine Opt. 1	Turbine Opt. 2		
Audubon's Shearwater	low (0.4)	low (0.4)	medium (0.6)	medium (0.73)
Cory's Shearwater	low (0.4)	low (0.4)	medium (0.6)	medium (0.6)
Great Shearwater	low (0.37)	low (0.37)	medium (0.6)	medium (0.67)
Leach's Storm-Petrel	low (0.43)	low (0.43)	medium (0.6)	low (0.47)
Manx Shearwater	low (0.4)	low (0.4)	medium (0.6)	medium (0.53)
Northern Fulmar	low (0.4)	low (0.4)	medium (0.6)	low (0.47)
Sooty Shearwater	low (0.37)	low (0.37)	medium (0.6)	medium (0.53)
Wilson's Storm-Petrel	low (0.43)	low (0.43)	medium (0.6)	low (0.4)

5.2.2.5 Candidate Petrel Species

5.2.2.5.1 Black-capped Petrel

Maps

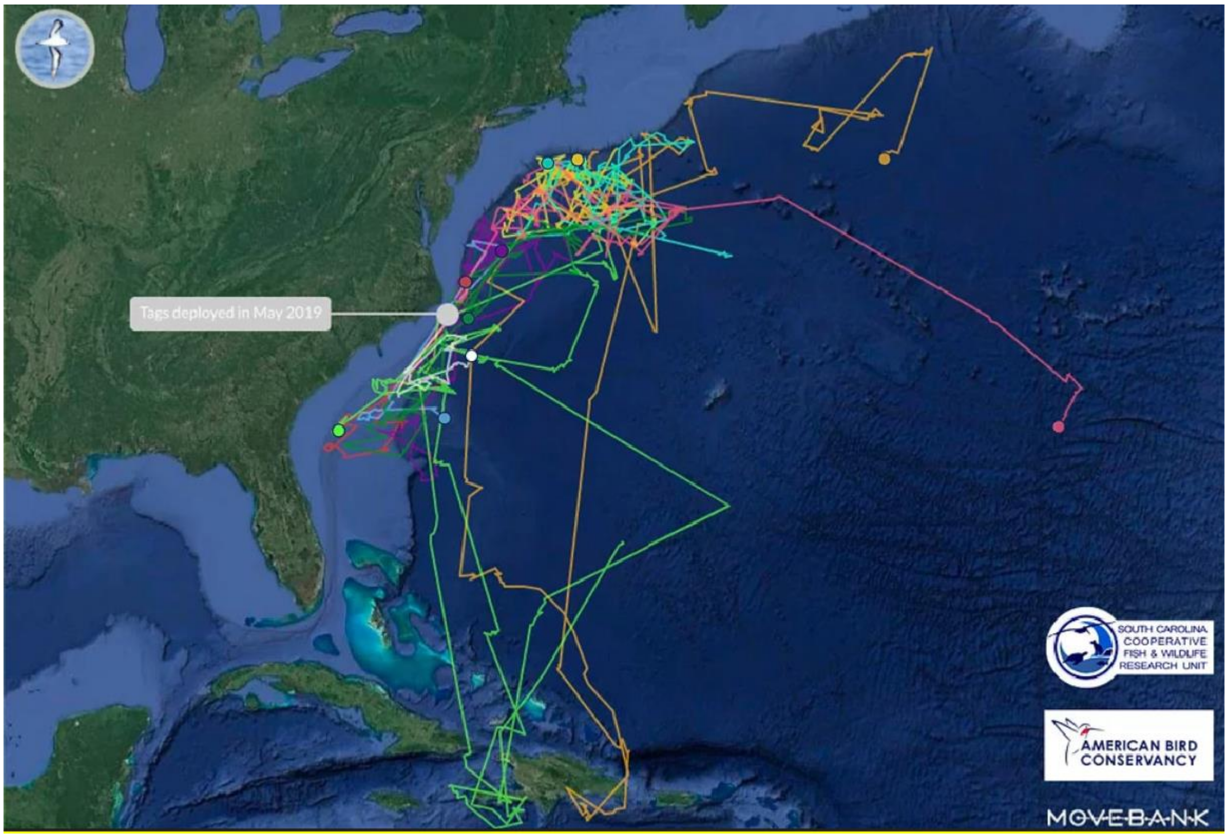

Figure 5-27: Track lines of 10 Black-capped Petrels tagged with solar satellite transmitters off of Cape Hatteras, North Carolina (Atlantic Seabirds 2020).

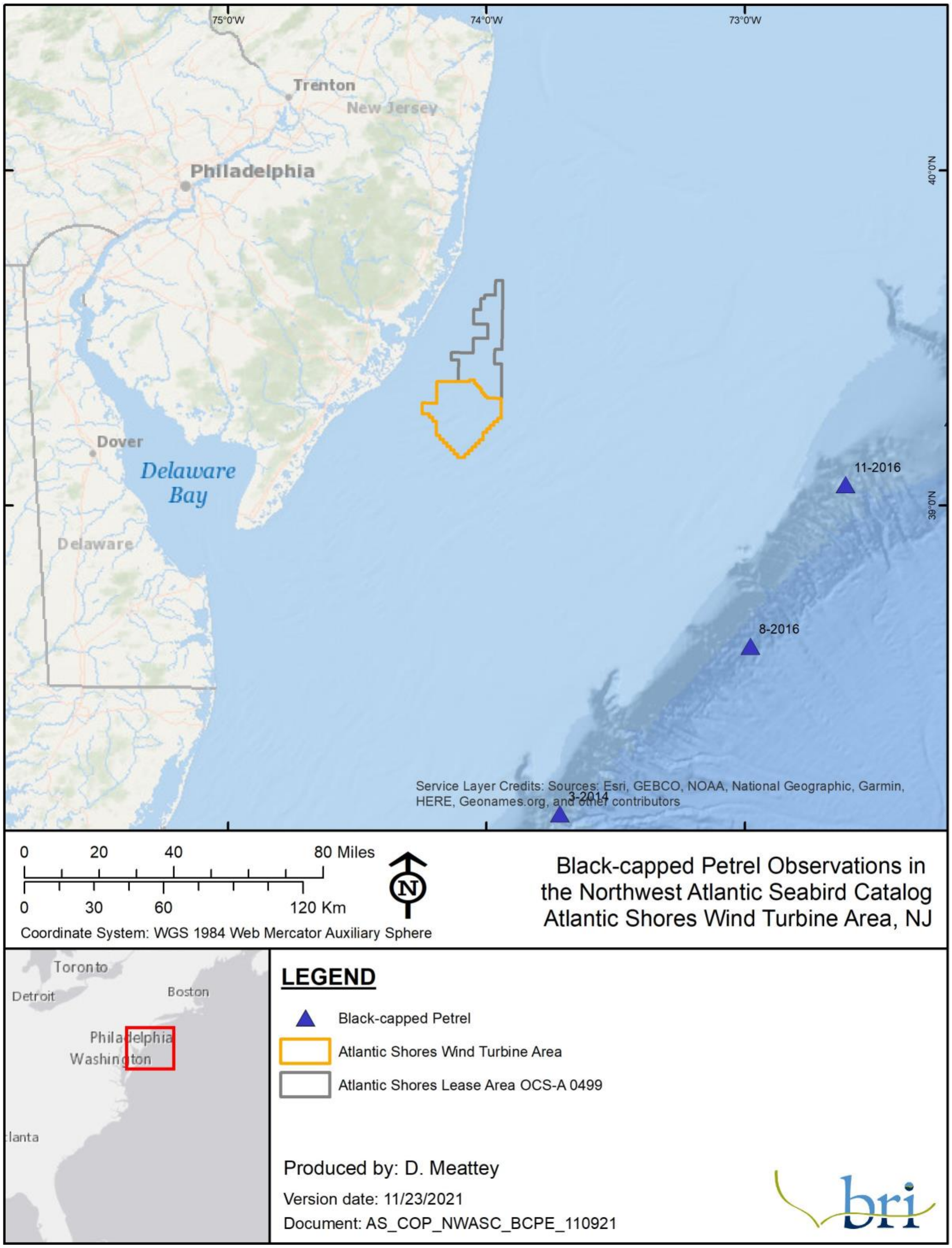

Figure 5-28: Black-capped Petrel observations from the Northwest Atlantic Seabird Catalog. Data provided by NOAA and used with permission.

5.2.3 <u>Gannets, Cormorants, and Pelicans</u>

5.2.3.1 Gannets

5.2.3.1.1 Exposure Tables, Maps, and Figures

Table 5-10: Seasonal exposure rankings for the Northern Gannet.

Species	Season	Local Rank	Regional Rank	Total Rank	Exposure Score
Northern Gannet	Winter	0	0	0	minimal
	Spring	0	1	1	low
	Summer	0	0	0	minimal
	Fall	0	0	0	minimal

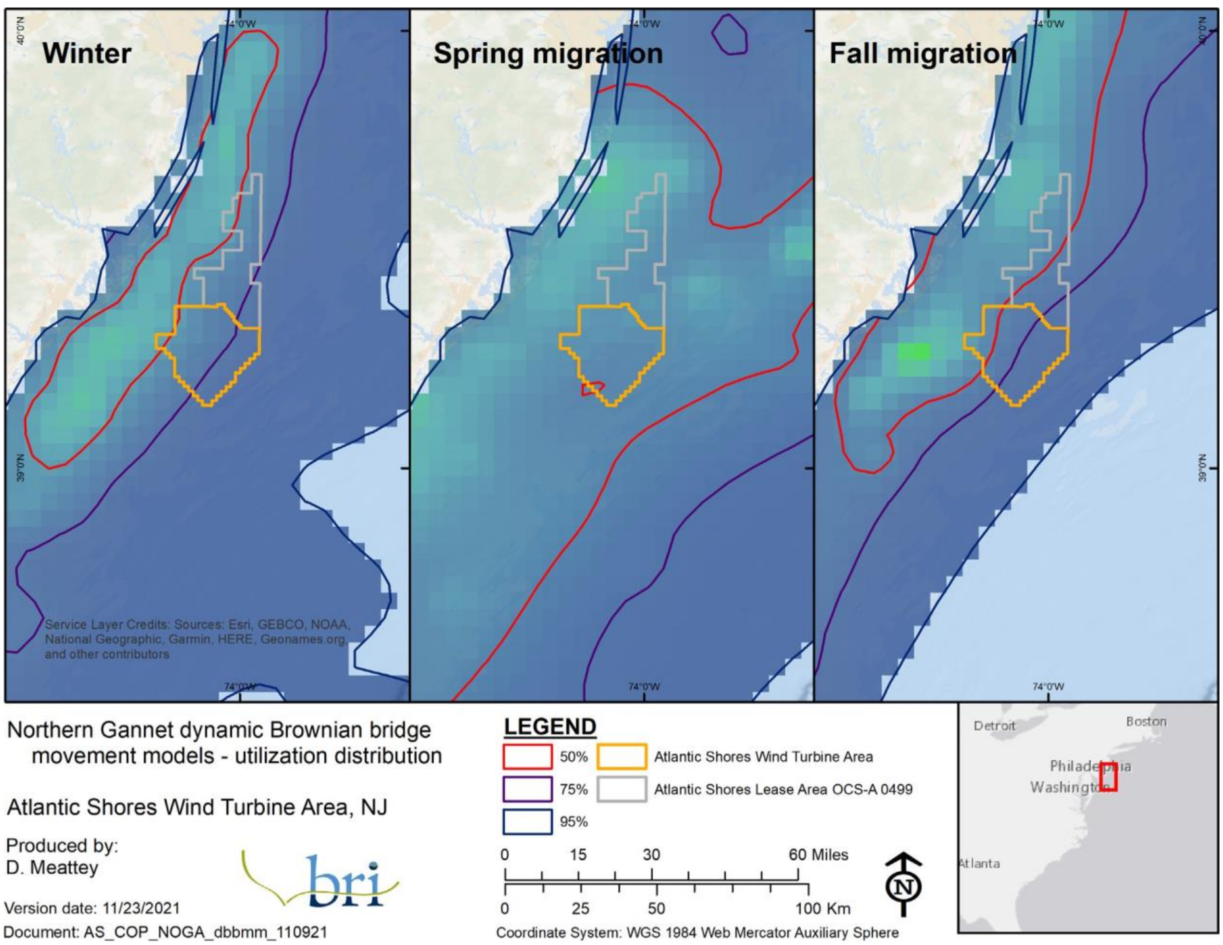

NOTE: (n=34, 35, 36 [winter, spring, fall]) that were tracked with satellite transmitters; the contours represent the percentage of the use area across the UD surface and represent various levels of use from 50% (core use) to 95% (home range). Data provided by BOEM and used with permission.

Figure 5-29: Dynamic Brownian bridge movement models for Northern Gannets

5.2.3.1.2 Relative Behavioral Vulnerability Figures and Tables

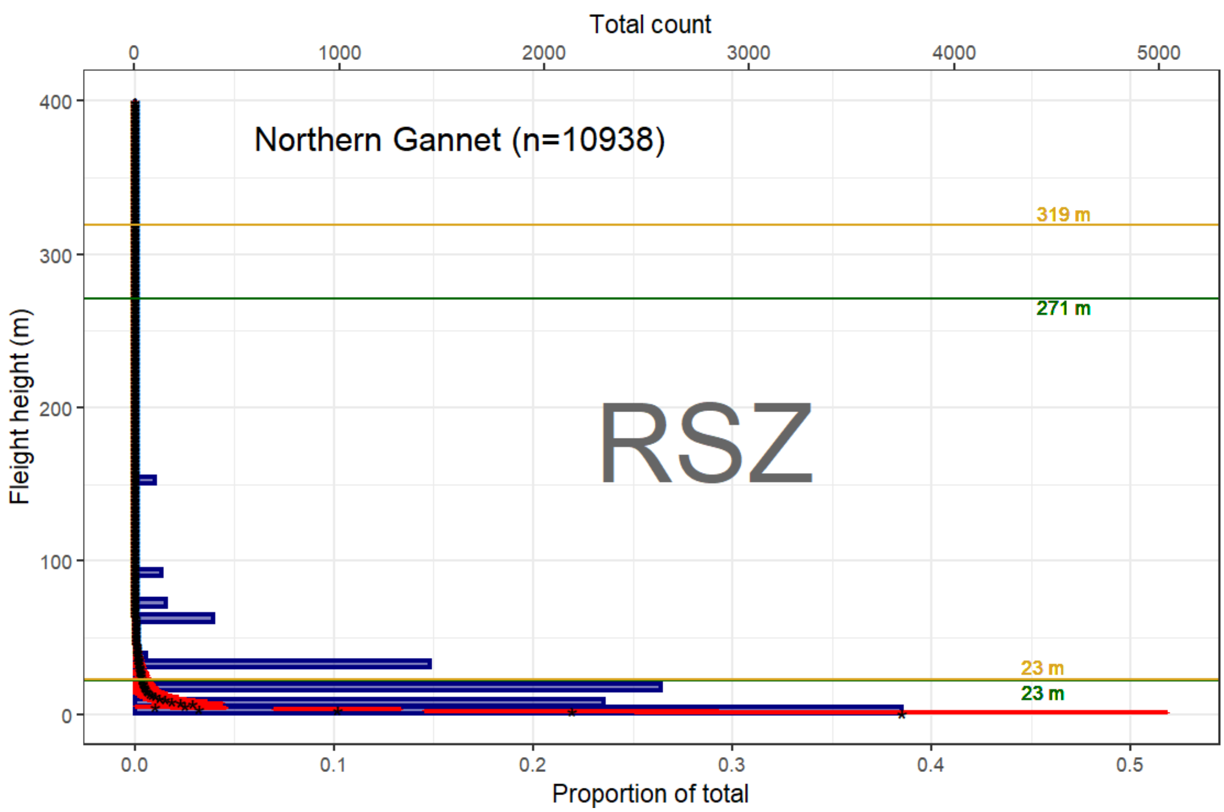

NOTE: Figure shows the actual number of birds in 5 m intervals (blue bars), and the modeled average flight height in 1 m intervals (asterisk) and the standard deviation (red lines), in relation to the upper and lower limits of the RSZ for a minimum (green: 23-271 m [75-889 ft]) and maximum WTG (gold: 23-319 m [75-1,046 ft]).

Figure 5-30: Flight heights of northern gannet (m) derived from the Northwest Atlantic Seabird Catalog,

Table 5-11: Vulnerability assessment rankings by species for the gannet group.

Species	Collision Vulnerability		DV	PV
	Turbine Opt. 1	Turbine Opt. 2		
Northern Gannet	low (0.47)	low (0.47)	medium (0.6)	low (0.47)

5.2.3.2 Cormorants and Pelicans

5.2.3.2.1 Exposure Tables, Maps, and Figures

Table 5-12: Seasonal exposure rankings for the cormorant and pelican group.

Species	Season	Local Rank	Regional Rank	Total Rank	Exposure Score
Double-crested Cormorant	Winter	0	1	1	low
	Spring	0	0	0	minimal
	Summer	0	1	1	low
	Fall	0	1	1	low
Great Cormorant	Winter	0	·	0	minimal
	Spring	0	·	0	minimal
	Summer	0	·	0	minimal
	Fall	0	·	0	minimal
Brown Pelican	Winter	0	0	0	minimal
	Spring	0	0	0	minimal
	Summer	0	0	0	minimal
	Fall	0	0	0	minimal

5.2.3.2.2 Relative Behavioral Vulnerability Figures and Tables

Table 5-13: Vulnerability assessment rankings by species for the cormorant and pelican group.

Species	Collision Vulnerability		DV	PV
	Turbine Opt. 1	Turbine Opt. 2		
Brown Pelican	medium (0.5)	medium (0.5)	medium (0.5)	low (0.4)
Double-crested Cormorant	medium (0.73)	medium (0.73)	low (0.4)	minimal (0.13)

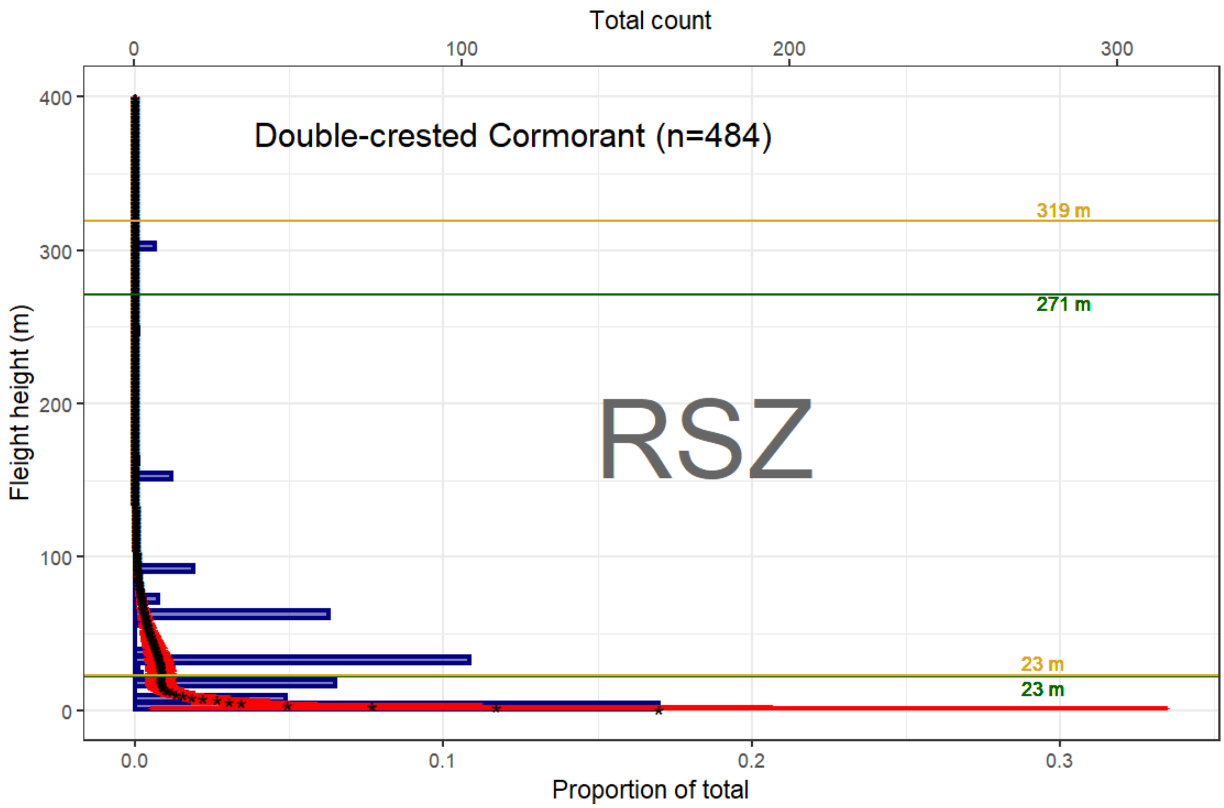

NOTE: Figure shows the actual number of birds in 5 m intervals (blue bars), and the modeled average flight height in 1 m intervals (asterisk) and the standard deviation (red lines), in relation to the upper and lower limits of the RSZ for a minimum (green: 23-271 m [75-889 ft]) and maximum WTG (gold: 23-319 m [75-1,046 ft]).

Figure 5-31: Flight heights of Double-crested Cormorant (m) derived from the Northwest Atlantic Seabird Catalog.

5.2.4 Gulls, Skuas, and Jaegers

5.2.4.1 Exposure Tables, Maps, and Figures

Table 5-14: Seasonal exposure rankings for the gull group.

Species	Season	Local Rank	Regional Rank	Total Rank	Exposure Score
Pomarine Jaeger	Winter	0	·	0	minimal
	Spring	0	0	0	minimal
	Summer	0	0	0	minimal
	Fall	0	0	0	minimal
Parasitic Jaeger	Winter	0	·	0	minimal
	Spring	3	1	4	medium
	Summer	0	0	0	minimal
	Fall	0	0	0	minimal
Black-legged Kittiwake	Winter	3	0	3	medium
	Spring	0	0	0	minimal
	Summer	0	·	0	minimal
	Fall	0	0	0	minimal
Sabine's Gull	Winter	0	·	0	minimal
	Spring	0	·	0	minimal
	Summer	0	·	0	minimal
	Fall	0	·	0	minimal
Bonaparte's Gull	Winter	1	0	1	low
	Spring	3	1	4	medium
	Summer	0	·	0	minimal
	Fall	0	1	1	low
Little Gull	Winter	0	·	0	minimal
	Spring	0	·	0	minimal
	Summer	0	·	0	minimal
	Fall	0	·	0	minimal
Laughing Gull	Winter	0	0	0	minimal
	Spring	1	0	1	low
	Summer	1	2	3	medium
	Fall	0	0	0	minimal
Ring-billed Gull	Winter	0	1	1	low
	Spring	3	0	3	medium
	Summer	0	2	2	low
	Fall	0	1	1	low
Herring Gull	Winter	1	1	2	low
	Spring	0	2	2	low
	Summer	0	0	0	minimal
	Fall	0	0	0	minimal
Iceland Gull	Winter	0	·	0	minimal
	Spring	0	·	0	minimal
	Summer	0	·	0	minimal
	Fall	0	·	0	minimal
Lesser Black-backed Gull	Winter	0	·	0	minimal
	Spring	0	·	0	minimal
	Summer	0	·	0	minimal

Species	Season	Local Rank	Regional Rank	Total Rank	Exposure Score
	Fall	0	·	0	minimal
Great Black-backed Gull	Winter	0	0	0	minimal
	Spring	0	0	0	minimal
	Summer	0	0	0	minimal
	Fall	0	0	0	minimal

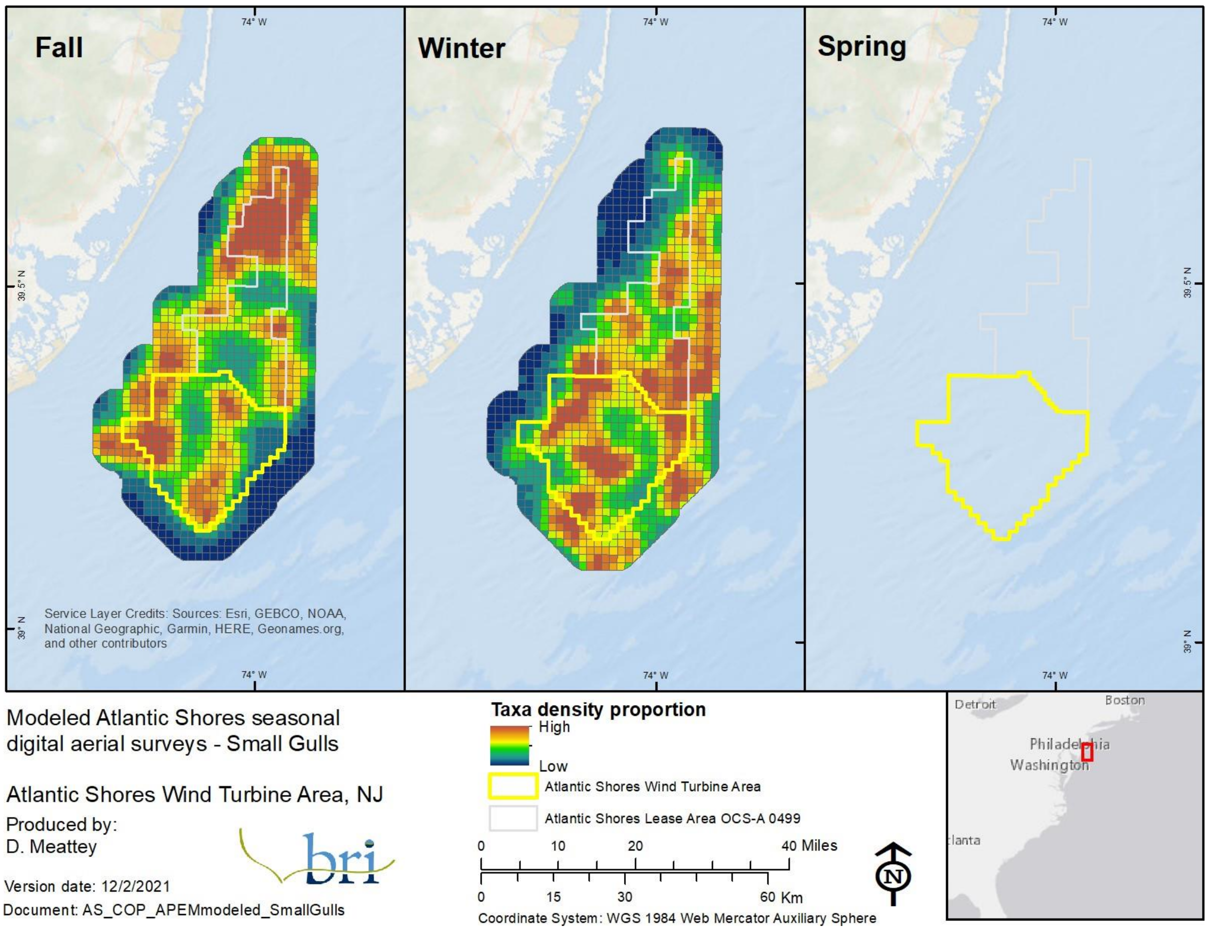

Figure 5-32: Seasonal distributions of small gulls across the WTA and broader Lease Area, modeled from monthly digital aerial surveys carried out in the area from October 2020–May 2021.

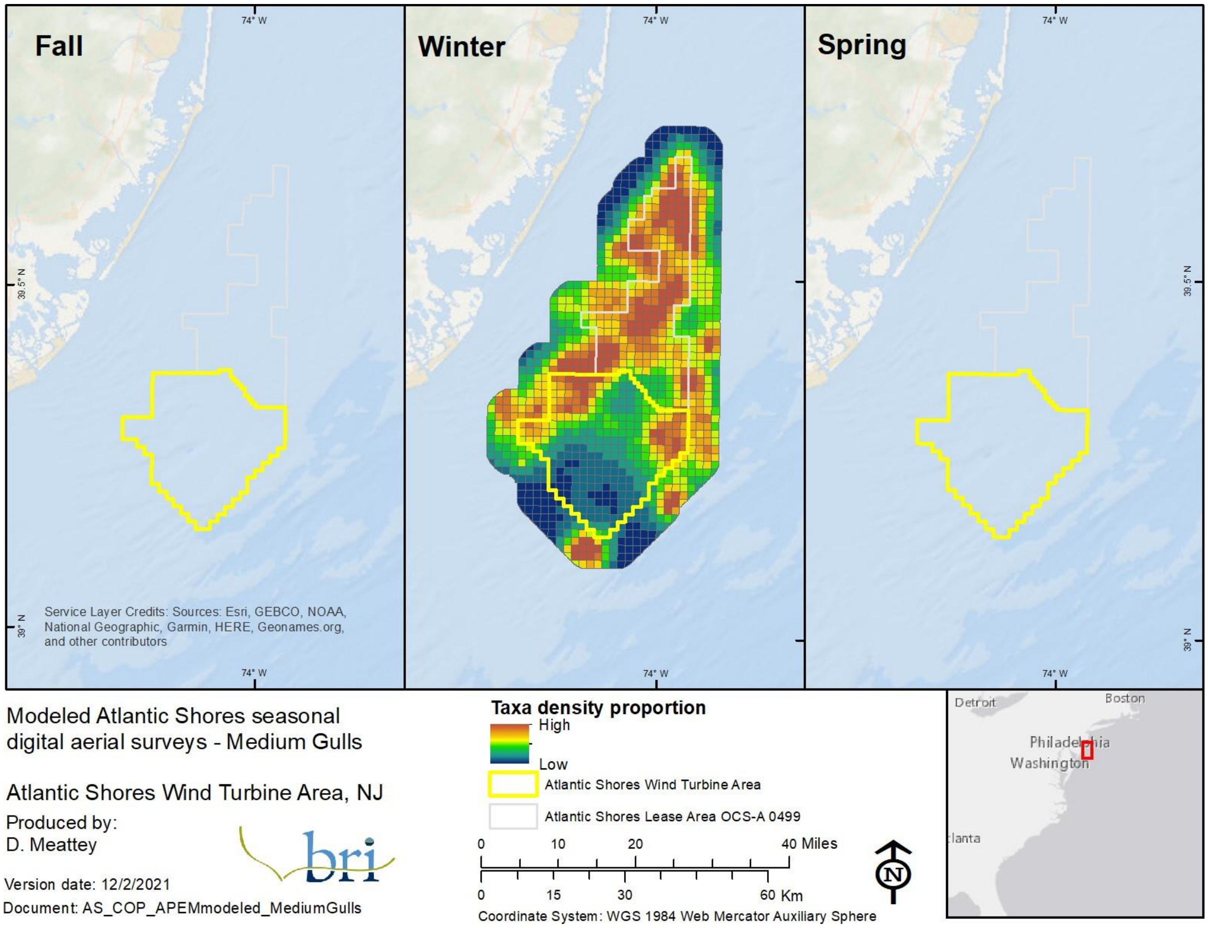

Figure 5-33: Seasonal distributions of medium gulls across the WTA and broader Lease Area, modeled from monthly digital aerial surveys carried out in the area from October 2020–May 2021.

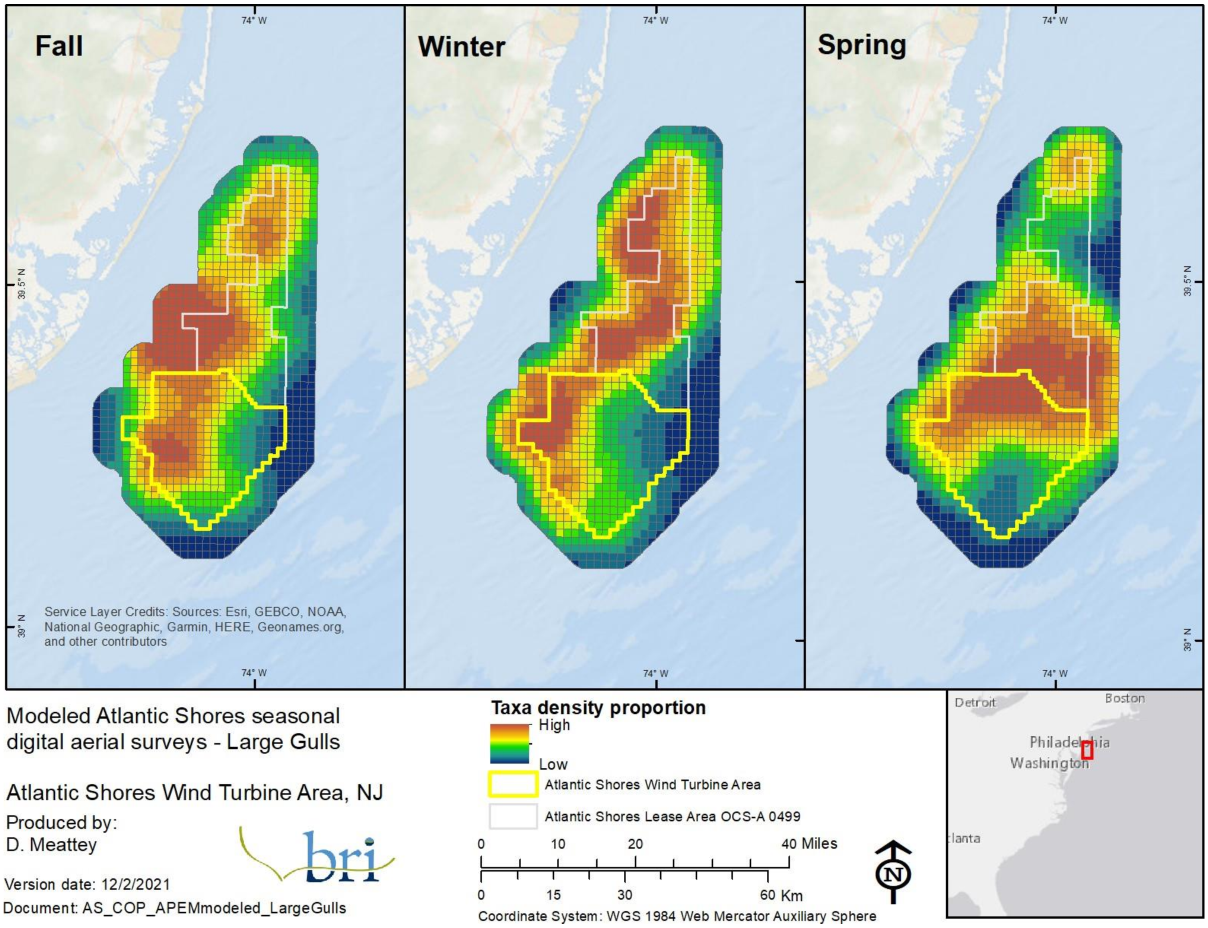

Figure 5-34: Seasonal distributions of large gulls across the WTA and broader Lease Area, modeled from monthly digital aerial surveys carried out in the area from October 2020–May 2021.

5.2.4.2 Relative Behavioral Vulnerability Figures and Tables

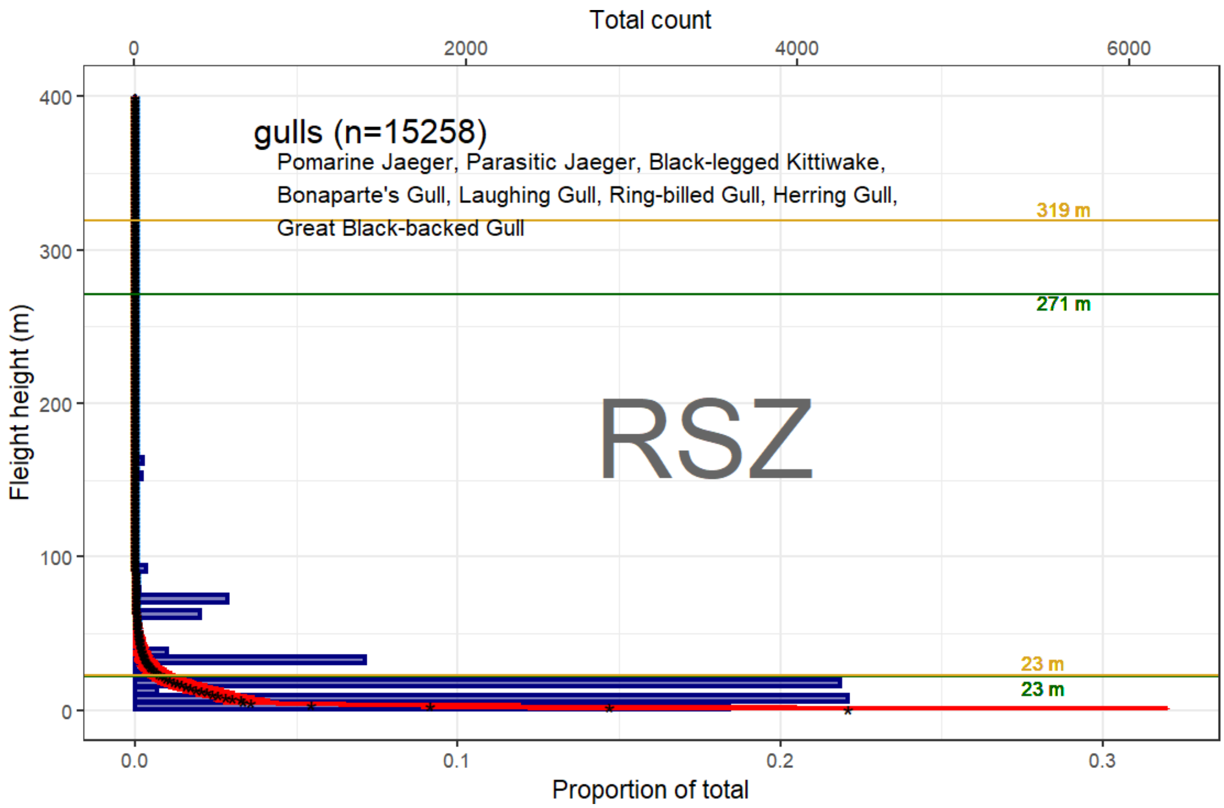

NOTE: Figure shows the actual number of birds in 5 m intervals (blue bars), and the modeled average flight height in 1 m intervals (asterisk) and the standard deviation (red lines), in relation to the upper and lower limits of the RSZ for a minimum (green: 23-271 m [75-889 ft]) and maximum WTG (gold: 23-319 m [75-1,046 ft]).

Figure 5-35: Flight heights of jaegers and gulls (m) derived from the Northwest Atlantic Seabird Catalog.

Table 5-15: Vulnerability assessment rankings by species for the gull group.

Species	Collision Vulnerability		DV	PV
	Turbine Opt. 1	Turbine Opt. 2		
Black-legged Kittiwake	low (0.43)	low (0.43)	medium (0.6)	low (0.33)
Bonaparte's Gull	low (0.43)	low (0.43)	medium (0.5)	low (0.33)
Great Black-backed Gull	medium (0.6)	medium (0.6)	medium (0.7)	minimal (0.2)
Herring Gull	medium (0.67)	medium (0.67)	medium (0.5)	medium (0.53)
Laughing Gull	medium (0.53)	medium (0.53)	medium (0.5)	low (0.4)
Ring-billed Gull	medium (0.6)	medium (0.6)	low (0.4)	low (0.33)
Parasitic Jaeger	medium (0.57)	medium (0.57)	low (0.3)	low (0.4)
Pomarine Jaeger	medium (0.67)	medium (0.67)	low (0.3)	low (0.4)

5.2.5 Terns

5.2.5.1 Exposure Tables, Maps, and Figures

Table 5-16: Seasonal exposure rankings for the tern group.

Species	Season	Local Rank	Regional Rank	Total Rank	Exposure Score
Least Tern	Winter	0	·	0	minimal
	Spring	0	·	0	minimal
	Summer	0	0	0	minimal
	Fall	0	0	0	minimal
Caspian Tern	Winter	0	·	0	minimal
	Spring	0	·	0	minimal
	Summer	0	·	0	minimal
	Fall	0	·	0	minimal
Black Tern	Winter	0	·	0	minimal
	Spring	0	·	0	minimal
	Summer	0	·	0	minimal
	Fall	0	·	0	minimal
Common Tern	Winter	0	·	0	minimal
	Spring	1	3	4	medium
	Summer	0	2	2	low
	Fall	0	1	1	low
Forster's Tern	Winter	0	·	0	minimal
	Spring	0	·	0	minimal
	Summer	0	·	0	minimal
	Fall	0	·	0	minimal
Royal Tern	Winter	0	·	0	minimal
	Spring	0	0	0	minimal
	Summer	0	0	0	minimal
	Fall	0	0	0	minimal

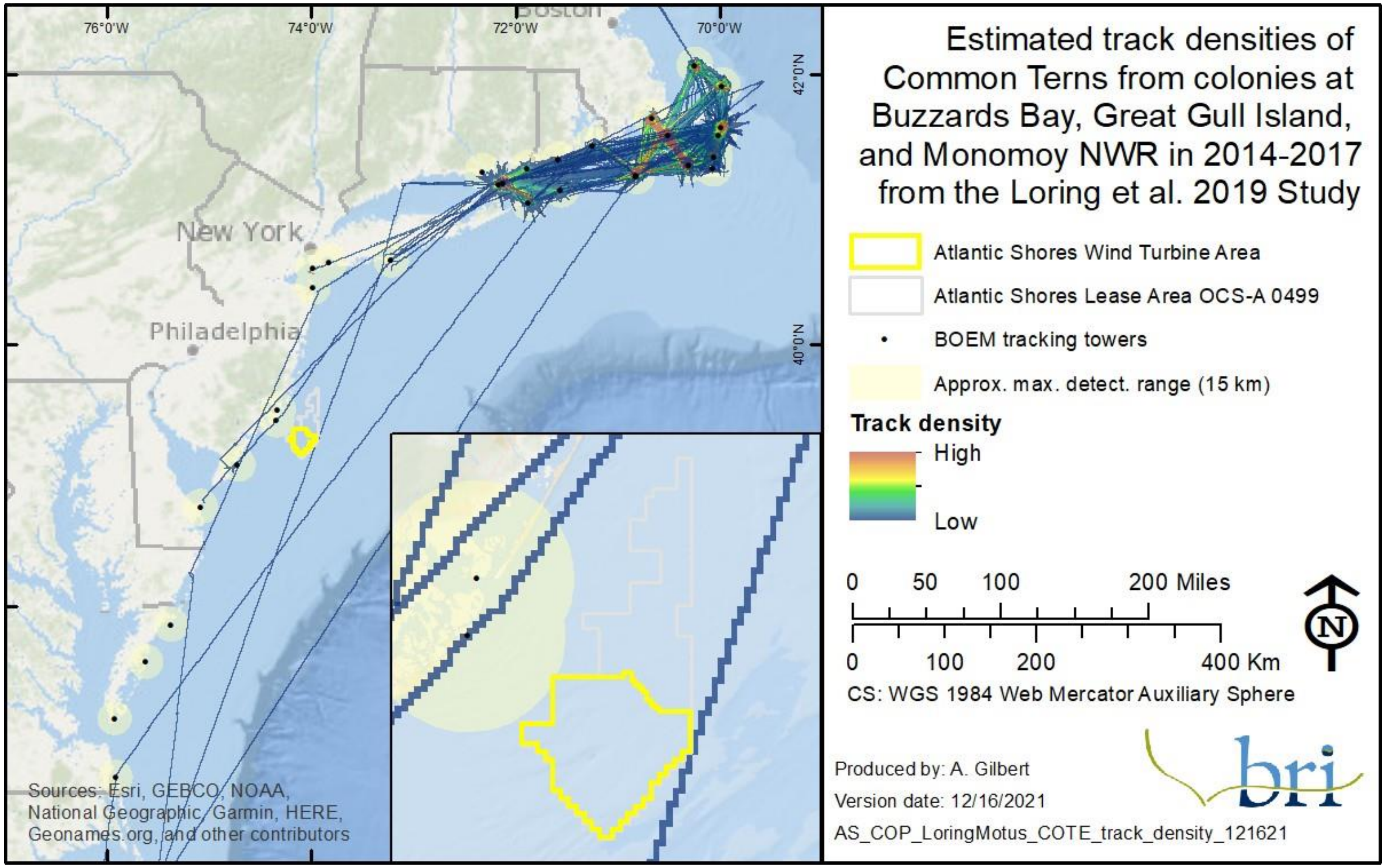

NOTE: All data are not actual flight paths but interpolated (model generated) flight paths. Flight paths were modeled by detections of movements between land-based towers. Towers had a typical detection range < 15 km, so birds were only detected when flying within approximately 15 km of one of the towers. (See Fig 5 [tower locations] in Loring et al. [2019] and Appendix K [detection probability] for details. Appendices are found at: https://espis.boem.gov/final%20reports/BOEM_2019-017a.pdf. Data provided by USFWS and used with permission.

Figure 5-36: Modeled flight paths of migratory Common Terns equipped with nanotags (Loring et al. 2019).

5.2.5.2 Behavioral Vulnerability Figures and Tables

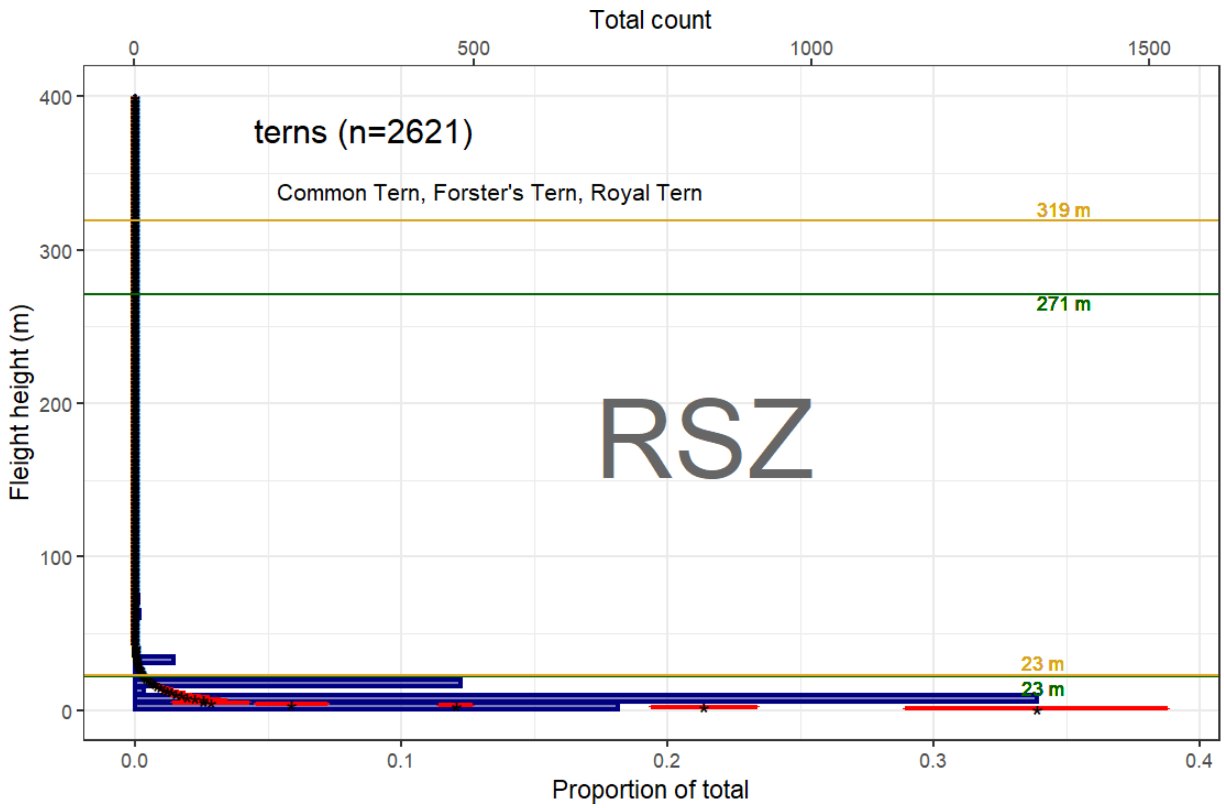

NOTE: Figure shows the actual number of birds in 5 m intervals (blue bars), and the modeled average flight height in 1 m intervals (asterisk) and the standard deviation (red lines), in relation to the upper and lower limits of the RSZ for a minimum (green: 23-271 m [75-889 ft]) and maximum WTG (gold: 23-319 m [75-1,046 ft]).

Figure 5-37: Flight heights of terns (m) derived from the Northwest Atlantic Seabird Catalog.

Figure 5-38: Vulnerability assessment rankings by species for the tern group.

Species	Collision Vulnerability		DV	PV
	Turbine Opt. 1	Turbine Opt. 2		
Common Tern	low (0.33)	low (0.33)	high (0.8)	medium (0.6)
Forster's Tern	low (0.47)	low (0.47)	medium (0.5)	low (0.4)
Roseate Tern	low (0.3)	low (0.3)	high (0.8)	high (0.87)
Royal Tern	low (0.43)	low (0.43)	medium (0.5)	medium (0.53)

5.2.5.3 Federally Endangered Tern Species

5.2.5.4 Roseate Tern

5.2.5.5 Exposure Tables, Maps, and Figures

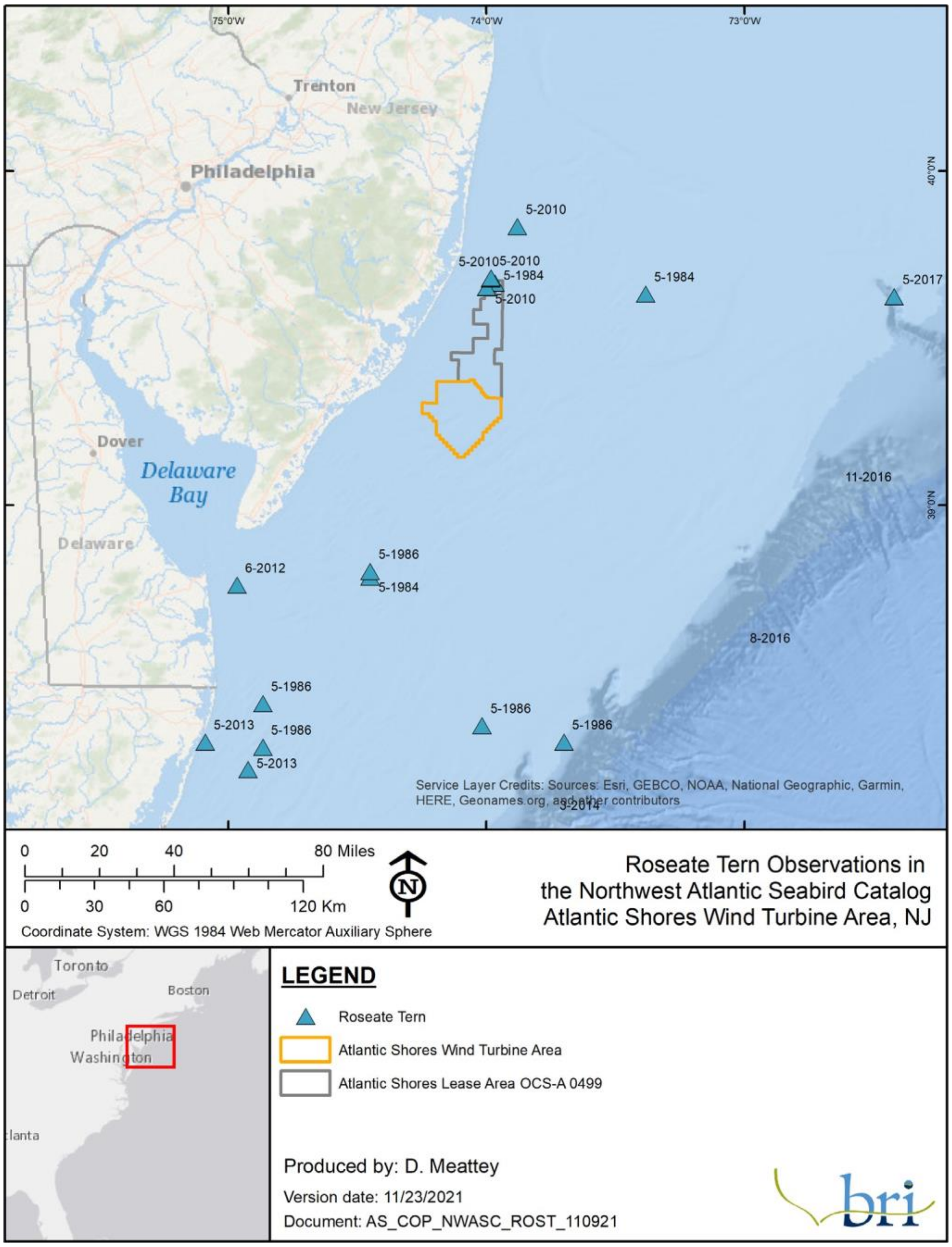

Figure 5-39: Roseate Tern observations from the Northwest Atlantic Seabird Catalog. Data provided by NOAA and used with permission.

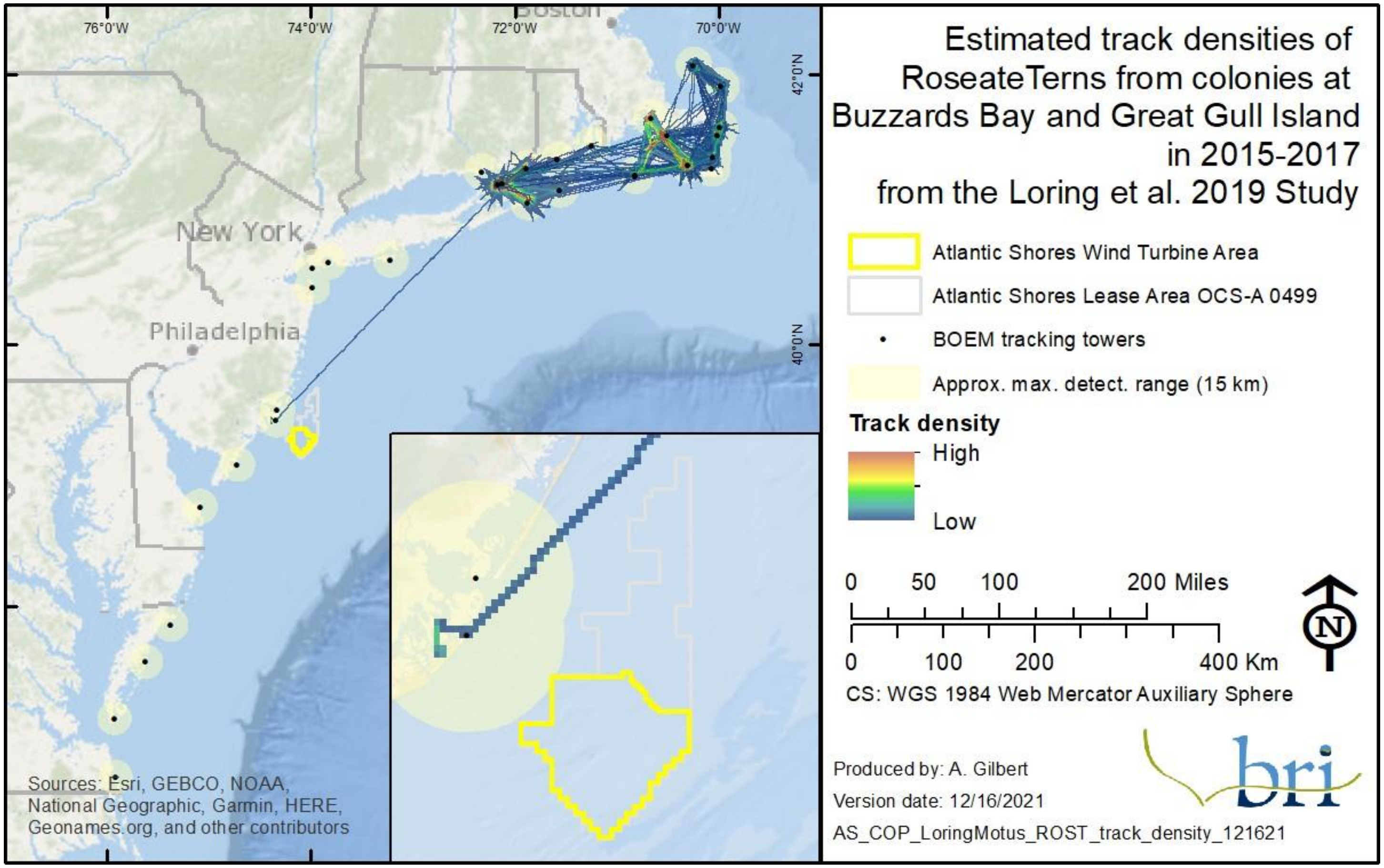

NOTE: All data are not actual flight paths but interpolated (model generated) flight paths. Flight paths were modeled by detections of movements between land-based towers. Towers had a typical detection range < 15 km, so birds were only detected when flying within approximately 15 km of one of the towers. (See Fig 5 [tower locations] in Loring et al. [2019] and Appendix K [detection probability] for details. Appendices are found at: https://espis.boem.gov/final%20reports/BOEM_2019-017a.pdf. Data provided by USFWS and used with permission.

Figure 5-40: Modeled flight paths of migratory Roseate Terns equipped with nanotags (Loring et al. 2019).

5.2.5.5.1 Relative Behavioral Vulnerability Figures and Tables

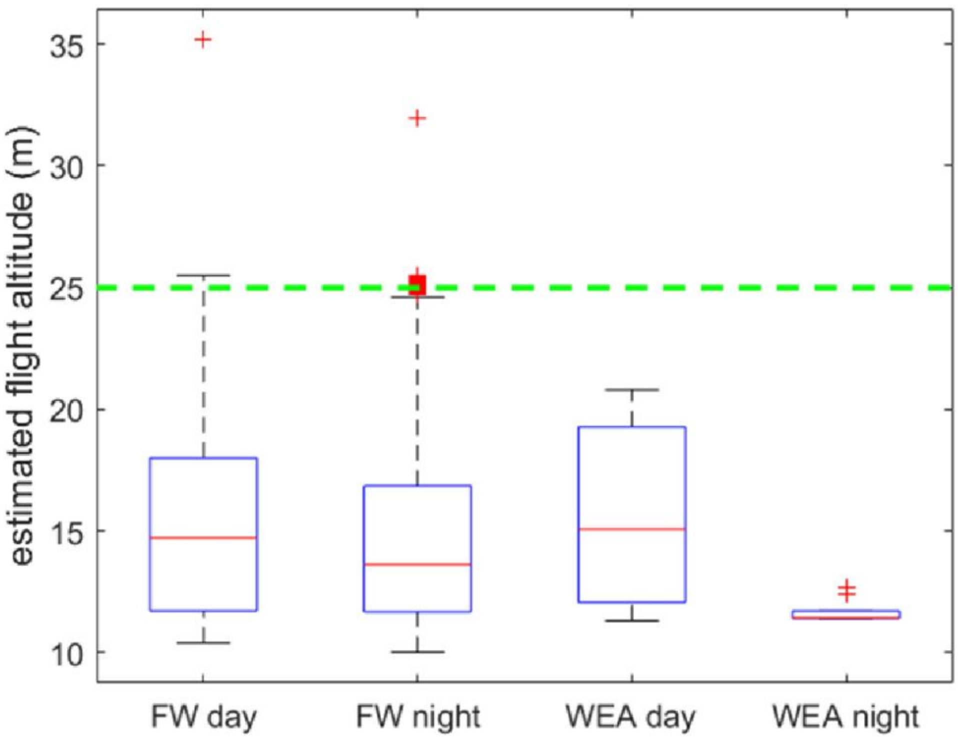

NOTE: During exposure to federal waters and Atlantic OCS WEAs during day and night. The green-dashed line represents the lower limit of an idealized RSZ used in the study (25 m [82 ft]; from Loring et al. [2019]).

Figure 5-41: Model-estimated flight altitude ranges (m) of Roseate Terns.

5.2.6 Auks

5.2.6.1 Exposure Tables, Maps, and Figures

Table 5-17: Seasonal exposure rankings for the auk group.

Species	Season	Local Rank	Regional Rank	Total Rank	Exposure Score
Dovekie	Winter	0	0	0	minimal
	Spring	1	0	1	low
	Summer	0	0	0	minimal
	Fall	0	0	0	minimal
Common Murre	Winter	0	0	0	minimal
	Spring	0	0	0	minimal
	Summer	0	·	0	minimal
	Fall	0	·	0	minimal
Thick-billed Murre	Winter	0	0	0	minimal
	Spring	0	0	0	minimal
	Summer	0	·	0	minimal
	Fall	0	·	0	minimal
Razorbill	Winter	2	1	3	medium
	Spring	1	1	2	low
	Summer	0	0	0	minimal
	Fall	0	0	0	minimal
Black Guillemot	Winter	0	·	0	minimal
	Spring	0	·	0	minimal
	Summer	0	0	0	minimal
	Fall	0	·	0	minimal
Atlantic Puffin	Winter	3	0	3	medium
	Spring	0	0	0	minimal
	Summer	0	0	0	minimal
	Fall	0	0	0	minimal

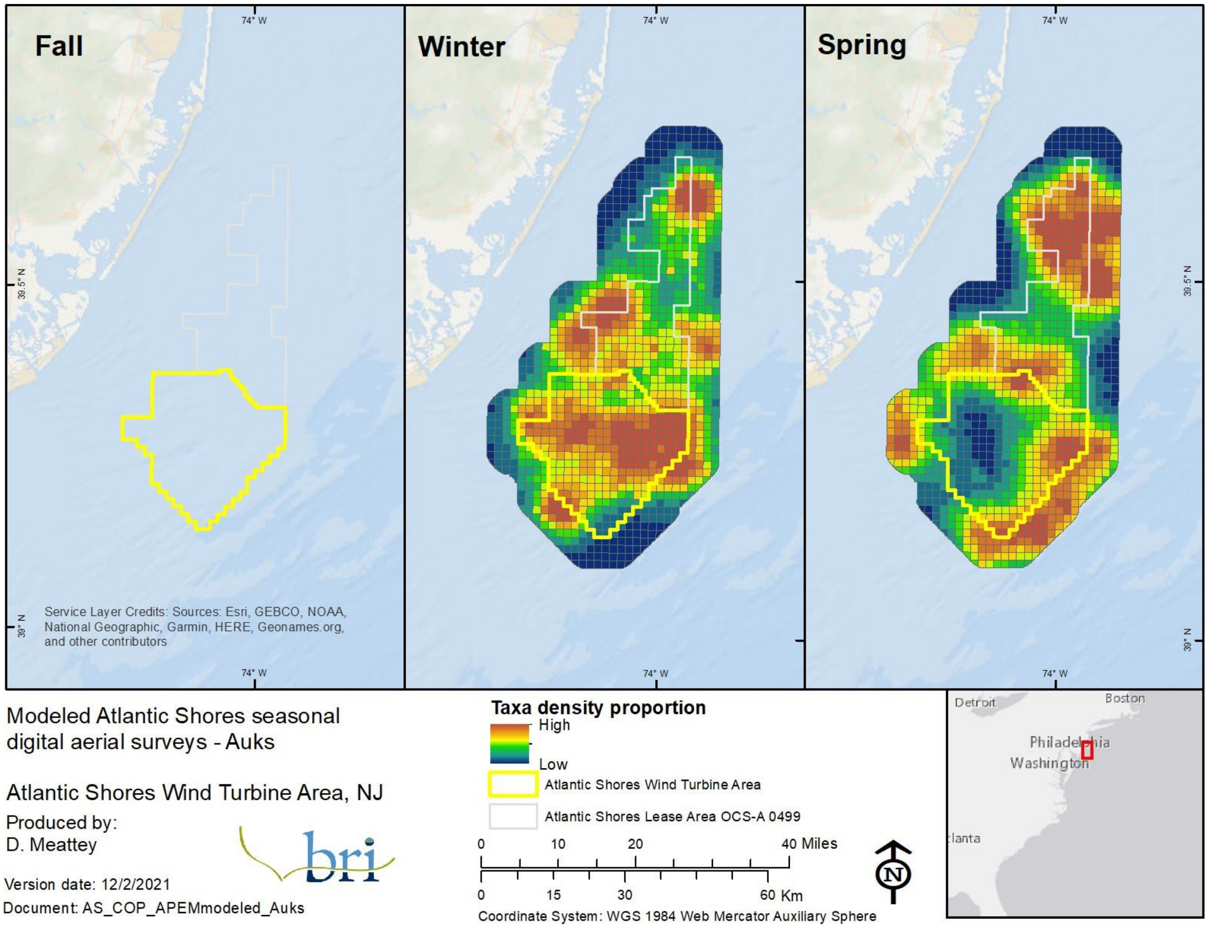

Figure 5-42: Seasonal distributions of auks across the WTA and broader Lease Area, modeled from monthly digital aerial surveys carried out in the area from October 2020–May 2021.

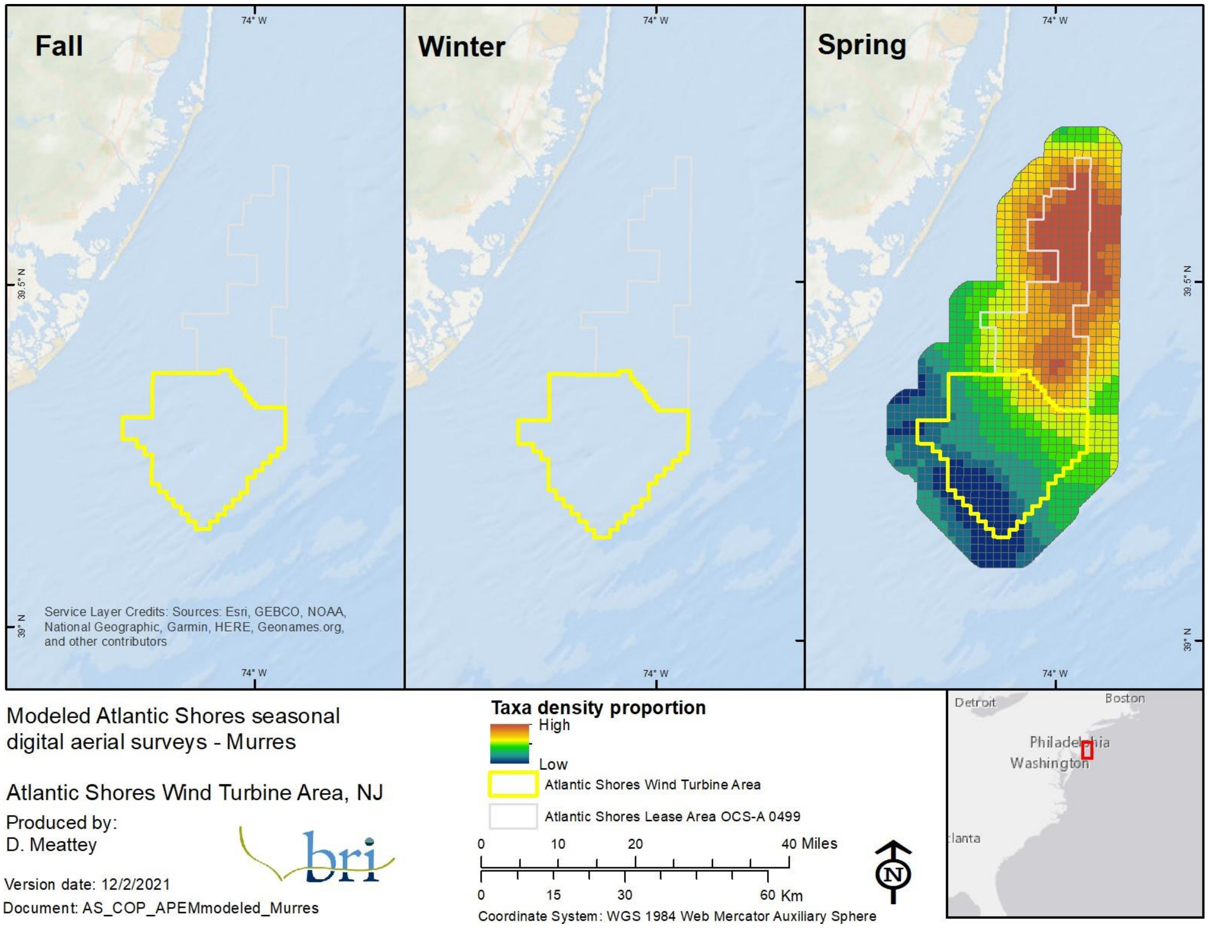

Figure 5-43: Seasonal distributions of murres across the WTA and broader Lease Area, modeled from monthly digital aerial surveys carried out in the area from October 2020–May 2021.

5.2.6.2 *Relative Behavioral Vulnerability Figures and Tables*

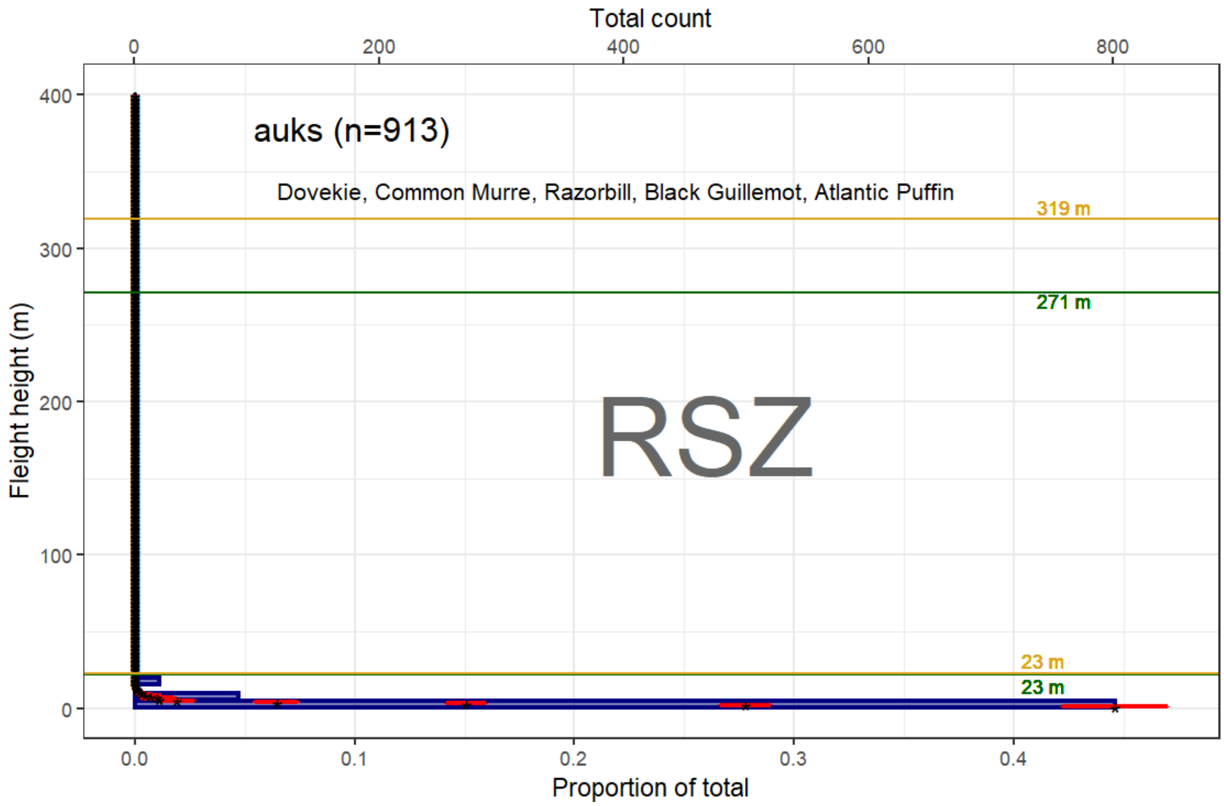

NOTE: Figure shows the actual number of birds in 5 m intervals (blue bars), and the modeled average flight height in 1 m intervals (asterisk) and the standard deviation (red lines), in relation to the upper and lower limits of the RSZ for a minimum (green: 23-271 m [75-889 ft]) and maximum WTG (gold: 23-319 m [75-1,046 ft]).

Figure 5-44: Flight heights of auks (m) derived from the Northwest Atlantic Seabird Catalog.

Table 5-18: Vulnerability assessment rankings by species for the auk group.

Species	Collision Vulnerability		DV	PV
	Turbine Opt. 1	Turbine Opt. 2		
Atlantic Puffin	minimal (0.2)	minimal (0.2)	high (0.8)	medium (0.53)
Black Guillemot	low (0.33)	low (0.33)	high (0.9)	low (0.4)
Common Murre	low (0.27)	low (0.27)	high (0.8)	low (0.4)
Dovekie	low (0.27)	low (0.27)	medium (0.7)	low (0.4)
Razorbill	minimal (0.23)	minimal (0.23)	high (0.8)	medium (0.6)

6 References

Adams J, Kelsey EC, Felis J, Pereksta DM. 2016. Collision and displacement vulnerability among marine birds of the California Current System associated with offshore wind energy infrastructure. U.S. Geological Survey Open-File Report 2016-1154.

Anderson JR. 1976. A Land Use and Land Cover Classification System For Use WIth Remote Sensor Data. Vol. 964. US Government Printing Office.

Bachl FE, Lindgren F, Borchers DL, Illian JB. 2019. inlabru: an R package for Bayesian spatial modelling from ecological survey data. Methods Ecol Evol. 10(6):760–766. doi:10.1111/2041-210X.13168. [accessed 2021 Nov 22]. https://onlinelibrary.wiley.com/doi/full/10.1111/2041-210X.13168.

Band W. 2012. Using a collision risk model to assess bird collision risk for offshore windfarms. Report commissioned by The Crown Estate, through the British Trust for Ornithology, via its Strategic Ornithological Support Services, Project SOSS-02. http://www.bto.org/sites/default/files/u28/downloads/Projects/Final_Report_SOSS02_Band1ModelGuidance.pdf.

Bolduc F, Fifield DA. 2017. Seabirds at-sea surveys: The line-transect method outperforms the point-transect alternative. Open Ornithol J. 10(1):42–52. doi:10.2174/1874453201710010042.

Bradbury G, Trinder M, Furness B, Banks AN, Caldow RWG, Hume D. 2014. Mapping seabird sensitivity to offshore wind farms. PLoS One. 9(9):e106366. doi:10.1371/journal.pone.0106366.

Buckland ST, Anderson DR, Burnham KP, Laake JL, Borchers DL, Thomas L. 2001. Introduction to distance sampling: estimating abundance of biological populations. Oxford, UK: Oxford University Press.

Camphuysen KCJ, Fox TAD, Mardik LMF, Petersen IK. 2004. Toward standardised seabirds at sea census techniques in connection with environmental impact assessments for offshore wind farms in the U.K. COWRIE BAM 02-2002. Report by Royal Netherlands Institute for Sea Research and the Danish National Environmental Research Institute to Crown Estate Commissioners, London, UK. 38 pp. http://www.thecrownestate.co.uk/1352_bird_survey_phase1_final_04_05_06.pdf.

Chamberlain DE, Rehfisch MR, Fox AD, Desholm M, Anthony SJ. 2006. The effect of avoidance rates on bird mortality predictions made by wind turbine collision risk models. Ibis (Lond 1859). 148:198–202. doi:10.1111/j.1474-919X.2006.00507.x.

Cook ASCP, Humphreys EM, Bennet F, Masden EA, Burton NHK. 2018. Quantifying avian avoidance of offshore wind turbines: Current evidence and key knowledge gaps. Mar Environ Res. 140:278–288. doi:https://doi.org/10.1016/j.marenvres.2018.06.017.

http://www.sciencedirect.com/science/article/pii/S014111361830179X.

Cook ASCP, Johnston A, Wright LJ, Burton NHK. 2012. A Review of Flight Heights and Avoidance Rates of Birds in Relation to Offshore Wind Farms. BTO Research Report Number 618. British Trust for Ornithology, Thetford, UK. 61 pp. http://www.bto.org/sites/default/files/u28/downloads/Projects/Final_Report_SOSS02_BTOReview.pdf.

Curtice C, Cleary J, Scumchenia E, Halpin PN. 2019. Marine-life Data and Analysis Team (MDAT) technical report on the methods and development of marine-life data to support regional ocean planning and management. Prepared on behalf of the Marine-life Data and Analysis Team (MDAT).

Desholm M. 2009. Avian sensitivity to mortality: Prioritising migratory bird species for assessment at proposed wind farms. J Environ Manage. 90(8):2672–2679.

DeSorbo CR, Gilpatrick L, Persico C, Hanson W. 2018. Pilot Study: Establishing a Migrant Raptor Research Station at the Naval and Telecommunications Area Master Station Atlantic Detachment Cutler, Cutler Maine. Biodiversity Research Institute, Portland, Maine. 6 pp.

DeSorbo CR, Persico C, Gilpatrick L. 2018. Studying migrant raptors using the Atlantic Flyway. Block Island Raptor Research Station, Block Island, RI: 2017 season. BRI Report # 2018-12 submitted to The Nature Conservancy, Block Island, Rhode Island, and The Bailey Wildlife Foundation, Cambridge, Massachusetts. Biodiversity Research Institute, Portland, Maine. 35 pp.

DeSorbo CR, Wright KG, Gray R. 2012. Bird Migration Stopover Sites: Ecology of Nocturnal and Diurnal Raptors at Monhegan Island. Report BRI 2012-09 submitted to the Maine Outdoor Heritage Fund, Pittston, Maine, and the Davis Conservation Foundation, Yarmouth, Maine. Biodiversity Research Institute, Gorham, Maine. 43 pp. http://www.briloon.org/raptors/monhegan.

Douglas DC, Weinzierl R, Davidson SC, Kays R, Wikelski M, Bohrer G. 2012. Moderating Argos location errors in animal tracking data. Methods Ecol Evol. 3(6):999–1007. doi:10.1111/j.2041-210X.2012.00245.x.

Fliessbach KL, Borkenhagen K, Guse N, Markones N, Schwemmer P, Garthe S. 2019. A ship traffic disturbance vulnerability index for Northwest European seabirds as a tool for marine spatial planning. Front Mar Sci. 6:192.

Fox AD, Desholm M, Kahlert J, Christensen TK, Petersen IK. 2006. Information needs to support environmental impact assessment of the effects of European marine offshore wind farms on birds. Ibis (Lond 1859). 148:129–144. doi:10.1111/j.1474-919X.2006.00510.x.

Fuglstad GA, Simpson D, Lindgren F, Rue H. 2018. Constructing Priors that Penalize the Complexity of Gaussian Random Fields. https://doi.org/101080/0162145920171415907. 114(525):445–452. doi:10.1080/01621459.2017.1415907. [accessed 2021 Nov 22].

https://www.tandfonline.com/doi/abs/10.1080/01621459.2017.1415907.

Furness RW, Wade HM, Masden EA. 2013. Assessing vulnerability of marine bird populations to offshore wind farms. J Environ Manage. 119:56–66. doi:10.1016/j.jenvman.2013.01.025. http://dx.doi.org/10.1016/j.jenvman.2013.01.025.

Garthe S, Hüppop O. 2004. Scaling possible adverse effects of marine wind farms on seabirds: developing and applying a vulnerability index. J Appl Ecol. 41(4):724–734. doi:10.1111/j.0021-8901.2004.00918.x.

Geo-Marine. 2010. Ocean/Wind Power Ecological Baseline Studies, January 2008 - December 2009 - Final Report. Volume II: Avian Studies. Geo-Marine, Inc., Plano, TX. 2109 pp.

Goodale MW, Stenhouse IJ. 2016. A conceptual model to determine vulnerability of wildlife populations to offshore wind energy development. Human-Wildlife Interact. 10(1):53–61. doi:10.26077/1d31-m472.

Heiser E, Davis C. 2020. Piping Plover Nesting Results in New Jersey: 2020. Conserve Wildlife Foundation of New Jersey & New Jersey Division of Fish and Wildlife Endangered and Nongame Species Program.

Horton TW, Bierregaard RO, Zawar-Reza P, Holdaway RN, Sagar P. 2014. Juvenile Osprey navigation during trans-oceanic migration. PLoS One. 9(12). doi:10.1371/journal.pone.0114557.

Johnston A, Cook ASCP, Wright LJ, Humphreys EM, Burton NHK. 2014. Modelling flight heights of marine birds to more accurately assess collision risk with offshore wind turbines. J Appl Ecol. 51(1):31–41. doi:10.1111/1365-2664.12191.

Kelsey EC, Felis JJ, Czapanskiy M, Pereksta DM, Adams J. 2018. Collision and displacement vulnerability to offshore wind energy infrastructure among marine birds of the Pacific Outer Continental Shelf. J Environ Manage. 227:229–247. doi:10.1016/j.jenvman.2018.08.051.

Krainski E, Gómez-Rubio V, Bakka H, Lenzi A, Castro-Camilo D, Simpson D, Lindgren F, Rue H. 2018 Dec 7. Advanced Spatial Modeling with Stochastic Partial Differential Equations Using R and INLA. Adv Spat Model with Stoch Partial Differ Equations Using R INLA. doi:10.1201/9780429031892. [accessed 2021 Nov 22]. https://www.taylorfrancis.com/books/mono/10.1201/9780429031892/advanced-spatial-modeling-stochastic-partial-differential-equations-using-inla-elias-krainski-virgilio-gómez-rubio-haakon-bakka-amanda-lenzi-daniela-castro-camilo-daniel-simpson-finn-lindgren-.

Kranstauber B, Kays R, Lapoint SD, Wikelski M, Safi K. 2012. A dynamic Brownian bridge movement model to estimate utilization distributions for heterogeneous animal movement. J Anim Ecol. 81(4):738–46. doi:10.1111/j.1365-2656.2012.01955.x.

Kranstauber B, Smolla M. 2016. Move: Visualizing and Analyzing Animal Track Data. R package version 2.1.0. https://cran.r-project.org/package=move.

Krijgsveld KL, Fljn RC, Japink M, van Horssen PW, Heunks C, Collier MP, Poot MJM, Beuker D, Birksen S. 2011. Effect Studies Offshore Wind Farm Egmond aan Zee: Final Report on Fluxes, Flight Altitudes and Behaviour of Flying Birds. Bureau Waardenburg report no. 10-219. Institute for Marine Resources & Ecosystem Studies, Wageningen UR, Netherlands.

Lindgren F, Rue H. 2015. Bayesian Spatial Modelling with R - INLA . J Stat Softw. 63(19). doi:10.18637/jss.v063.i19.

Lindgren F, Rue H, Lindstrom J. 2011. An explicit link between gaussian fields and gaussian Markov random fields: the stochastic partial differential equation approach (with discussion). J R Stat Soc B. 73(4):423–498. doi:10.1111/j.1467-9868.2011.00777.x.

Loring P, Goyert H, Griffin C, Sievert P, Paton P. 2017. Tracking Movements of Common Terns, Endangered Roseate Terns, and Threatened Piping Plovers in the Northwest Atlantic. 2017 Annual Report to the Bureau of Ocean Energy Management. US Fish and Wildlife Service, Hadley, MA. 134 pp.

Loring PH, McLaren JD, Smith PA, Niles LJ, Koch SL, Goyert HF, Bai H. 2018. Tracking Movements of Threatened Migratory rufa Red Knots in U.S. Atlantic Outer Continental Shelf Waters. OCS Study BOEM 2018-046. U.S. Department of the Interior, Bureau of Ocean Energy Management, Sterling, VA. 145 pp.

Loring PH, Paton PWC, McLaren JD, Bai H, Janaswamy R, Goyert HF, Griffin CR, Sievert PR. 2019. Tracking offshore occurrence of Common Terns, endangered Roseate Terns, and threatened Piping Plovers with VHF arrays. OCS Study BOEM 2019-017. US Department of the Interior, Bureau of Ocean Energy Management, Sterling, VA. 140 pp. https://espis.boem.gov/final reports/BOEM_2019-017.pdf.

Loring PH, Paton PWC, Osenkowski JE, Gilliland SG, Savard J-PL, Mcwilliams SR. 2014. Habitat use and selection of black scoters in southern New England and siting of offshore wind energy facilities. J Wildl Manage. 78(4):645–656. doi:10.1002/jwmg.696.

Martell MS, Douglas D. 2019. Data from: Fall migration routes, timing, and wintering sites of North American Ospreys as determined by satellite telemetry. Movebank Data Repos. doi:doi:10.5441/001/1.sv6335t3.

Martell MS, Henny CJ, Nye PE, Solensky MJ. 2001. Fall migration routes, timing, and wintering sites of North American Ospreys as determined by satellite telemetry. Condor. 103(4):715–724. doi:doi:10.1650/0010-5422(2001)103[0715:FMRTAW]2.0.CO;2 url:https://sora.unm.edu/node/54078.

Masden EA. 2019. Avian Stochastic CRM v2.3.1.

Masden EA, McCluskie A, Owen E, Langston RHW. 2015. Renewable energy developments in an uncertain world: The case of offshore wind and birds in the UK. Mar Policy. 51:169–172. doi:https://doi.org/10.1016/j.marpol.2014.08.006.

Meattey DE, Mcwilliams SR, Paton PWC, Lepage C, Gilliland SG, Savoy L, Olsen GH, Osenkowski JE. 2019. Resource selection and wintering phenology of White-winged Scoters in southern New England : Implications for offshore wind energy development. 121:1–18. doi:10.1093/condor/duy014.

Meattey DE, McWilliams SR, Paton PWC, Lepage C, Gilliland SG, Savoy L, Olsen GH, Osenkowski JE. 2018. Annual cycle of White-winged Scoters (*Melanitta fusca*) in eastern North America: migratory phenology, population delineation, and connectivity. Can J Zool. 96:1353–1365.

Møller J, Waagepetersen RP. 2007. Modern Statistics for Spatial Point Processes*. Scand J Stat. 34(4):643–684. doi:10.1111/J.1467-9469.2007.00569.X. [accessed 2021 Nov 22]. https://onlinelibrary.wiley.com/doi/full/10.1111/j.1467-9469.2007.00569.x.

Panjabi AO, Easton WE, Blancher PJ, Shaw AE, Andres BA, Beardmore CJ, Camfield AF, Demarest DW, Dettmers R, Keller RH, et al. 2019. Avian Conservation Assessment Database Handbook, Version 2019. Partners in Flight Technical Series No. 8. Available from pif.birdconservancy.org/acad_handbook.pdf.

R Core Team. 2020. R: a language and environment for statistical computing. http://www.r-project.org.

Rue H, Martino S, Chopin N. 2009. Approximate Bayesian inference for latent Gaussian models using integrated nested Laplace approximations (with discussion). J R Stat Soc B. 71:319–392. doi:10.1111/j.1467-9868.2008.00700.x.

SDJV. 2015. Atlantic and Great Lakes Sea Duck Migration Study: progress report June 2015.

Skov H, Heinanen S, Norman T, Ward RM, Mendez-Roldan S, Ellis I. 2018. ORJIP Bird Collision and Avoidance Study. Final Report - April 2018. Report by NIRAS and DHI to The Cabon Trust, U.K. 247 pp.

Sollmann R, Gardner B, Williams KA, Gilbert AT, Veit RR. 2016. A hierarchical distance sampling model to estimate abundance and covariate associations of species and communities. Methods Ecol Evol. 7(5):529–537.

Spiegel CS, Berlin AM, Gilbert AT, Gray CO, Montevecchi WA, Stenhouse IJ, Ford SL, Olsen GH, Fiely JL, Savoy L, et al. 2017. Determining fine-scale use and movement patterns of diving bird species in federal waters of the Mid-Atlantic United States using satellite telemetry. OCS Study BOEM 2017-069. Department of the Interior, Bureau of Ocean Energy Management, Sterling, VA. 293 pp. https://www.boem.gov/espis/5/5635.pdf.

Stenhouse IJ, Berlin AM, Gilbert AT, Goodale MW, Gray CE, Montevecchi WA, Savoy L, Spiegel CS. 2020. Assessing the exposure of three diving bird species to offshore wind areas on the U.S. Atlantic Outer Continental Shelf using satellite telemetry. Divers Distrib. n/a(n/a). doi:10.1111/ddi.13168. https://doi.org/10.1111/ddi.13168.

Sullivan BL, Wood CL, Iliff MJ, Bonney RE, Fink D, Kelling S. 2009. eBird: A citizen-based bird observation network in the biological sciences. Biol Conserv. 142(10):2282–2292. doi:10.1016/j.biocon.2009.05.006. http://dx.doi.org/10.1016/j.biocon.2009.05.006.

Thaxter CB, Ross-Smith VH, Bouten W. 2015. Seabird – wind farm interactions during the breeding season vary within and between years: A case study of lesser black-backed gull *Larus fuscus* in the UK. Biol Conserv. 186:347–358. doi:10.1016/j.biocon.2015.03.027.

U.S. Fish and Wildlife Service. 2015. Status of the Species - Red Knot.

U.S. Fish and Wildlife Service. 2020. Information for Planning and Consultation (IPaC). Retrieved from: https://ecos.fws.gov/ipac/user/login.

Vanermen N, Onkelinx T, Courtens W, Van de walle M, Verstraete H, Stienen EWM. 2015. Seabird avoidance and attraction at an offshore wind farm in the Belgian part of the North Sea. Hydrobiologia. 756(1):51–61. doi:10.1007/s10750-014-2088-x.

Wade HM, Masden EA, Jackson AC, Furness RW. 2016. Incorporating data uncertainty when estimating potential vulnerability of Scottish seabirds to marine renewable energy developments. Mar Policy. 70:108–113. doi:10.1016/j.marpol.2016.04.045.

Walker WE, Harremoes P, Rotmans J, Van Der Sluijs JP, Van Asselt MBA, Janssen P, Krayer Von Krauss MP. 2003. Defining Uncertainty. Integr Assess. https://www.narcis.nl/publication/RecordID/oai:tudelft.nl:uuid:fdc0105c-e601-402a-8f16-ca97e9963592.

Willmott JR, Forcey G, Kent A. 2013. The Relative Vulnerability of Migratory Bird Species to Offshore Wind Energy Projects on the Atlantic Outer Continental Shelf: An Assessment Method and Database. OCS Study BOEM 2013-207. Final Report to the U.S. Department of the Interior, Bureau of Ocean Energy Management, Herndon, VA. 275 pp.

Winship AJ, Kinlan BP, White TP, Leirness JB, Christensen J. 2018. Modeling At-Sea Density of Marine Birds to Support Atlantic Marine Renewable Energy Planning: Final Report. OCS Study BOEM 2018-010. U.S. Department of the Interior, Bureau of Ocean Energy Management, Office of Renewable Energy Programs, Sterling, VA. 67 pp.

7 Applying a Community Distance Model to Correct Density Estimates of Seabirds in New Jersey Waters

Background

Boat-based surveys are a standardized methodology to describe patterns of distribution and abundance in the marine environment. A known bias in this method is that individuals further from the transect line are more difficult to detect than those closer to the center (Buckland et al. 2001). This bias causes surveyors to underestimate the total number of animals in the survey area. Importantly, this bias can be variable by species and survey conditions, where it can be challenging to compare detection-naïve density estimates among species or surveys (Camphuysen et al. 2004). Estimating detection probability for rare species can be difficult due to a lack of observations, so researchers have developed new methods for estimating detection probabilities of communities have to address this issue (Sollmann et al. 2016). These community-based methods can be beneficial for surveys of wind energy projects as they can help account for problems relating to surveys of relatively small areas or including data from rare species.

Objectives

This analysis aims to correct the density estimates for all bird species detected boat surveys in and around the project area. We used a community distance modeling approach to obtain estimates of detection probability for species groups found in the surveys. After we evaluate the efficacy of the modeling technique, we can then use these estimates to correct the estimates of total population size (or density) in the region to account for this source of bias. These estimates can then inform collision risk models or other conservation or management applications.

Methods

Boat-based survey data from New Jersey were collected as part of the New Jersey Offshore Wind Power Ecological Baseline Study (New Jersey Department of Environmental Protection) in 2008-2009. Surveys from the ‘Offshore’ and ‘Sawtooth’ protocols were selected to avoid issues in data collection that came from other surveys types in the project (e.g., coastal seawatch surveys). A distance survey protocol was implemented in these surveys (Buckland et al. 2001), where the distance from the transect line to the animal was estimated for all detected animals. A 300 m strip transect was surveyed off the boat, but animals outside the strip were also included if detected and time allowed for observation outside this primary observation area (the 300 m strip). Species were assigned a taxonomic group that ranged from multi-species ‘sea ducks’ to single species ‘gannets.’ Detections could be of individual animals or groups, and the group size was estimated for most detections.

To estimate detection probabilities for each taxonomic group, thus estimating the total population size of the group using the study area, a community distance model was parameterized in nimble (www.r-nimble.org) within R (R Core Team 2020). The observed data were parsed into transects, truncated to those less than 400 m from the transect line, then placed in eight 50 m distance bins to parameterize the model. The core of the model is a distance detection model (Buckland et al. 2001) that uses a key function to describe the change in detection probability with distance from the transect line. The community distance model generalizes this detection function across multiple species and assumes that each species has a similar functional relationship with detection probability (Sollmann et al. 2016). While Sollmann et al. (2016) uses a half-normal detection function, here we expanded their approach to also include a hazard rate function:

$$pp_{iiiii} = 1 - \exp - \frac{MM_{ii}}{\sigma\sigma_{iiii}}^{2 - \theta\theta_{jj}}$$

Where, pp_{iiiii} is the detection probability of a given distance band for survey transect *i*, species *j*, and distance band *b*; pp_{iiiiii} is the mean distance to the transect line, MM_{ii} is the distance from the middle of the distance band to the transect centerline, while $\sigma\sigma$ and $\theta\theta$ are the shape and scale parameters that vary by species and transect. These probabilities are then summed across all distance bands to determine the detection probability for a given species and transect. The general form of the community distance sampling model shares information across species using a random effects approach. This process works similarly across both half-normal and hazard detection functions, here we use a shrinkage model to share information across the hazard model shape parameter:

$$\log \sigma\sigma_{ii} = \alpha\alpha_{iiii} + \beta\beta_{iiii} XX \; \alpha\alpha_{iiii} \sim NNNNrrCCCCM(\mu\mu_{\alpha\alpha}, \sigma\sigma_{\alpha\alpha}) \; \beta\beta_{iiii} \sim NNNNrrCCCCM \mu\mu_{\beta\beta}, \sigma\sigma_{\beta\beta}$$

Where $\alpha\alpha_{ii}$ is the species j intercept for the hazard rate function and $\boldsymbol{\beta\beta_{iiii}}$ is a vector of parameters that describe relationships to a vector of covariates (**X**). Information can be shared among taxonomic groups can be shared in both the intercept and slope parameter estimates and facilitates estimation of detection probabilities even in species with small sample sizes. These data are used to calculate the detection probability for each distance band, which are then summed to estimate the detection probability for the entire survey. In this case, we do not use additional covariates to explain detection probability, and the description is present to describe future possibilities.

Finally, group size estimates are also known to be influenced by detection probability. Groups farther away from the boat tend to be underestimated, particularly if the species spends time underwater. To estimate this effect, we use a linear model:

$$\log (M_{i}) = \beta\beta_{0} + \beta\beta_{pppppppp} pp_{ii}$$

Where M_{i} is the average detection-corrected group size for transect *i* and the $\beta\beta$ parameters are either the intercept or the slope of the linear equation. However, like the detection functions, we use a shrinkage effect to share data among taxa groups:

$$\log (M_{ii}) = \beta\beta_{0ii} + \beta\beta_{pppppppp,ii} pp_{ii}$$
$$\beta\beta_{0ii} \sim NNNNrrCCCCM(\mu\mu_{gggg0}, \sigma\sigma_{gggg0})$$
$$\beta\beta_{pppppppp,ii} \sim NNNNrrCCCCM(\mu\mu_{gggg1}, \sigma\sigma_{gggg1})$$

We are now sharing information on the intercept and slope parameters across j species using the two μ and σ parameters. The mean group size when detection probability is one is estimated by adding β_0 and β_{pppp} for each species.

Once the survey specific detection probability is estimated for each taxonomic group, then a Horvitz-Thompson estimator is used to calculate the total population size for each species on each survey:

$$\hat{N}_{ki} = \frac{\bar{m}_{ki} A}{C} \frac{y_{ki}}{p_{ki}}$$

Where, $\hat{N}_{ki}$ is the estimated total population size for survey *k* and species *j*, p_{ki} is the detection probability, and $\bar{m}_{ki}$ is the average detection-corrected group size for survey *k* and species *j*. The ratio the total study area (A) over the surveyed area (a) scales the estimate to the total study area. Note that if no individuals are found on the survey, then this estimator cannot provide non-zero estimates of $\hat{N}_{ki}$. Density estimates were obtained by dividing $\hat{N}_{ki}$ by the study area (km^2).

Both half-normal and hazard detection functions were tested on the survey data. Additionally, observation data were filtered based on flight height. Initial model criticism suggested that flying birds were frequently detected 0 m from the transect line, which indicated that assumptions of distance sampling were violated (i.e., that animals were observed when first detected and randomly within the survey area). Therefore, we decided to analyze data from animals 25 m above sea level or lower to limit the issues associated with large numbers of birds detected on the transect line. Model fit was assessed using visual comparison of the detection curve and empirical data.

Results and Discussion

Model fit was variable across species using a hazard detection function. Some species showed reasonable fit (terns or gannets; Figure 7-1 and Figure 7-2), while others did not (loons; Figure 7-3). The group size model did not indicate that group size was strongly influenced by detection probability for any species.

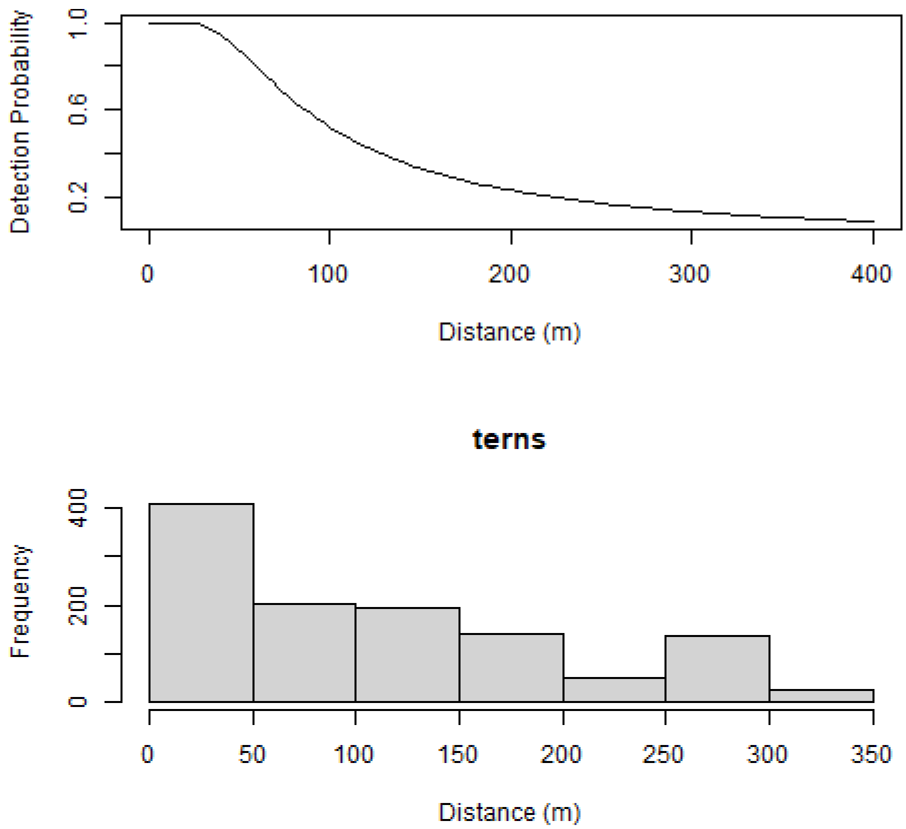

NOTE: Only birds 25 m or less from the ocean's surface were used in this analysis.

Figure 7-1: Detection curve estimated using a hazard function from a community distance sampling model (top) and a histogram of detection distances (bottom) for all tern species.

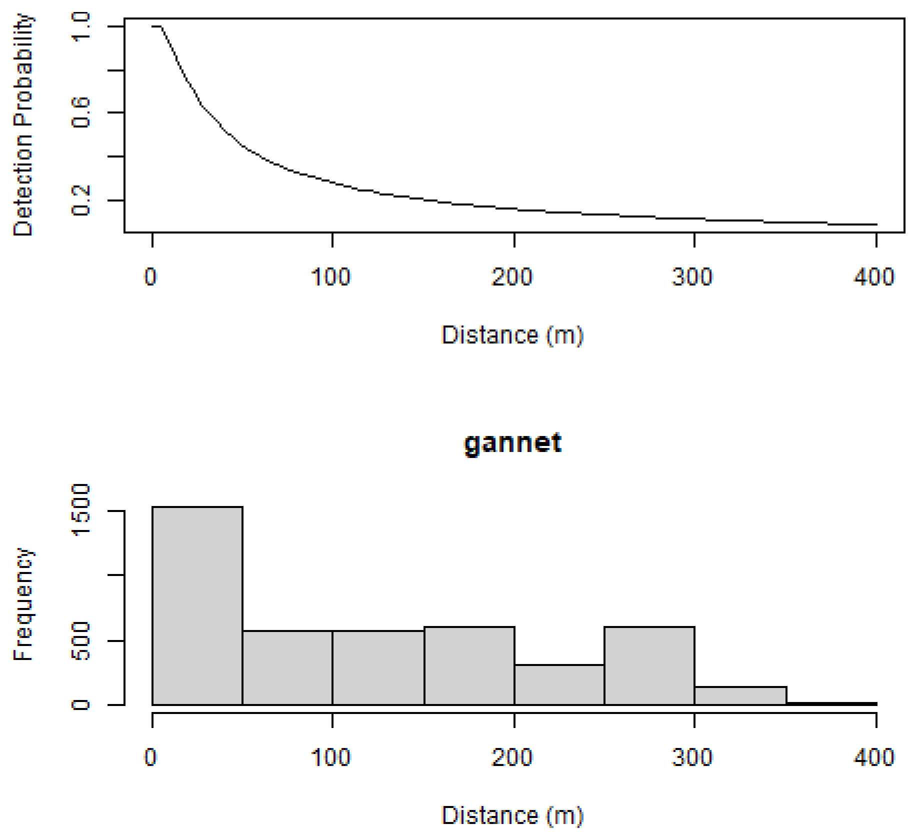

NOTE: Only birds 25 m or less from the ocean's surface were used in this analysis.

Figure 7-2: Detection curve estimated using a hazard function from a community distance sampling model (top) and a histogram of detection distances (bottom) for Northern Gannets.

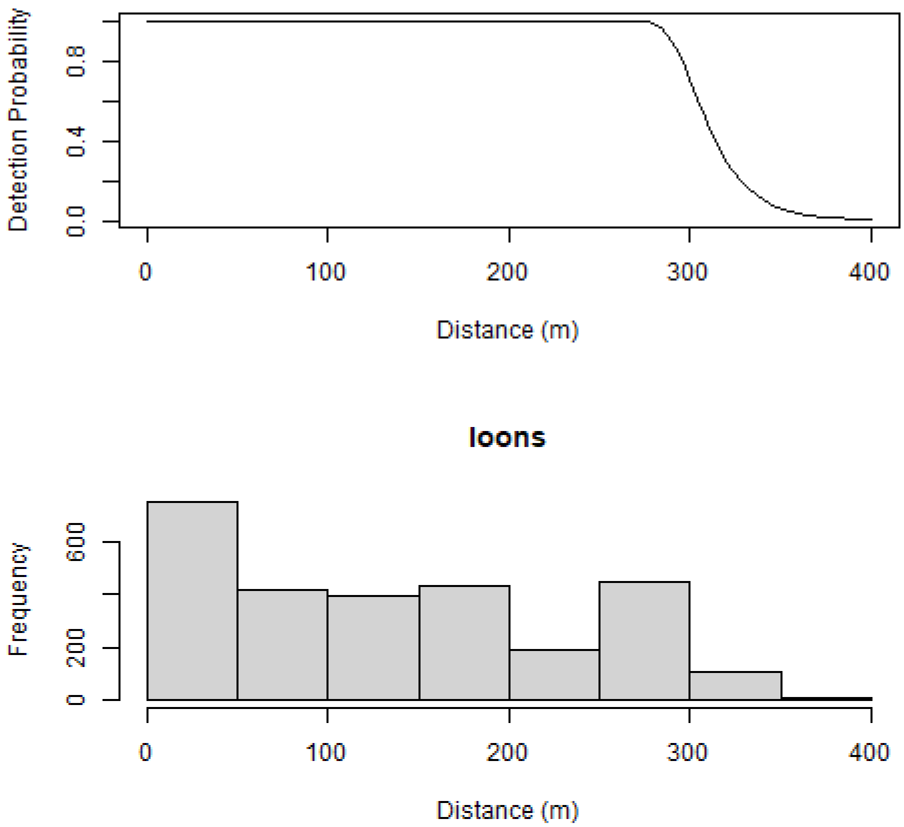

NOTE: Only birds 25 m or less from the ocean's surface were used in this analysis.

Figure 7-3: Detection curve estimated using a hazard function from a community distance sampling model (top) and a histogram of detection distances (bottom) for the two loon species.

Note with these examples the significant drop in detections from the 0-50 m range to 50-100 m. Many species showed evidence of a large number of detections on the transect line. Additionally, there is often a spike in detections from 250-300 m, which could indicate observers were underestimating the distance of the first detection to include the species in the survey area (0-300 m).

The half-normal model did not appear to fit these data well, as most species show rapid detection declines at some point in the detection curve. As such, we are not describing those results here. But the issues with this endeavor do not lie with model fit specifically, the model results also appeared to suggest that there are issues with these data. We found that detection probabilities varied significantly by species and that species that often are easy to detect (e.g., Northern Gannets) were challenging in this survey (Table 7-1). They were the second most difficult to detect taxonomic group, even more than smaller birds like terns, gulls, and sea ducks. Outside of gannets, the loon model also appeared to produce nonsensical results, with nearly

100% of loons detected within the 300 m survey strip. This outcome is extremely unlikely and these results do not make sense given what we know about these species in this region.

Table 7-1: Estimates of detection probability for each taxonomic group tested using a hazard detection function from a community distance sampling model.

Taxonomic Group	Detection Probability
Shearwaters and petrels	0.62
Gulls	0.47
Northern Gannet	0.29
Terns	0.45
Loons	0.99
Seaducks	0.35
Dabblers, geese, and swans	0.23
Shorebirds	0.20
Cormorants and pelicans	0.62
Auks	0.28

NOTE: Detection probability is estimated over a 300 m strip transect.

Taken together, these results indicate that there is an issue with the distance sampling protocols employed. It is likely that animals are not detected immediately upon entry into the study area, or there is bias in the observers' distance estimates. Further, it seems likely that some animals are attracted to the boat and likely biasing the distance estimates low. In sum, we suspect there are some significant issues with these data that make distance sampling models challenging to fit and the values that come from them possibly spurious. As such, we chose not to use these estimates of detection probability to correct the densities of seabirds in the study area.

Conclusions

While model convergence was adequate, and this modeling approach often fitted reasonable detection curves for these species groups, there are several reasons why we do not think that these results are useful for correcting density estimates. Our past experience with boat surveys suggests that Northern Gannets are one of the easiest to detect species in the region. Their large white bodies are notable in the air and on the water from a significant distance. Moreover, other issues with the data lead to equally unlikely models where detection probability was nearly perfect for 300 m for loons. Our experience with these types of data suggests that both of these outcomes are extremely unlikely. With additional time, some of these issues might be addressed to correct some of these issues, but the current state of the analysis is concerning enough for us to avoid using them at the moment.

These issues in data collection, paired with the knowledge that these data are almost 15 years out of date, we think that results from this model are not worth inclusion in the risk analysis. While there are also issues with using uncorrected density estimates from boat surveys with known distance biases, the most parsimonious solution is to use the uncorrected density estimates as this action involves the fewest number of assumptions. Future work should consider collecting more survey data from this area to update our understanding of regional seabird density patterns.

8 Analysis of NJDEP boat-based survey density estimates relative to a 15-mile offshore boundary.

In order to address recent criticism involving the placement of offshore wind development within 15 miles of shore, we conducted a brief analysis of naïve density estimates from the NJDEP boat-based surveys inside and outside the 15-mile boundary. We examined these data to determine if there was any indication of strong density differences between the NJDEP boat-based survey area and that offshore of the 15-mile boundary and as well comparing the Atlantic Shores WTA including and excluding the area inside of the 15-mile boundary. We calculated density estimates for each species where data was available, but do not present those results here. Instead, we provide a summary of the number of species within each taxa group where densities were equal, lesser, or greater between areas (NJDEP survey area vs. NJDEP survey area outside of 15 miles and WTA including 15 miles and excluding it, Table 8-1). There were no clear patterns in the results that would suggest that excluding the area shore-word of 15 miles would result in overall lower densities of animals. Depending on the taxa, some increased, some decreased, and some remained the same.

Table 8-1: Comparison of differences in naïve density estimates between NJDEP survey area vs. NJDEP survey area outside of 15 miles and WTA including 15 miles and excluding it.

Group	equal density in survey area	outside 15 miles greater density in survey area	outside 15 miles smaller density in survey area	equal density in WTA	outside 15 miles greater density in WTA	outside 15 miles smaller density in WTA
Dabblers, Geese, and Swans	NA	4	7	10	1	NA
Sea ducks	NA	1	6	3	4	NA
Coastal Diving Ducks	1	2	NA	2	1	NA
Loons	NA	1	2	NA	3	NA
Grebes	NA	NA	1	1	NA	NA
Herons and Egrets	NA	NA	2	2	NA	NA
Shearwaters and Petrels	6	2	1	5	2	2
Gannet	NA	NA	1	NA	NA	1
Cormorants and Pelicans	NA	NA	3	2	NA	1
Gulls	1	5	6	4	4	4
Terns	1	NA	5	1	1	4
Auks	2	2	2	2	2	2
Shorebirds	4	6	4	12	2	NA
Raptors	2	NA	NA	2	NA	NA
Passerines	9	8	8	13	7	5

9 Birds – Offshore: Seasonal Maps

Table of Maps

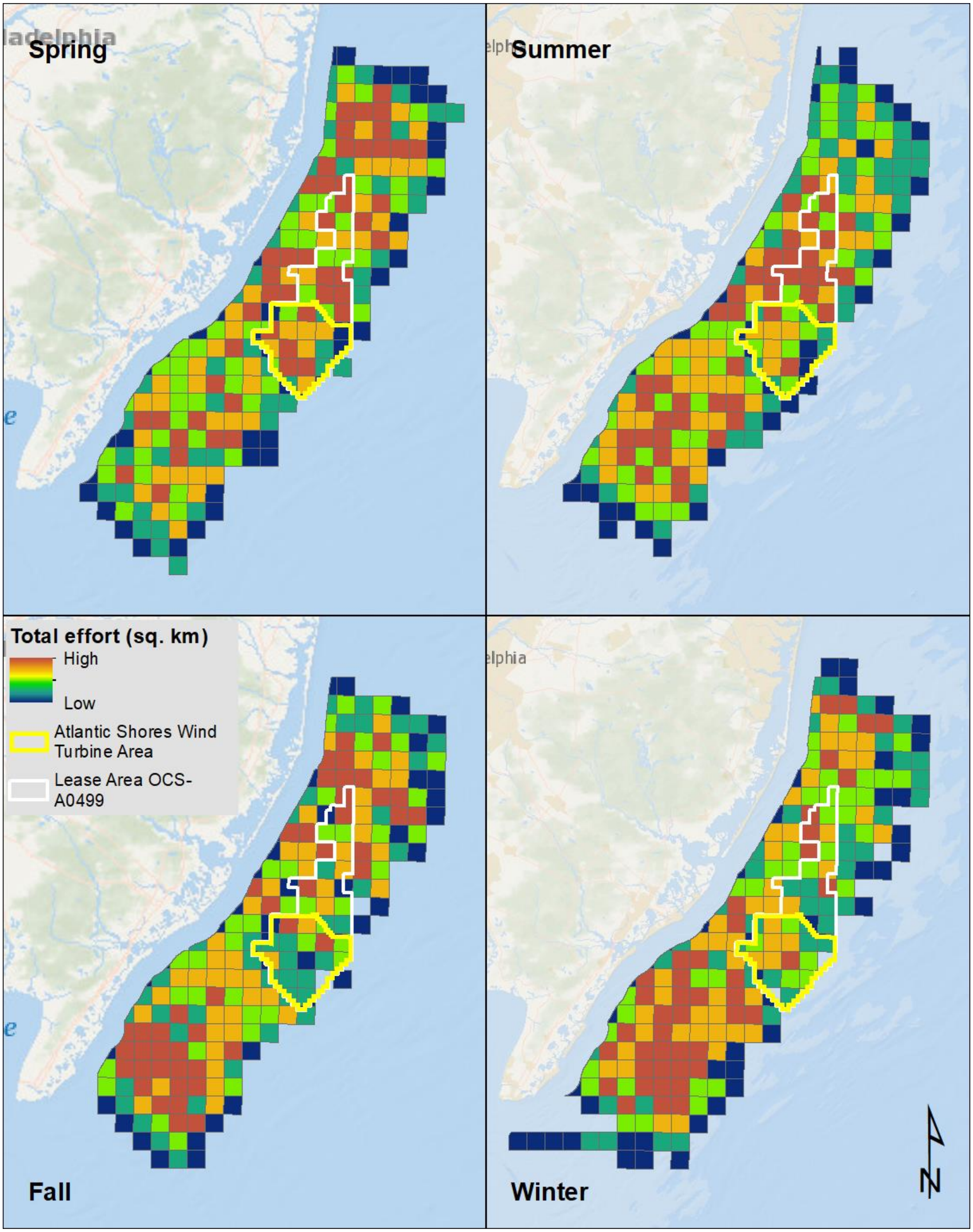

Map 1. NJDEP baseline seasonal survey effort. Survey effort totaled within each full or partial lease block inside and outside the Atlantic Shores Wind Turbine Area.

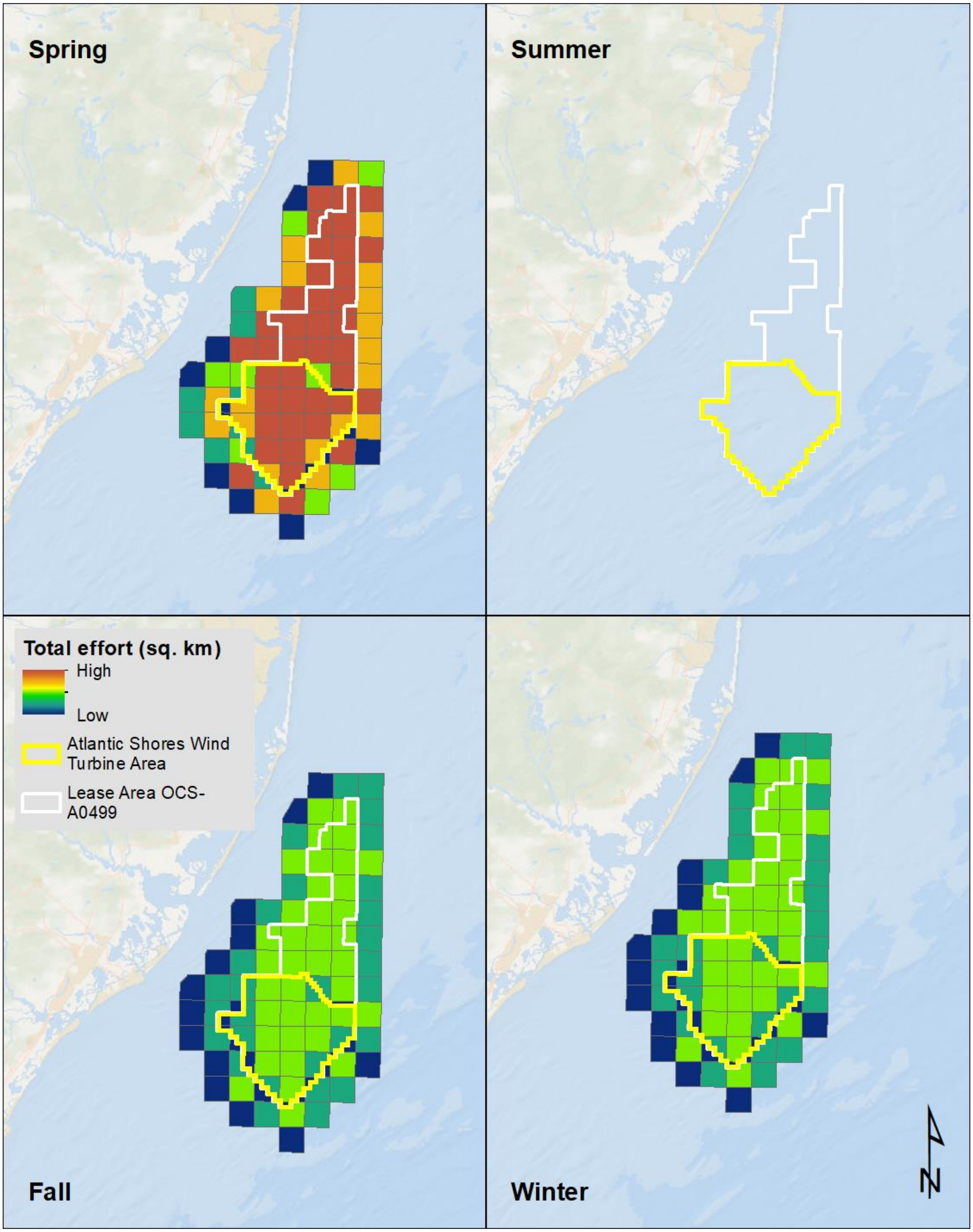

Map 2. Atlantic Shores digital aerial seasonal survey effort. Survey effort totaled within each full or partial lease block inside and outside the Atlantic Shores Wind Turbine Area.

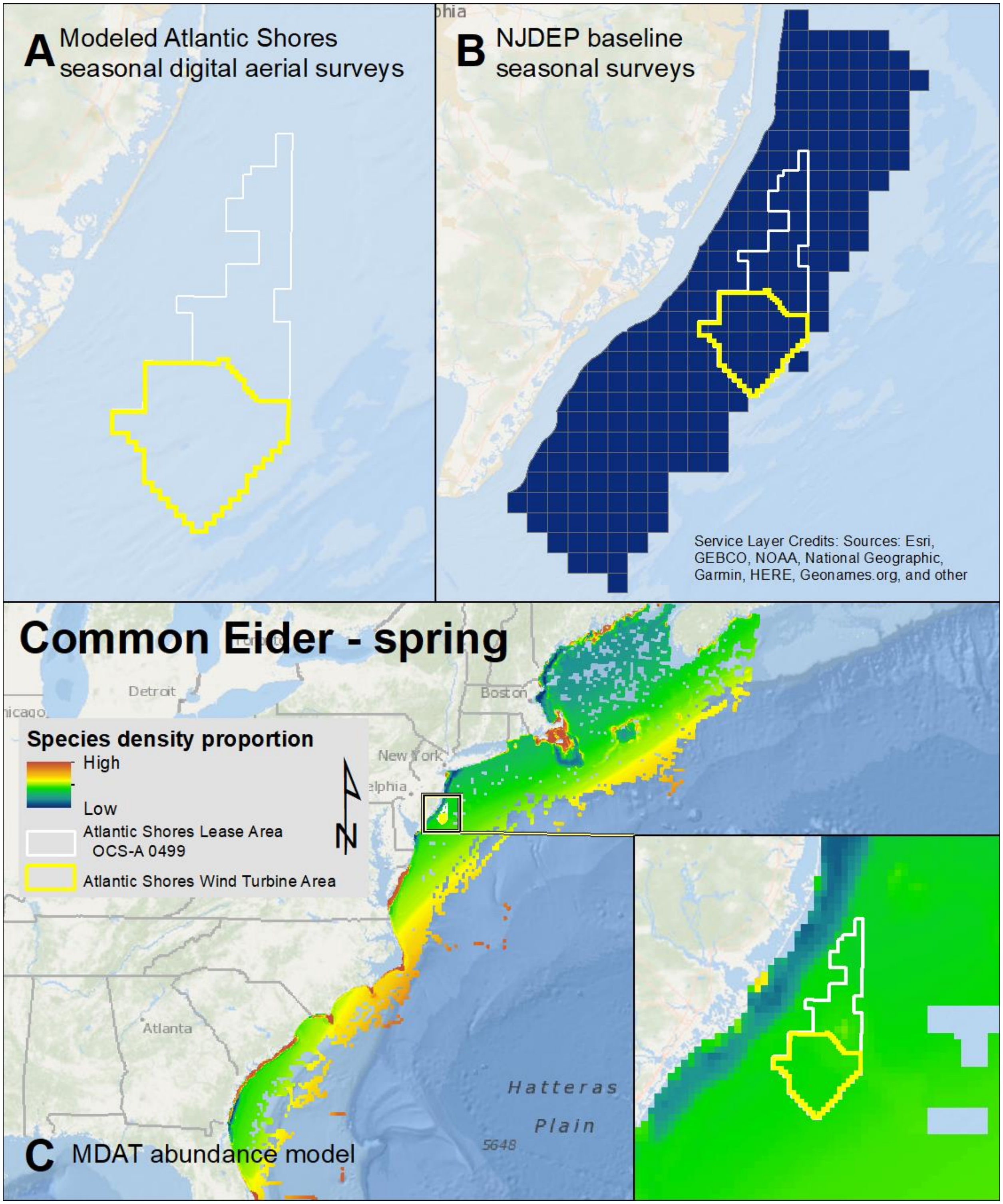

Map 3. Spring Common Eider modeled density proportions in the Atlantic Shores seasonal digital aerial surveys (A), density proportions in the NJDEP baseline survey data (B), and the MDAT data at local and regional scales (C). The scale for all maps is representative of relative spatial variation in the sites within the season for each data source.

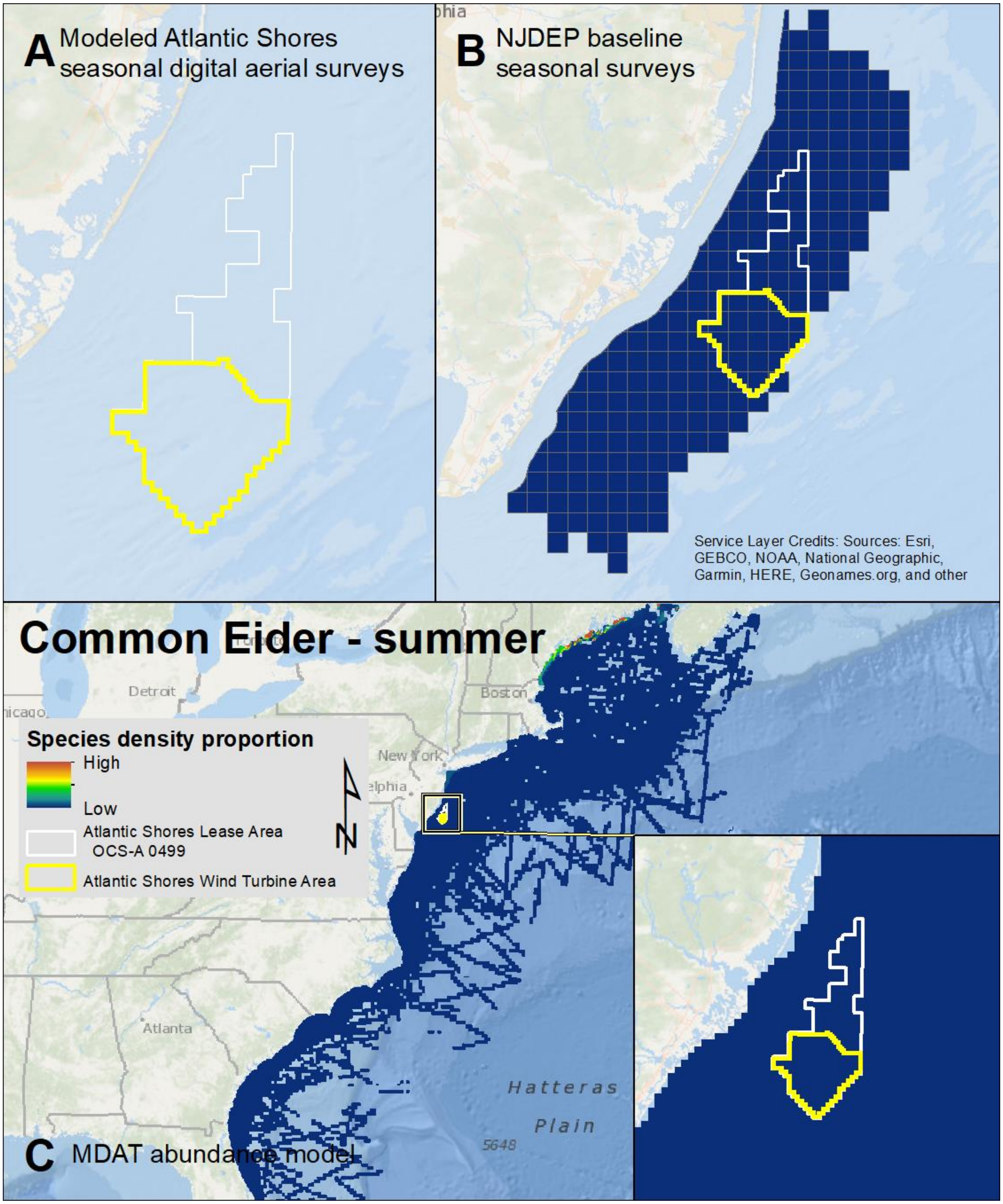

Map 4. Summer Common Eider modeled density proportions in the Atlantic Shores seasonal digital aerial surveys (A), density proportions in the NJDEP baseline survey data (B), and the MDAT data at local and regional scales (C). The scale for all maps is representative of relative spatial variation in the sites within the season for each data source.

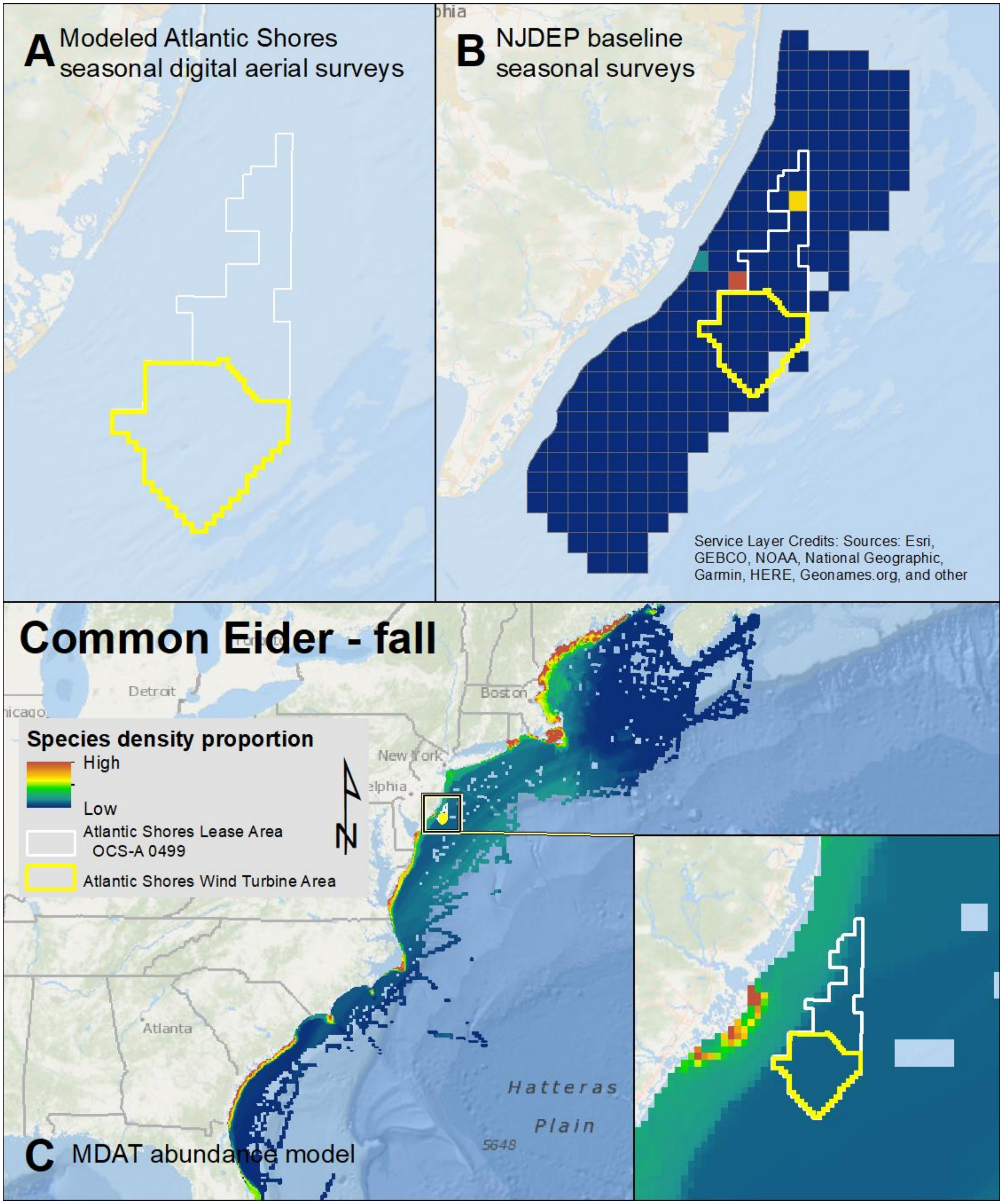

Map 5. Fall Common Eider modeled density proportions in the Atlantic Shores seasonal digital aerial surveys (A), density proportions in the NJDEP baseline survey data (B), and the MDAT data at local and regional scales (C). The scale for all maps is representative of relative spatial variation in the sites within the season for each data source.

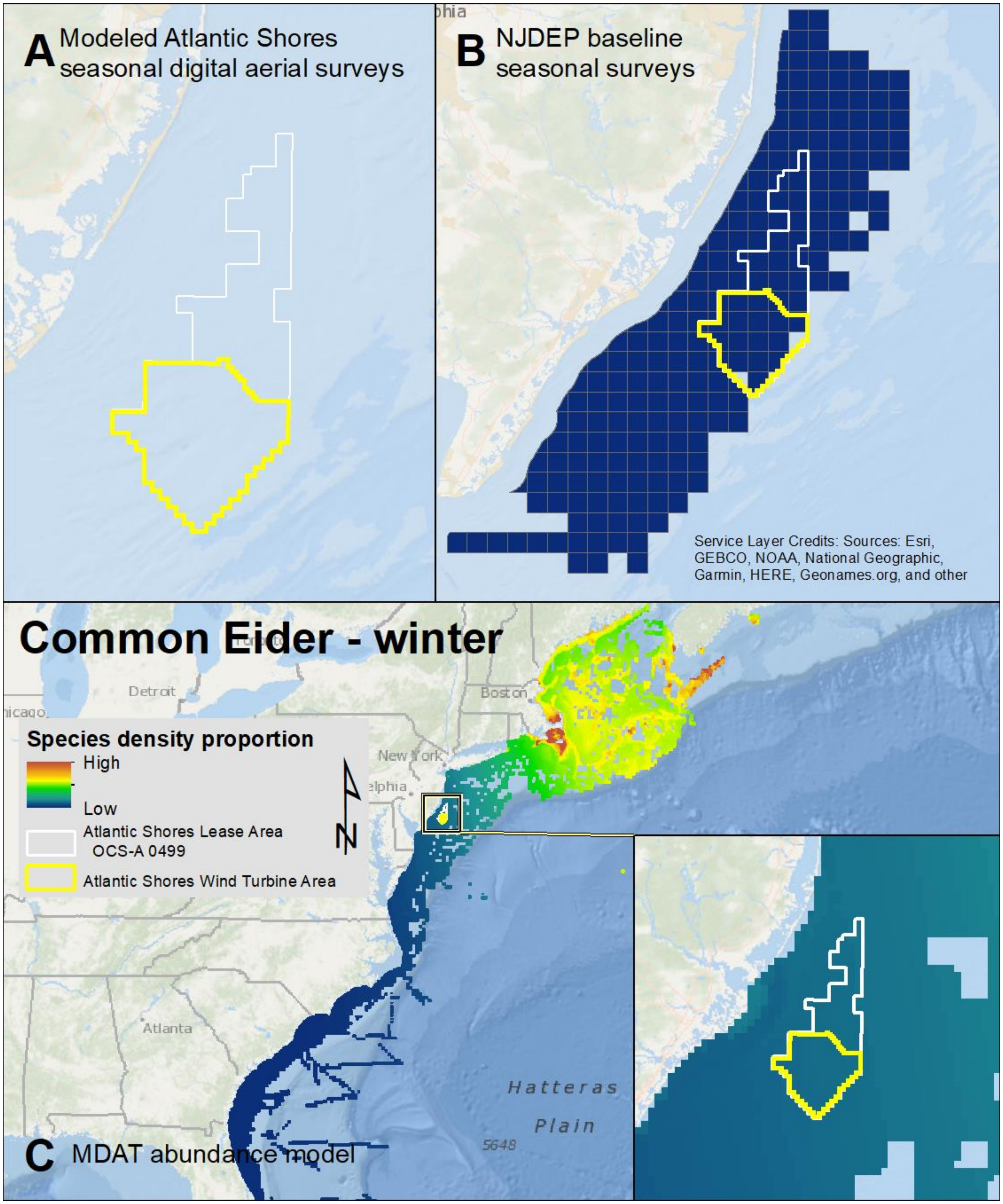

Map 6. Winter Common Eider modeled density proportions in the Atlantic Shores seasonal digital aerial surveys (A), density proportions in the NJDEP baseline survey data (B), and the MDAT data at local and regional scales (C). The scale for all maps is representative of relative spatial variation in the sites within the season for each data source.

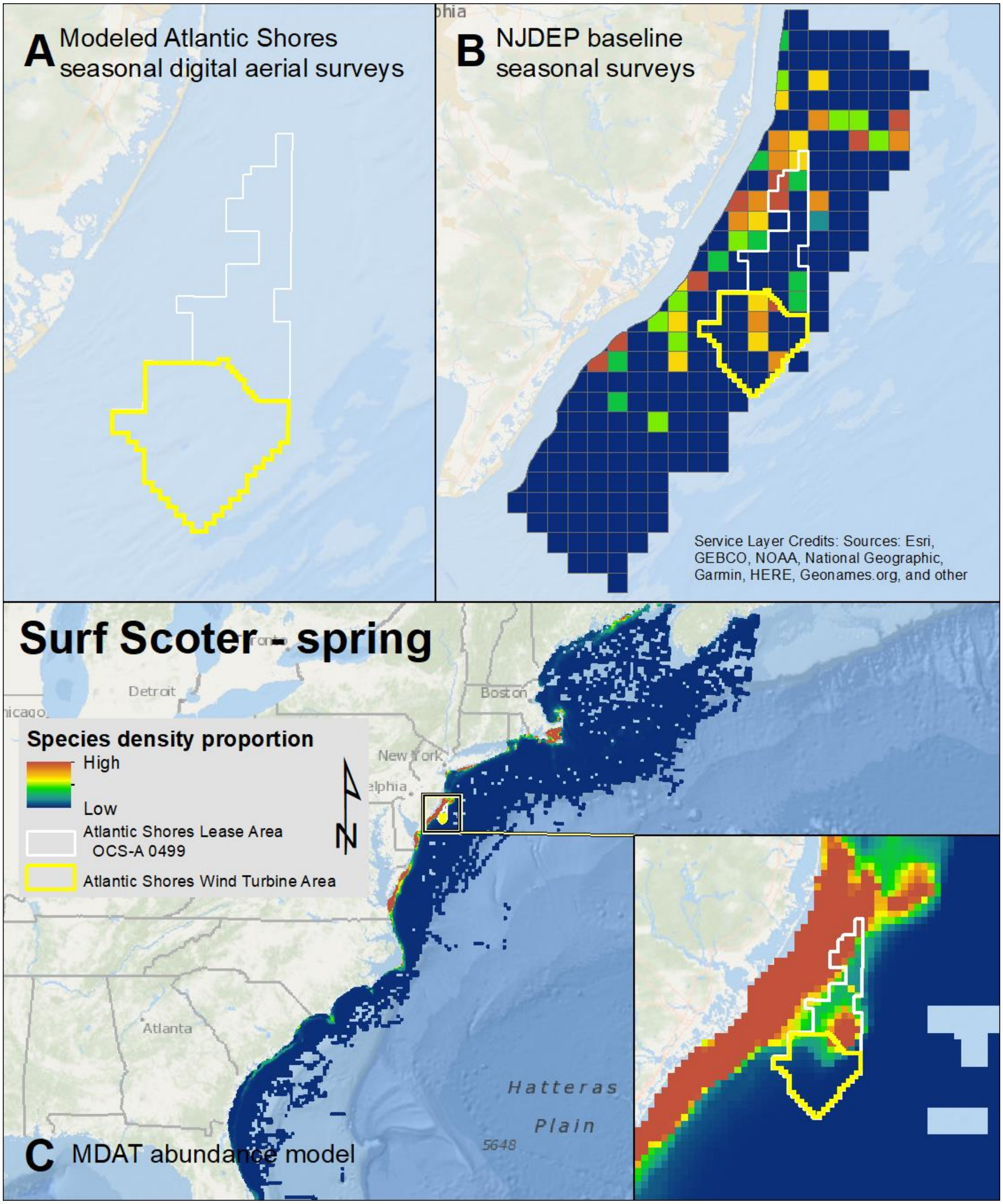

Map 7. Spring Surf Scoter modeled density proportions in the Atlantic Shores seasonal digital aerial surveys (A), density proportions in the NJDEP baseline survey data (B), and the MDAT data at local and regional scales (C). The scale for all maps is representative of relative spatial variation in the sites within the season for each data source.

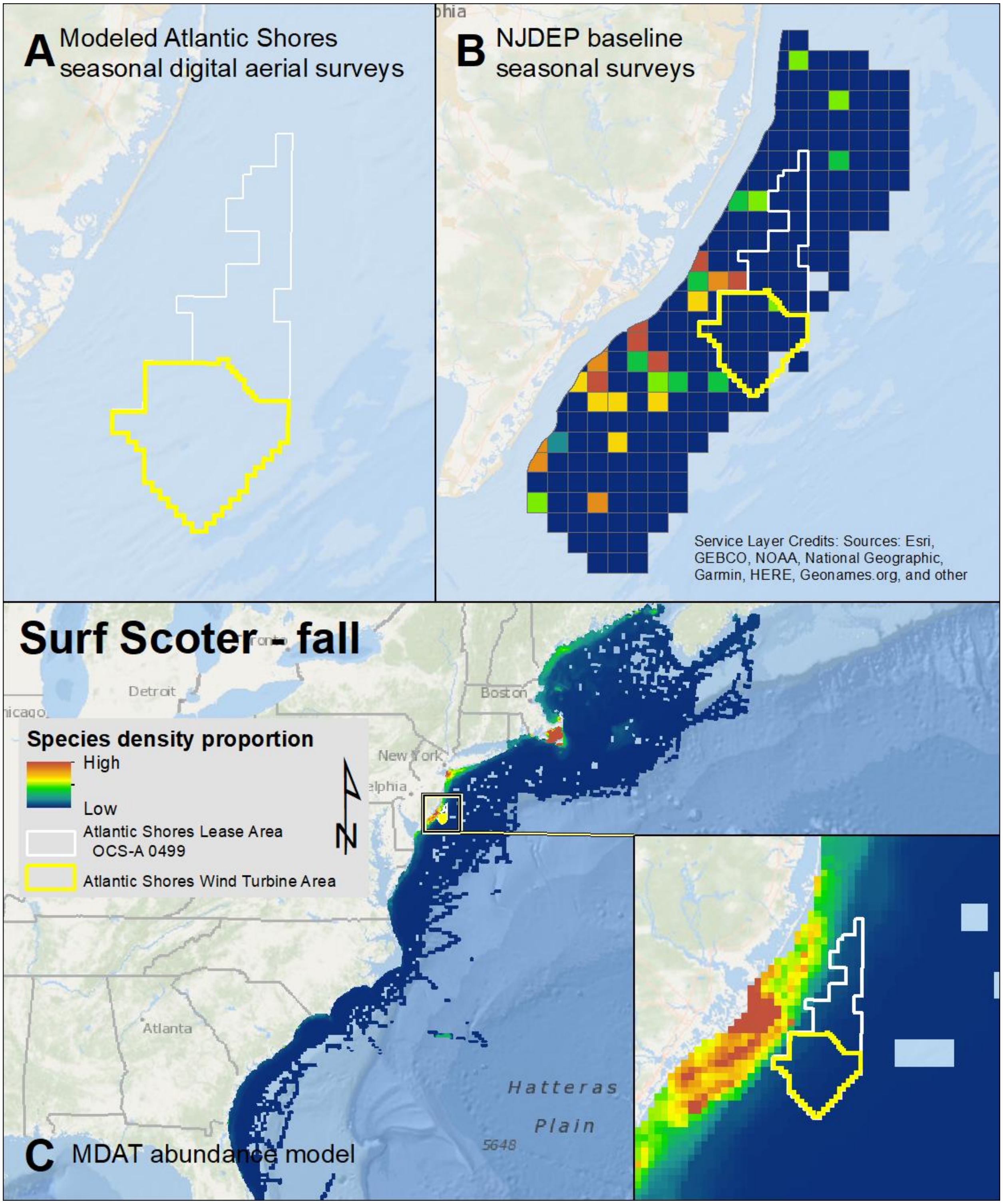

Map 8. Fall Surf Scoter modeled density proportions in the Atlantic Shores seasonal digital aerial surveys (A), density proportions in the NJDEP baseline survey data (B), and the MDAT data at local and regional scales (C). The scale for all maps is representative of relative spatial variation in the sites within the season for each data source.

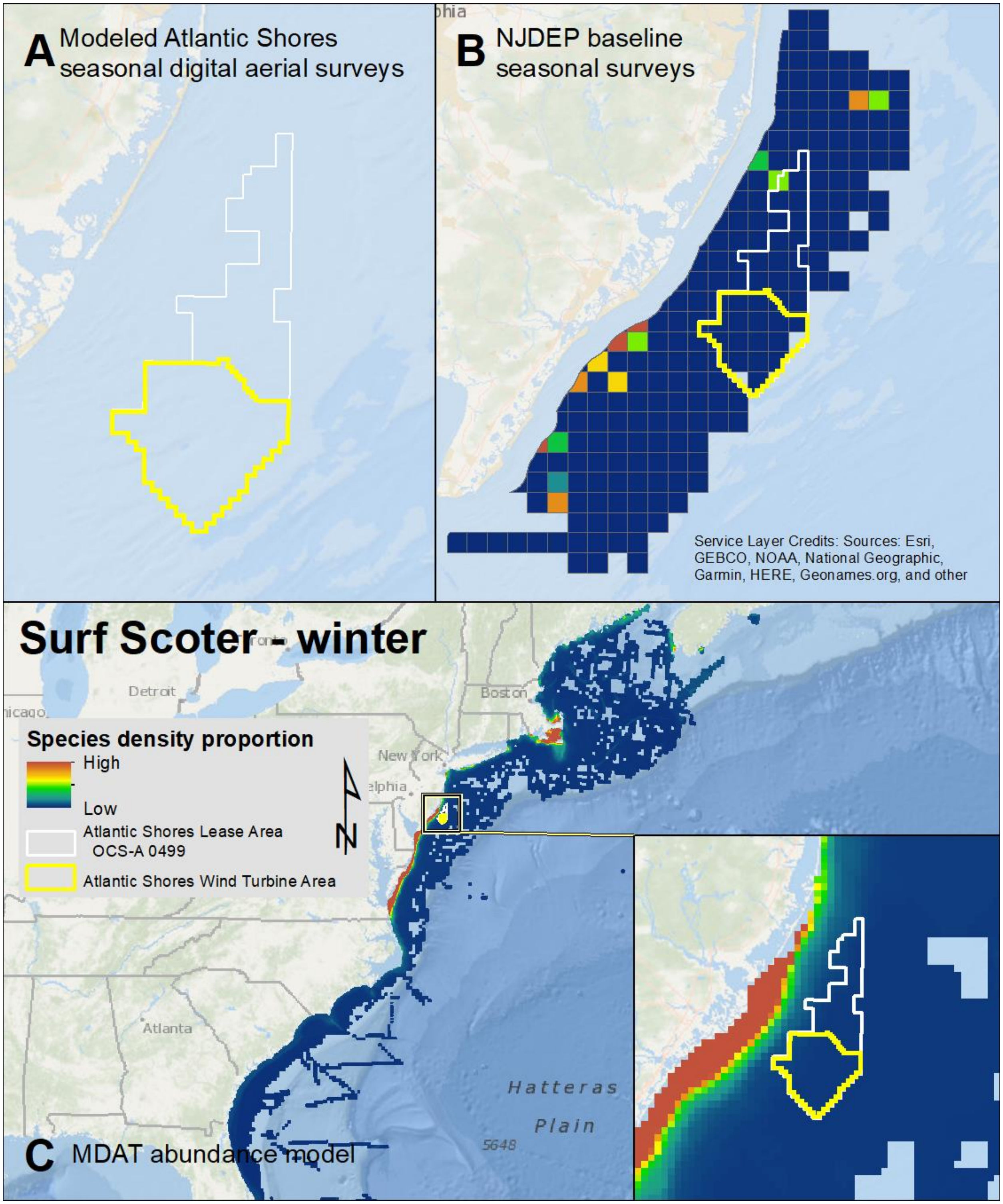

Map 9. Winter Surf Scoter modeled density proportions in the Atlantic Shores seasonal digital aerial surveys (A), density proportions in the NJDEP baseline survey data (B), and the MDAT data at local and regional scales (C). The scale for all maps is representative of relative spatial variation in the sites within the season for each data source.

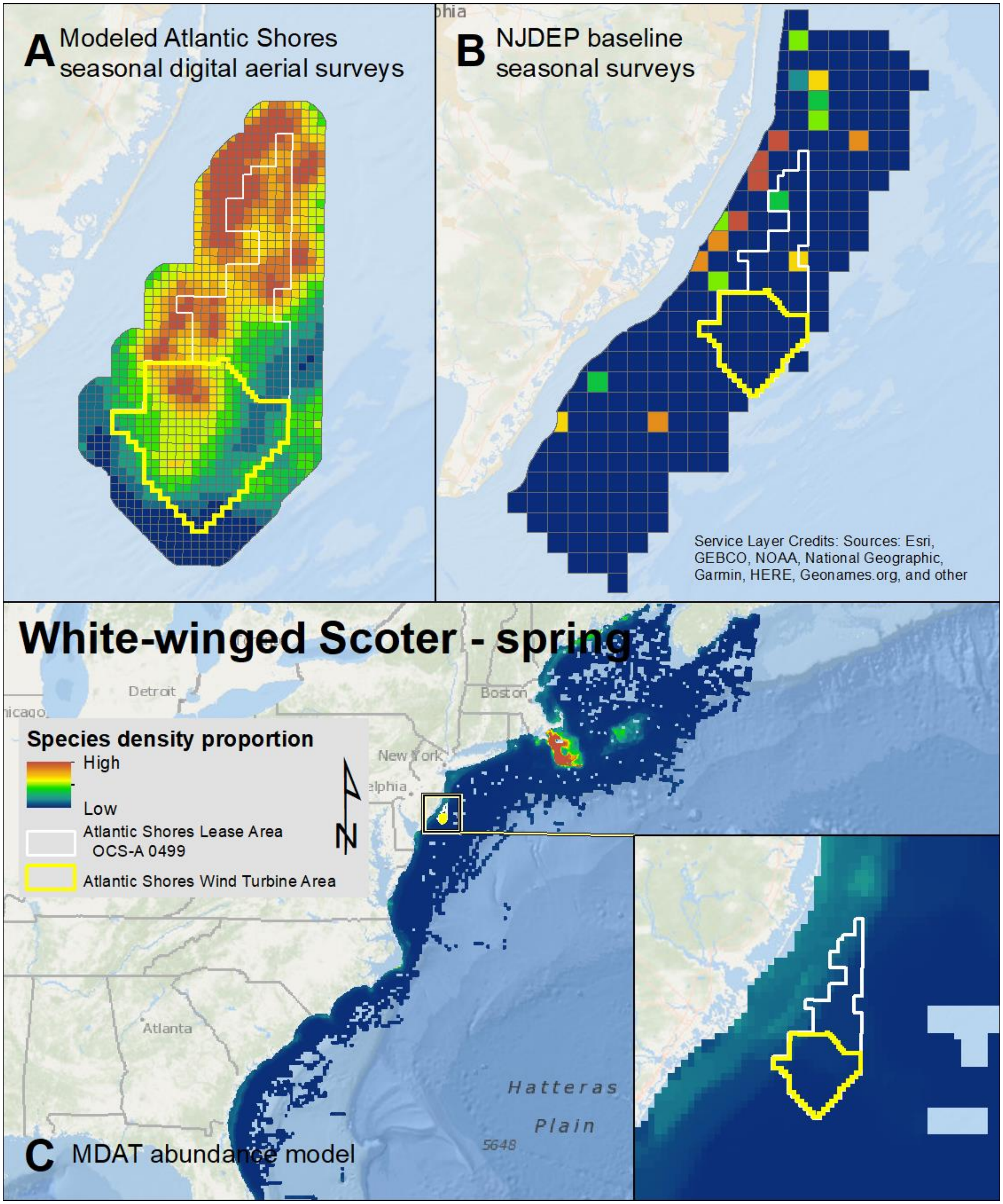

Map 10. Spring White-winged Scoter modeled density proportions in the Atlantic Shores seasonal digital aerial surveys (A), density proportions in the NJDEP baseline survey data (B), and the MDAT data at local and regional scales (C). The scale for all maps is representative of relative spatial variation in the sites within the season for each data source.

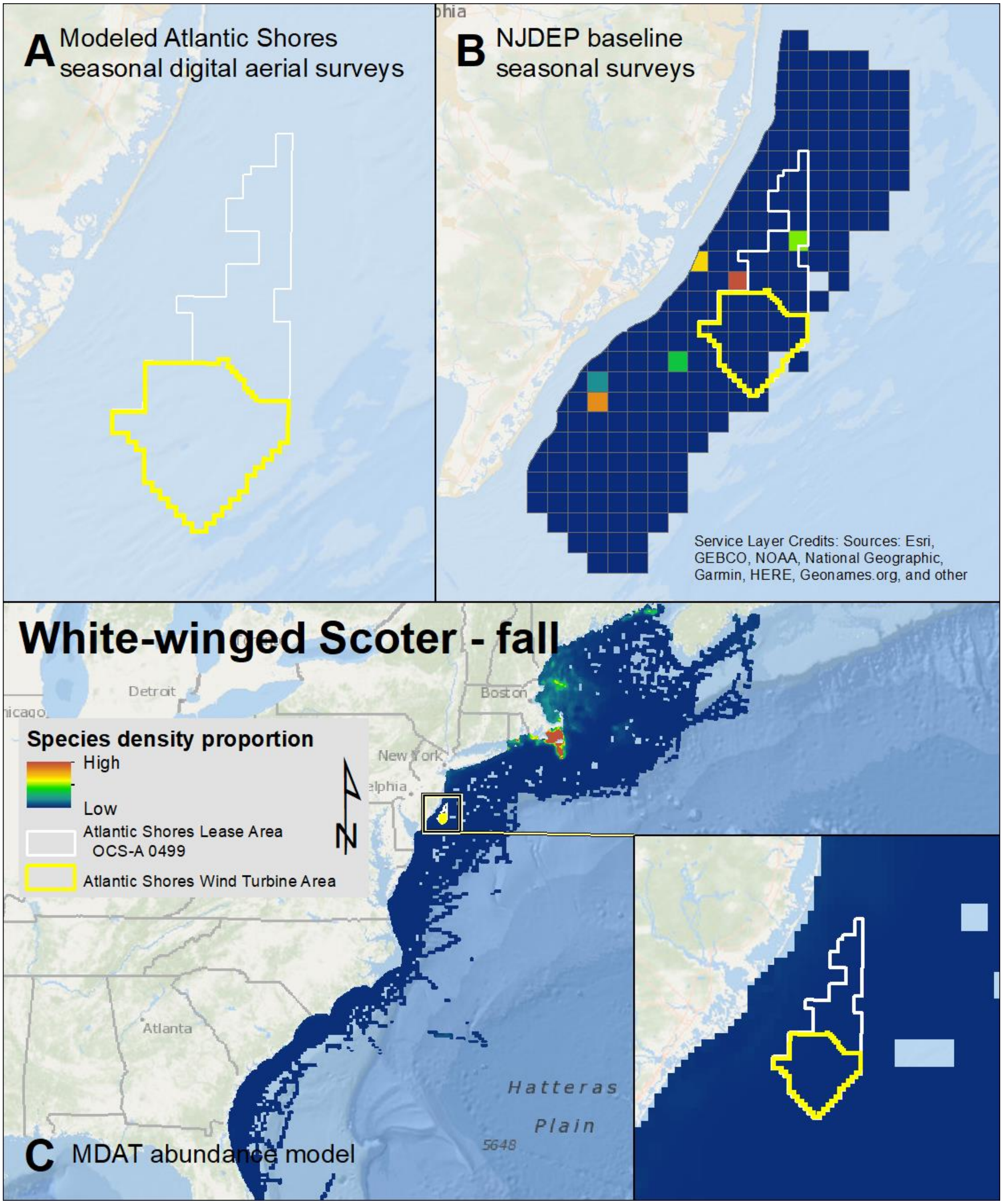

Map 11. Fall White-winged Scoter modeled density proportions in the Atlantic Shores seasonal digital aerial surveys (A), density proportions in the NJDEP baseline survey data (B), and the MDAT data at local and regional scales (C). The scale for all maps is representative of relative spatial variation in the sites within the season for each data source.

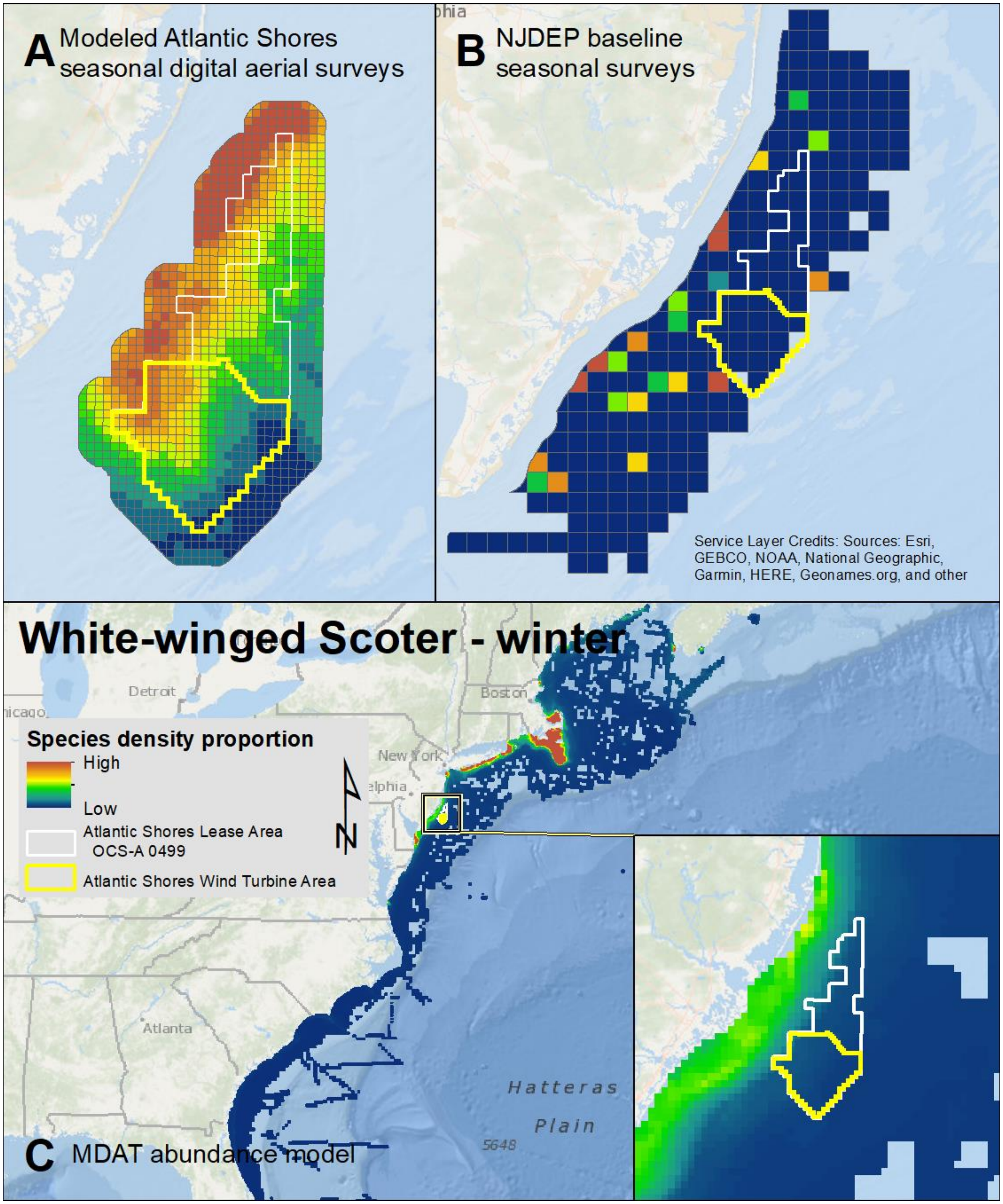

Map 12. Winter White-winged Scoter modeled density proportions in the Atlantic Shores seasonal digital aerial surveys (A), density proportions in the NJDEP baseline survey data (B), and the MDAT data at local and regional scales (C). The scale for all maps is representative of relative spatial variation in the sites within the season for each data source.

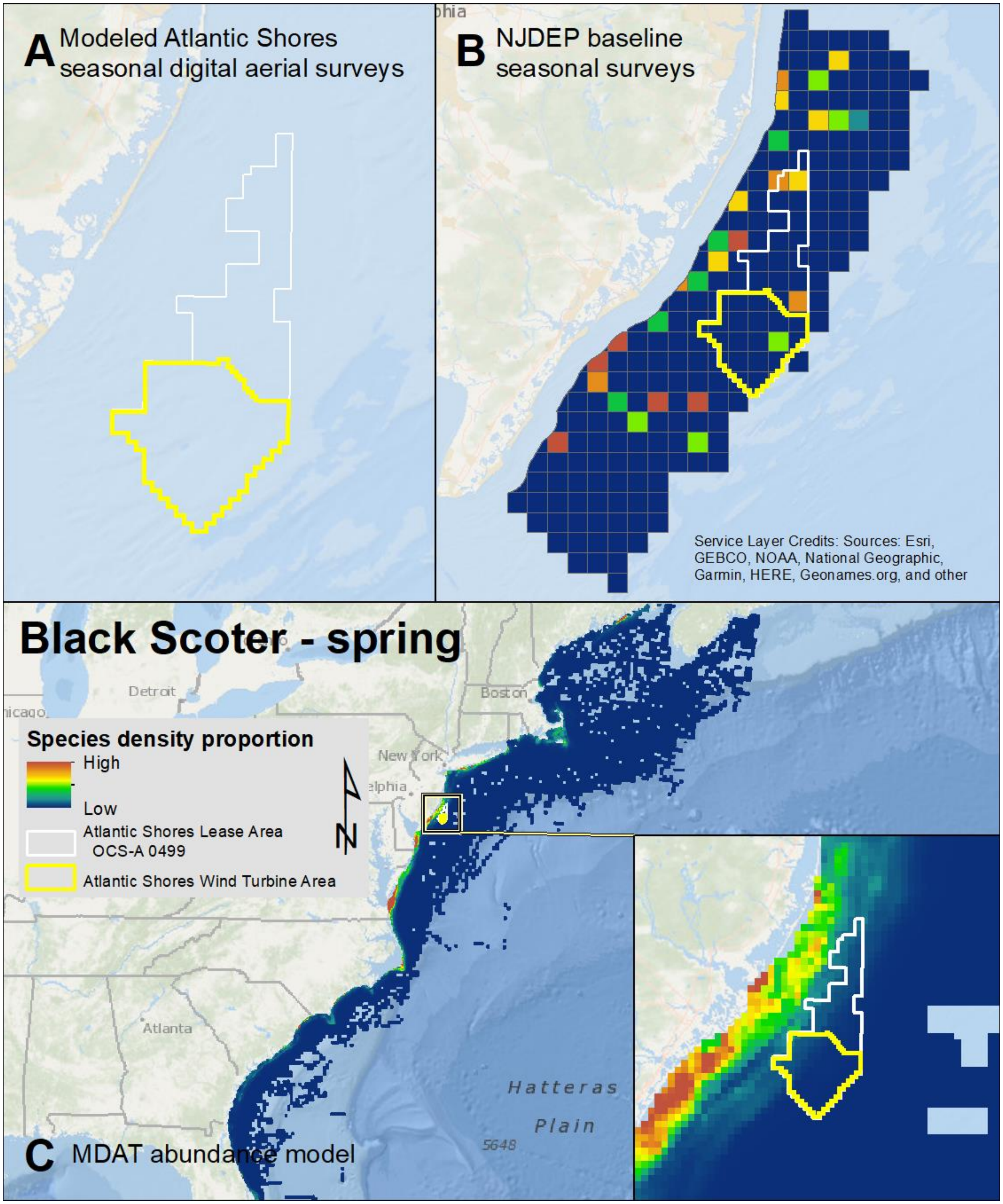

Map 13. Spring Black Scoter modeled density proportions in the Atlantic Shores seasonal digital aerial surveys (A), density proportions in the NJDEP baseline survey data (B), and the MDAT data at local and regional scales (C). The scale for all maps is representative of relative spatial variation in the sites within the season for each data source.

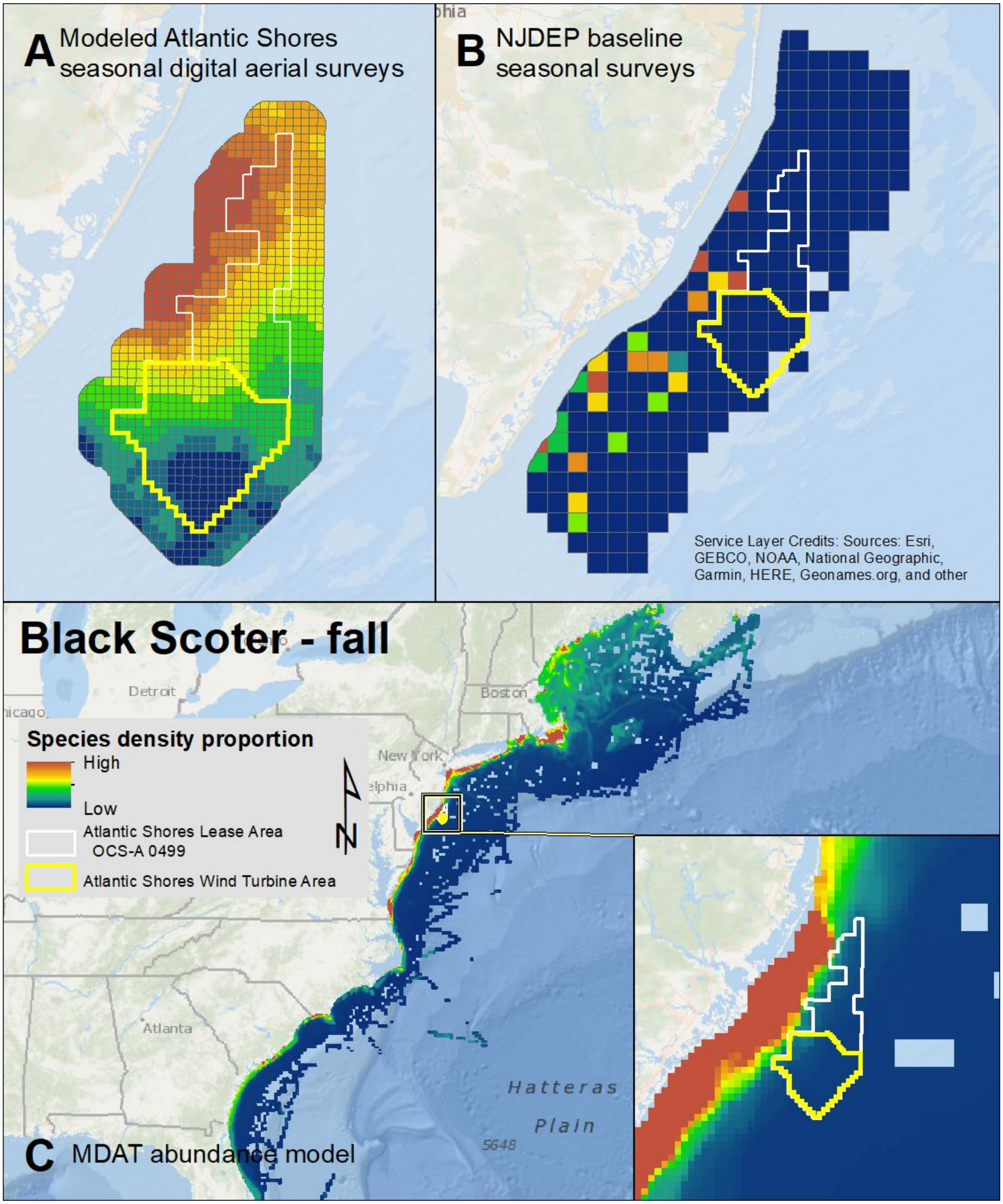

Map 14. Fall Black Scoter modeled density proportions in the Atlantic Shores seasonal digital aerial surveys (A), density proportions in the NJDEP baseline survey data (B), and the MDAT data at local and regional scales (C). The scale for all maps is representative of relative spatial variation in the sites within the season for each data source.

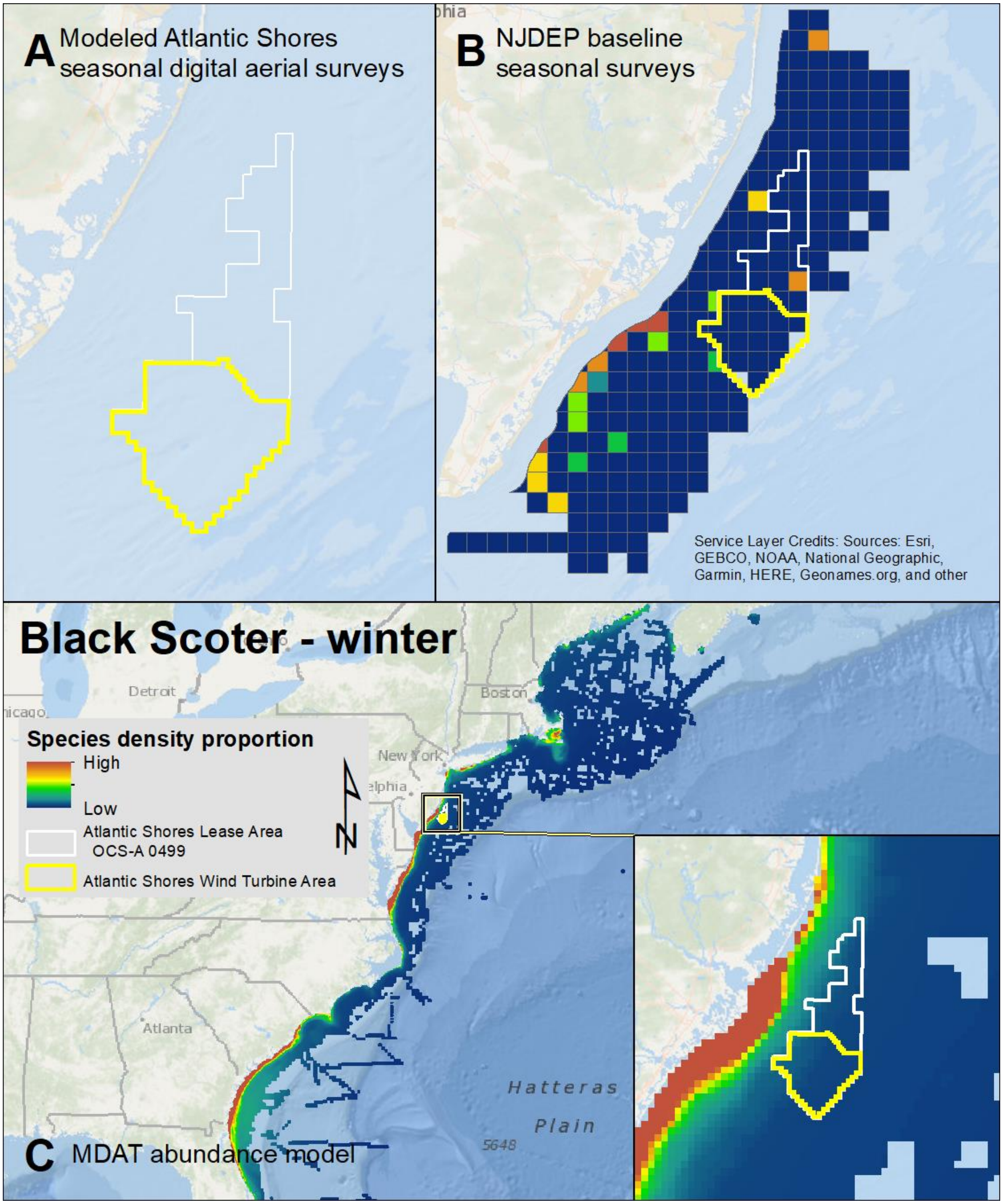

Map 15. Winter Black Scoter modeled density proportions in the Atlantic Shores seasonal digital aerial surveys (A), density proportions in the NJDEP baseline survey data (B), and the MDAT data at local and regional scales (C). The scale for all maps is representative of relative spatial variation in the sites within the season for each data source.

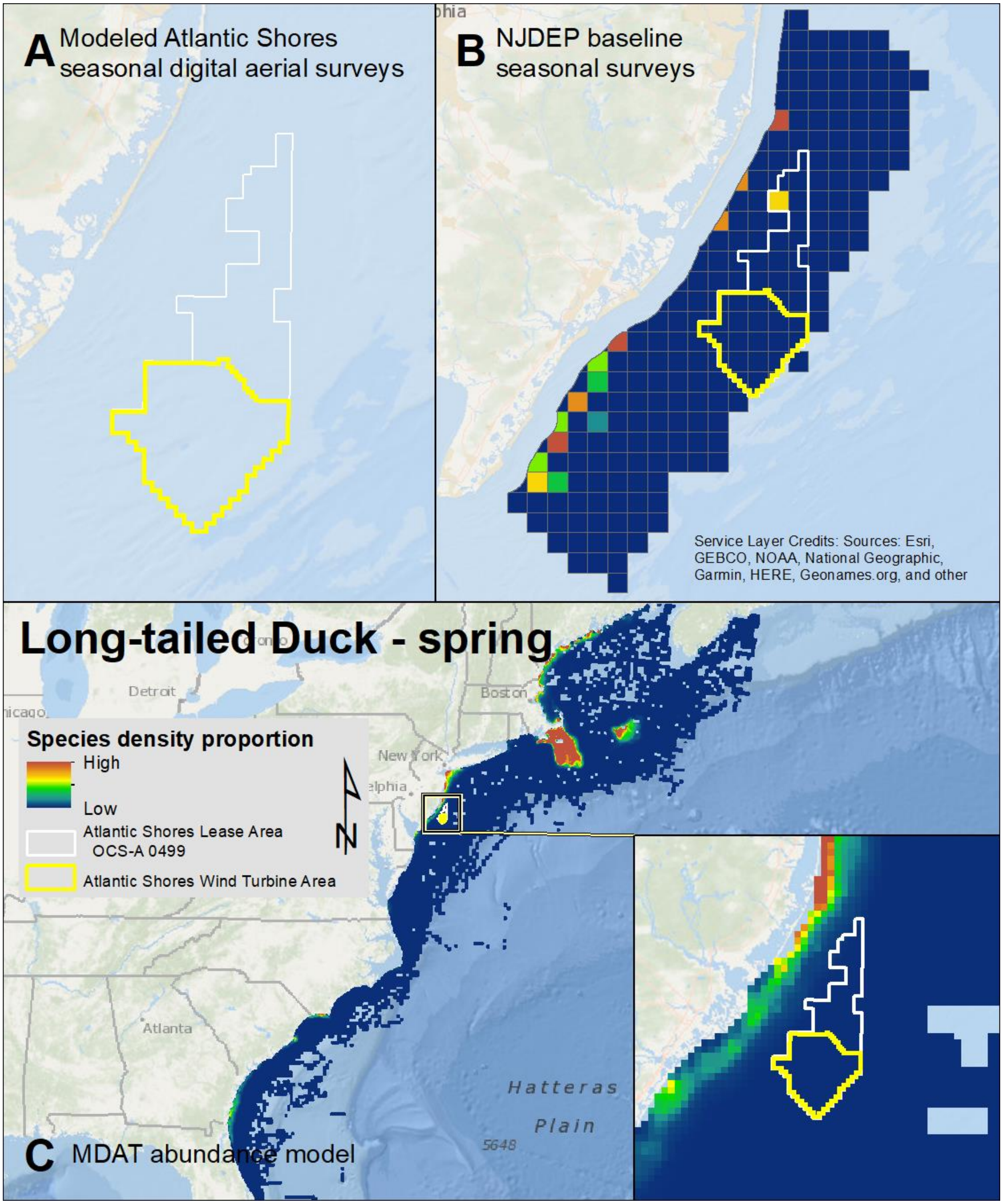

Map 16. Spring Long-tailed Duck modeled density proportions in the Atlantic Shores seasonal digital aerial surveys (A), density proportions in the NJDEP baseline survey data (B), and the MDAT data at local and regional scales (C). The scale for all maps is representative of relative spatial variation in the sites within the season for each data source.

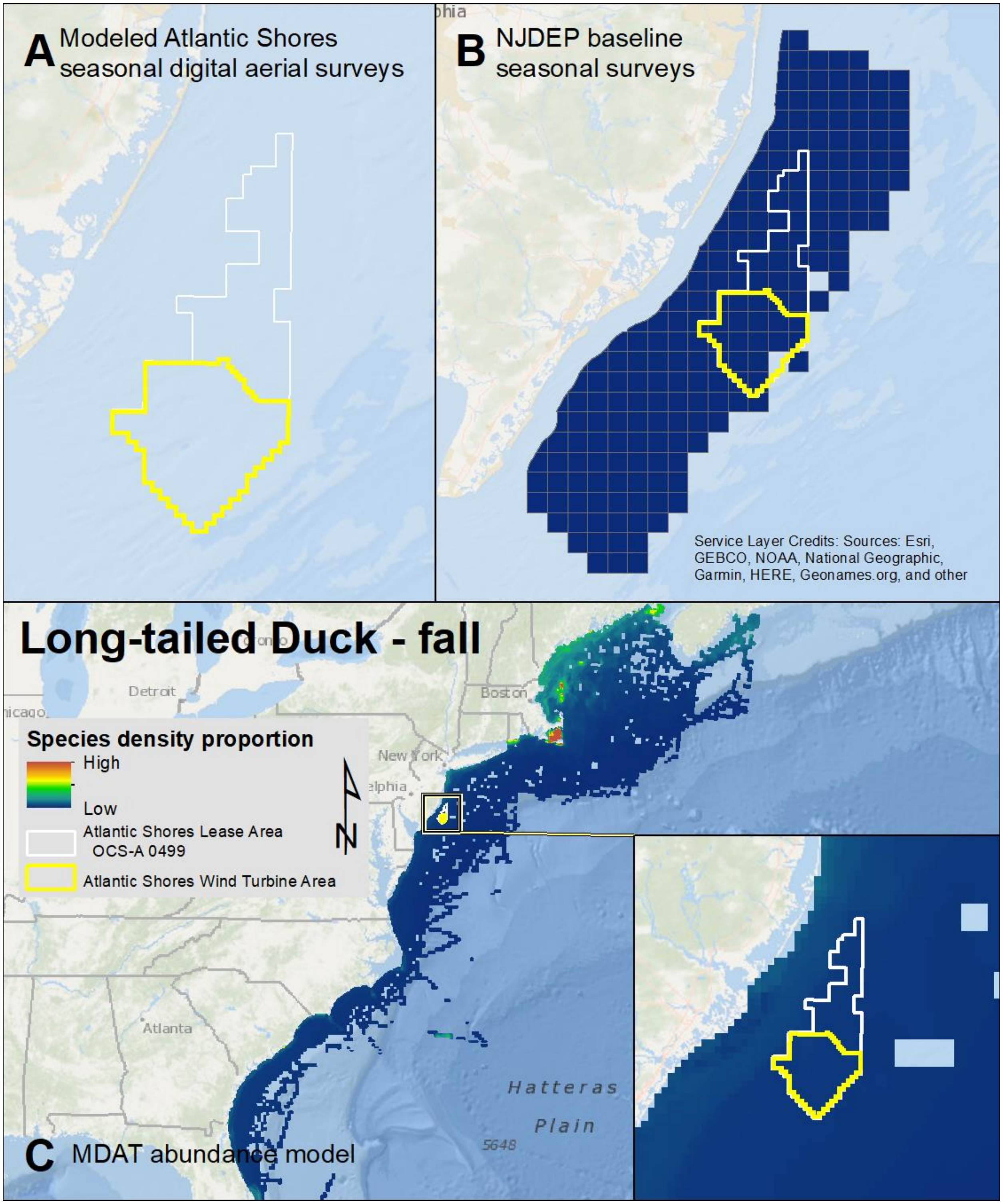

Map 17. Fall Long-tailed Duck modeled density proportions in the Atlantic Shores seasonal digital aerial surveys (A), density proportions in the NJDEP baseline survey data (B), and the MDAT data at local and regional scales (C). The scale for all maps is representative of relative spatial variation in the sites within the season for each data source.

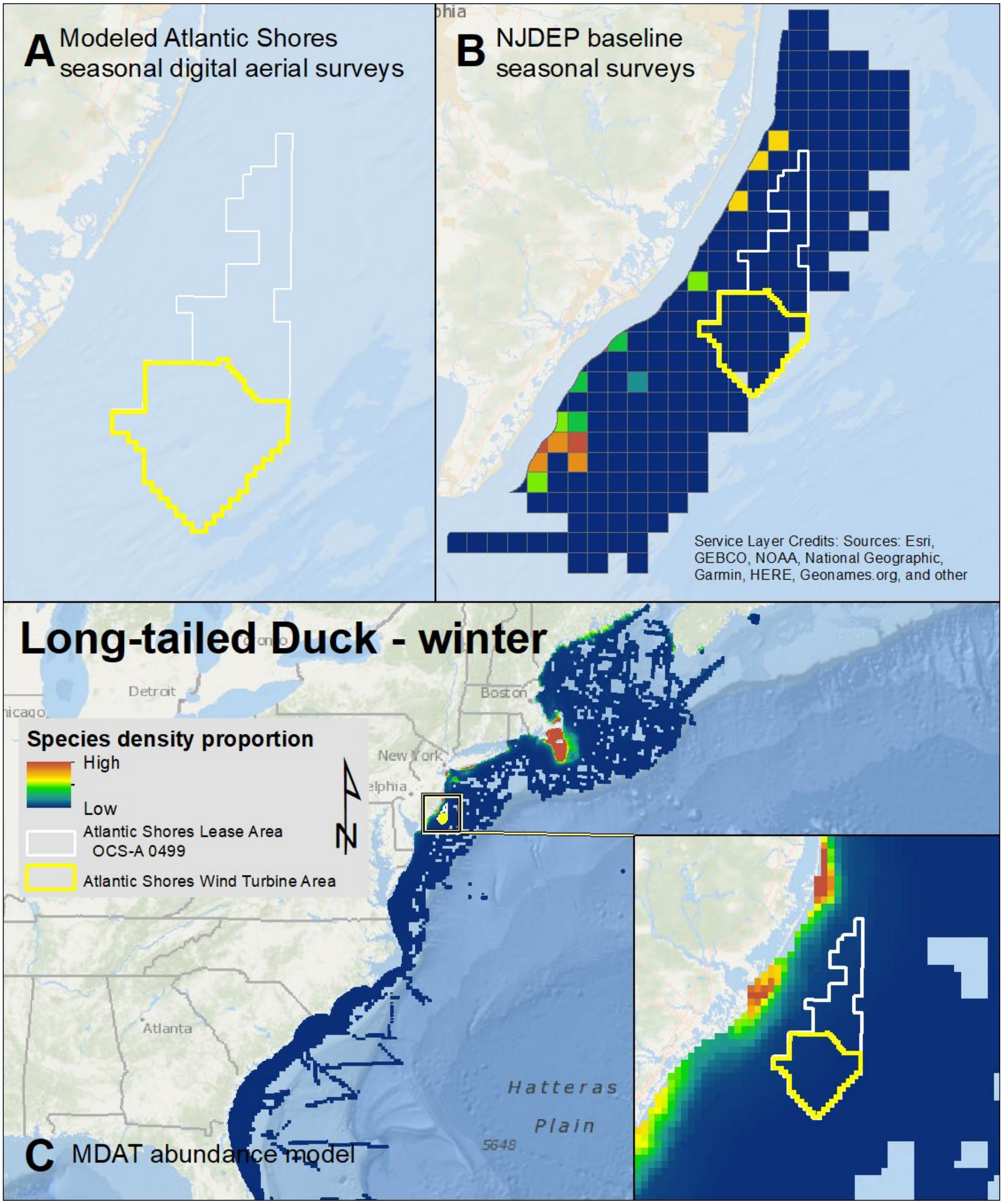

Map 18. Winter Long-tailed Duck modeled density proportions in the Atlantic Shores seasonal digital aerial surveys (A), density proportions in the NJDEP baseline survey data (B), and the MDAT data at local and regional scales (C). The scale for all maps is representative of relative spatial variation in the sites within the season for each data source.

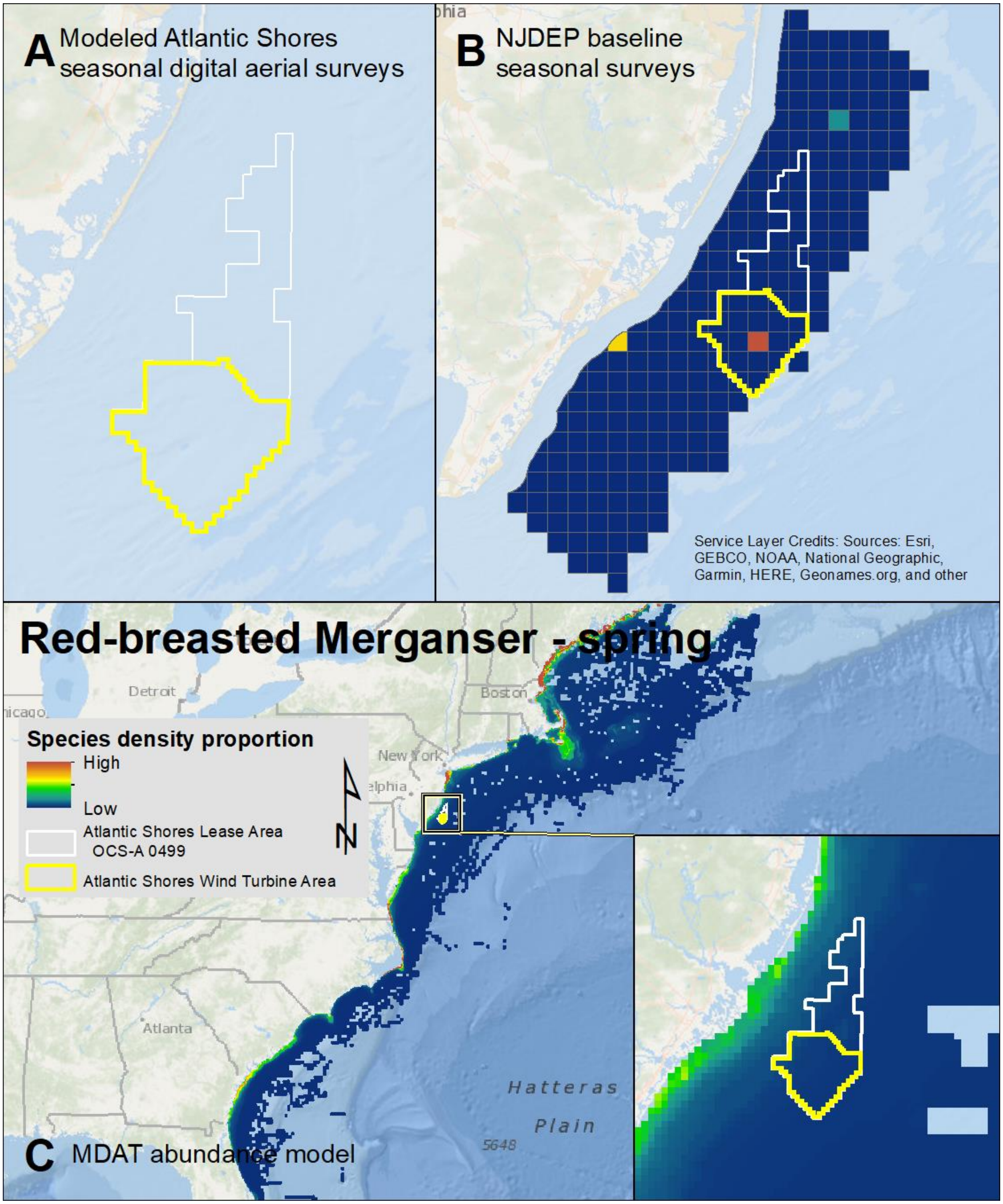

Map 19. Spring Red-breasted Merganser modeled density proportions in the Atlantic Shores seasonal digital aerial surveys (A), density proportions in the NJDEP baseline survey data (B), and the MDAT data at local and regional scales (C). The scale for all maps is representative of relative spatial variation in the sites within the season for each data source.

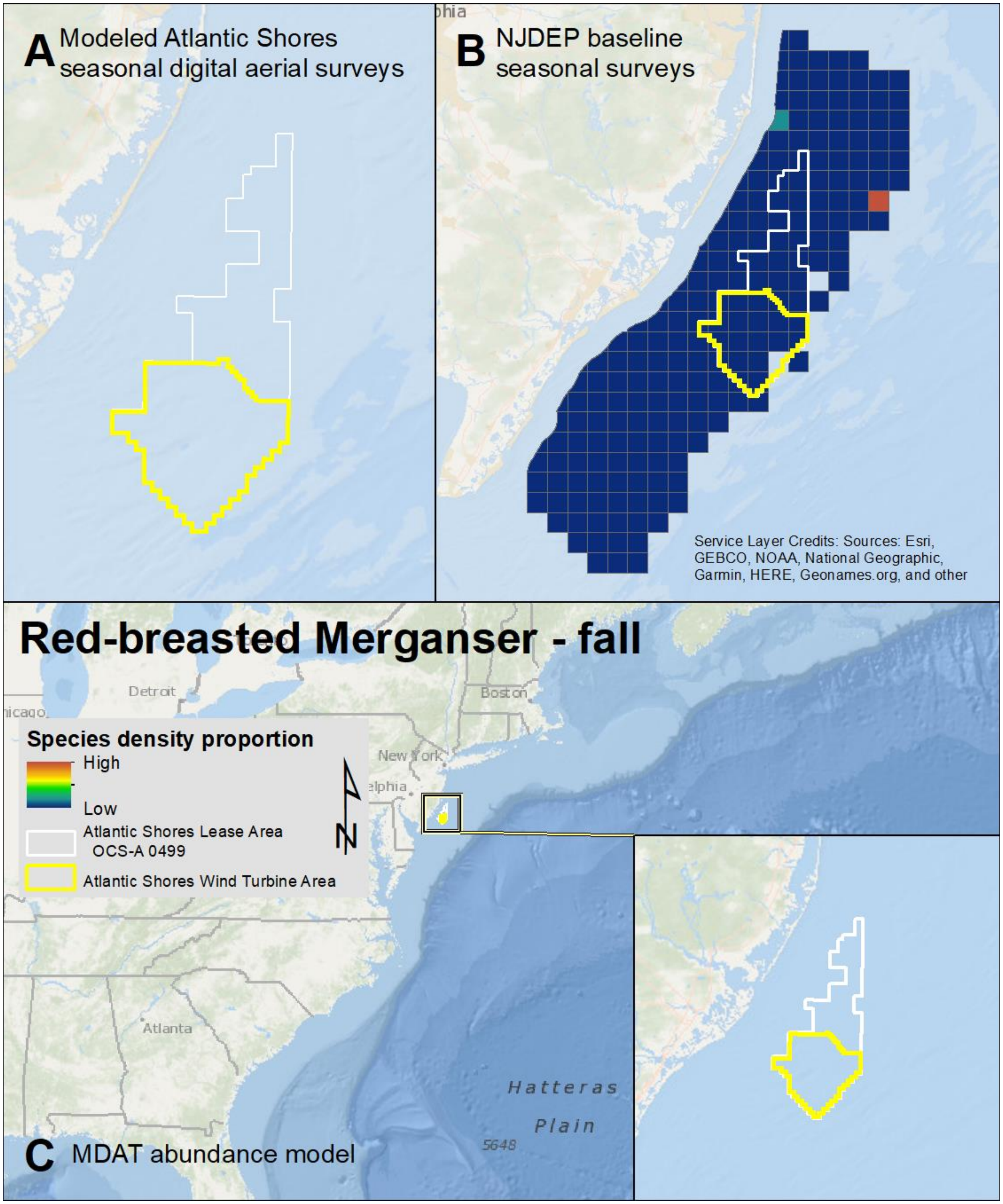

Map 20. Fall Red-breasted Merganser modeled density proportions in the Atlantic Shores seasonal digital aerial surveys (A), density proportions in the NJDEP baseline survey data (B), and the MDAT data at local and regional scales (C). The scale for all maps is representative of relative spatial variation in the sites within the season for each data source.

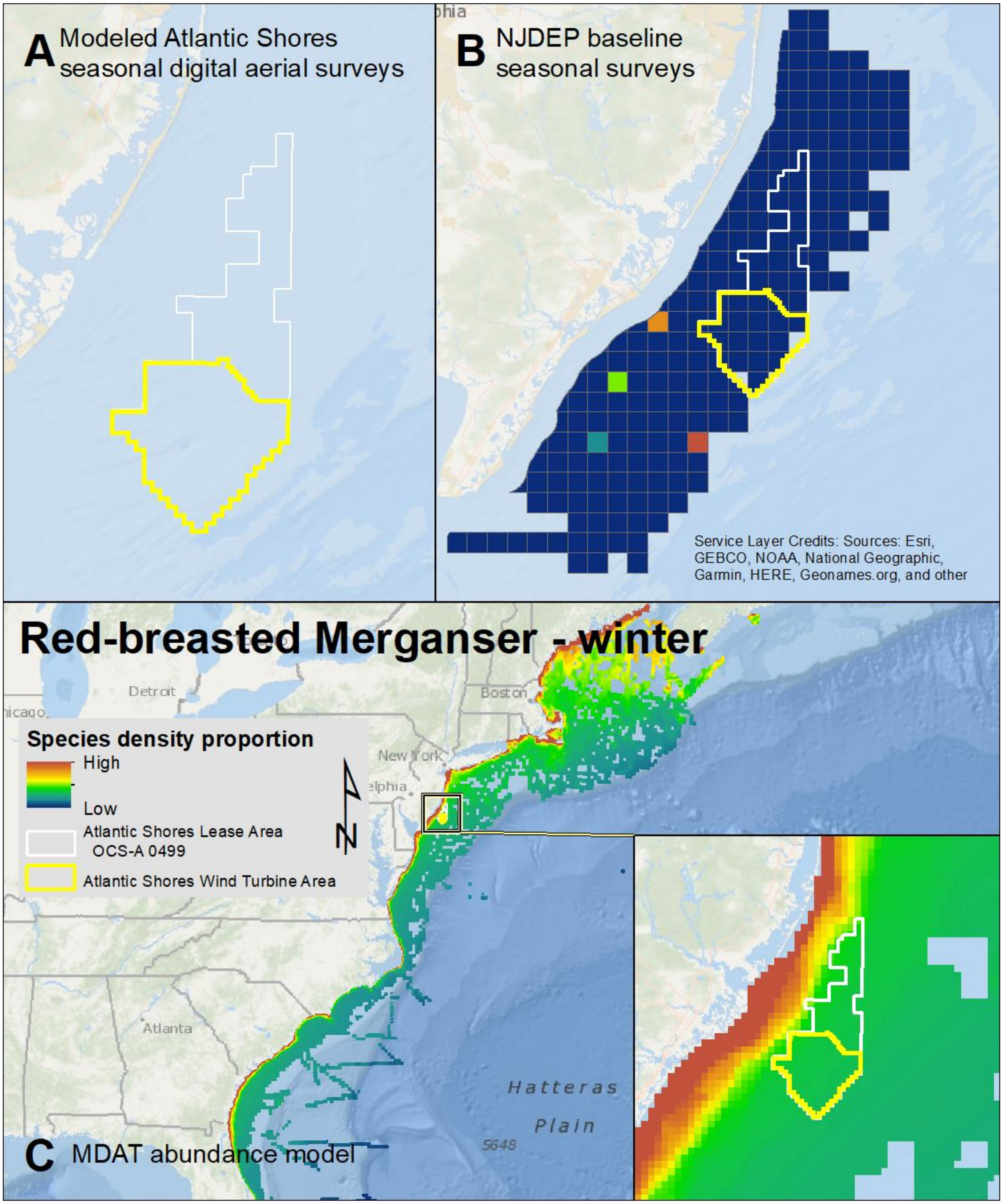

Map 21. Winter Red-breasted Merganser modeled density proportions in the Atlantic Shores seasonal digital aerial surveys (A), density proportions in the NJDEP baseline survey data (B), and the MDAT data at local and regional scales (C). The scale for all maps is representative of relative spatial variation in the sites within the season for each data source.

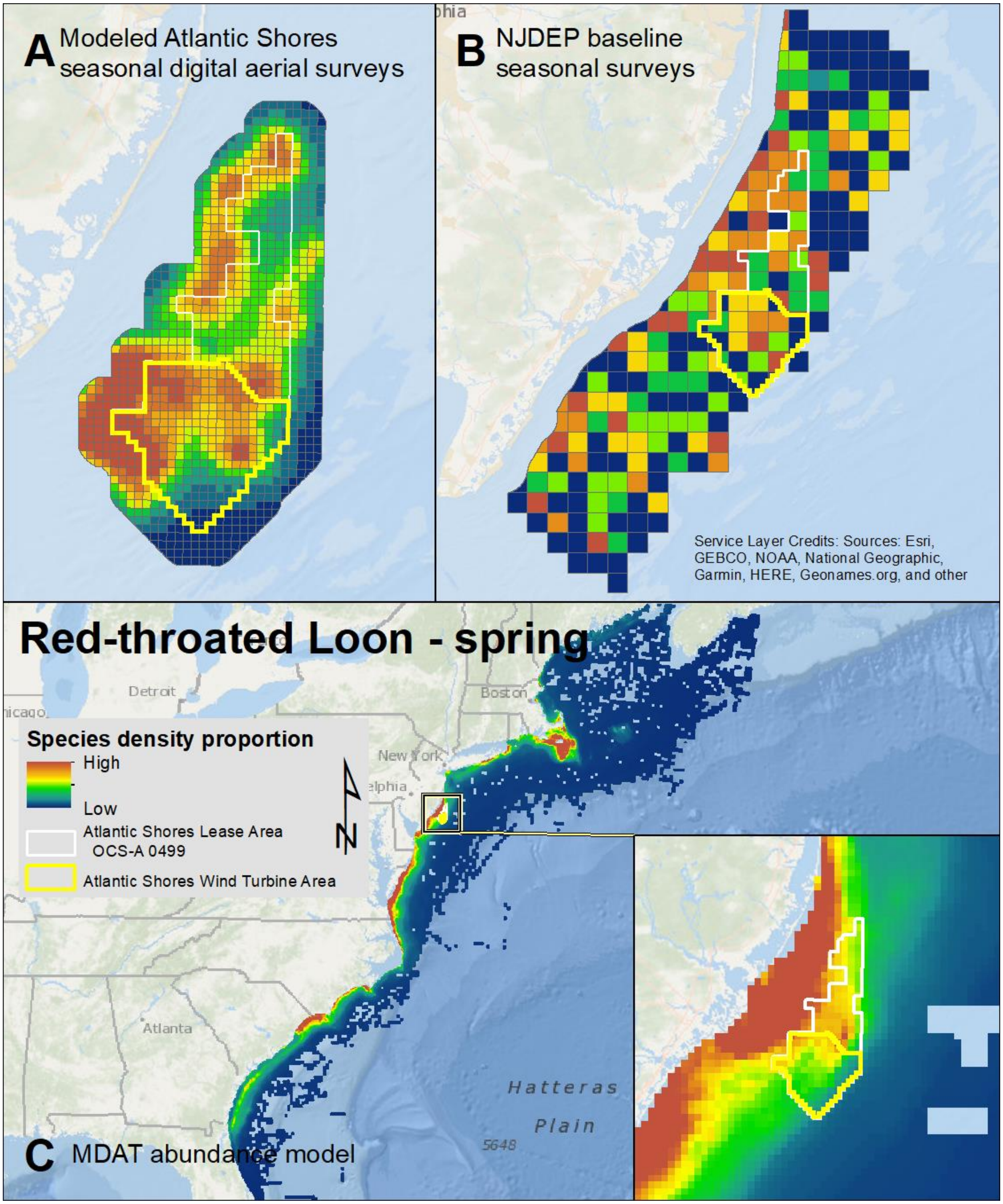

Map 22. Spring Red-throated Loon modeled density proportions in the Atlantic Shores seasonal digital aerial surveys (A), density proportions in the NJDEP baseline survey data (B), and the MDAT data at local and regional scales (C). The scale for all maps is representative of relative spatial variation in the sites within the season for each data source.

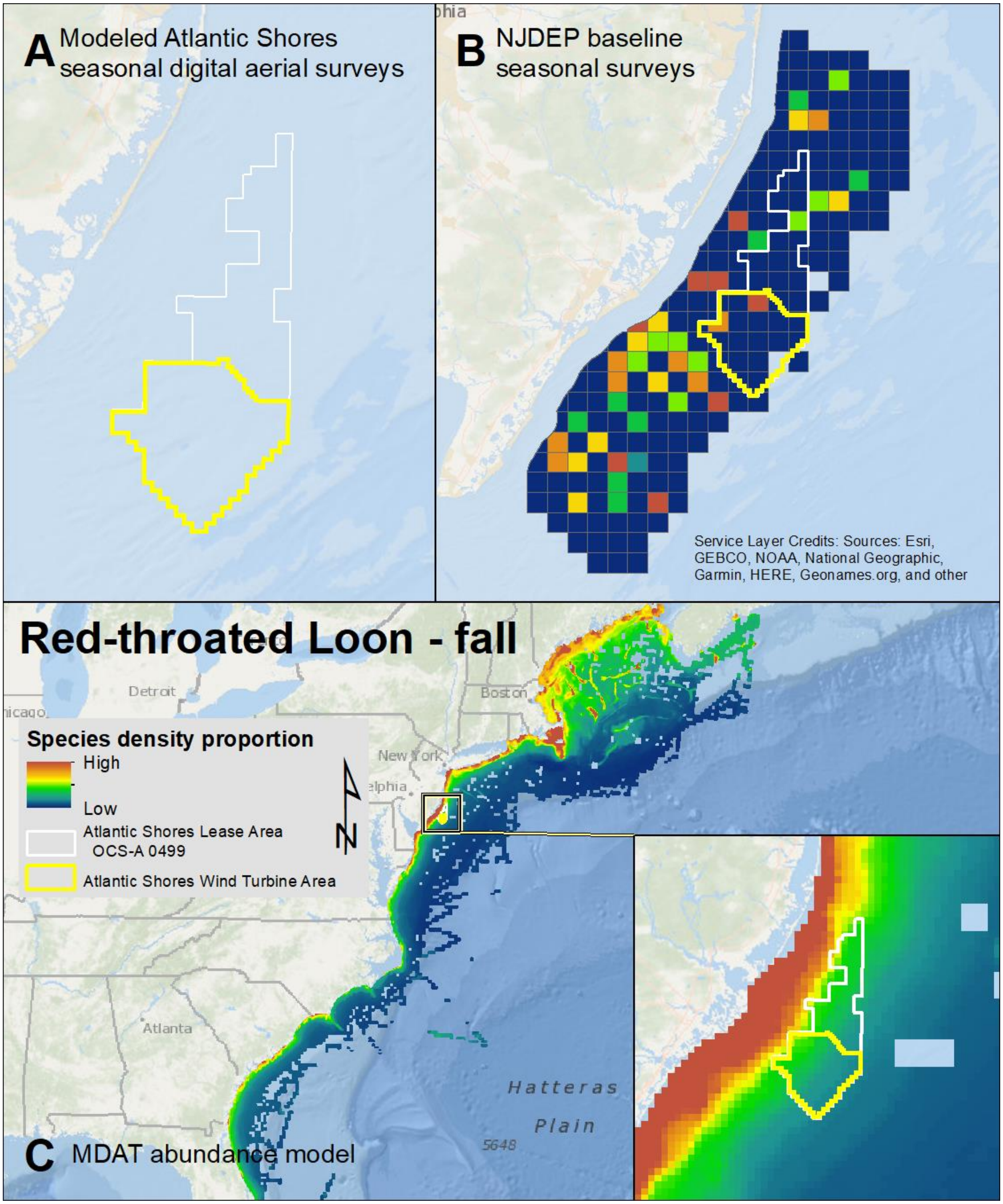

Map 23. Fall Red-throated Loon modeled density proportions in the Atlantic Shores seasonal digital aerial surveys (A), density proportions in the NJDEP baseline survey data (B), and the MDAT data at local and regional scales (C). The scale for all maps is representative of relative spatial variation in the sites within the season for each data source.

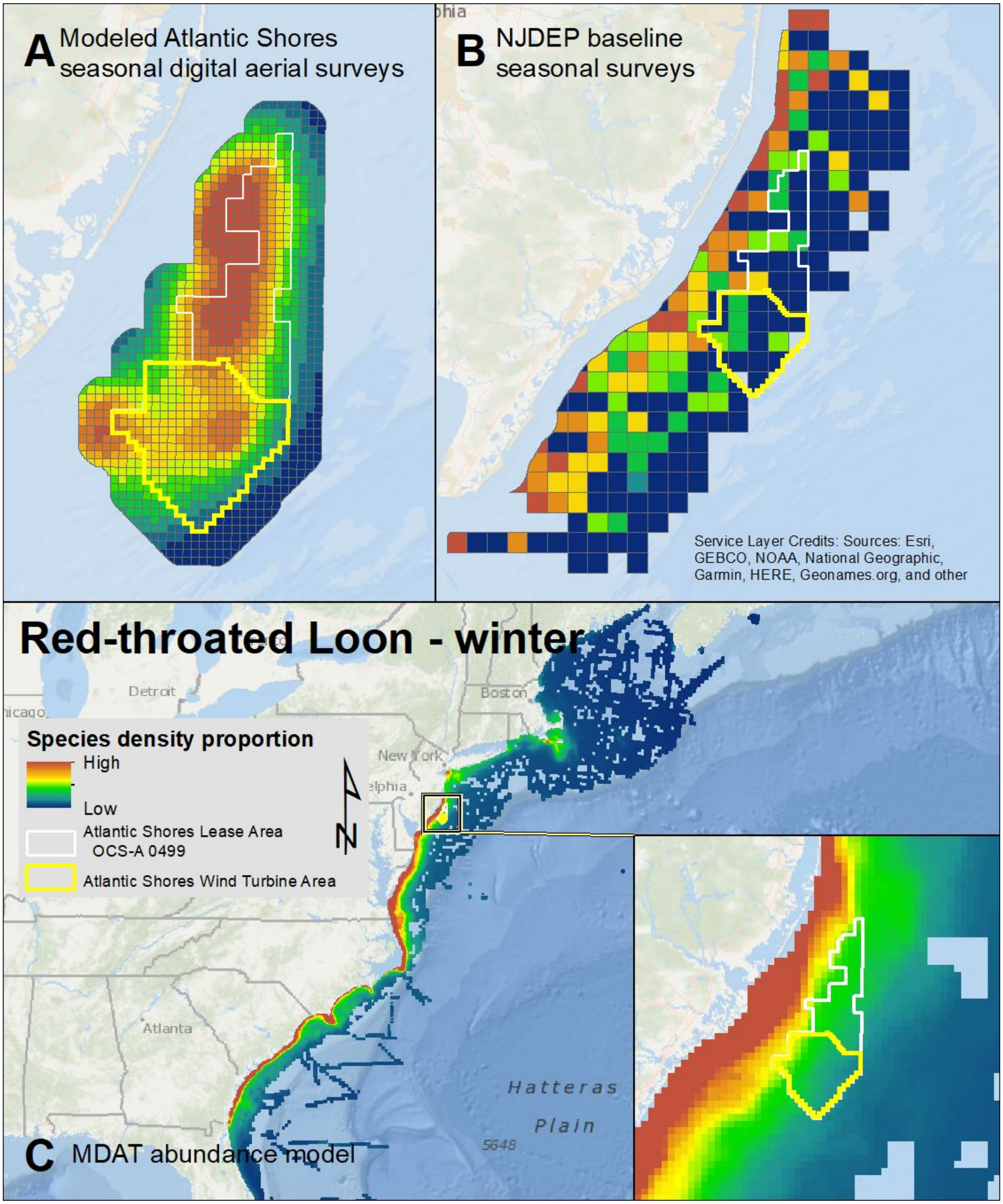

Map 24. Winter Red-throated Loon modeled density proportions in the Atlantic Shores seasonal digital aerial surveys (A), density proportions in the NJDEP baseline survey data (B), and the MDAT data at local and regional scales (C). The scale for all maps is representative of relative spatial variation in the sites within the season for each data source.

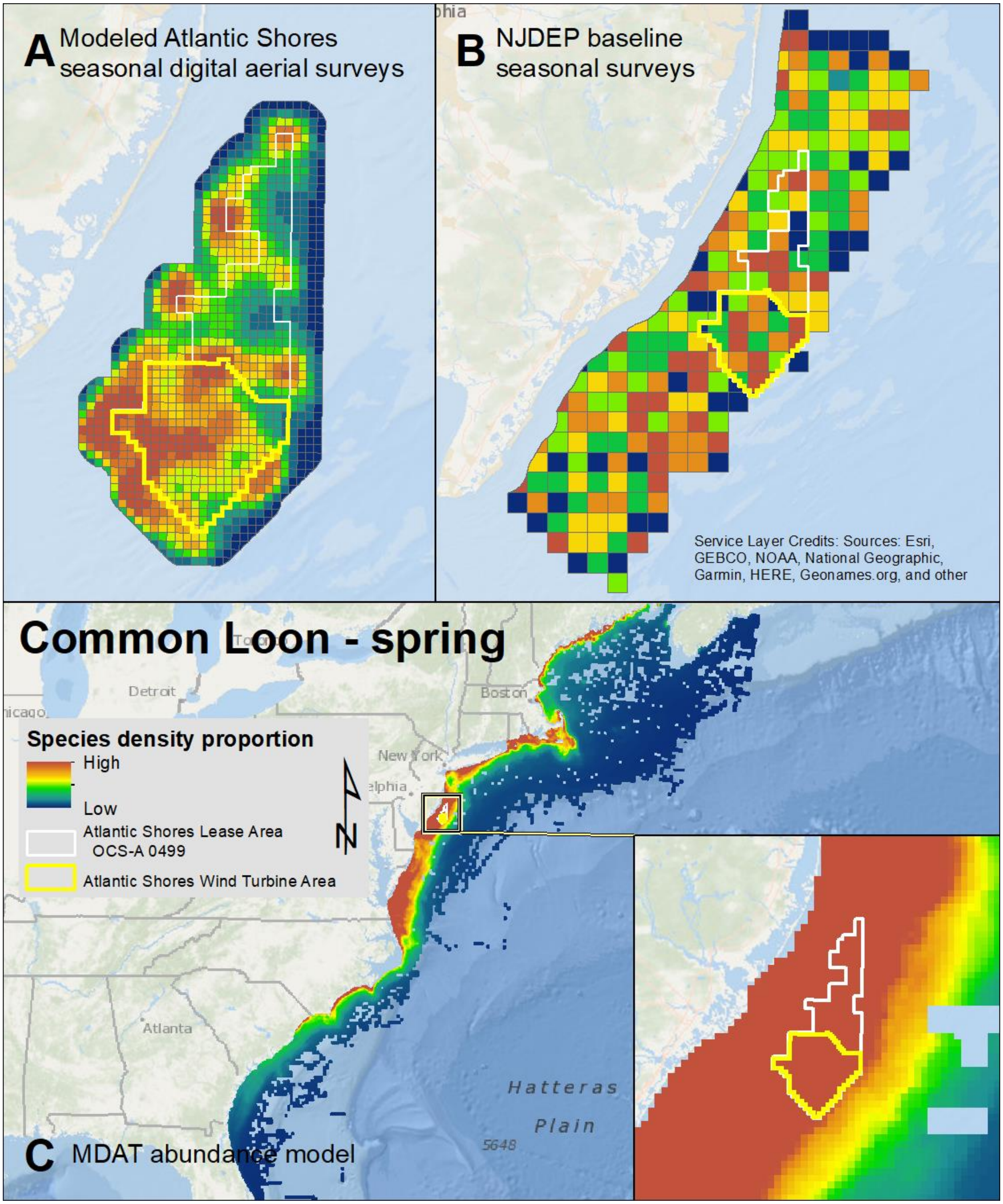

Map 25. Spring Common Loon modeled density proportions in the Atlantic Shores seasonal digital aerial surveys (A), density proportions in the NJDEP baseline survey data (B), and the MDAT data at local and regional scales (C). The scale for all maps is representative of relative spatial variation in the sites within the season for each data source.

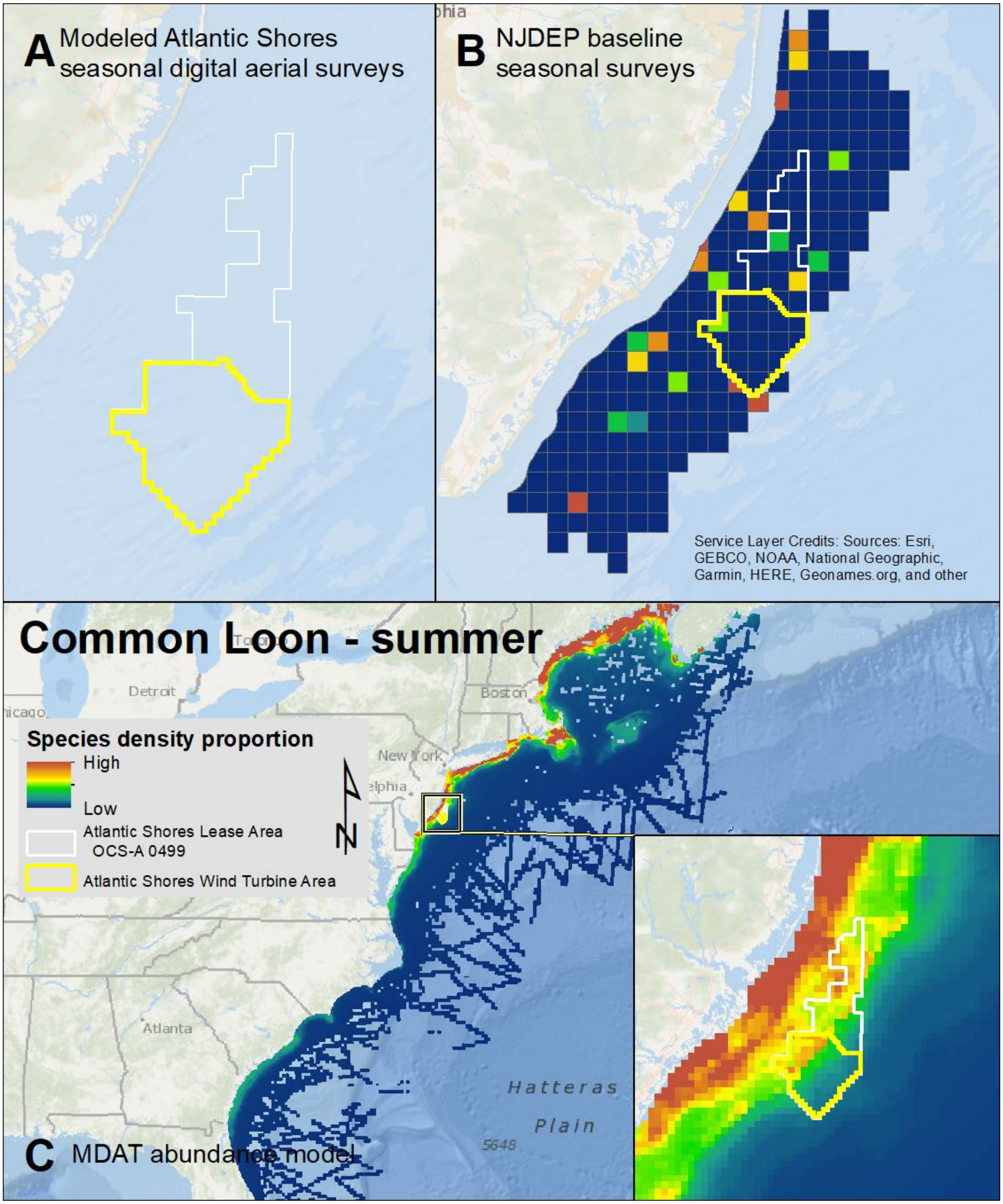

Map 26. Summer Common Loon modeled density proportions in the Atlantic Shores seasonal digital aerial surveys (A), density proportions in the NJDEP baseline survey data (B), and the MDAT data at local and regional scales (C). The scale for all maps is representative of relative spatial variation in the sites within the season for each data source.

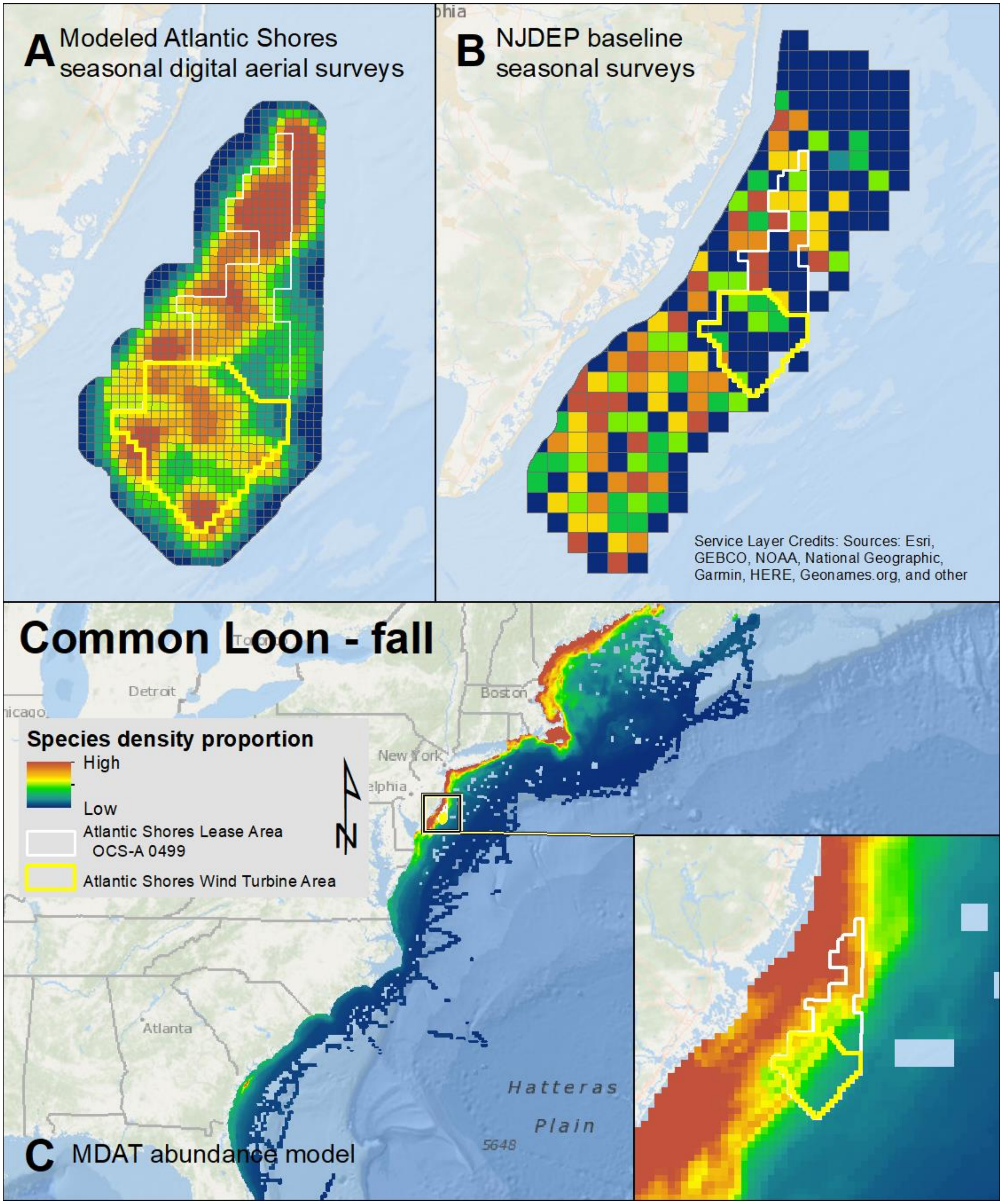

Map 27. Fall Common Loon modeled density proportions in the Atlantic Shores seasonal digital aerial surveys (A), density proportions in the NJDEP baseline survey data (B), and the MDAT data at local and regional scales (C). The scale for all maps is representative of relative spatial variation in the sites within the season for each data source.

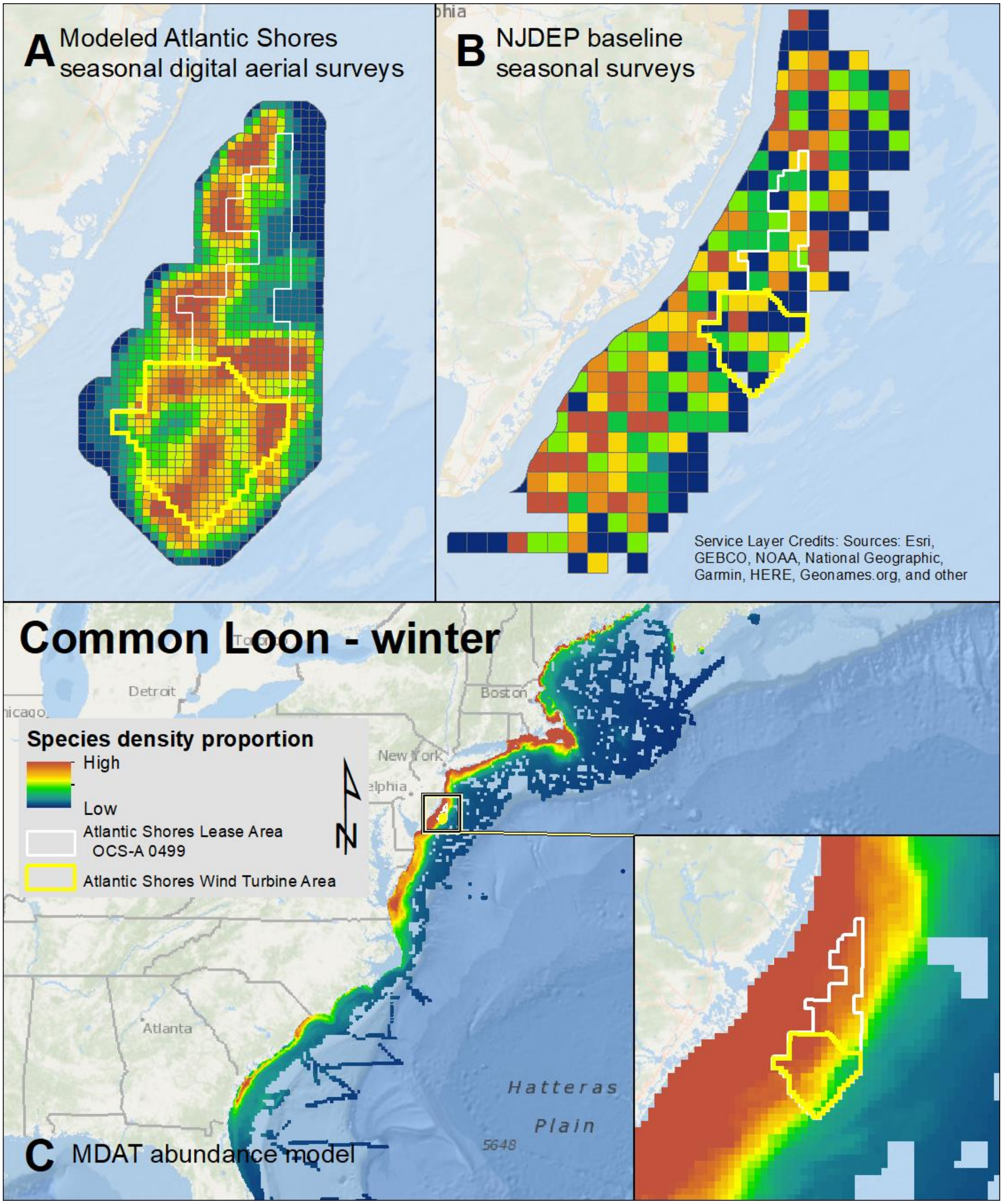

Map 28. Winter Common Loon modeled density proportions in the Atlantic Shores seasonal digital aerial surveys (A), density proportions in the NJDEP baseline survey data (B), and the MDAT data at local and regional scales (C). The scale for all maps is representative of relative spatial variation in the sites within the season for each data source.

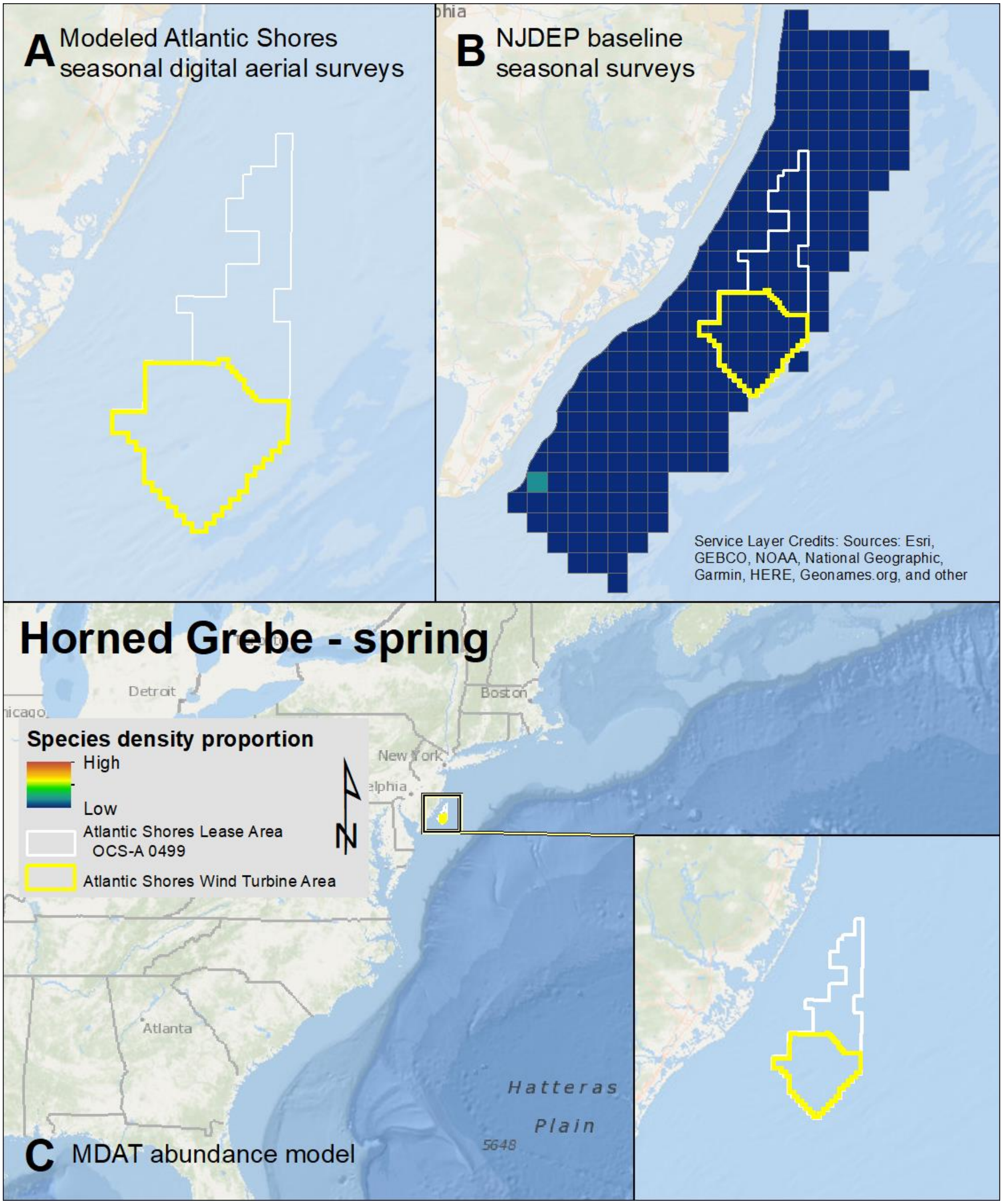

Map 29. Spring Horned Grebe modeled density proportions in the Atlantic Shores seasonal digital aerial surveys (A), density proportions in the NJDEP baseline survey data (B), and the MDAT data at local and regional scales (C). The scale for all maps is representative of relative spatial variation in the sites within the season for each data source.

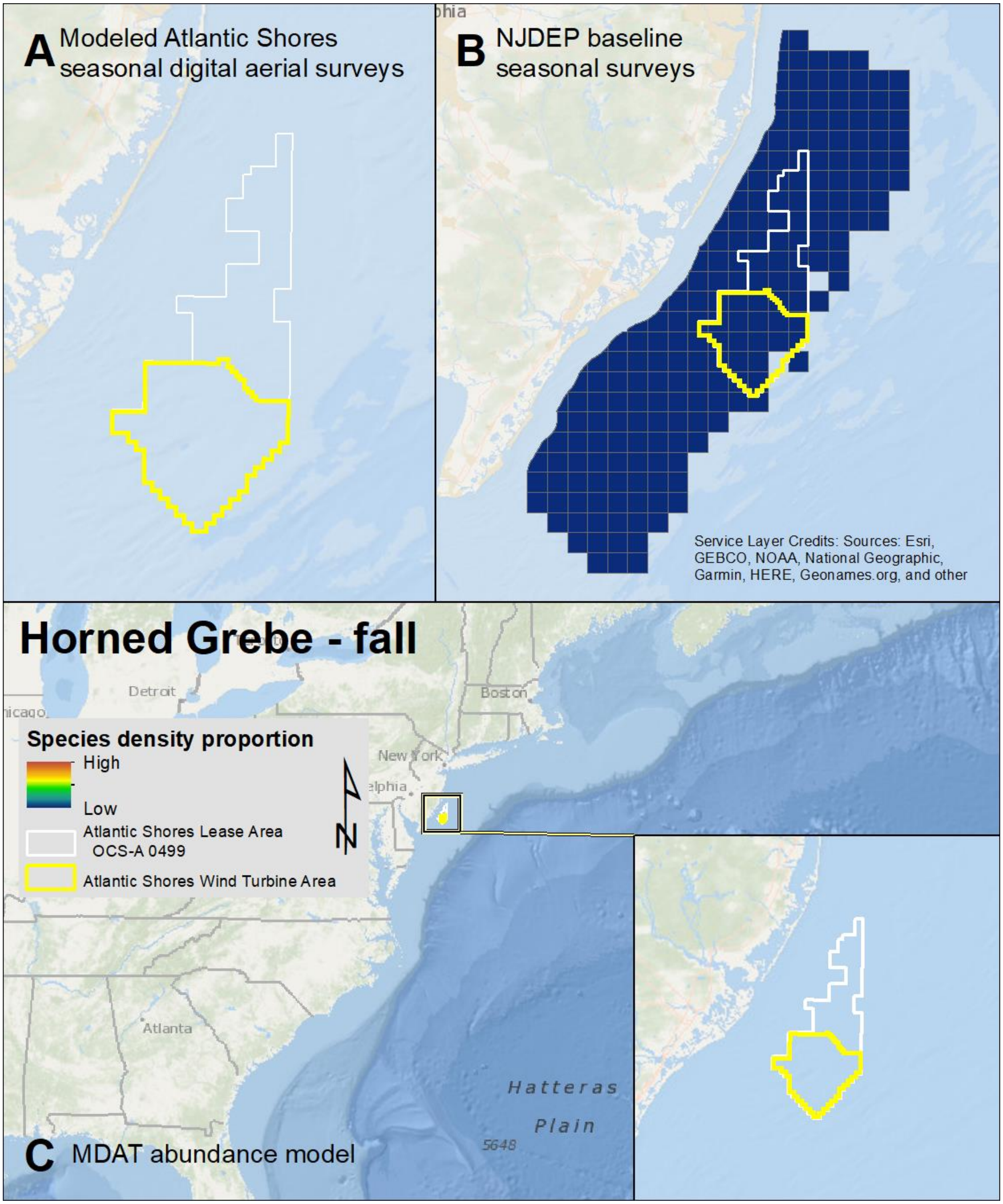

Map 30. Fall Horned Grebe modeled density proportions in the Atlantic Shores seasonal digital aerial surveys (A), density proportions in the NJDEP baseline survey data (B), and the MDAT data at local and regional scales (C). The scale for all maps is representative of relative spatial variation in the sites within the season for each data source.

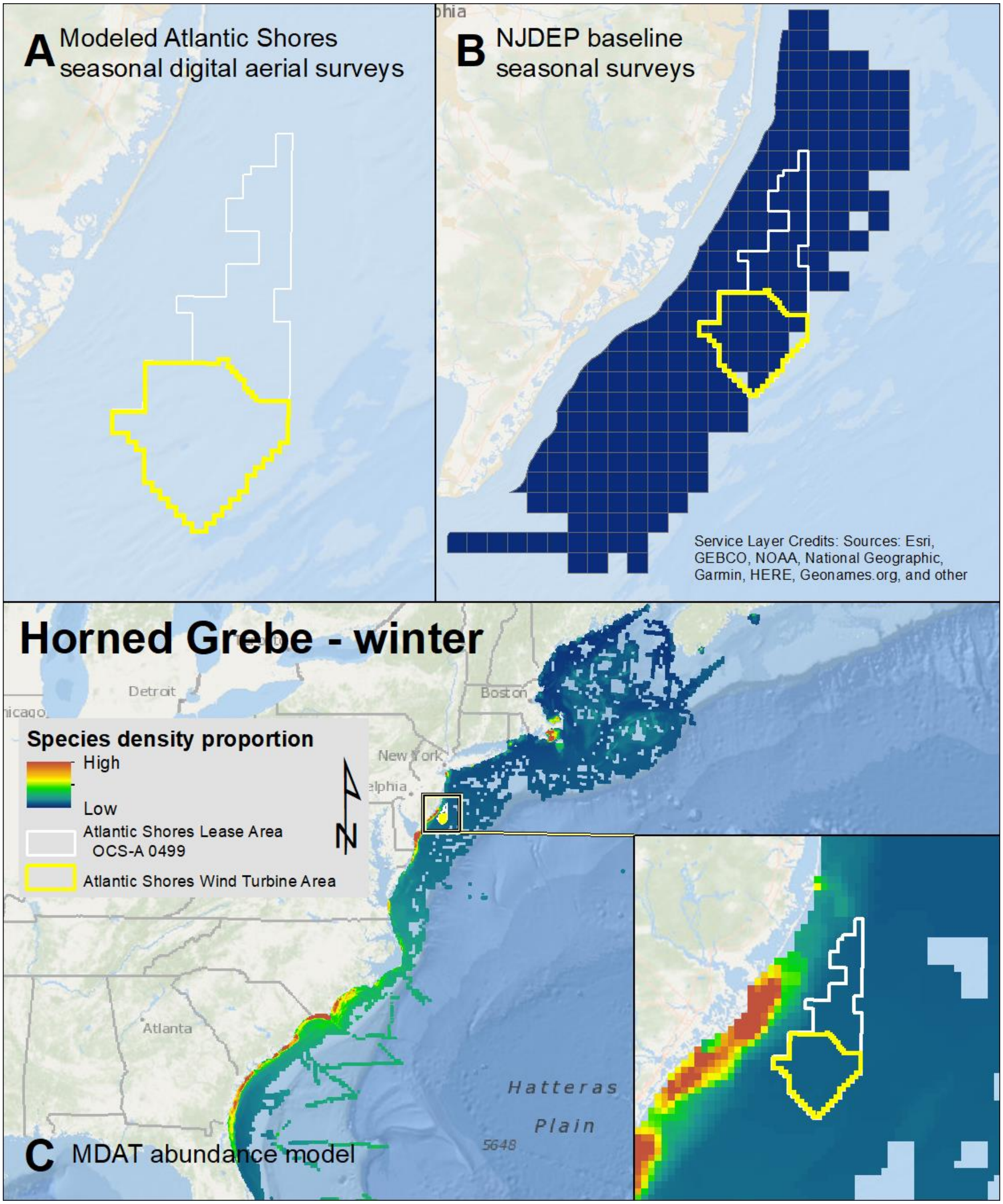

Map 31. Winter Horned Grebe modeled density proportions in the Atlantic Shores seasonal digital aerial surveys (A), density proportions in the NJDEP baseline survey data (B), and the MDAT data at local and regional scales (C). The scale for all maps is representative of relative spatial variation in the sites within the season for each data source.

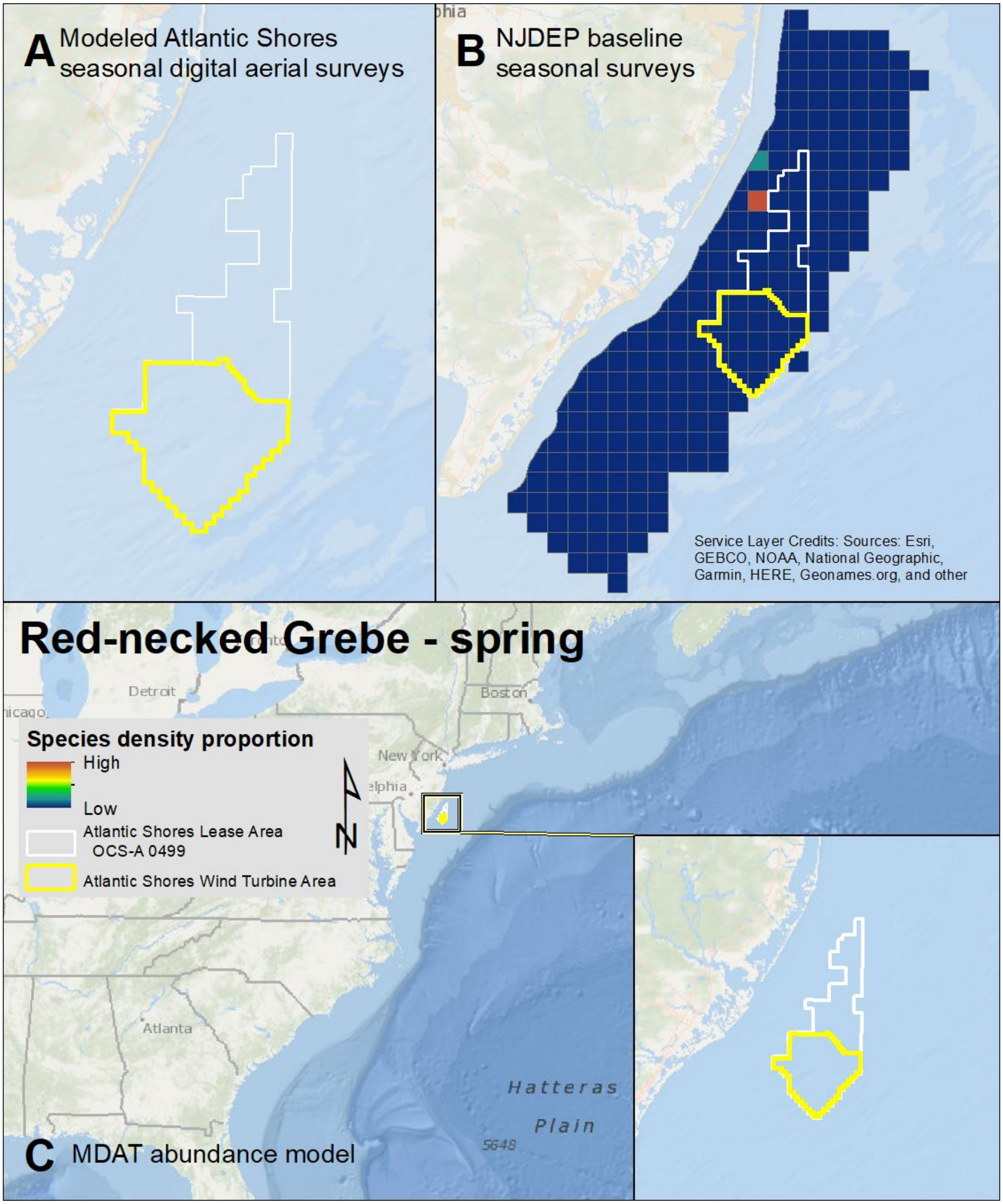

Map 32. Spring Red-necked Grebe modeled density proportions in the Atlantic Shores seasonal digital aerial surveys (A), density proportions in the NJDEP baseline survey data (B), and the MDAT data at local and regional scales (C). The scale for all maps is representative of relative spatial variation in the sites within the season for each data source.

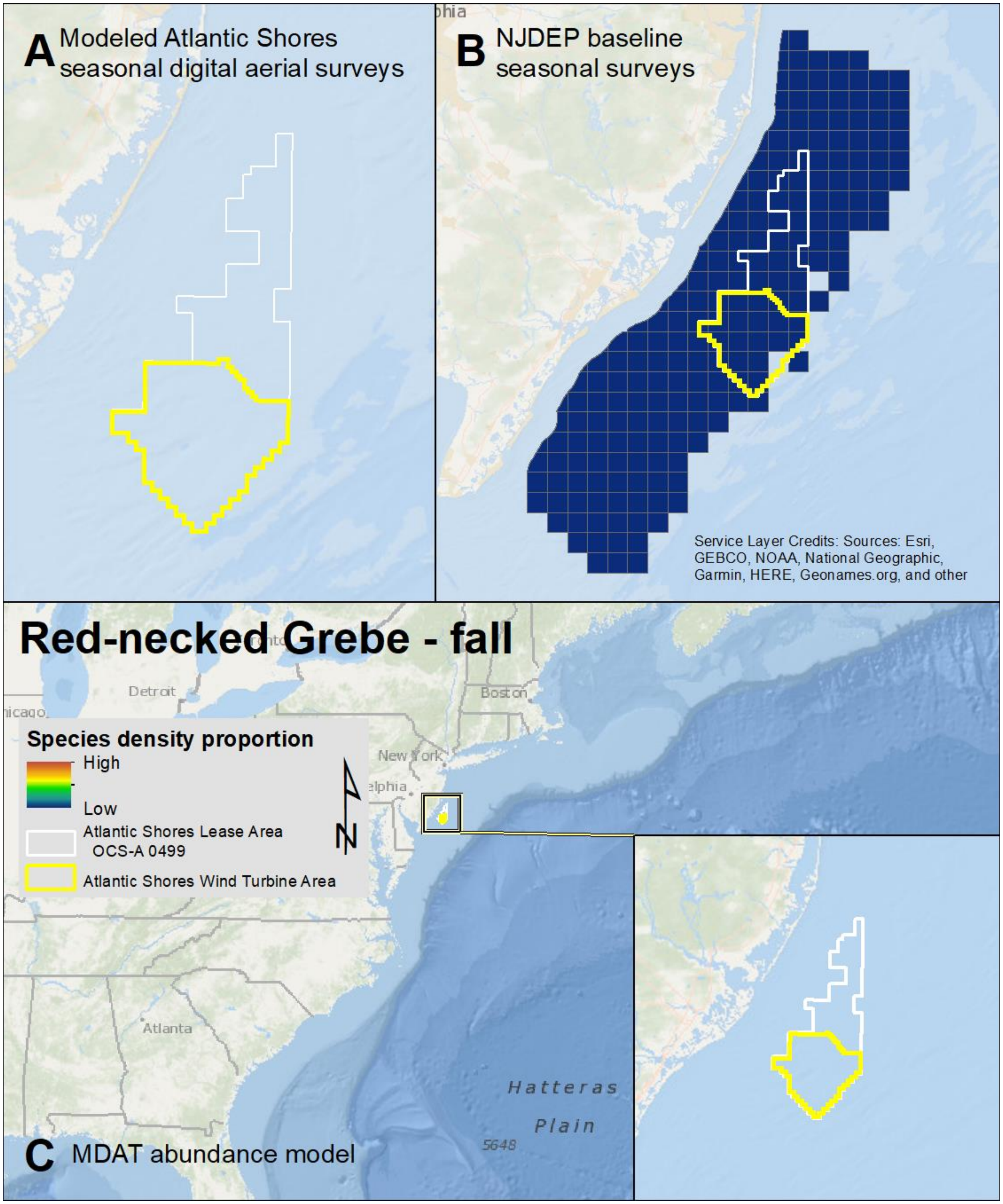

Map 33. Fall Red-necked Grebe modeled density proportions in the Atlantic Shores seasonal digital aerial surveys (A), density proportions in the NJDEP baseline survey data (B), and the MDAT data at local and regional scales (C). The scale for all maps is representative of relative spatial variation in the sites within the season for each data source.

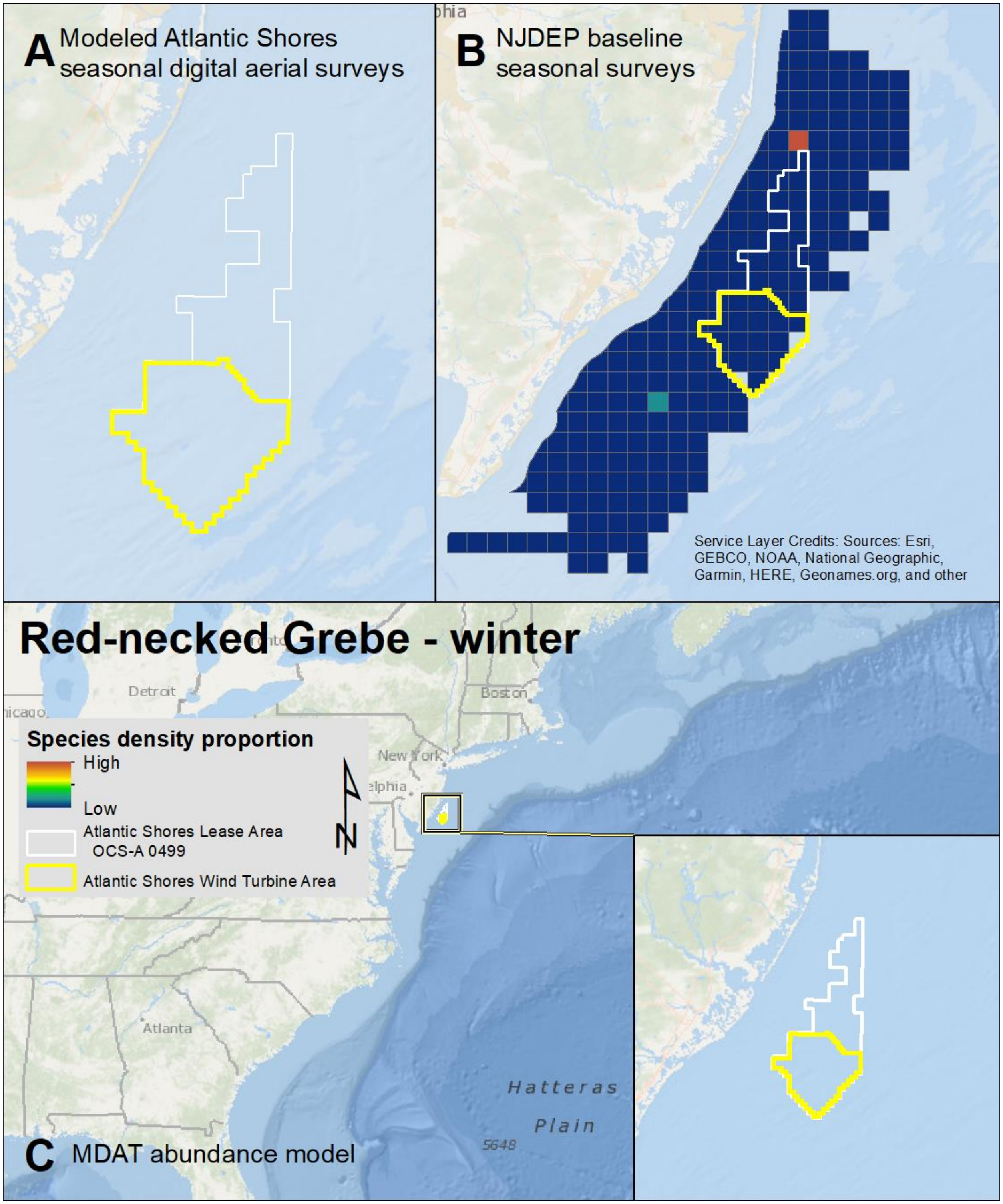

Map 34. Winter Red-necked Grebe modeled density proportions in the Atlantic Shores seasonal digital aerial surveys (A), density proportions in the NJDEP baseline survey data (B), and the MDAT data at local and regional scales (C). The scale for all maps is representative of relative spatial variation in the sites within the season for each data source.

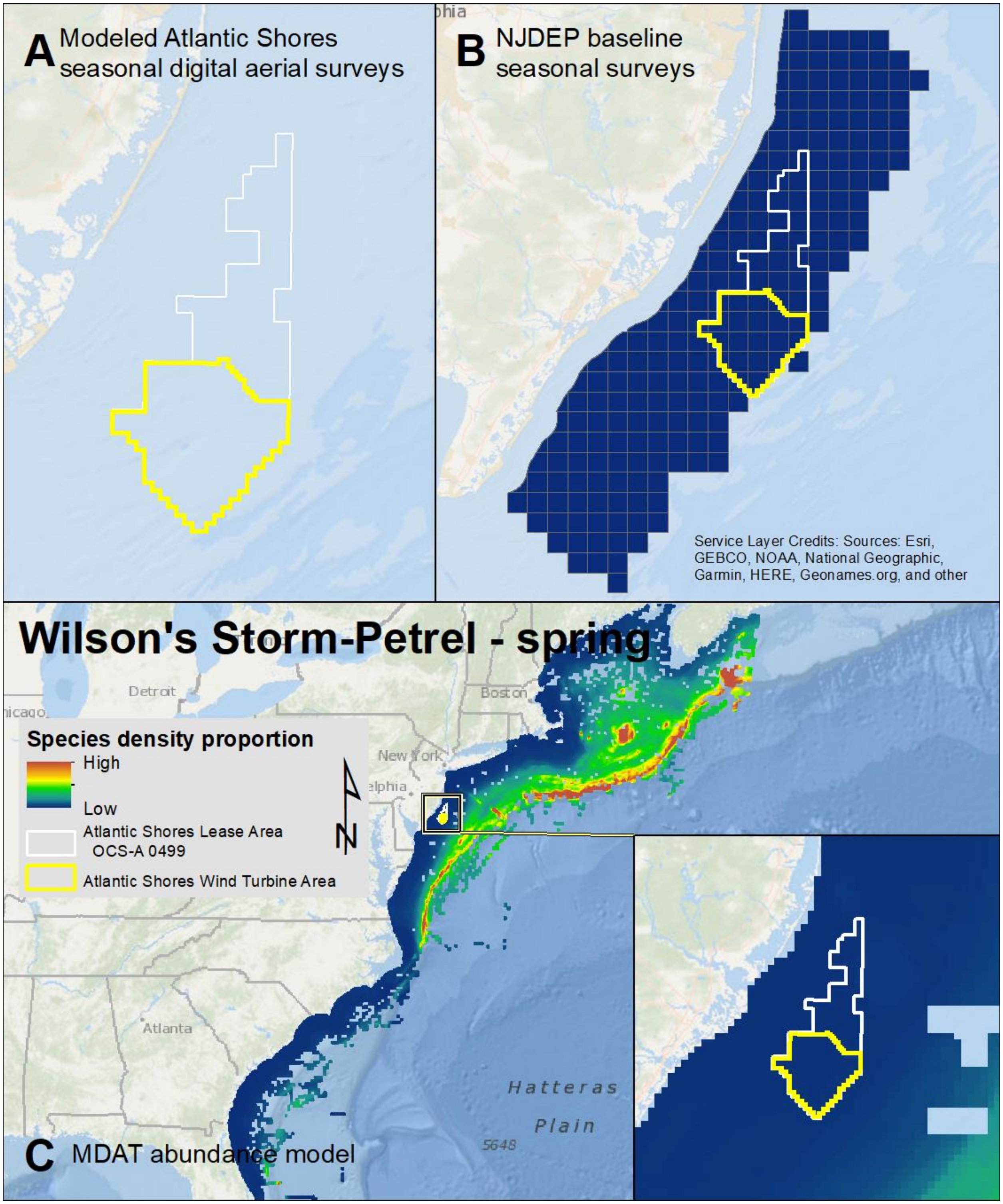

Map 35. Spring Wilson's Storm-Petrel modeled density proportions in the Atlantic Shores seasonal digital aerial surveys (A), density proportions in the NJDEP baseline survey data (B), and the MDAT data at local and regional scales (C). The scale for all maps is representative of relative spatial variation in the sites within the season for each data source.

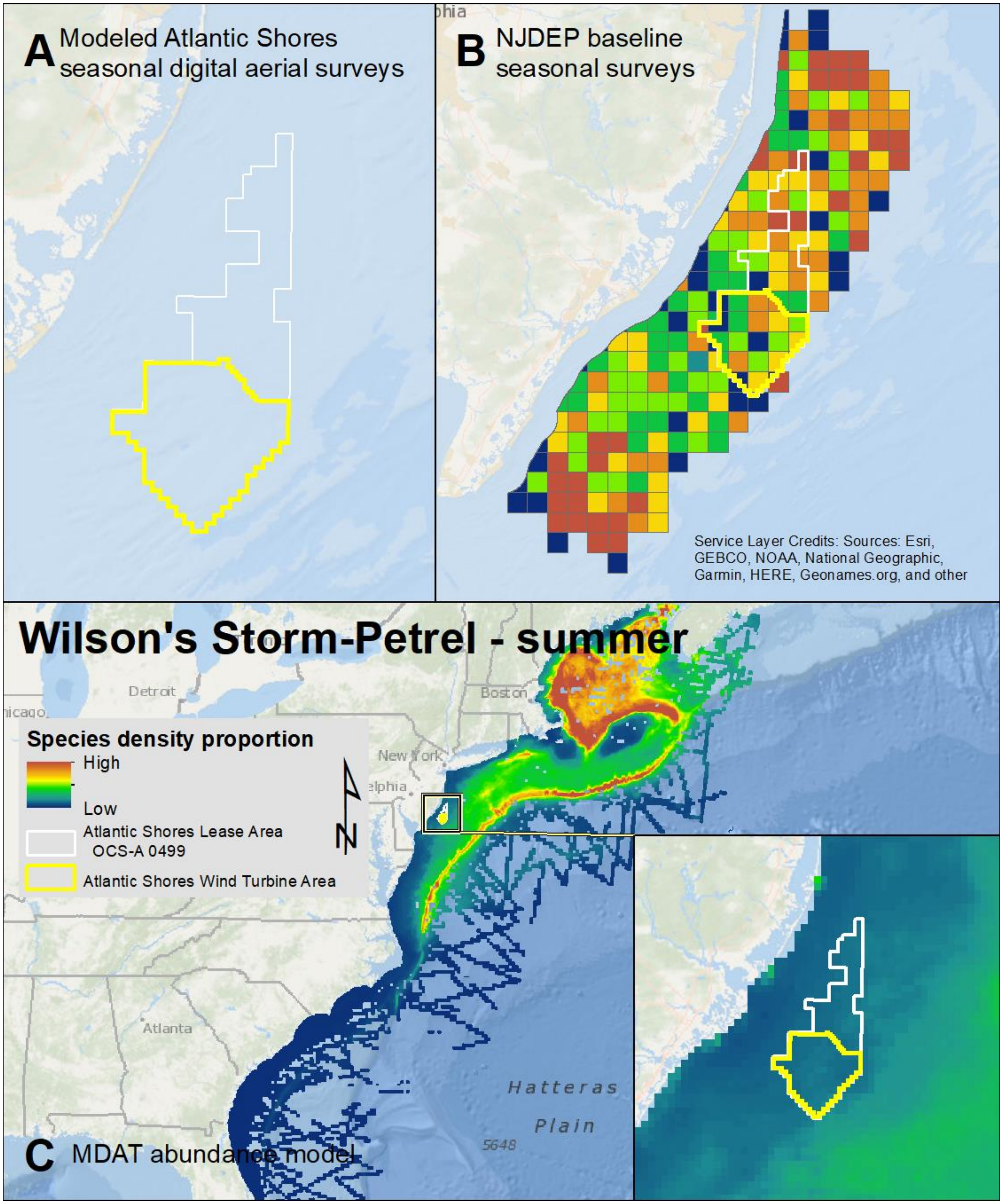

Map 36. Summer Wilson's Storm-Petrel modeled density proportions in the Atlantic Shores seasonal digital aerial surveys (A), density proportions in the NJDEP baseline survey data (B), and the MDAT data at local and regional scales (C). The scale for all maps is representative of relative spatial variation in the sites within the season for each data source.

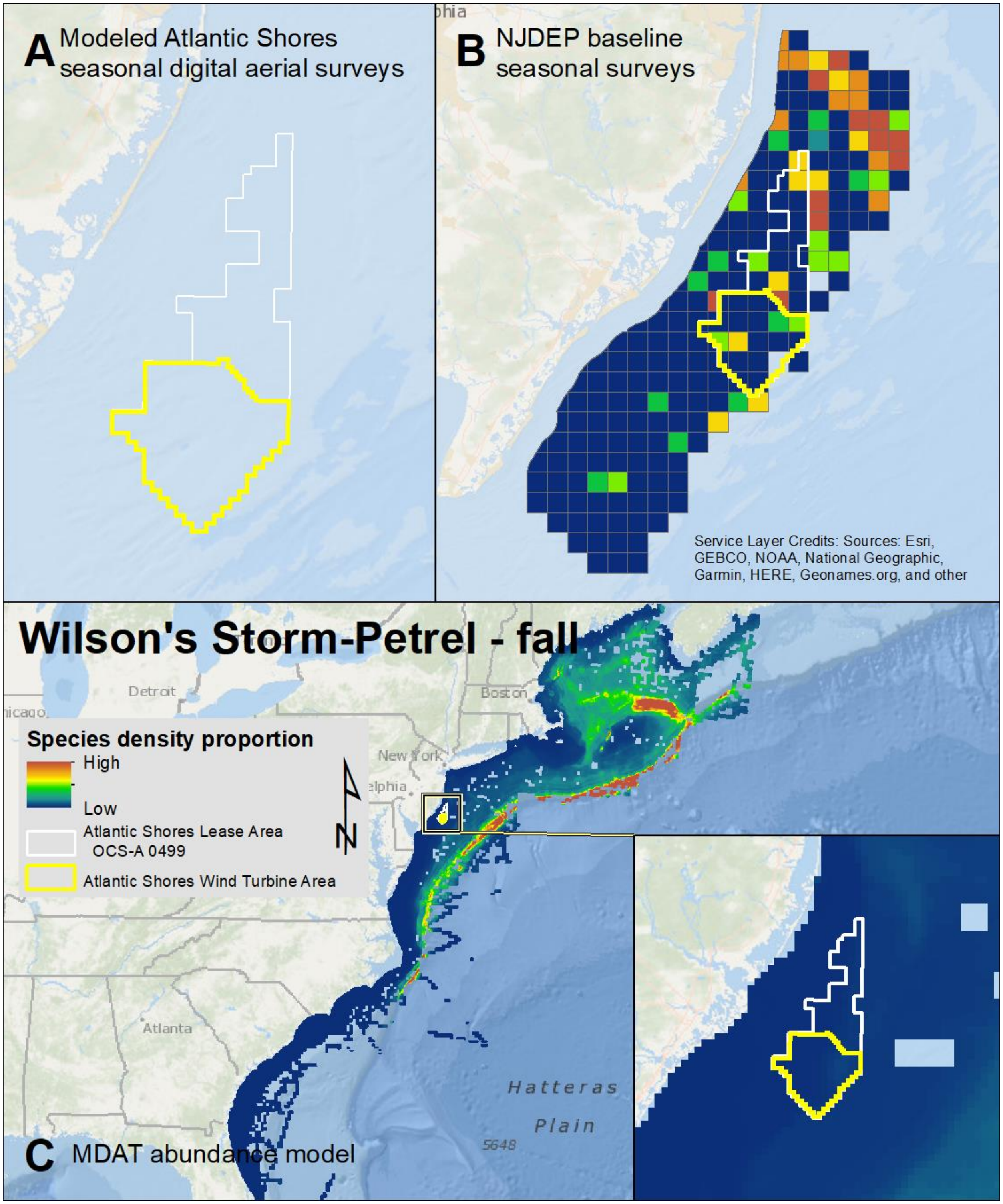

Map 37. Fall Wilson's Storm-Petrel modeled density proportions in the Atlantic Shores seasonal digital aerial surveys (A), density proportions in the NJDEP baseline survey data (B), and the MDAT data at local and regional scales (C). The scale for all maps is representative of relative spatial variation in the sites within the season for each data source.

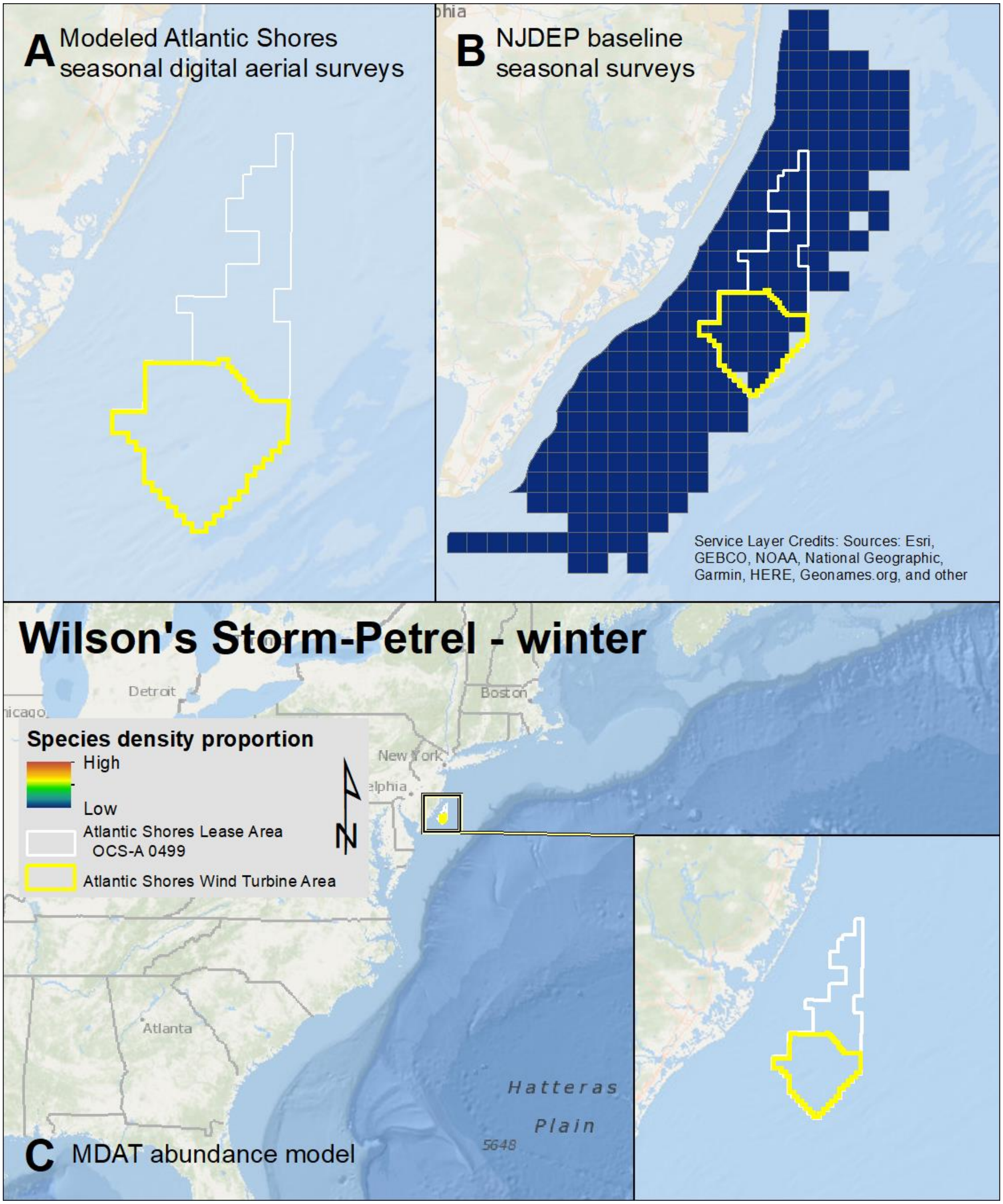

Map 38. Winter Wilson's Storm-Petrel modeled density proportions in the Atlantic Shores seasonal digital aerial surveys (A), density proportions in the NJDEP baseline survey data (B), and the MDAT data at local and regional scales (C). The scale for all maps is representative of relative spatial variation in the sites within the season for each data source.

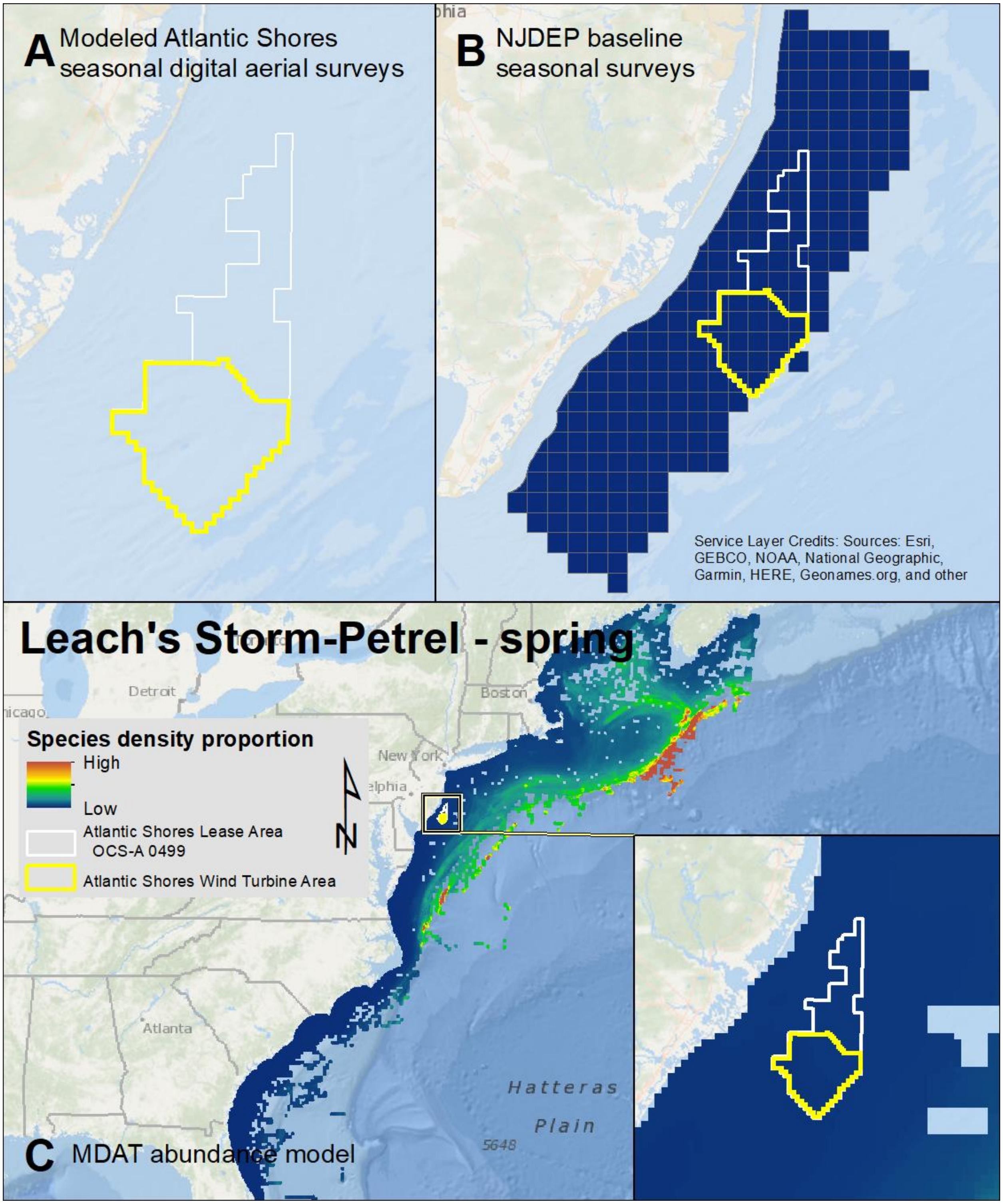

Map 39. Spring Leach's Storm-Petrel modeled density proportions in the Atlantic Shores seasonal digital aerial surveys (A), density proportions in the NJDEP baseline survey data (B), and the MDAT data at local and regional scales (C). The scale for all maps is representative of relative spatial variation in the sites within the season for each data source.

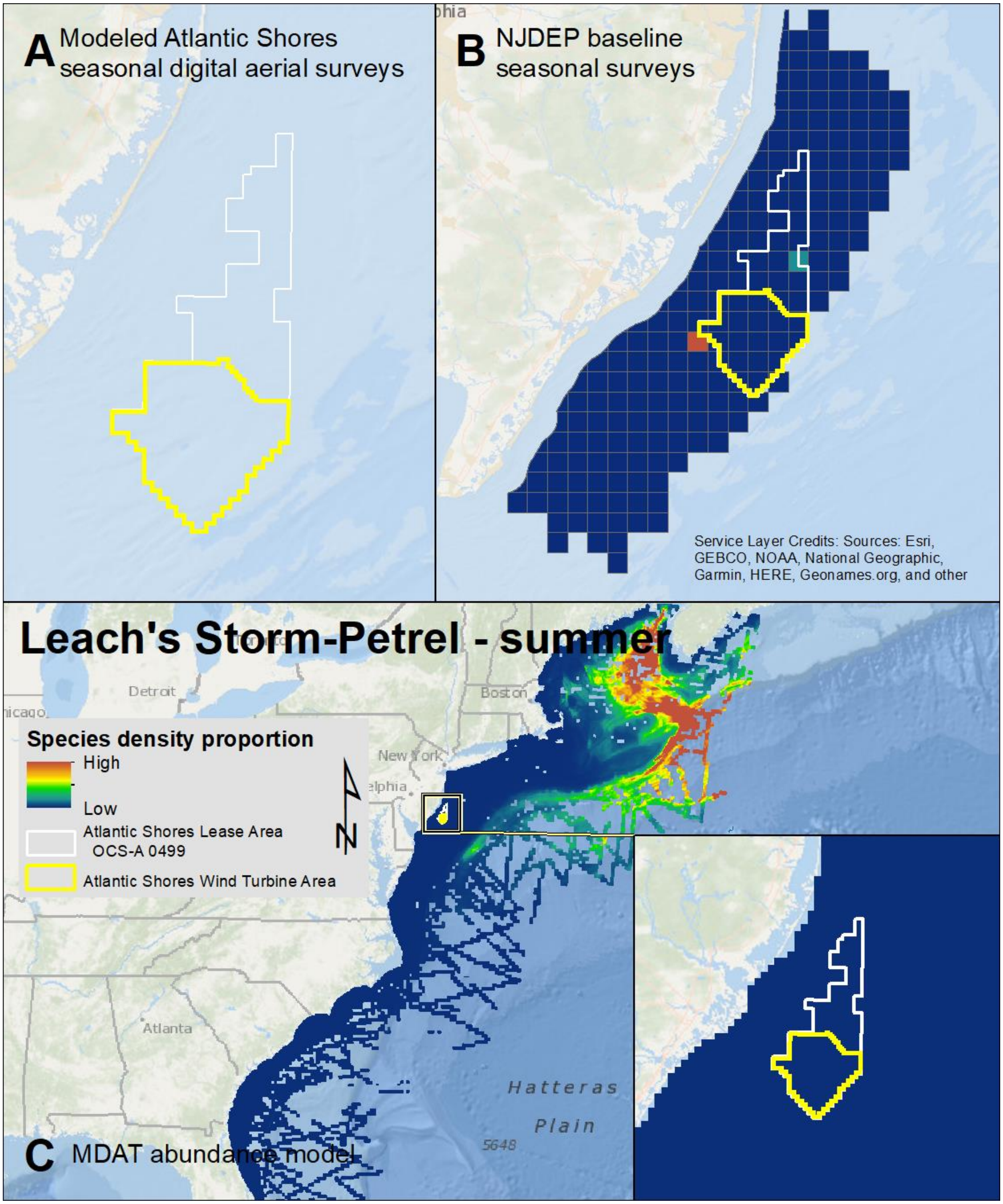

Map 40. Summer Leach's Storm-Petrel modeled density proportions in the Atlantic Shores seasonal digital aerial surveys (A), density proportions in the NJDEP baseline survey data (B), and the MDAT data at local and regional scales (C). The scale for all maps is representative of relative spatial variation in the sites within the season for each data source.

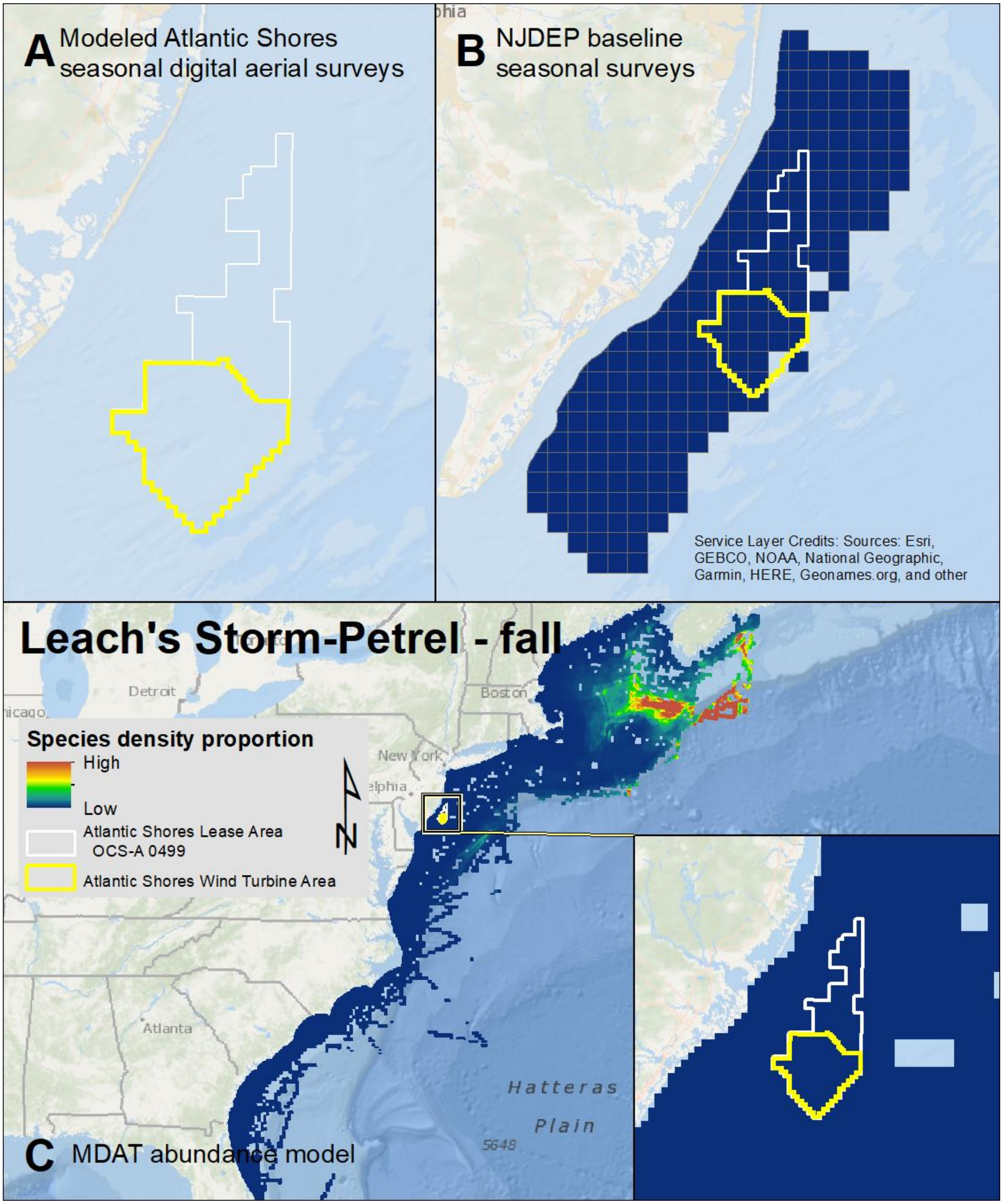

Map 41. Fall Leach's Storm-Petrel modeled density proportions in the Atlantic Shores seasonal digital aerial surveys (A), density proportions in the NJDEP baseline survey data (B), and the MDAT data at local and regional scales (C). The scale for all maps is representative of relative spatial variation in the sites within the season for each data source.

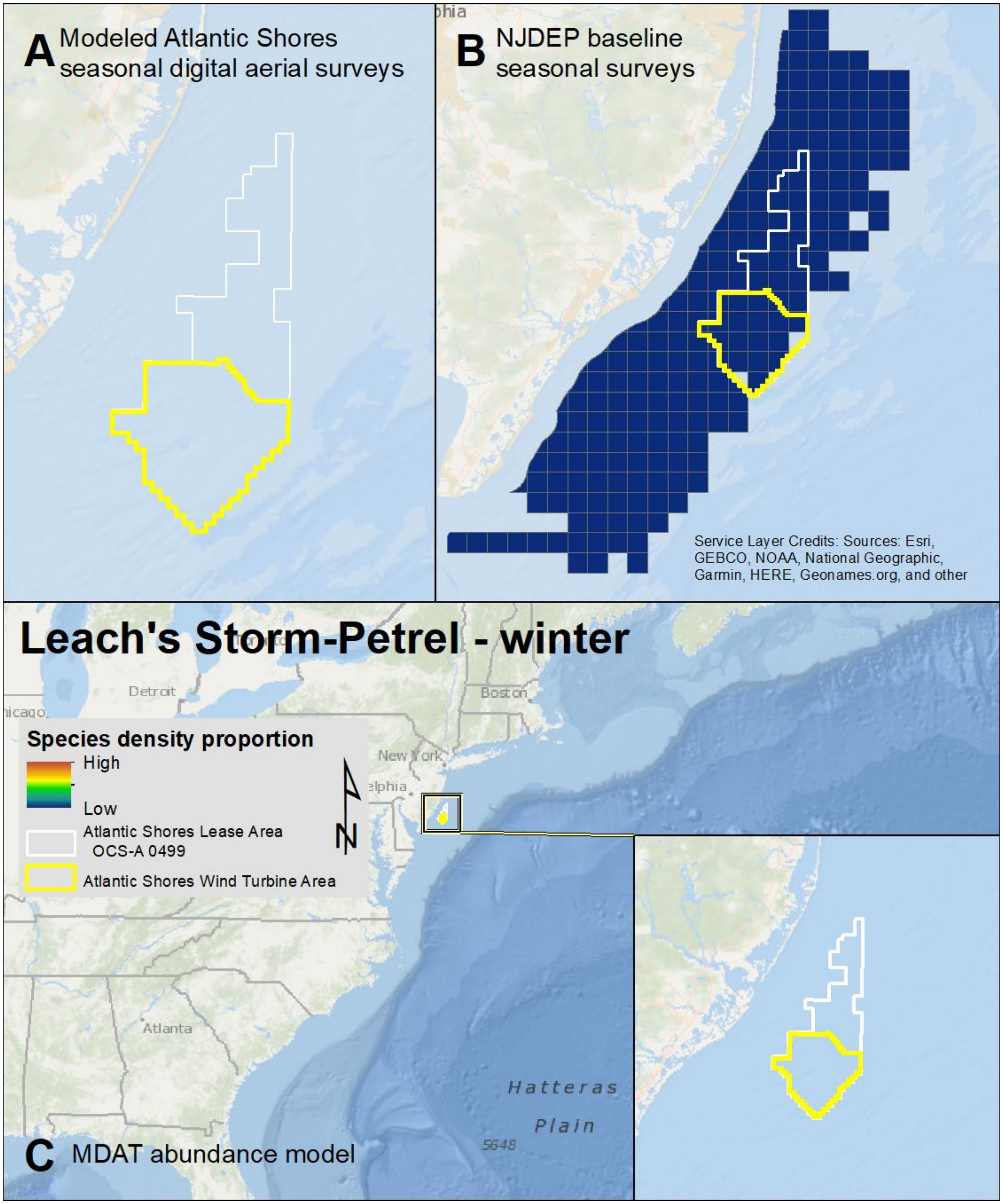

Map 42. Winter Leach's Storm-Petrel modeled density proportions in the Atlantic Shores seasonal digital aerial surveys (A), density proportions in the NJDEP baseline survey data (B), and the MDAT data at local and regional scales (C). The scale for all maps is representative of relative spatial variation in the sites within the season for each data source.

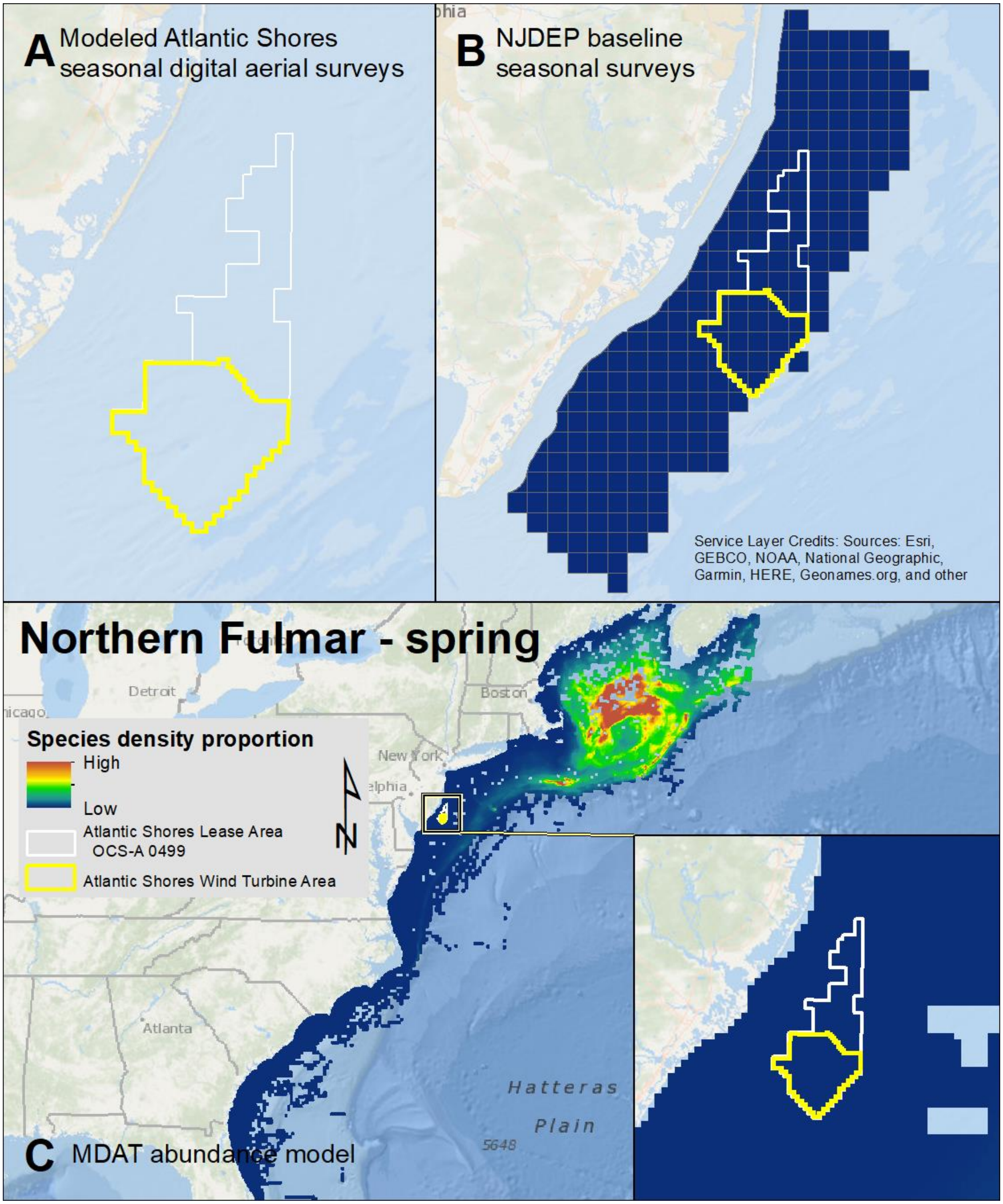

Map 43. Spring Northern Fulmar modeled density proportions in the Atlantic Shores seasonal digital aerial surveys (A), density proportions in the NJDEP baseline survey data (B), and the MDAT data at local and regional scales (C). The scale for all maps is representative of relative spatial variation in the sites within the season for each data source.

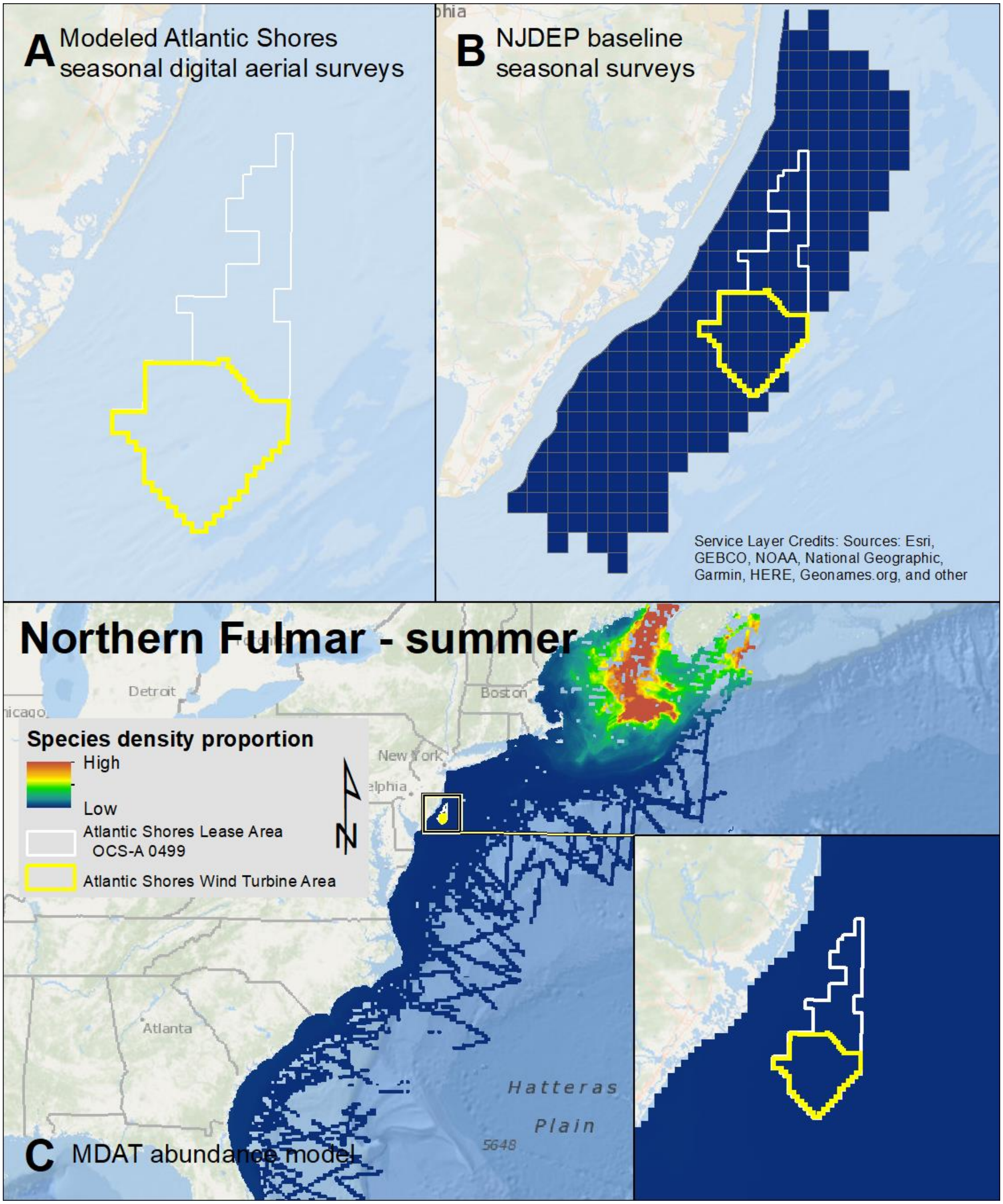

Map 44. Summer Northern Fulmar modeled density proportions in the Atlantic Shores seasonal digital aerial surveys (A), density proportions in the NJDEP baseline survey data (B), and the MDAT data at local and regional scales (C). The scale for all maps is representative of relative spatial variation in the sites within the season for each data source.

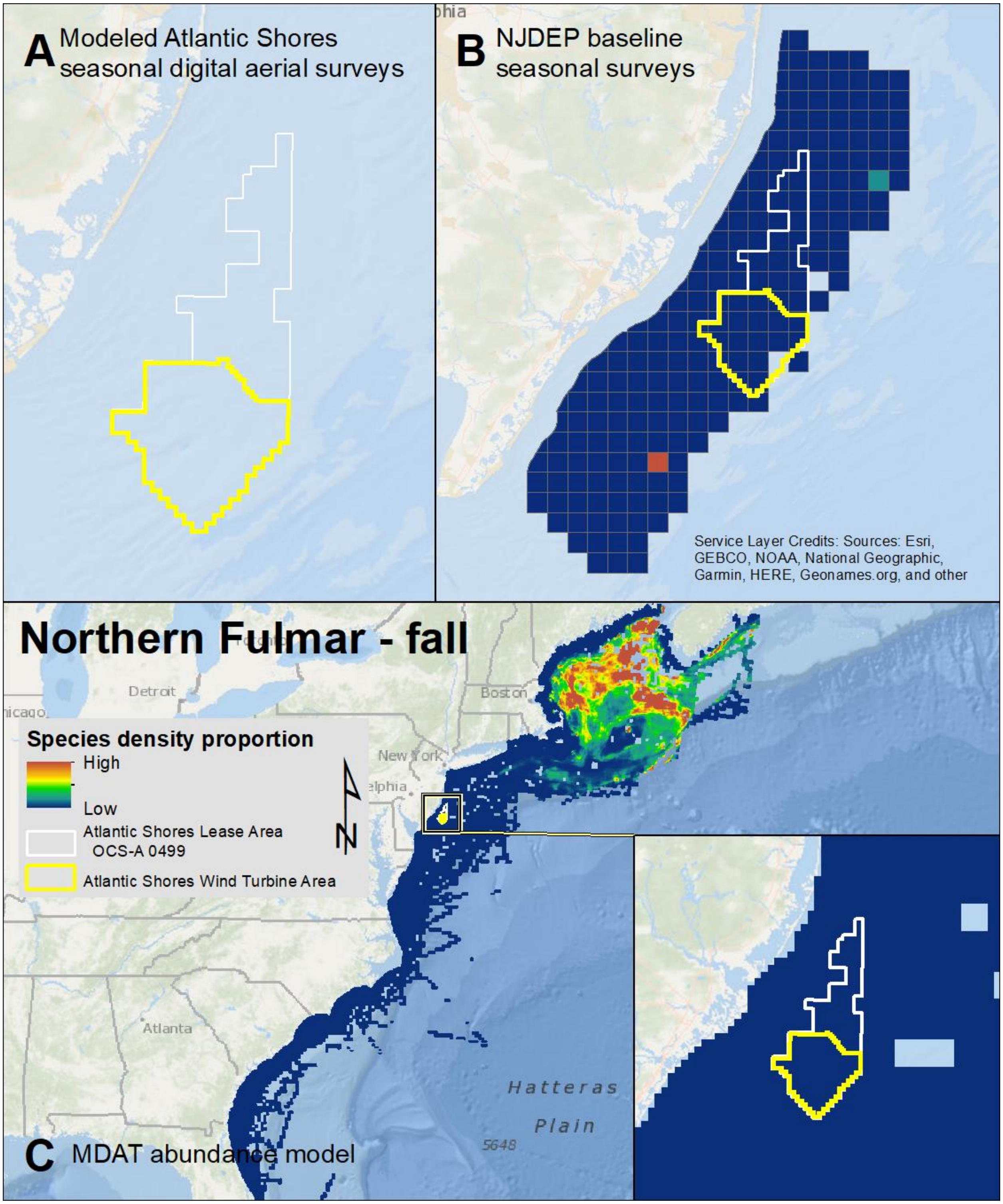

Map 45. Fall Northern Fulmar modeled density proportions in the Atlantic Shores seasonal digital aerial surveys (A), density proportions in the NJDEP baseline survey data (B), and the MDAT data at local and regional scales (C). The scale for all maps is representative of relative spatial variation in the sites within the season for each data source.

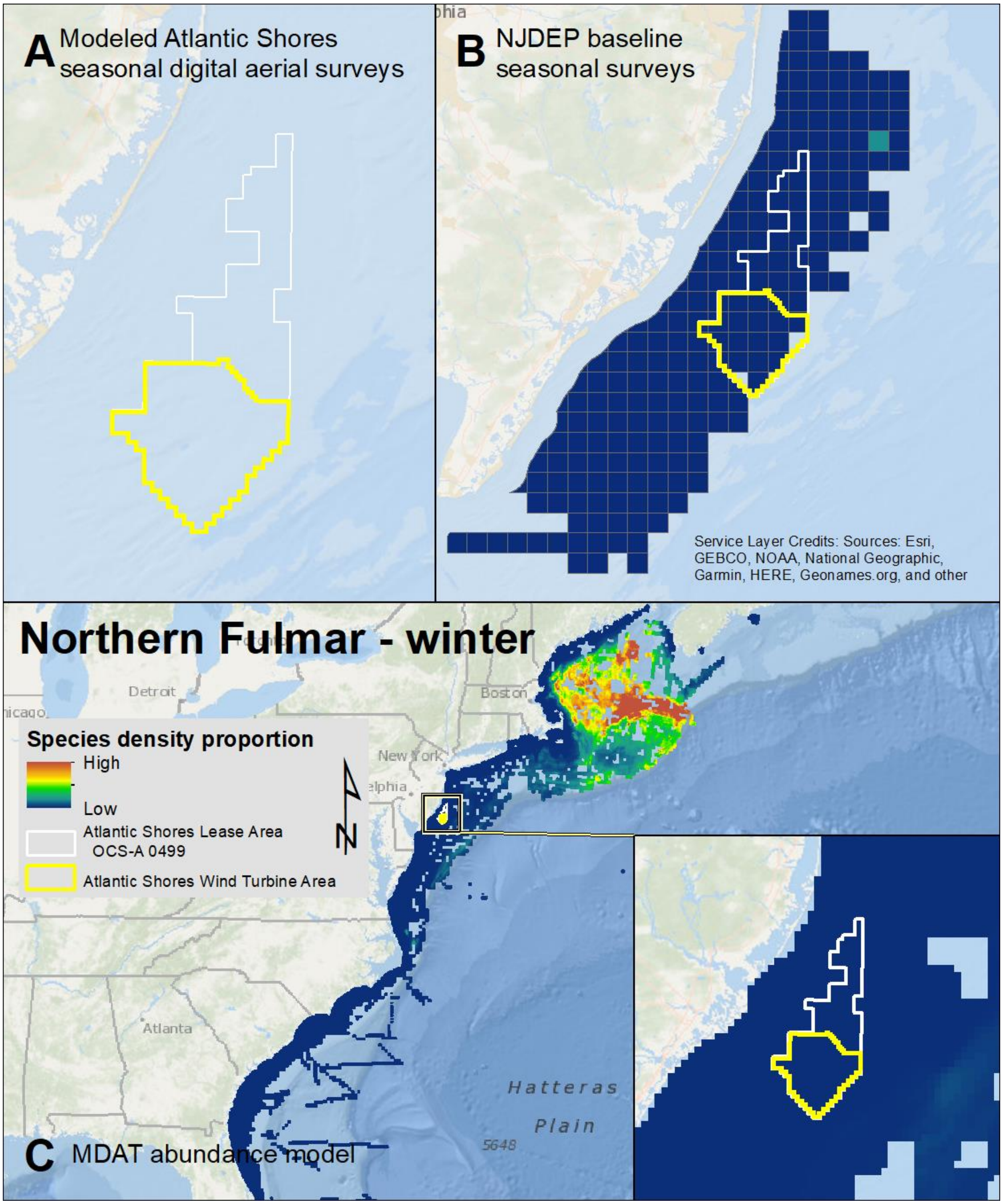

Map 46. Winter Northern Fulmar modeled density proportions in the Atlantic Shores seasonal digital aerial surveys (A), density proportions in the NJDEP baseline survey data (B), and the MDAT data at local and regional scales (C). The scale for all maps is representative of relative spatial variation in the sites within the season for each data source.

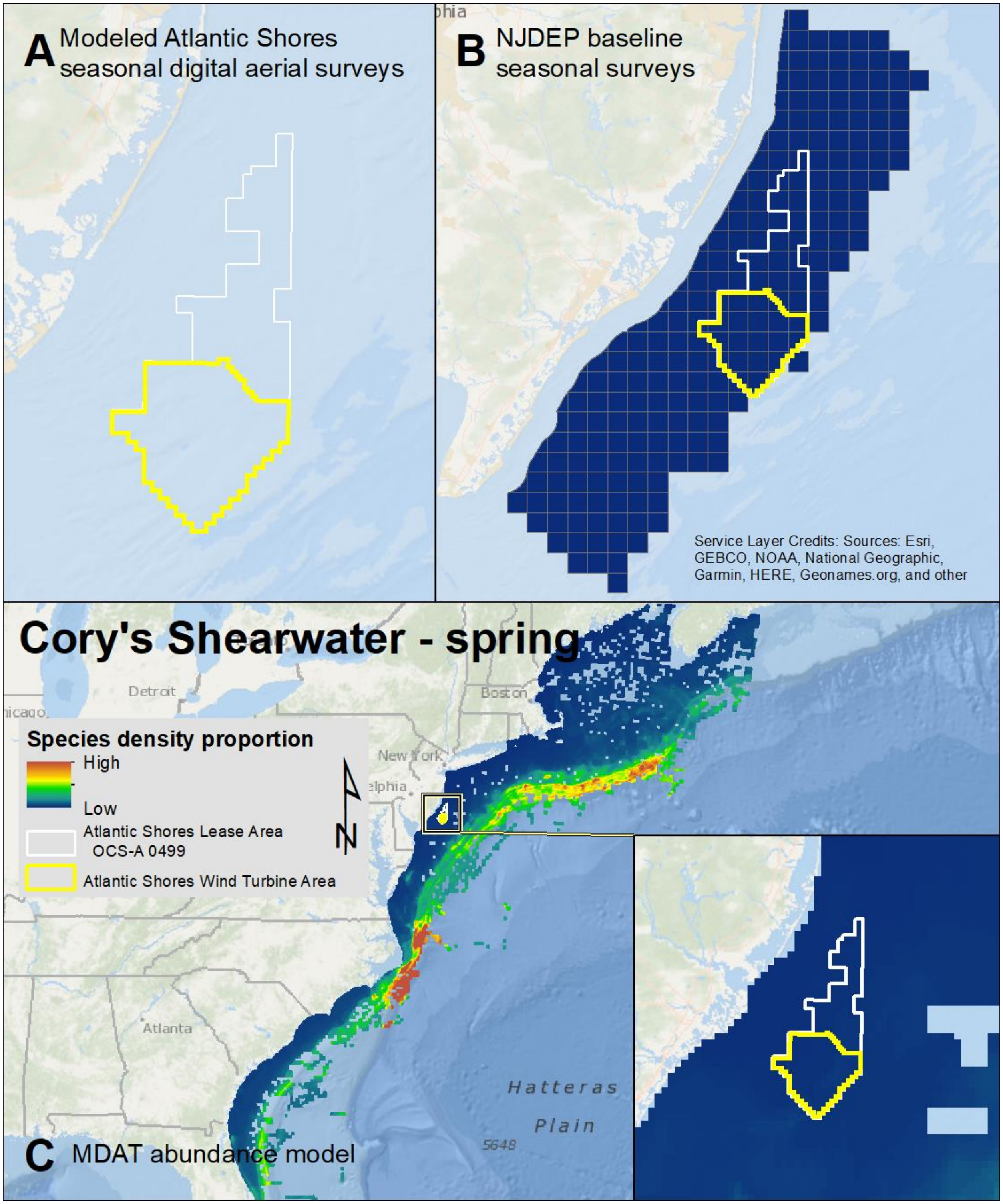

Map 47. Spring Cory's Shearwater modeled density proportions in the Atlantic Shores seasonal digital aerial surveys (A), density proportions in the NJDEP baseline survey data (B), and the MDAT data at local and regional scales (C). The scale for all maps is representative of relative spatial variation in the sites within the season for each data source.

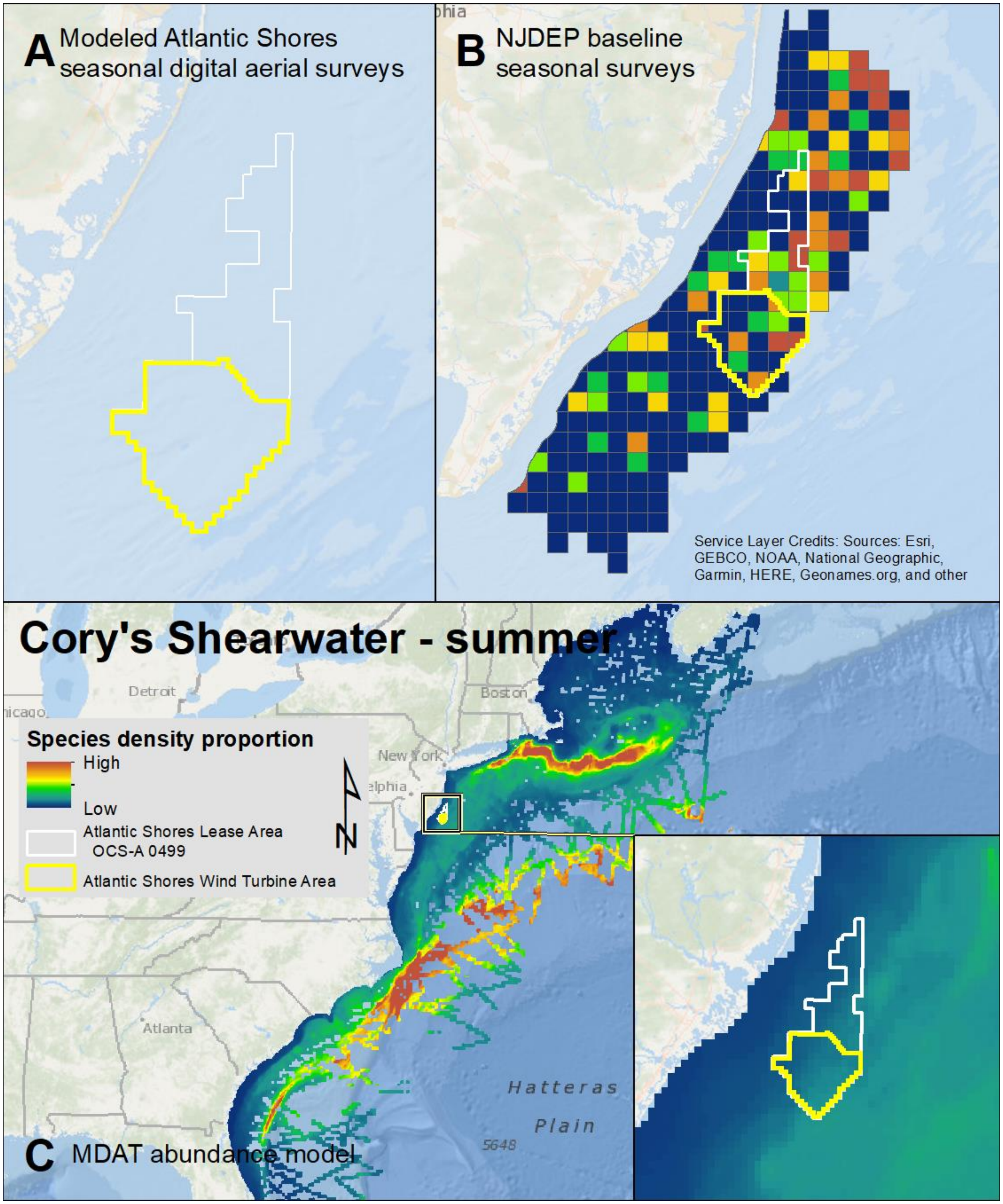

Map 48. Summer Cory's Shearwater modeled density proportions in the Atlantic Shores seasonal digital aerial surveys (A), density proportions in the NJDEP baseline survey data (B), and the MDAT data at local and regional scales (C). The scale for all maps is representative of relative spatial variation in the sites within the season for each data source.

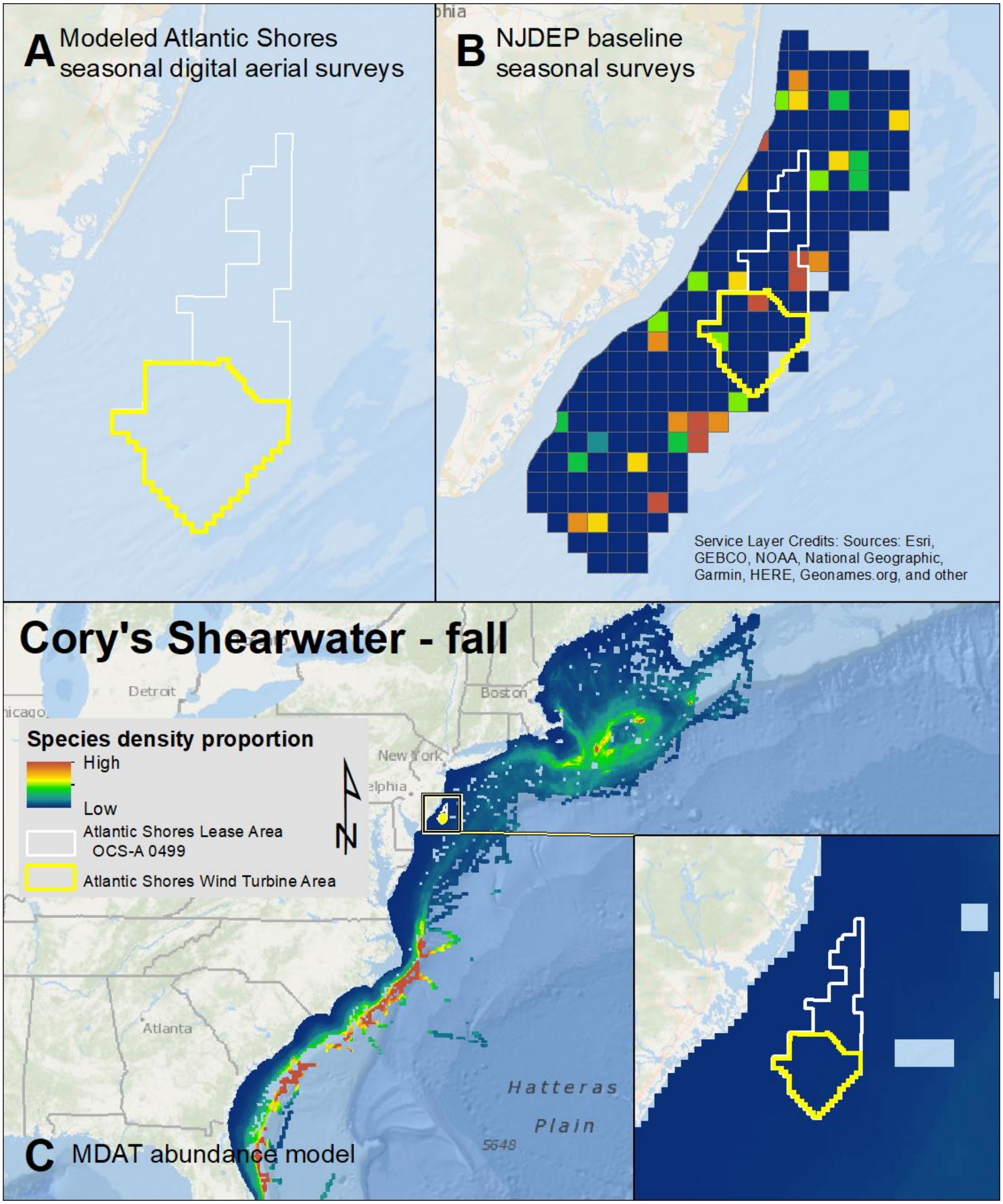

Map 49. Fall Cory's Shearwater modeled density proportions in the Atlantic Shores seasonal digital aerial surveys (A), density proportions in the NJDEP baseline survey data (B), and the MDAT data at local and regional scales (C). The scale for all maps is representative of relative spatial variation in the sites within the season for each data source.

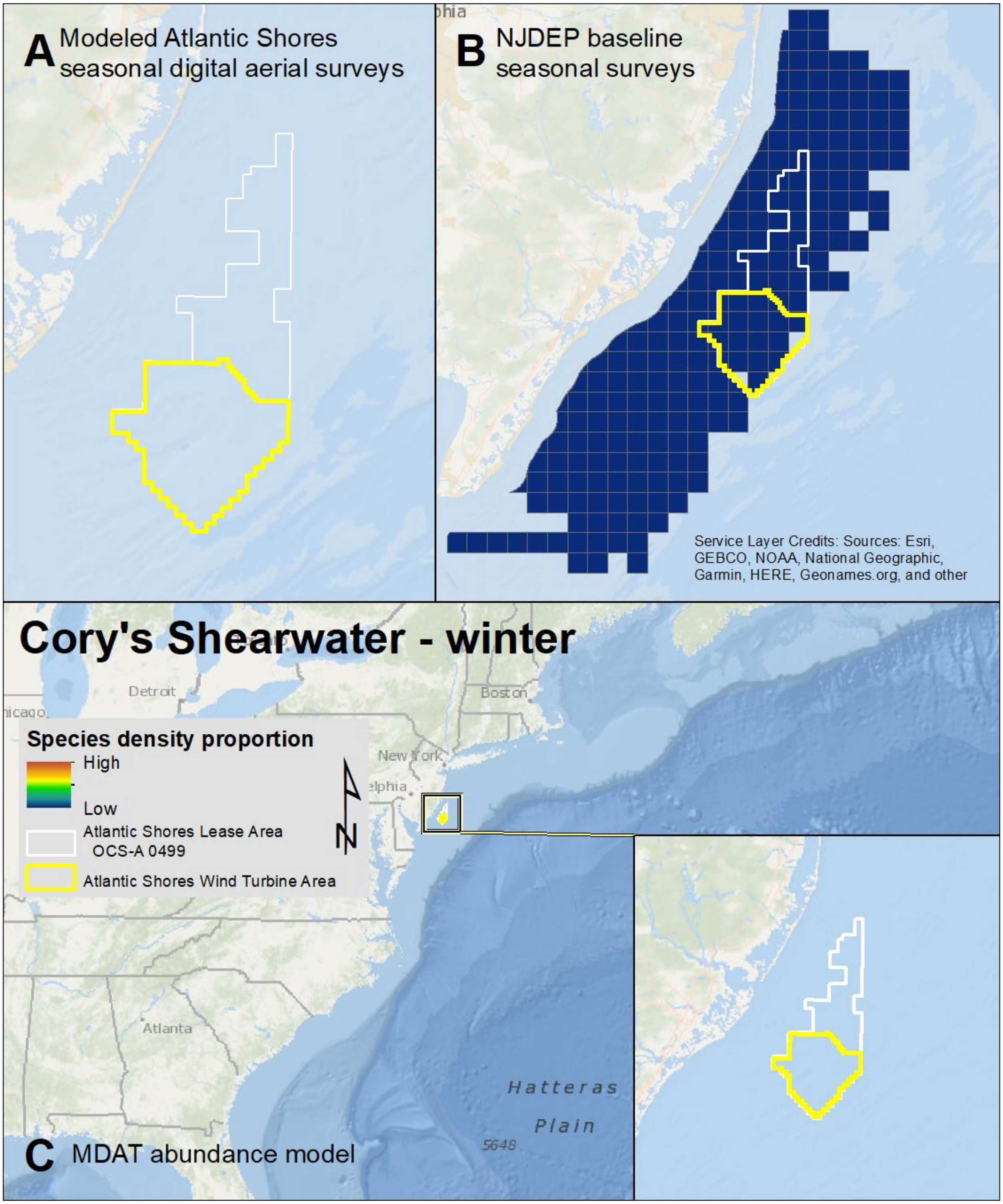

Map 50. Winter Cory's Shearwater modeled density proportions in the Atlantic Shores seasonal digital aerial surveys (A), density proportions in the NJDEP baseline survey data (B), and the MDAT data at local and regional scales (C). The scale for all maps is representative of relative spatial variation in the sites within the season for each data source.

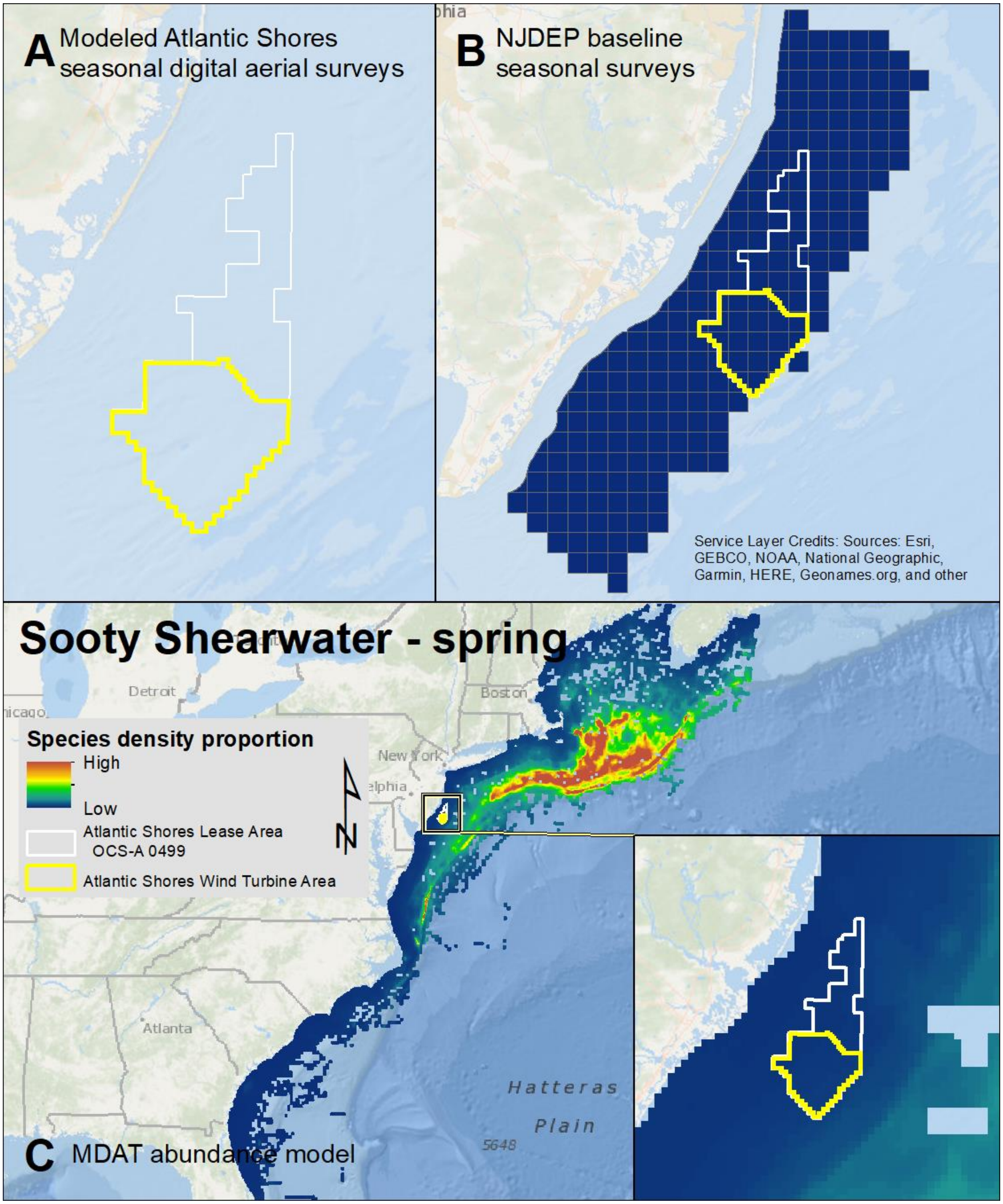

Map 51. Spring Sooty Shearwater modeled density proportions in the Atlantic Shores seasonal digital aerial surveys (A), density proportions in the NJDEP baseline survey data (B), and the MDAT data at local and regional scales (C). The scale for all maps is representative of relative spatial variation in the sites within the season for each data source.

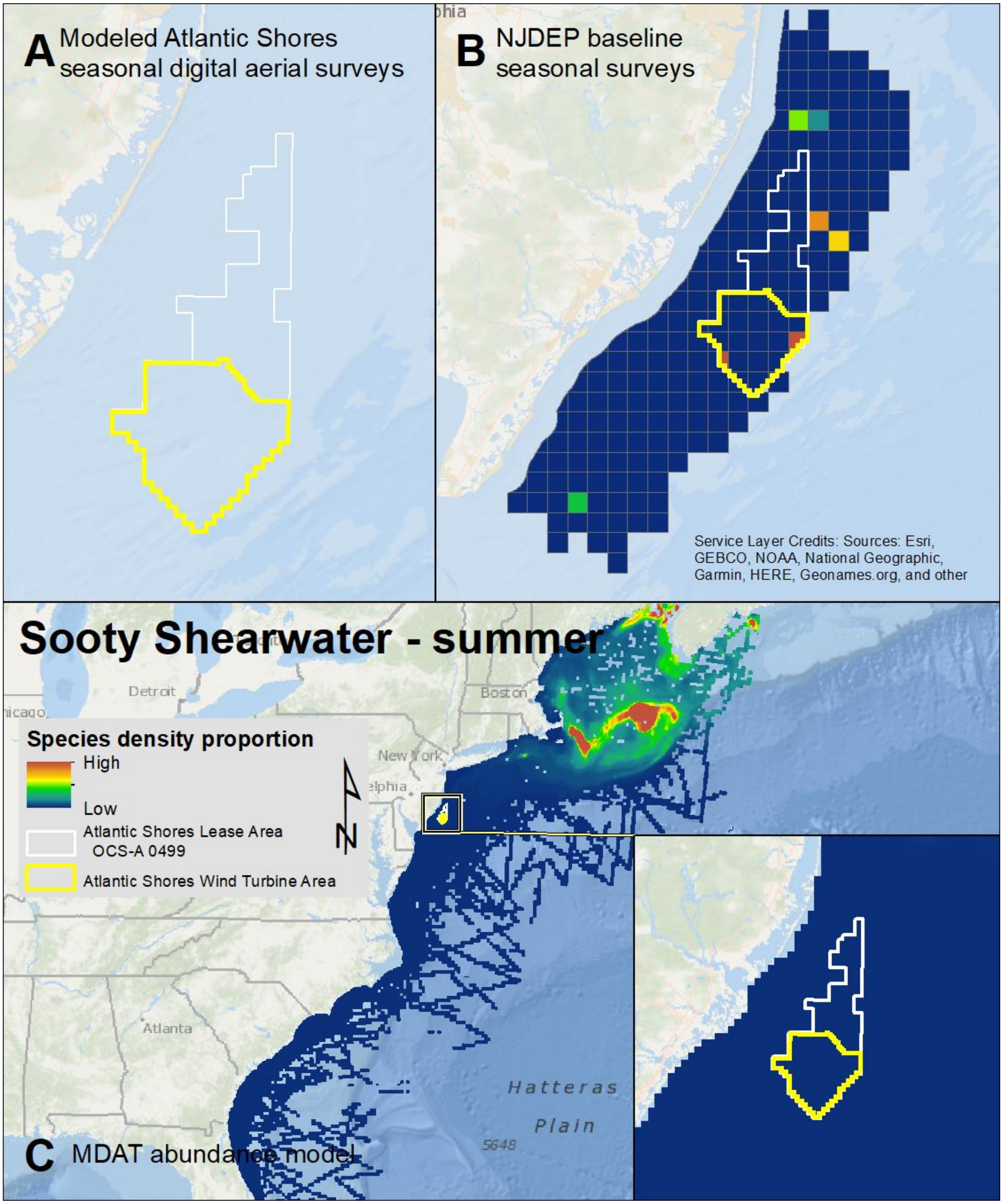

Map 52. Summer Sooty Shearwater modeled density proportions in the Atlantic Shores seasonal digital aerial surveys (A), density proportions in the NJDEP baseline survey data (B), and the MDAT data at local and regional scales (C). The scale for all maps is representative of relative spatial variation in the sites within the season for each data source.

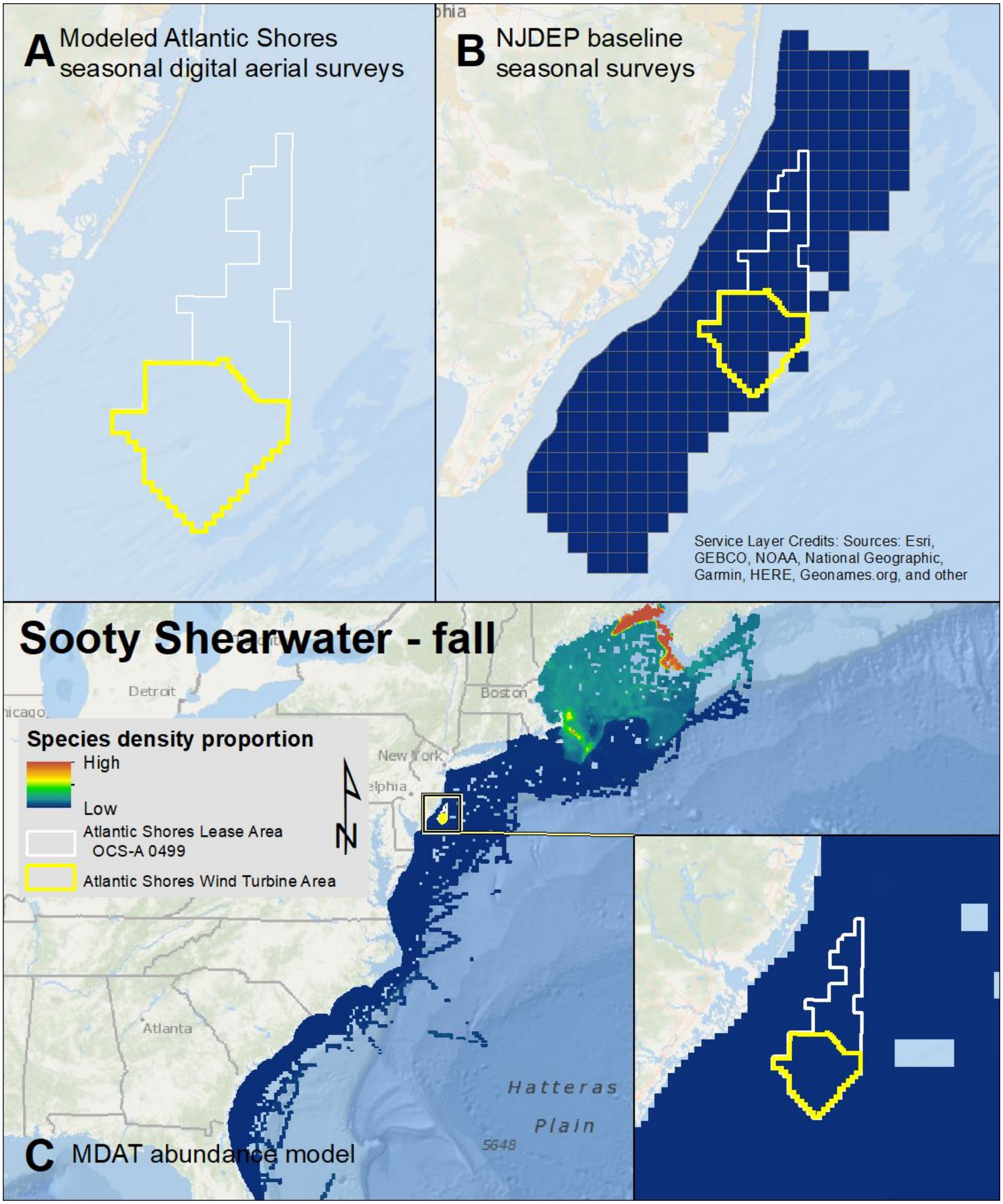

Map 53. Fall Sooty Shearwater modeled density proportions in the Atlantic Shores seasonal digital aerial surveys (A), density proportions in the NJDEP baseline survey data (B), and the MDAT data at local and regional scales (C). The scale for all maps is representative of relative spatial variation in the sites within the season for each data source.

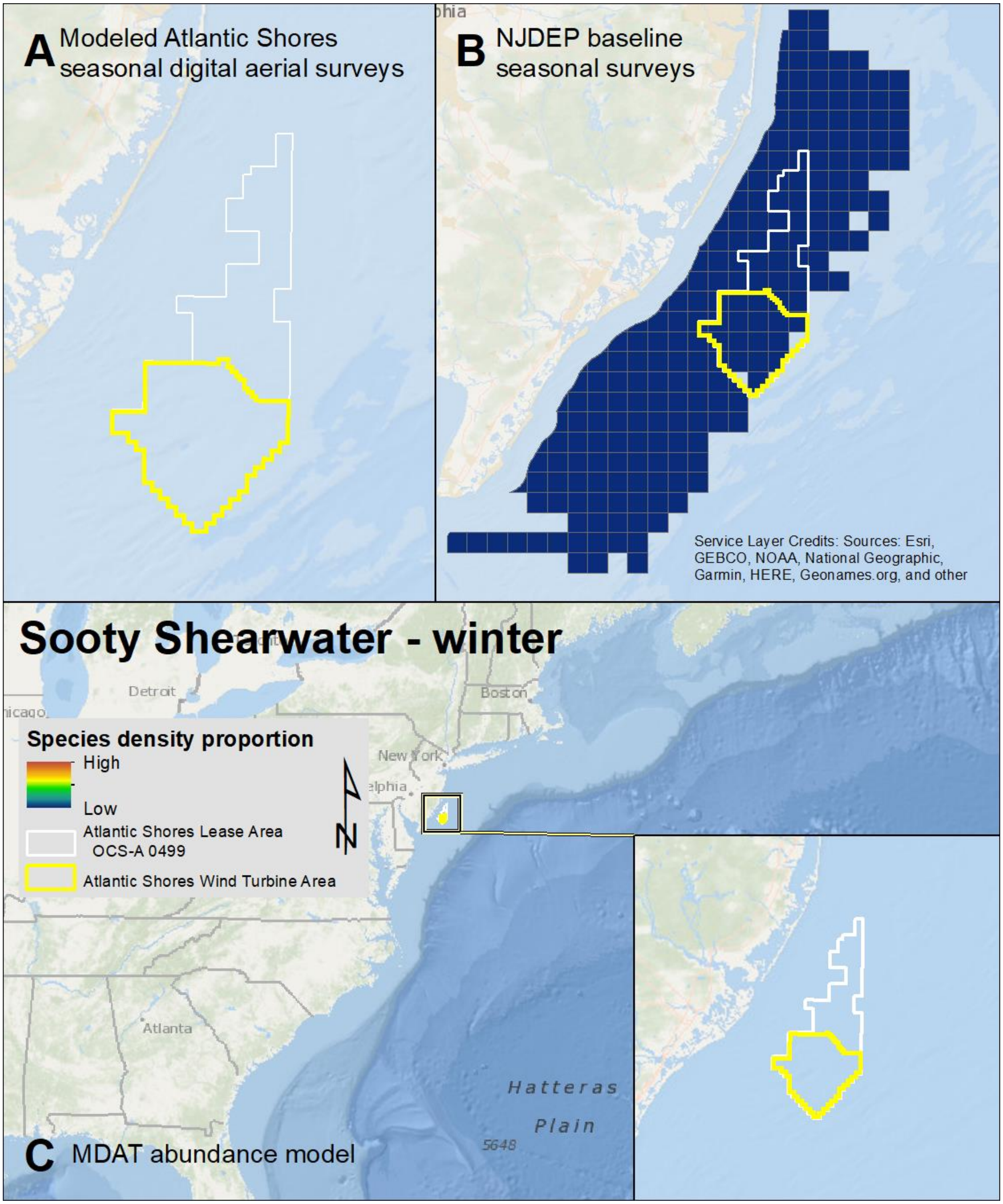

Map 54. Winter Sooty Shearwater modeled density proportions in the Atlantic Shores seasonal digital aerial surveys (A), density proportions in the NJDEP baseline survey data (B), and the MDAT data at local and regional scales (C). The scale for all maps is representative of relative spatial variation in the sites within the season for each data source.

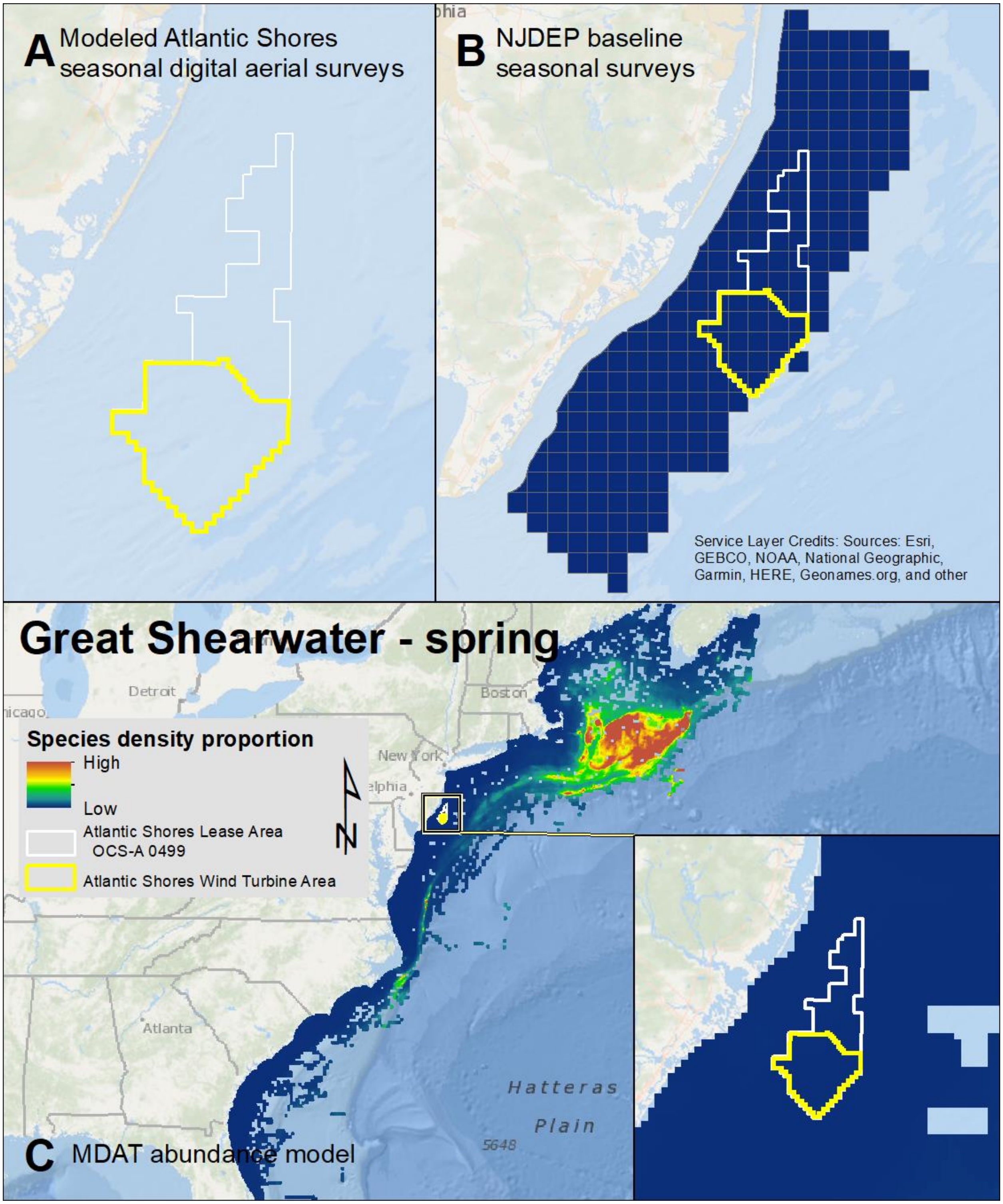

Map 55. Spring Great Shearwater modeled density proportions in the Atlantic Shores seasonal digital aerial surveys (A), density proportions in the NJDEP baseline survey data (B), and the MDAT data at local and regional scales (C). The scale for all maps is representative of relative spatial variation in the sites within the season for each data source.

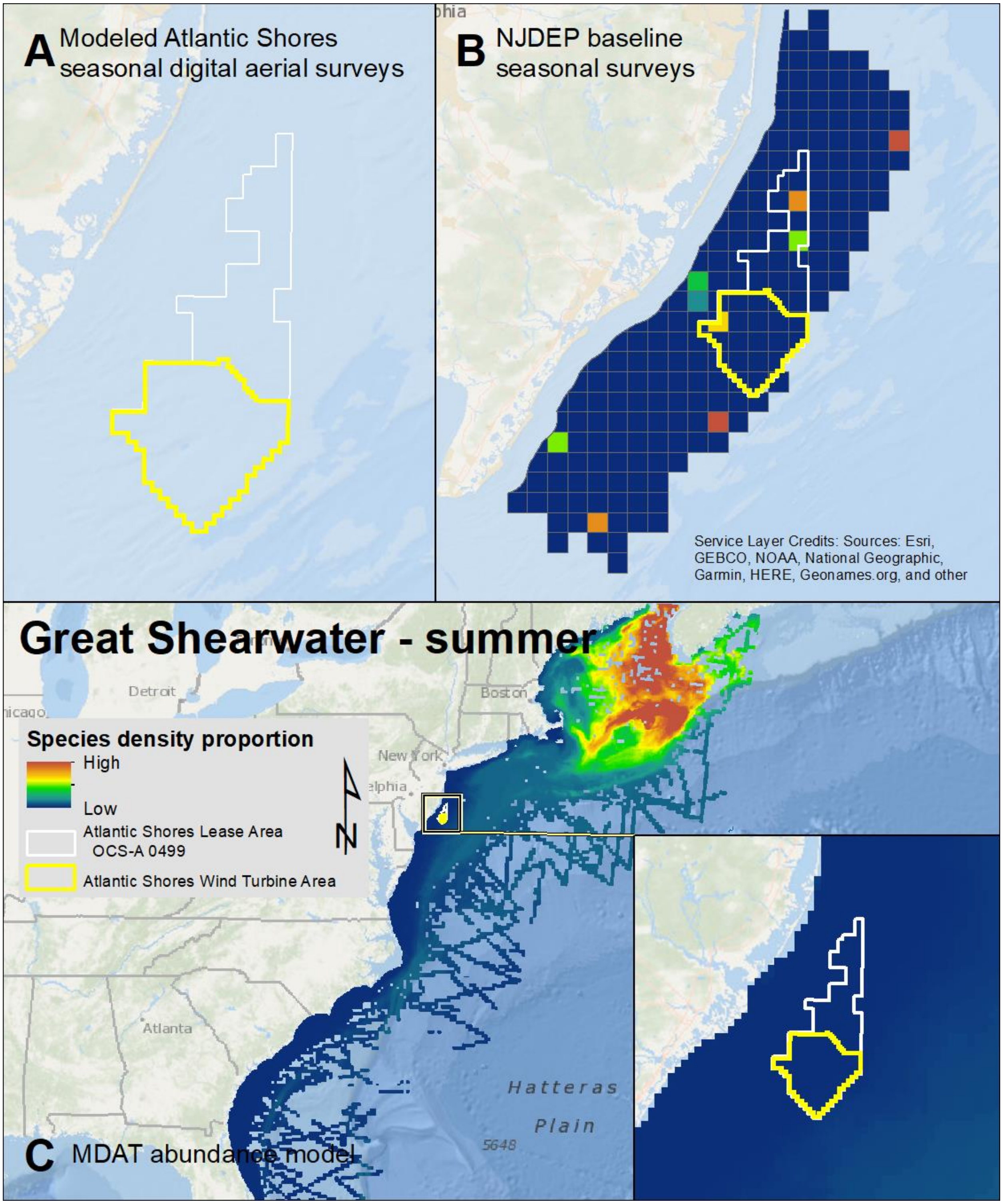

Map 56. Summer Great Shearwater modeled density proportions in the Atlantic Shores seasonal digital aerial surveys (A), density proportions in the NJDEP baseline survey data (B), and the MDAT data at local and regional scales (C). The scale for all maps is representative of relative spatial variation in the sites within the season for each data source.

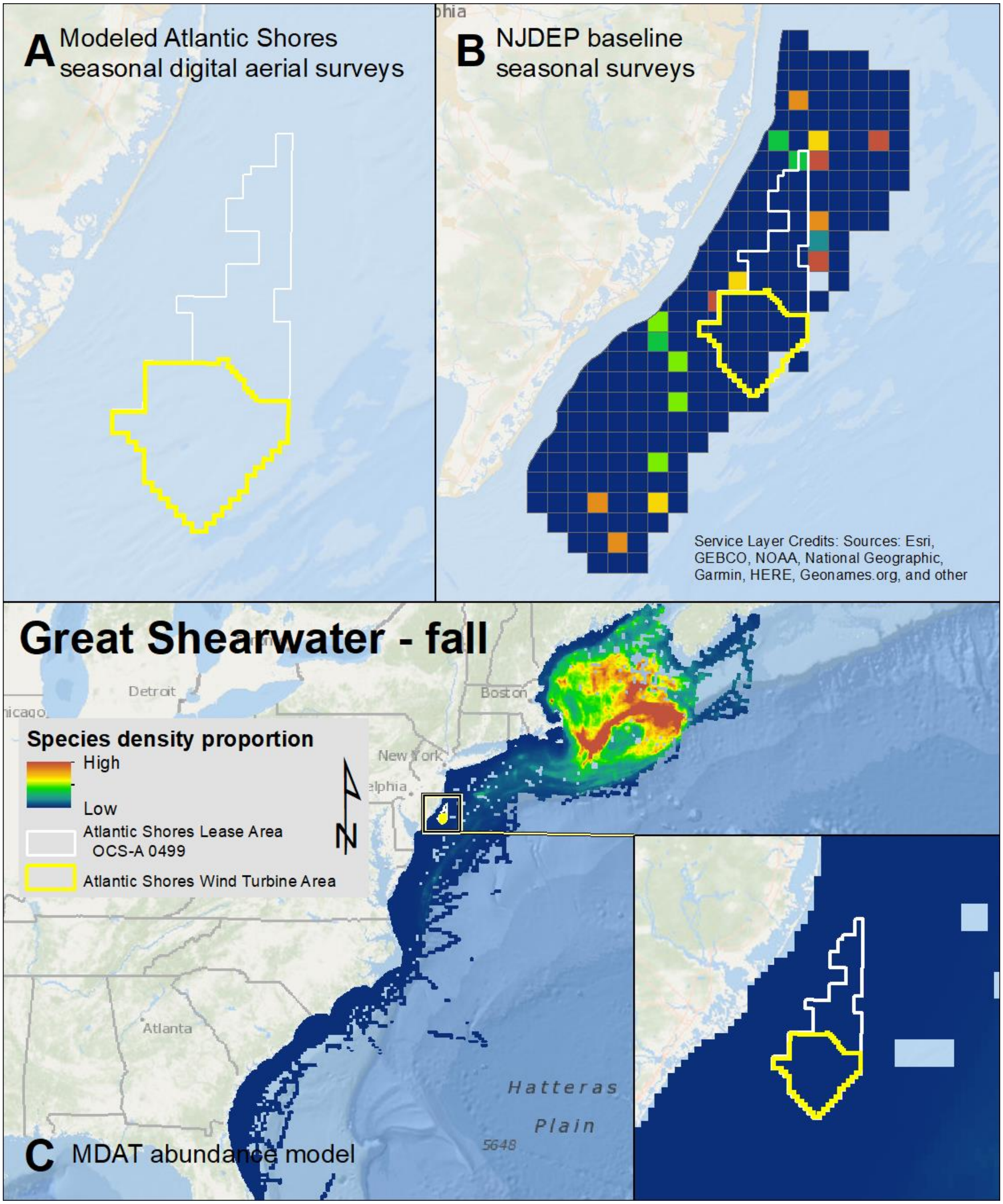

Map 57. Fall Great Shearwater modeled density proportions in the Atlantic Shores seasonal digital aerial surveys (A), density proportions in the NJDEP baseline survey data (B), and the MDAT data at local and regional scales (C). The scale for all maps is representative of relative spatial variation in the sites within the season for each data source.

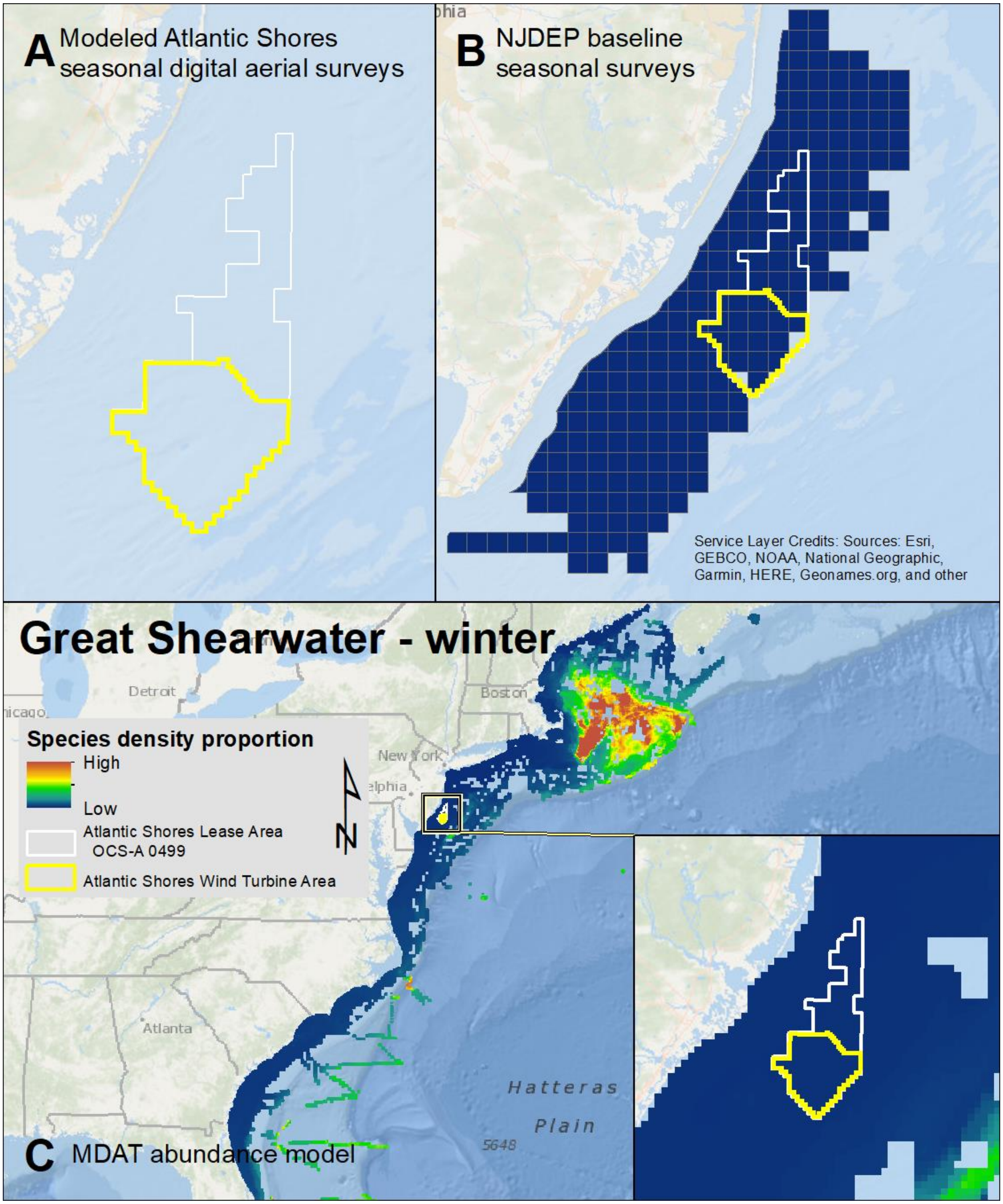

Map 58. Winter Great Shearwater modeled density proportions in the Atlantic Shores seasonal digital aerial surveys (A), density proportions in the NJDEP baseline survey data (B), and the MDAT data at local and regional scales (C). The scale for all maps is representative of relative spatial variation in the sites within the season for each data source.

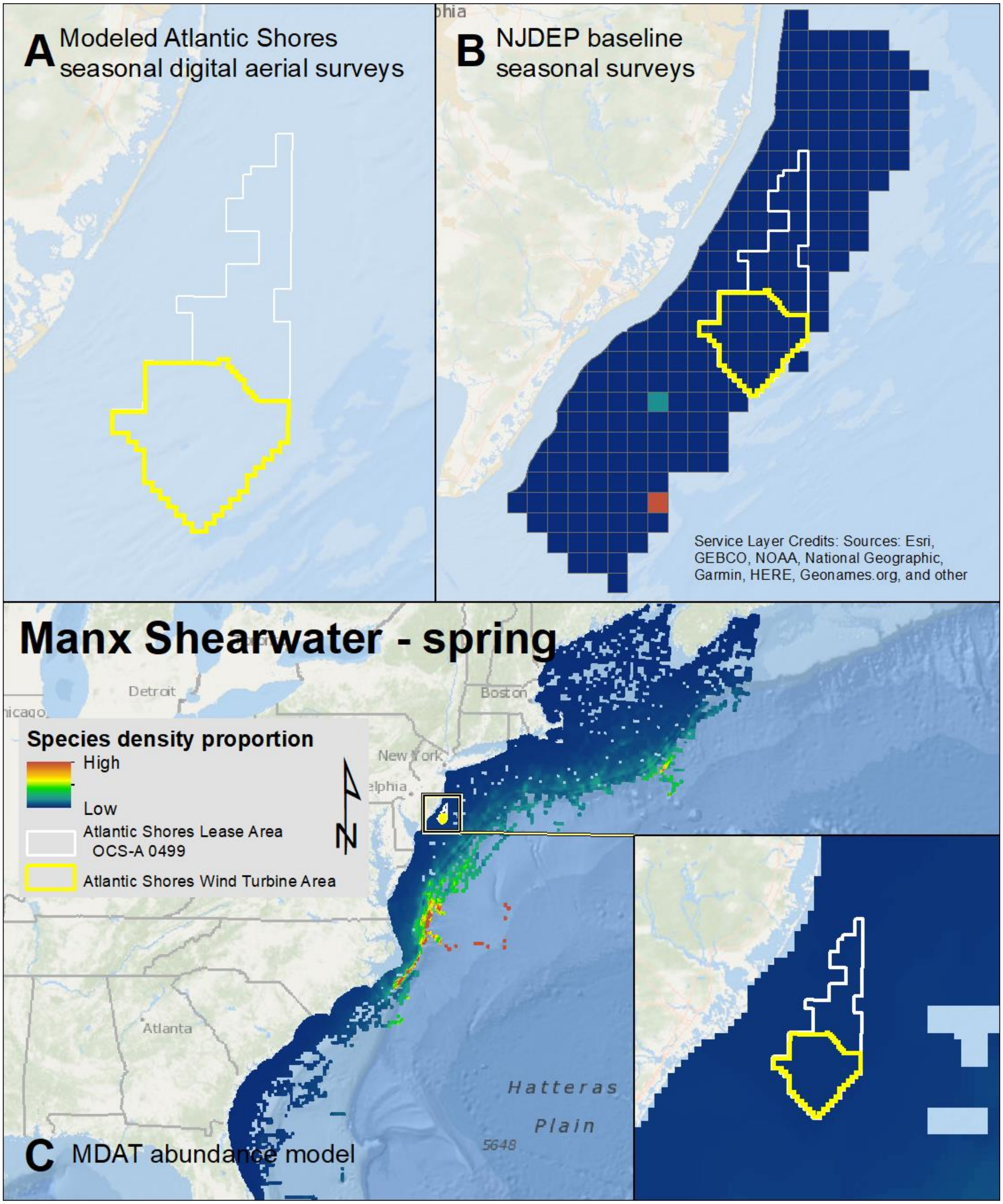

Map 59. Spring Manx Shearwater modeled density proportions in the Atlantic Shores seasonal digital aerial surveys (A), density proportions in the NJDEP baseline survey data (B), and the MDAT data at local and regional scales (C). The scale for all maps is representative of relative spatial variation in the sites within the season for each data source.

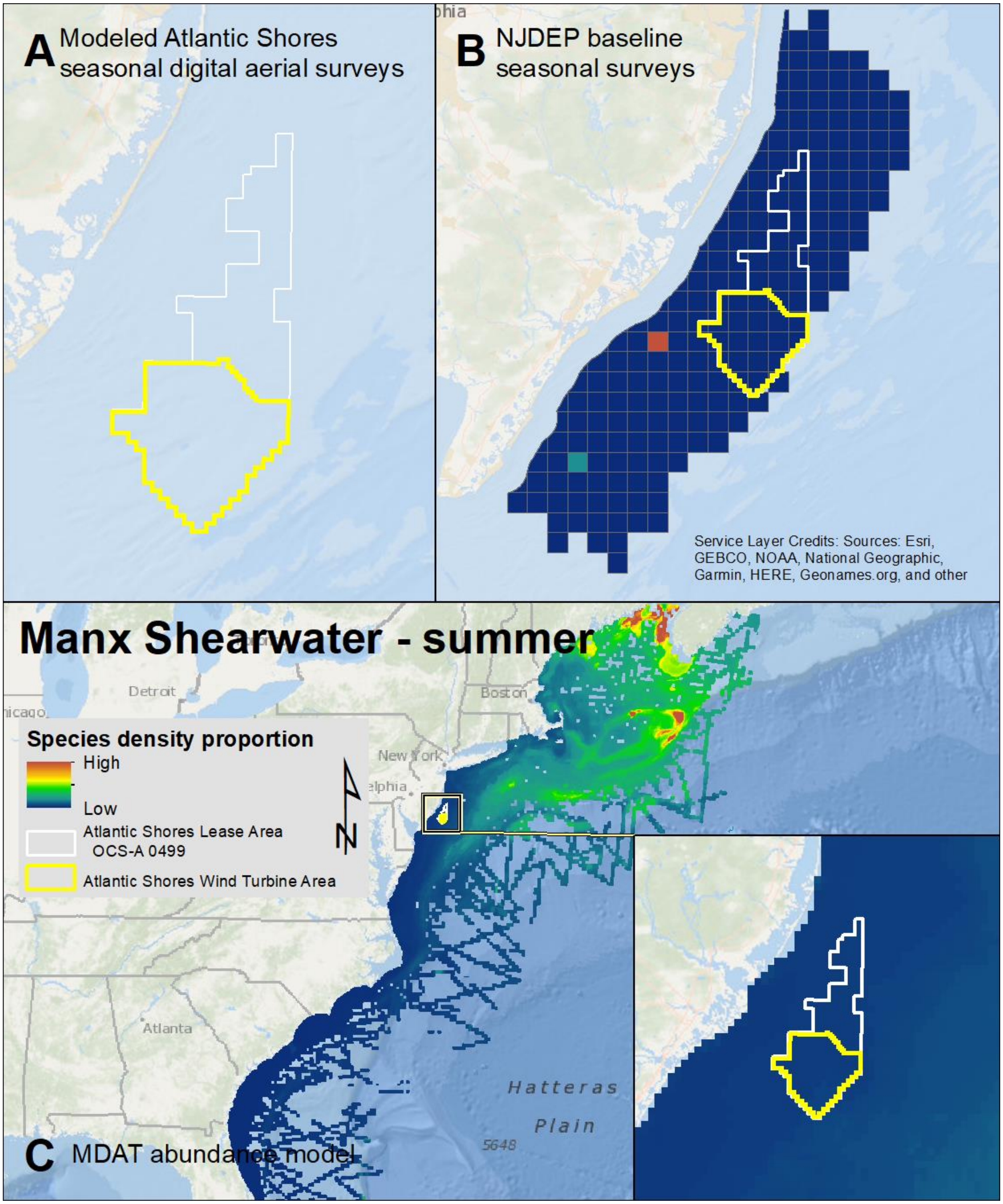

Map 60. Summer Manx Shearwater modeled density proportions in the Atlantic Shores seasonal digital aerial surveys (A), density proportions in the NJDEP baseline survey data (B), and the MDAT data at local and regional scales (C). The scale for all maps is representative of relative spatial variation in the sites within the season for each data source.

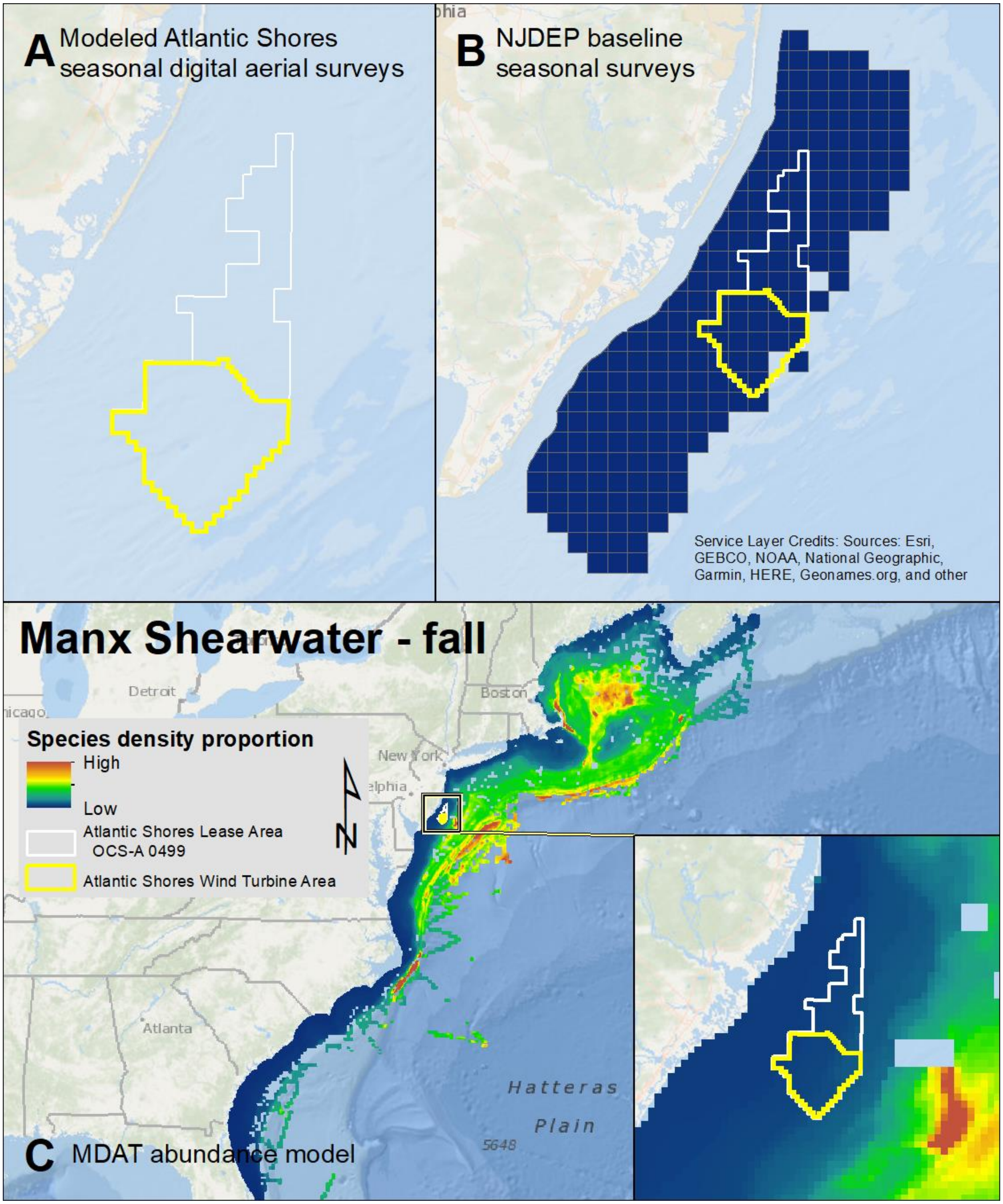

Map 61. Fall Manx Shearwater modeled density proportions in the Atlantic Shores seasonal digital aerial surveys (A), density proportions in the NJDEP baseline survey data (B), and the MDAT data at local and regional scales (C). The scale for all maps is representative of relative spatial variation in the sites within the season for each data source.

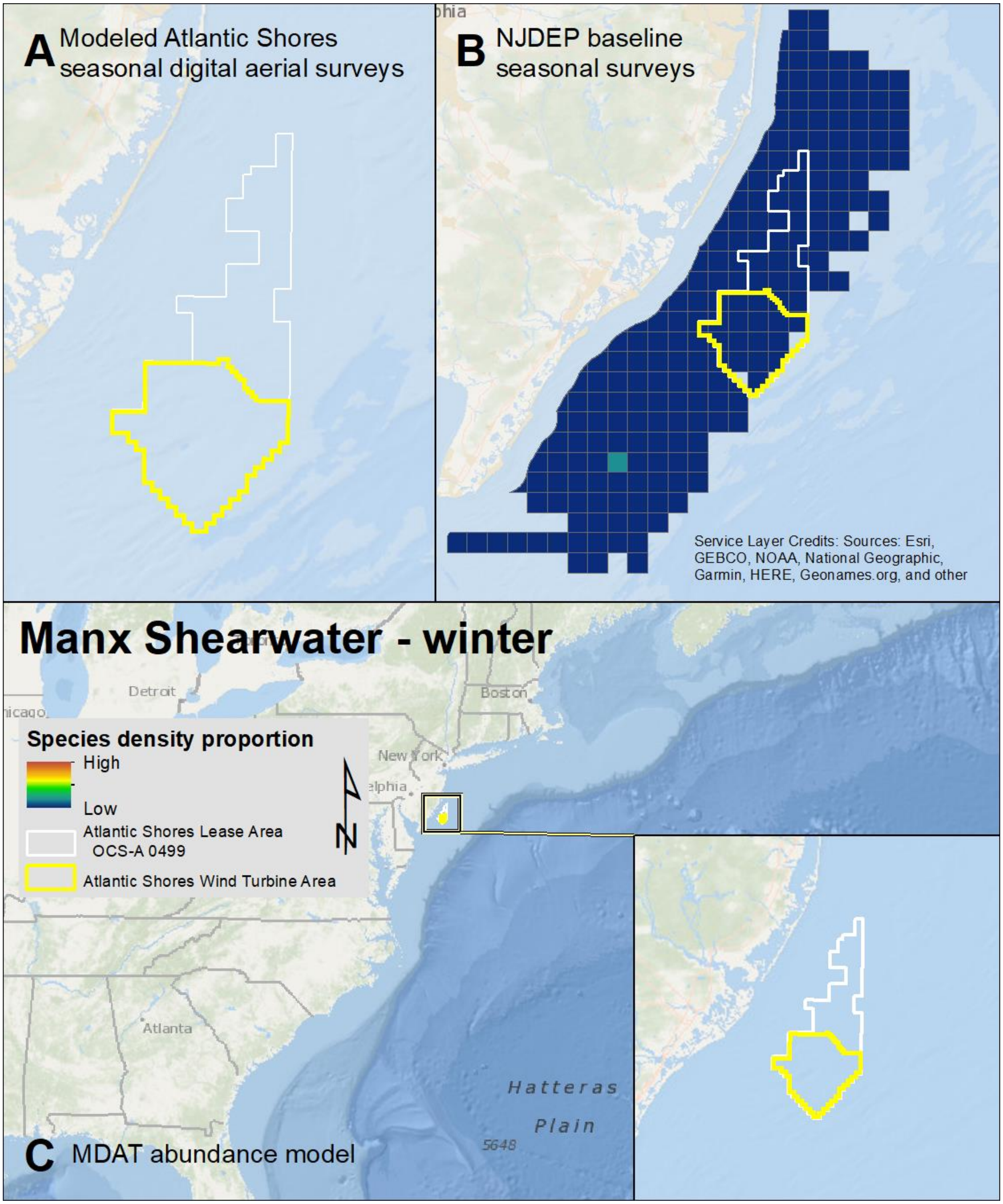

Map 62. Winter Manx Shearwater modeled density proportions in the Atlantic Shores seasonal digital aerial surveys (A), density proportions in the NJDEP baseline survey data (B), and the MDAT data at local and regional scales (C). The scale for all maps is representative of relative spatial variation in the sites within the season for each data source.

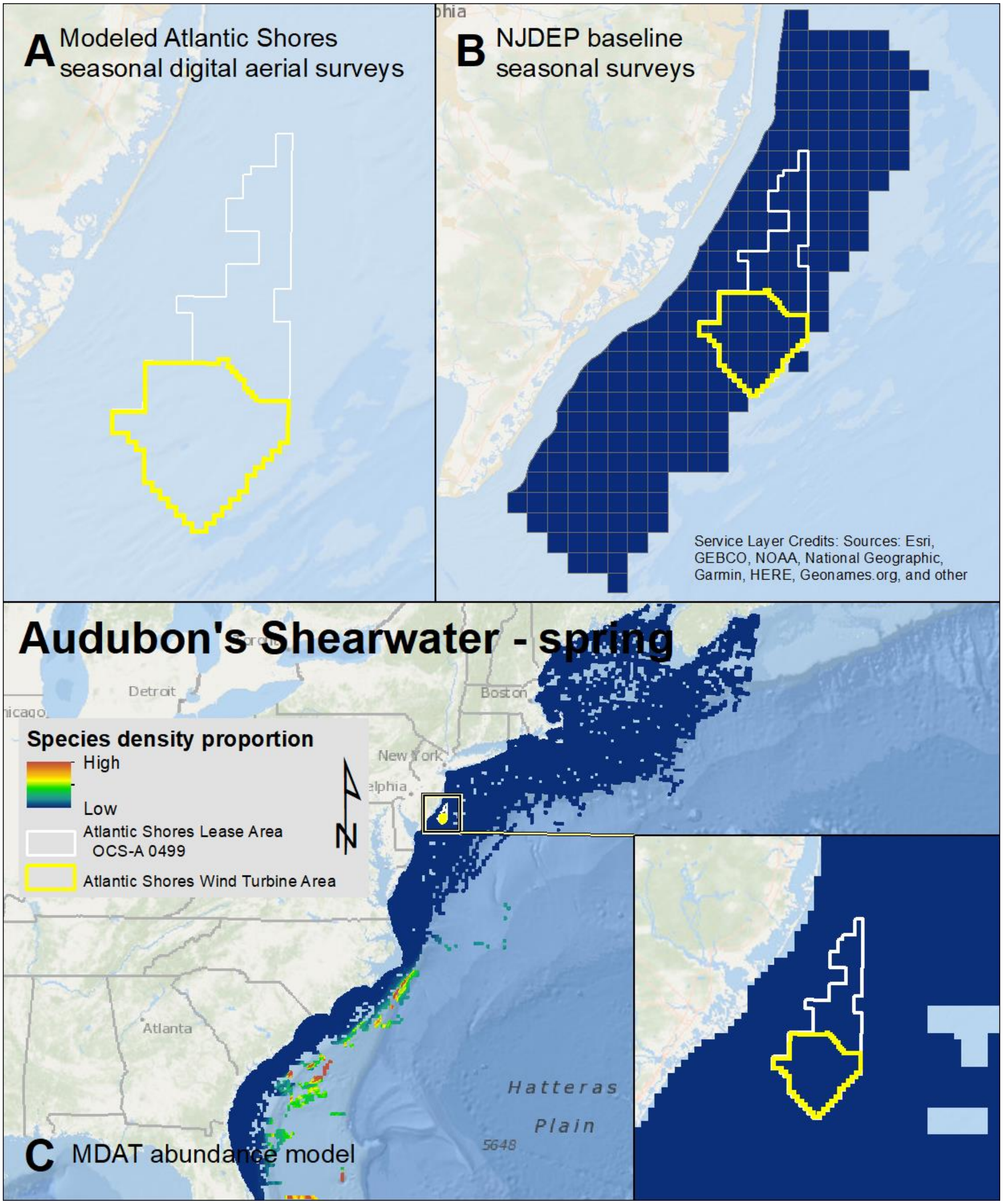

Map 63. Spring Audubon's Shearwater modeled density proportions in the Atlantic Shores seasonal digital aerial surveys (A), density proportions in the NJDEP baseline survey data (B), and the MDAT data at local and regional scales (C). The scale for all maps is representative of relative spatial variation in the sites within the season for each data source.

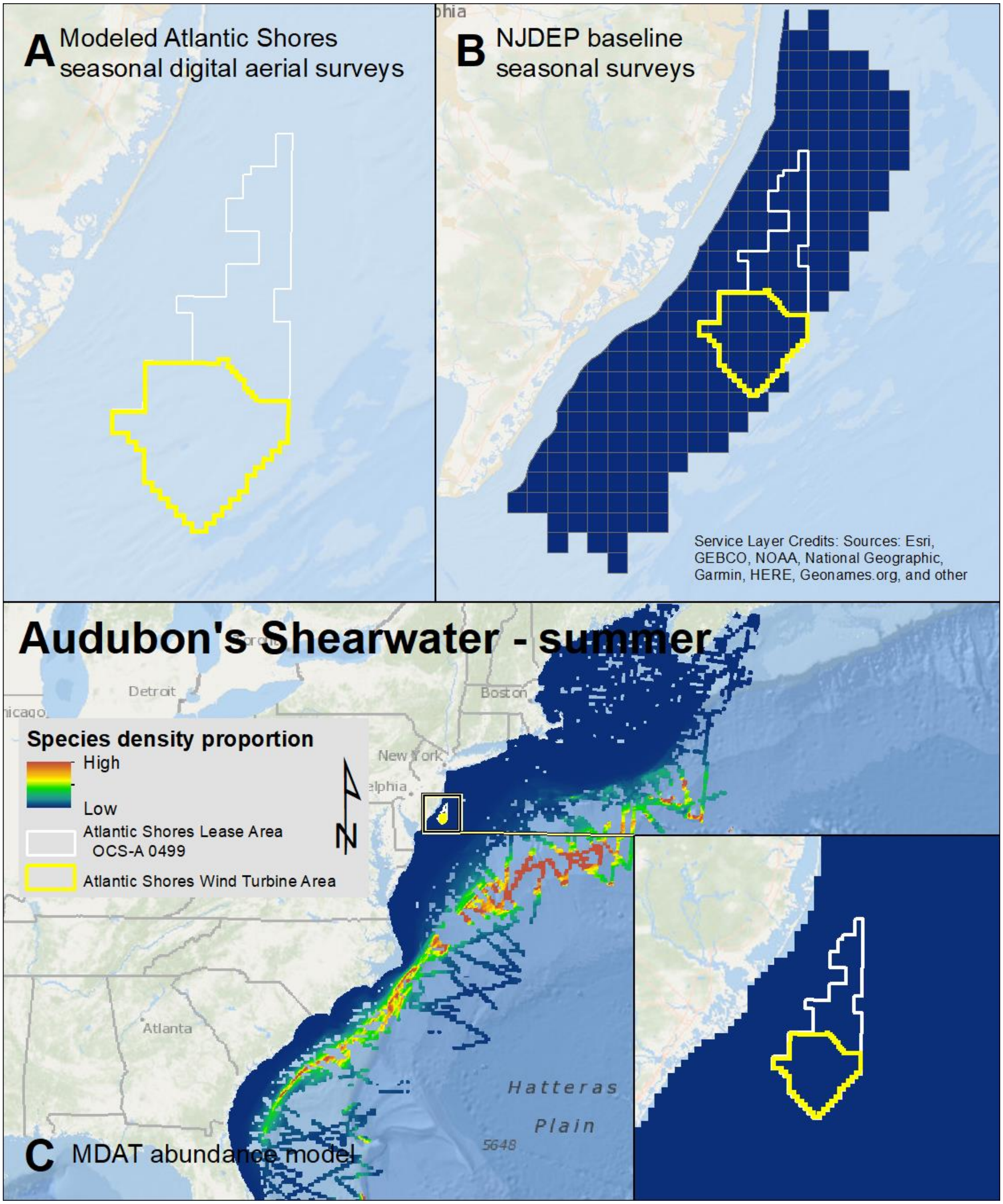

Map 64. Summer Audubon's Shearwater modeled density proportions in the Atlantic Shores seasonal digital aerial surveys (A), density proportions in the NJDEP baseline survey data (B), and the MDAT data at local and regional scales (C). The scale for all maps is representative of relative spatial variation in the sites within the season for each data source.

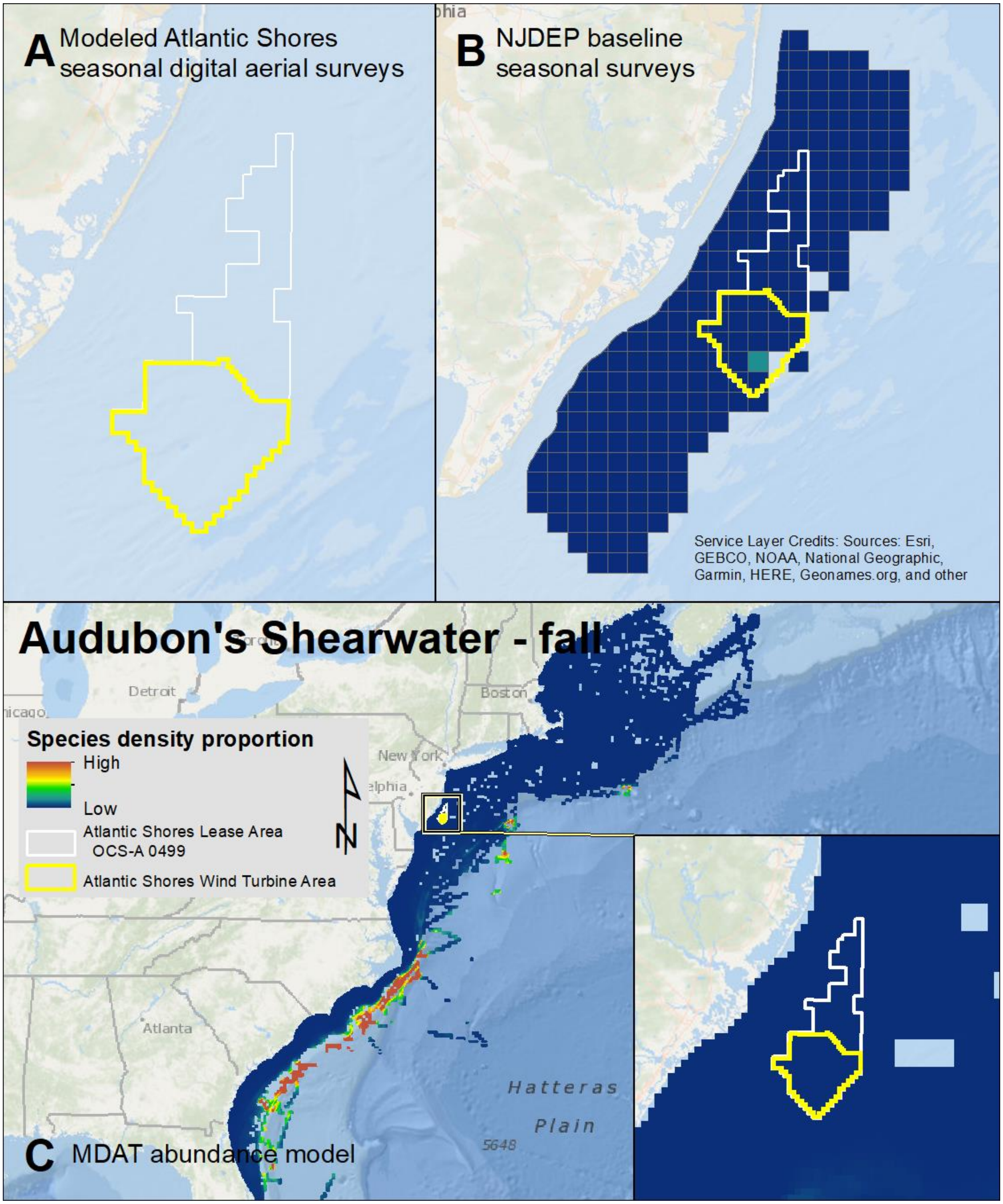

Map 65. Fall Audubon's Shearwater modeled density proportions in the Atlantic Shores seasonal digital aerial surveys (A), density proportions in the NJDEP baseline survey data (B), and the MDAT data at local and regional scales (C). The scale for all maps is representative of relative spatial variation in the sites within the season for each data source.

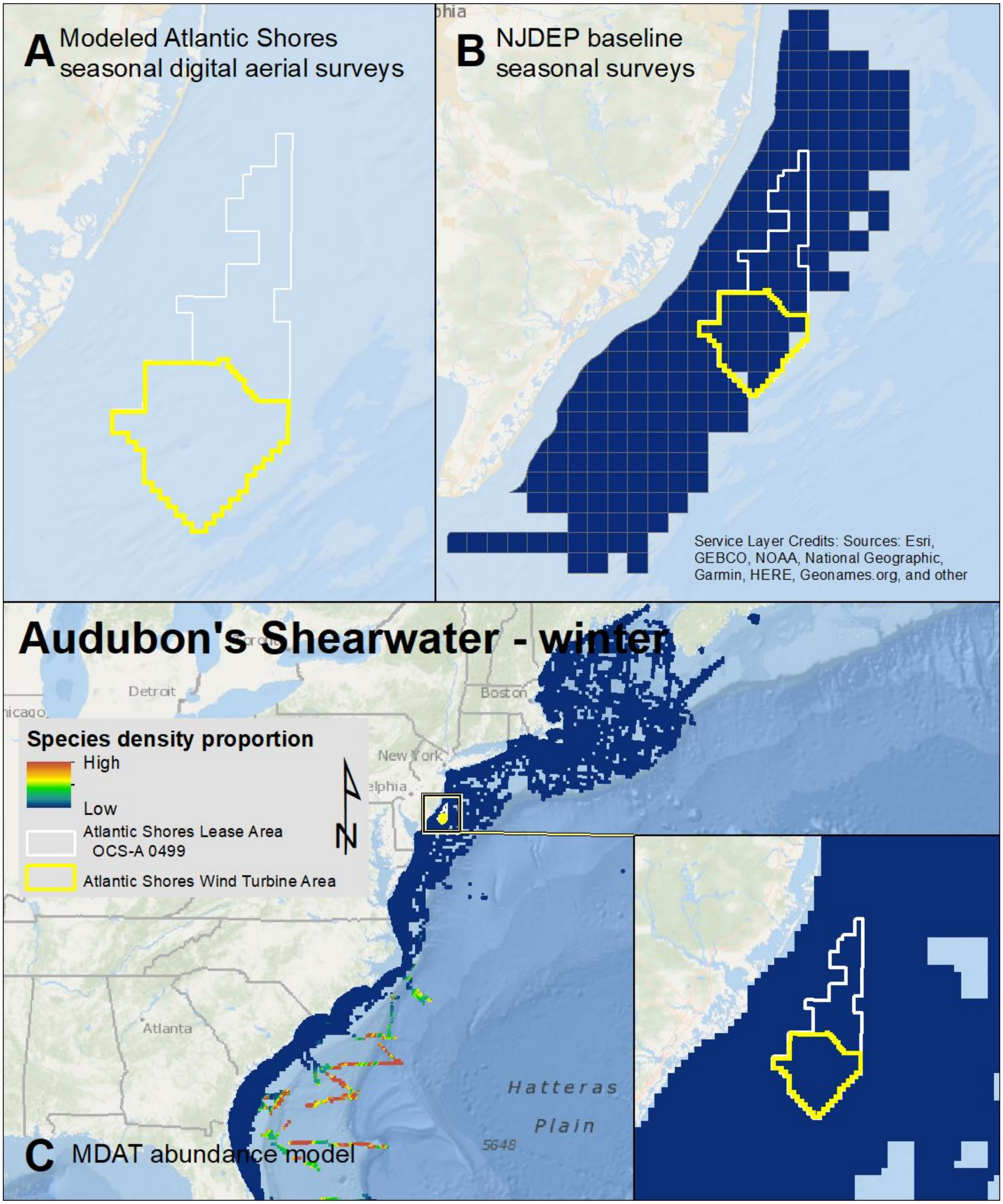

Map 66. Winter Audubon's Shearwater modeled density proportions in the Atlantic Shores seasonal digital aerial surveys (A), density proportions in the NJDEP baseline survey data (B), and the MDAT data at local and regional scales (C). The scale for all maps is representative of relative spatial variation in the sites within the season for each data source.

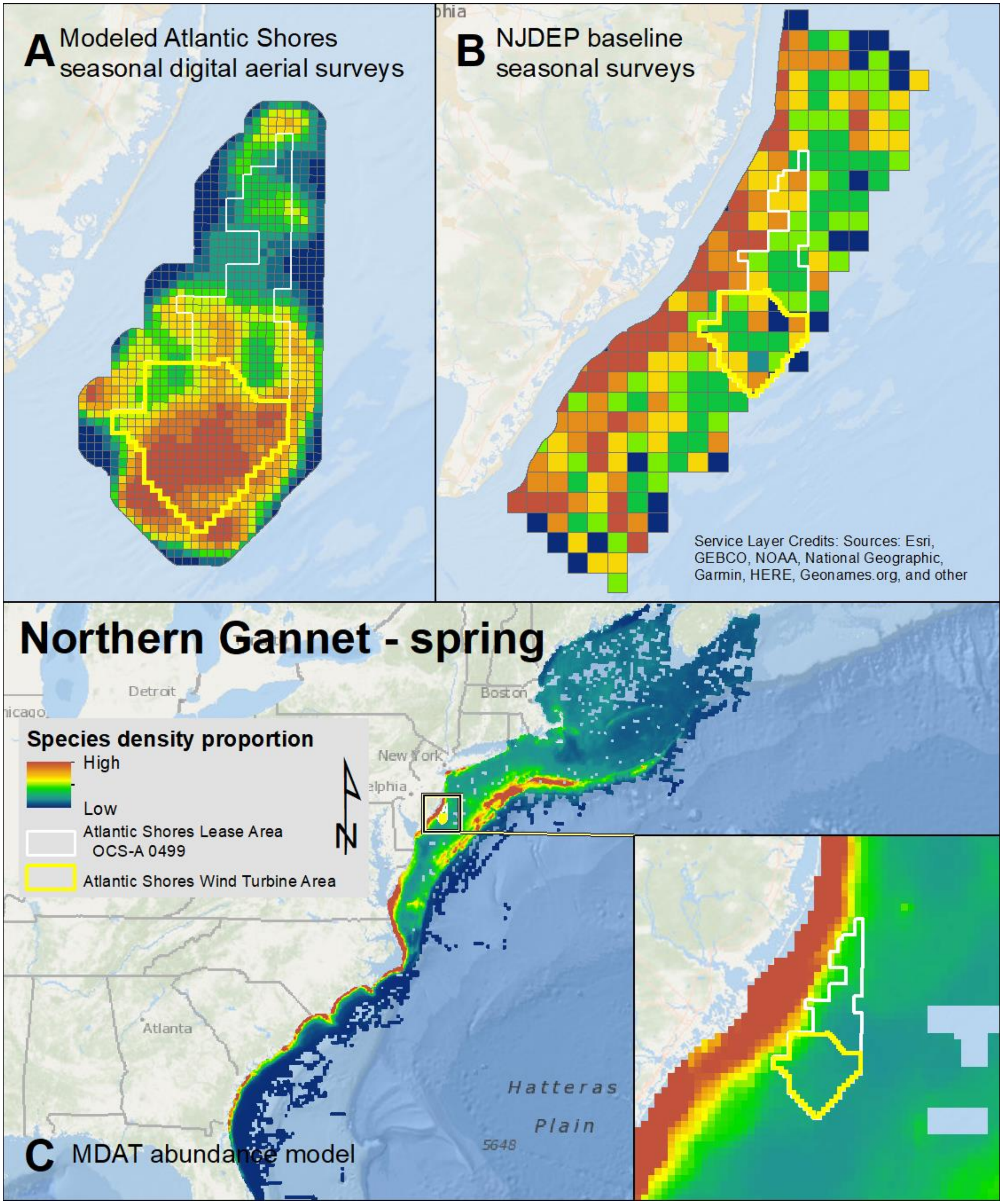

Map 67. Spring Northern Gannet modeled density proportions in the Atlantic Shores seasonal digital aerial surveys (A), density proportions in the NJDEP baseline survey data (B), and the MDAT data at local and regional scales (C). The scale for all maps is representative of relative spatial variation in the sites within the season for each data source.

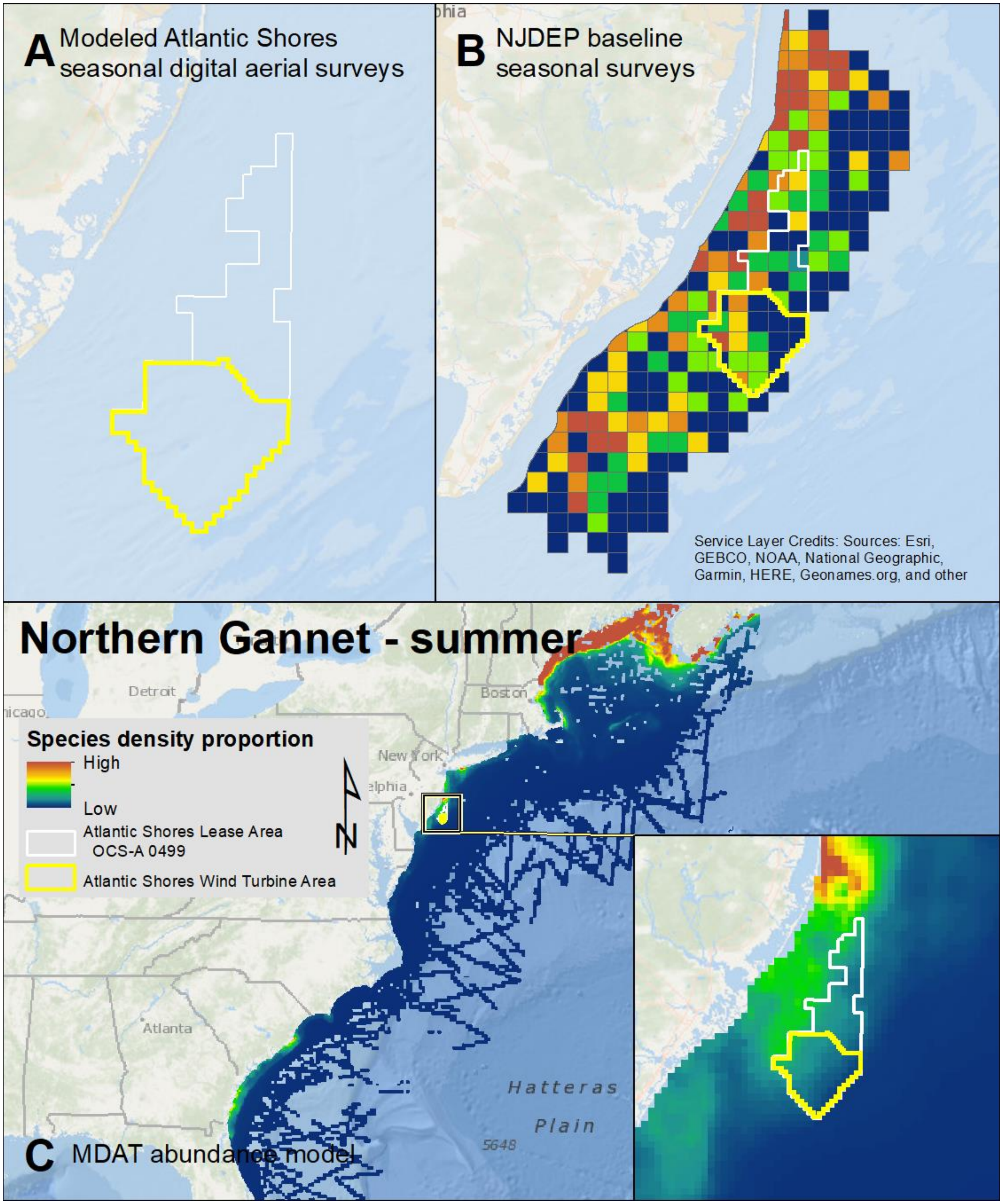

Map 68. Summer Northern Gannet modeled density proportions in the Atlantic Shores seasonal digital aerial surveys (A), density proportions in the NJDEP baseline survey data (B), and the MDAT data at local and regional scales (C). The scale for all maps is representative of relative spatial variation in the sites within the season for each data source.

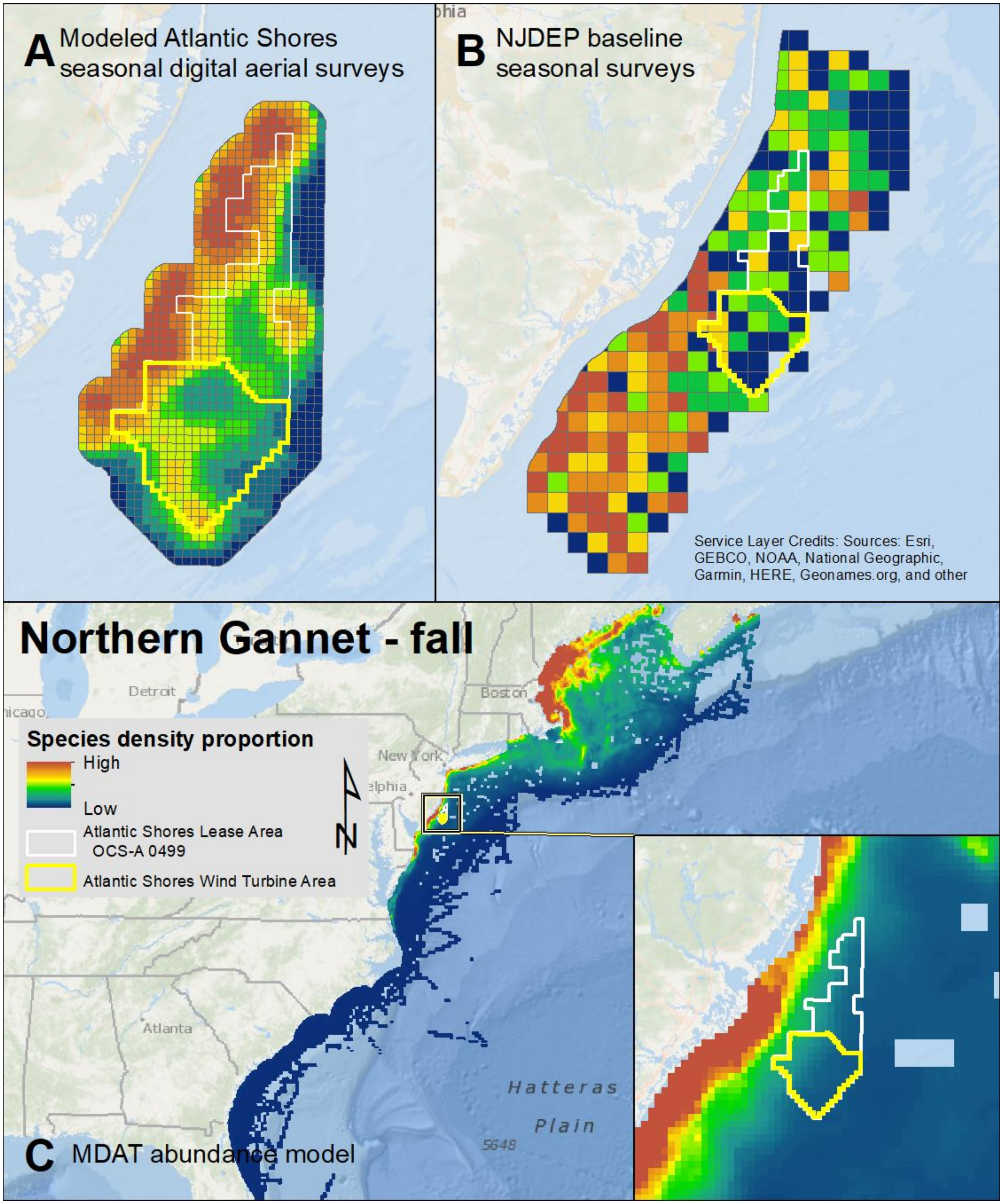

Map 69. Fall Northern Gannet modeled density proportions in the Atlantic Shores seasonal digital aerial surveys (A), density proportions in the NJDEP baseline survey data (B), and the MDAT data at local and regional scales (C). The scale for all maps is representative of relative spatial variation in the sites within the season for each data source.

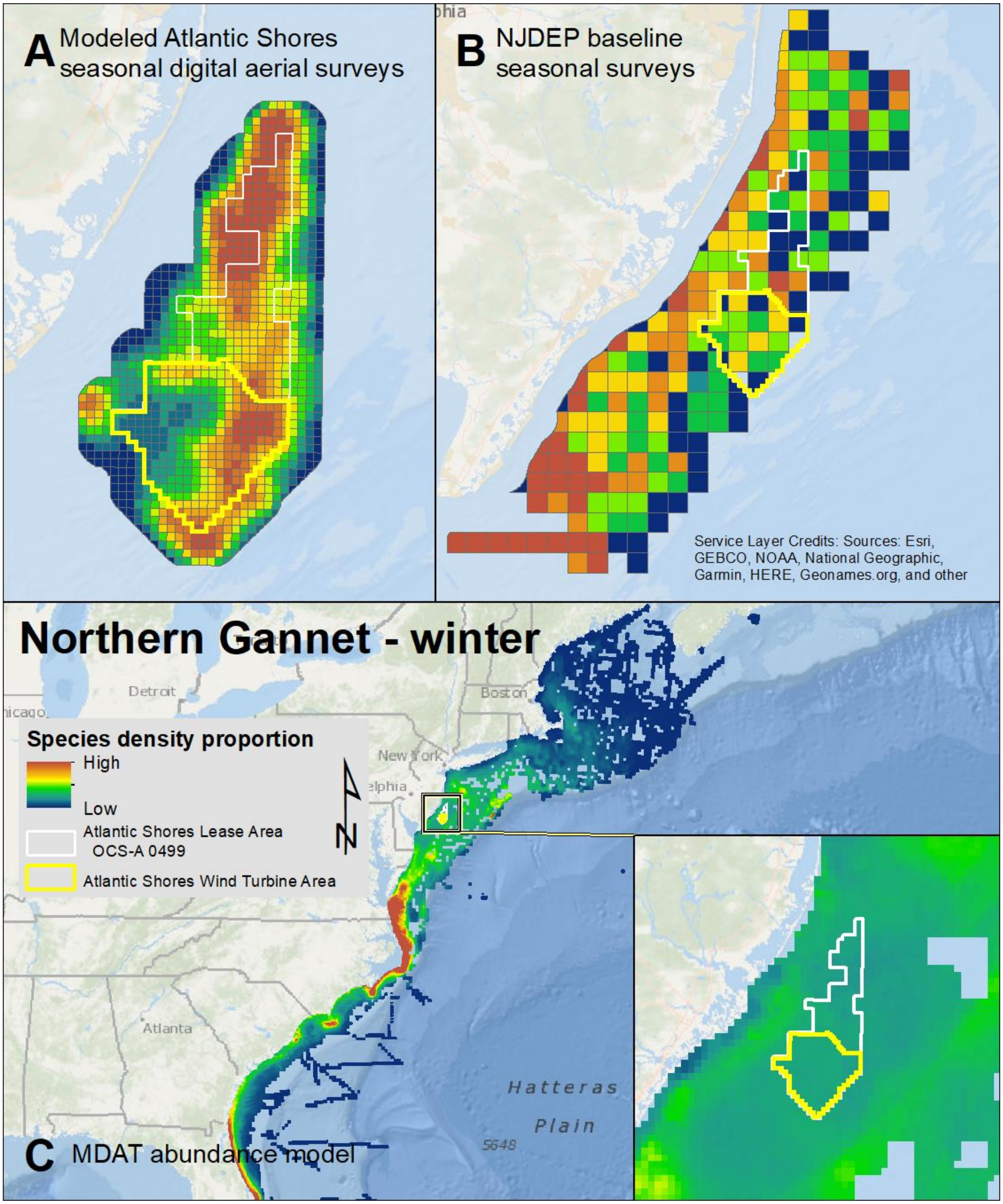

Map 70. Winter Northern Gannet modeled density proportions in the Atlantic Shores seasonal digital aerial surveys (A), density proportions in the NJDEP baseline survey data (B), and the MDAT data at local and regional scales (C). The scale for all maps is representative of relative spatial variation in the sites within the season for each data source.

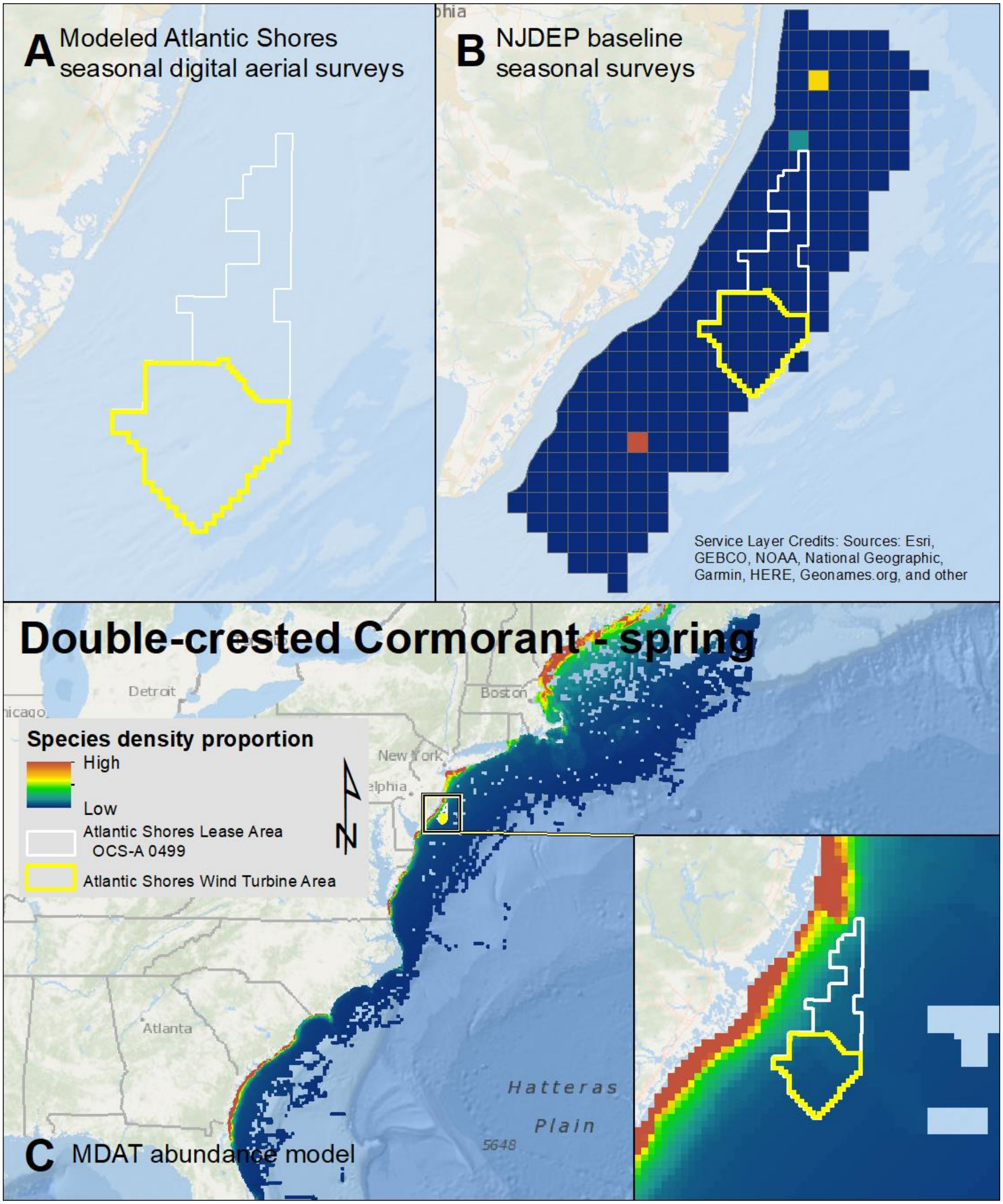

Map 71. Spring Double-crested Cormorant modeled density proportions in the Atlantic Shores seasonal digital aerial surveys (A), density proportions in the NJDEP baseline survey data (B), and the MDAT data at local and regional scales (C). The scale for all maps is representative of relative spatial variation in the sites within the season for each data source.

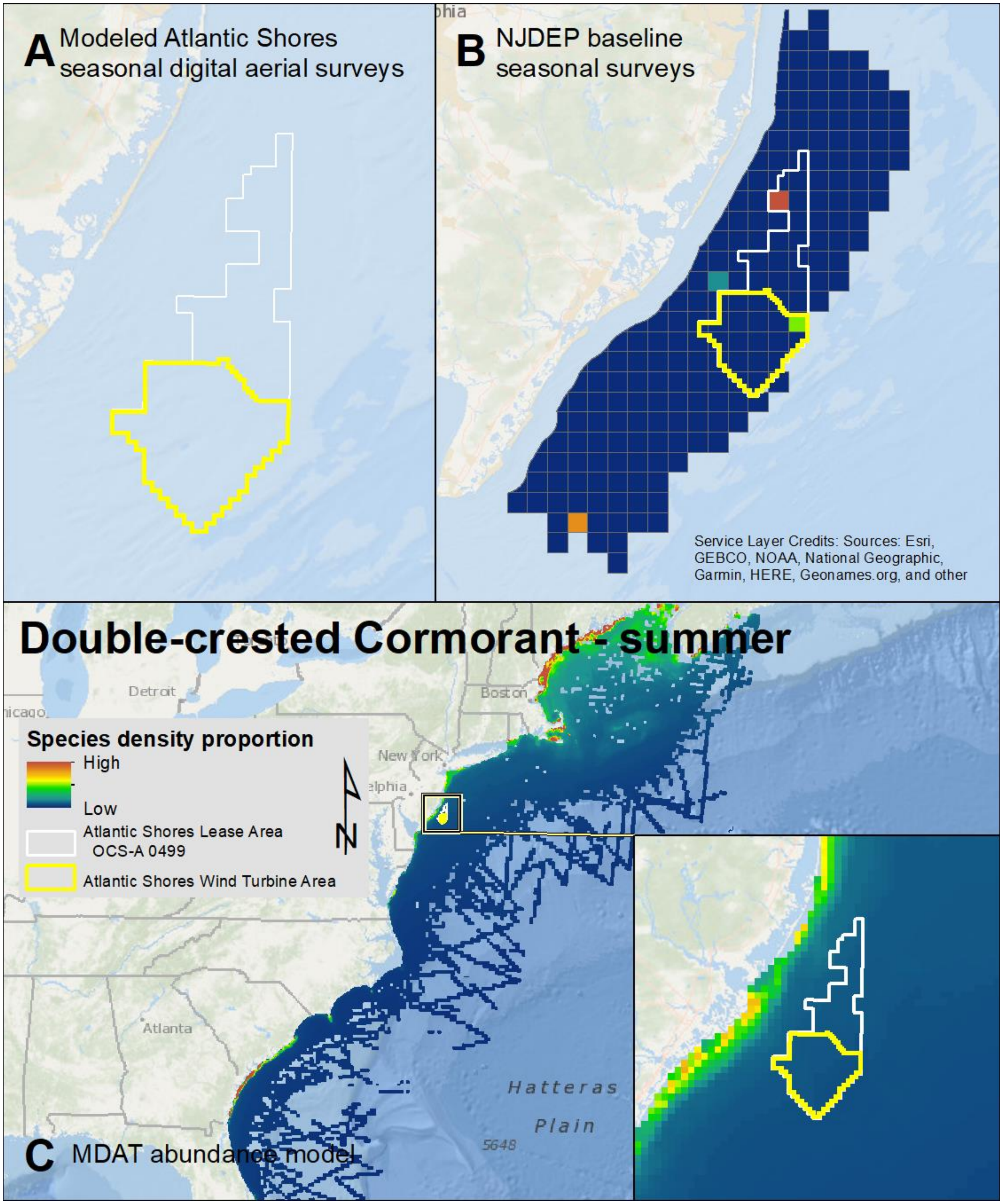

Map 72. Summer Double-crested Cormorant modeled density proportions in the Atlantic Shores seasonal digital aerial surveys (A), density proportions in the NJDEP baseline survey data (B), and the MDAT data at local and regional scales (C). The scale for all maps is representative of relative spatial variation in the sites within the season for each data source.

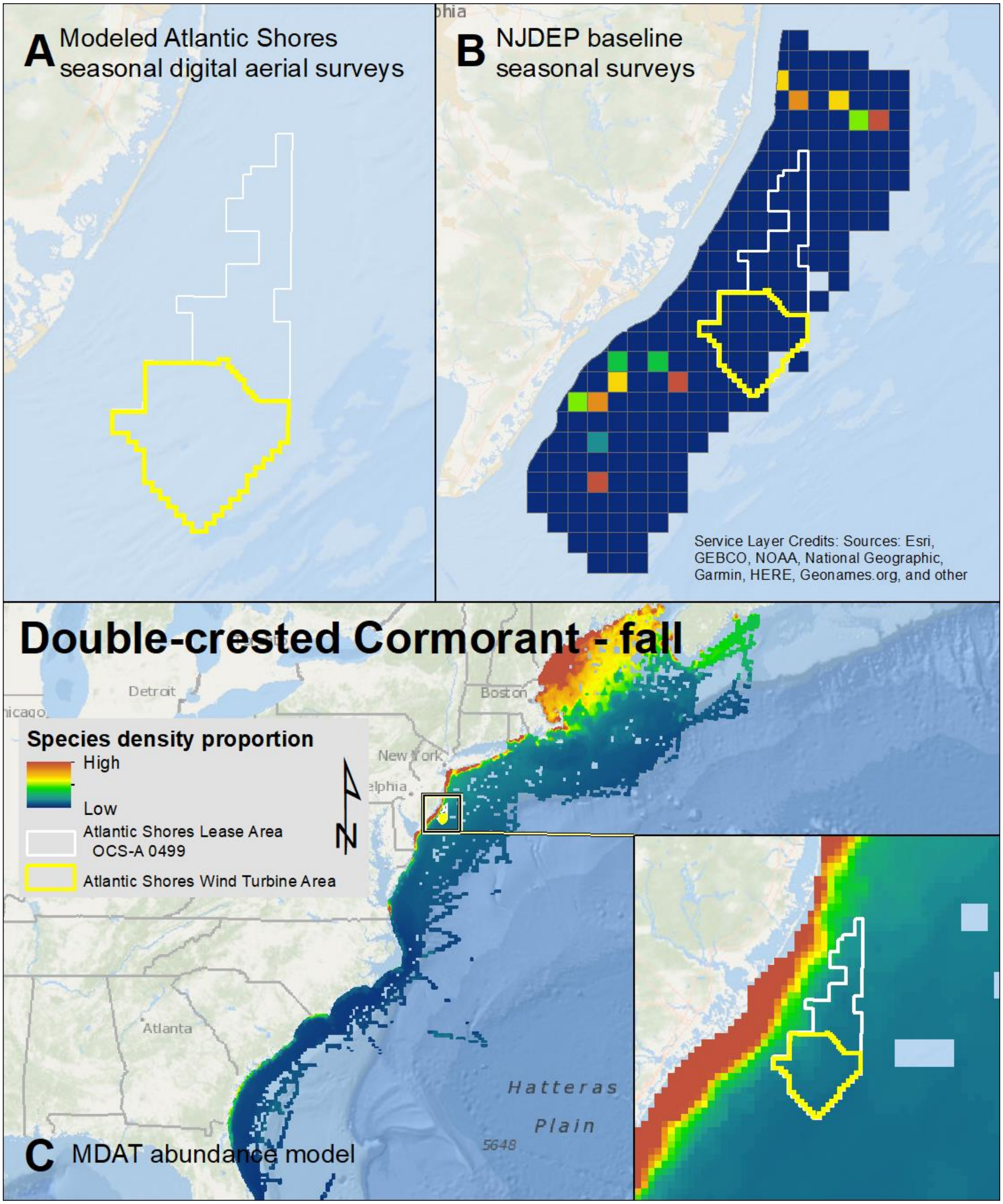

Map 73. Fall Double-crested Cormorant modeled density proportions in the Atlantic Shores seasonal digital aerial surveys (A), density proportions in the NJDEP baseline survey data (B), and the MDAT data at local and regional scales (C). The scale for all maps is representative of relative spatial variation in the sites within the season for each data source.

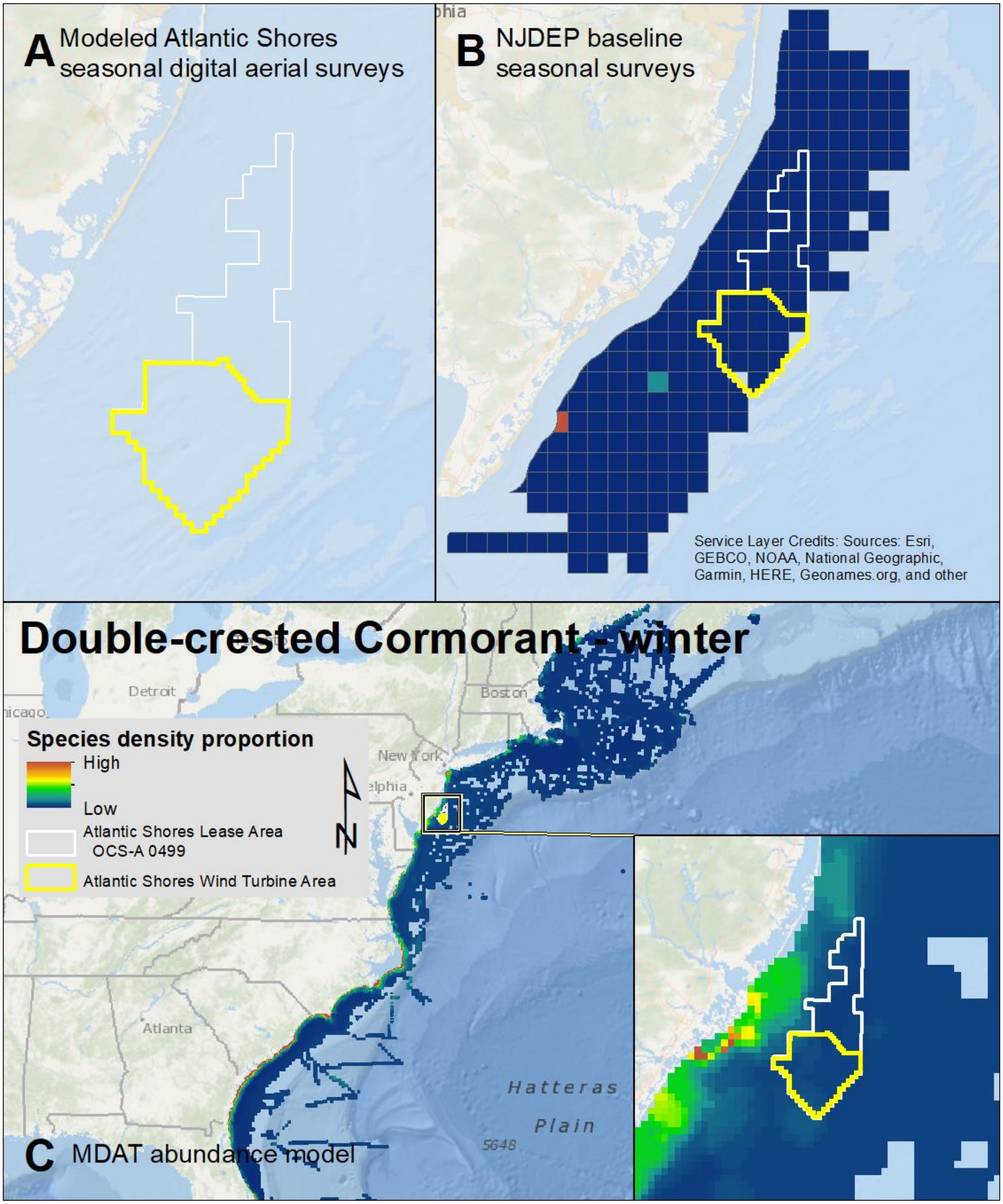

Map 74. Winter Double-crested Cormorant modeled density proportions in the Atlantic Shores seasonal digital aerial surveys (A), density proportions in the NJDEP baseline survey data (B), and the MDAT data at local and regional scales (C). The scale for all maps is representative of relative spatial variation in the sites within the season for each data source.

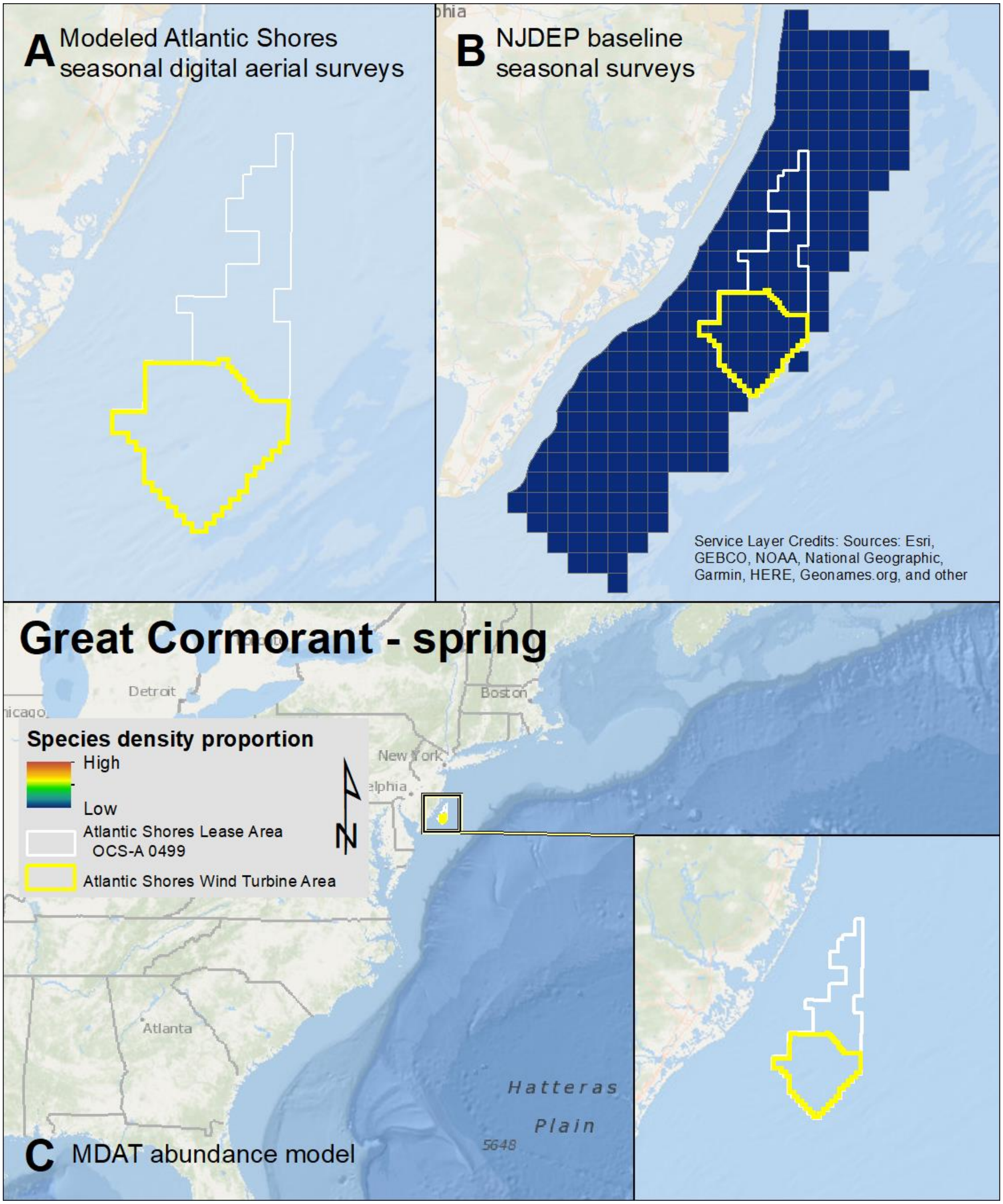

Map 75. Spring Great Cormorant modeled density proportions in the Atlantic Shores seasonal digital aerial surveys (A), density proportions in the NJDEP baseline survey data (B), and the MDAT data at local and regional scales (C). The scale for all maps is representative of relative spatial variation in the sites within the season for each data source.

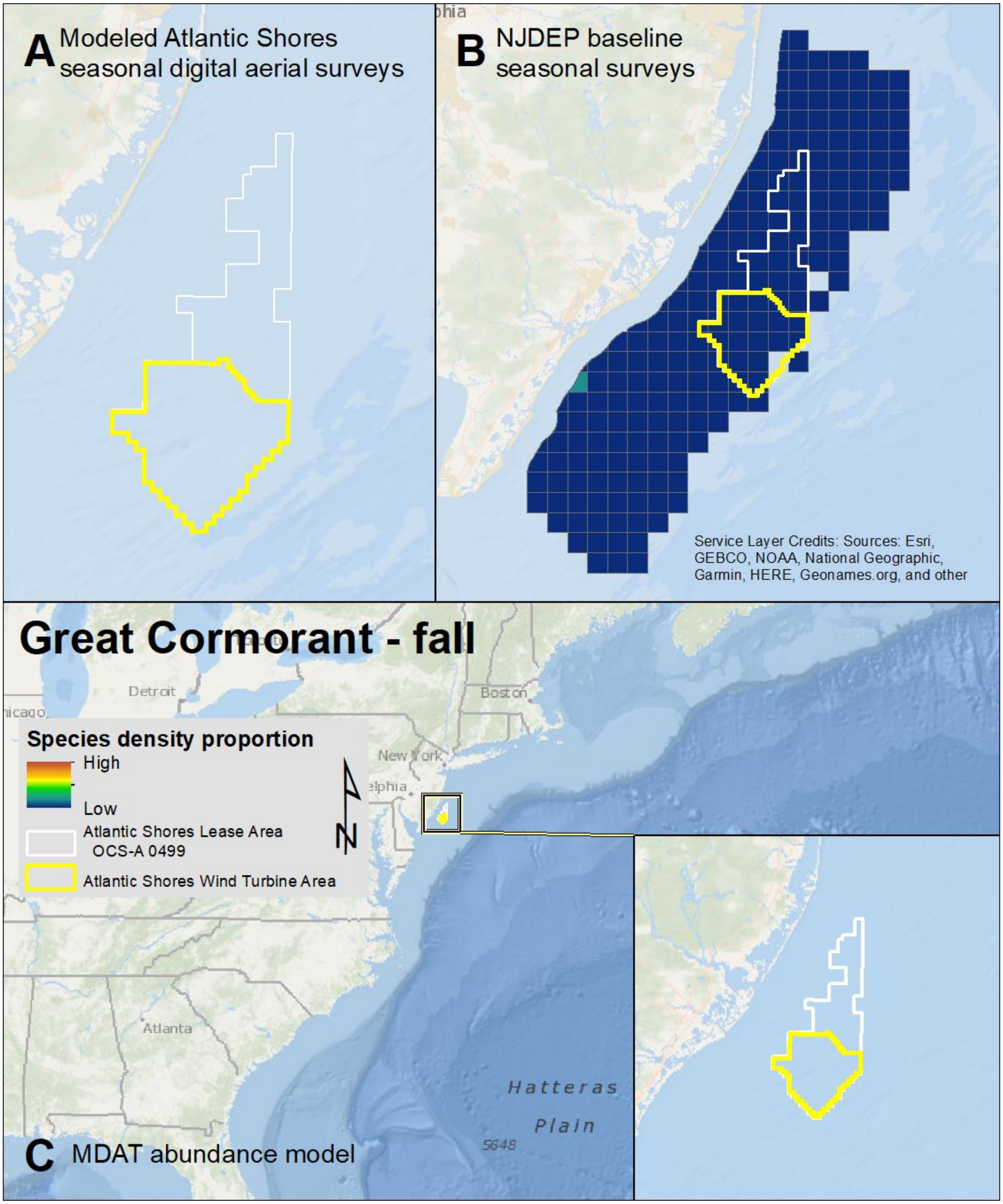

Map 76. Fall Great Cormorant modeled density proportions in the Atlantic Shores seasonal digital aerial surveys (A), density proportions in the NJDEP baseline survey data (B), and the MDAT data at local and regional scales (C). The scale for all maps is representative of relative spatial variation in the sites within the season for each data source.

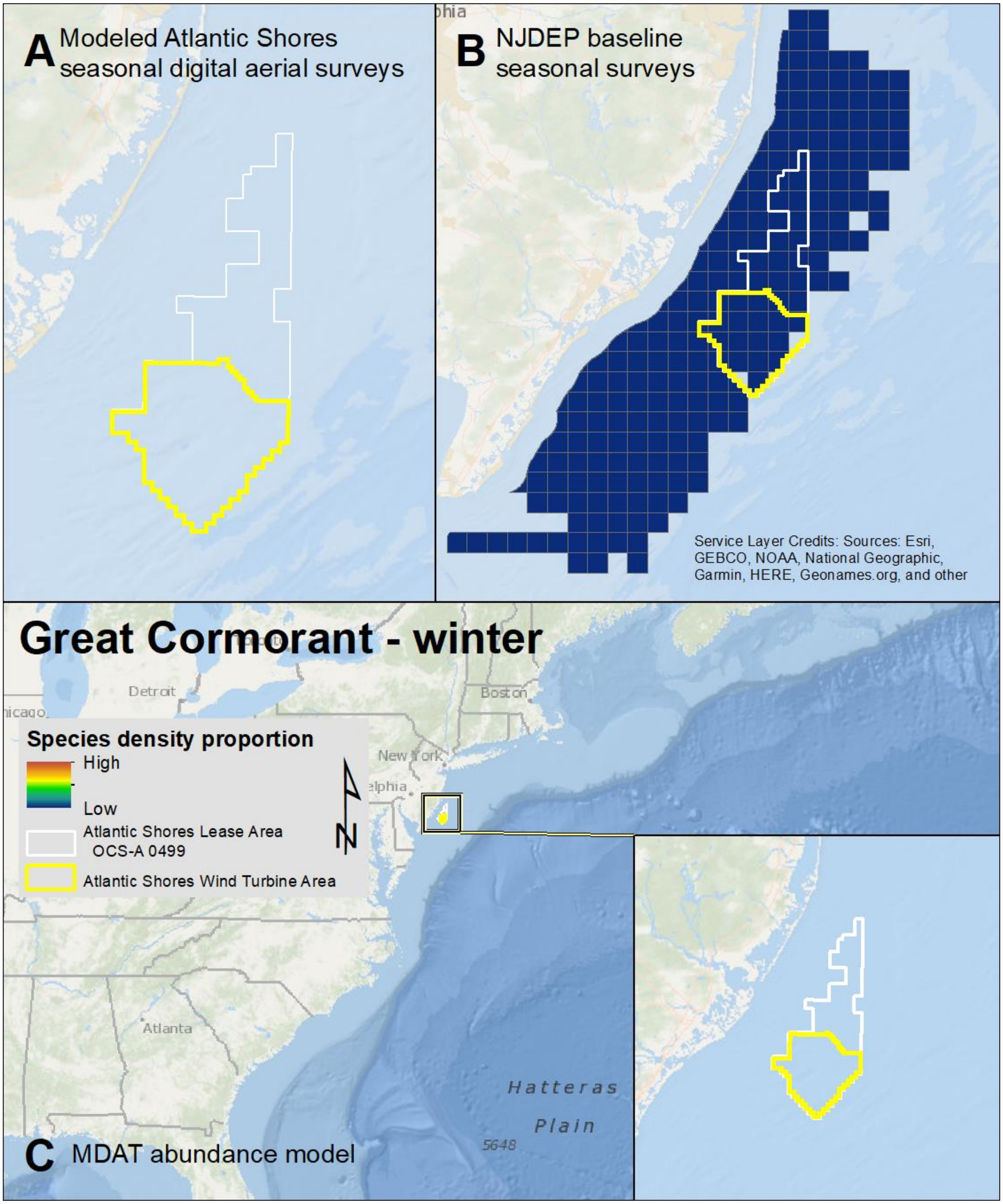

Map 77. Winter Great Cormorant modeled density proportions in the Atlantic Shores seasonal digital aerial surveys (A), density proportions in the NJDEP baseline survey data (B), and the MDAT data at local and regional scales (C). The scale for all maps is representative of relative spatial variation in the sites within the season for each data source.

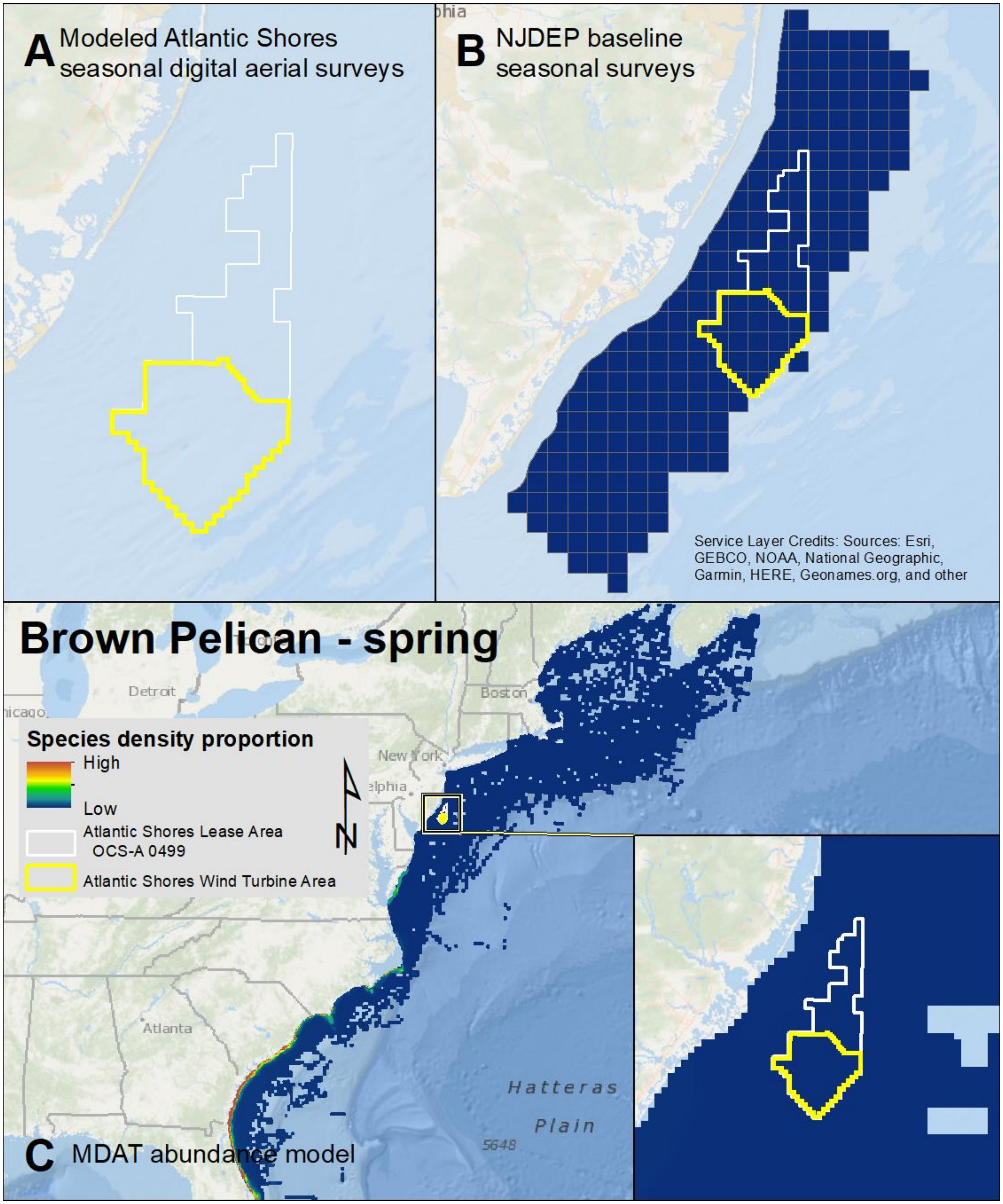

Map 78. Spring Brown Pelican modeled density proportions in the Atlantic Shores seasonal digital aerial surveys (A), density proportions in the NJDEP baseline survey data (B), and the MDAT data at local and regional scales (C). The scale for all maps is representative of relative spatial variation in the sites within the season for each data source.

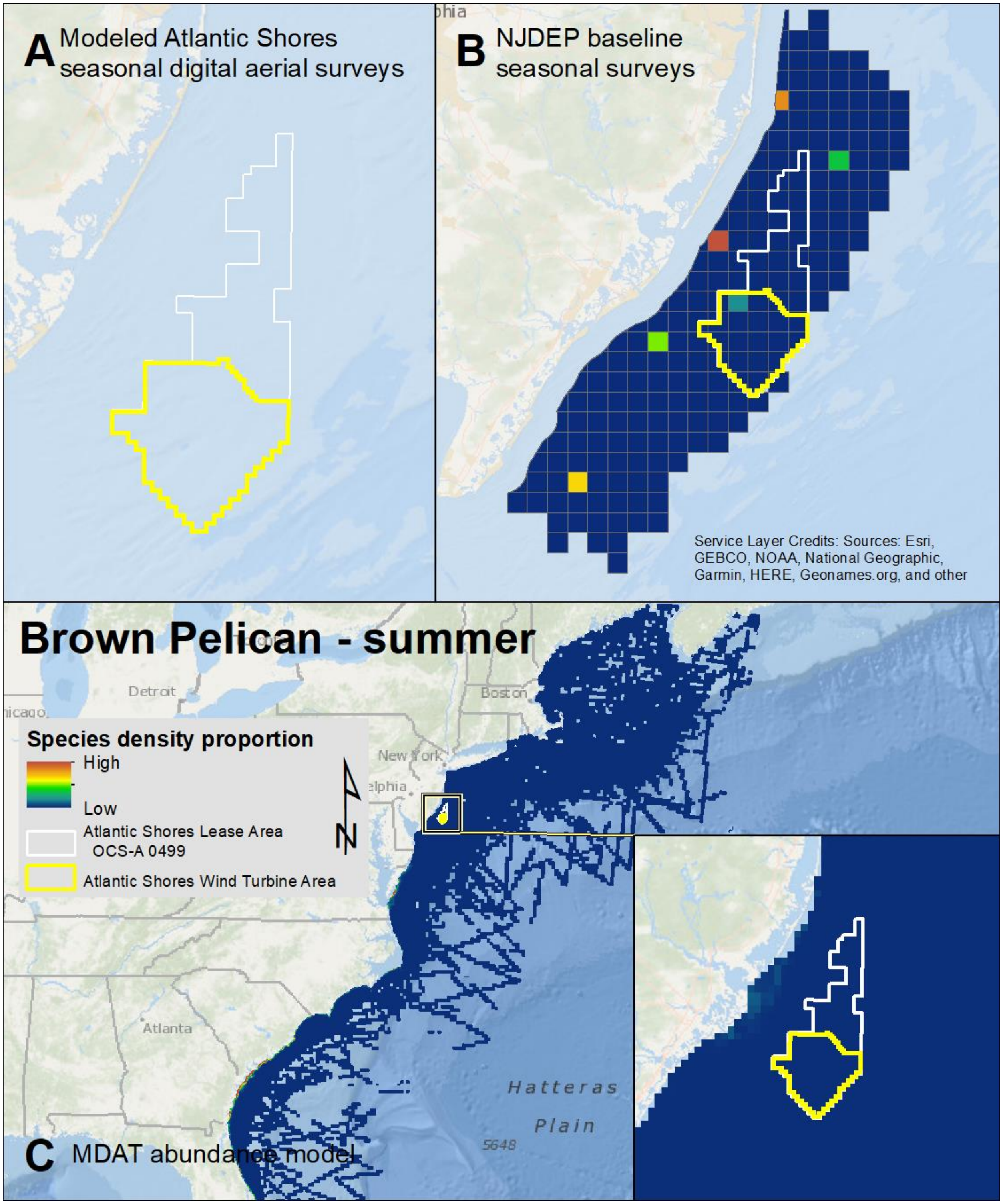

Map 79. Summer Brown Pelican modeled density proportions in the Atlantic Shores seasonal digital aerial surveys (A), density proportions in the NJDEP baseline survey data (B), and the MDAT data at local and regional scales (C). The scale for all maps is representative of relative spatial variation in the sites within the season for each data source.

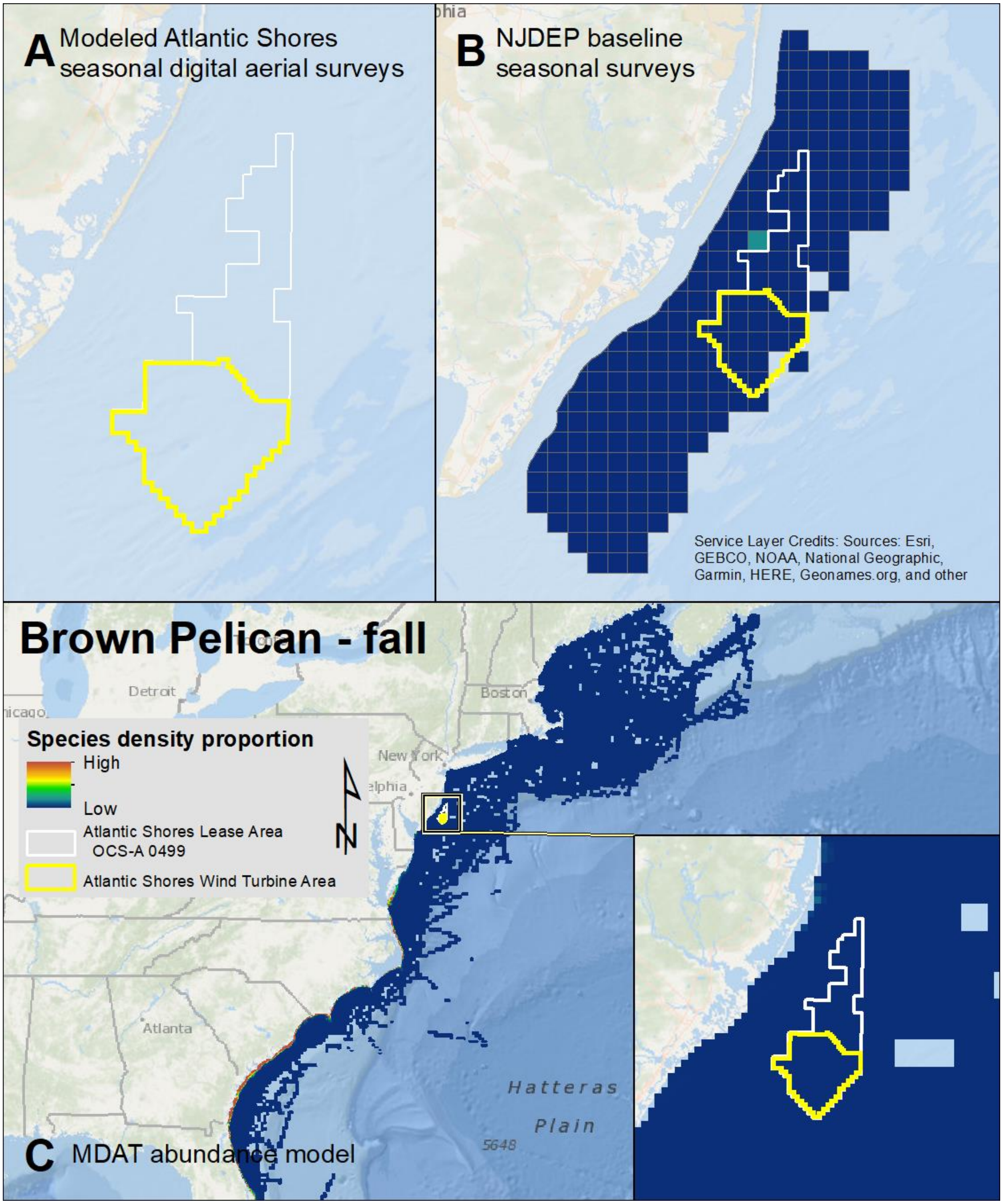

Map 80. Fall Brown Pelican modeled density proportions in the Atlantic Shores seasonal digital aerial surveys (A), density proportions in the NJDEP baseline survey data (B), and the MDAT data at local and regional scales (C). The scale for all maps is representative of relative spatial variation in the sites within the season for each data source.

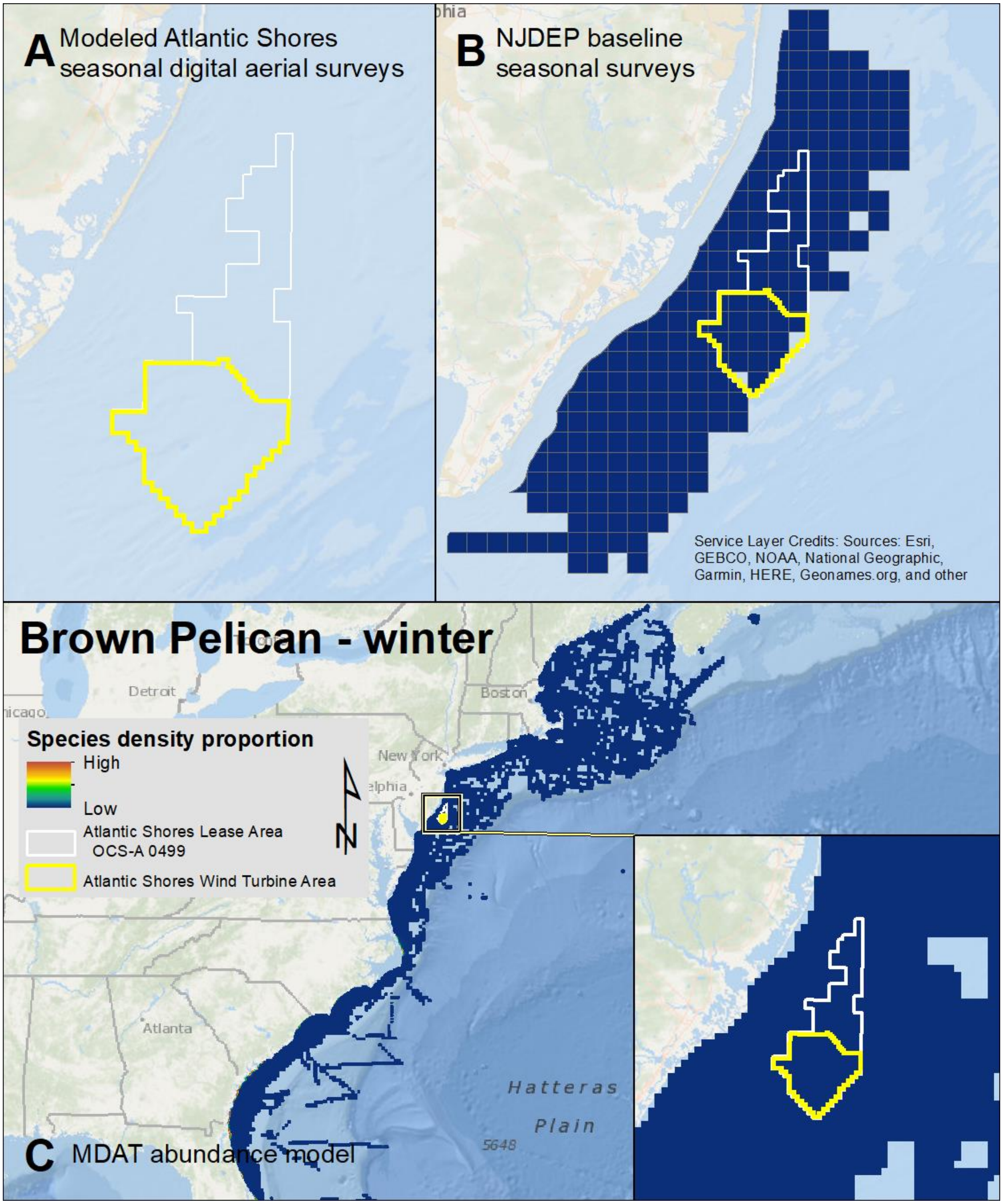

Map 81. Winter Brown Pelican modeled density proportions in the Atlantic Shores seasonal digital aerial surveys (A), density proportions in the NJDEP baseline survey data (B), and the MDAT data at local and regional scales (C). The scale for all maps is representative of relative spatial variation in the sites within the season for each data source.

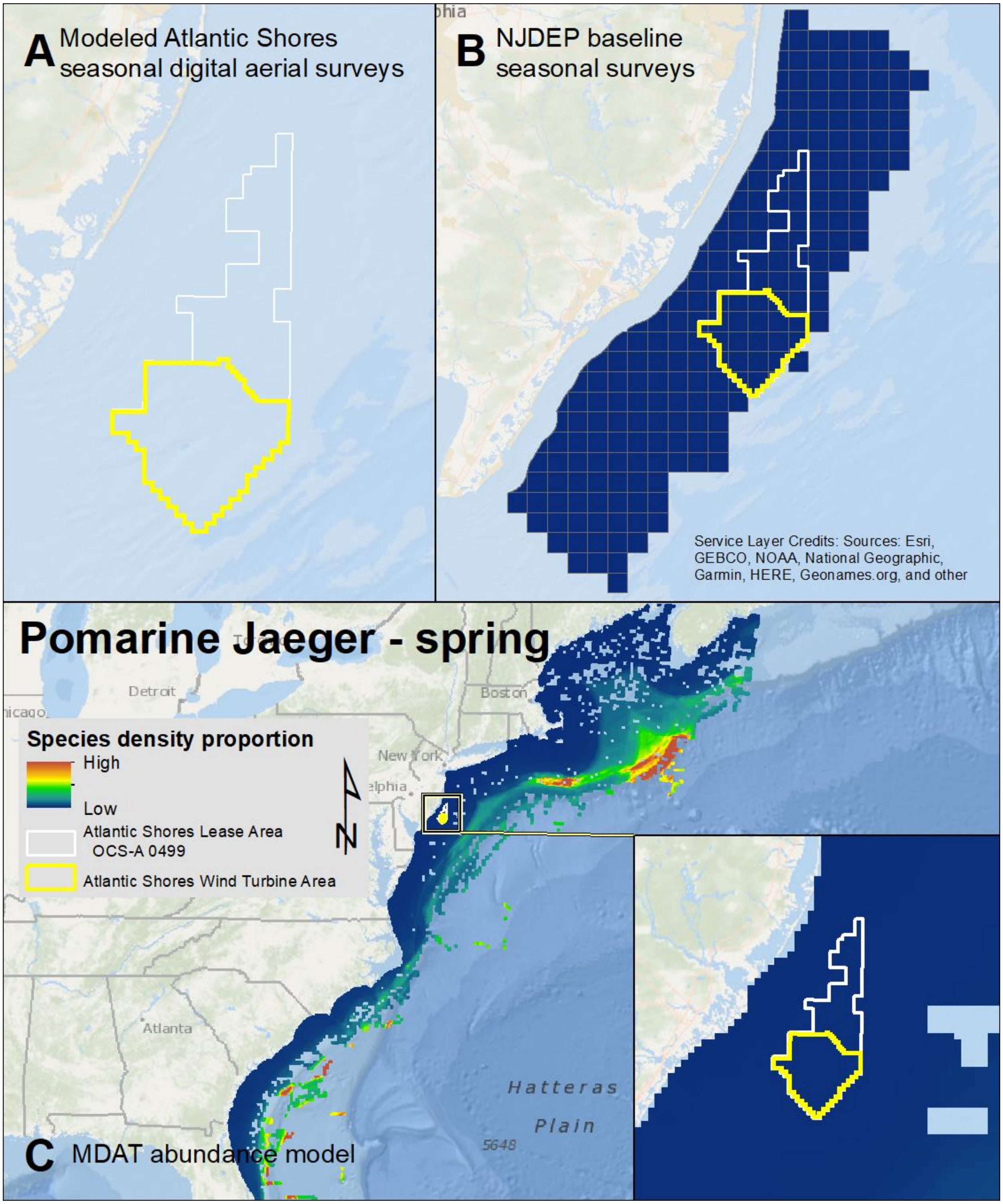

Map 82. Spring Pomarine Jaeger modeled density proportions in the Atlantic Shores seasonal digital aerial surveys (A), density proportions in the NJDEP baseline survey data (B), and the MDAT data at local and regional scales (C). The scale for all maps is representative of relative spatial variation in the sites within the season for each data source.

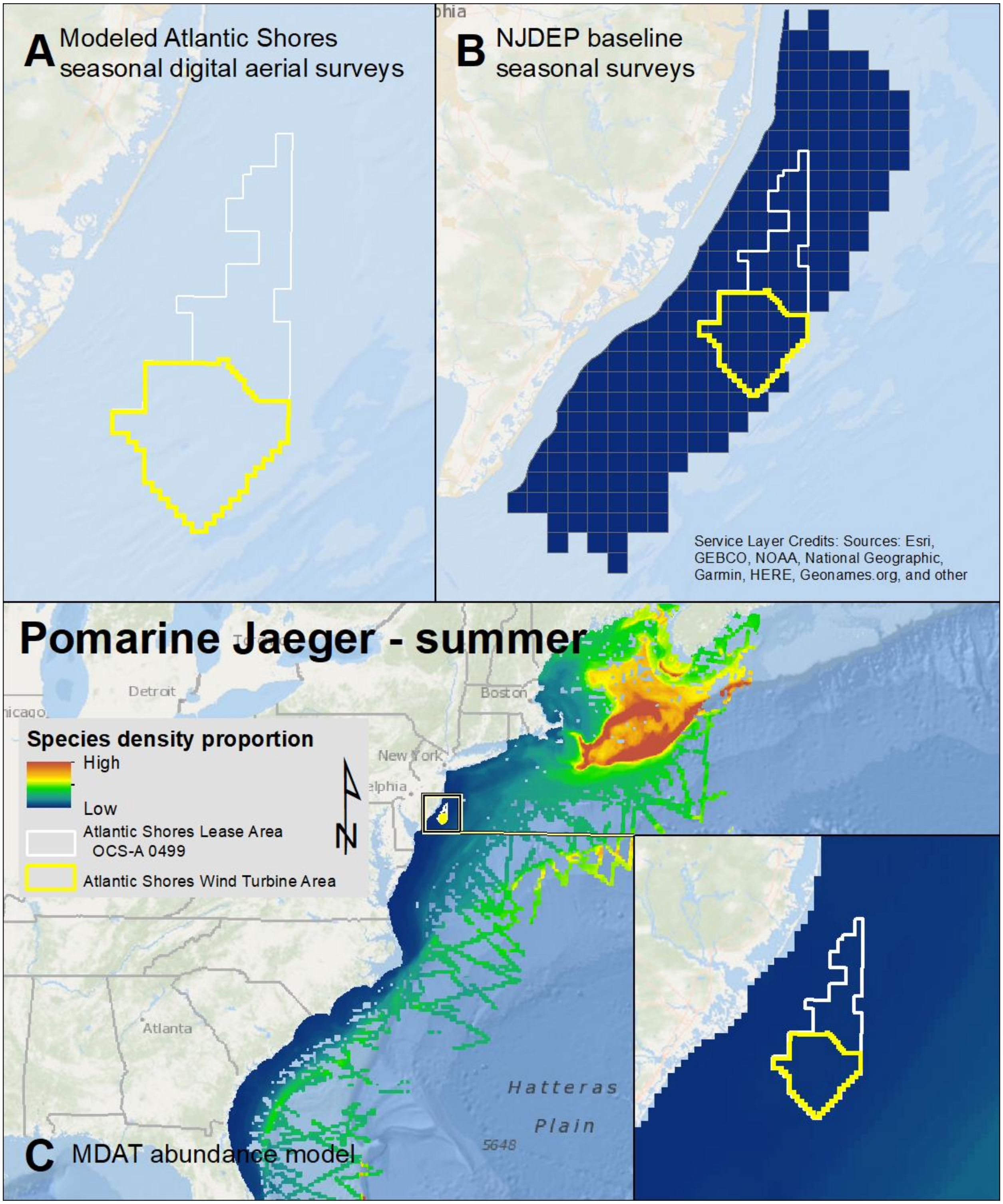

Map 83. Summer Pomarine Jaeger modeled density proportions in the Atlantic Shores seasonal digital aerial surveys (A), density proportions in the NJDEP baseline survey data (B), and the MDAT data at local and regional scales (C). The scale for all maps is representative of relative spatial variation in the sites within the season for each data source.

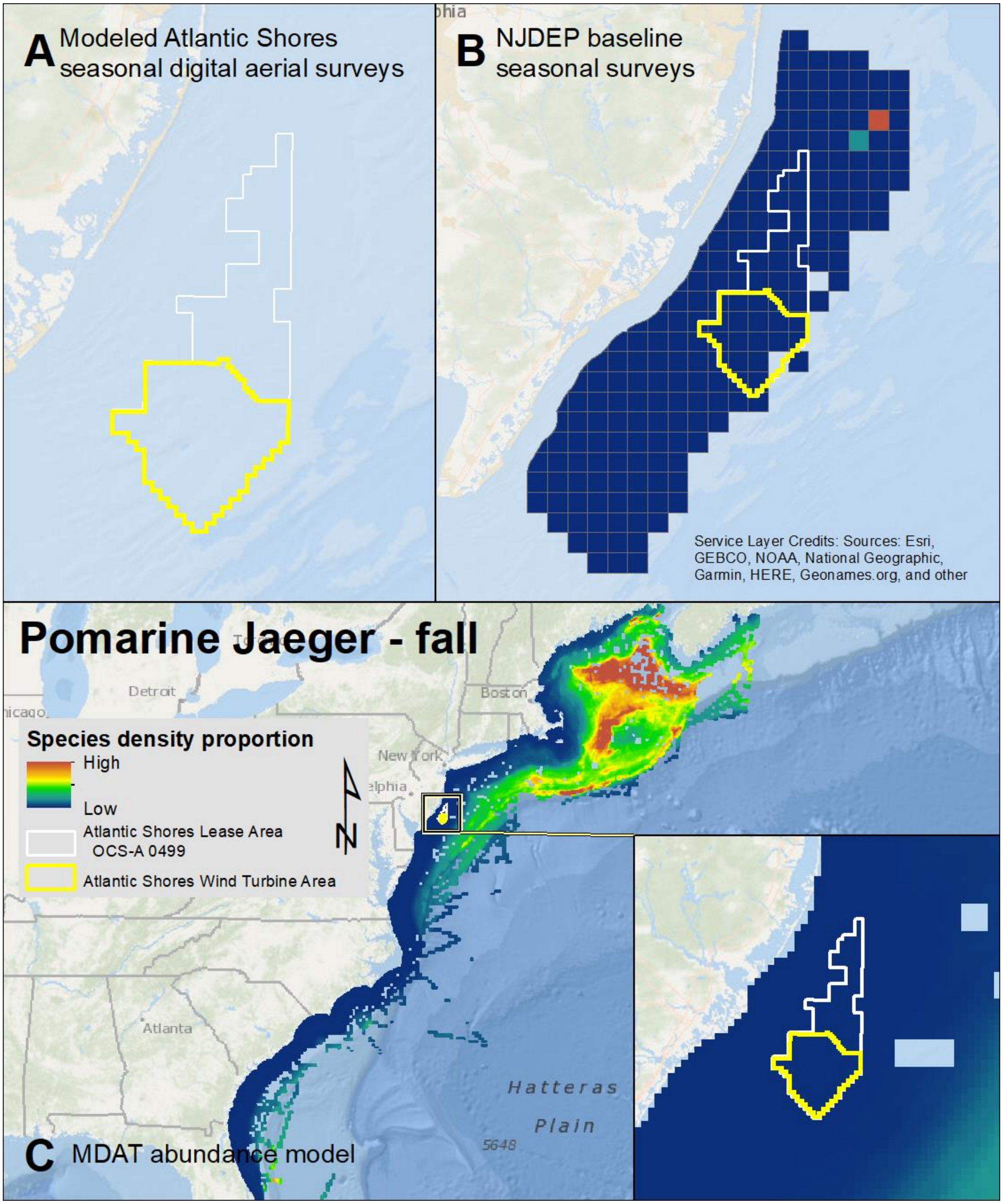

Map 84. Fall Pomarine Jaeger modeled density proportions in the Atlantic Shores seasonal digital aerial surveys (A), density proportions in the NJDEP baseline survey data (B), and the MDAT data at local and regional scales (C). The scale for all maps is representative of relative spatial variation in the sites within the season for each data source.

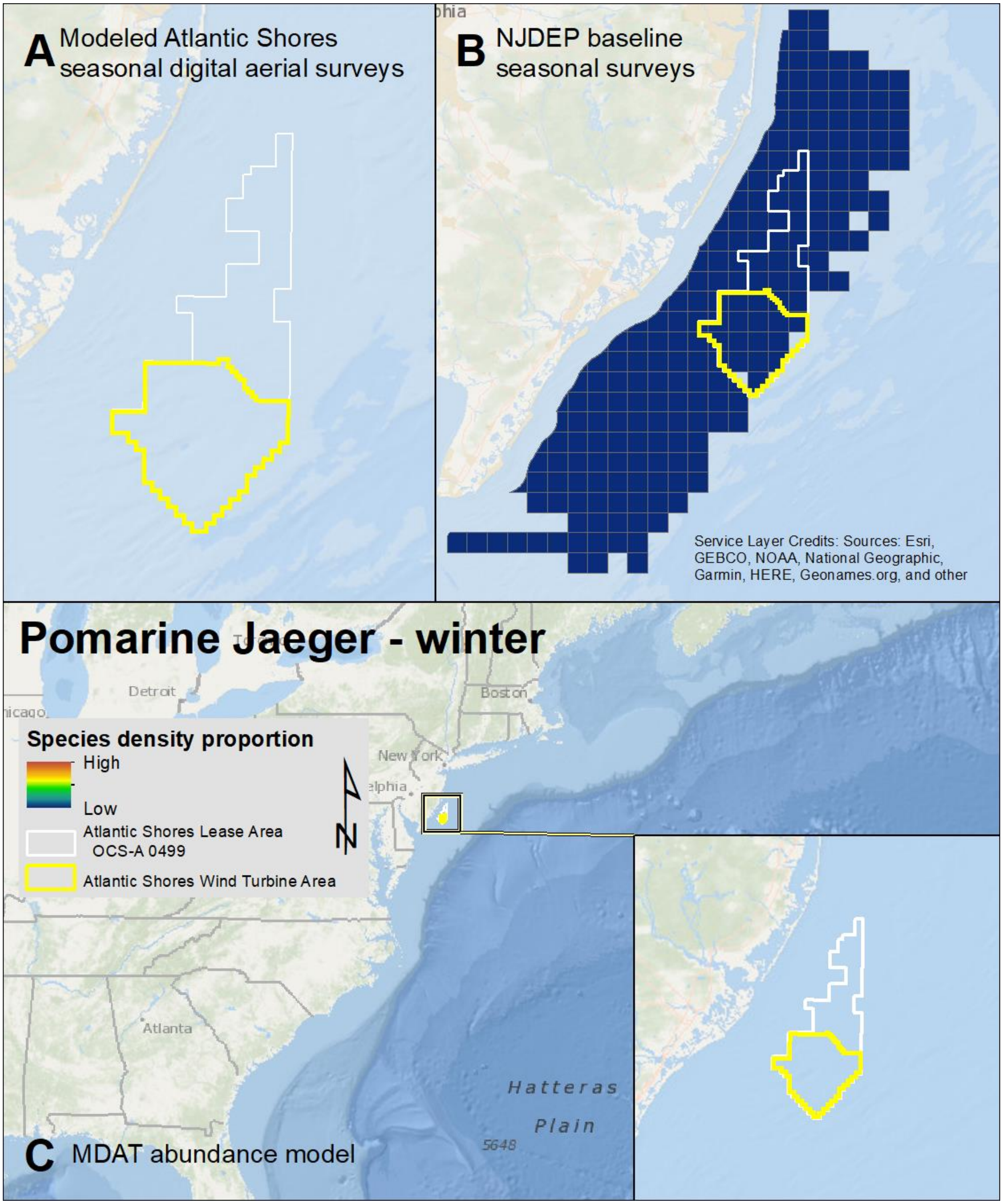

Map 85. Winter Pomarine Jaeger modeled density proportions in the Atlantic Shores seasonal digital aerial surveys (A), density proportions in the NJDEP baseline survey data (B), and the MDAT data at local and regional scales (C). The scale for all maps is representative of relative spatial variation in the sites within the season for each data source.

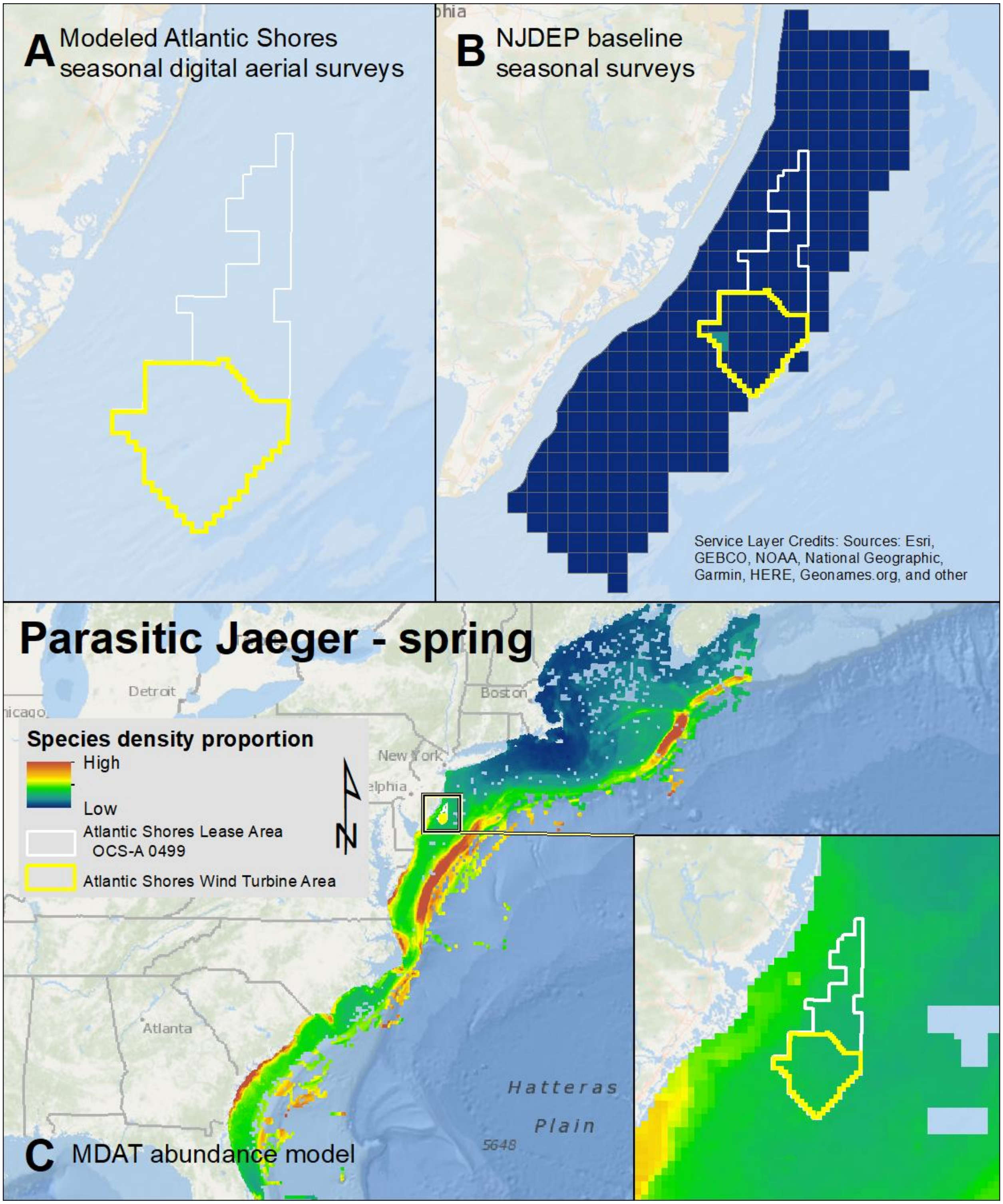

Map 86. Spring Parasitic Jaeger modeled density proportions in the Atlantic Shores seasonal digital aerial surveys (A), density proportions in the NJDEP baseline survey data (B), and the MDAT data at local and regional scales (C). The scale for all maps is representative of relative spatial variation in the sites within the season for each data source.

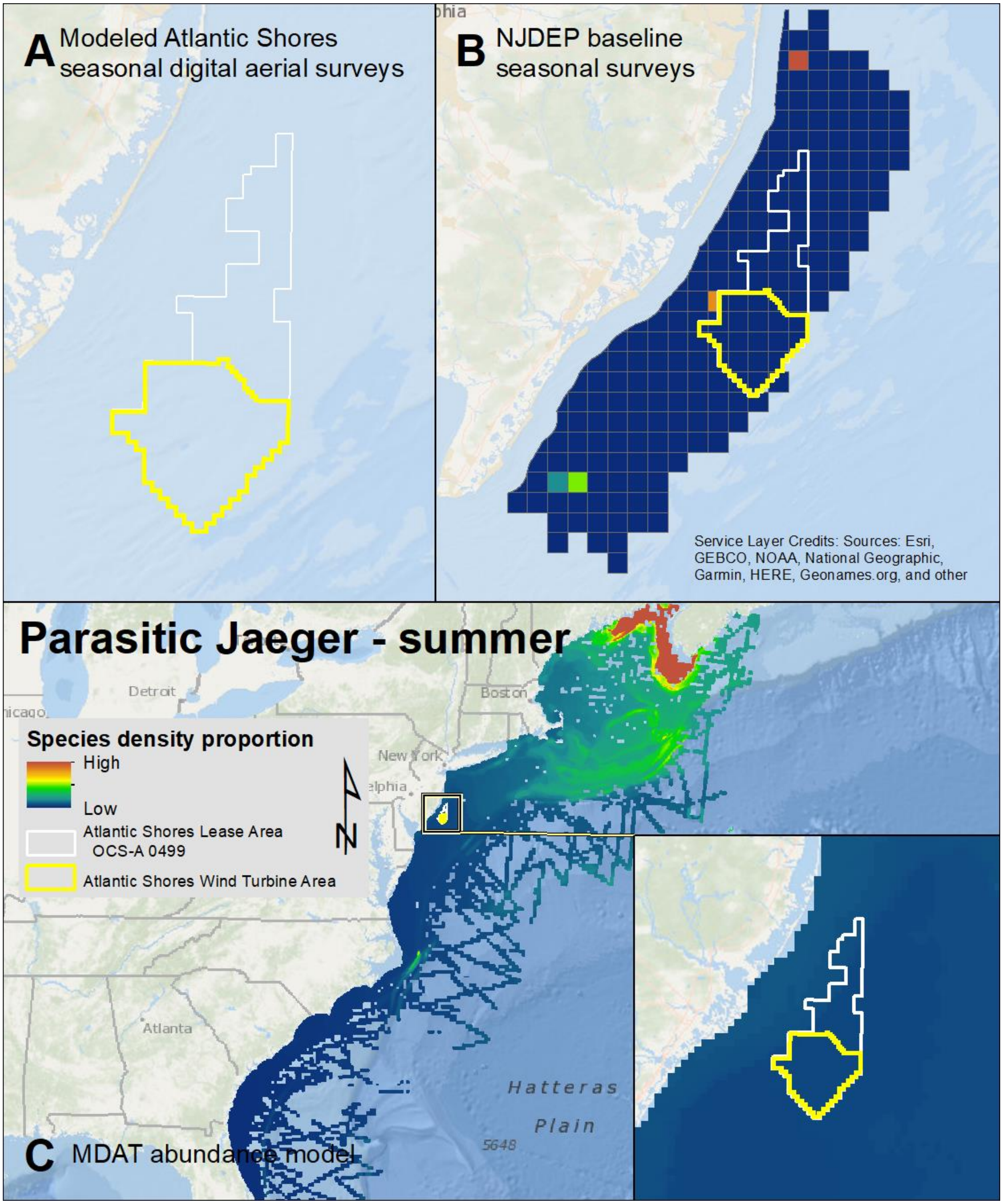

Map 87. Summer Parasitic Jaeger modeled density proportions in the Atlantic Shores seasonal digital aerial surveys (A), density proportions in the NJDEP baseline survey data (B), and the MDAT data at local and regional scales (C). The scale for all maps is representative of relative spatial variation in the sites within the season for each data source.

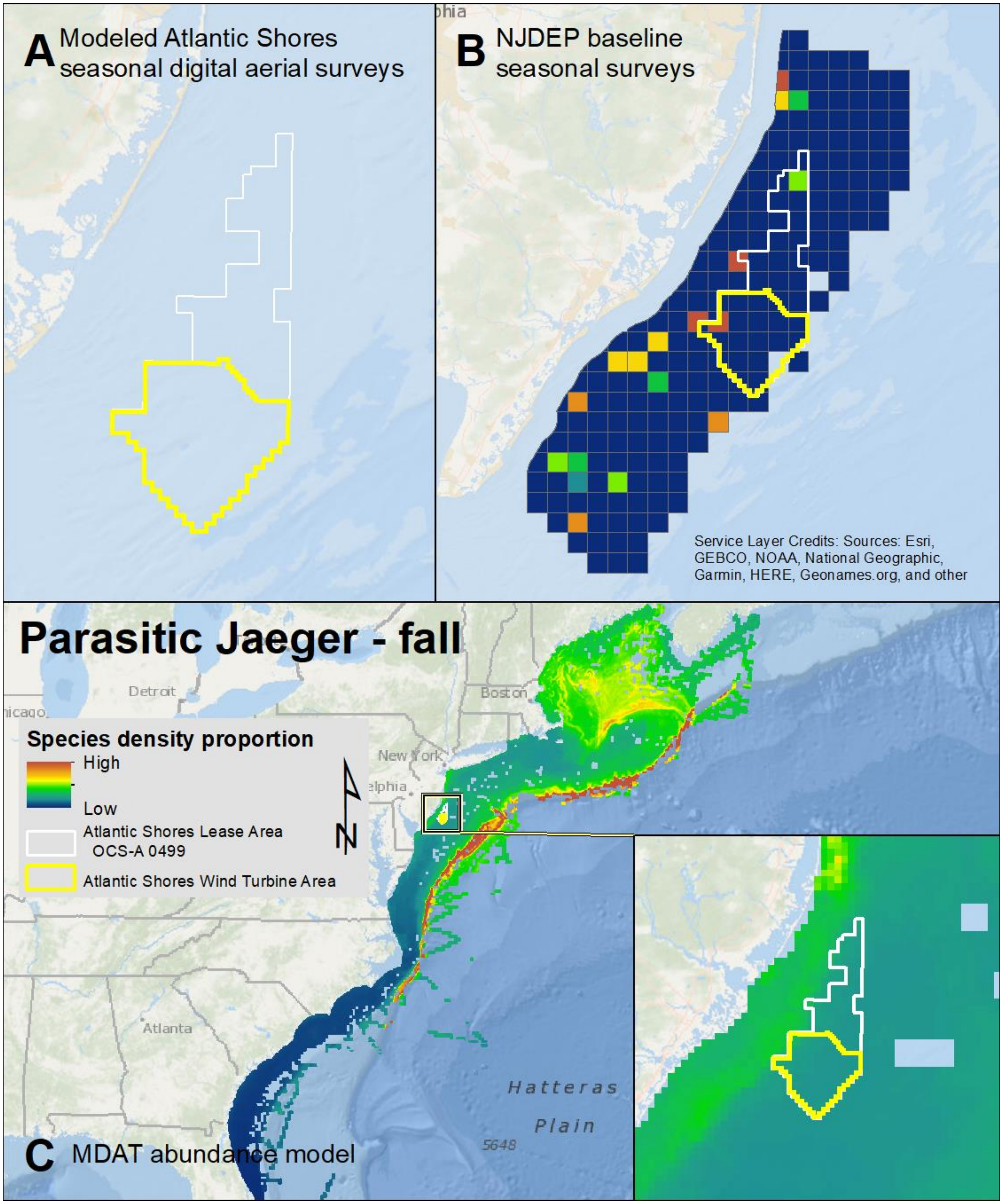

Map 88. Fall Parasitic Jaeger modeled density proportions in the Atlantic Shores seasonal digital aerial surveys (A), density proportions in the NJDEP baseline survey data (B), and the MDAT data at local and regional scales (C). The scale for all maps is representative of relative spatial variation in the sites within the season for each data source.

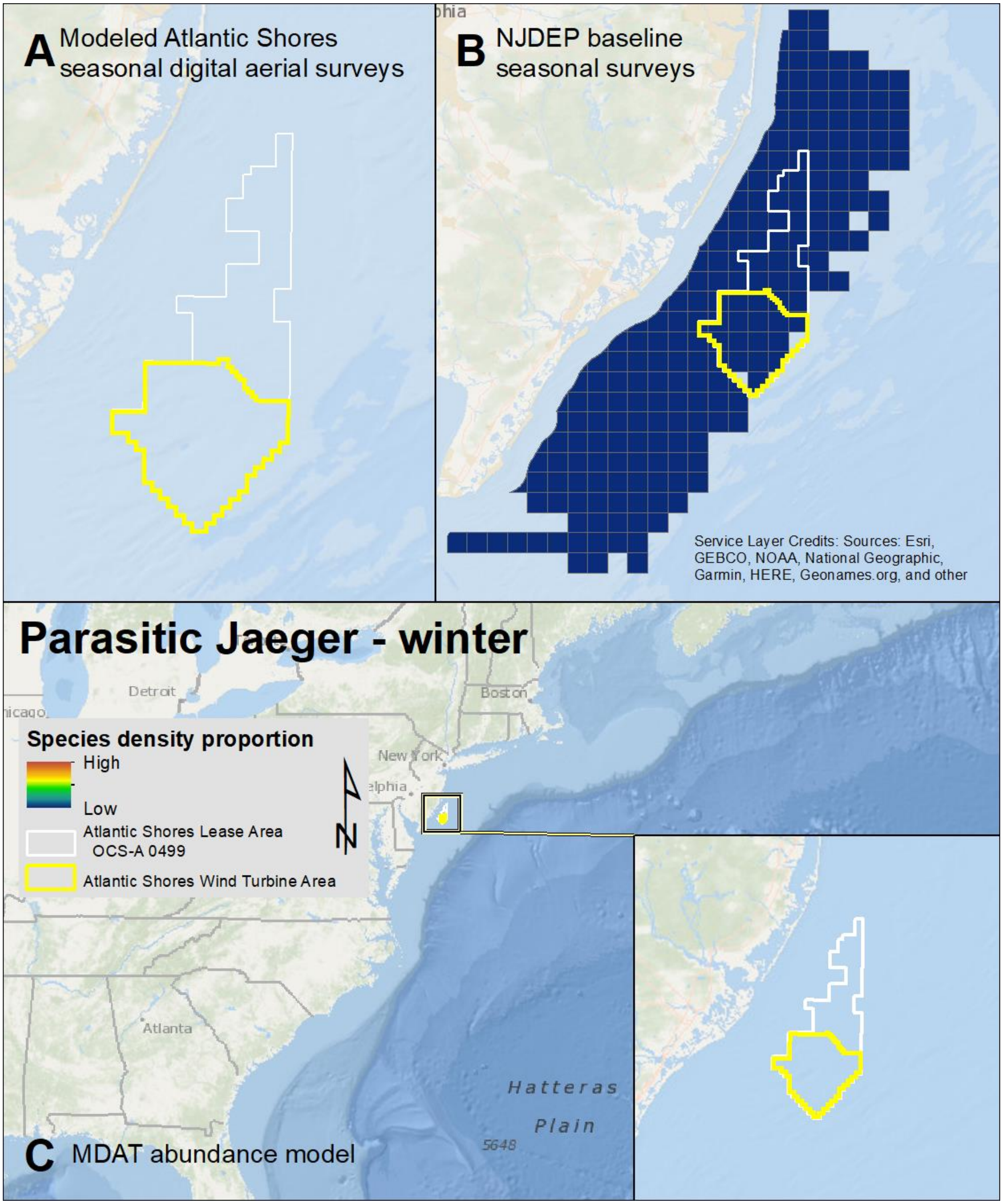

Map 89. Winter Parasitic Jaeger modeled density proportions in the Atlantic Shores seasonal digital aerial surveys (A), density proportions in the NJDEP baseline survey data (B), and the MDAT data at local and regional scales (C). The scale for all maps is representative of relative spatial variation in the sites within the season for each data source.

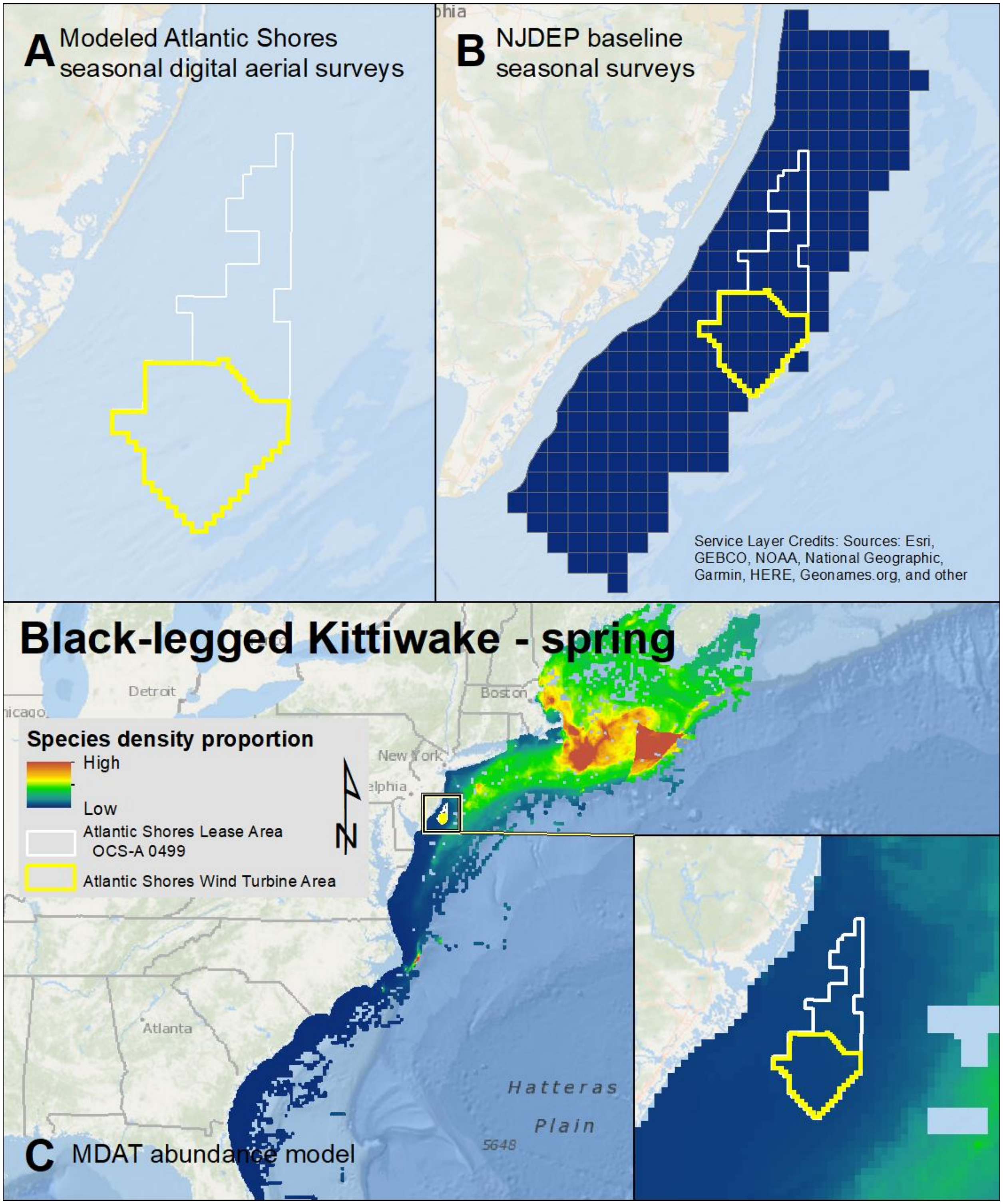

Map 90. Spring Black-legged Kittiwake modeled density proportions in the Atlantic Shores seasonal digital aerial surveys (A), density proportions in the NJDEP baseline survey data (B), and the MDAT data at local and regional scales (C). The scale for all maps is representative of relative spatial variation in the sites within the season for each data source.

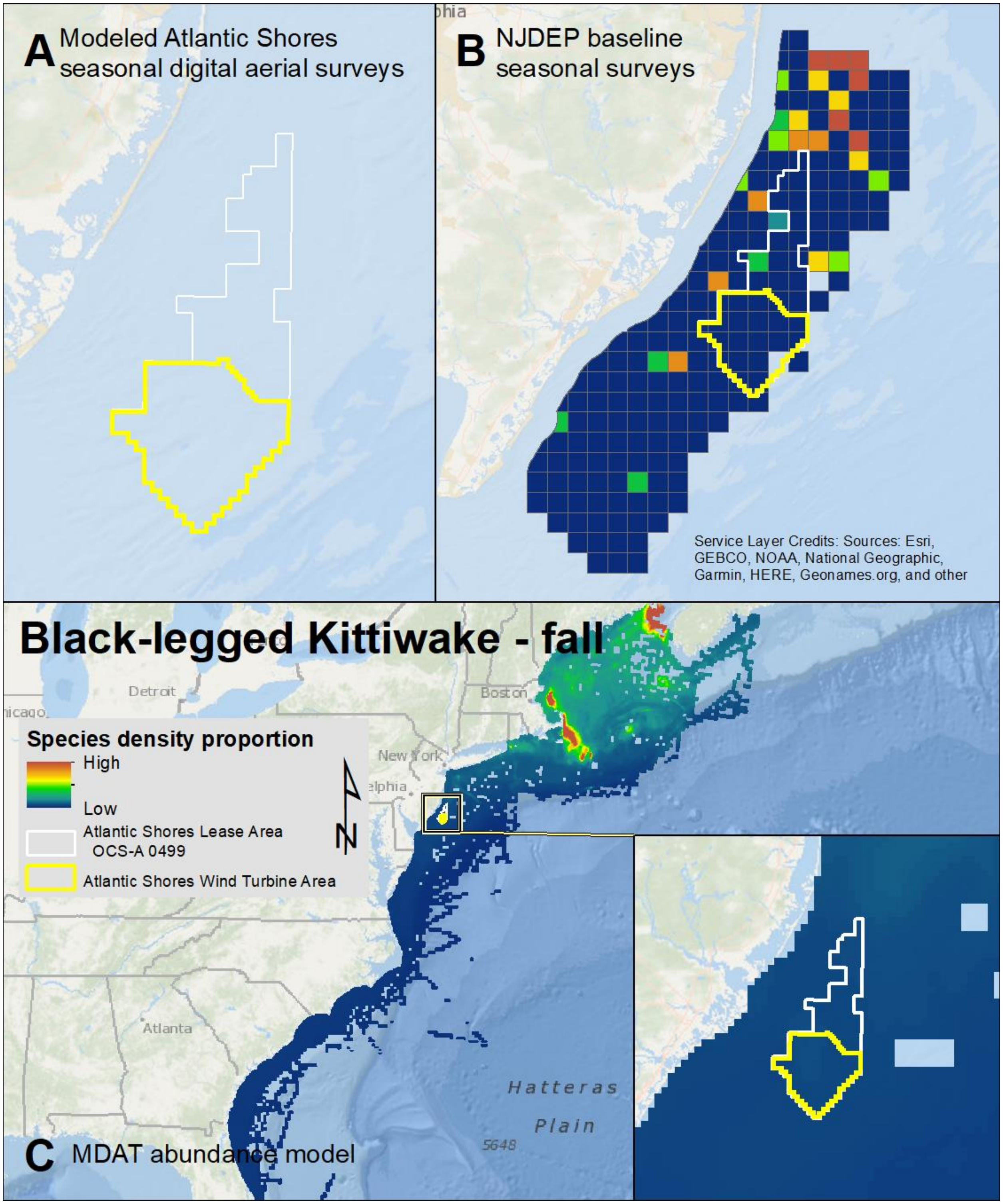

Map 91. Fall Black-legged Kittiwake modeled density proportions in the Atlantic Shores seasonal digital aerial surveys (A), density proportions in the NJDEP baseline survey data (B), and the MDAT data at local and regional scales (C). The scale for all maps is representative of relative spatial variation in the sites within the season for each data source.

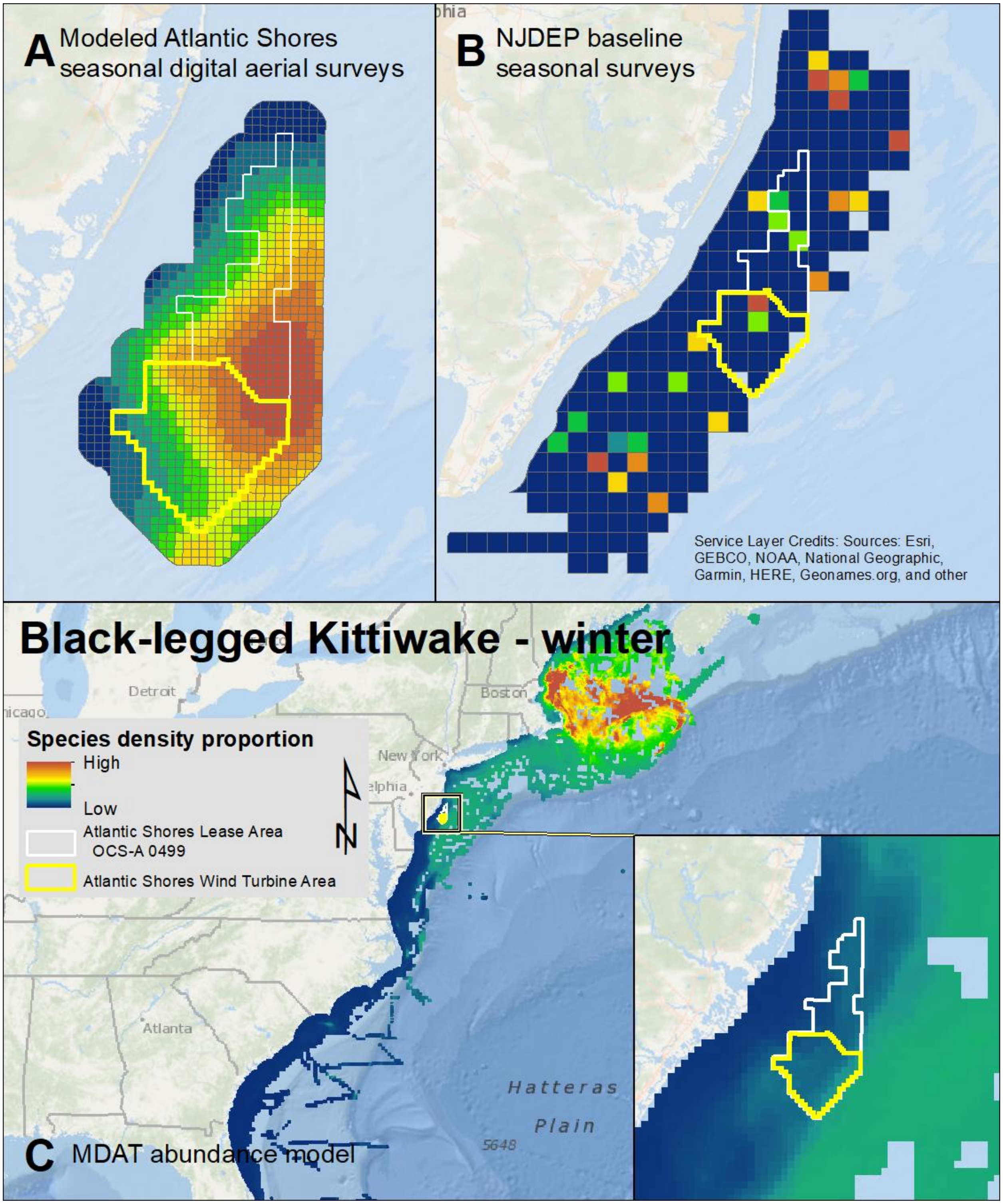

Map 92. Winter Black-legged Kittiwake modeled density proportions in the Atlantic Shores seasonal digital aerial surveys (A), density proportions in the NJDEP baseline survey data (B), and the MDAT data at local and regional scales (C). The scale for all maps is representative of relative spatial variation in the sites within the season for each data source.

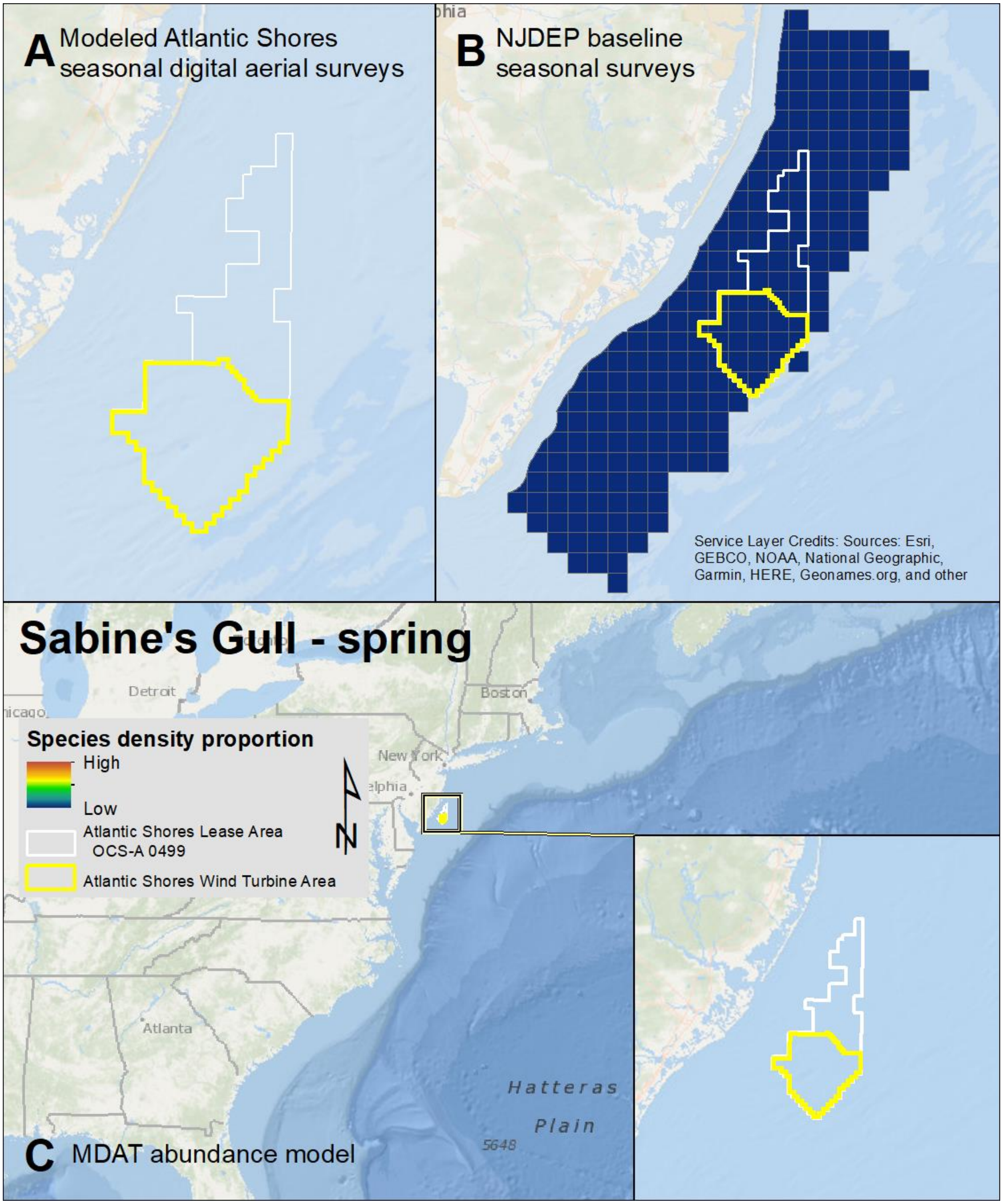

Map 93. Spring Sabine's Gull modeled density proportions in the Atlantic Shores seasonal digital aerial surveys (A), density proportions in the NJDEP baseline survey data (B), and the MDAT data at local and regional scales (C). The scale for all maps is representative of relative spatial variation in the sites within the season for each data source.

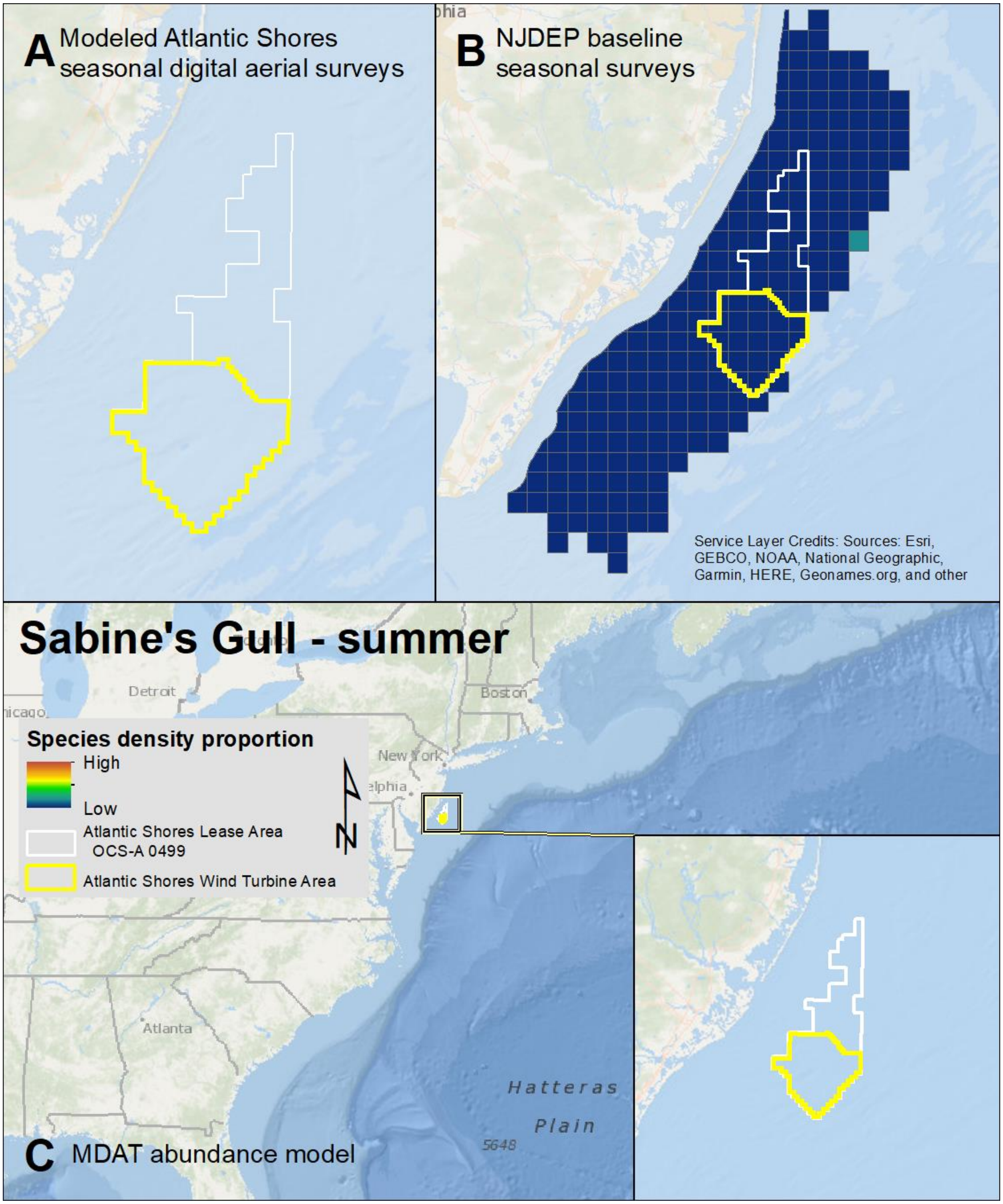

Map 94. Summer Sabine's Gull modeled density proportions in the Atlantic Shores seasonal digital aerial surveys (A), density proportions in the NJDEP baseline survey data (B), and the MDAT data at local and regional scales (C). The scale for all maps is representative of relative spatial variation in the sites within the season for each data source.

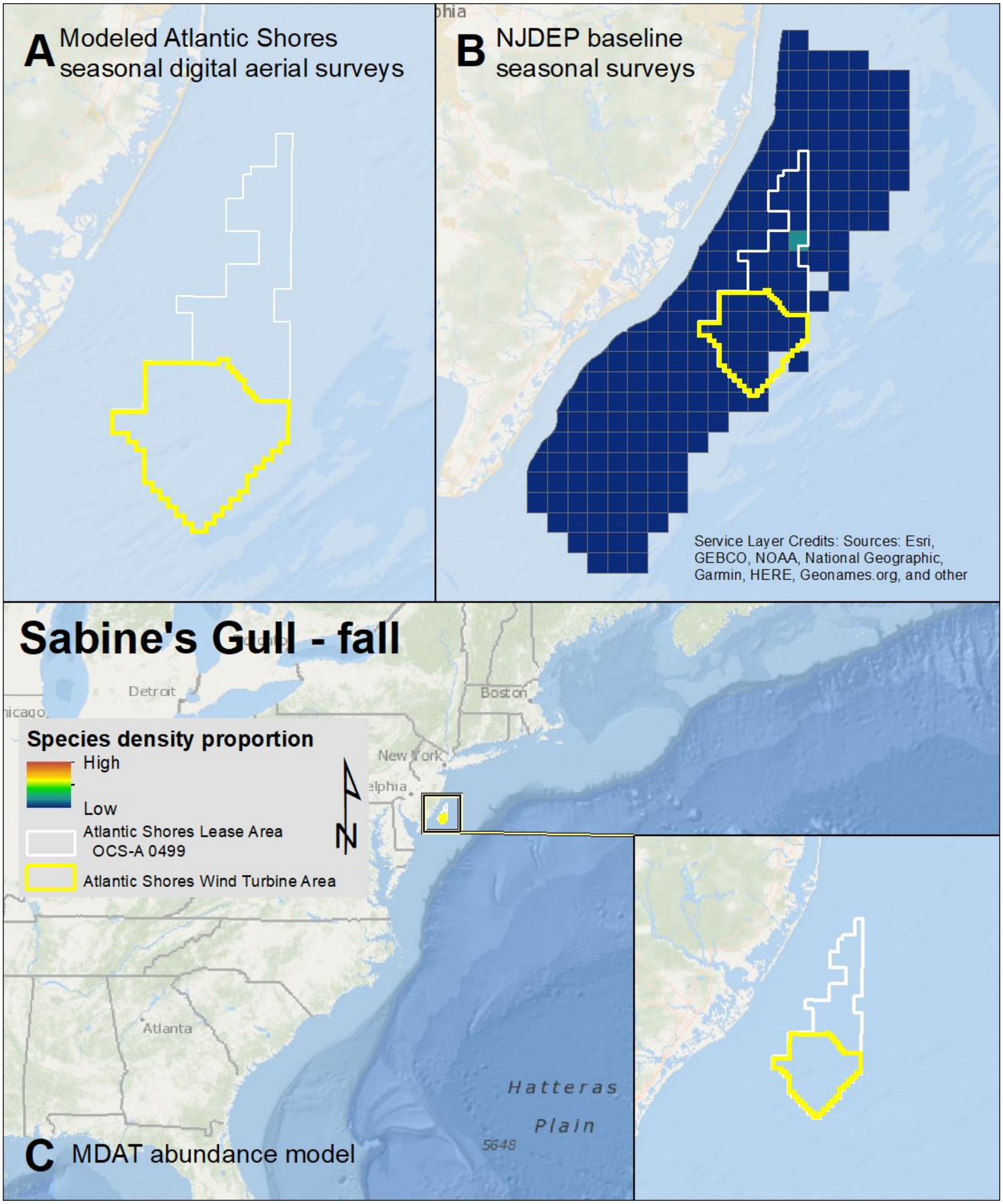

Map 95. Fall Sabine's Gull modeled density proportions in the Atlantic Shores seasonal digital aerial surveys (A), density proportions in the NJDEP baseline survey data (B), and the MDAT data at local and regional scales (C). The scale for all maps is representative of relative spatial variation in the sites within the season for each data source.

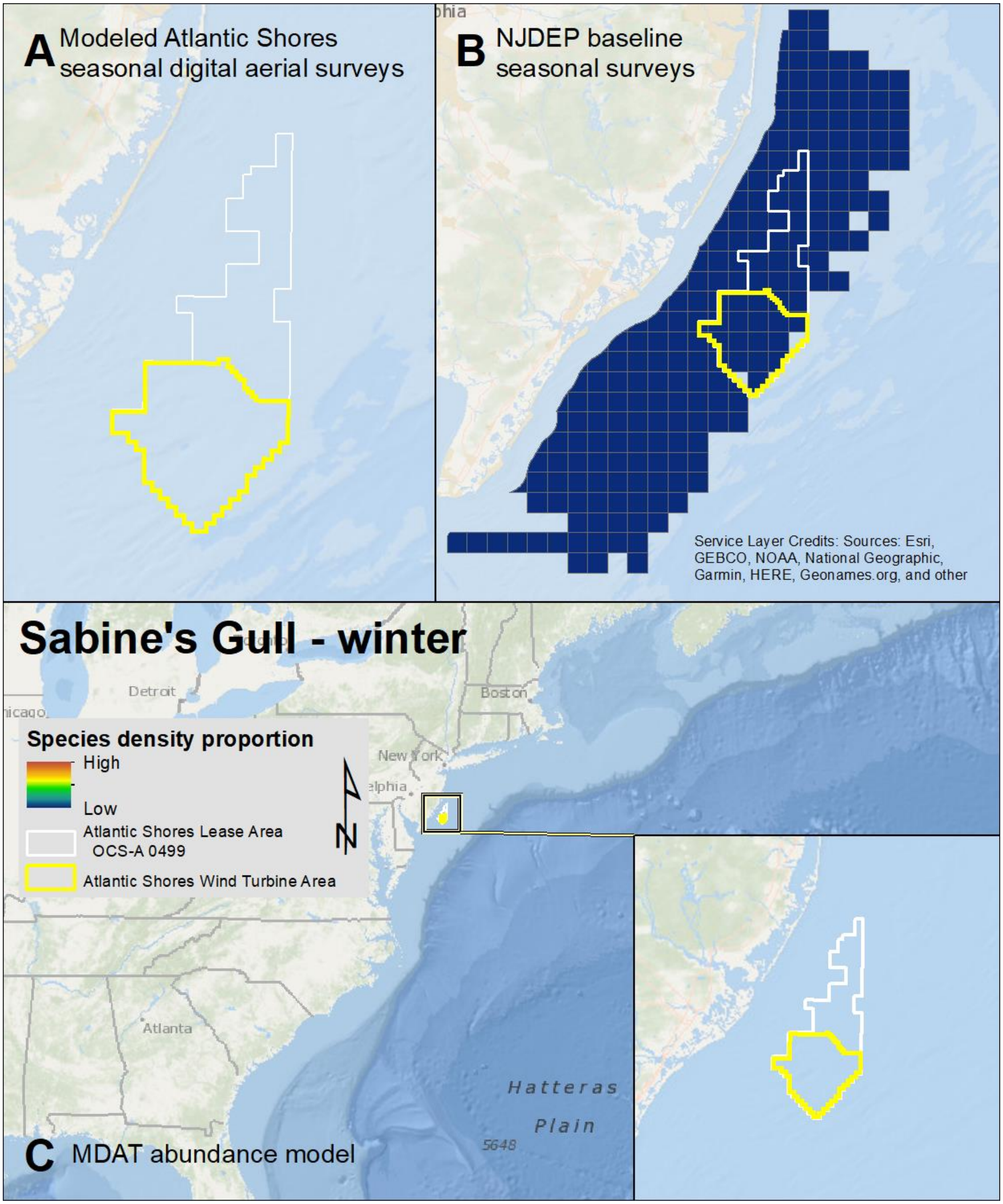

Map 96. Winter Sabine's Gull modeled density proportions in the Atlantic Shores seasonal digital aerial surveys (A), density proportions in the NJDEP baseline survey data (B), and the MDAT data at local and regional scales (C). The scale for all maps is representative of relative spatial variation in the sites within the season for each data source.

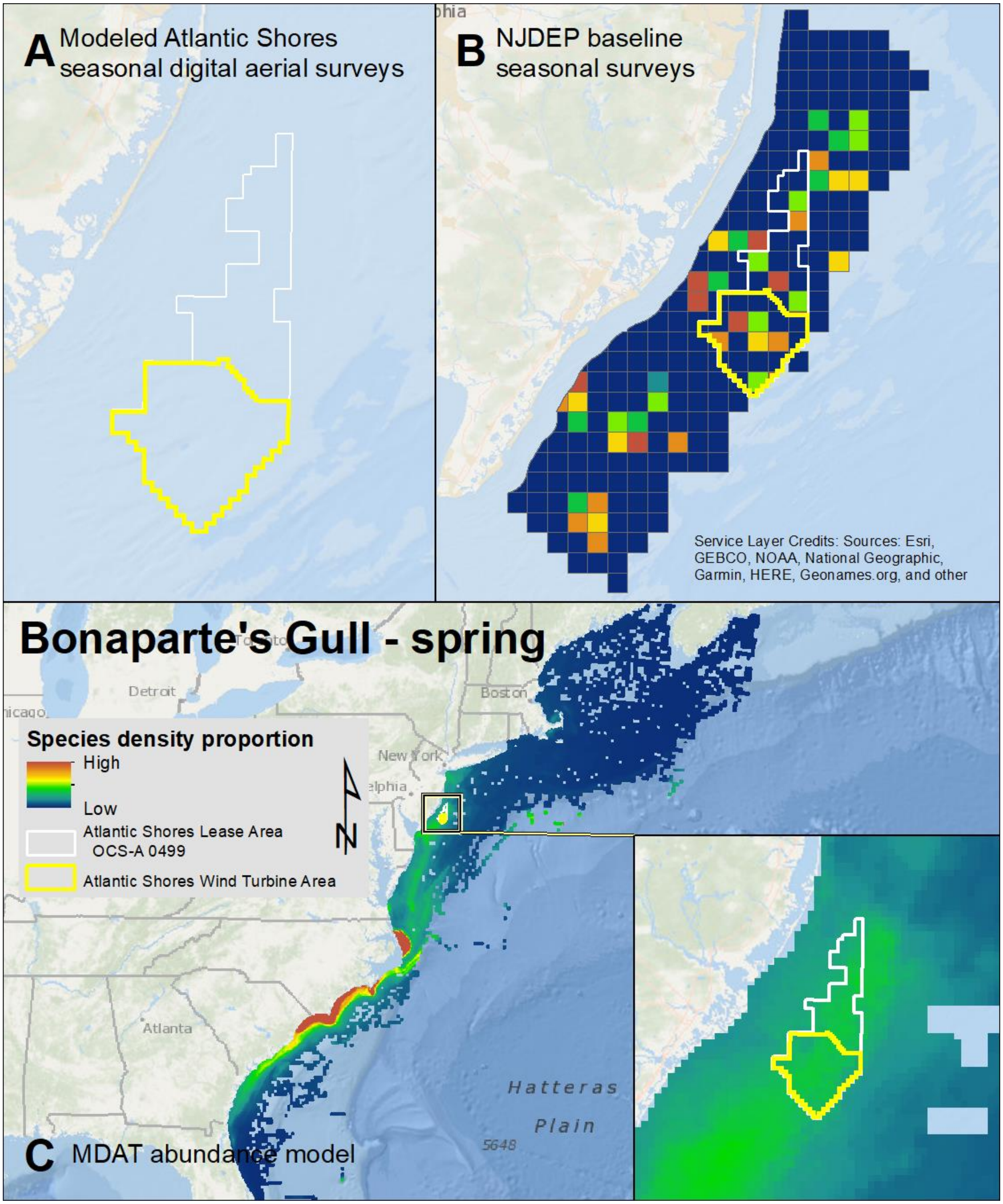

Map 97. Spring Bonaparte's Gull modeled density proportions in the Atlantic Shores seasonal digital aerial surveys (A), density proportions in the NJDEP baseline survey data (B), and the MDAT data at local and regional scales (C). The scale for all maps is representative of relative spatial variation in the sites within the season for each data source.

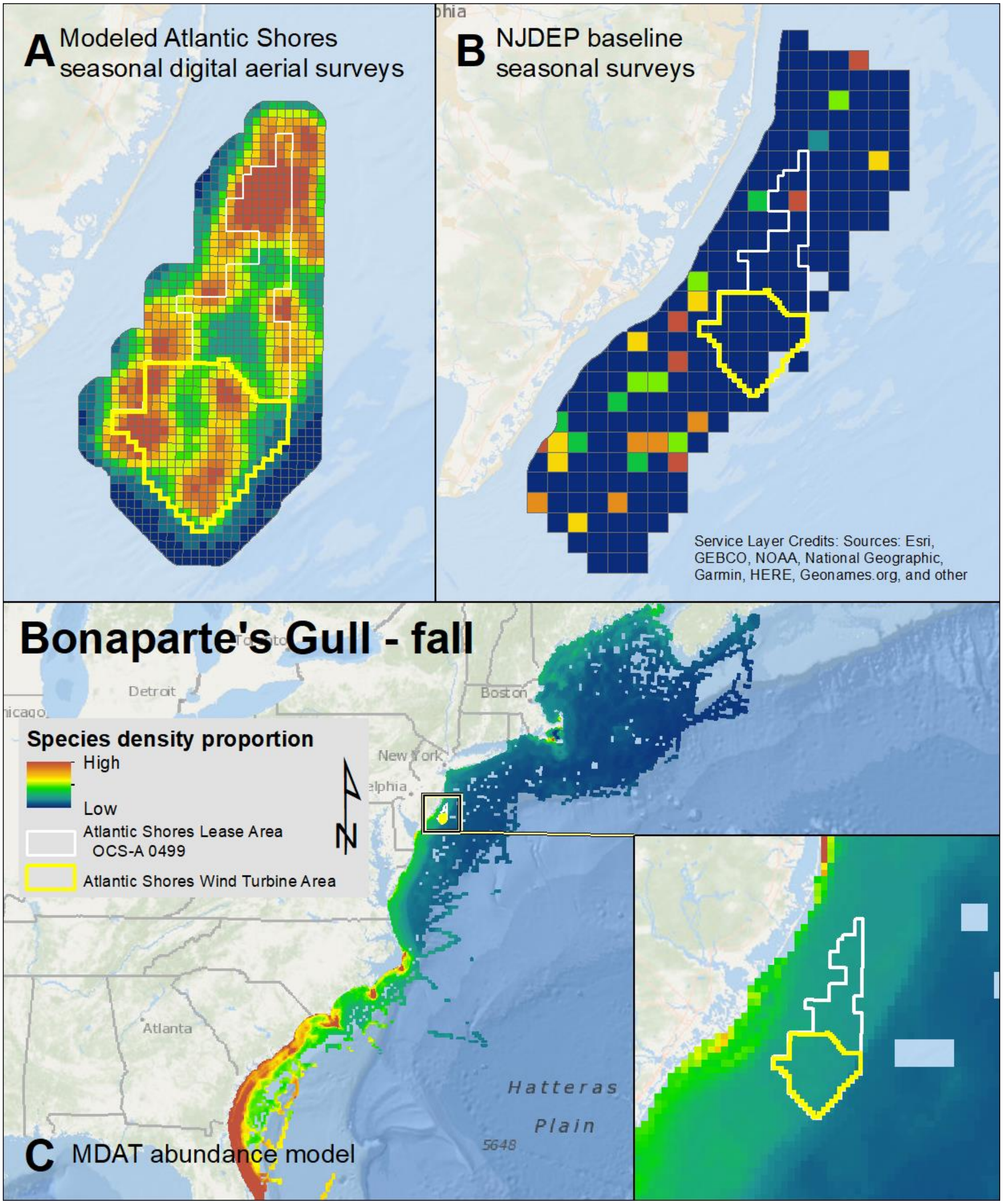

Map 98. Fall Bonaparte's Gull modeled density proportions in the Atlantic Shores seasonal digital aerial surveys (A), density proportions in the NJDEP baseline survey data (B), and the MDAT data at local and regional scales (C). The scale for all maps is representative of relative spatial variation in the sites within the season for each data source.

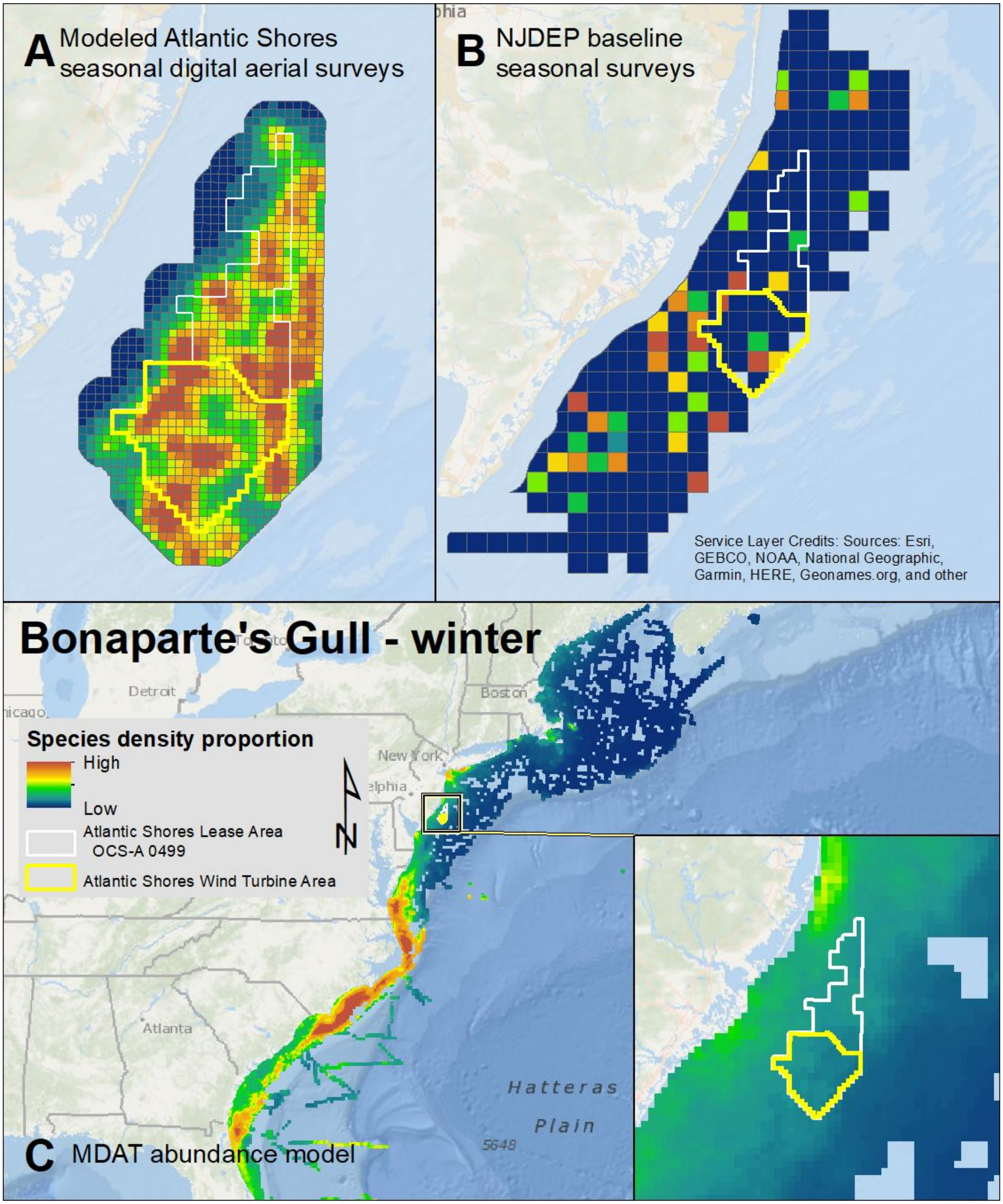

Map 99. Winter Bonaparte's Gull modeled density proportions in the Atlantic Shores seasonal digital aerial surveys (A), density proportions in the NJDEP baseline survey data (B), and the MDAT data at local and regional scales (C). The scale for all maps is representative of relative spatial variation in the sites within the season for each data source.

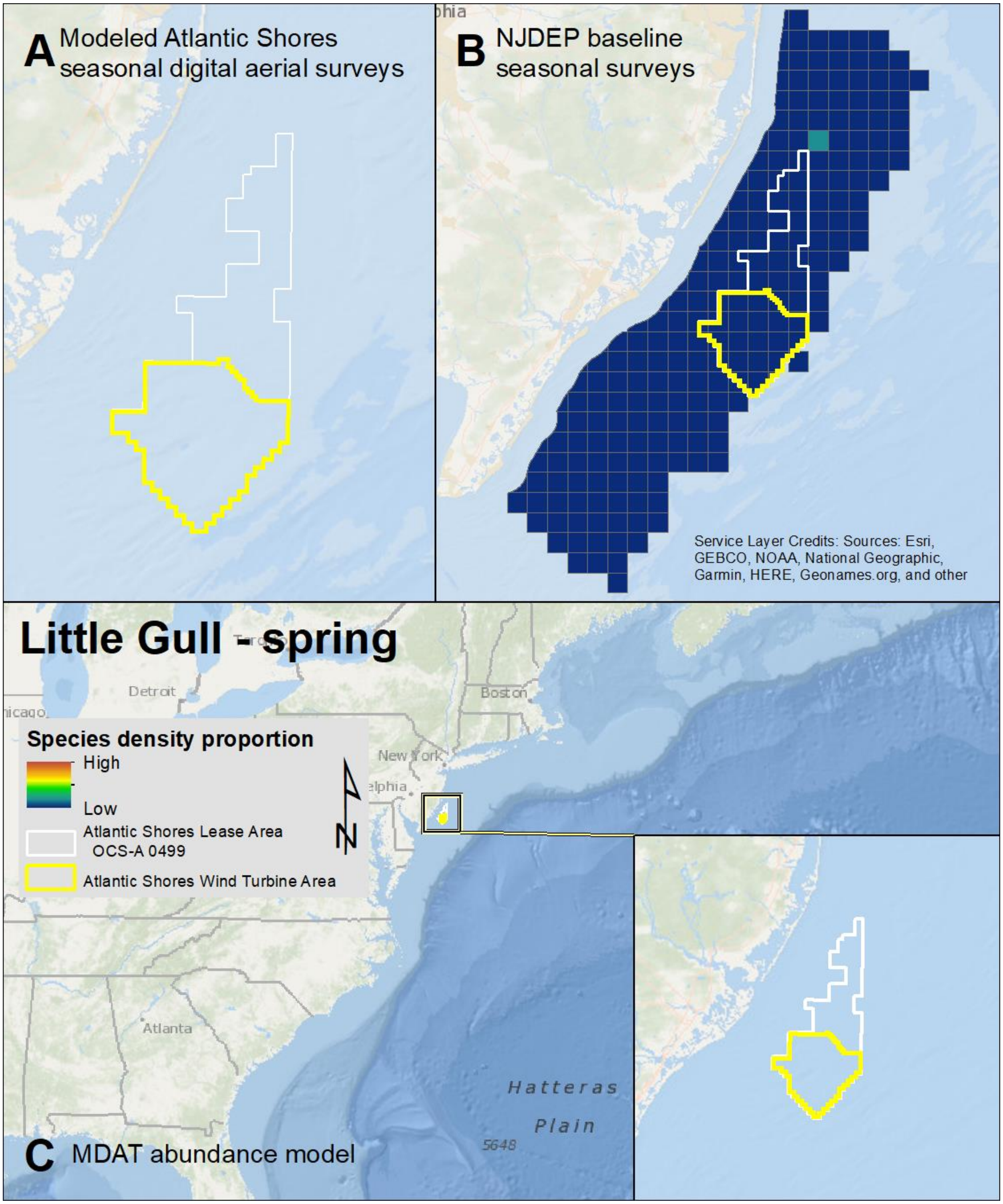

Map 100. Spring Little Gull modeled density proportions in the Atlantic Shores seasonal digital aerial surveys (A), density proportions in the NJDEP baseline survey data (B), and the MDAT data at local and regional scales (C). The scale for all maps is representative of relative spatial variation in the sites within the season for each data source.

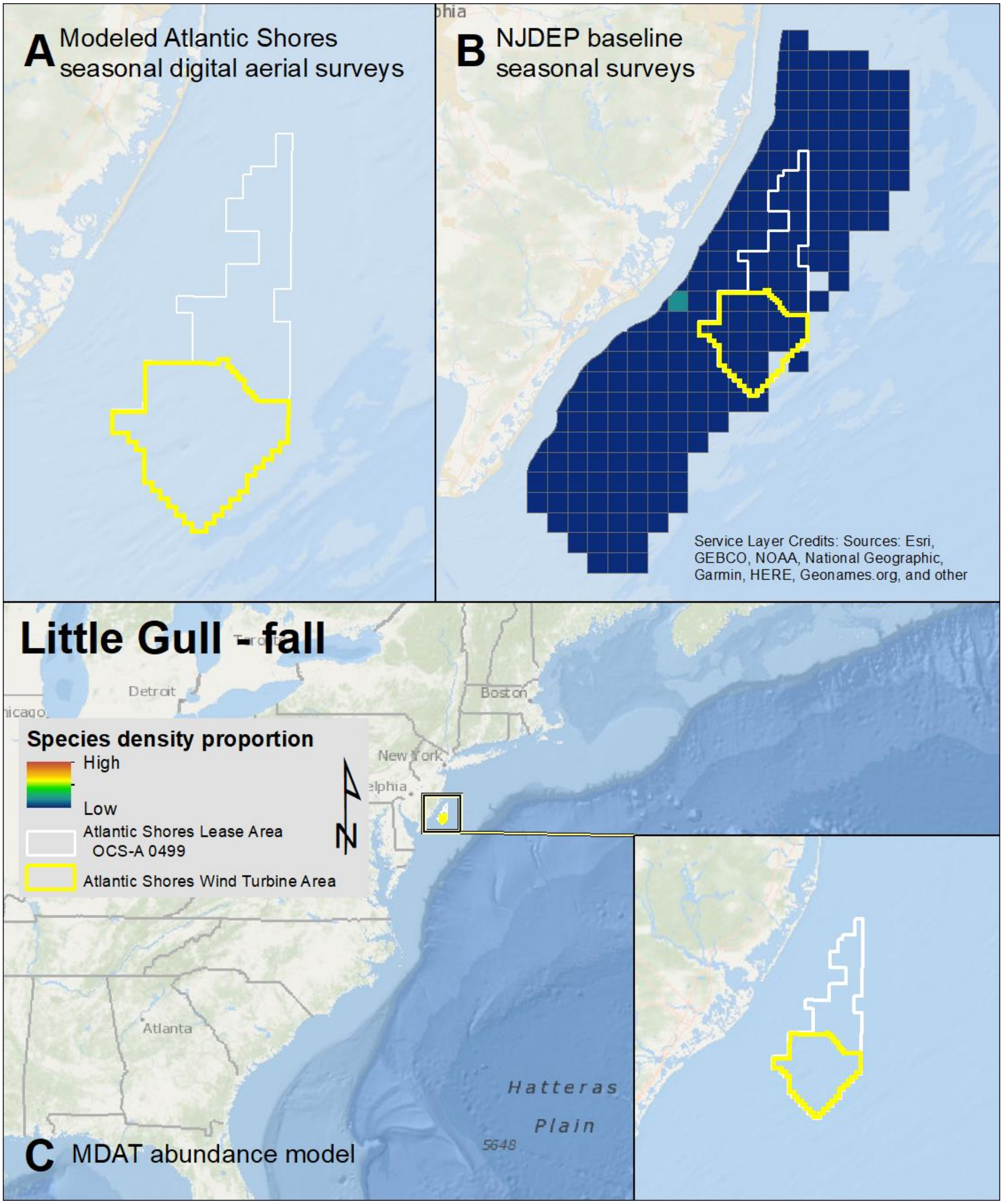

Map 101. Fall Little Gull modeled density proportions in the Atlantic Shores seasonal digital aerial surveys (A), density proportions in the NJDEP baseline survey data (B), and the MDAT data at local and regional scales (C). The scale for all maps is representative of relative spatial variation in the sites within the season for each data source.

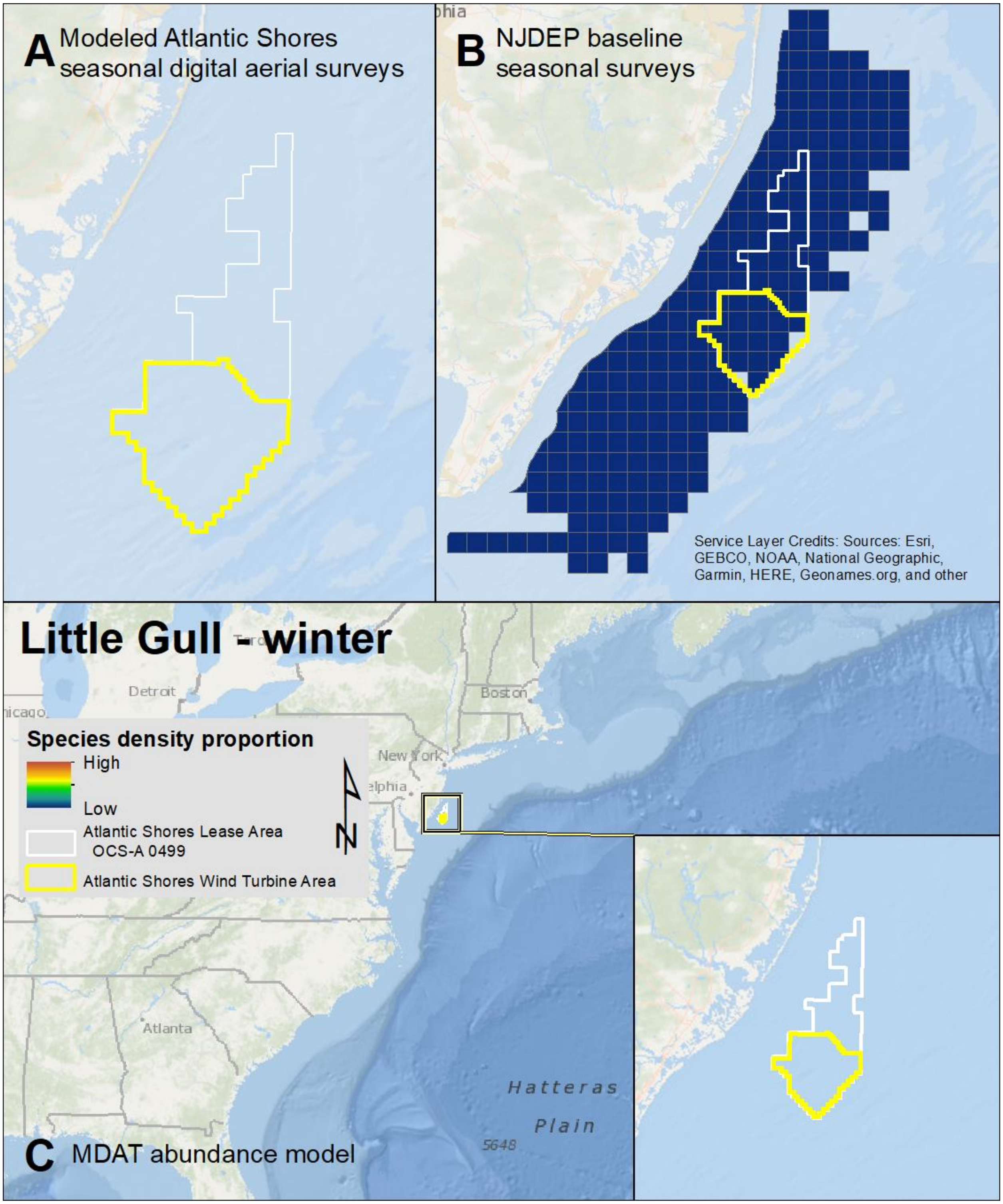

Map 102. Winter Little Gull modeled density proportions in the Atlantic Shores seasonal digital aerial surveys (A), density proportions in the NJDEP baseline survey data (B), and the MDAT data at local and regional scales (C). The scale for all maps is representative of relative spatial variation in the sites within the season for each data source.

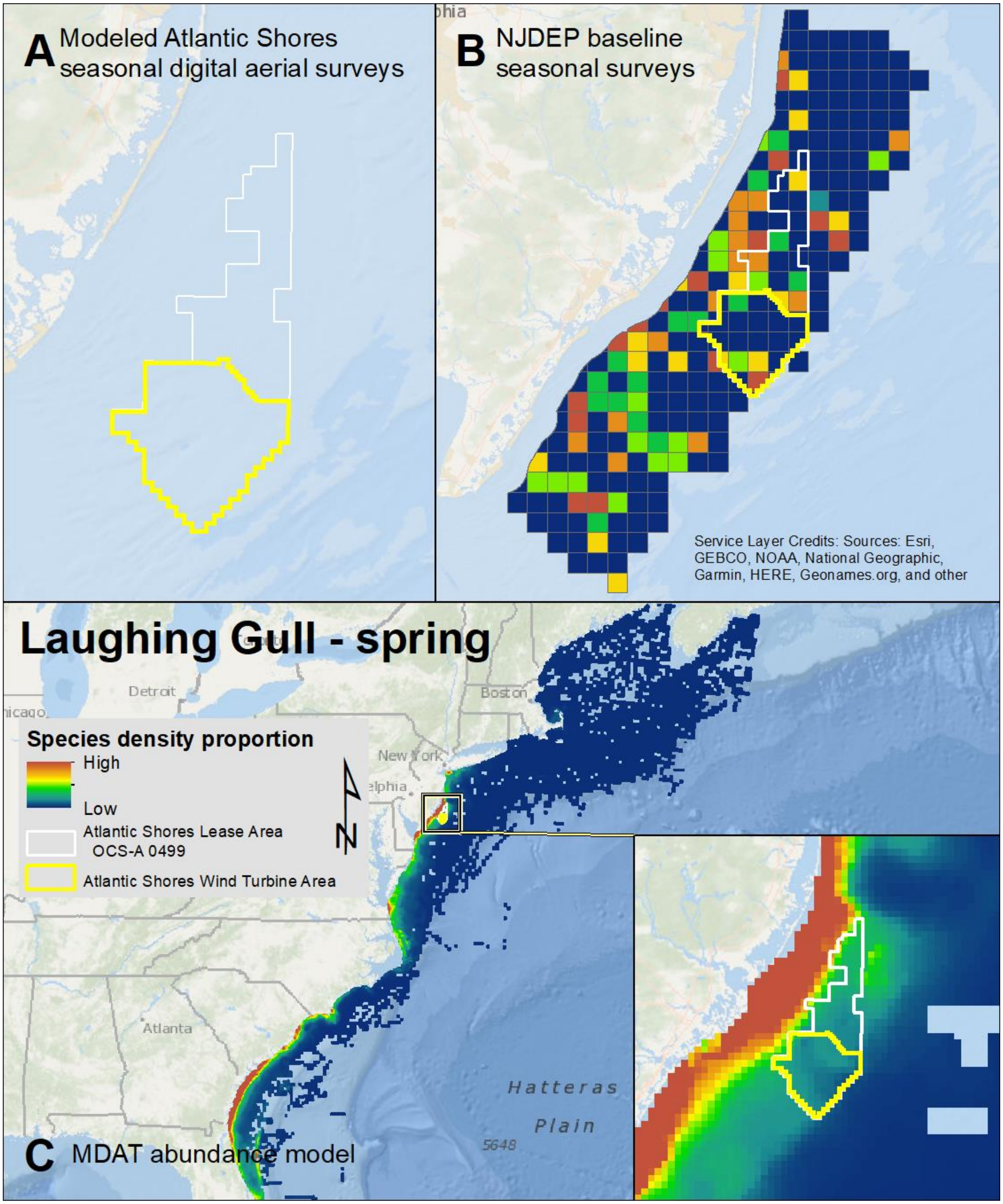

Map 103. Spring Laughing Gull modeled density proportions in the Atlantic Shores seasonal digital aerial surveys (A), density proportions in the NJDEP baseline survey data (B), and the MDAT data at local and regional scales (C). The scale for all maps is representative of relative spatial variation in the sites within the season for each data source.

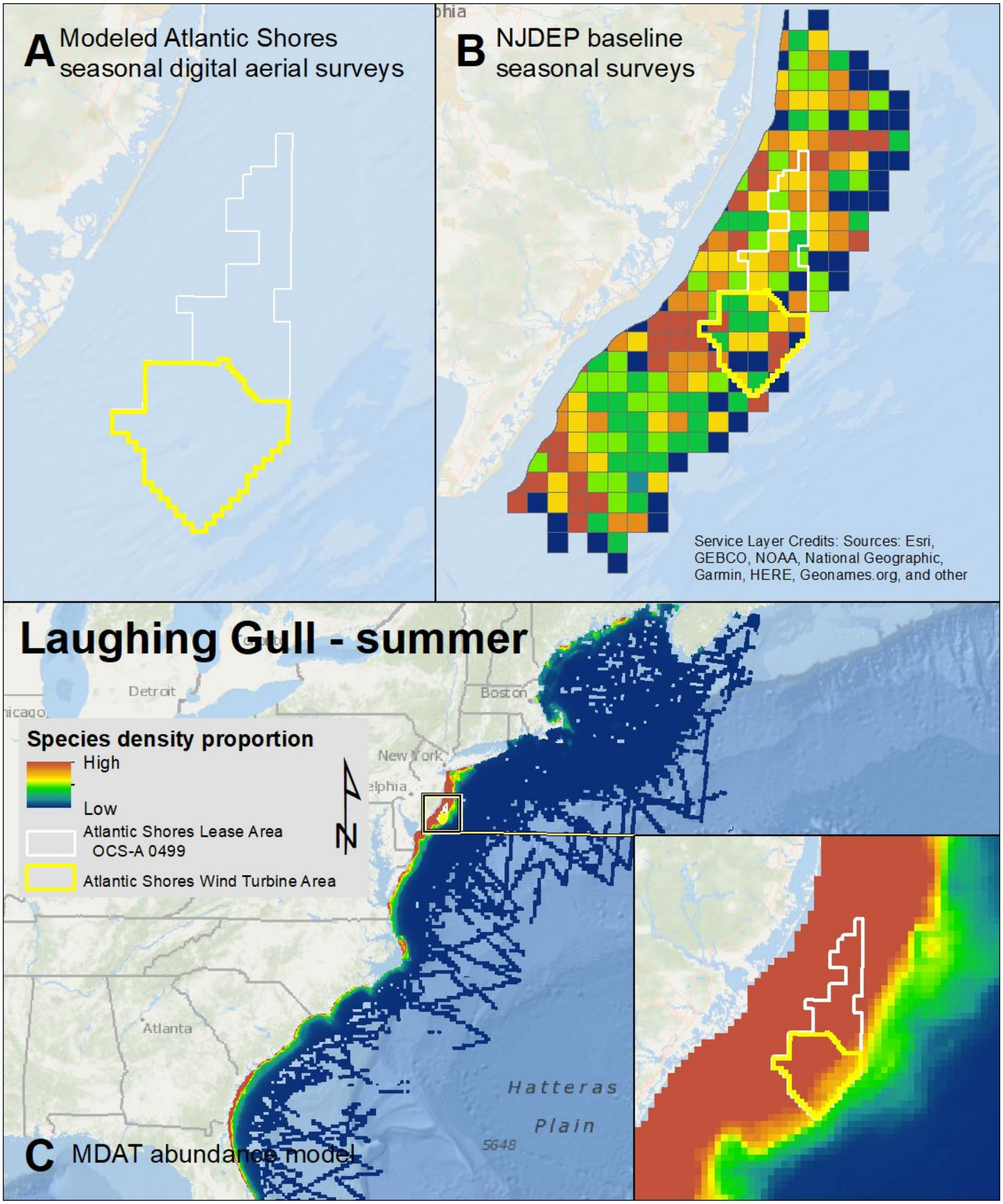

Map 104. Summer Laughing Gull modeled density proportions in the Atlantic Shores seasonal digital aerial surveys (A), density proportions in the NJDEP baseline survey data (B), and the MDAT data at local and regional scales (C). The scale for all maps is representative of relative spatial variation in the sites within the season for each data source.

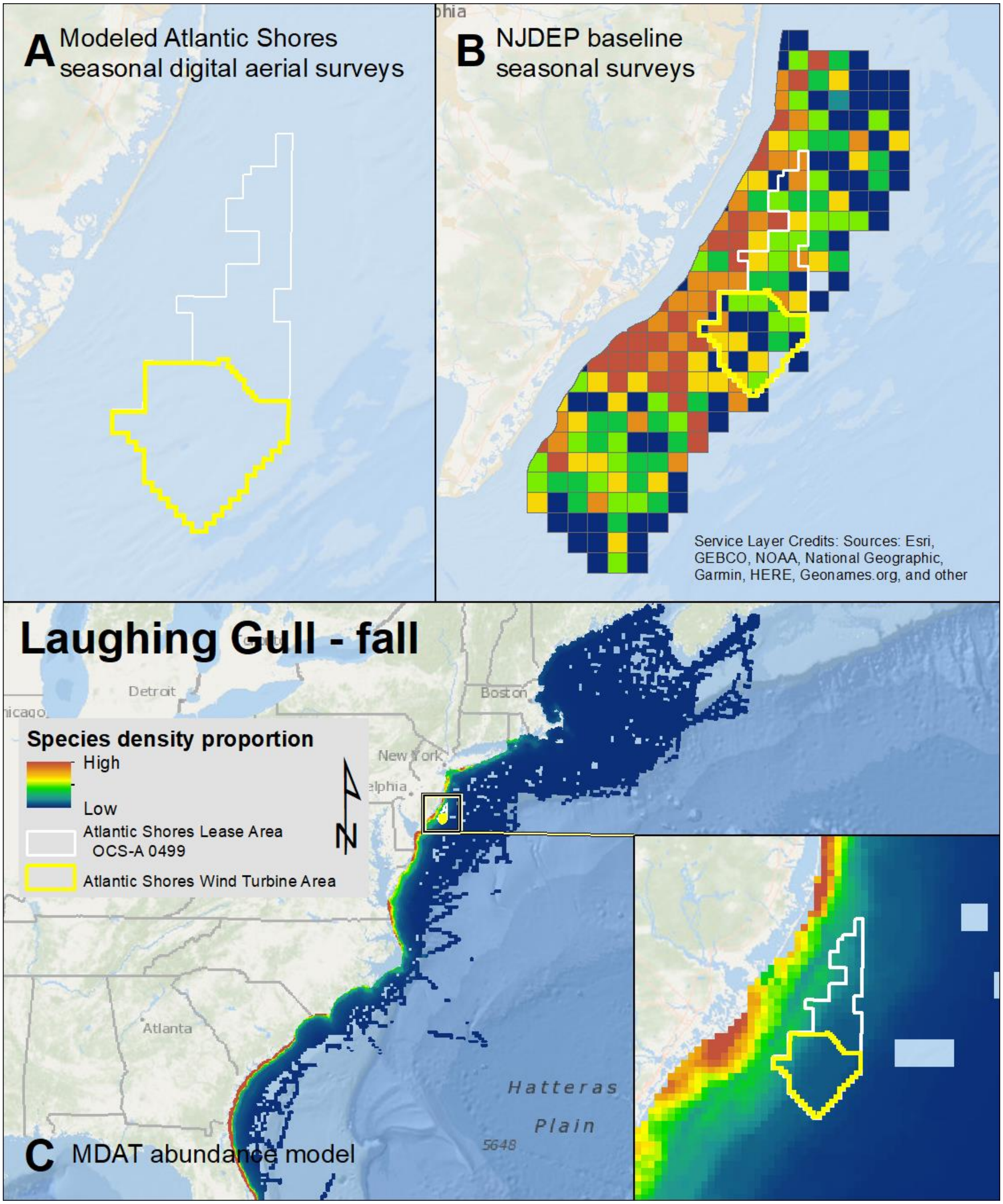

Map 105. Fall Laughing Gull modeled density proportions in the Atlantic Shores seasonal digital aerial surveys (A), density proportions in the NJDEP baseline survey data (B), and the MDAT data at local and regional scales (C). The scale for all maps is representative of relative spatial variation in the sites within the season for each data source.

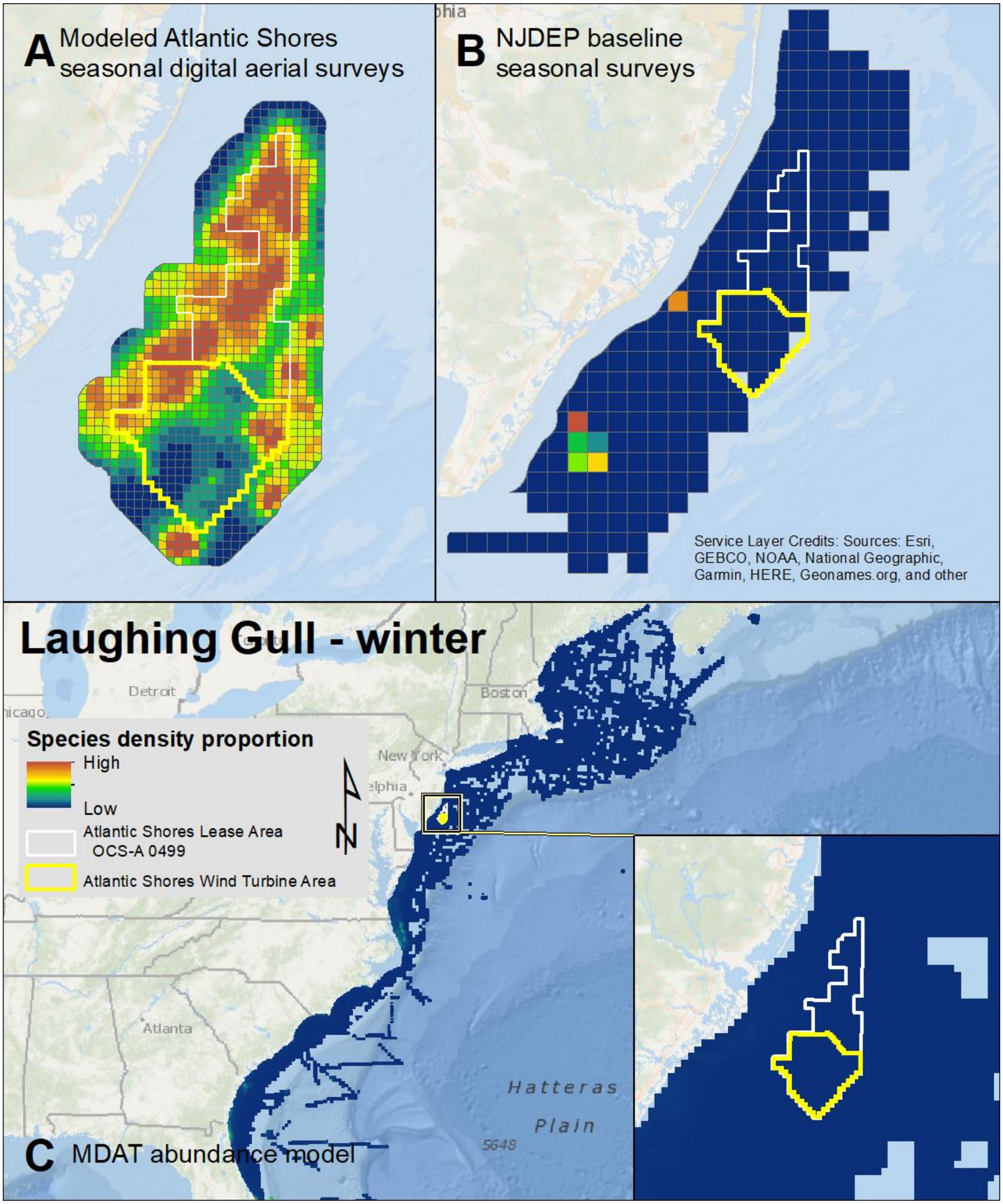

Map 106. Winter Laughing Gull modeled density proportions in the Atlantic Shores seasonal digital aerial surveys (A), density proportions in the NJDEP baseline survey data (B), and the MDAT data at local and regional scales (C). The scale for all maps is representative of relative spatial variation in the sites within the season for each data source.

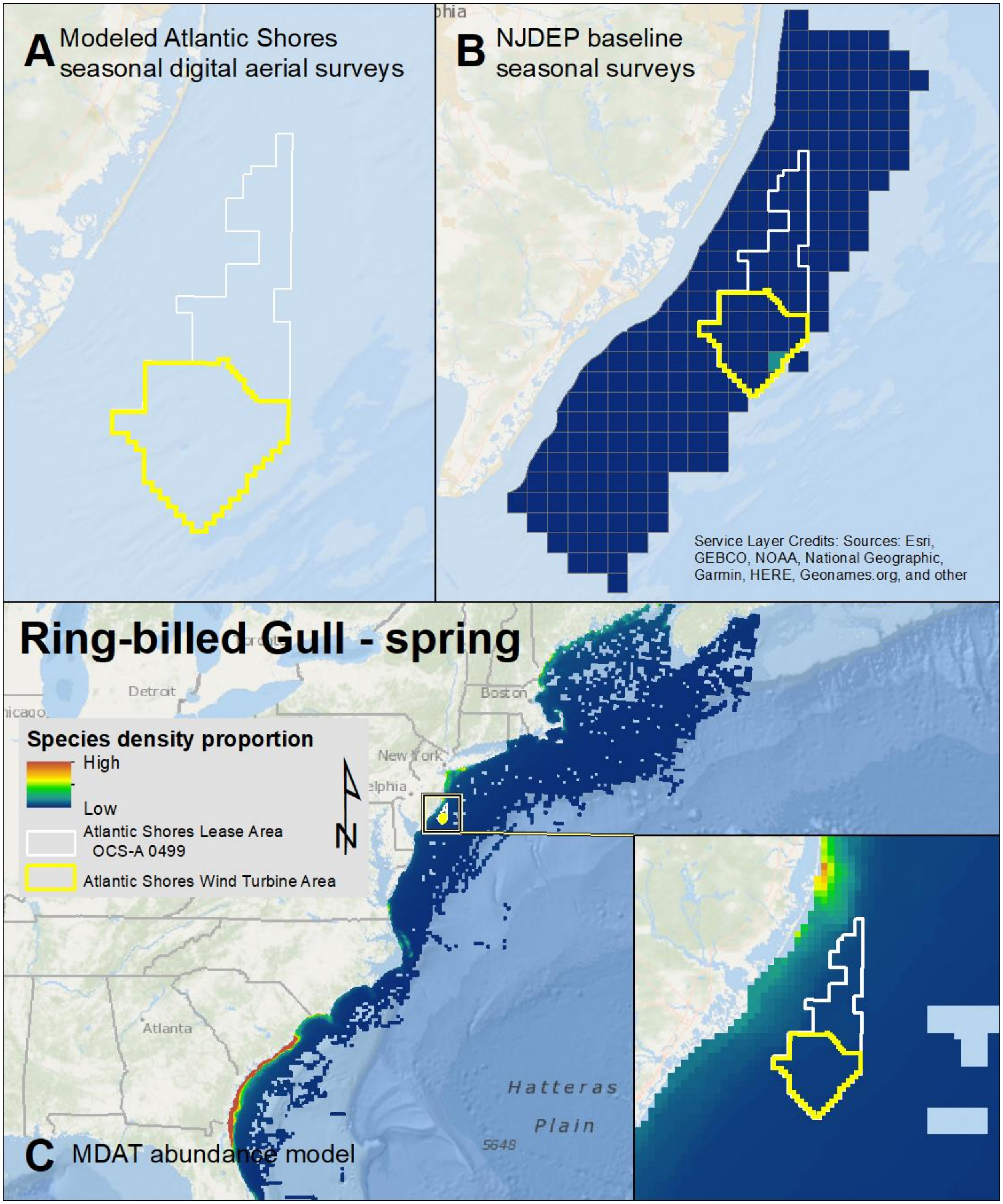

Map 107. Spring Ring-billed Gull modeled density proportions in the Atlantic Shores seasonal digital aerial surveys (A), density proportions in the NJDEP baseline survey data (B), and the MDAT data at local and regional scales (C). The scale for all maps is representative of relative spatial variation in the sites within the season for each data source.

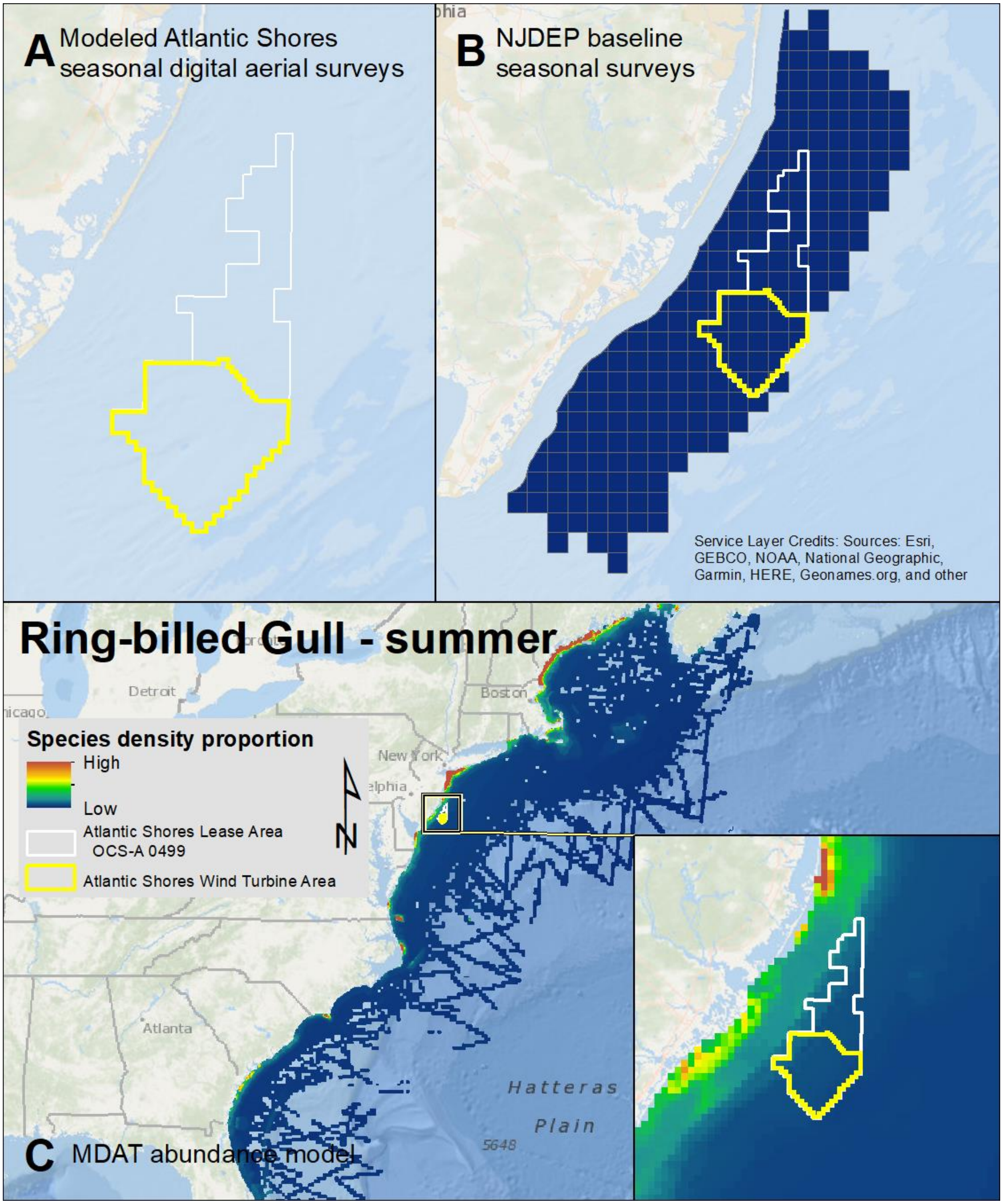

Map 108. Summer Ring-billed Gull modeled density proportions in the Atlantic Shores seasonal digital aerial surveys (A), density proportions in the NJDEP baseline survey data (B), and the MDAT data at local and regional scales (C). The scale for all maps is representative of relative spatial variation in the sites within the season for each data source.

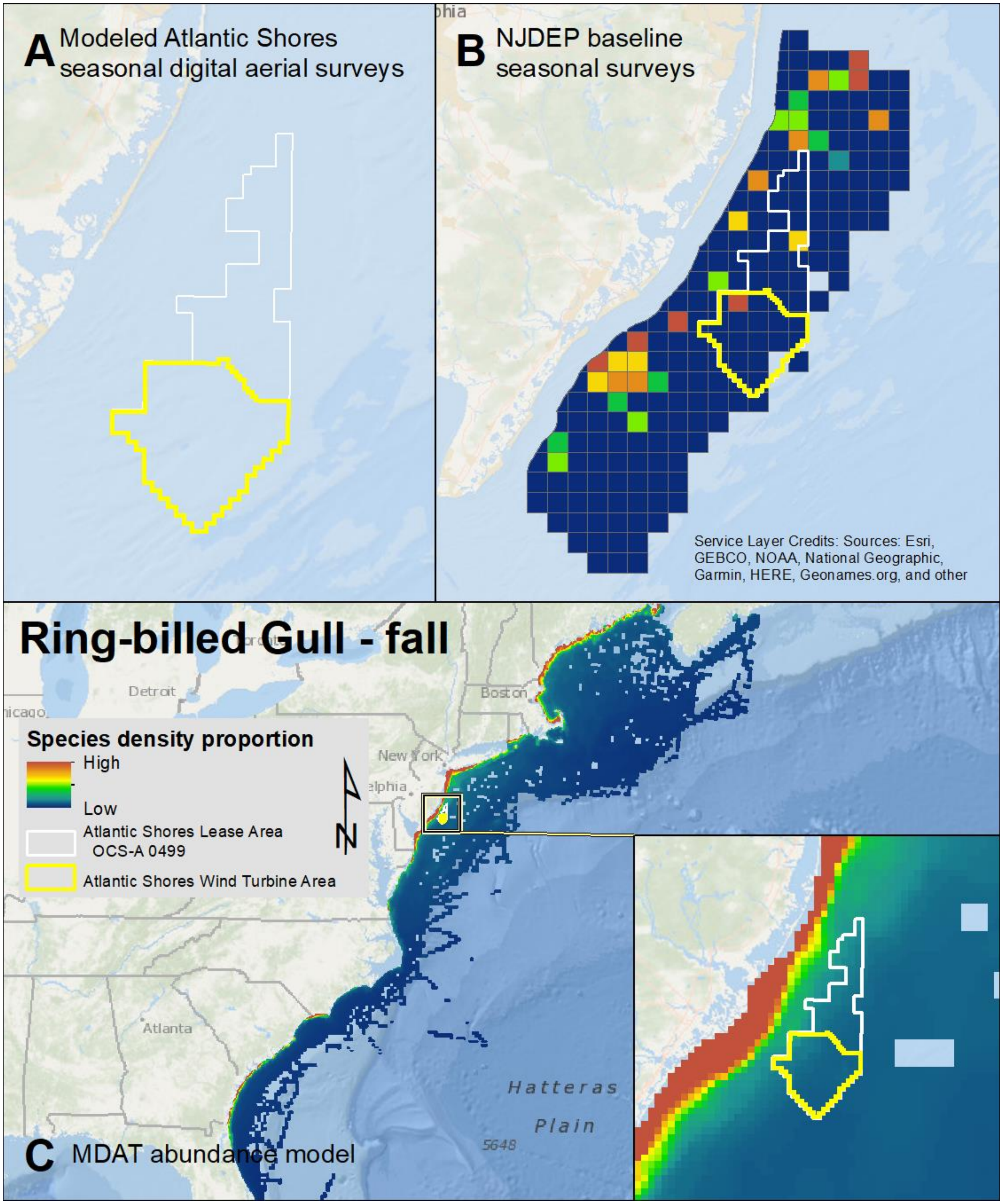

Map 109. Fall Ring-billed Gull modeled density proportions in the Atlantic Shores seasonal digital aerial surveys (A), density proportions in the NJDEP baseline survey data (B), and the MDAT data at local and regional scales (C). The scale for all maps is representative of relative spatial variation in the sites within the season for each data source.

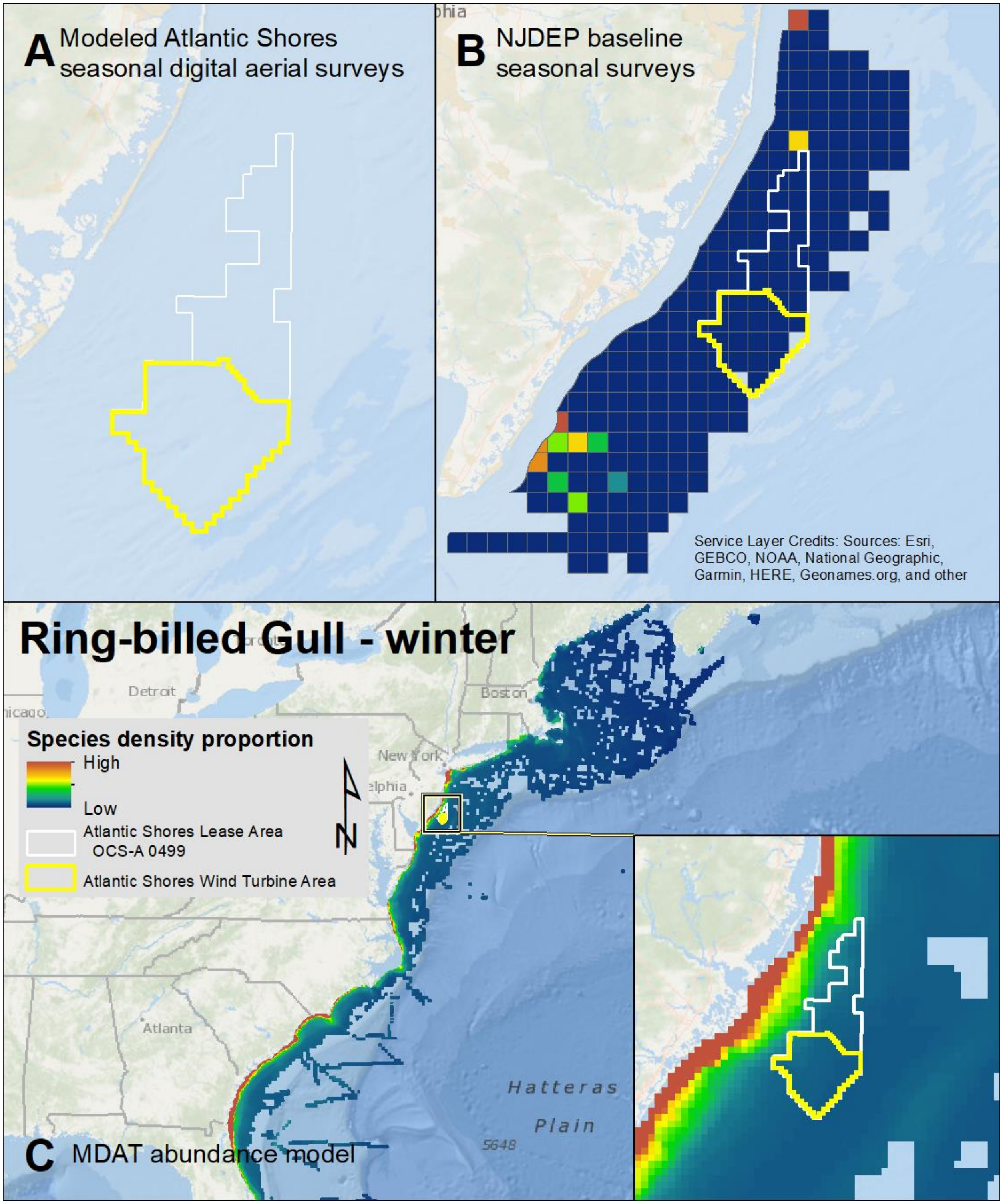

Map 110. Winter Ring-billed Gull modeled density proportions in the Atlantic Shores seasonal digital aerial surveys (A), density proportions in the NJDEP baseline survey data (B), and the MDAT data at local and regional scales (C). The scale for all maps is representative of relative spatial variation in the sites within the season for each data source.

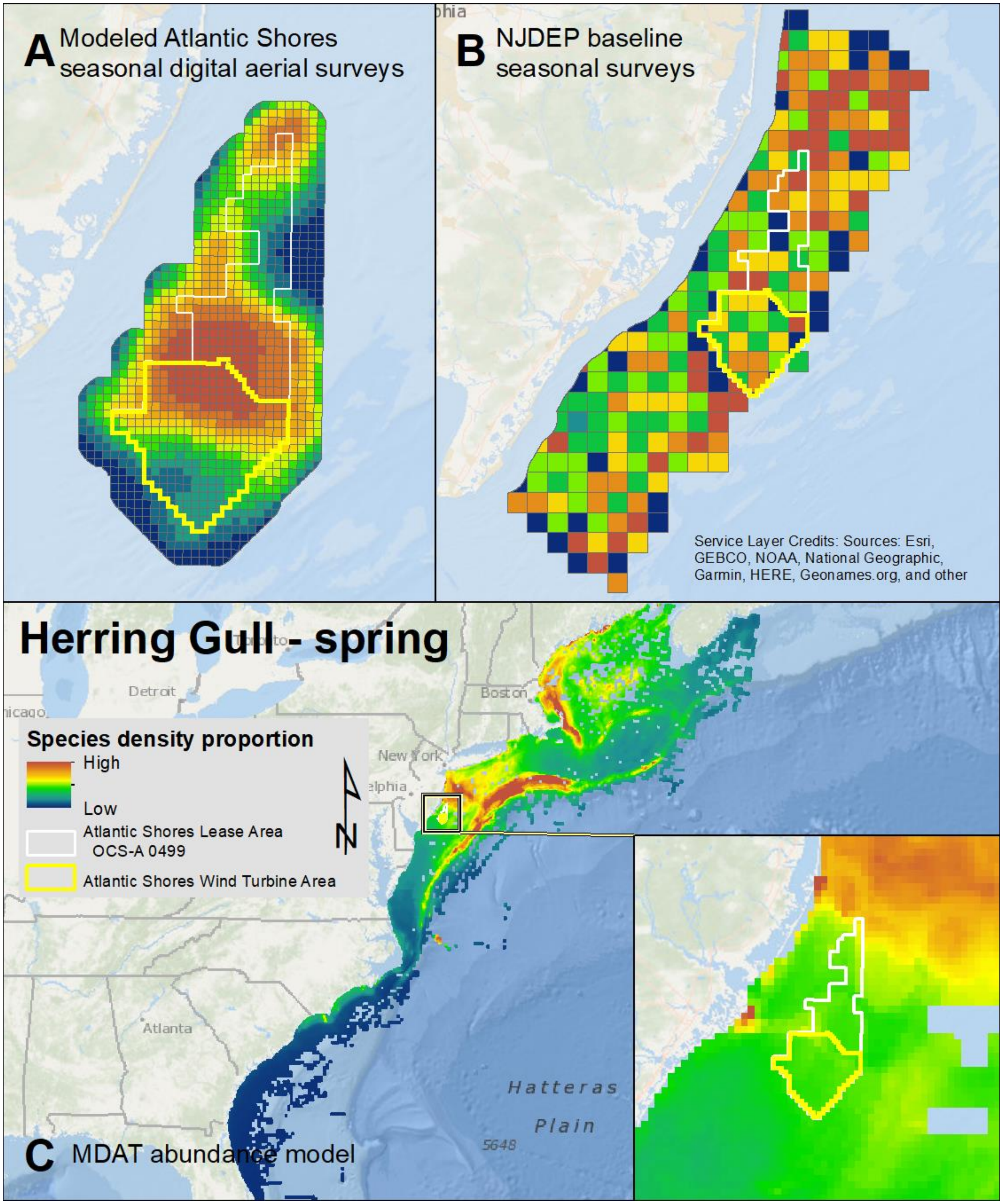

Map 111. Spring Herring Gull modeled density proportions in the Atlantic Shores seasonal digital aerial surveys (A), density proportions in the NJDEP baseline survey data (B), and the MDAT data at local and regional scales (C). The scale for all maps is representative of relative spatial variation in the sites within the season for each data source.

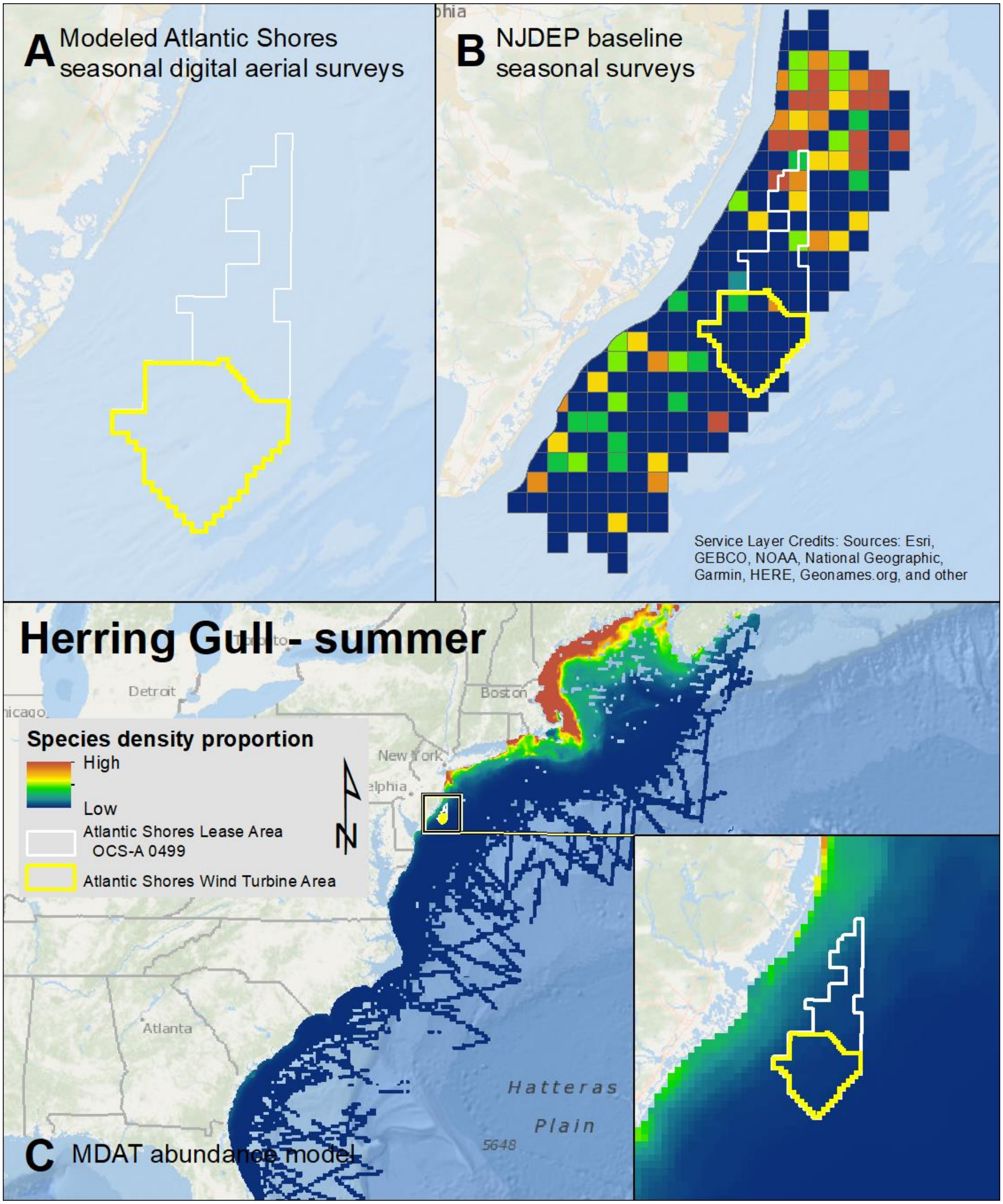

Map 112. Summer Herring Gull modeled density proportions in the Atlantic Shores seasonal digital aerial surveys (A), density proportions in the NJDEP baseline survey data (B), and the MDAT data at local and regional scales (C). The scale for all maps is representative of relative spatial variation in the sites within the season for each data source.

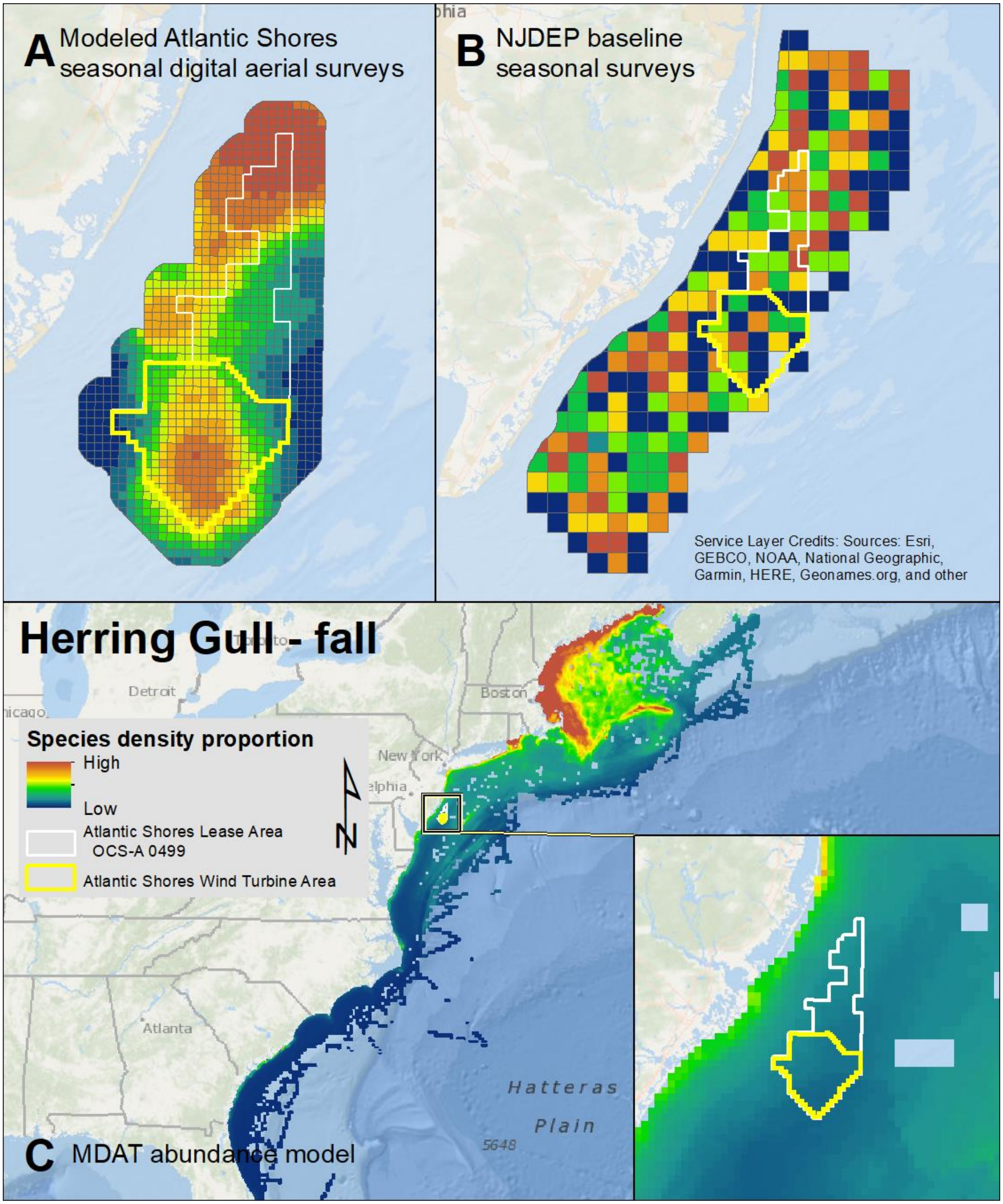

Map 113. Fall Herring Gull modeled density proportions in the Atlantic Shores seasonal digital aerial surveys (A), density proportions in the NJDEP baseline survey data (B), and the MDAT data at local and regional scales (C). The scale for all maps is representative of relative spatial variation in the sites within the season for each data source.

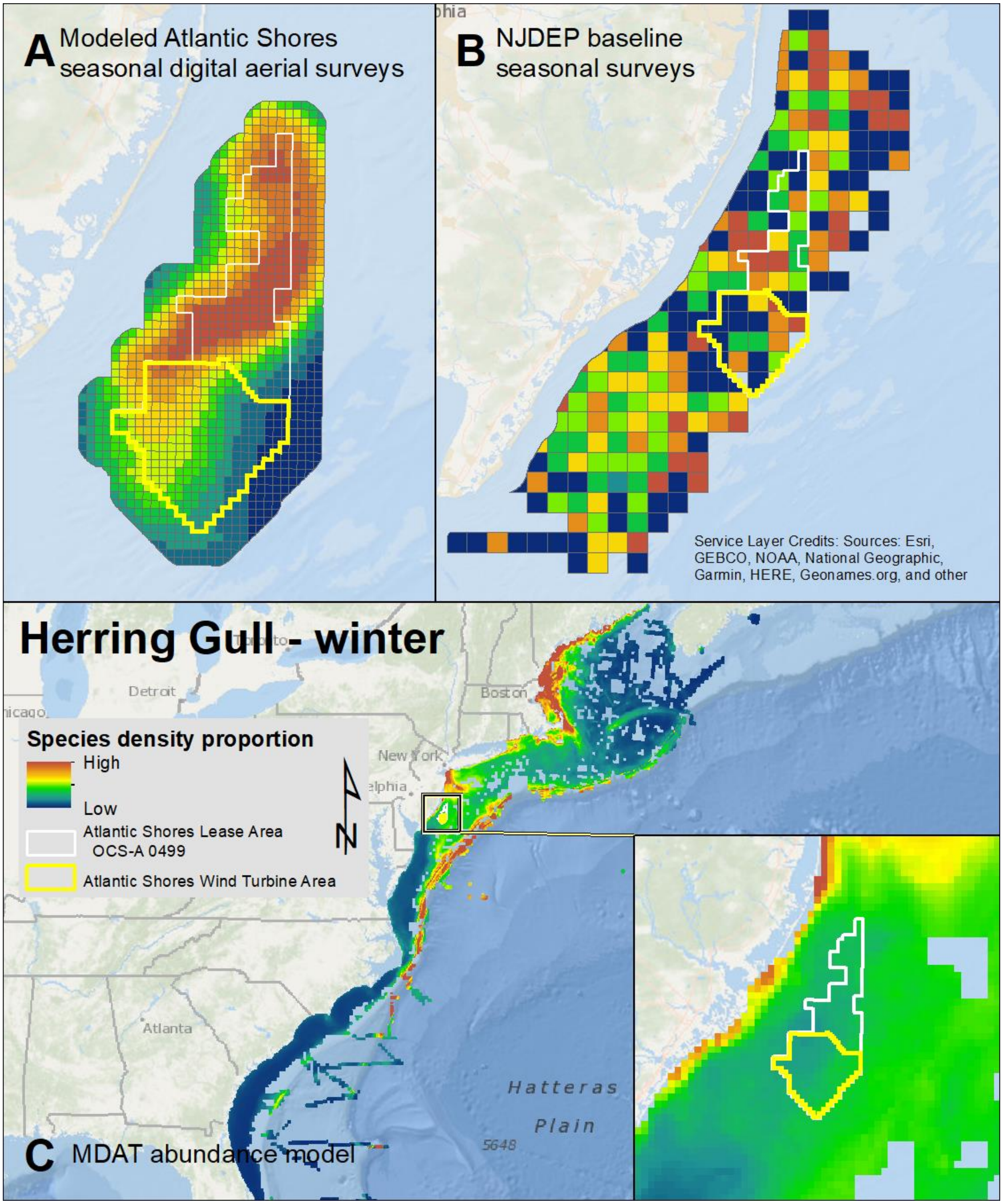

Map 114. Winter Herring Gull modeled density proportions in the Atlantic Shores seasonal digital aerial surveys (A), density proportions in the NJDEP baseline survey data (B), and the MDAT data at local and regional scales (C). The scale for all maps is representative of relative spatial variation in the sites within the season for each data source.

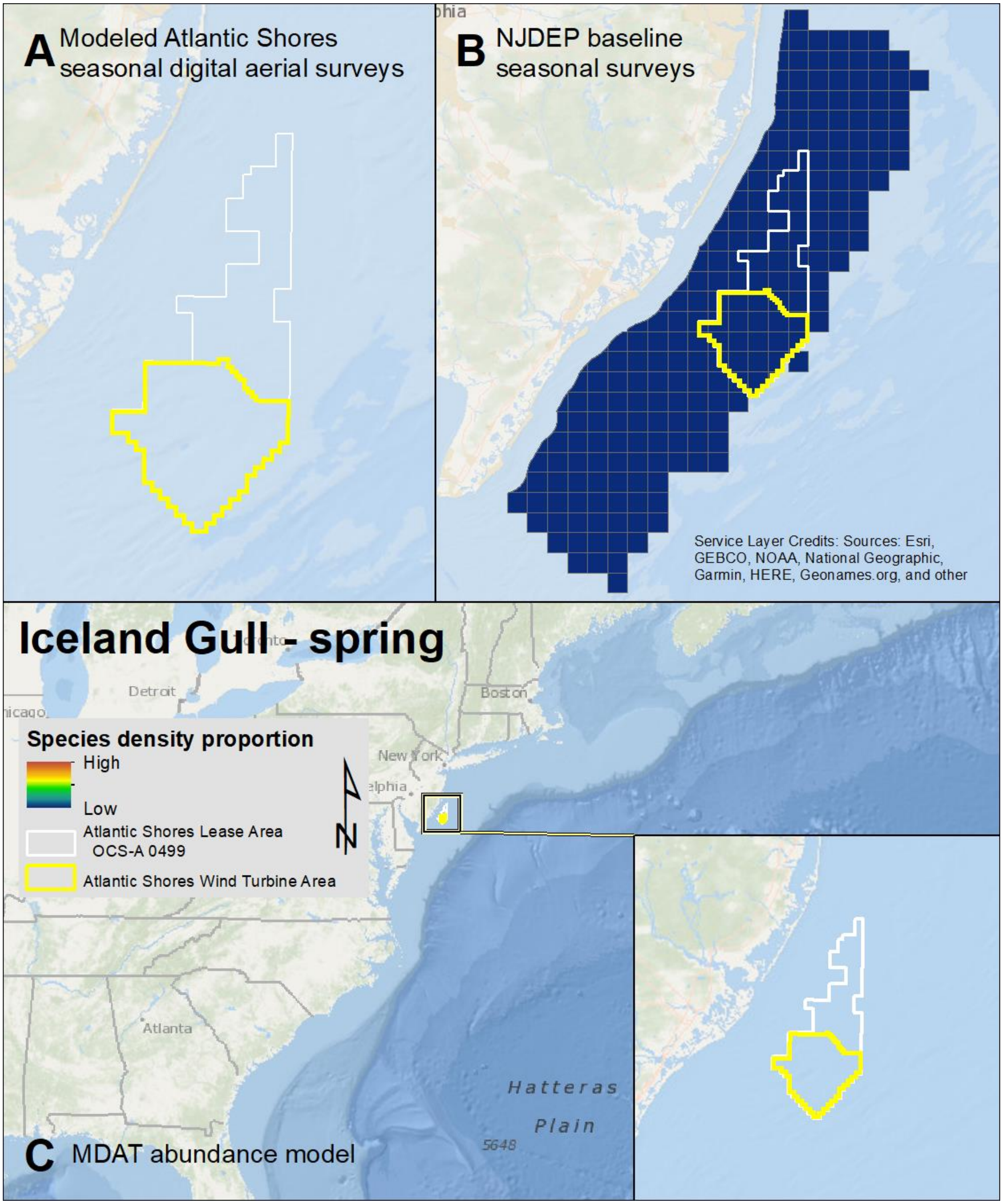

Map 115. Spring Iceland Gull modeled density proportions in the Atlantic Shores seasonal digital aerial surveys (A), density proportions in the NJDEP baseline survey data (B), and the MDAT data at local and regional scales (C). The scale for all maps is representative of relative spatial variation in the sites within the season for each data source.

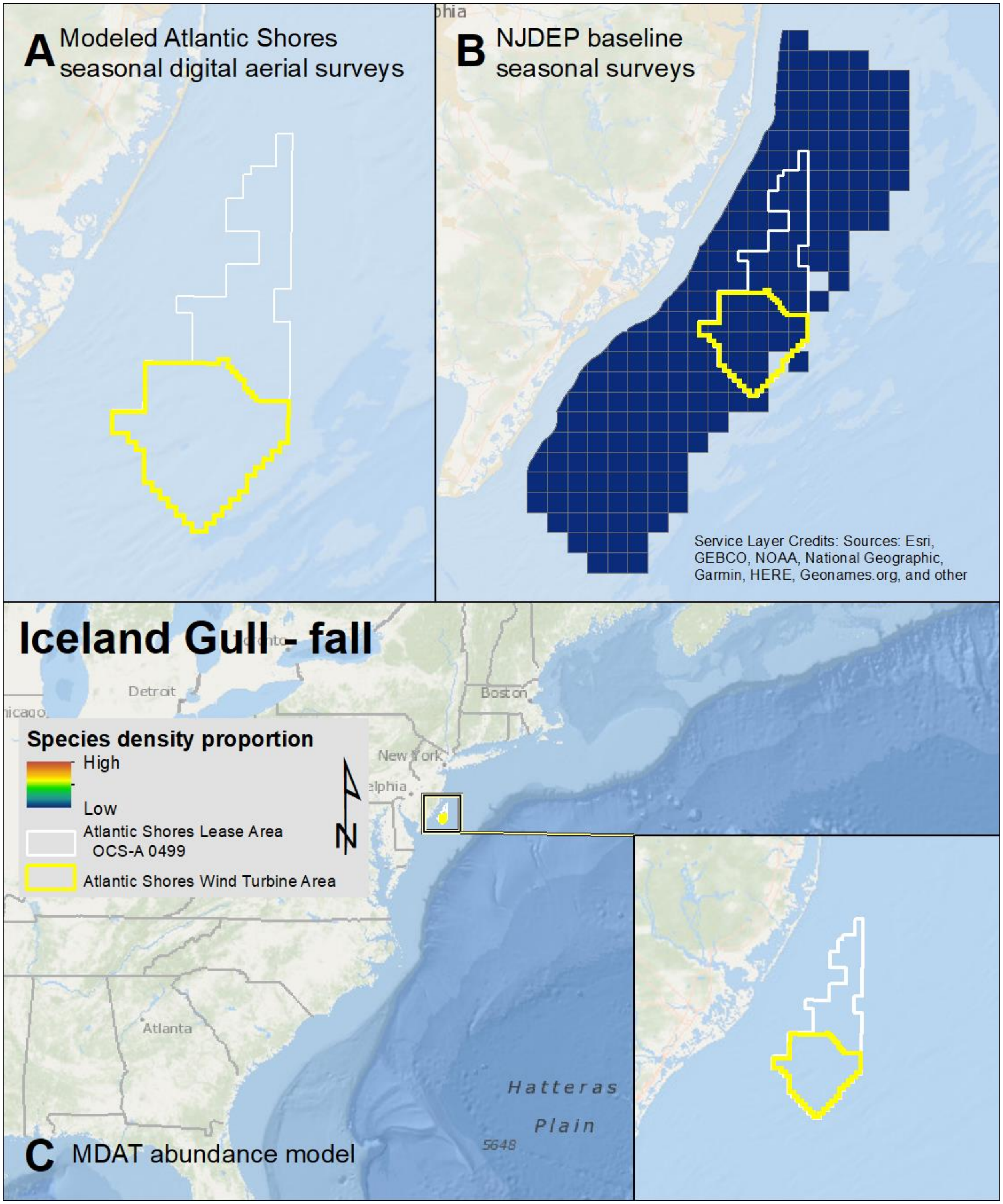

Map 116. Fall Iceland Gull modeled density proportions in the Atlantic Shores seasonal digital aerial surveys (A), density proportions in the NJDEP baseline survey data (B), and the MDAT data at local and regional scales (C). The scale for all maps is representative of relative spatial variation in the sites within the season for each data source.

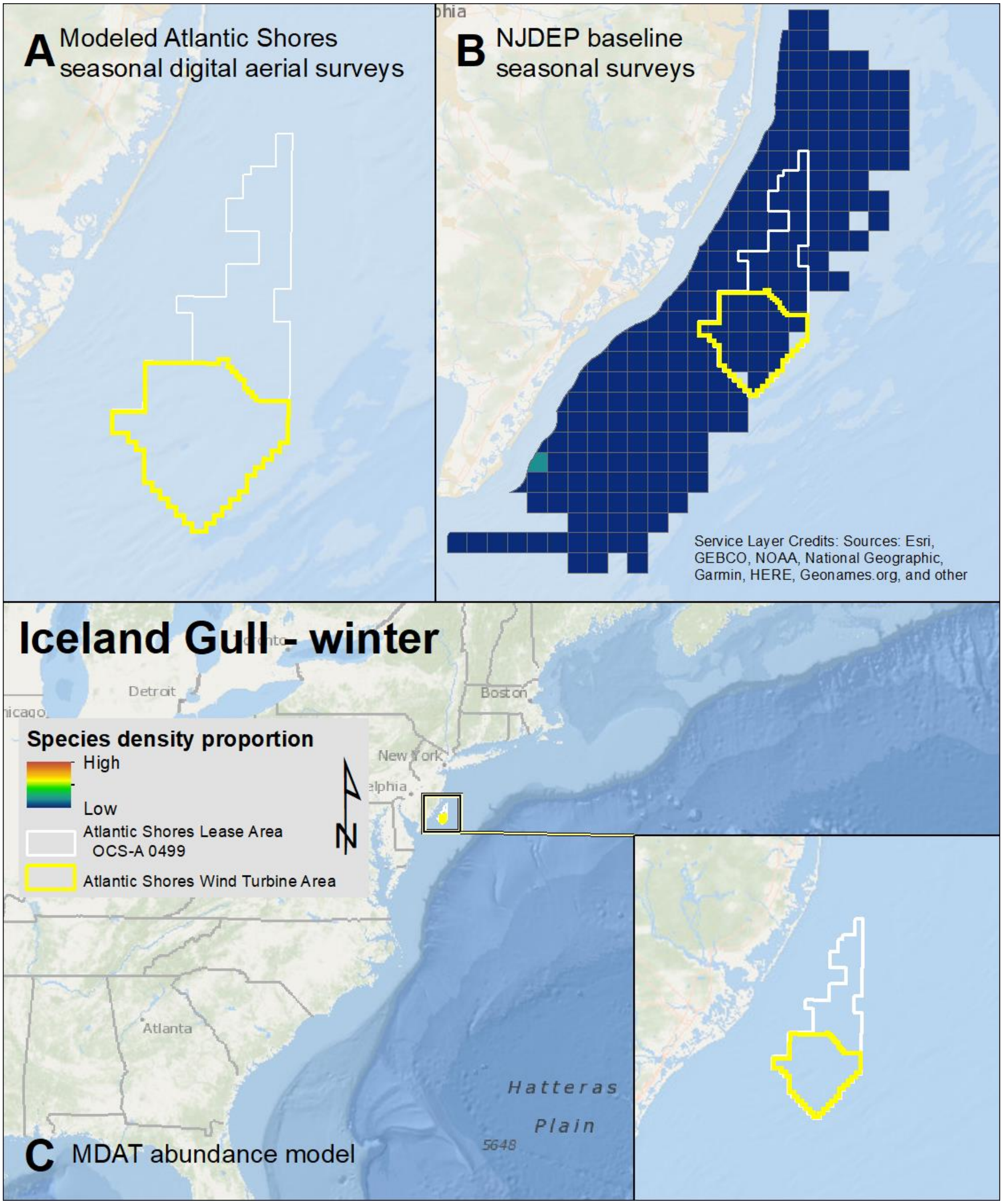

Map 117. Winter Iceland Gull modeled density proportions in the Atlantic Shores seasonal digital aerial surveys (A), density proportions in the NJDEP baseline survey data (B), and the MDAT data at local and regional scales (C). The scale for all maps is representative of relative spatial variation in the sites within the season for each data source.

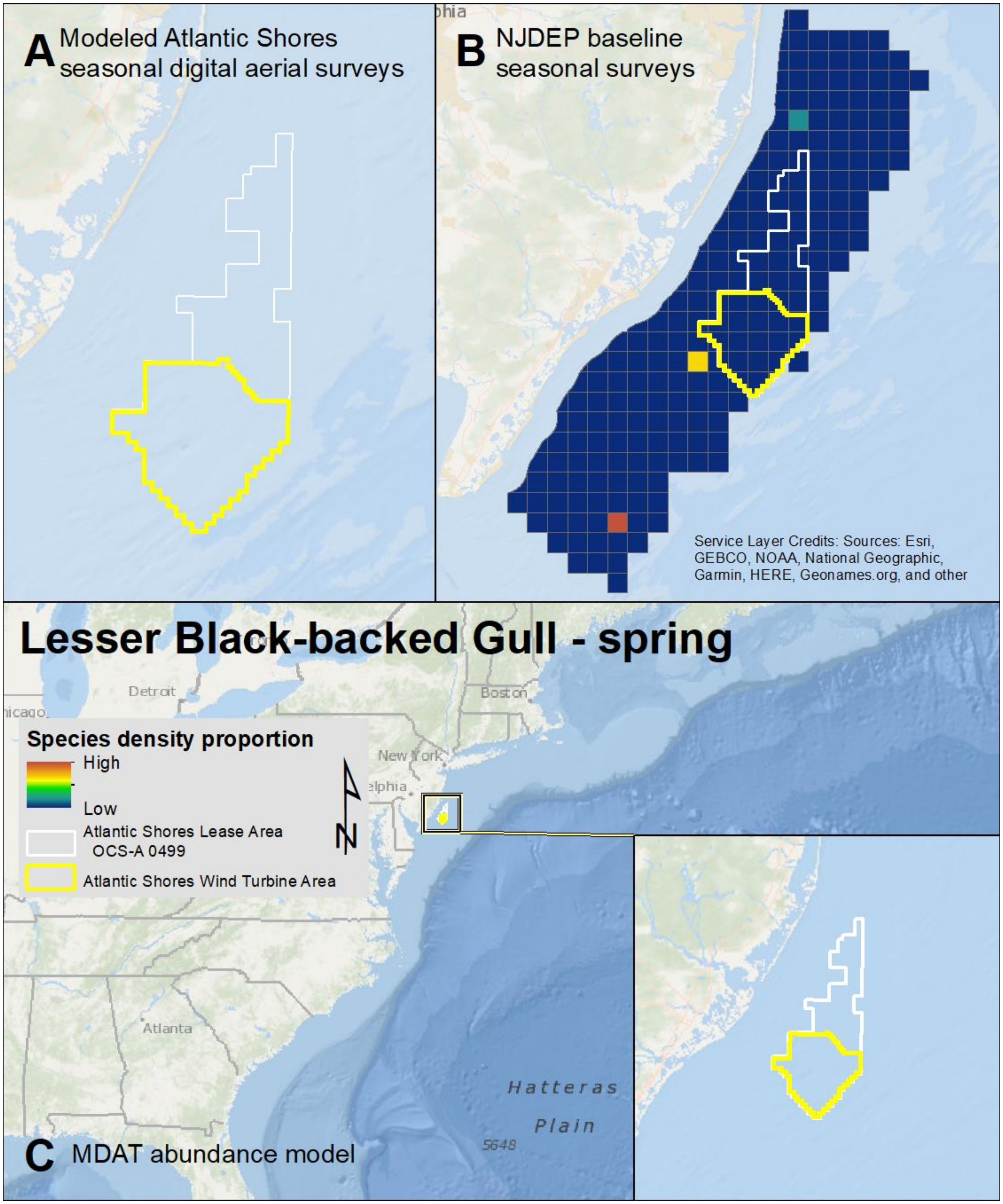

Map 118. Spring Lesser Black-backed Gull modeled density proportions in the Atlantic Shores seasonal digital aerial surveys (A), density proportions in the NJDEP baseline survey data (B), and the MDAT data at local and regional scales (C). The scale for all maps is representative of relative spatial variation in the sites within the season for each data source.

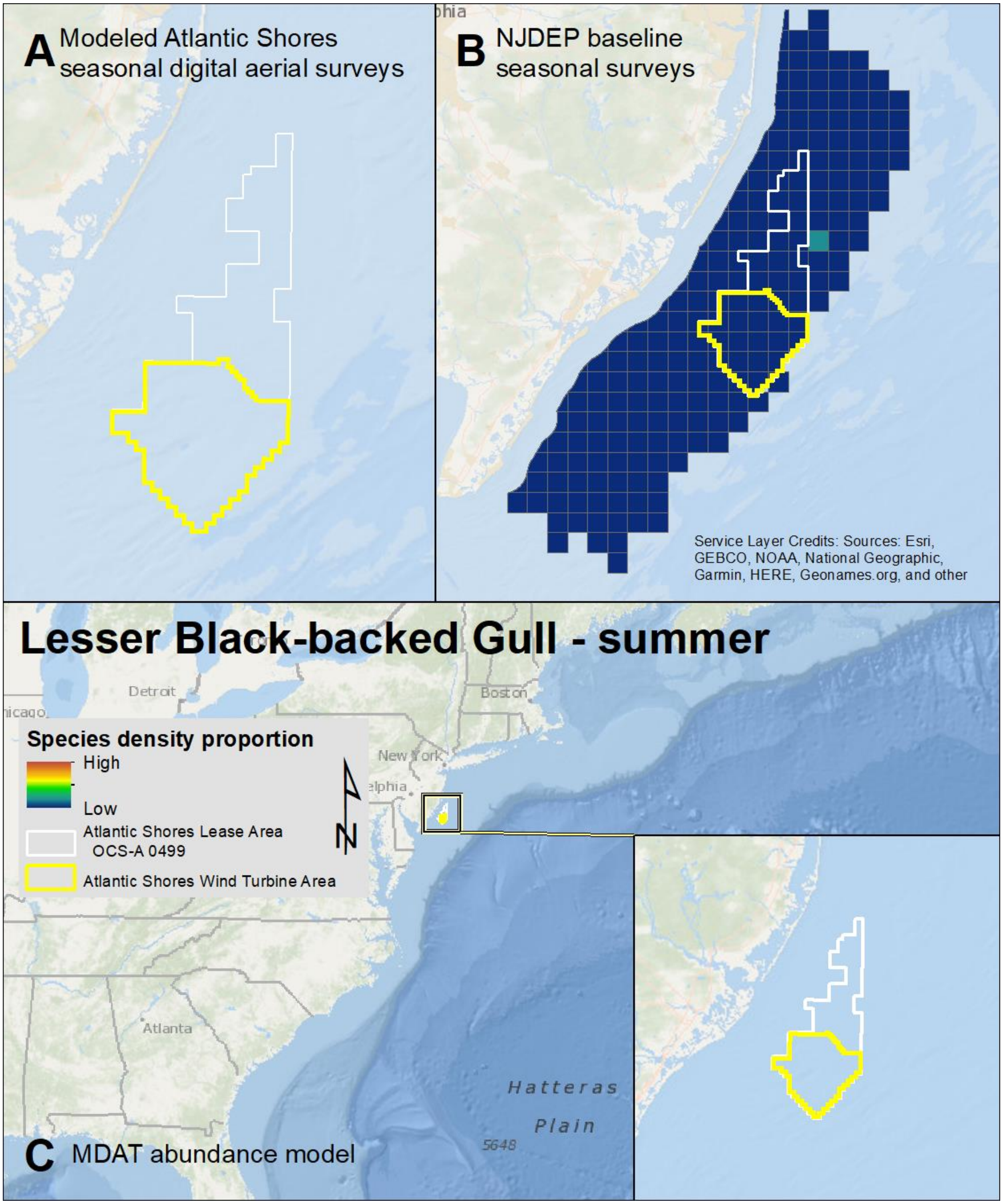

Map 119. Summer Lesser Black-backed Gull modeled density proportions in the Atlantic Shores seasonal digital aerial surveys (A), density proportions in the NJDEP baseline survey data (B), and the MDAT data at local and regional scales (C). The scale for all maps is representative of relative spatial variation in the sites within the season for each data source.

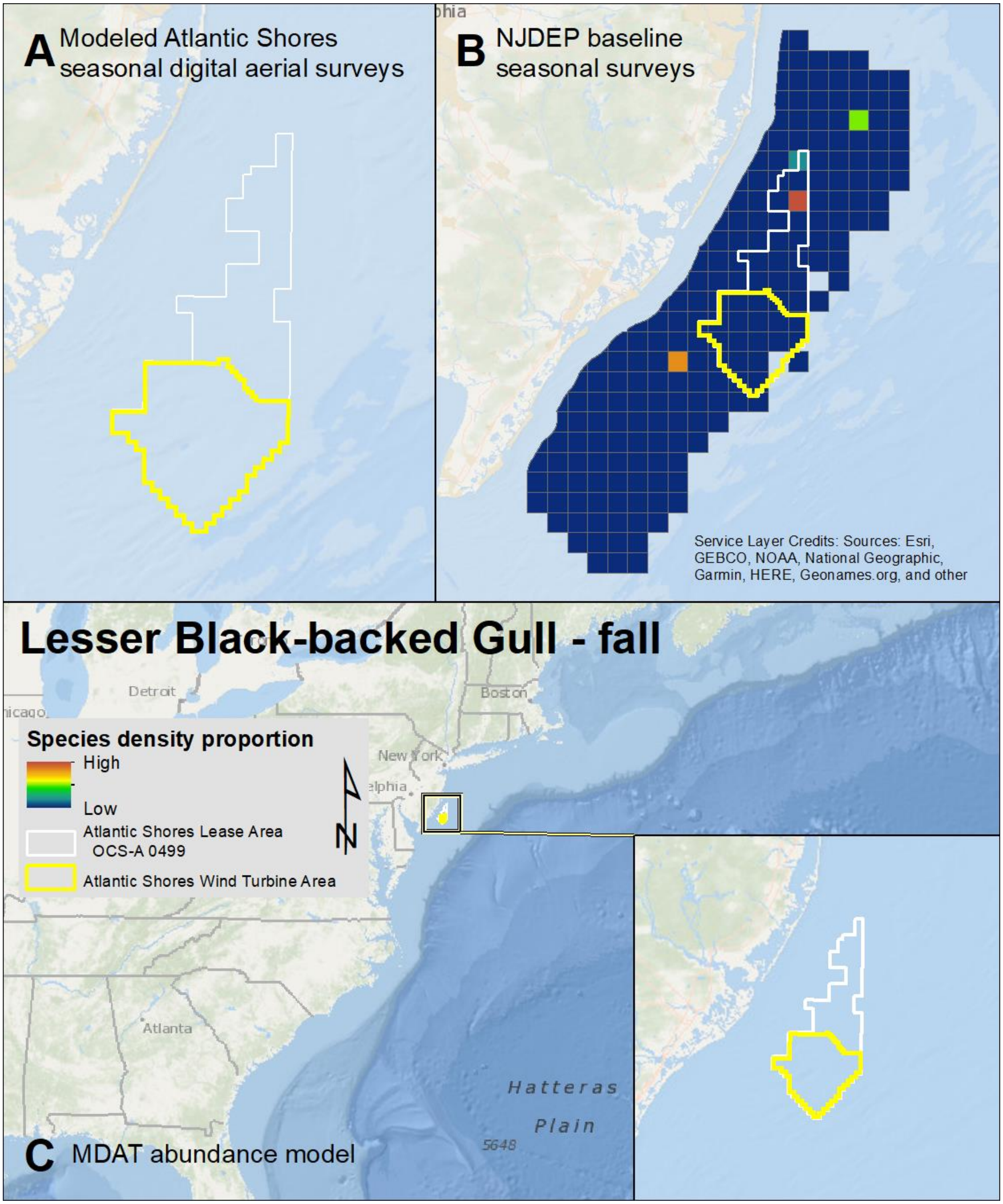

Map 120. Fall Lesser Black-backed Gull modeled density proportions in the Atlantic Shores seasonal digital aerial surveys (A), density proportions in the NJDEP baseline survey data (B), and the MDAT data at local and regional scales (C). The scale for all maps is representative of relative spatial variation in the sites within the season for each data source.

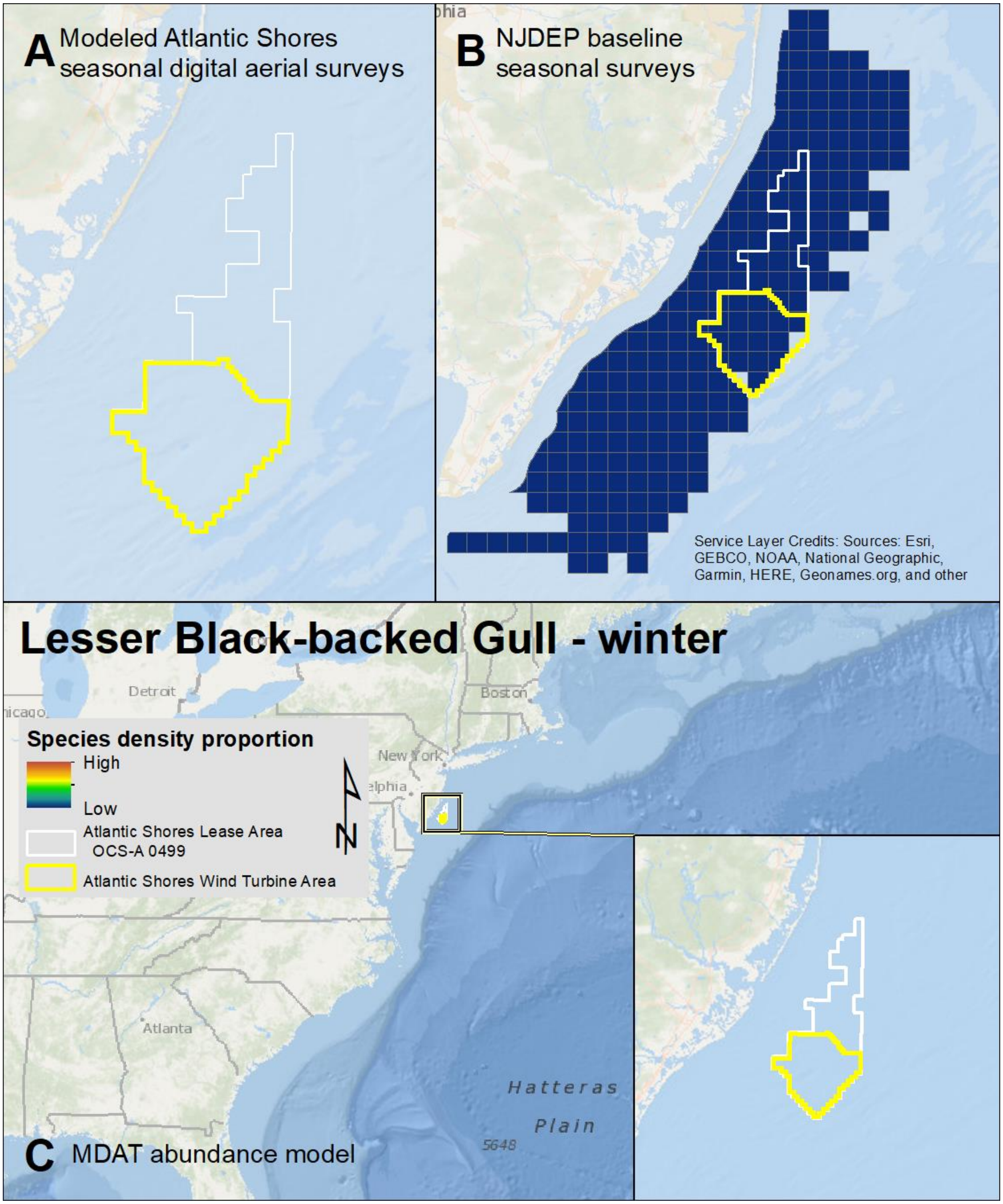

Map 121. Winter Lesser Black-backed Gull modeled density proportions in the Atlantic Shores seasonal digital aerial surveys (A), density proportions in the NJDEP baseline survey data (B), and the MDAT data at local and regional scales (C). The scale for all maps is representative of relative spatial variation in the sites within the season for each data source.

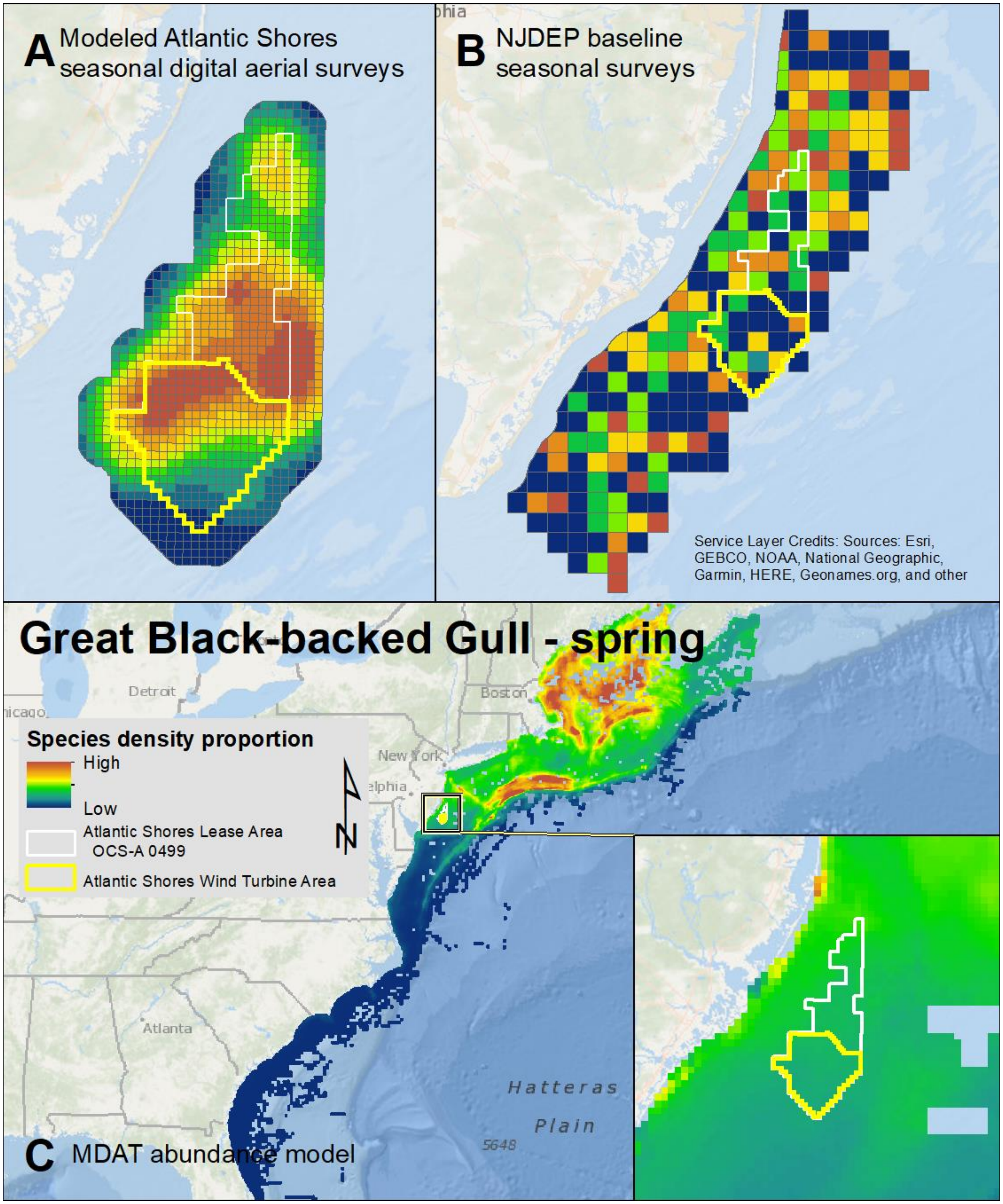

Map 122. Spring Great Black-backed Gull modeled density proportions in the Atlantic Shores seasonal digital aerial surveys (A), density proportions in the NJDEP baseline survey data (B), and the MDAT data at local and regional scales (C). The scale for all maps is representative of relative spatial variation in the sites within the season for each data source.

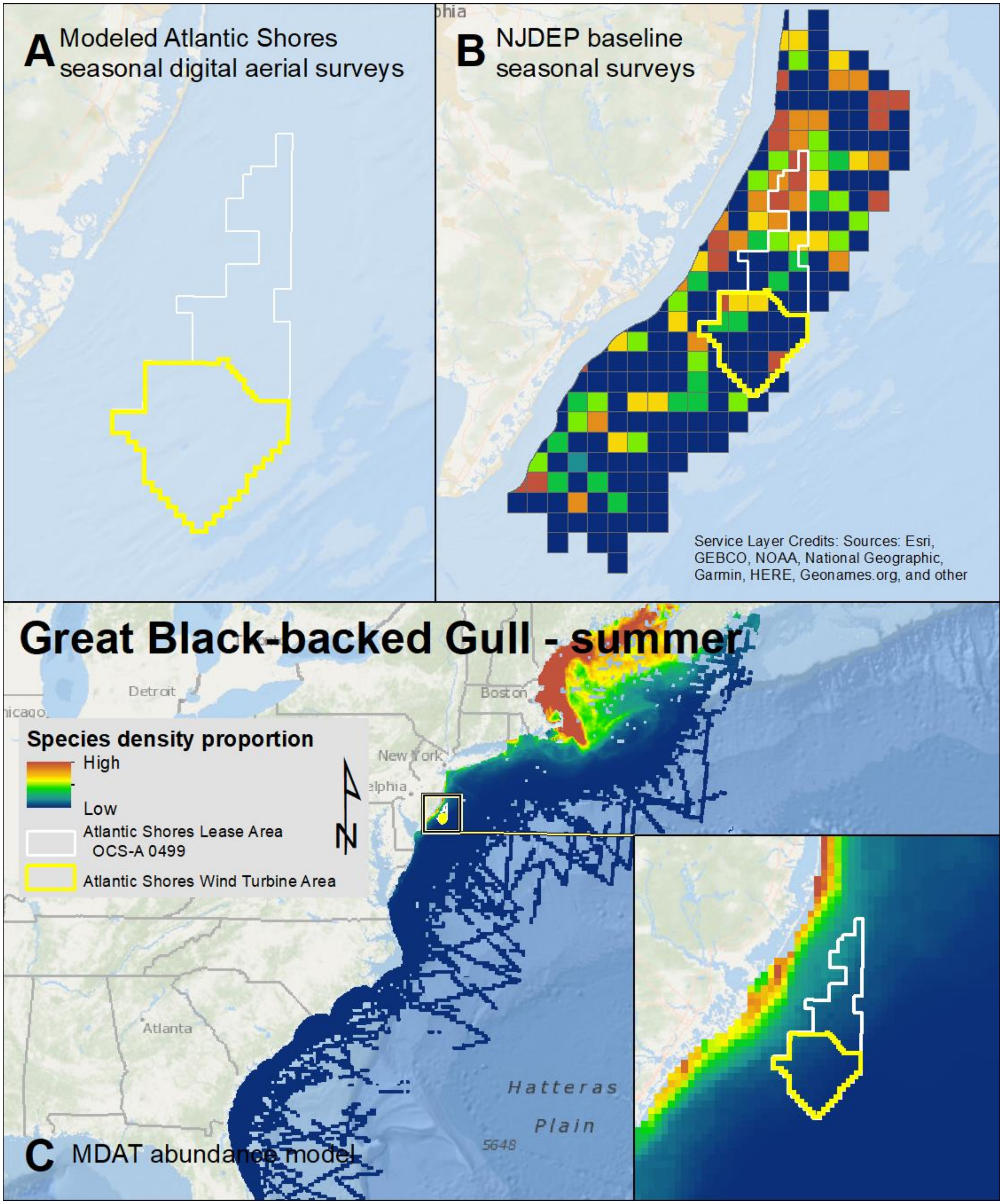

Map 123. Summer Great Black-backed Gull modeled density proportions in the Atlantic Shores seasonal digital aerial surveys (A), density proportions in the NJDEP baseline survey data (B), and the MDAT data at local and regional scales (C). The scale for all maps is representative of relative spatial variation in the sites within the season for each data source.

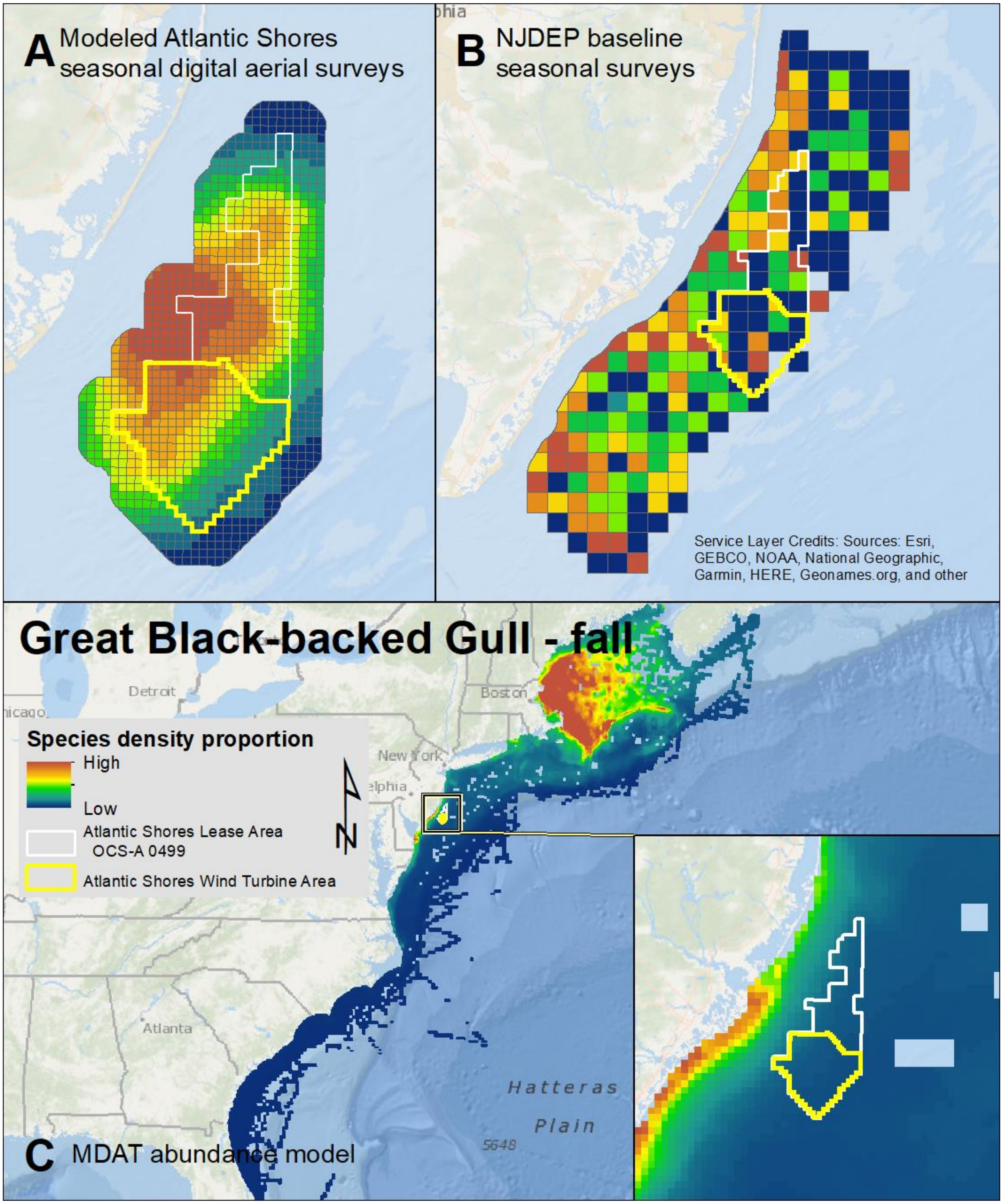

Map 124. Fall Great Black-backed Gull modeled density proportions in the Atlantic Shores seasonal digital aerial surveys (A), density proportions in the NJDEP baseline survey data (B), and the MDAT data at local and regional scales (C). The scale for all maps is representative of relative spatial variation in the sites within the season for each data source.

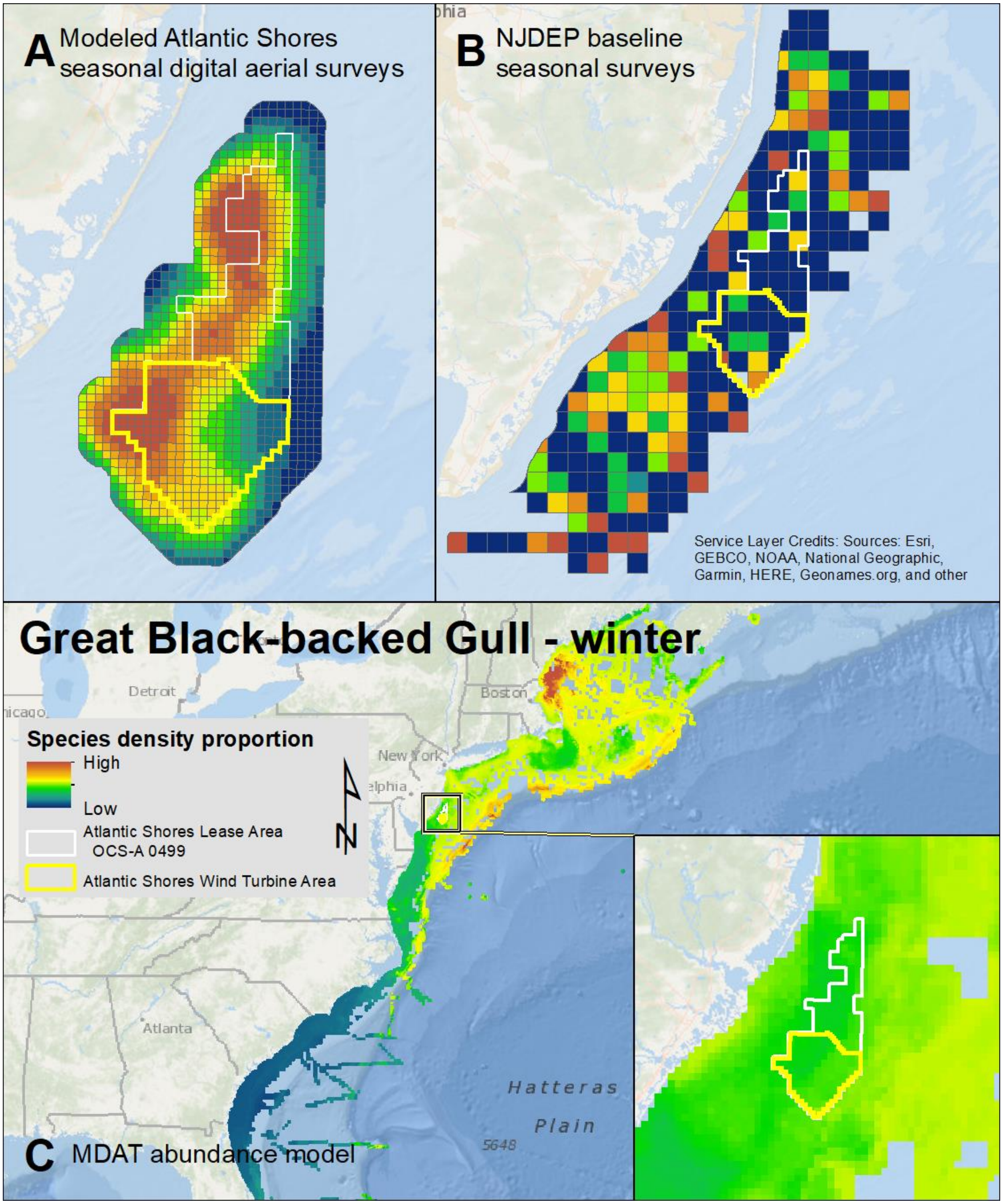

Map 125. Winter Great Black-backed Gull modeled density proportions in the Atlantic Shores seasonal digital aerial surveys (A), density proportions in the NJDEP baseline survey data (B), and the MDAT data at local and regional scales (C). The scale for all maps is representative of relative spatial variation in the sites within the season for each data source.

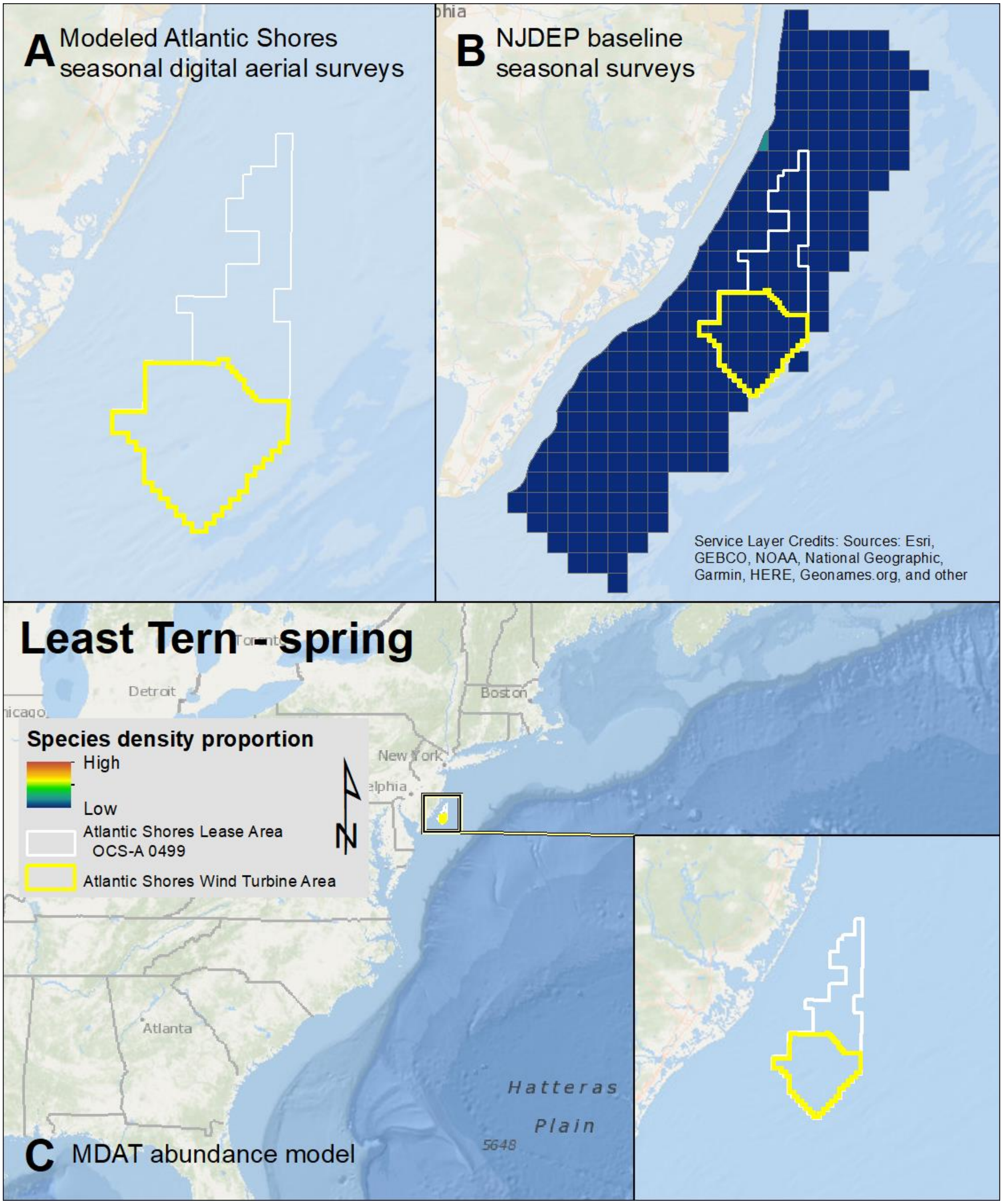

Map 126. Spring Least Tern modeled density proportions in the Atlantic Shores seasonal digital aerial surveys (A), density proportions in the NJDEP baseline survey data (B), and the MDAT data at local and regional scales (C). The scale for all maps is representative of relative spatial variation in the sites within the season for each data source.

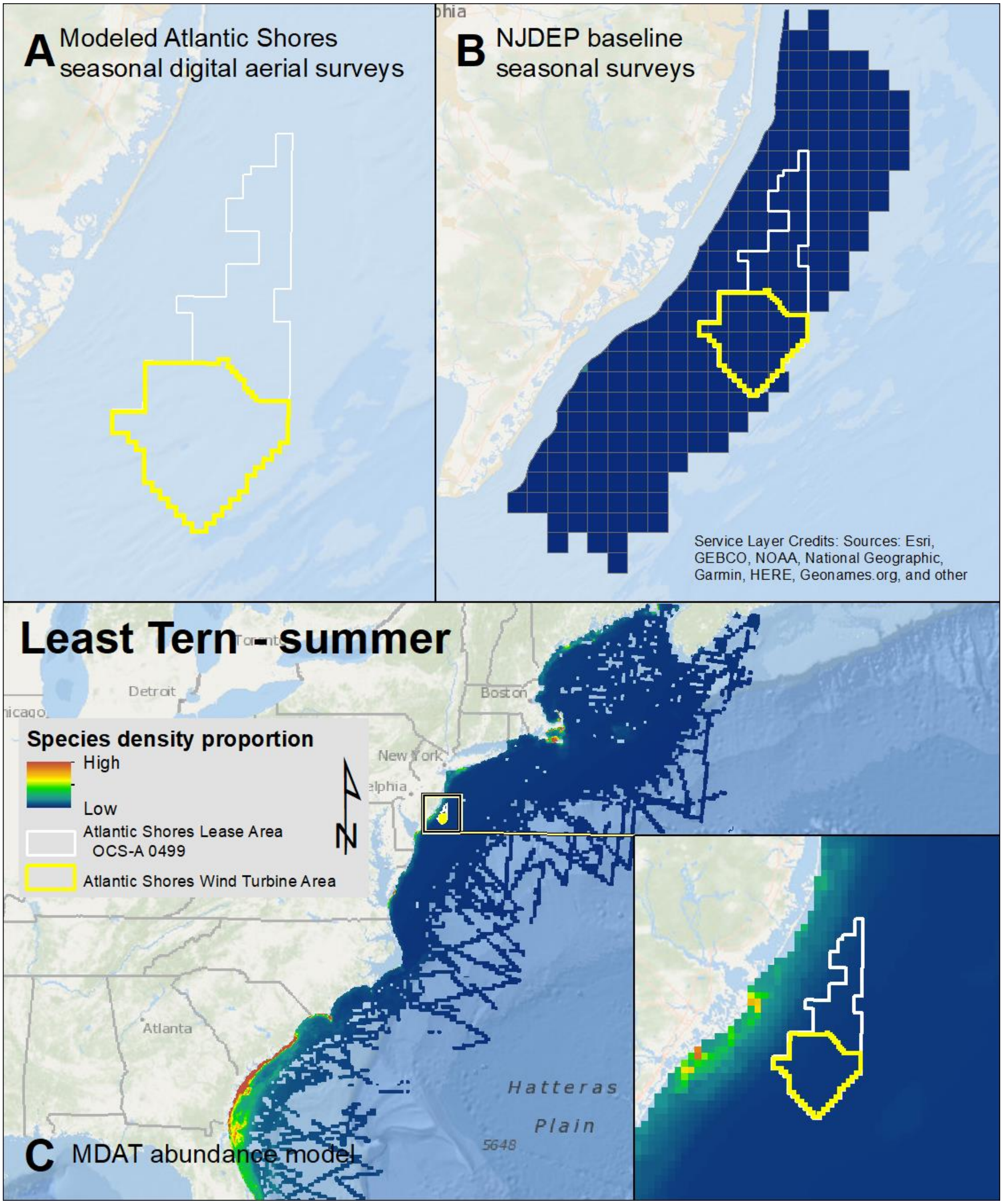

Map 127. Summer Least Tern modeled density proportions in the Atlantic Shores seasonal digital aerial surveys (A), density proportions in the NJDEP baseline survey data (B), and the MDAT data at local and regional scales (C). The scale for all maps is representative of relative spatial variation in the sites within the season for each data source.

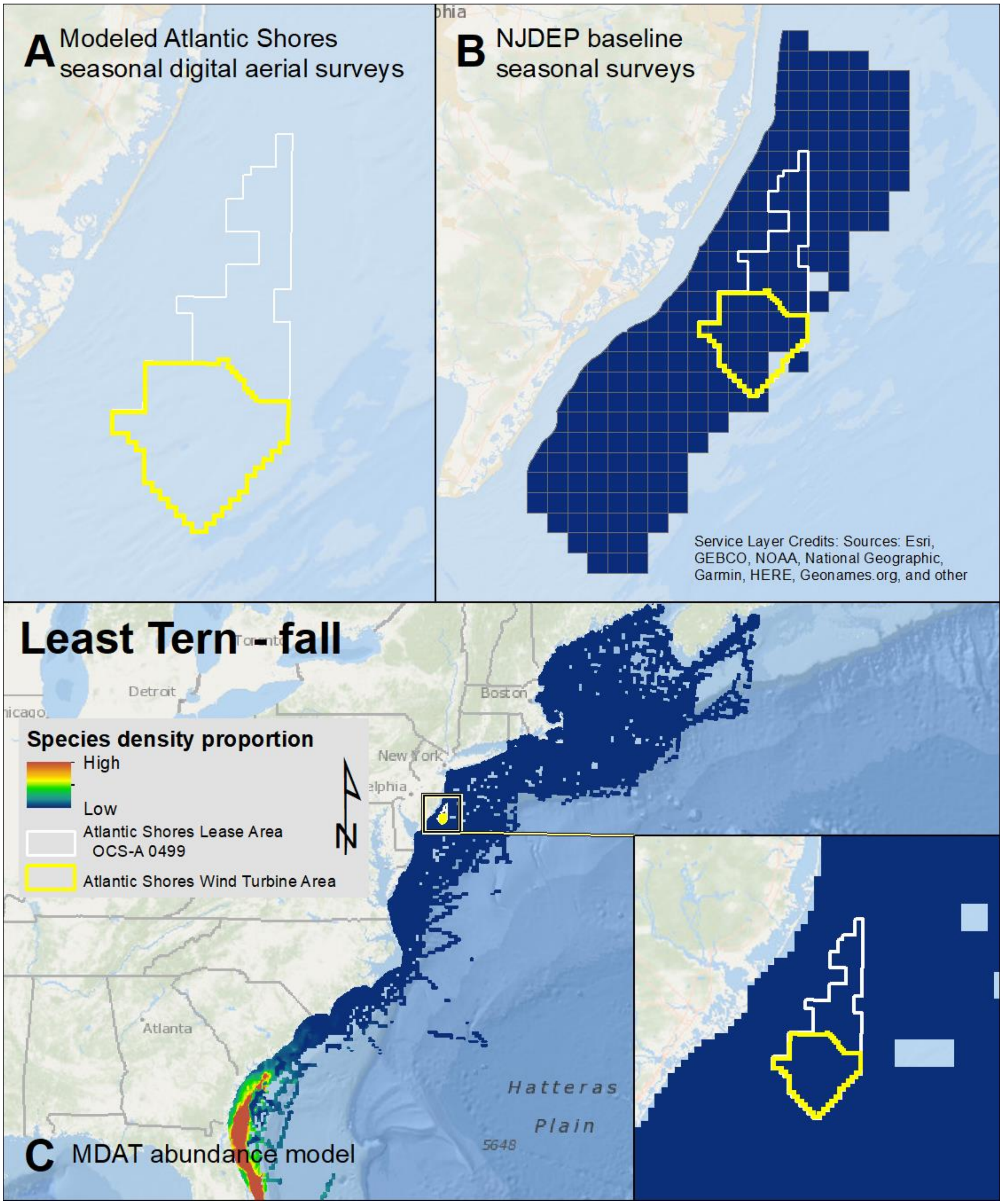

Map 128. Fall Least Tern modeled density proportions in the Atlantic Shores seasonal digital aerial surveys (A), density proportions in the NJDEP baseline survey data (B), and the MDAT data at local and regional scales (C). The scale for all maps is representative of relative spatial variation in the sites within the season for each data source.

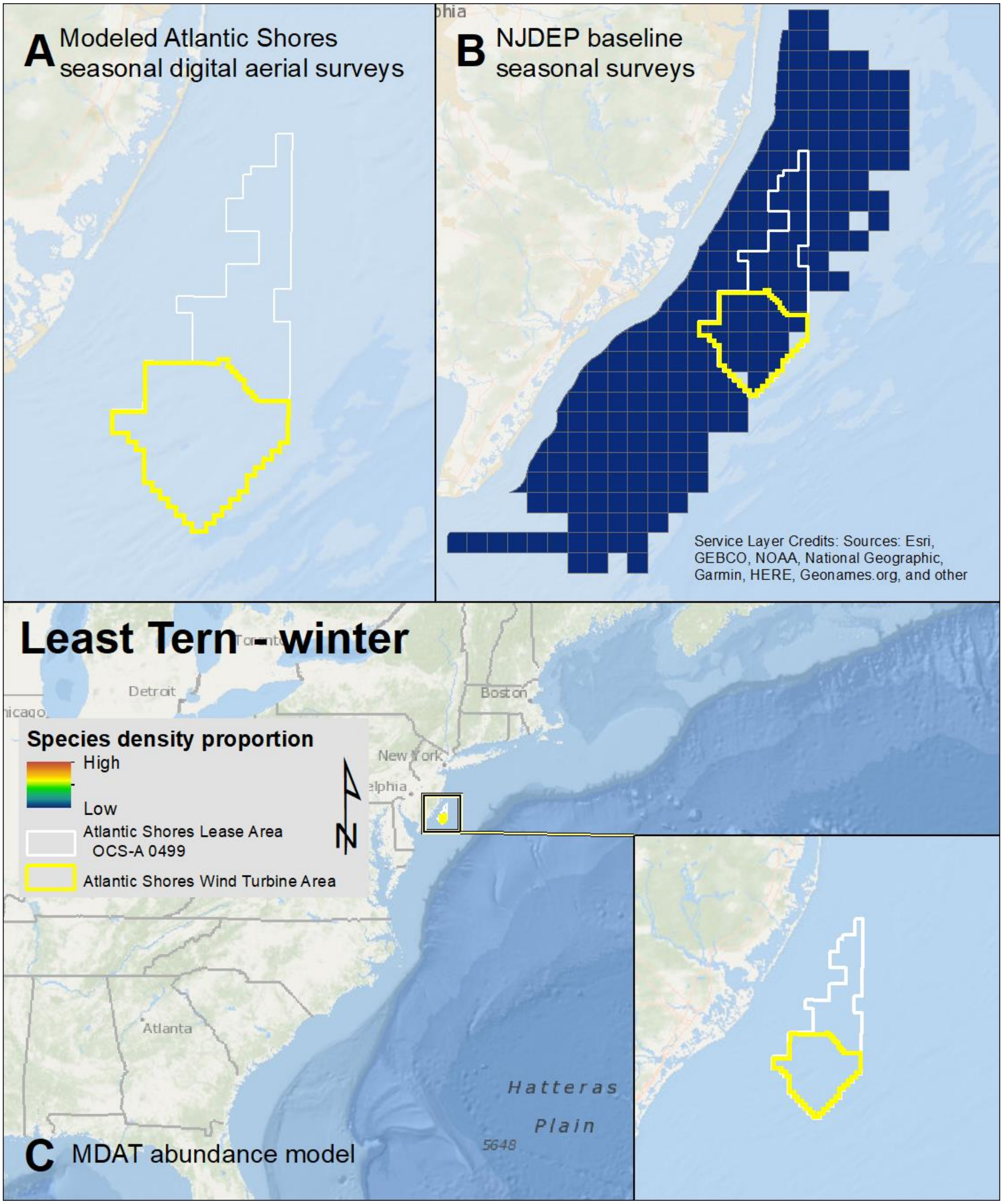

Map 129. Winter Least Tern modeled density proportions in the Atlantic Shores seasonal digital aerial surveys (A), density proportions in the NJDEP baseline survey data (B), and the MDAT data at local and regional scales (C). The scale for all maps is representative of relative spatial variation in the sites within the season for each data source.

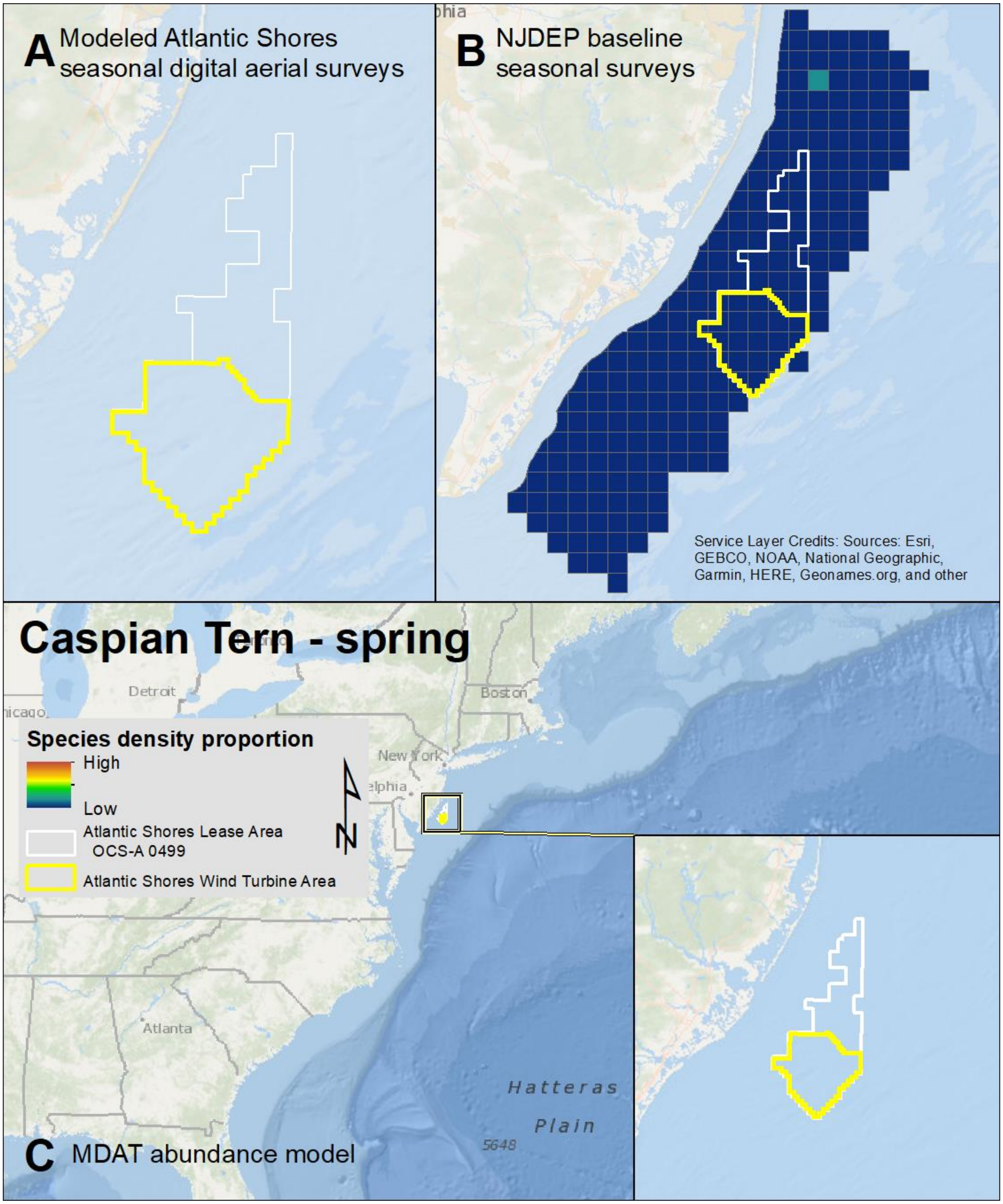

Map 130. Spring Caspian Tern modeled density proportions in the Atlantic Shores seasonal digital aerial surveys (A), density proportions in the NJDEP baseline survey data (B), and the MDAT data at local and regional scales (C). The scale for all maps is representative of relative spatial variation in the sites within the season for each data source.

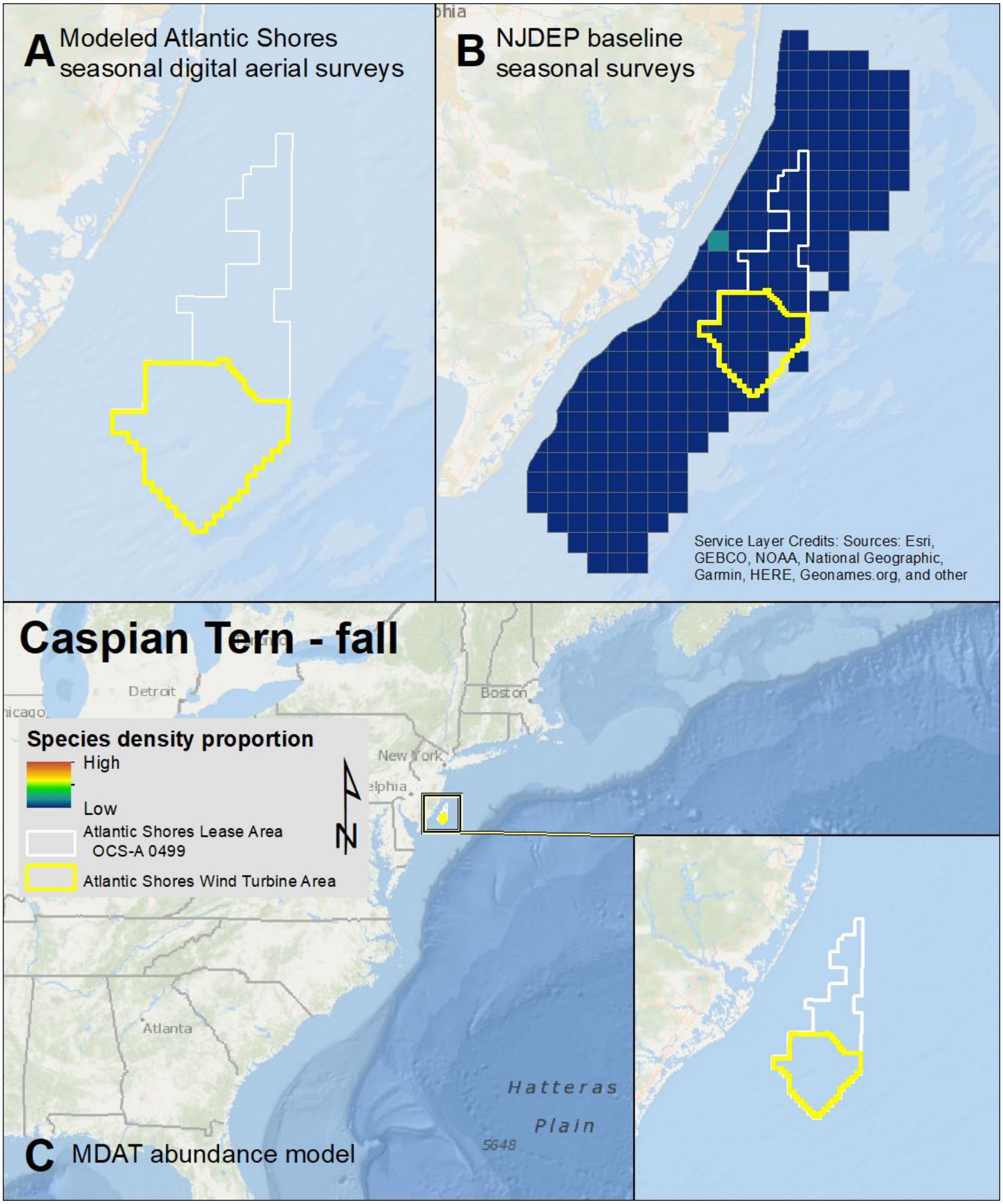

Map 131. Fall Caspian Tern modeled density proportions in the Atlantic Shores seasonal digital aerial surveys (A), density proportions in the NJDEP baseline survey data (B), and the MDAT data at local and regional scales (C). The scale for all maps is representative of relative spatial variation in the sites within the season for each data source.

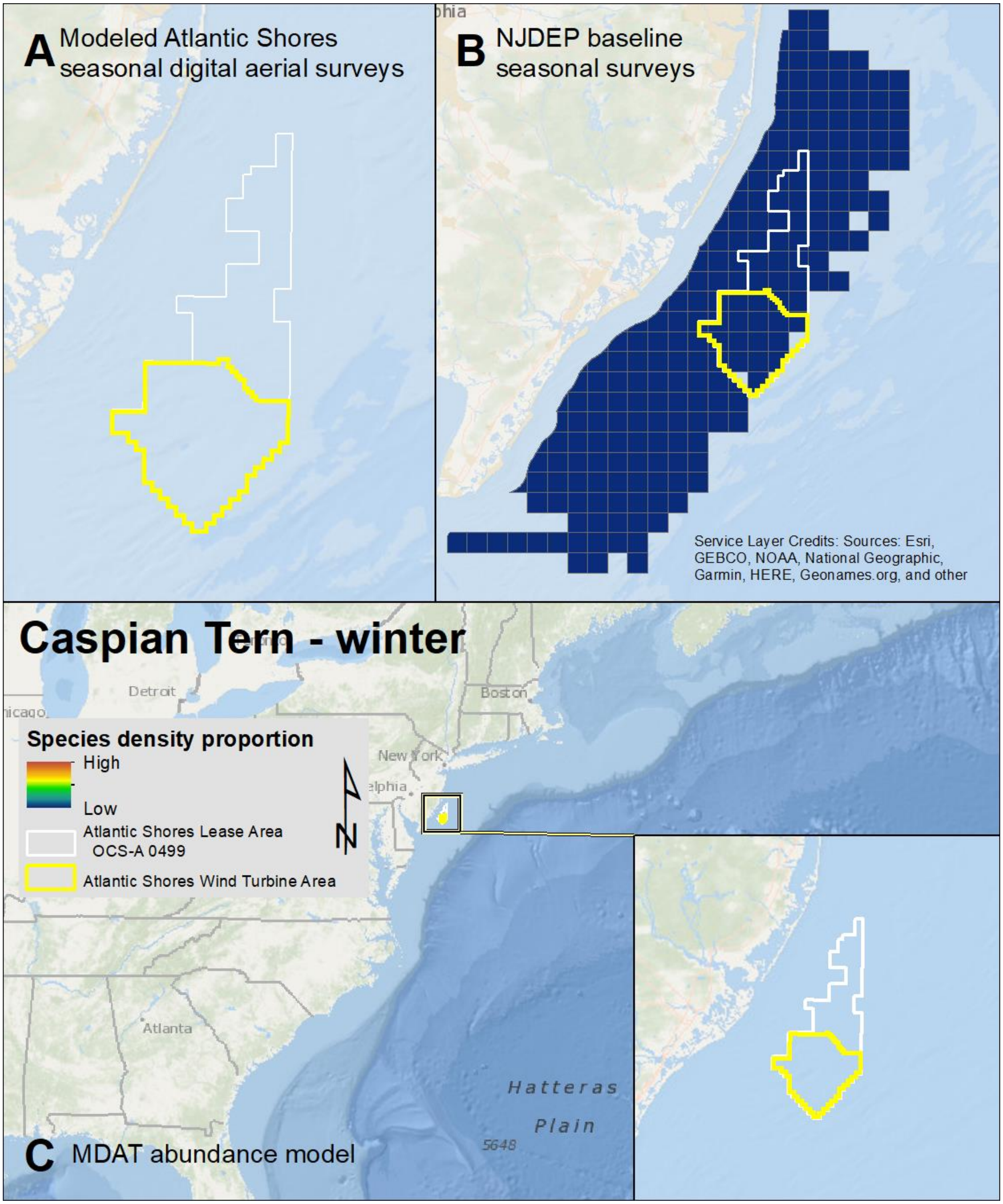

Map 132. Winter Caspian Tern modeled density proportions in the Atlantic Shores seasonal digital aerial surveys (A), density proportions in the NJDEP baseline survey data (B), and the MDAT data at local and regional scales (C). The scale for all maps is representative of relative spatial variation in the sites within the season for each data source.

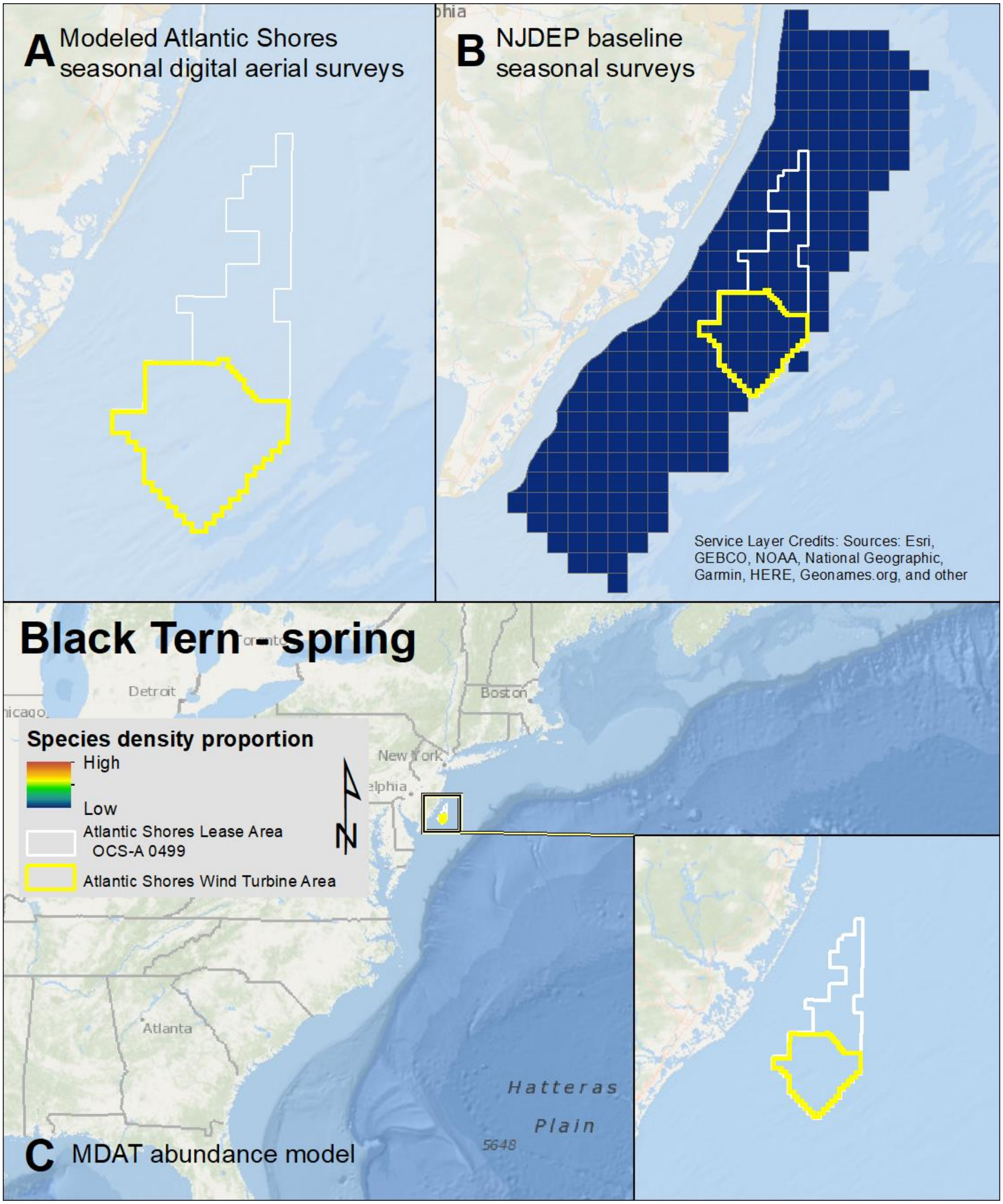

Map 133. Spring Black Tern modeled density proportions in the Atlantic Shores seasonal digital aerial surveys (A), density proportions in the NJDEP baseline survey data (B), and the MDAT data at local and regional scales (C). The scale for all maps is representative of relative spatial variation in the sites within the season for each data source.

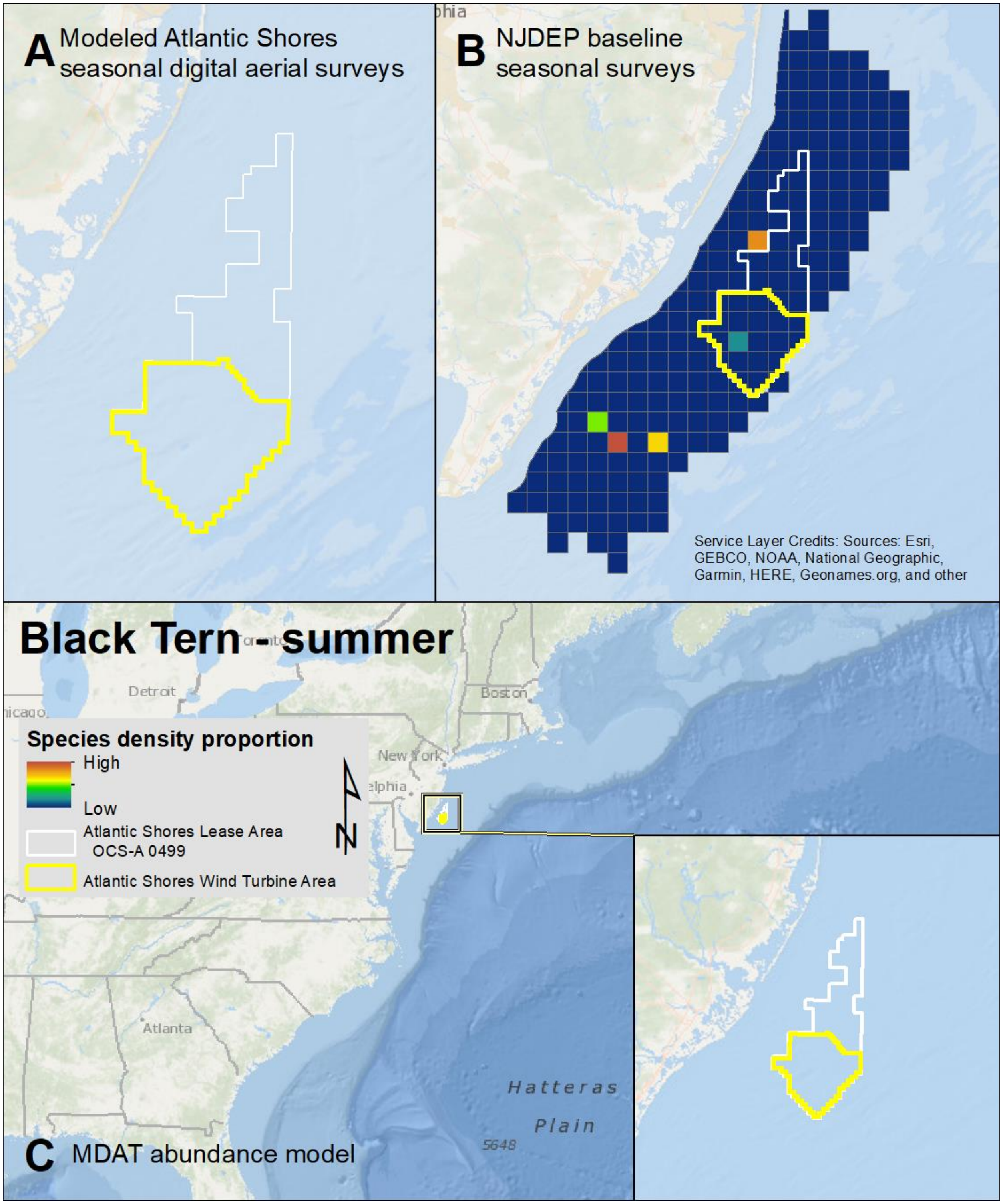

Map 134. Summer Black Tern modeled density proportions in the Atlantic Shores seasonal digital aerial surveys (A), density proportions in the NJDEP baseline survey data (B), and the MDAT data at local and regional scales (C). The scale for all maps is representative of relative spatial variation in the sites within the season for each data source.

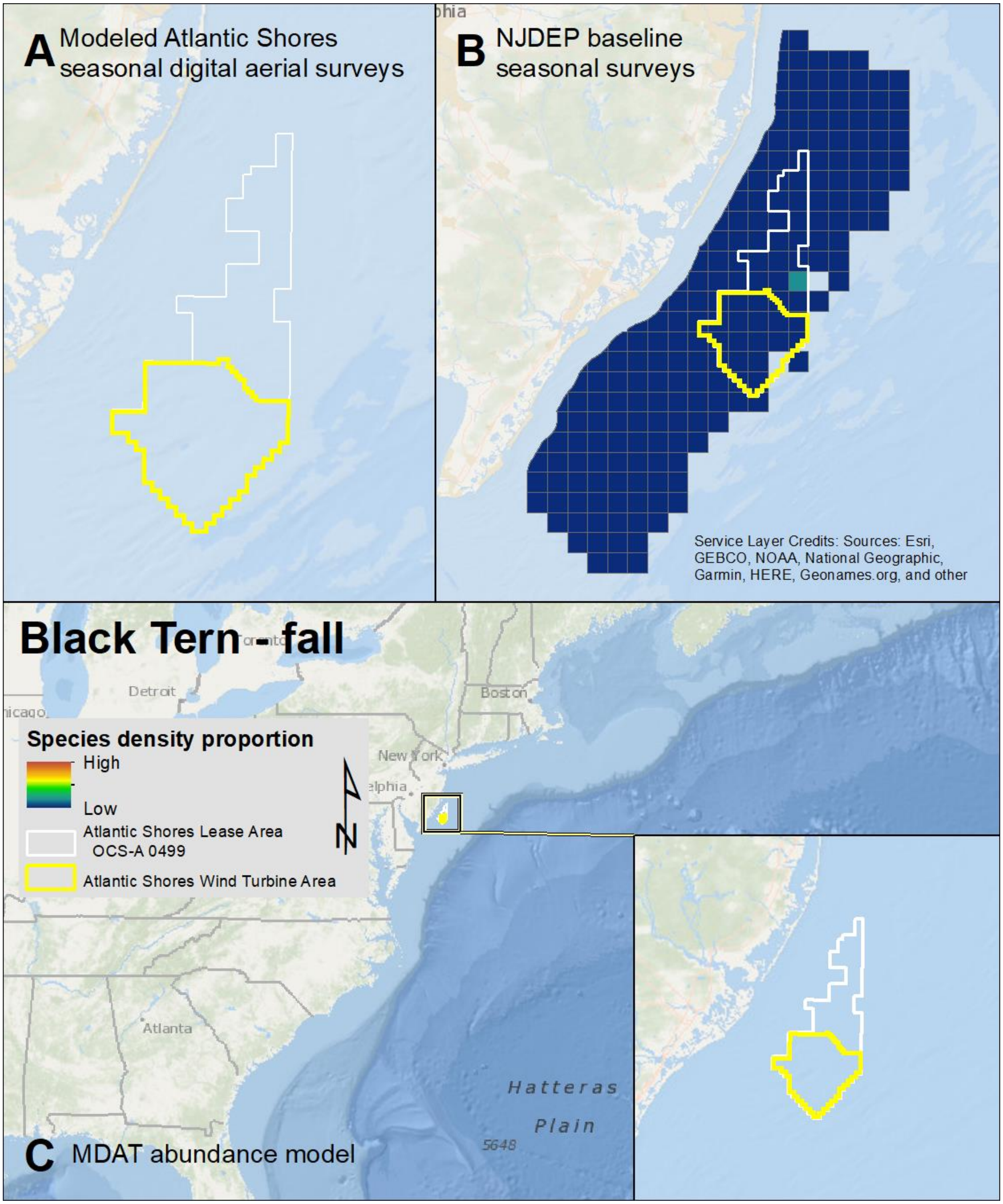

Map 135. Fall Black Tern modeled density proportions in the Atlantic Shores seasonal digital aerial surveys (A), density proportions in the NJDEP baseline survey data (B), and the MDAT data at local and regional scales (C). The scale for all maps is representative of relative spatial variation in the sites within the season for each data source.

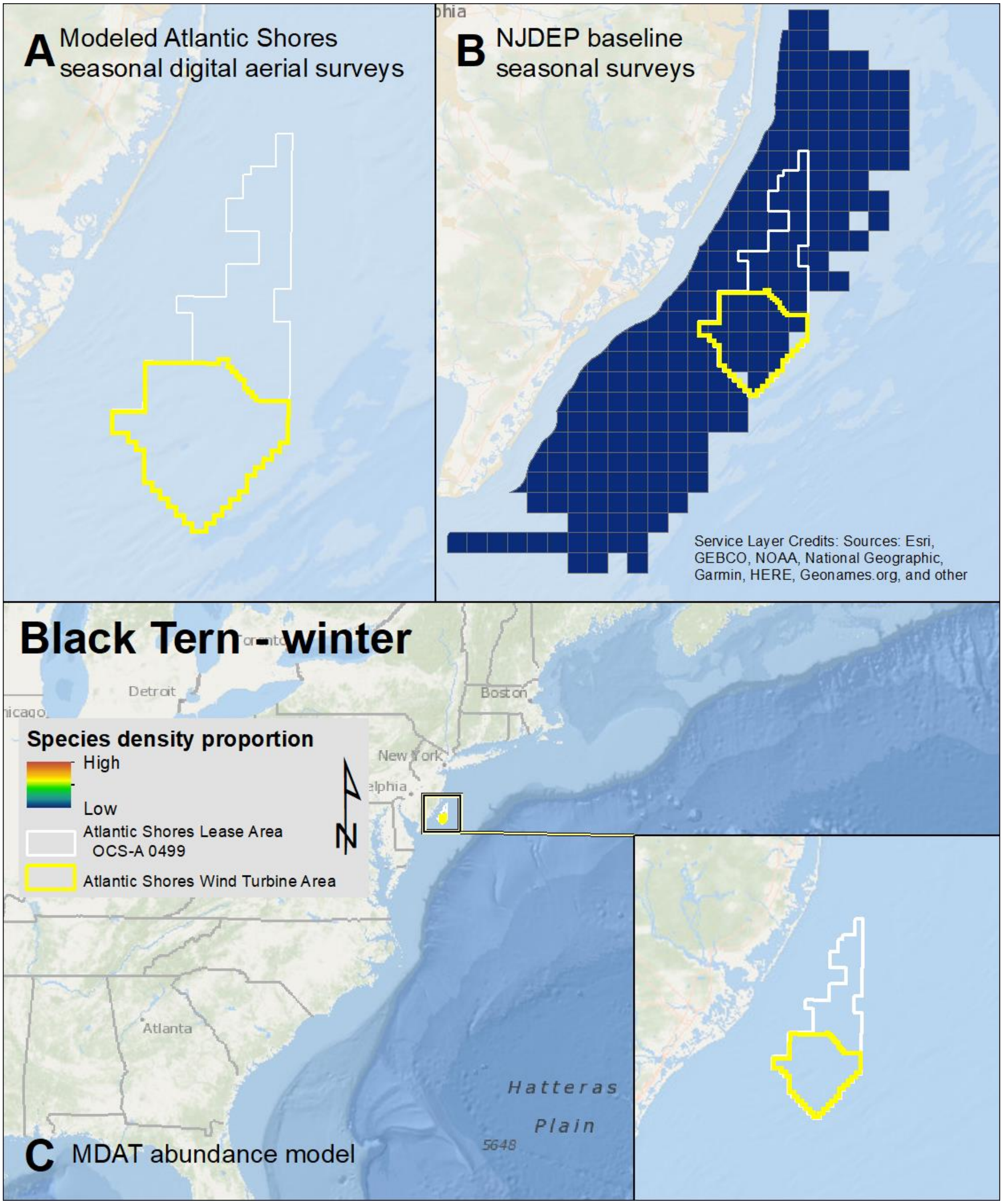

Map 136. Winter Black Tern modeled density proportions in the Atlantic Shores seasonal digital aerial surveys (A), density proportions in the NJDEP baseline survey data (B), and the MDAT data at local and regional scales (C). The scale for all maps is representative of relative spatial variation in the sites within the season for each data source.

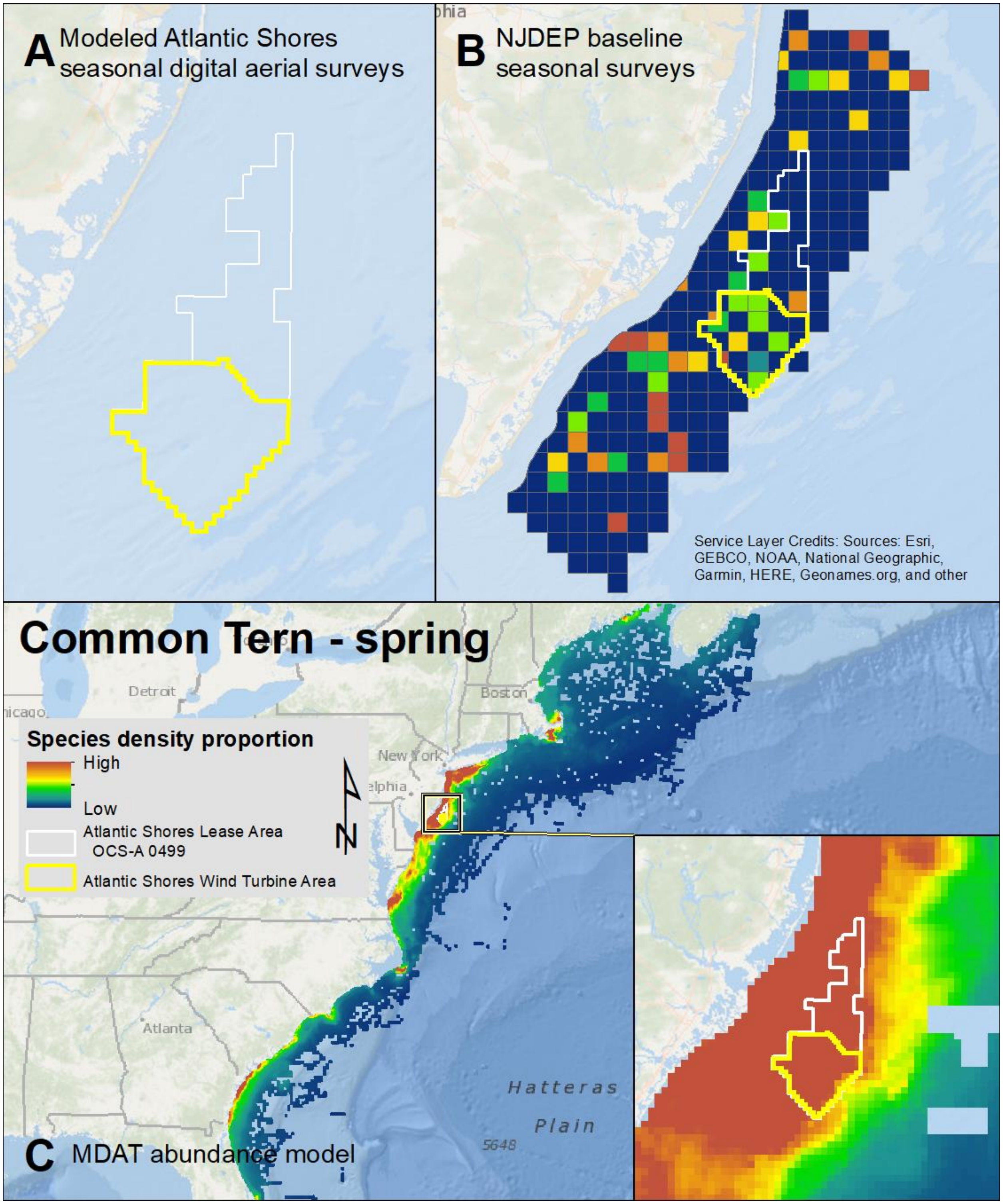

Map 137. Spring Common Tern modeled density proportions in the Atlantic Shores seasonal digital aerial surveys (A), density proportions in the NJDEP baseline survey data (B), and the MDAT data at local and regional scales (C). The scale for all maps is representative of relative spatial variation in the sites within the season for each data source.

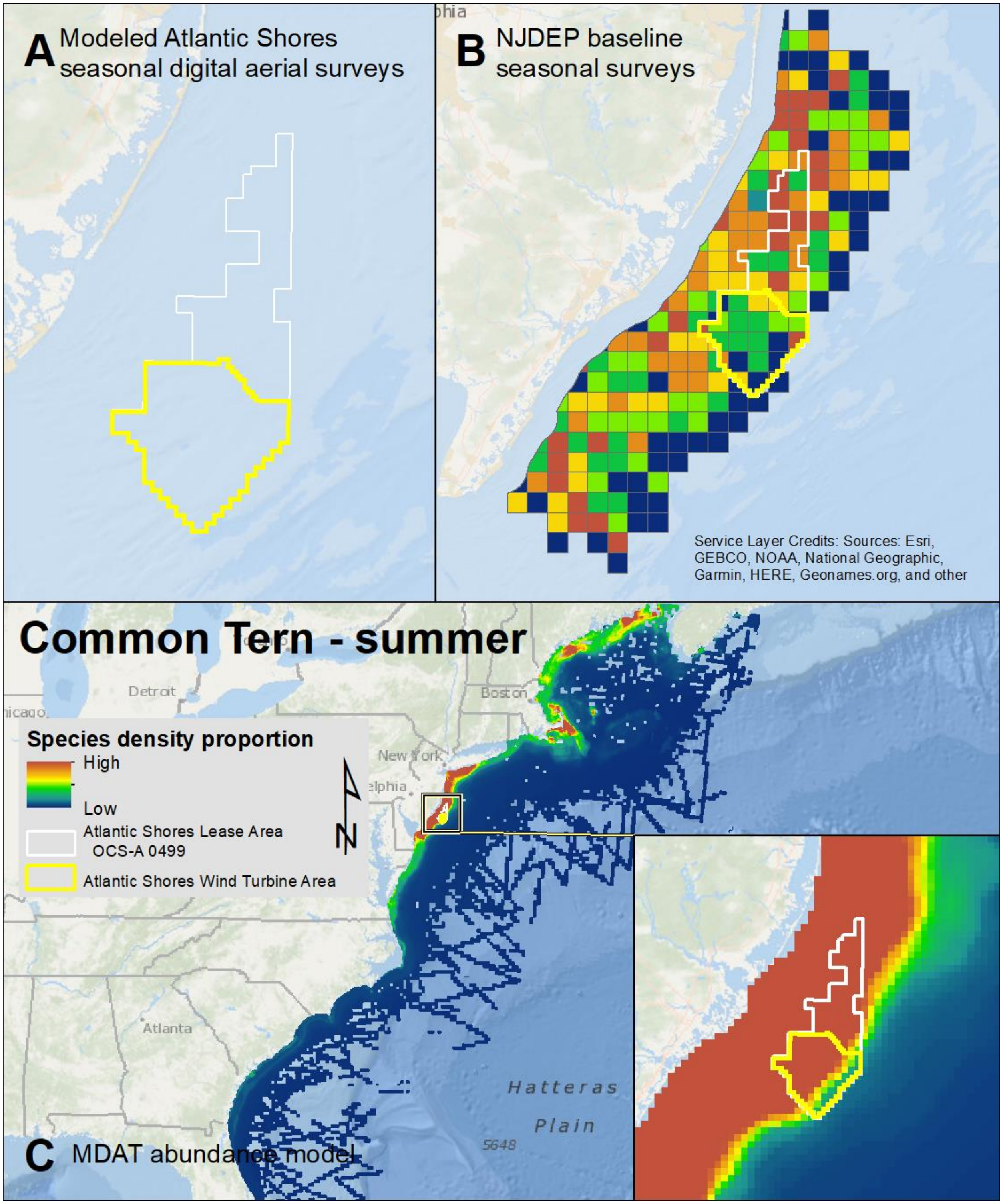

Map 138. Summer Common Tern modeled density proportions in the Atlantic Shores seasonal digital aerial surveys (A), density proportions in the NJDEP baseline survey data (B), and the MDAT data at local and regional scales (C). The scale for all maps is representative of relative spatial variation in the sites within the season for each data source.

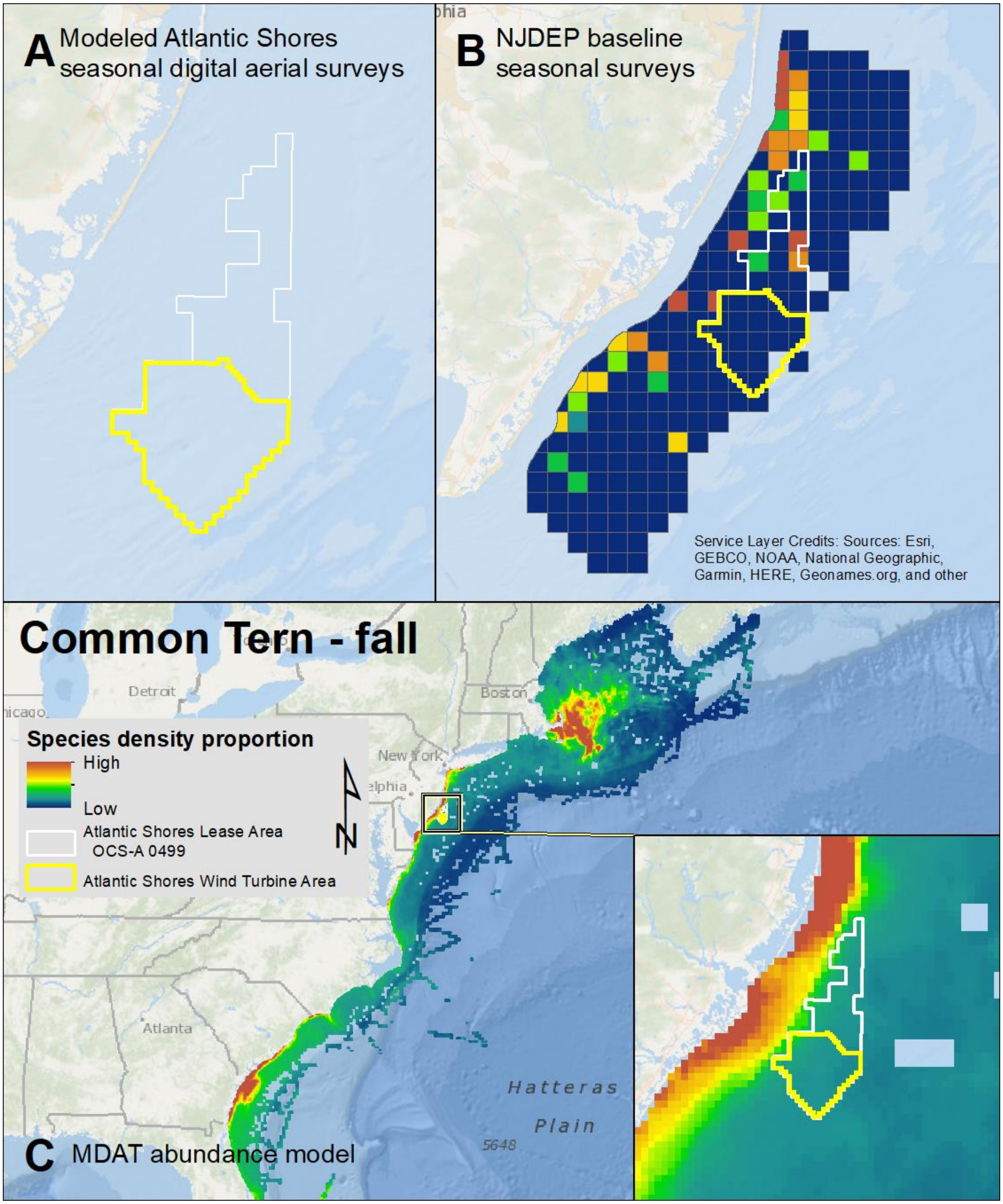

Map 139. Fall Common Tern modeled density proportions in the Atlantic Shores seasonal digital aerial surveys (A), density proportions in the NJDEP baseline survey data (B), and the MDAT data at local and regional scales (C). The scale for all maps is representative of relative spatial variation in the sites within the season for each data source.

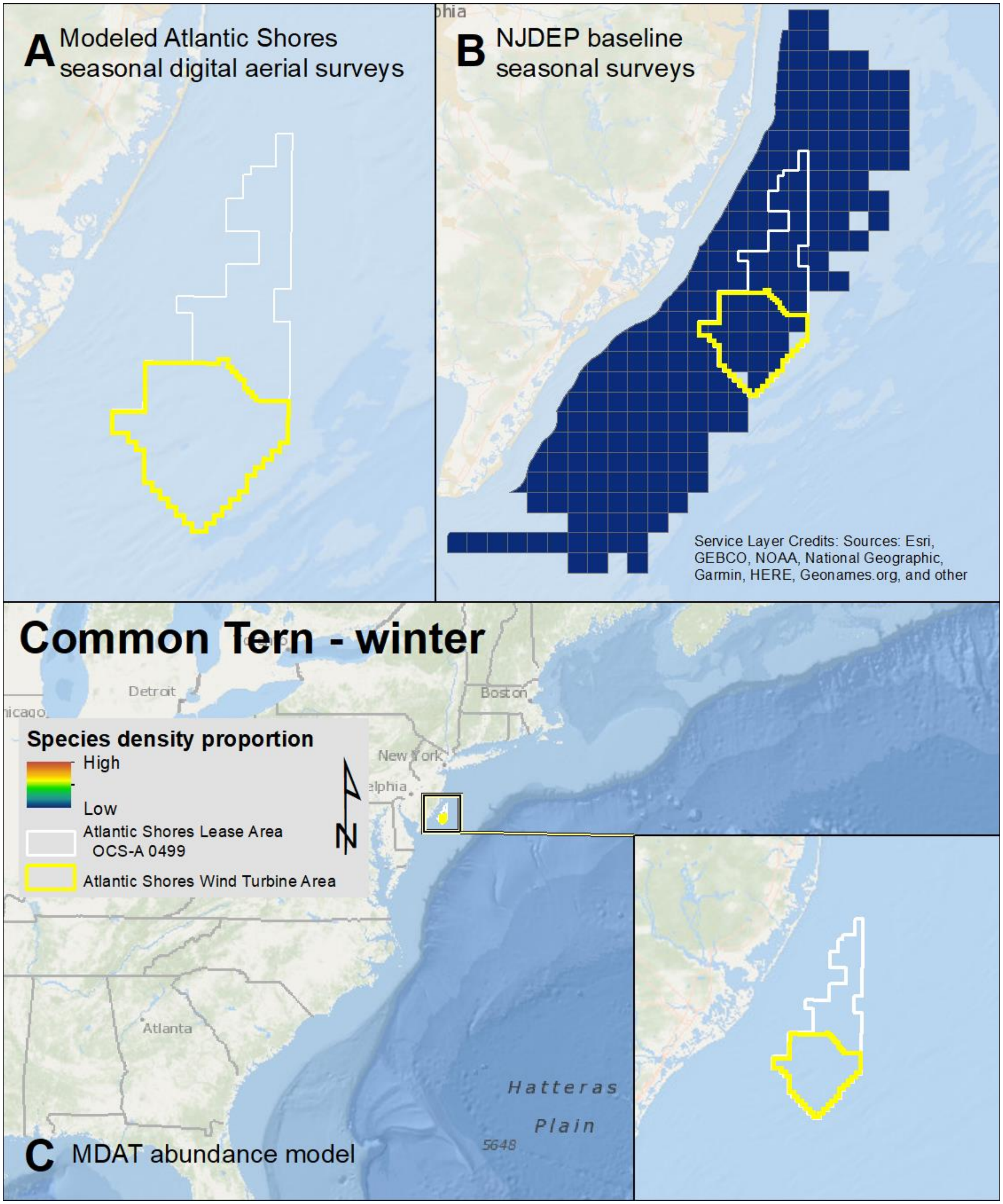

Map 140. Winter Common Tern modeled density proportions in the Atlantic Shores seasonal digital aerial surveys (A), density proportions in the NJDEP baseline survey data (B), and the MDAT data at local and regional scales (C). The scale for all maps is representative of relative spatial variation in the sites within the season for each data source.

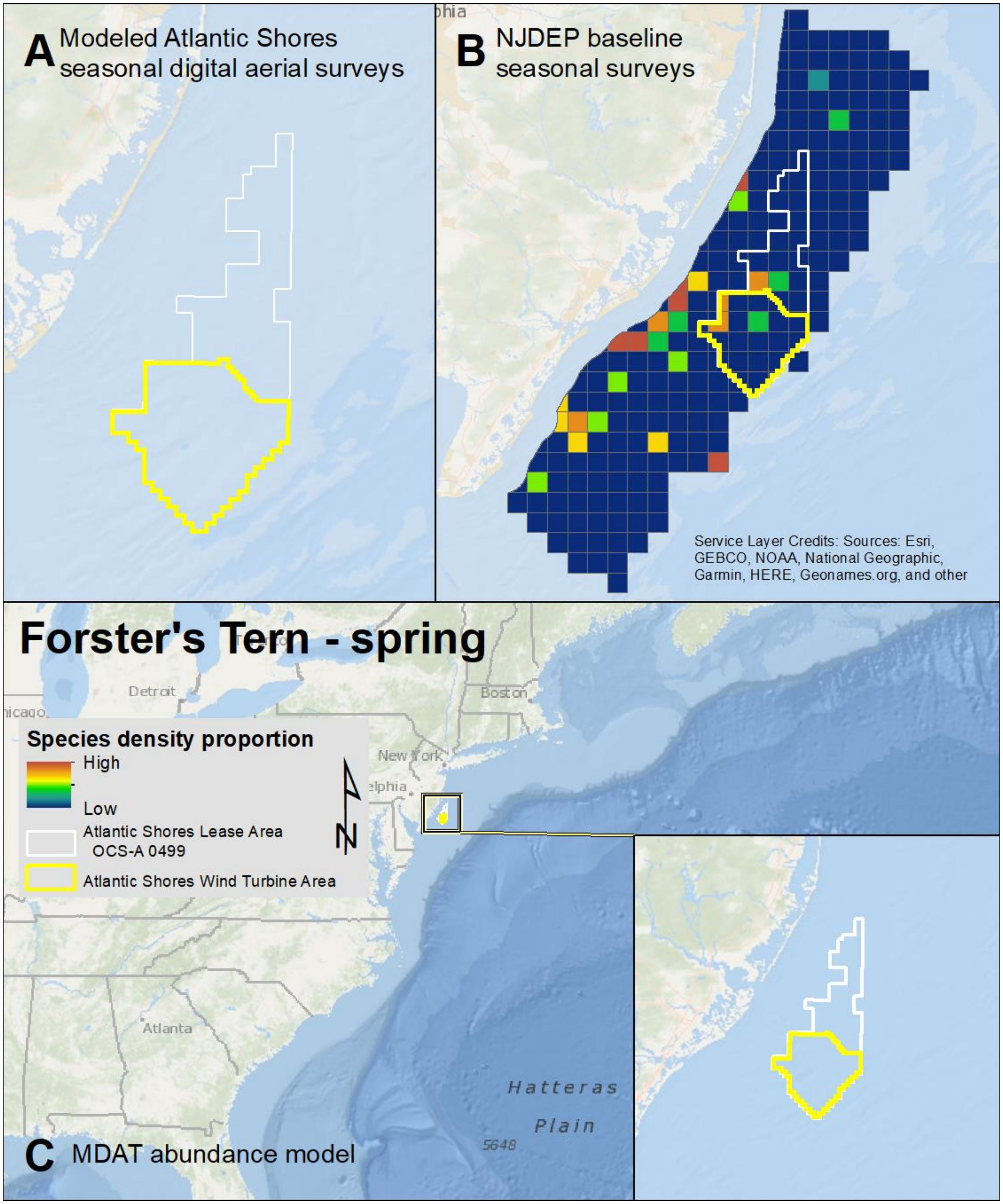

Map 141. Spring Forster's Tern modeled density proportions in the Atlantic Shores seasonal digital aerial surveys (A), density proportions in the NJDEP baseline survey data (B), and the MDAT data at local and regional scales (C). The scale for all maps is representative of relative spatial variation in the sites within the season for each data source.

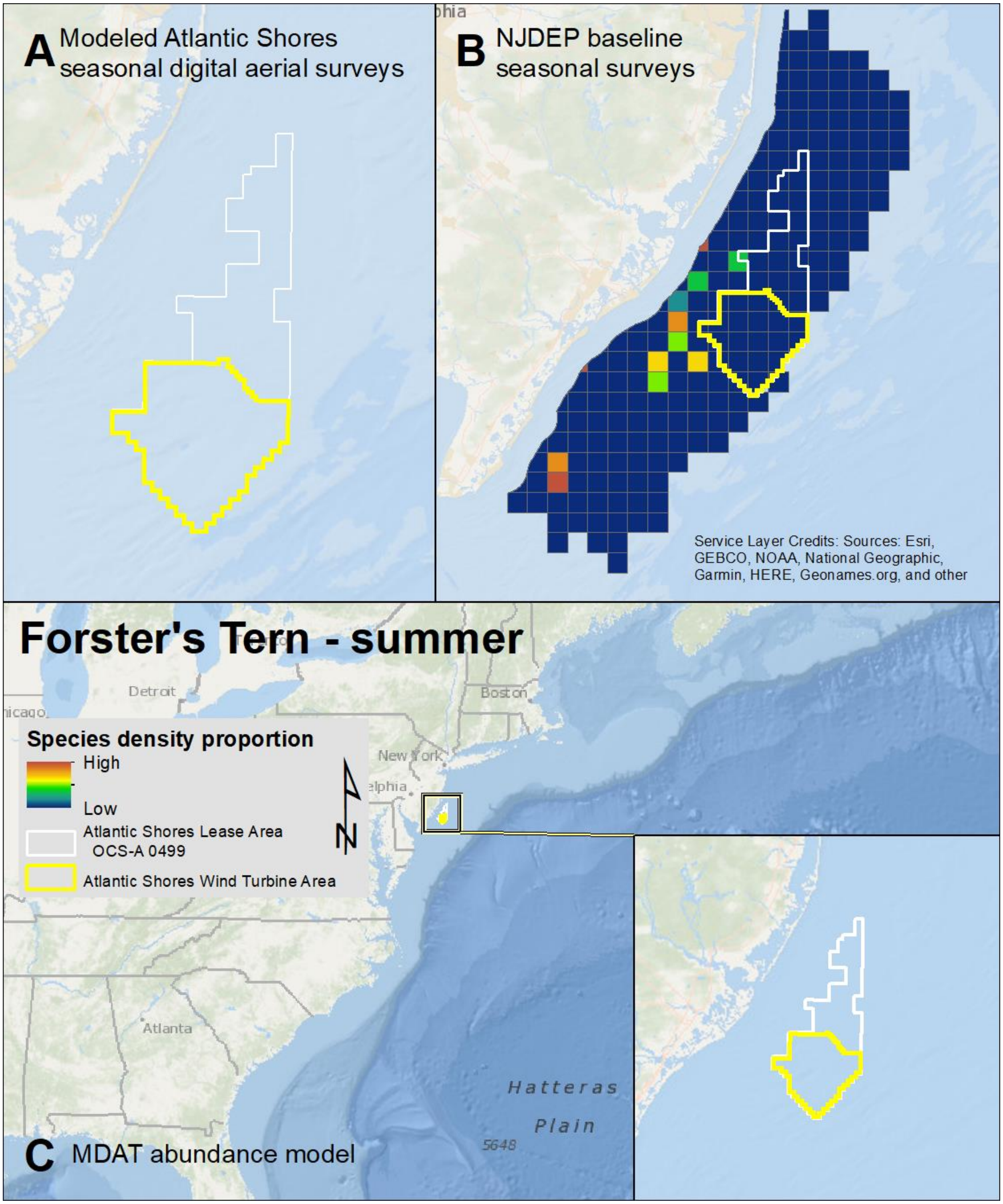

Map 142. Summer Forster's Tern modeled density proportions in the Atlantic Shores seasonal digital aerial surveys (A), density proportions in the NJDEP baseline survey data (B), and the MDAT data at local and regional scales (C). The scale for all maps is representative of relative spatial variation in the sites within the season for each data source.

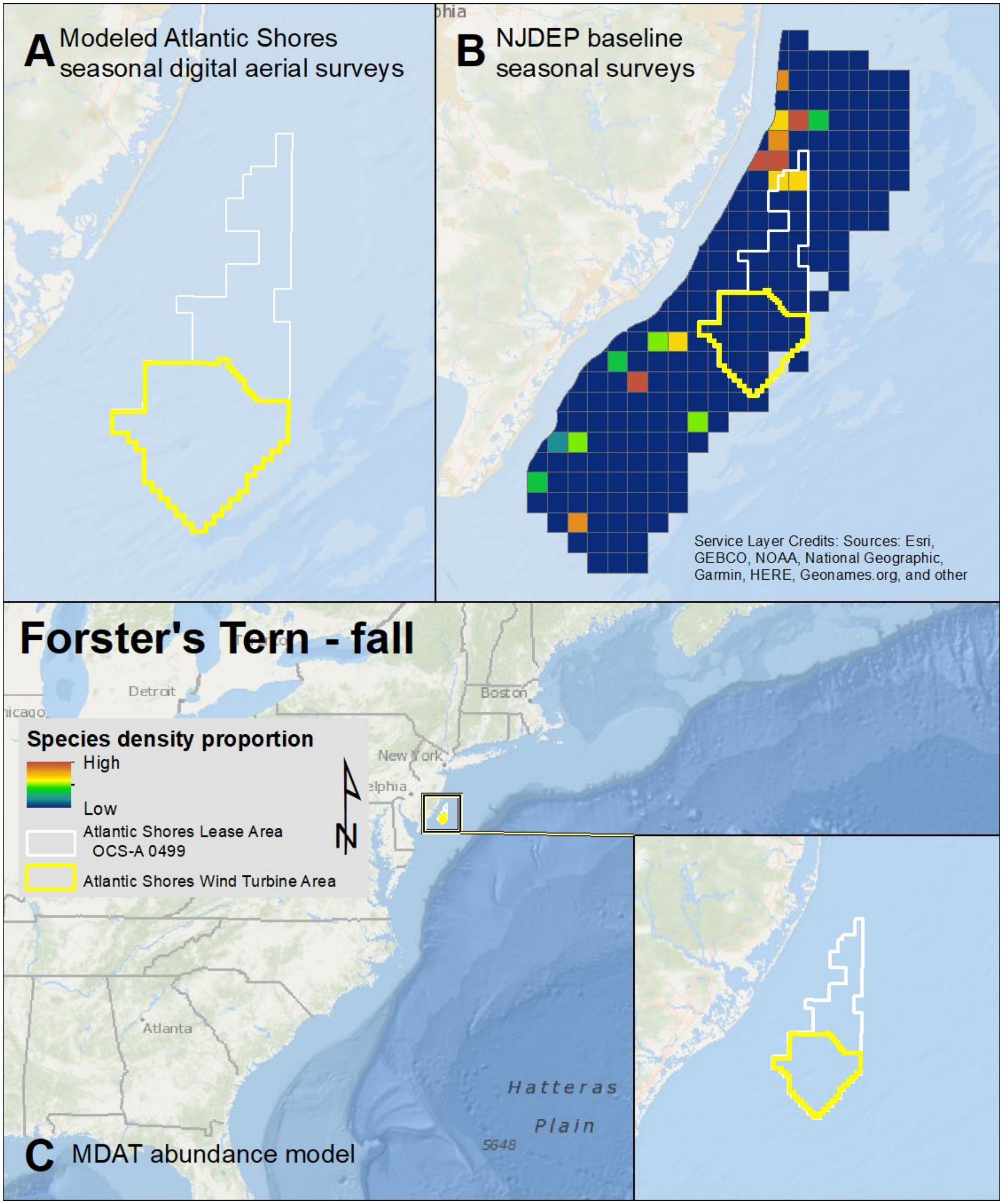

Map 143. Fall Forster's Tern modeled density proportions in the Atlantic Shores seasonal digital aerial surveys (A), density proportions in the NJDEP baseline survey data (B), and the MDAT data at local and regional scales (C). The scale for all maps is representative of relative spatial variation in the sites within the season for each data source.

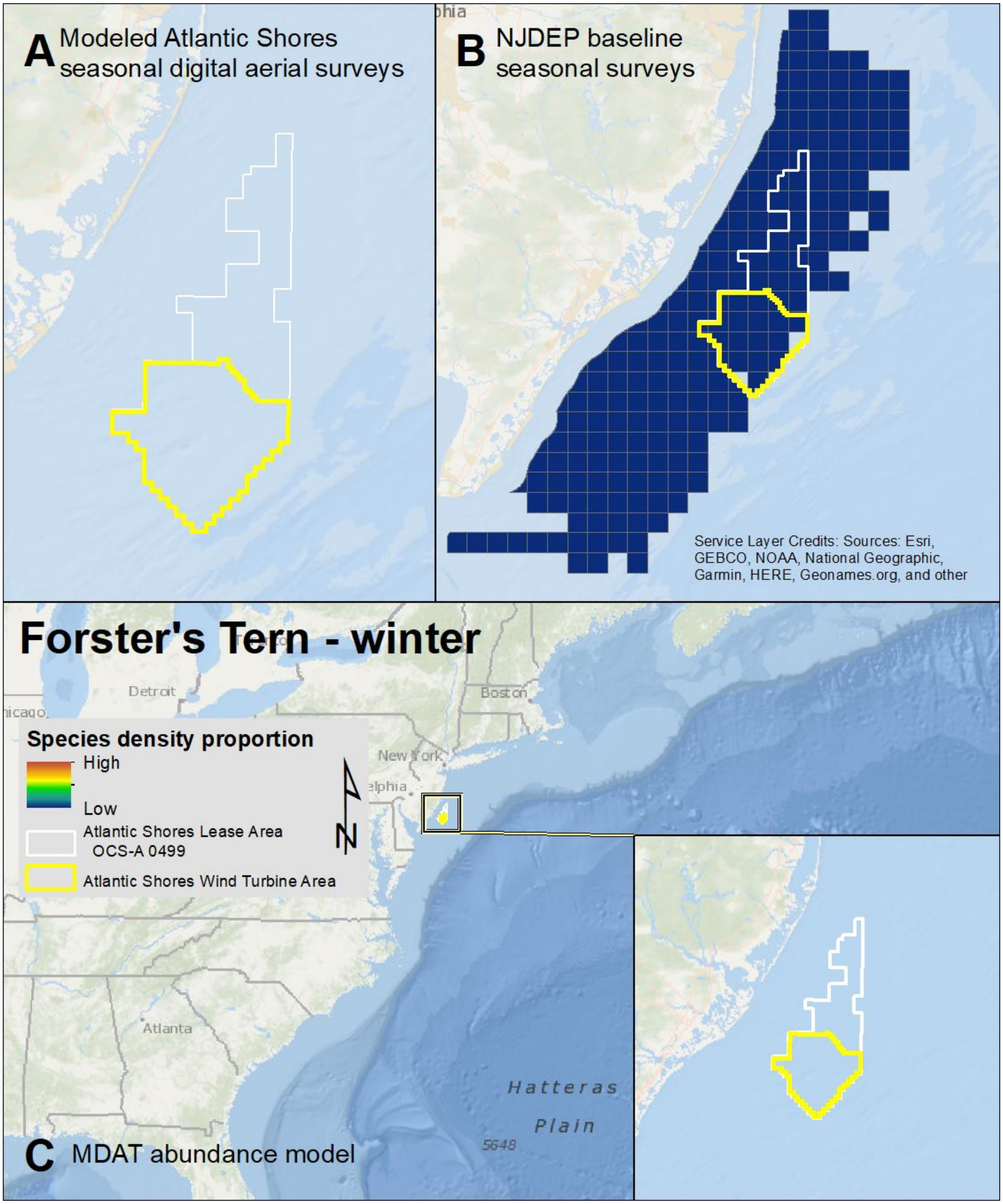

Map 144. Winter Forster's Tern modeled density proportions in the Atlantic Shores seasonal digital aerial surveys (A), density proportions in the NJDEP baseline survey data (B), and the MDAT data at local and regional scales (C). The scale for all maps is representative of relative spatial variation in the sites within the season for each data source.

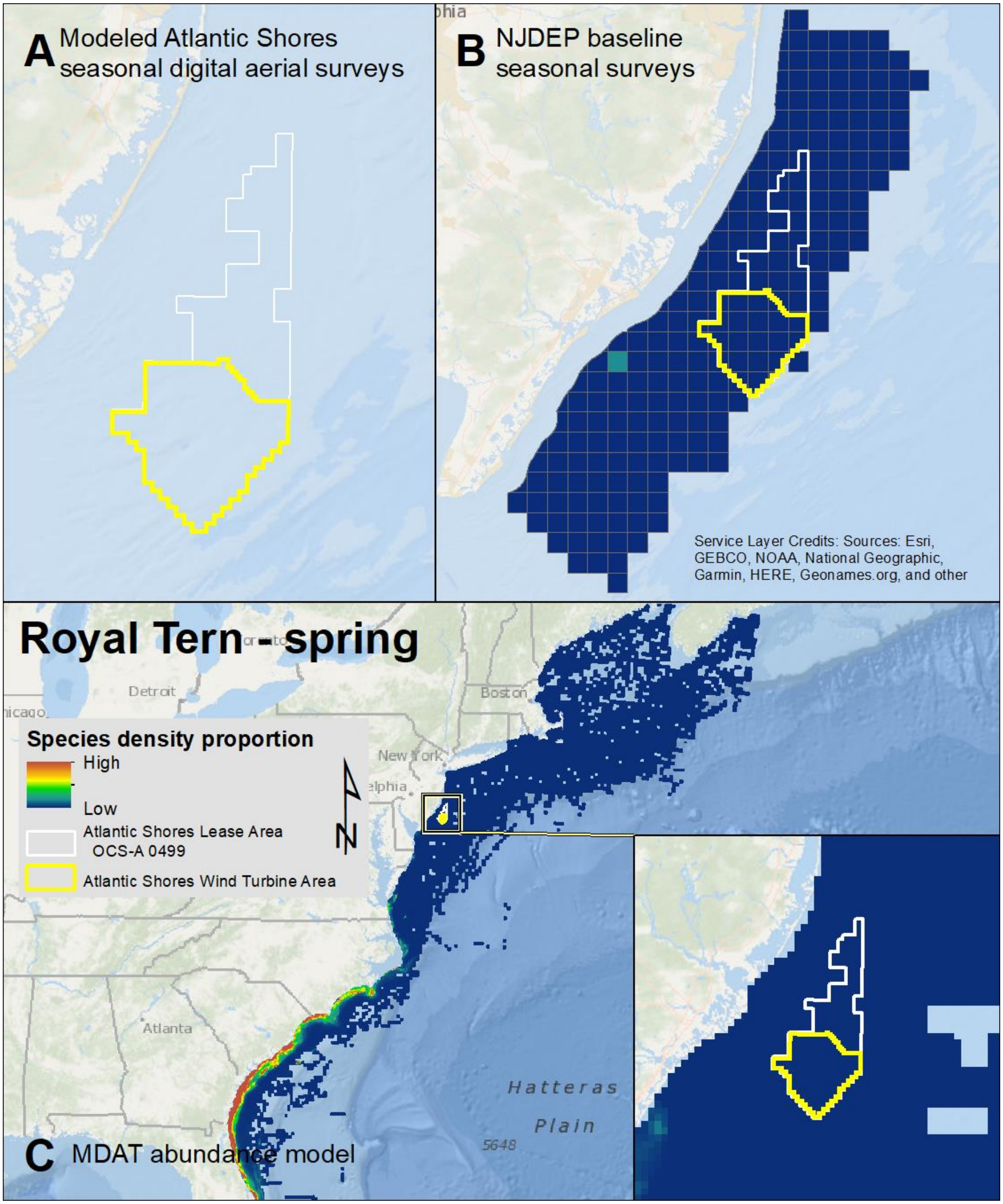

Map 145. Spring Royal Tern modeled density proportions in the Atlantic Shores seasonal digital aerial surveys (A), density proportions in the NJDEP baseline survey data (B), and the MDAT data at local and regional scales (C). The scale for all maps is representative of relative spatial variation in the sites within the season for each data source.

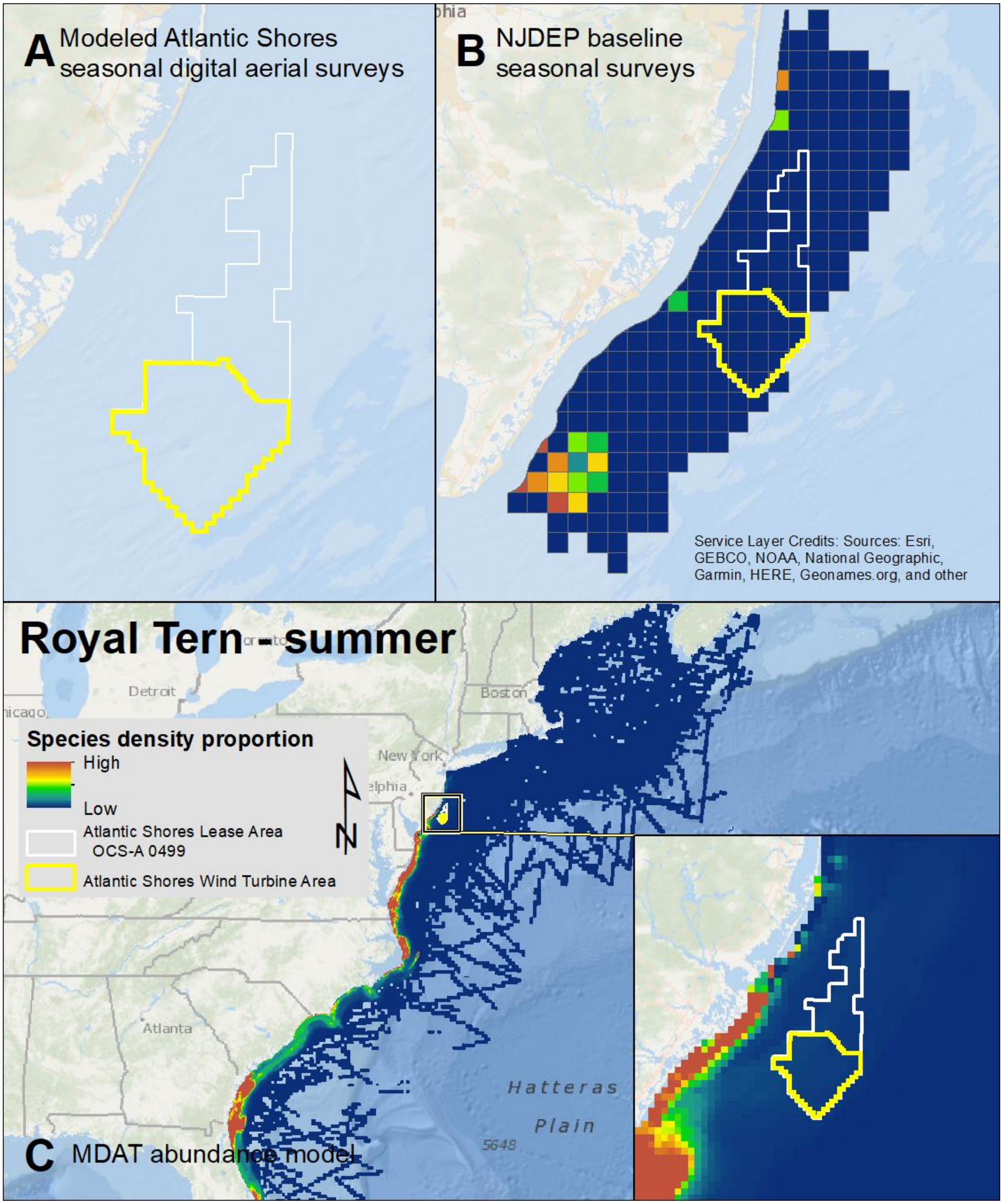

Map 146. Summer Royal Tern modeled density proportions in the Atlantic Shores seasonal digital aerial surveys (A), density proportions in the NJDEP baseline survey data (B), and the MDAT data at local and regional scales (C). The scale for all maps is representative of relative spatial variation in the sites within the season for each data source.

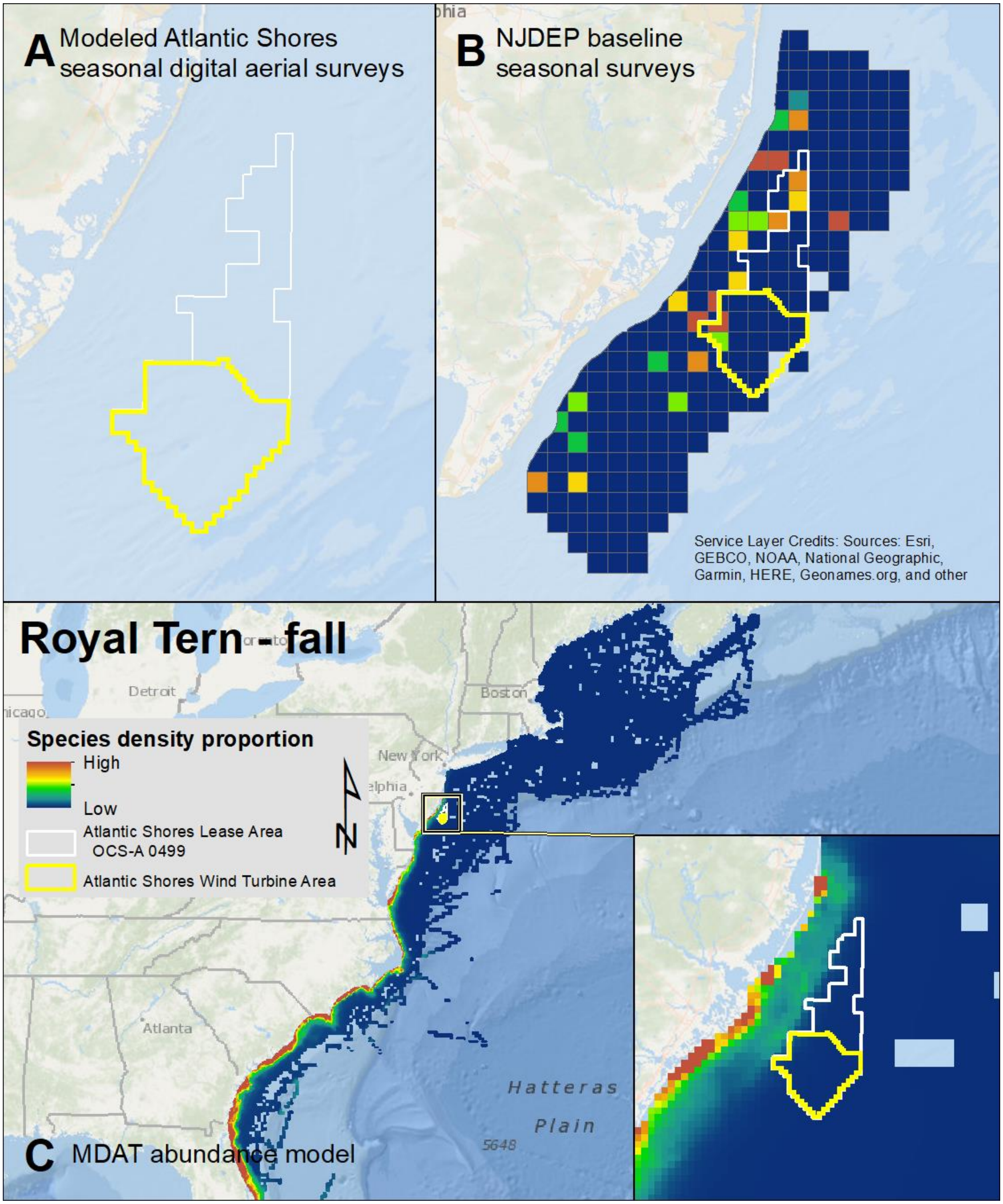

Map 147. Fall Royal Tern modeled density proportions in the Atlantic Shores seasonal digital aerial surveys (A), density proportions in the NJDEP baseline survey data (B), and the MDAT data at local and regional scales (C). The scale for all maps is representative of relative spatial variation in the sites within the season for each data source.

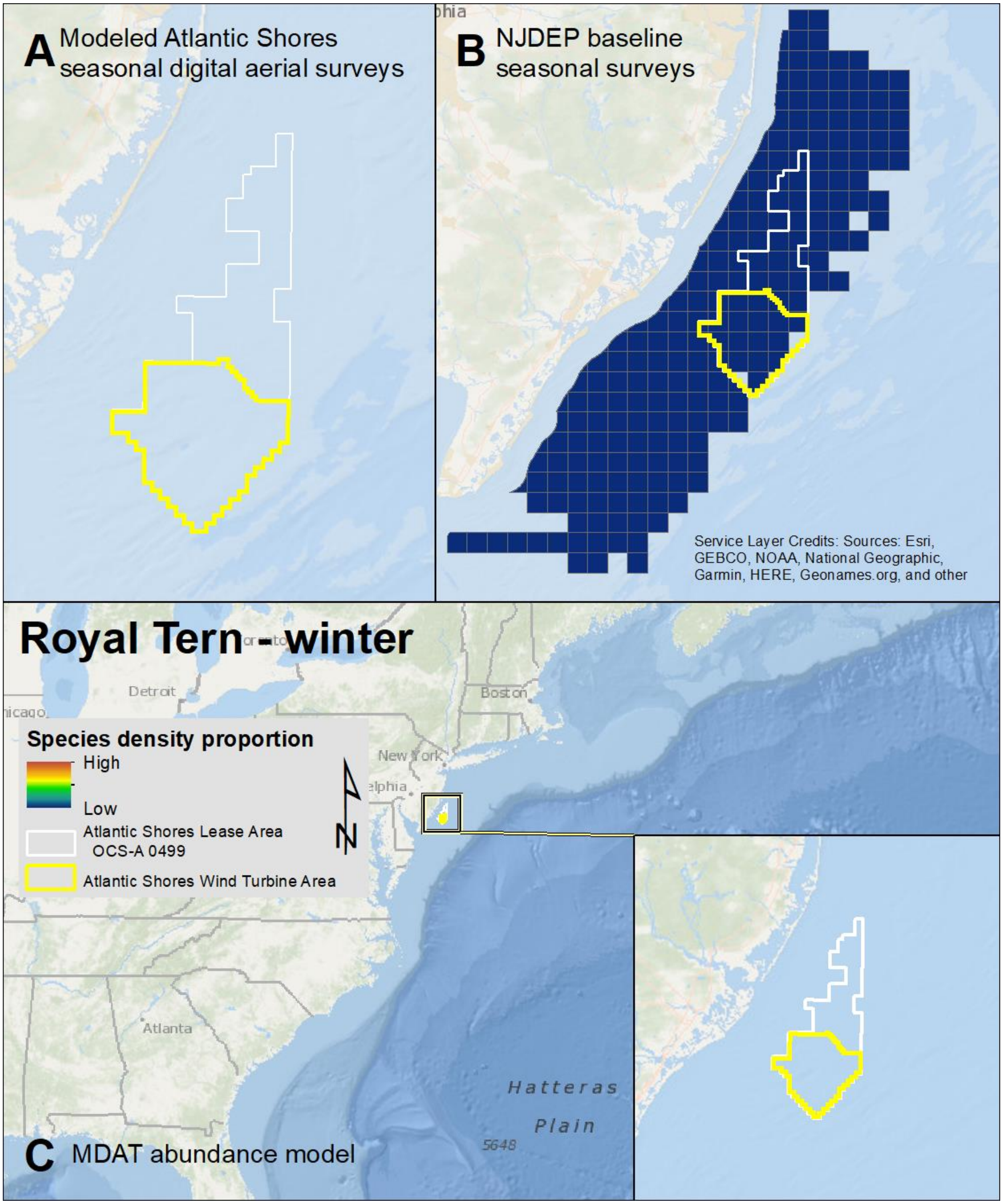

Map 148. Winter Royal Tern modeled density proportions in the Atlantic Shores seasonal digital aerial surveys (A), density proportions in the NJDEP baseline survey data (B), and the MDAT data at local and regional scales (C). The scale for all maps is representative of relative spatial variation in the sites within the season for each data source.

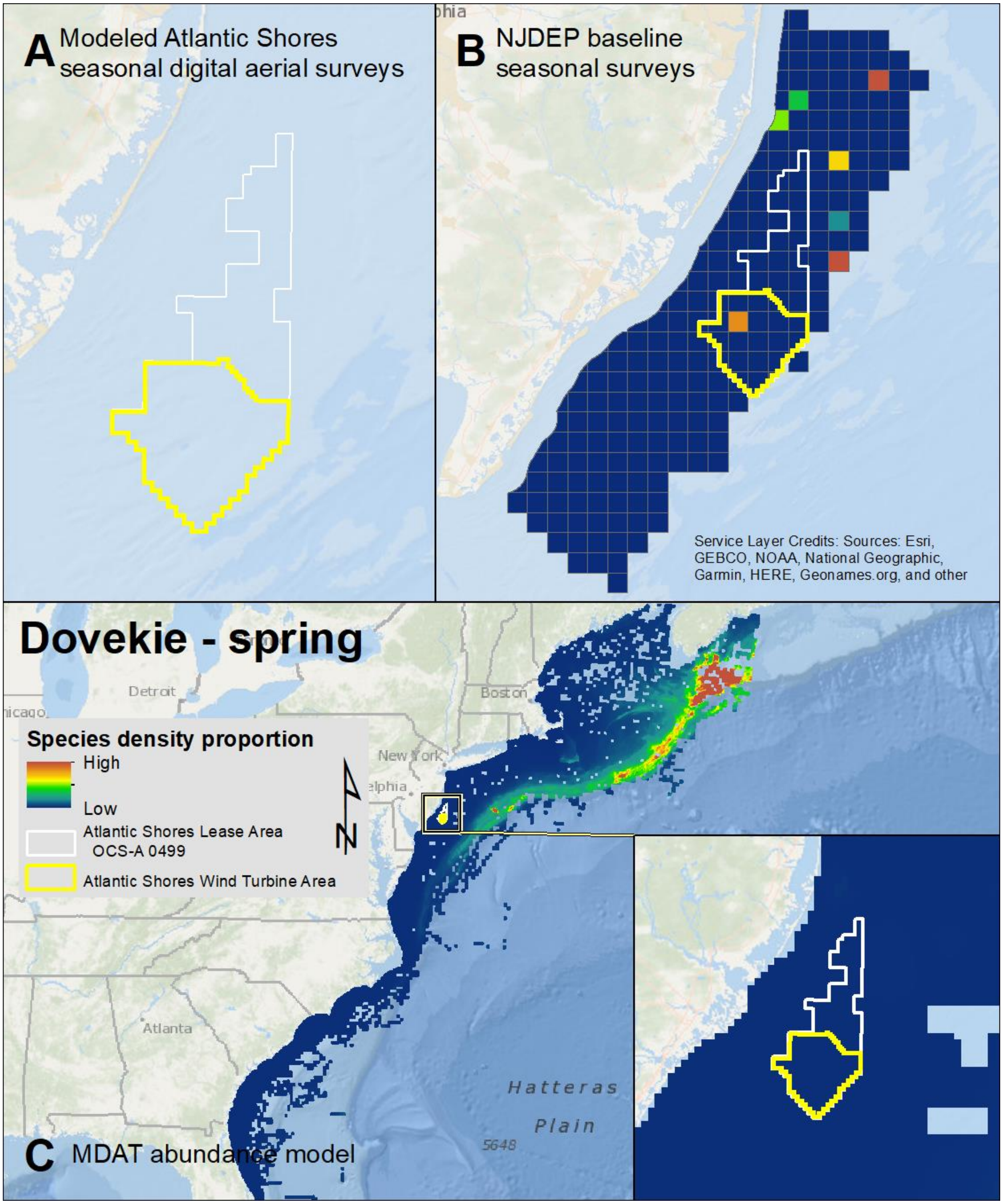

Map 149. Spring Dovekie modeled density proportions in the Atlantic Shores seasonal digital aerial surveys (A), density proportions in the NJDEP baseline survey data (B), and the MDAT data at local and regional scales (C). The scale for all maps is representative of relative spatial variation in the sites within the season for each data source.

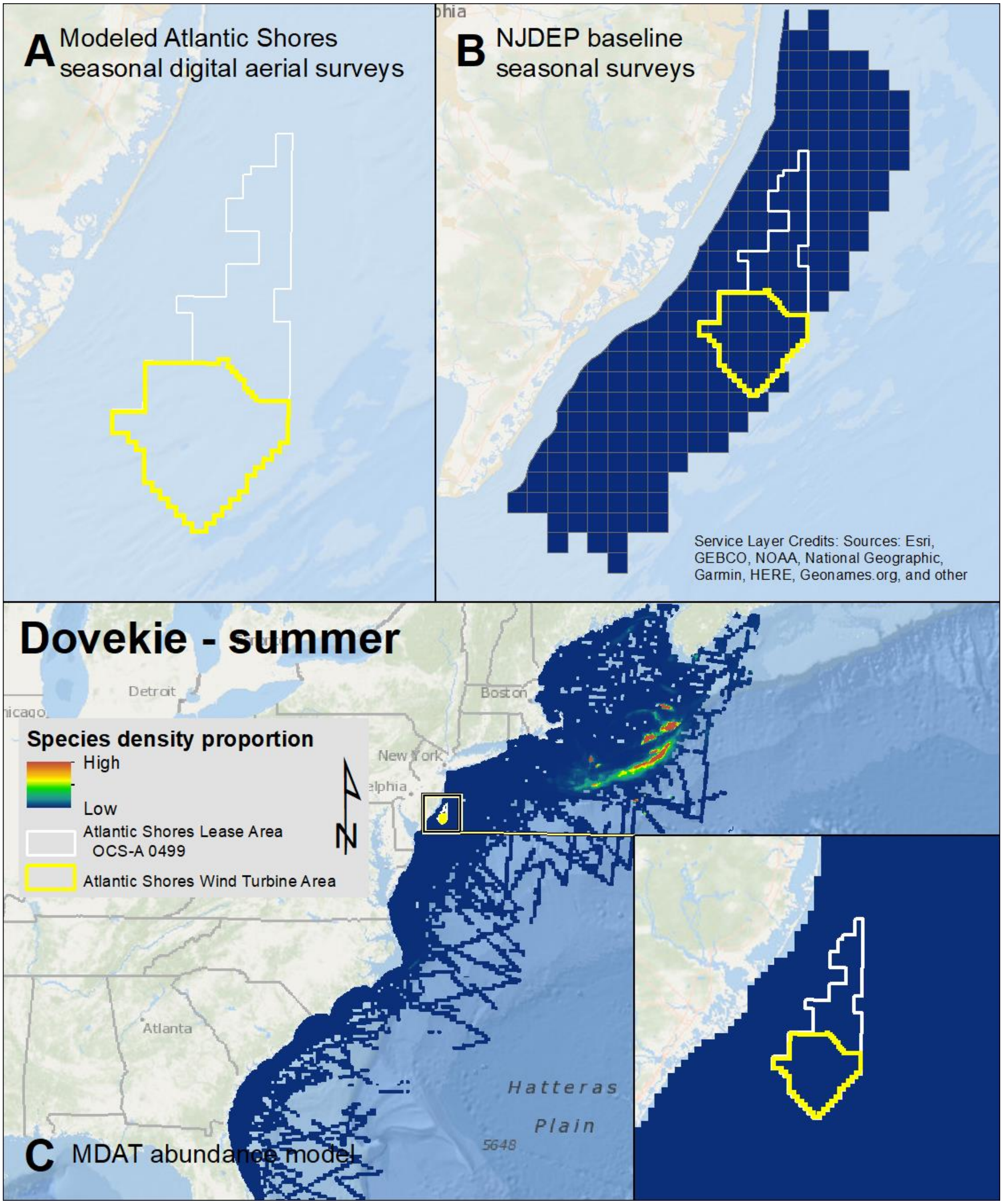

Map 150. Summer Dovekie modeled density proportions in the Atlantic Shores seasonal digital aerial surveys (A), density proportions in the NJDEP baseline survey data (B), and the MDAT data at local and regional scales (C). The scale for all maps is representative of relative spatial variation in the sites within the season for each data source.

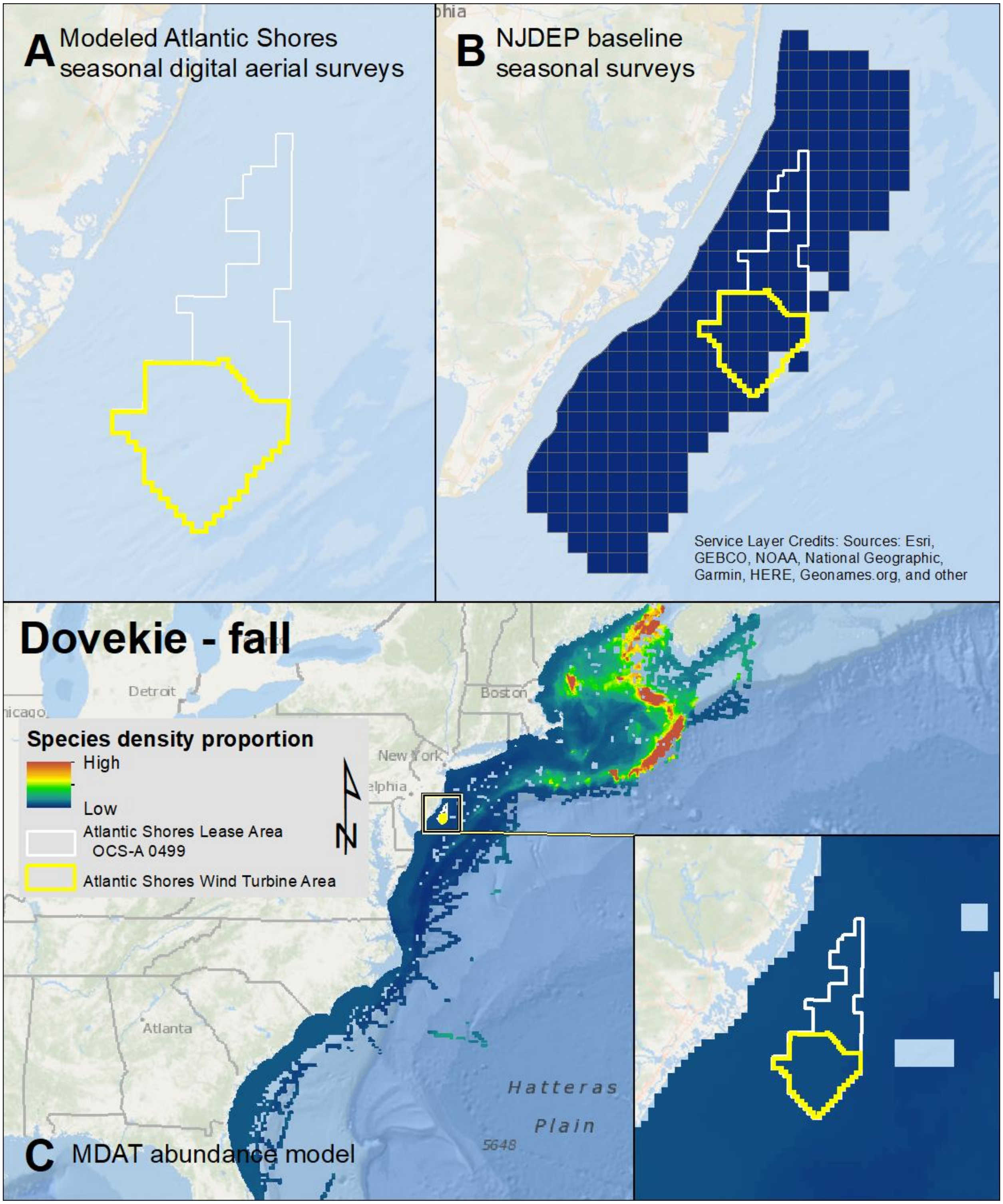

Map 151. Fall Dovekie modeled density proportions in the Atlantic Shores seasonal digital aerial surveys (A), density proportions in the NJDEP baseline survey data (B), and the MDAT data at local and regional scales (C). The scale for all maps is representative of relative spatial variation in the sites within the season for each data source.

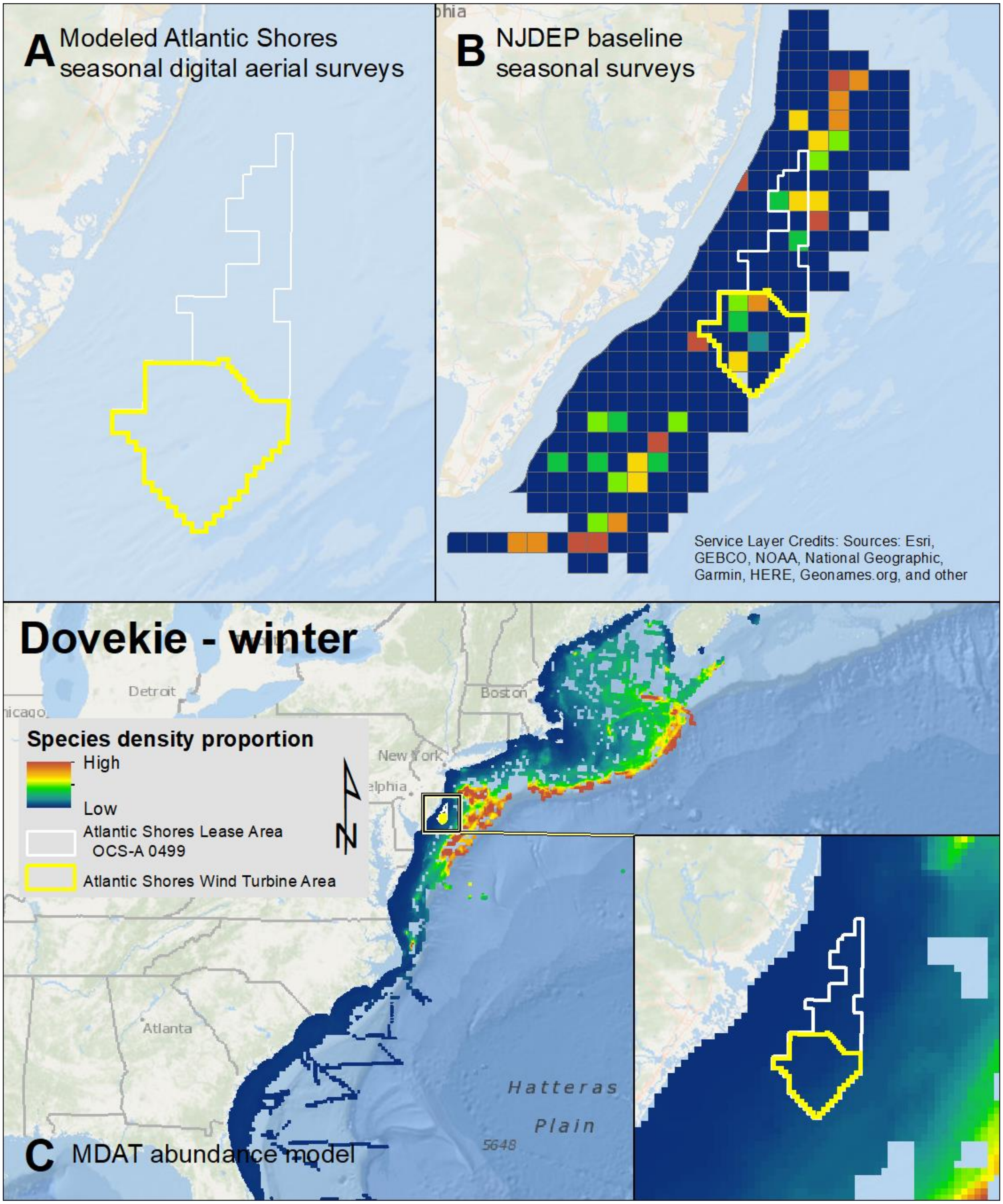

Map 152. Winter Dovekie modeled density proportions in the Atlantic Shores seasonal digital aerial surveys (A), density proportions in the NJDEP baseline survey data (B), and the MDAT data at local and regional scales (C). The scale for all maps is representative of relative spatial variation in the sites within the season for each data source.

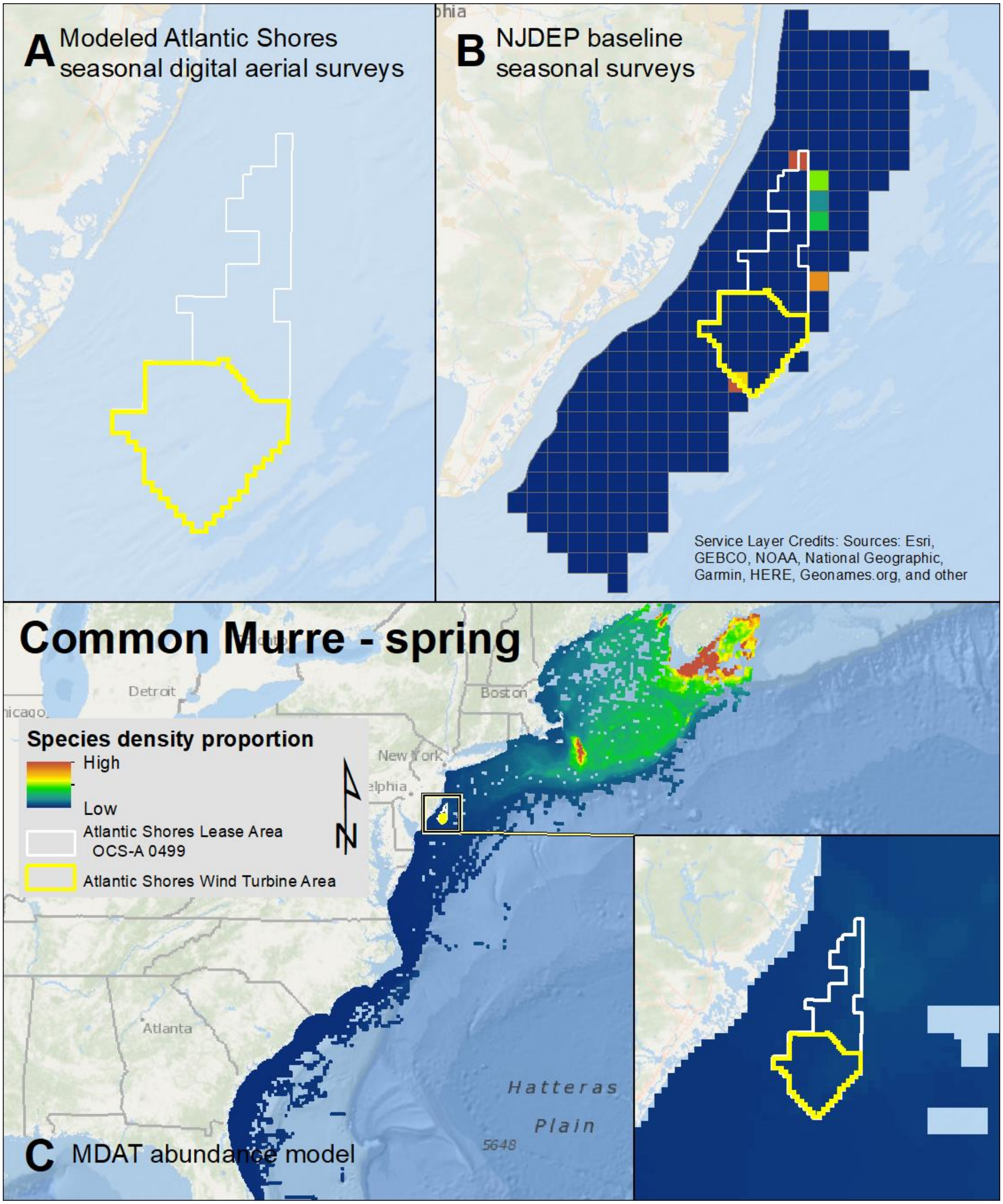

Map 153. Spring Common Murre modeled density proportions in the Atlantic Shores seasonal digital aerial surveys (A), density proportions in the NJDEP baseline survey data (B), and the MDAT data at local and regional scales (C). The scale for all maps is representative of relative spatial variation in the sites within the season for each data source.

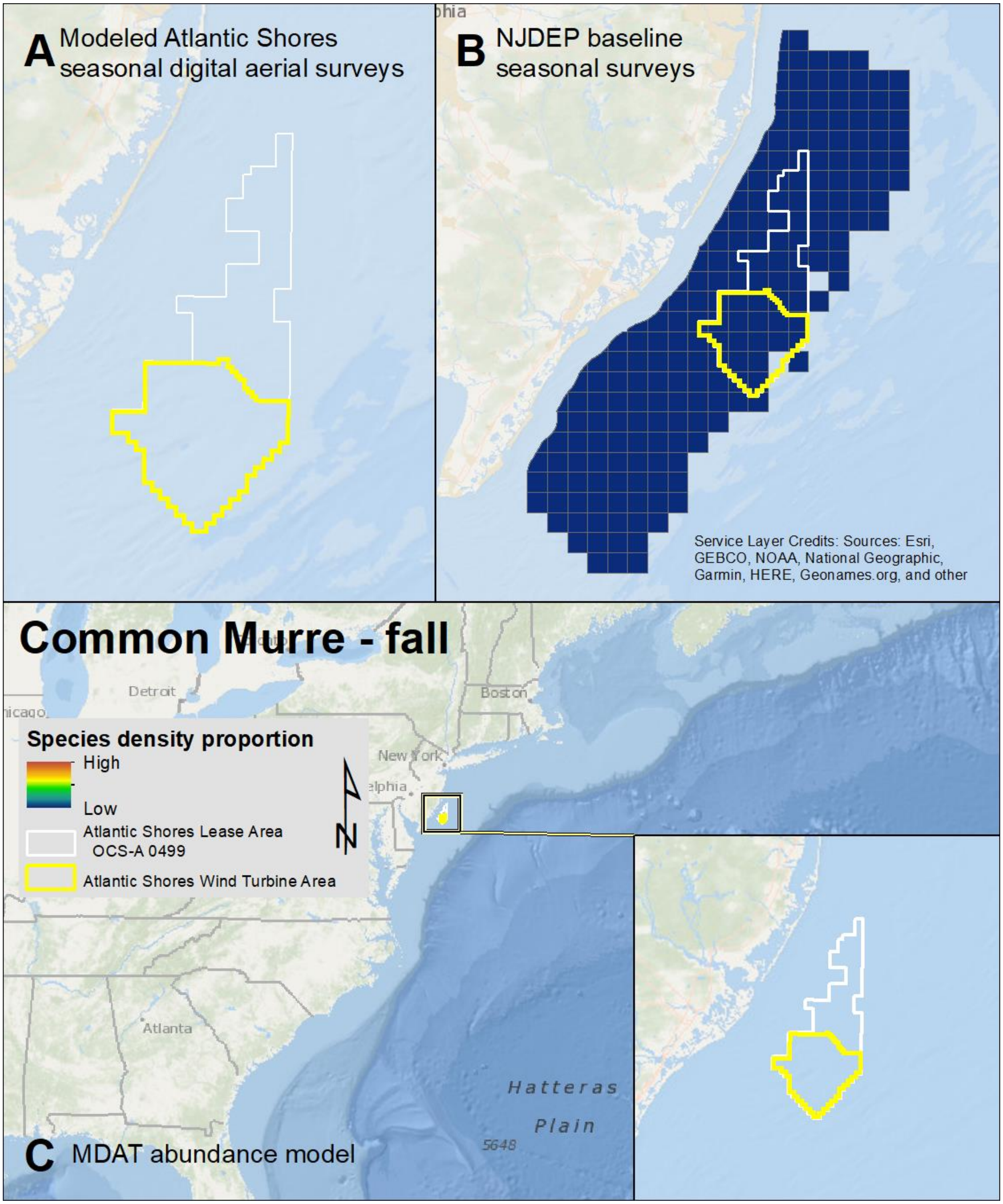

Map 154. Fall Common Murre modeled density proportions in the Atlantic Shores seasonal digital aerial surveys (A), density proportions in the NJDEP baseline survey data (B), and the MDAT data at local and regional scales (C). The scale for all maps is representative of relative spatial variation in the sites within the season for each data source.

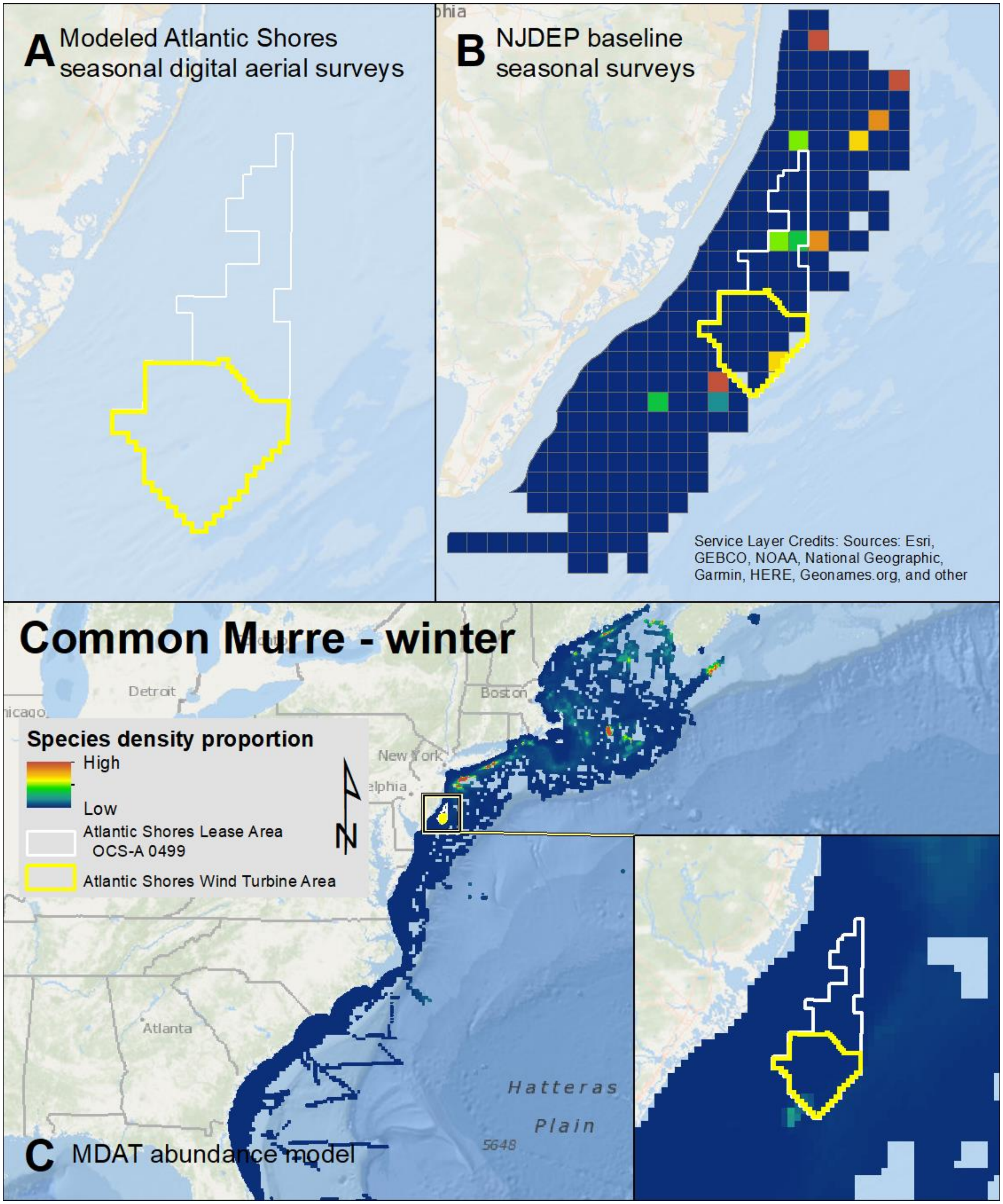

Map 155. Winter Common Murre modeled density proportions in the Atlantic Shores seasonal digital aerial surveys (A), density proportions in the NJDEP baseline survey data (B), and the MDAT data at local and regional scales (C). The scale for all maps is representative of relative spatial variation in the sites within the season for each data source.

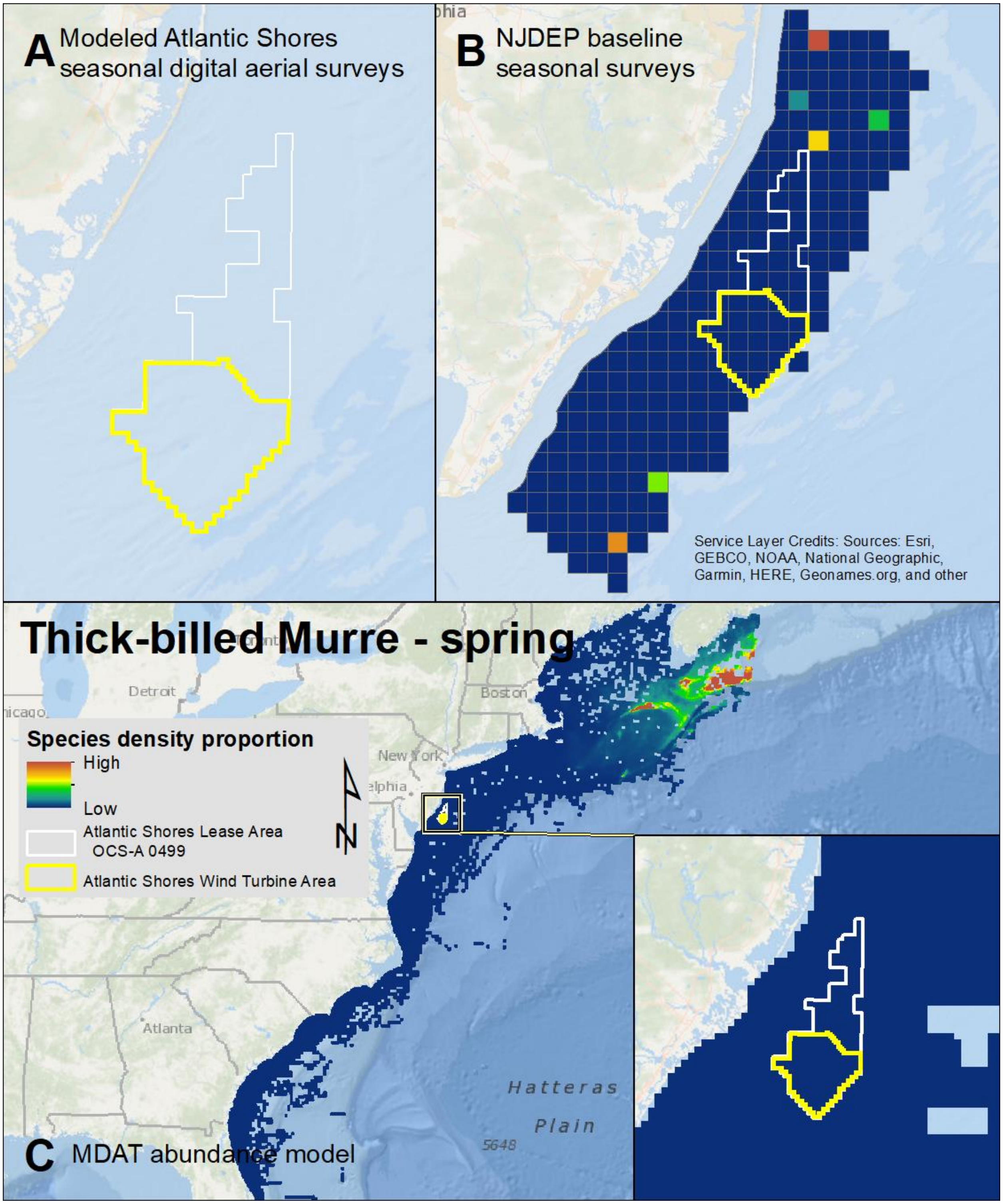

Map 156. Spring Thick-billed Murre modeled density proportions in the Atlantic Shores seasonal digital aerial surveys (A), density proportions in the NJDEP baseline survey data (B), and the MDAT data at local and regional scales (C). The scale for all maps is representative of relative spatial variation in the sites within the season for each data source.

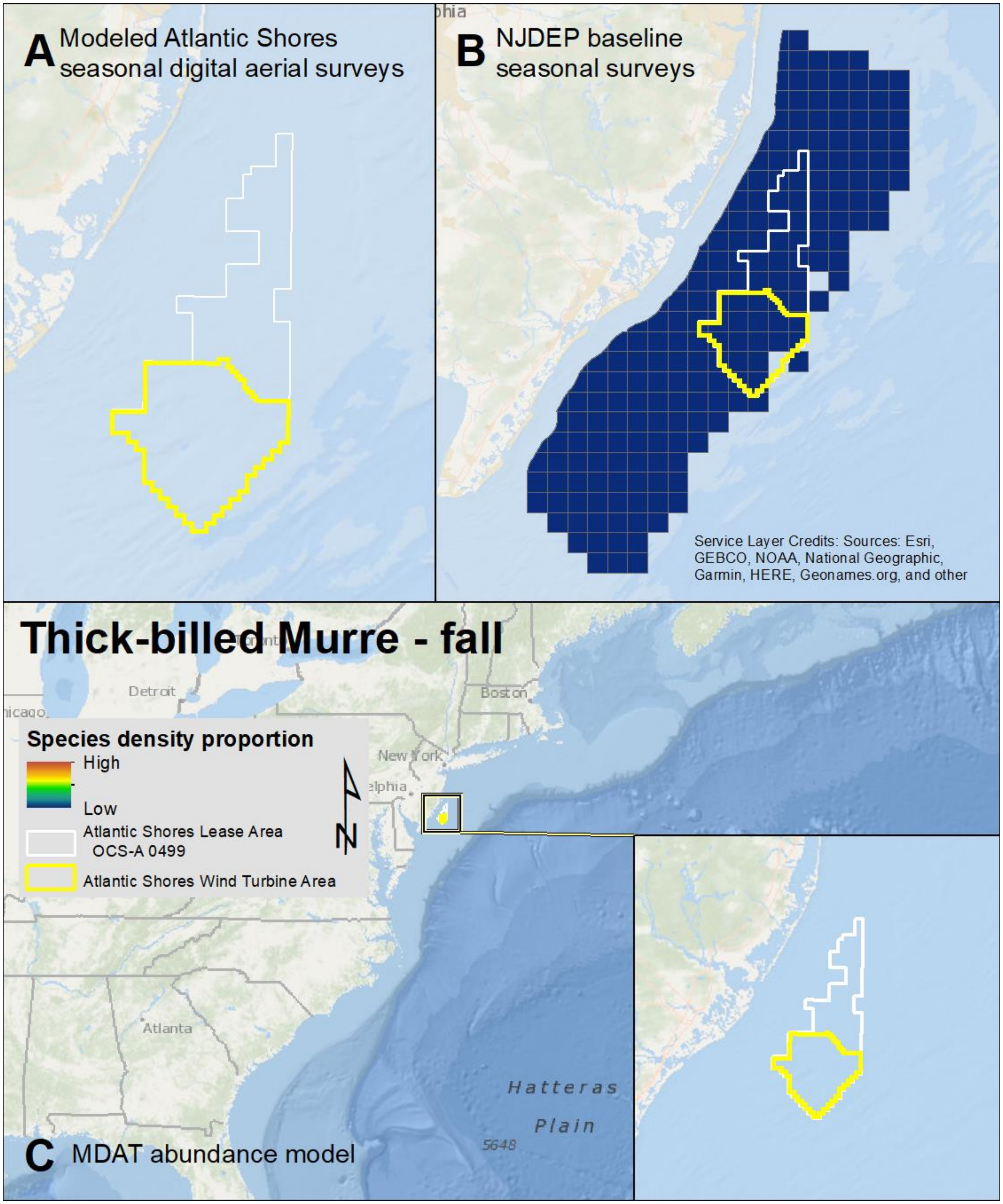

Map 157. Fall Thick-billed Murre modeled density proportions in the Atlantic Shores seasonal digital aerial surveys (A), density proportions in the NJDEP baseline survey data (B), and the MDAT data at local and regional scales (C). The scale for all maps is representative of relative spatial variation in the sites within the season for each data source.

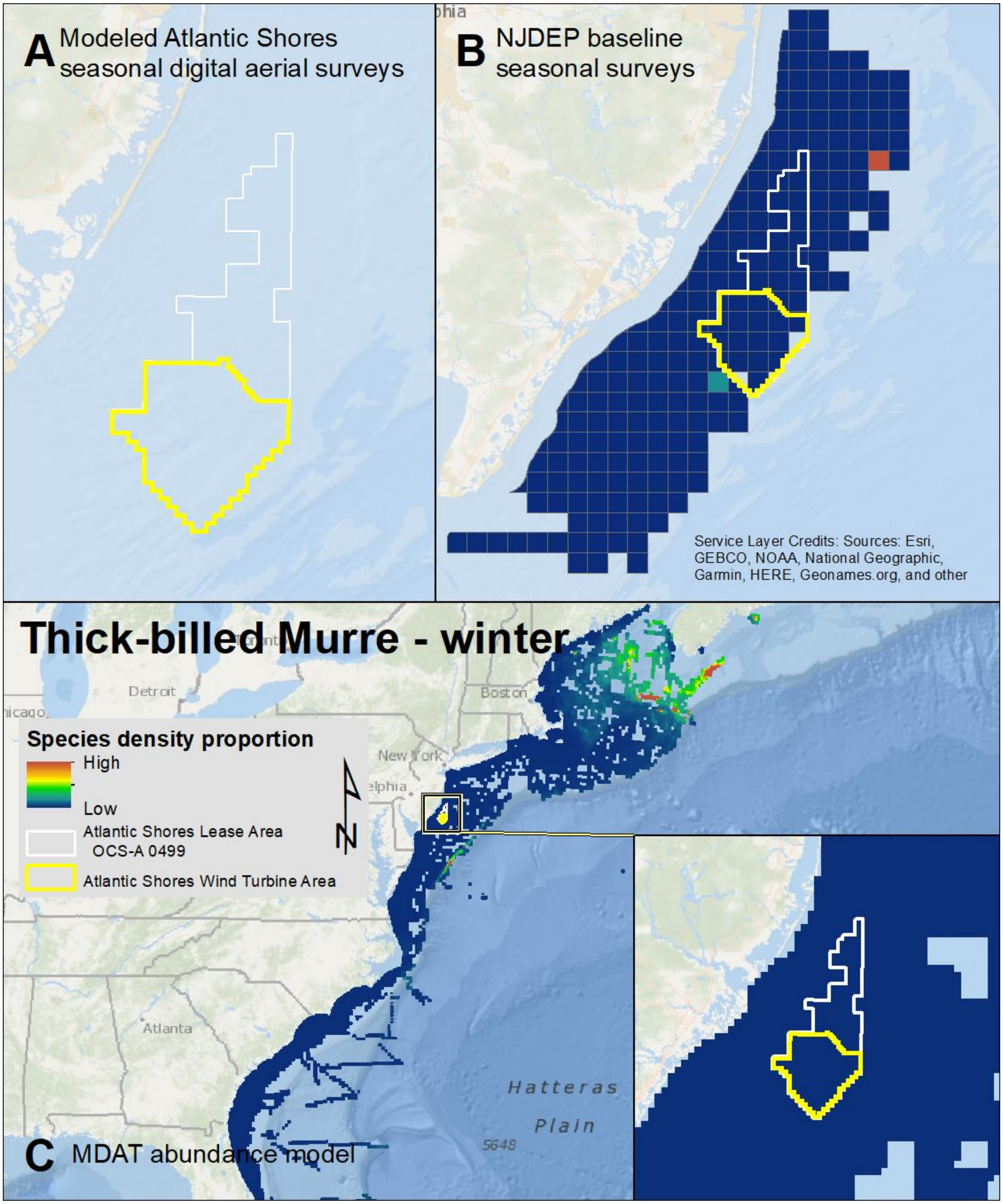

Map 158. Winter Thick-billed Murre modeled density proportions in the Atlantic Shores seasonal digital aerial surveys (A), density proportions in the NJDEP baseline survey data (B), and the MDAT data at local and regional scales (C). The scale for all maps is representative of relative spatial variation in the sites within the season for each data source.

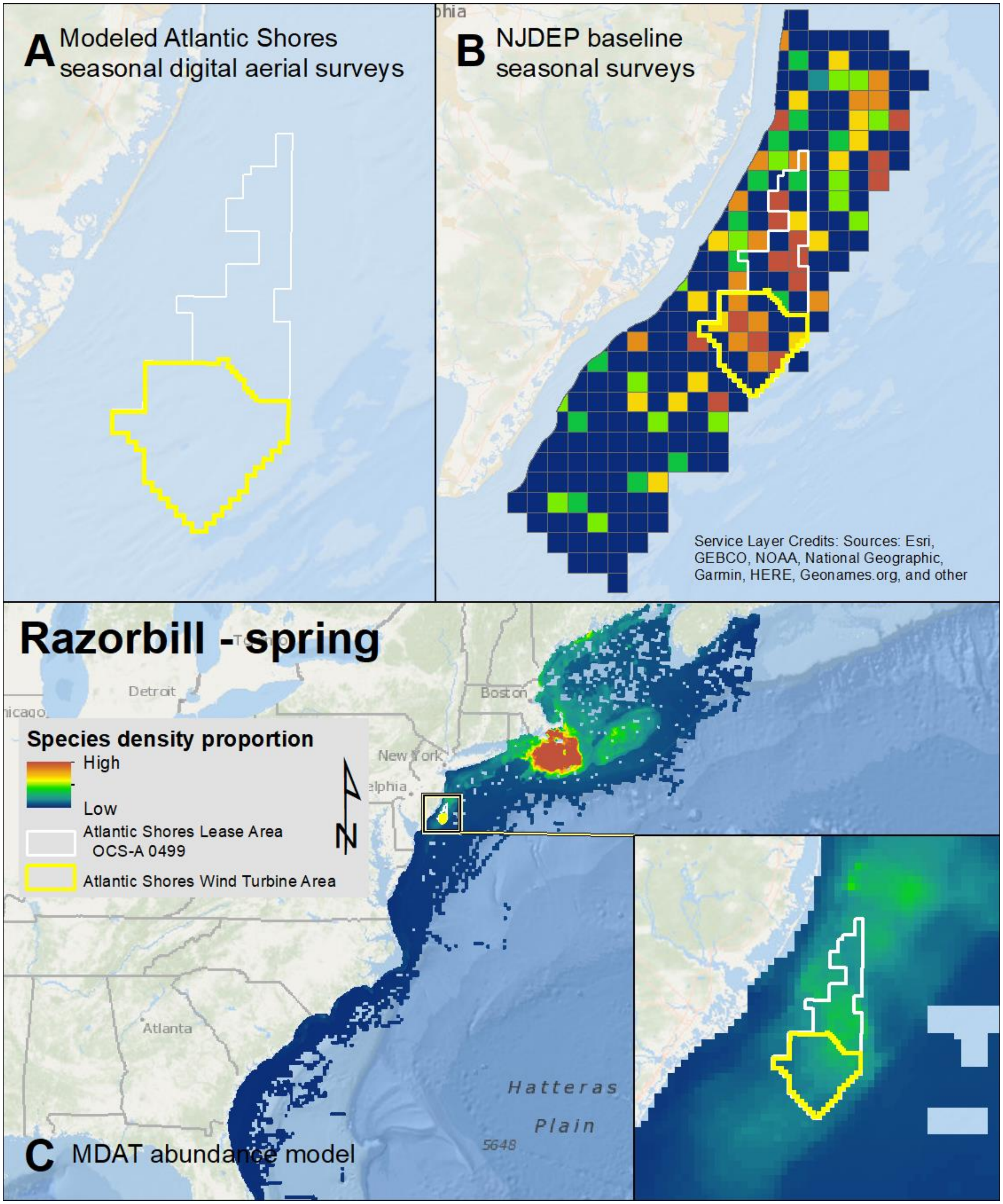

Map 159. Spring Razorbill modeled density proportions in the Atlantic Shores seasonal digital aerial surveys (A), density proportions in the NJDEP baseline survey data (B), and the MDAT data at local and regional scales (C). The scale for all maps is representative of relative spatial variation in the sites within the season for each data source.

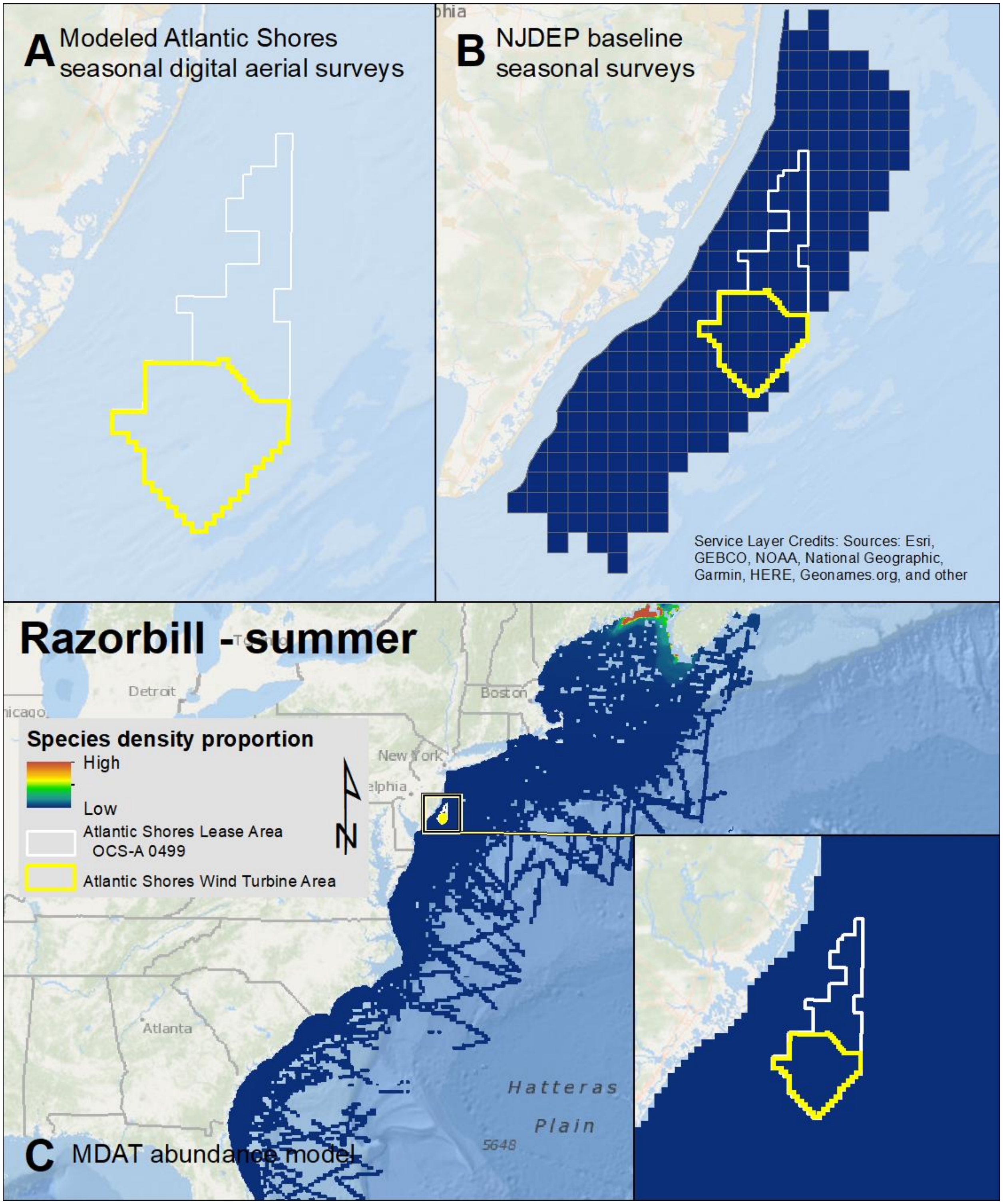

Map 160. Summer Razorbill modeled density proportions in the Atlantic Shores seasonal digital aerial surveys (A), density proportions in the NJDEP baseline survey data (B), and the MDAT data at local and regional scales (C). The scale for all maps is representative of relative spatial variation in the sites within the season for each data source.

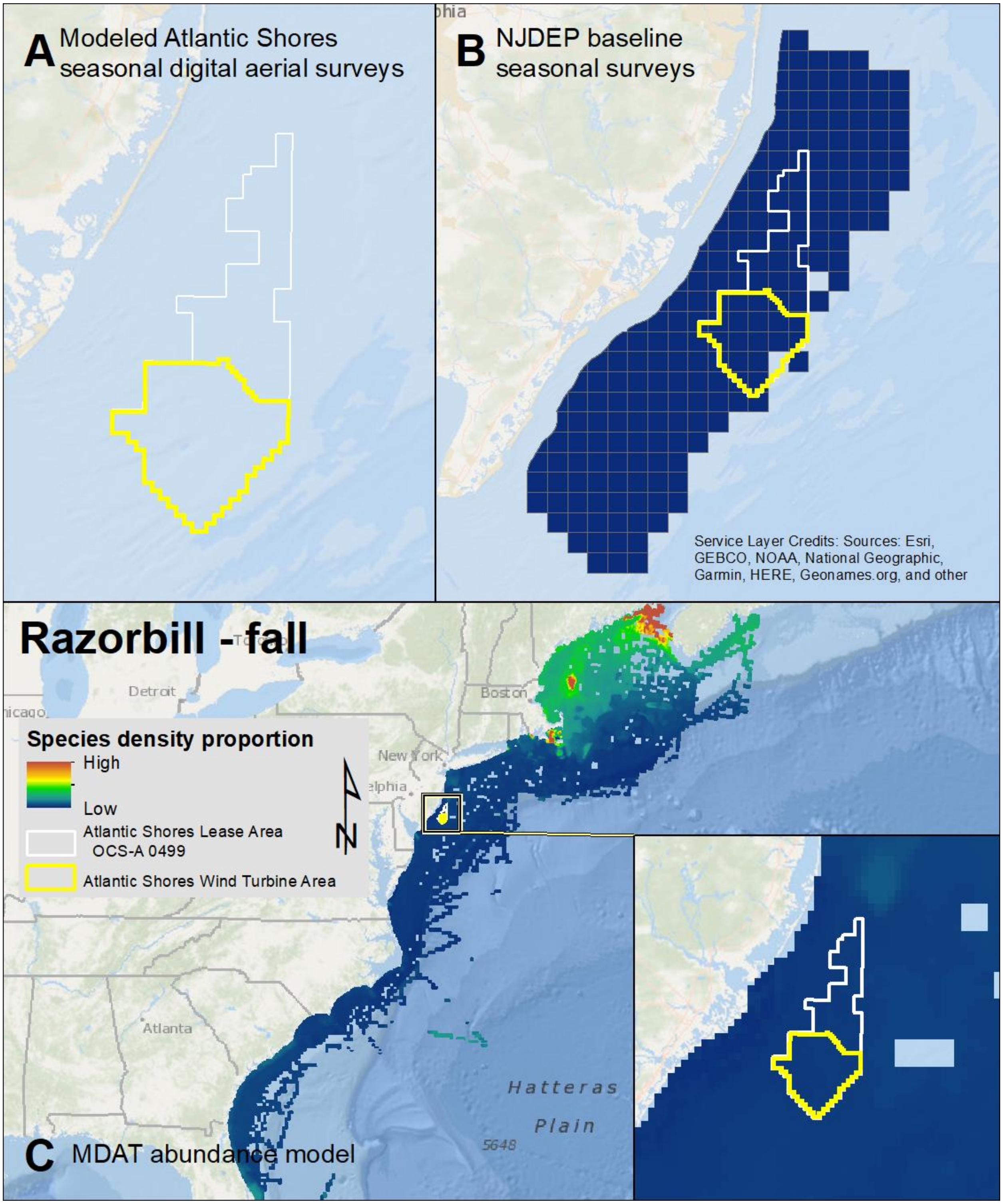

Map 161. Fall Razorbill modeled density proportions in the Atlantic Shores seasonal digital aerial surveys (A), density proportions in the NJDEP baseline survey data (B), and the MDAT data at local and regional scales (C). The scale for all maps is representative of relative spatial variation in the sites within the season for each data source.

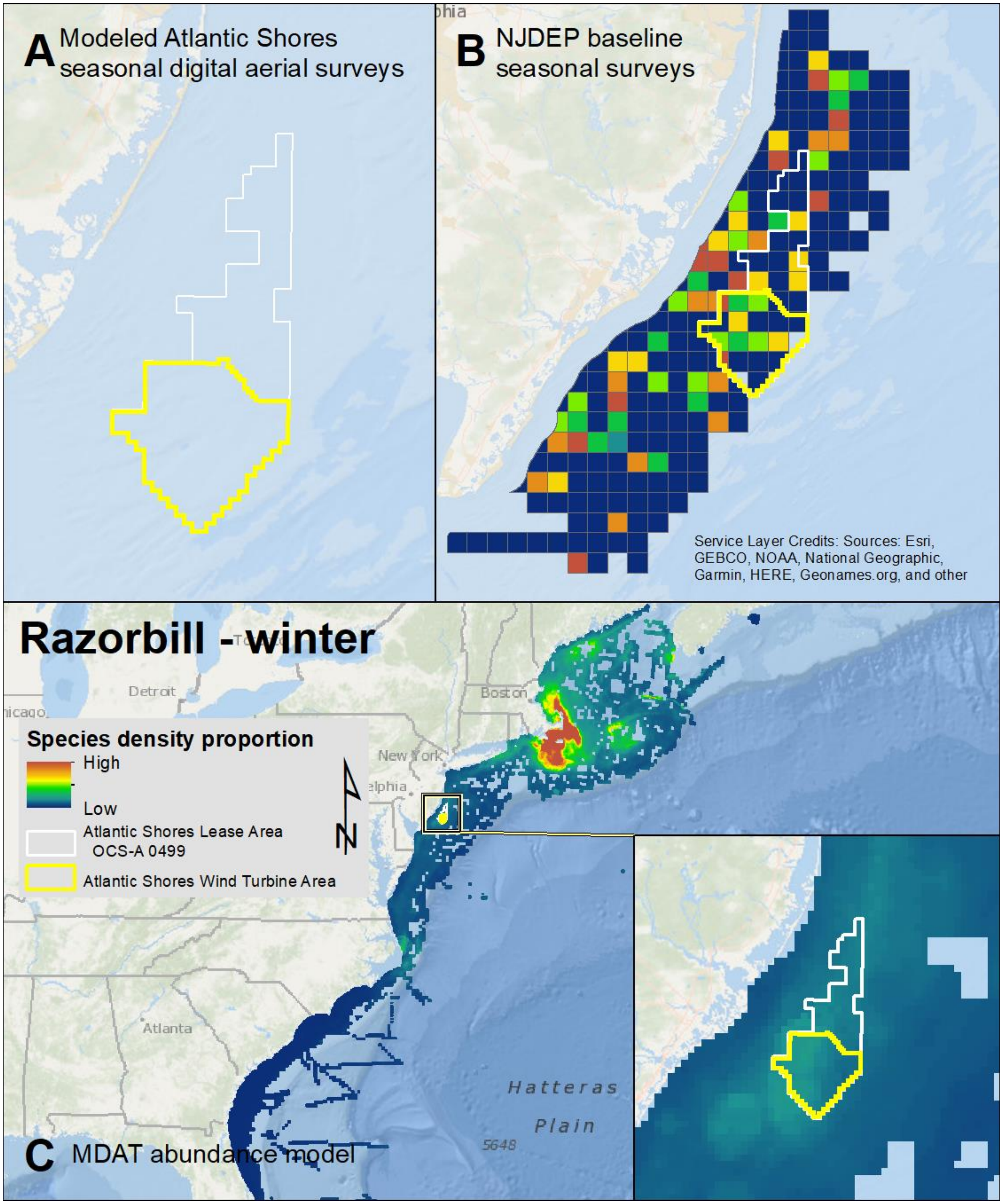

Map 162. Winter Razorbill modeled density proportions in the Atlantic Shores seasonal digital aerial surveys (A), density proportions in the NJDEP baseline survey data (B), and the MDAT data at local and regional scales (C). The scale for all maps is representative of relative spatial variation in the sites within the season for each data source.

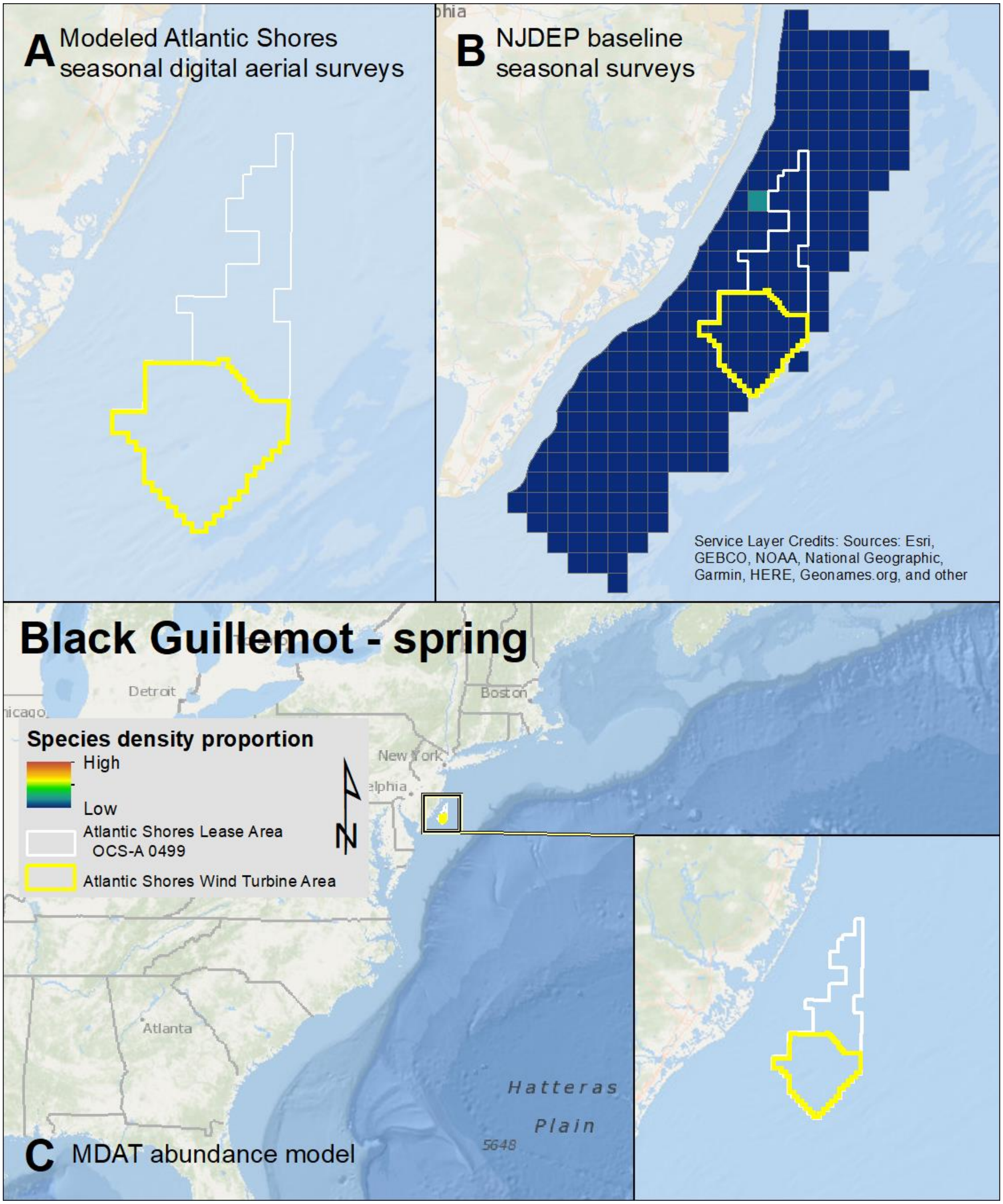

Map 163. Spring Black Guillemot modeled density proportions in the Atlantic Shores seasonal digital aerial surveys (A), density proportions in the NJDEP baseline survey data (B), and the MDAT data at local and regional scales (C). The scale for all maps is representative of relative spatial variation in the sites within the season for each data source.

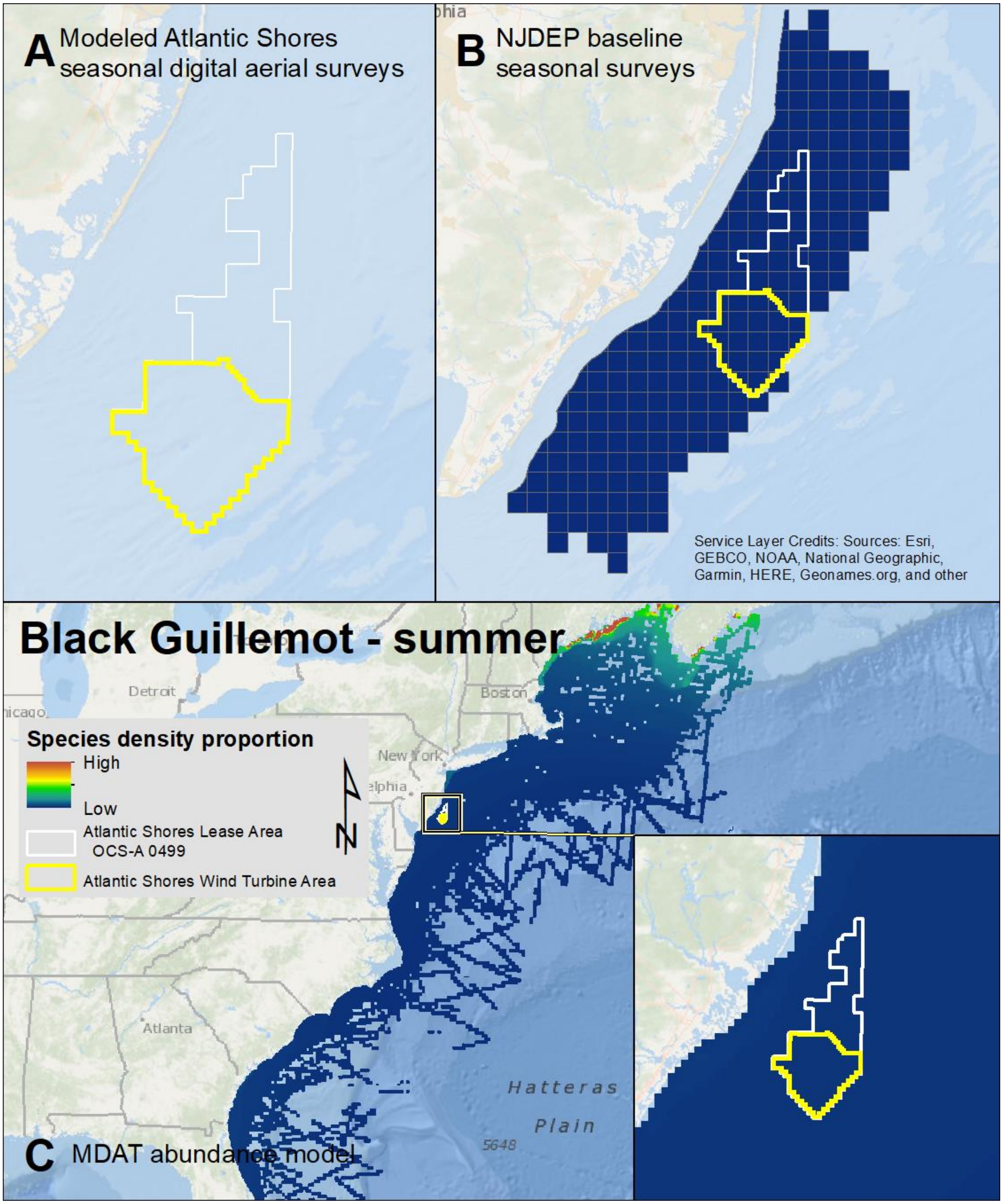

Map 164. Summer Black Guillemot modeled density proportions in the Atlantic Shores seasonal digital aerial surveys (A), density proportions in the NJDEP baseline survey data (B), and the MDAT data at local and regional scales (C). The scale for all maps is representative of relative spatial variation in the sites within the season for each data source.

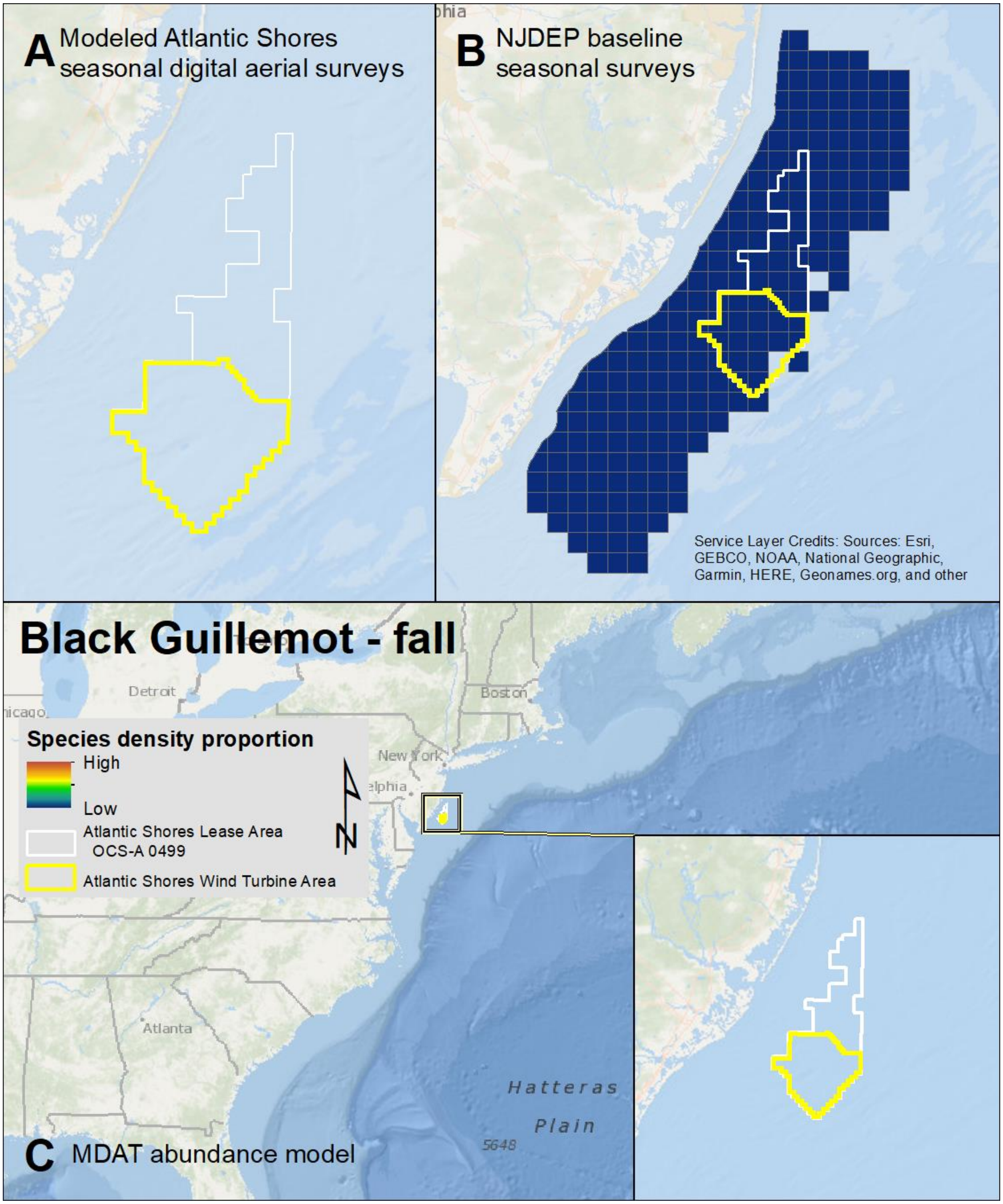

Map 165. Fall Black Guillemot modeled density proportions in the Atlantic Shores seasonal digital aerial surveys (A), density proportions in the NJDEP baseline survey data (B), and the MDAT data at local and regional scales (C). The scale for all maps is representative of relative spatial variation in the sites within the season for each data source.

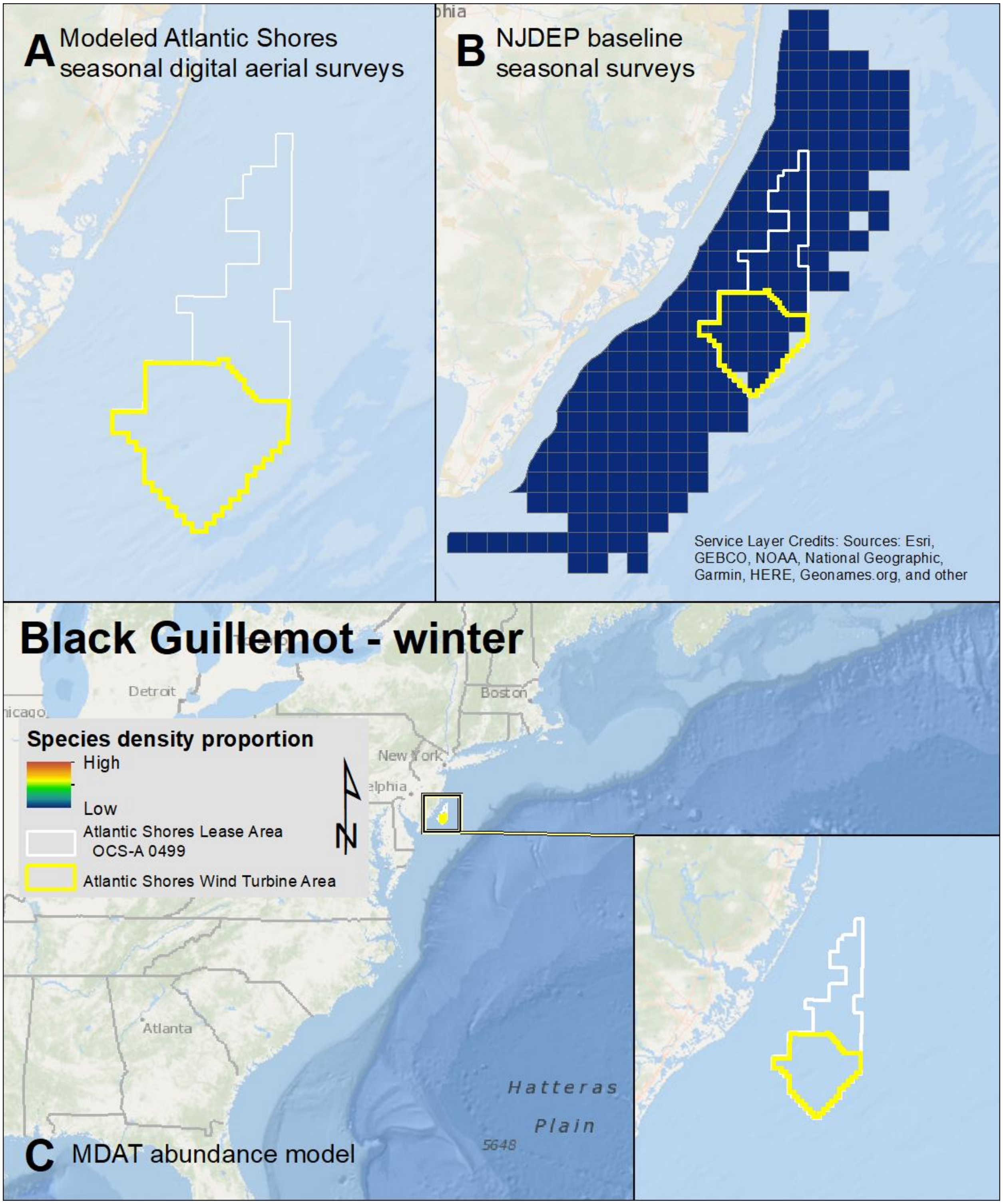

Map 166. Winter Black Guillemot modeled density proportions in the Atlantic Shores seasonal digital aerial surveys (A), density proportions in the NJDEP baseline survey data (B), and the MDAT data at local and regional scales (C). The scale for all maps is representative of relative spatial variation in the sites within the season for each data source.

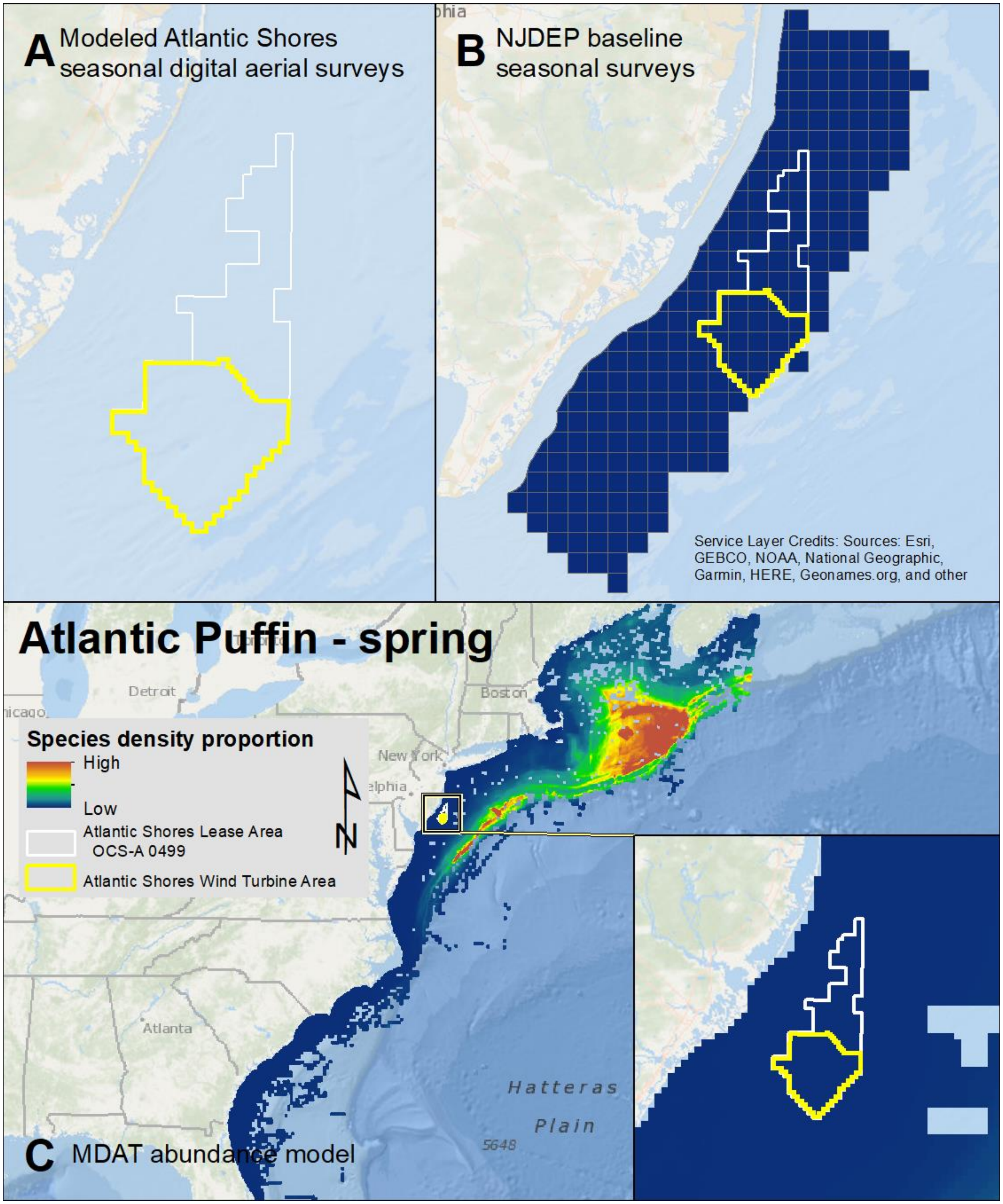

Map 167. Spring Atlantic Puffin modeled density proportions in the Atlantic Shores seasonal digital aerial surveys (A), density proportions in the NJDEP baseline survey data (B), and the MDAT data at local and regional scales (C). The scale for all maps is representative of relative spatial variation in the sites within the season for each data source.

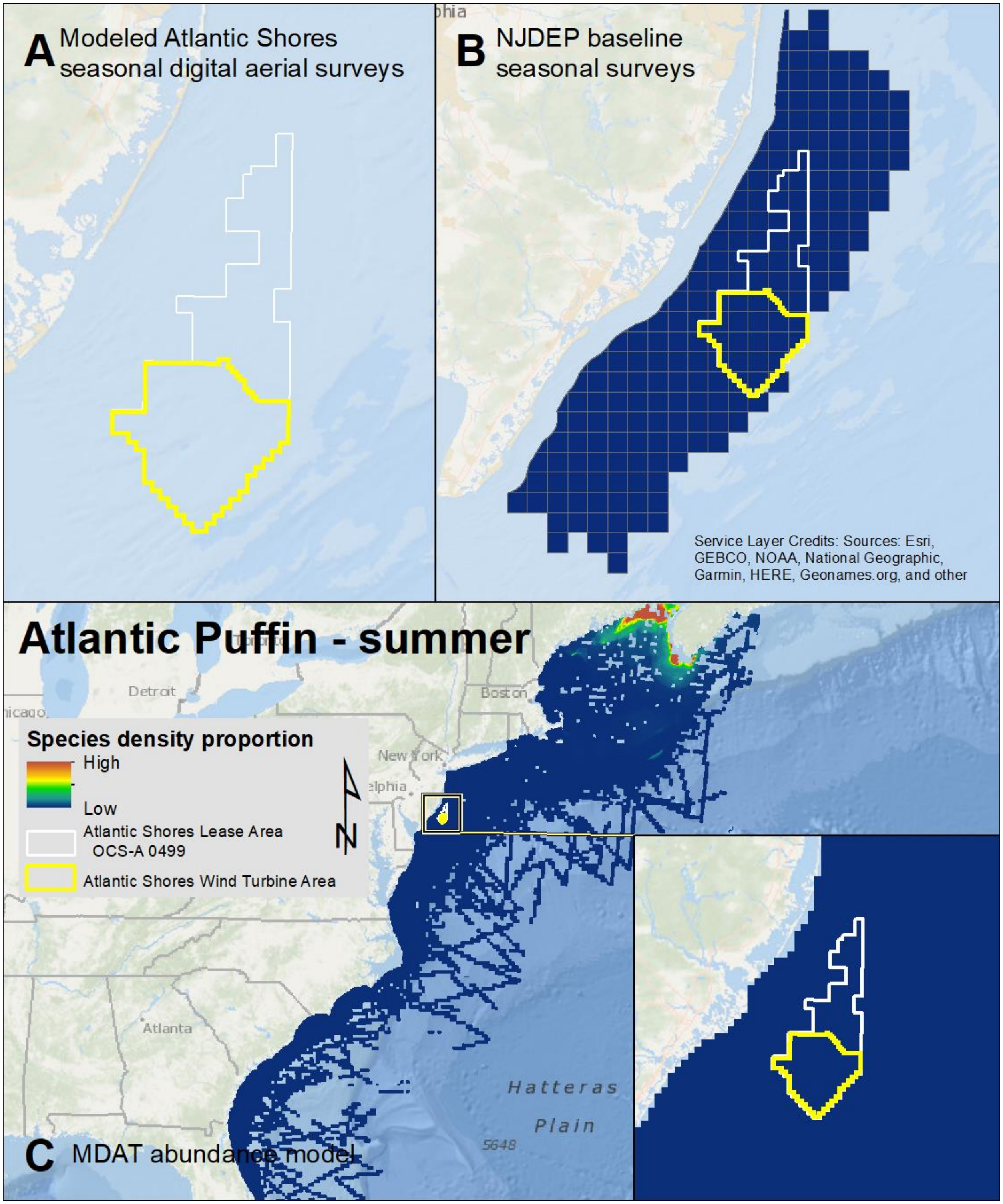

Map 168. Summer Atlantic Puffin modeled density proportions in the Atlantic Shores seasonal digital aerial surveys (A), density proportions in the NJDEP baseline survey data (B), and the MDAT data at local and regional scales (C). The scale for all maps is representative of relative spatial variation in the sites within the season for each data source.

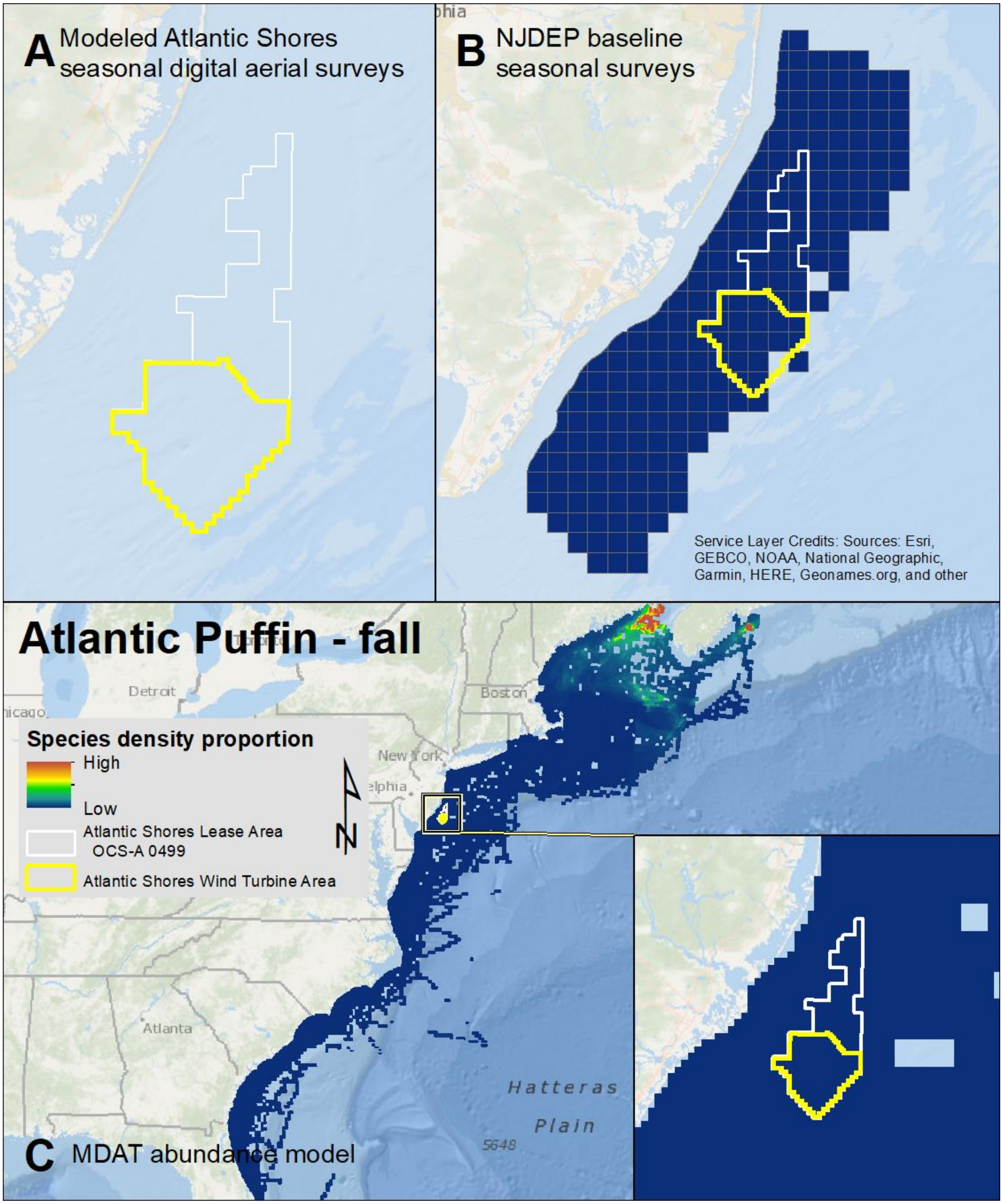

Map 169. Fall Atlantic Puffin modeled density proportions in the Atlantic Shores seasonal digital aerial surveys (A), density proportions in the NJDEP baseline survey data (B), and the MDAT data at local and regional scales (C). The scale for all maps is representative of relative spatial variation in the sites within the season for each data source.

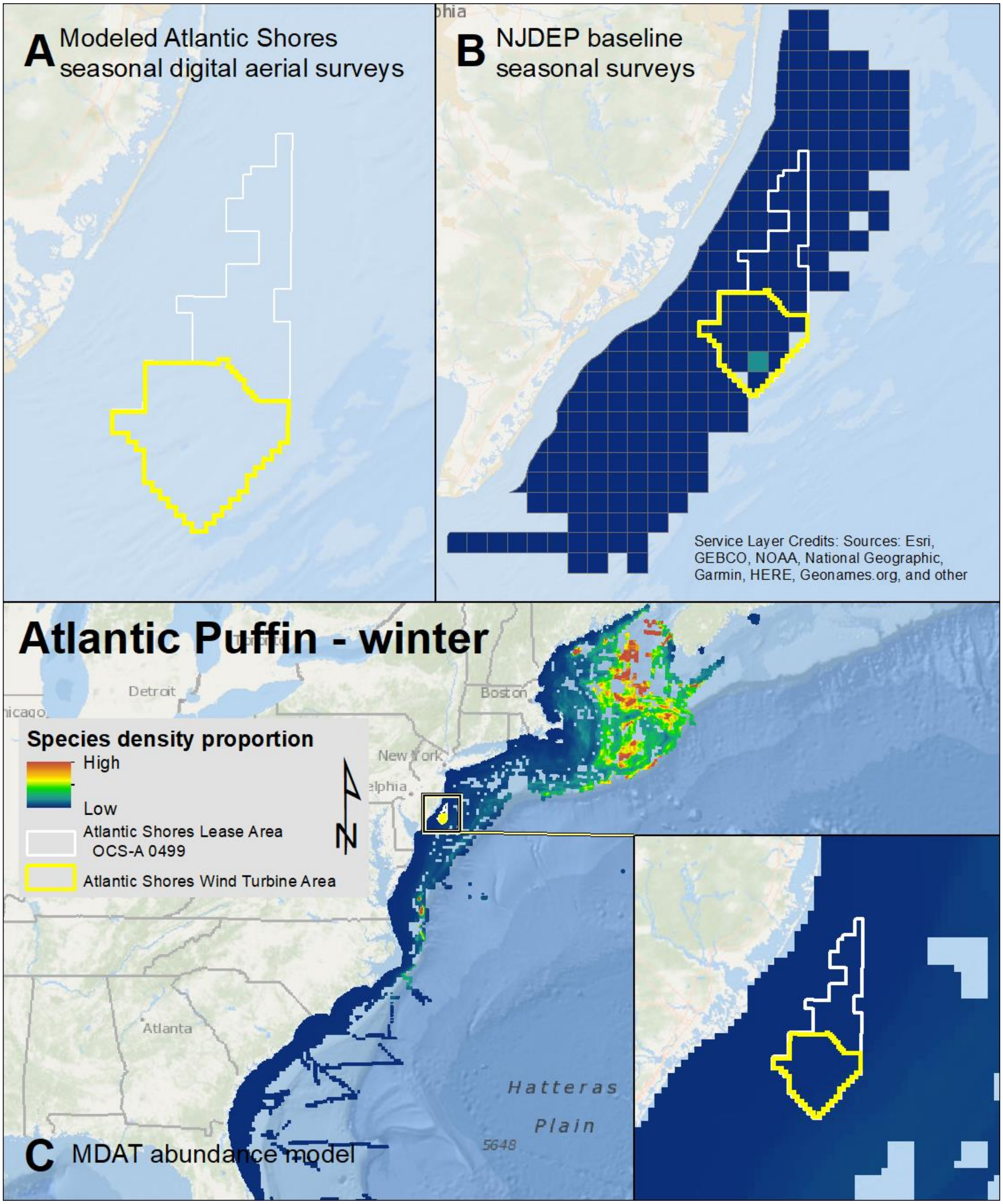

Map 170. Winter Atlantic Puffin modeled density proportions in the Atlantic Shores seasonal digital aerial surveys (A), density proportions in the NJDEP baseline survey data (B), and the MDAT data at local and regional scales (C). The scale for all maps is representative of relative spatial variation in the sites within the season for each data source.

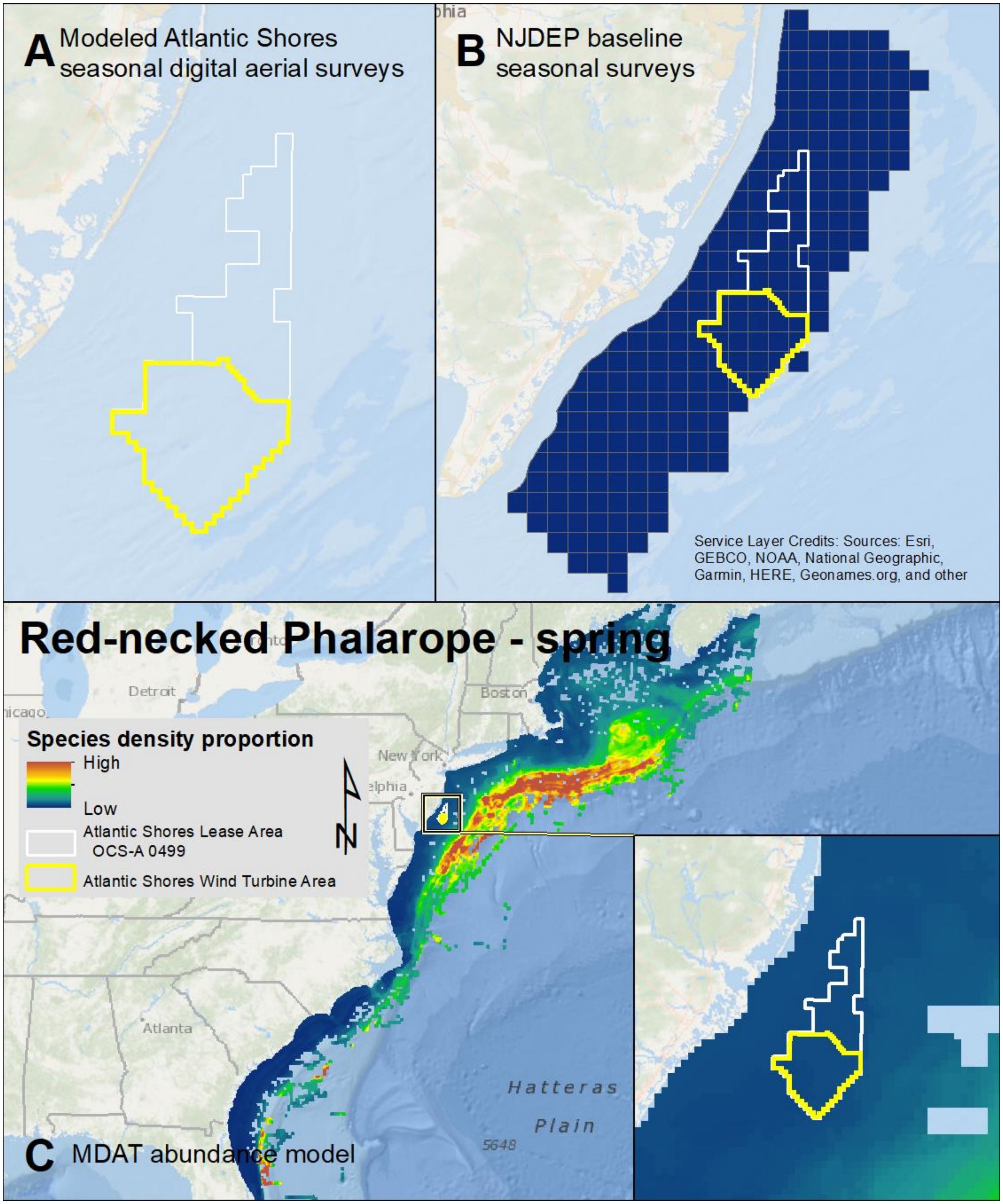

Map 171. Spring Red-necked Phalarope modeled density proportions in the Atlantic Shores seasonal digital aerial surveys (A), density proportions in the NJDEP baseline survey data (B), and the MDAT data at local and regional scales (C). The scale for all maps is representative of relative spatial variation in the sites within the season for each data source.

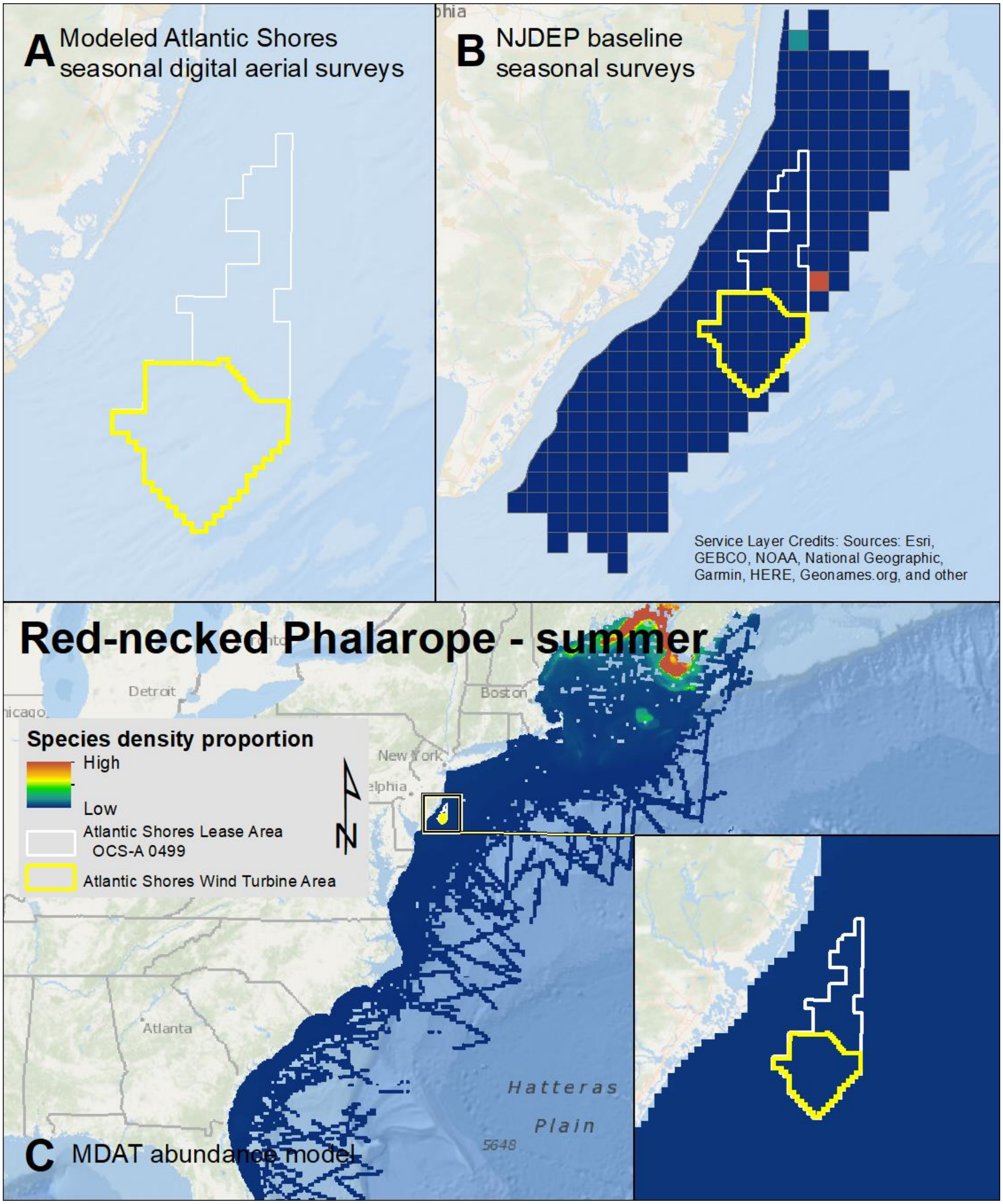

Map 172. Summer Red-necked Phalarope modeled density proportions in the Atlantic Shores seasonal digital aerial surveys (A), density proportions in the NJDEP baseline survey data (B), and the MDAT data at local and regional scales (C). The scale for all maps is representative of relative spatial variation in the sites within the season for each data source.

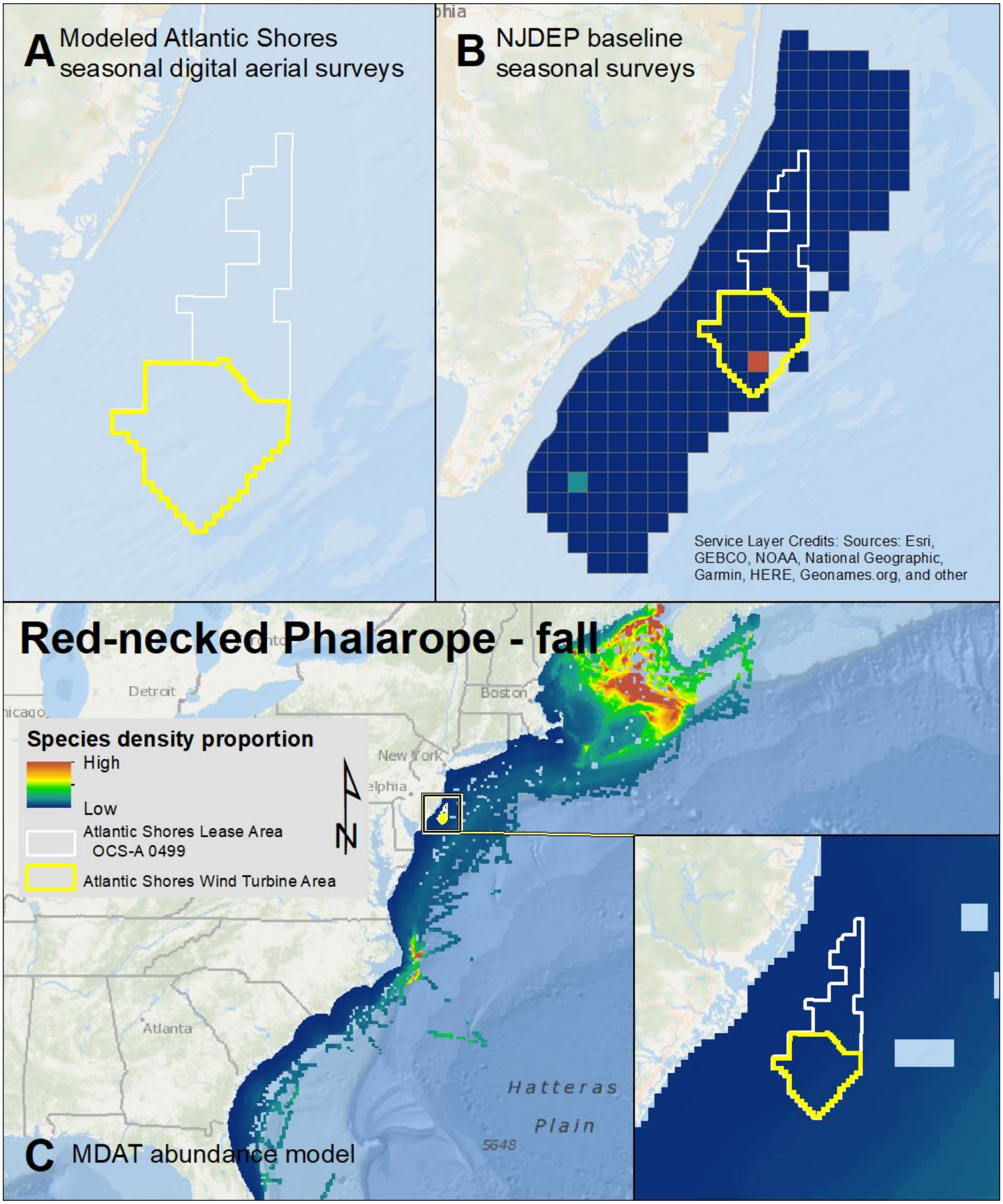

Map 173. Fall Red-necked Phalarope modeled density proportions in the Atlantic Shores seasonal digital aerial surveys (A), density proportions in the NJDEP baseline survey data (B), and the MDAT data at local and regional scales (C). The scale for all maps is representative of relative spatial variation in the sites within the season for each data source.

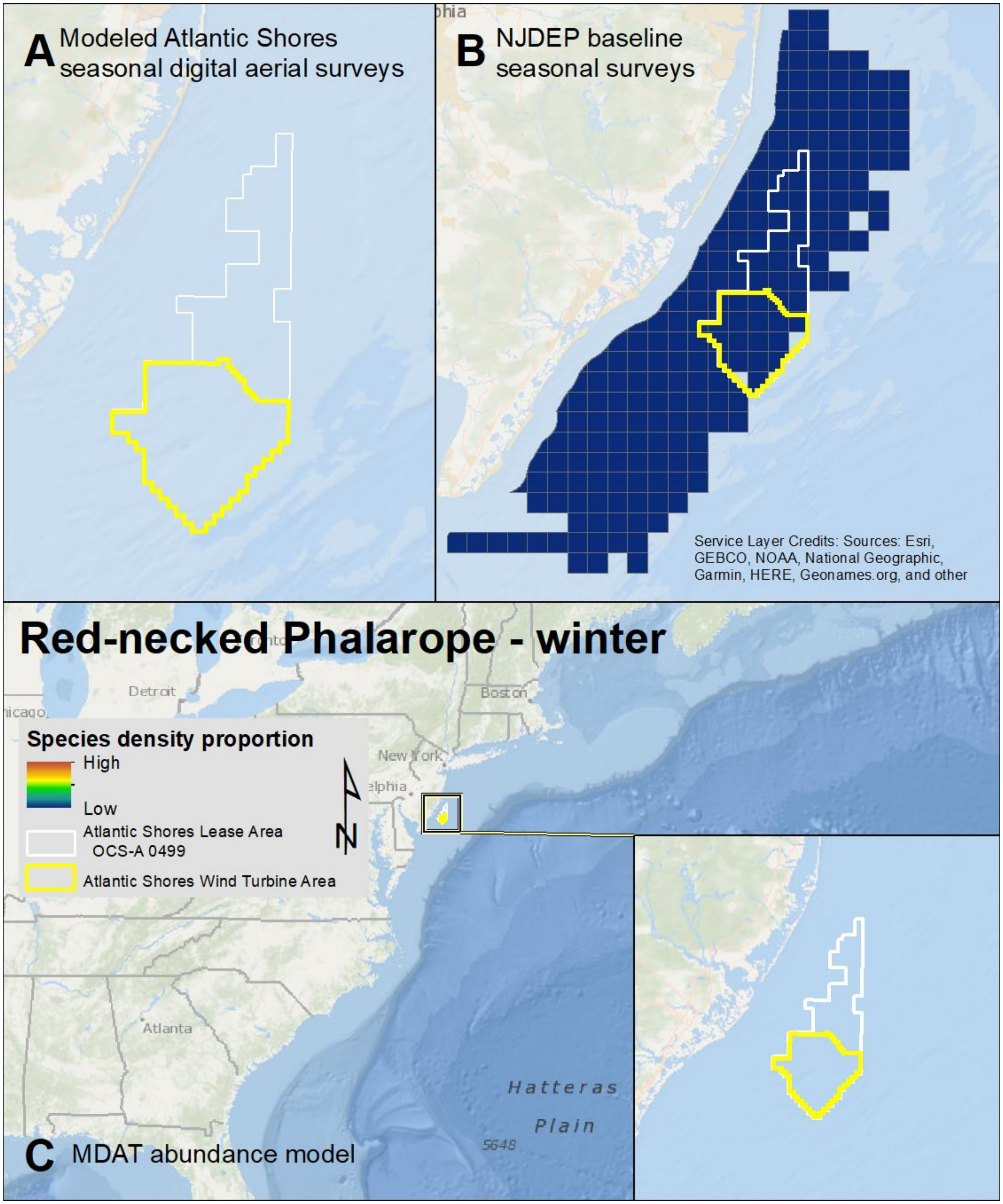

Map 174. Winter Red-necked Phalarope modeled density proportions in the Atlantic Shores seasonal digital aerial surveys (A), density proportions in the NJDEP baseline survey data (B), and the MDAT data at local and regional scales (C). The scale for all maps is representative of relative spatial variation in the sites within the season for each data source.

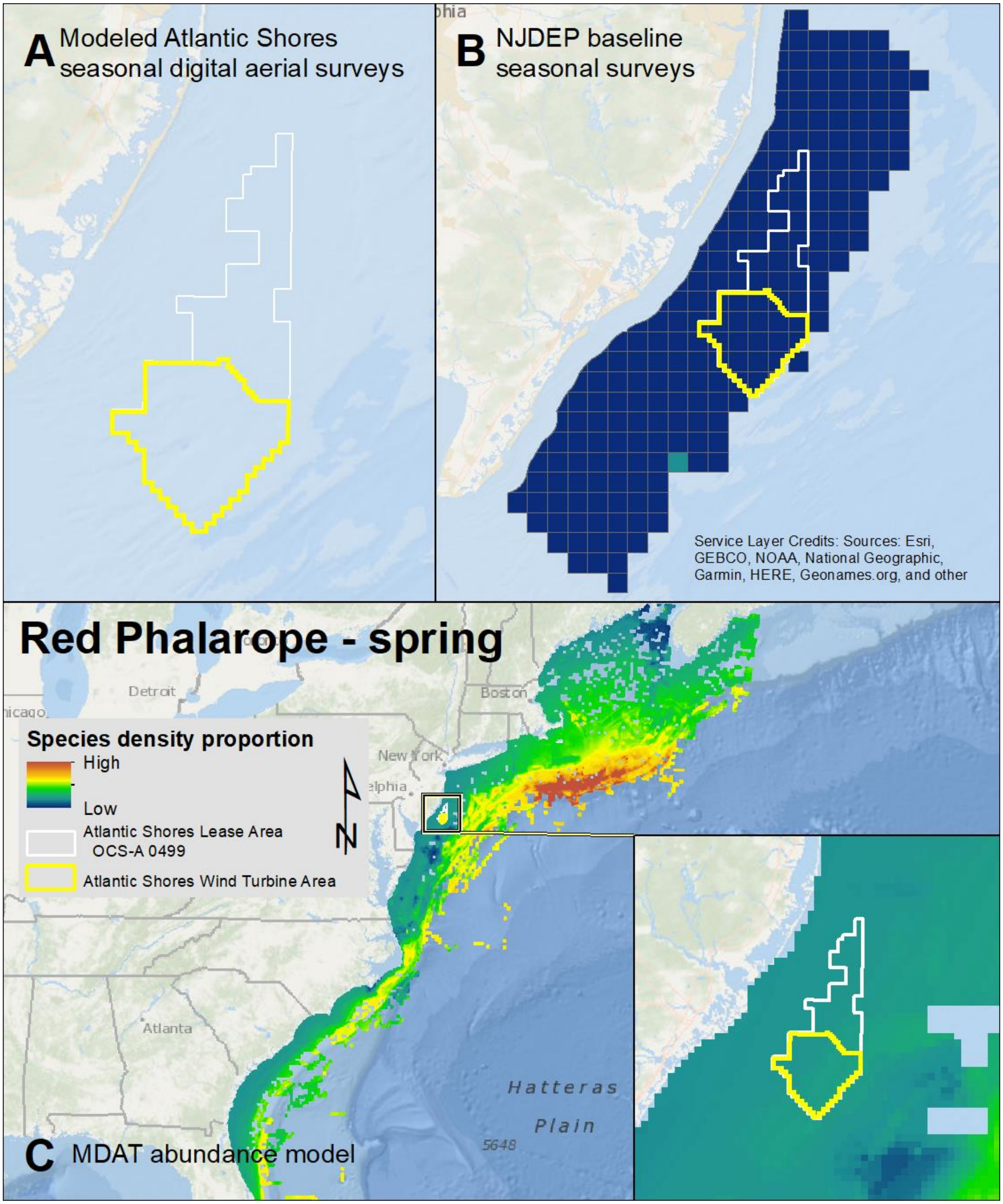

Map 175. Spring Red Phalarope modeled density proportions in the Atlantic Shores seasonal digital aerial surveys (A), density proportions in the NJDEP baseline survey data (B), and the MDAT data at local and regional scales (C). The scale for all maps is representative of relative spatial variation in the sites within the season for each data source.

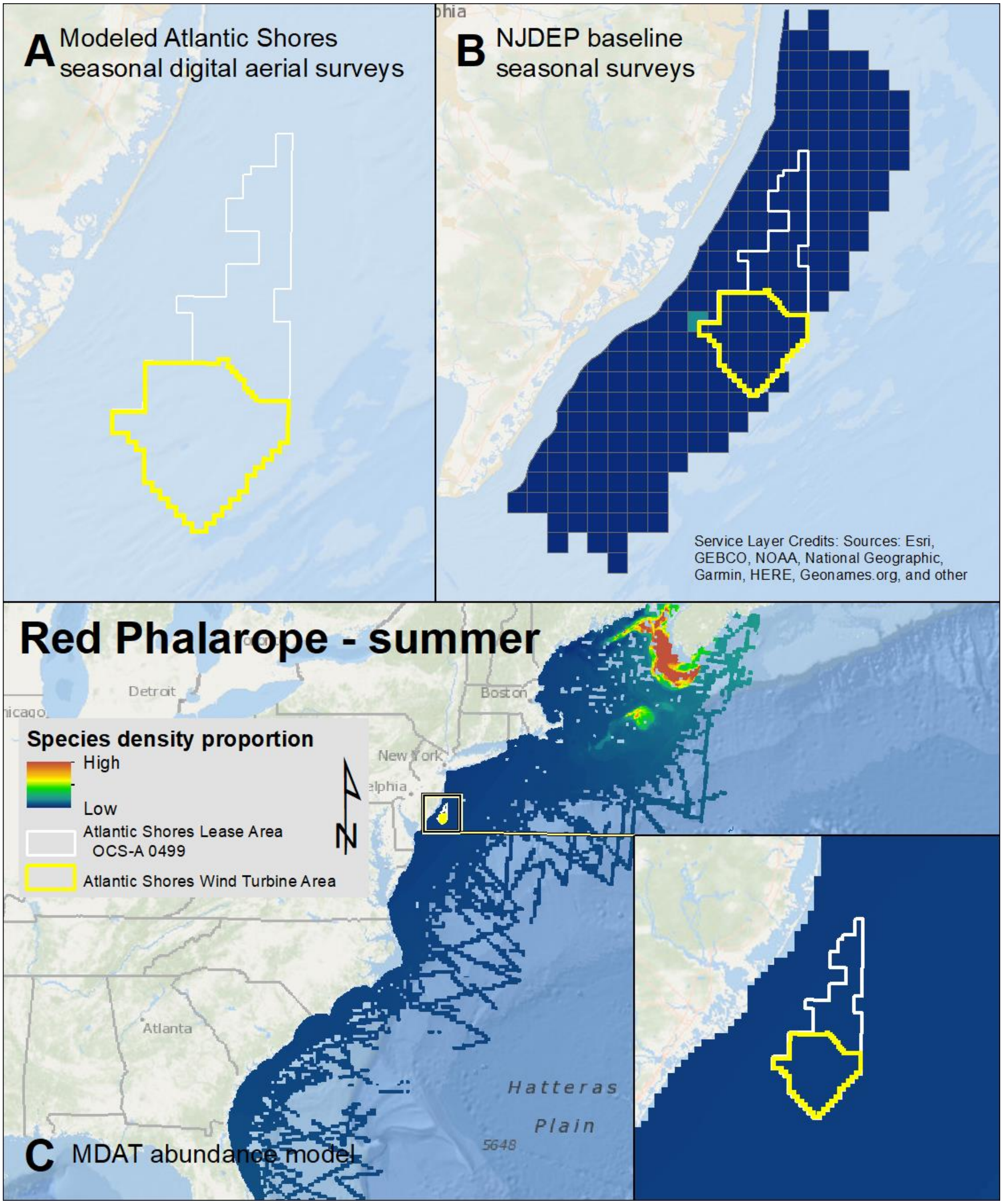

Map 176. Summer Red Phalarope modeled density proportions in the Atlantic Shores seasonal digital aerial surveys (A), density proportions in the NJDEP baseline survey data (B), and the MDAT data at local and regional scales (C). The scale for all maps is representative of relative spatial variation in the sites within the season for each data source.

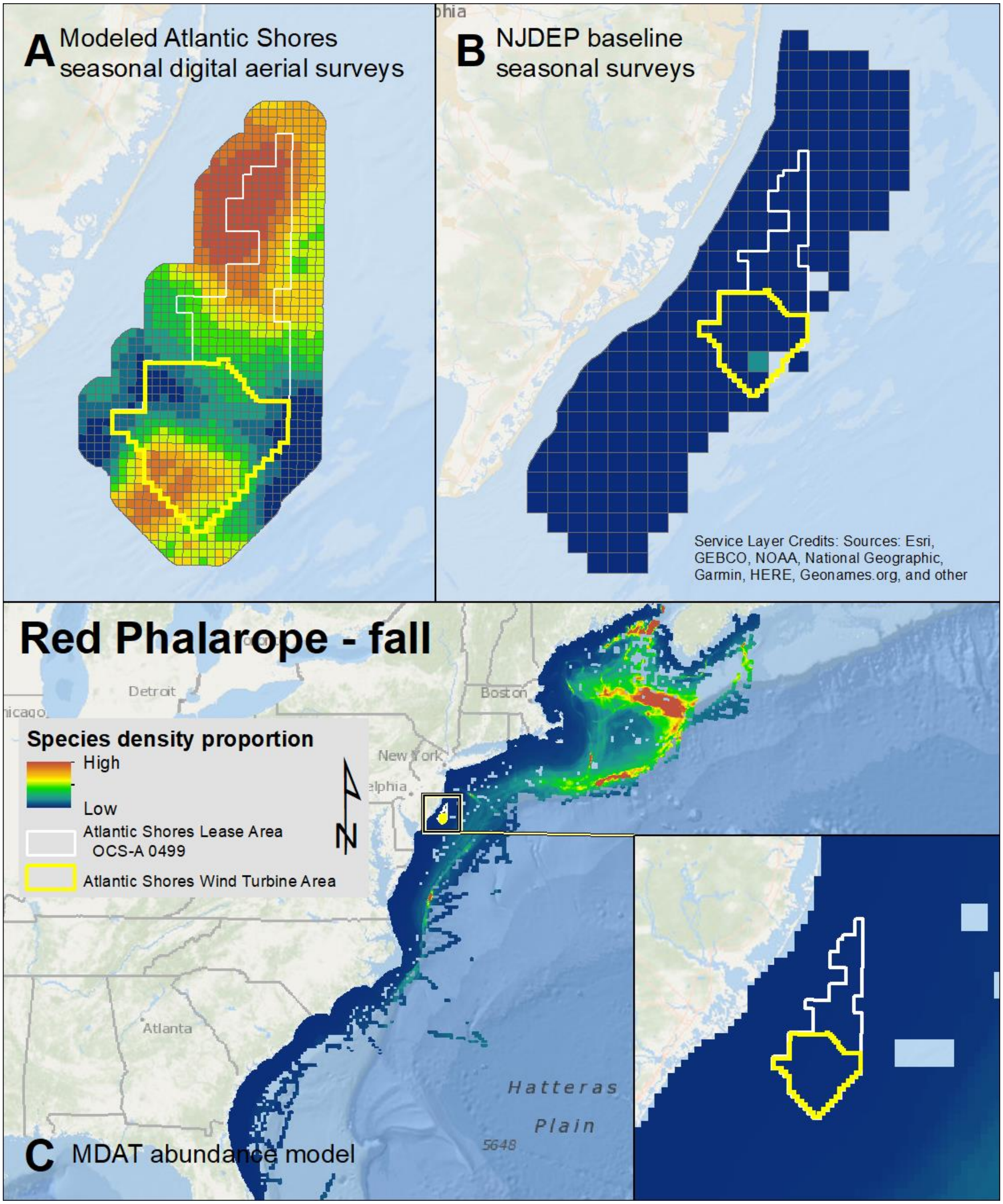

Map 177. Fall Red Phalarope modeled density proportions in the Atlantic Shores seasonal digital aerial surveys (A), density proportions in the NJDEP baseline survey data (B), and the MDAT data at local and regional scales (C). The scale for all maps is representative of relative spatial variation in the sites within the season for each data source.

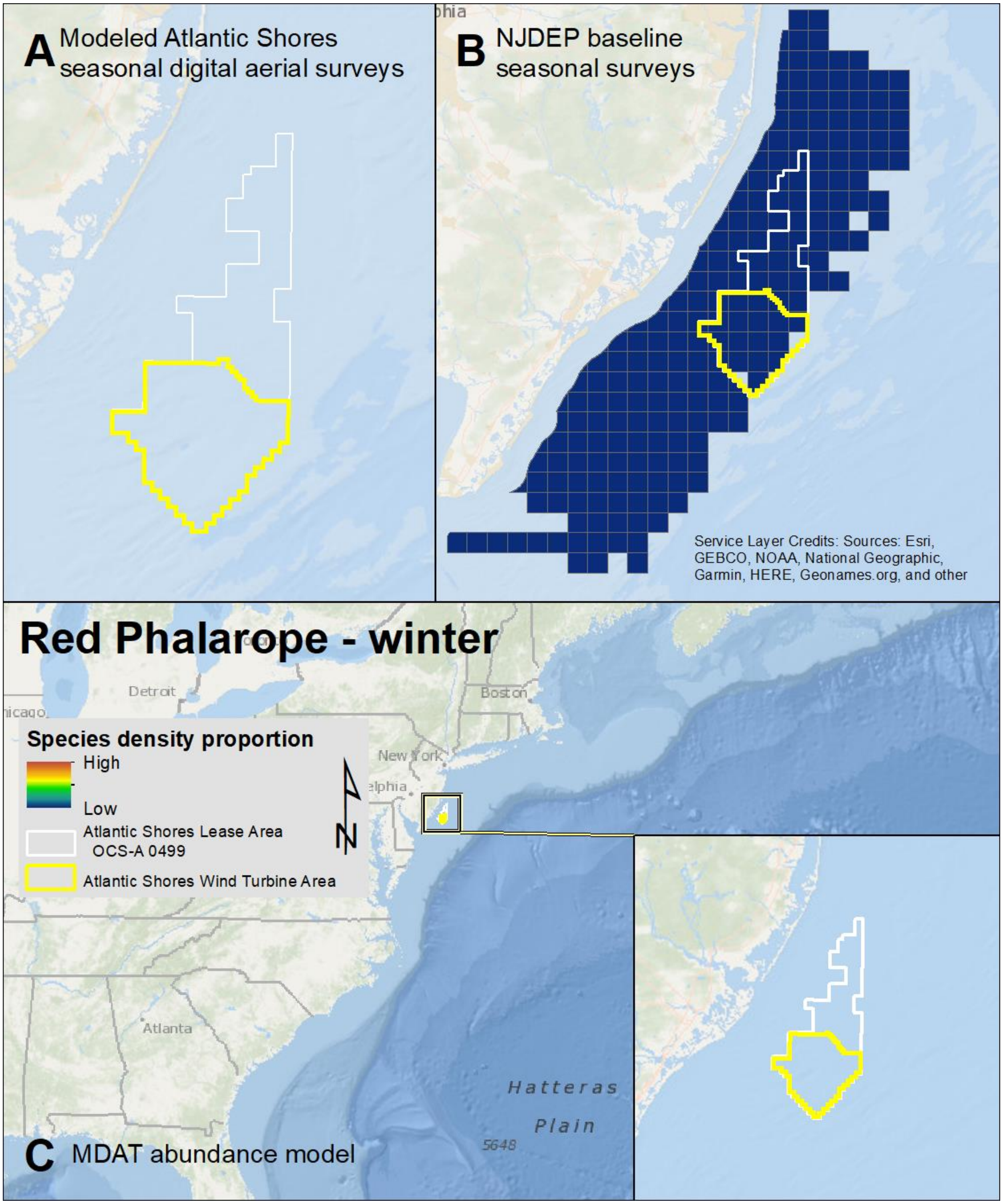

Map 178. Winter Red Phalarope modeled density proportions in the Atlantic Shores seasonal digital aerial surveys (A), density proportions in the NJDEP baseline survey data (B), and the MDAT data at local and regional scales (C). The scale for all maps is representative of relative spatial variation in the sites within the season for each data source.